

ANALYSIS AND CHARACTERIZATION OF PERFORATED NEUTRON DETECTORS

by

CLELL J. SOLOMON, JR.

B.S., Kansas State University, 2005

A THESIS

submitted in partial fulfillment of the

requirements for the degree

MASTER OF SCIENCE

Department of Mechanical and Nuclear Engineering

College of Engineering

KANSAS STATE UNIVERSITY

Manhattan, Kansas

2007

Approved by:

Major Professor

J. Kenneth Shultis

Abstract

Perforated neutron detectors suffer the unfortunate effect that their efficiency is a strong function of the direction of neutron incidence. It is found, by Monte Carlo simulation of many perforation shapes, that sinusoidal-type perforations greatly reduce the variation of detector efficiency. Detectors with rod-type perforations are modeled using a hybrid transport method linking the MCNP transport code and a specialized ion-transport code to calculate the probability that a neutron is detected. Channel, chevron, and sinusoidal perforations are modeled using other customized transport codes. Detector efficiency calculations are performed for neutrons incident at various polar and azimuthal angles. It is discovered that the efficiency losses of the detectors result from the decreasing solid angle subtended by the detector from the source and streaming through the detector at specific azimuthal angles. Detectors achieving an efficiency in excess of 10% and having a relatively flat $\pm 1\%$ angular dependence in all azimuthal angles and polar angles between 0 and 60° are predicted. Efficiencies up to 25% are achievable at the loss of directional independence.

In addition to minimizing the directional dependence of the perforated detectors, the feasibility of developing a neutron detector for deployment in cargo containers to locate nuclear weapon pits is investigated using the MCNP transport code. The detector considered is a 7-mm diameter, ^6LiF , rod-perforated detector surrounded in a cylinder of polyethylene. The optimum thicknesses of surrounding polyethylene, to maximize the response of the detector, is determined to be 10 cm of radial, 5 cm of front, and 5 cm of back polyethylene for end-on neutron incidence. Such a detector is predicted to produce a count rate between 12 and 15 cpm from a nuclear-weapon pit composed of 90% ^{239}Pu and 10% ^{240}Pu at a distance of 3 m. Side incidence is also considered, and the optimum moderator dimensions are 8 cm of radial, 10 cm of front, and 10 cm of back polyethylene that produce approximately the same count rate.

Table of Contents

Table of Contents	iii
List of Figures	v
List of Tables	ix
Acknowledgements	xi
1 Introduction	1
2 Detector Modeling Theory	3
2.1 Neutron Interaction in ^{10}B , ^6LiF , and Si	3
2.1.1 Basics of Neutron Interaction	3
2.1.2 Thermal Neutron Interactions in ^{10}B	6
2.1.3 Thermal Neutron Interactions in ^6LiF	7
2.1.4 Neutron Interactions in Si	8
2.2 Ion Producing Reaction for ^{10}B and ^6LiF	9
2.2.1 The $^{10}\text{B}(\text{n},\alpha)^7\text{Li}$ Reaction	9
2.2.2 The $^6\text{Li}(\text{n},\text{t})^4\text{He}$ Reaction	9
2.3 Ion Interactions	10
2.3.1 The Interaction and Energy Loss of Charged Particles	10
2.3.2 Stopping Power, Range, and Residual Energy of Ions	11
2.3.3 Ion Straggling	13
2.3.4 Energy Deposition and Spectra	14
2.4 Detector Efficiency Considerations	17
2.4.1 Neutron Absorption Probability	17
2.4.2 Ion Detection Probability	18
2.4.3 Normalizing the Efficiencies	19
2.5 Monte Carlo Transport Simulation	19
2.5.1 Neutron Transport in Specialized Codes	20
2.5.2 Neutron Transport in MCNP	21
2.5.3 Monte Carlo Simulation of Ion Energy Deposition	21

3	Directional Sensitivity of Perforated Detectors	24
3.1	Motivation	24
3.2	Hybrid Method with MCNP and Specialized Ion Transport Code	25
3.2.1	The MCNP Model	25
3.2.2	The Ion Code Model	30
3.2.3	Marriage of the MCNP and Ion Transport Codes	31
3.2.4	Verification and Validation of the Hybrid Model	36
3.3	Specialized Detector Efficiency Calculation Codes	38
3.3.1	General Description of the Customized Codes	39
3.3.2	Unit Cell for Sinusoidal Perforations	41
3.3.3	Ray Intersections with Sinusoidal Planes	41
3.3.4	Verification and Validation of the Customized Codes	43
3.4	Angular Efficiency Results	45
3.4.1	Neutron Absorption Efficiencies	46
3.4.2	Ion Detection Probabilities	57
3.4.3	Total Neutron Detection Efficiencies	62
3.5	Normal Incidence Optimization	65
3.5.1	Chevron Detector Optimization	65
3.5.2	Sinusoidal Detector Optimization	70
3.6	Conclusions and Recommendations	72
4	Cargo Detector	74
4.1	Motivation	74
4.2	Cargo-container Detector Optimization	74
4.2.1	Detector Model	75
4.2.2	Results of Cargo-Detector Simulations	76
4.3	Nuclear Weapon Pit Modeling	81
4.3.1	Nuclear Weapon Pit Model	83
4.3.2	Results of Nuclear Pit Modeling	85
4.4	Feasibility of Pit Detection	88
4.5	Conclusions, Recommendations, and Suggested Future Work	91
A	Perforated Detector Efficiency Calculation Scripts and Codes	94
B	Perforated Detector Efficiency Tabulated Data	132
C	Cargo Detector Calculation Scripts and Codes	278
D	Cargo Detector Tabulated Data	294

List of Figures

1.1	A diagram of a perforated detector cross section	2
2.1	A parallel neutron beam incident on a medium of thickness a	4
2.2	Microscopic cross section for ^{10}B [X-5 Monte Carlo Team, 2003]	6
2.3	Microscopic cross section for ^6Li [X-5 Monte Carlo Team, 2003]	7
2.4	Microscopic cross section for F [X-5 Monte Carlo Team, 2003]	8
2.5	Microscopic cross section for Si [X-5 Monte Carlo Team, 2003]	9
2.6	The stopping power of an α particle in boron calculated from the Bethe-Bloche formula of Eq. (2.23)	12
2.7	Residual energy of a 1.47 MeV α particle in boron	13
2.8	Diagram of energy and range straggling. Adapted from Evans [1955]	15
2.9	Expected spectrum from a ^6LiF coated diode with a film thickness of $20\ \mu\text{m}$	16
2.10	Expected spectrum from a ^6LiF $20\ \mu\text{m}$ wide channel perforated detector with a $20\ \mu\text{m}$ cap	17
2.11	Neutron incidence to perforated detector	18
2.12	Fluence and flow relation. Adapted from Shultis and Faw [2000].	20
2.13	Alpha and triton residual energies in LiF [Shultis and McGregor, 2004]	22
2.14	Hypothetical ion transport situation	23
3.1	Unit cell cross sections	26
3.2	Creating repeated structures in MCNP	27
3.3	Rotation of source about the perforated detector	29
3.4	3D diagram of rod-type perforation unit cell	32
3.5	Calculation of unit-cell absorption locations	36
3.6	3D rod-type unit-cell absorption locations for a $50 \times 50 \times 120\text{-}\mu\text{m}^3$ unit cell with a $20\text{-}\mu\text{m}$ cap thickness and $30\text{-}\mu\text{m}$ diameter rods	37
3.7	2D neutron absorption distributions for the normal incidence case. The data of Fig. 3.6 has been projected onto the (a) x - y and (b) y - z planes	37
3.8	2D neutron absorption distributions for nearly glancing incidence	38
3.9	Comparison of numerical calculation to analytical solution for a coated diode detector with a $3.54\text{-}\mu\text{m}$ thick film	39
3.10	A sinusoidal plane having a y offset of P_y , an amplitude of Δ , and a period of w	42

3.11	Sinusoidal unit-cell surface crossing locations for neutrons randomly positioned and isotropically directed throughout the unit cell. (a) is the projection of the crossing locations on the x - y plane, and (b) is their projection on the x - z plane.	43
3.12	3D sinusoidal unit cell showing the absorption locations	44
3.13	2D projections of the sinusoidal unit-cell absorption locations from Fig. 3.12 onto the (a) x - y plane and (b) x - z plane	44
3.14	Comparison of numerical and analytical solutions for coated diode detector efficiencies for a 26- μm ^6LiF film and a 2.4- μm ^{10}B film	45
3.15	The neutron absorption efficiency of a ^{10}B rod perforated detector with 30- μm perforation depth, 6- μm diameter rods, and no cap	46
3.16	The neutron absorption efficiency of a ^6LiF rod perforated detector with 100- μm perforation depth, 30- μm diameter rods, and no cap	47
3.17	The neutron absorption efficiency of a ^6LiF rod perforated detector with 300- μm perforation depth, 30- μm diameter rods, and no cap	48
3.18	Streaming in rod perforated detectors	48
3.19	The neutron absorption efficiency of a ^6LiF rod perforated detector with 100- μm perforation depth, 30- μm diameter rods, and a 20- μm cap	49
3.20	The neutron absorption efficiency of a ^{10}B channel perforated detector with 30- μm perforation depth, 4- μm wide channels, and no cap	50
3.21	The neutron absorption efficiency of a ^6LiF channel perforated detector with 100- μm perforation depth, 20- μm wide channels, and no cap	50
3.22	Streaming in channel perforated detectors	51
3.23	The neutron absorption efficiency of a ^{10}B chevron perforated detector with 30- μm perforation depth, 4- μm wide channels, and no cap	52
3.24	The neutron absorption efficiency of a ^6LiF chevron perforated detector with 100- μm perforation depth, 20- μm wide channels, and no cap	52
3.25	The neutron absorption efficiency of a ^6LiF sinusoid perforated detector with 100- μm perforation depth, 130- μm sine period, 40- μm sine amplitude, 35- μm sine wave separation, and no cap	53
3.26	The neutron absorption efficiency of a ^{10}B sinusoid perforated detector with 30- μm perforation depth, 4- μm sine period, 4- μm sine amplitude, 4- μm sine wave separation, and no cap	54
3.27	The neutron absorption efficiency of a ^6LiF sinusoid perforated detector with 100- μm perforation depth, 20- μm sine period, 20- μm sine amplitude, 20- μm sine wave separation, and no cap	54
3.28	The neutron absorption efficiency of a ^6LiF sinusoid perforated detector with 100- μm perforation depth, 30- μm sine period, 40- μm sine amplitude, 30- μm sine wave separation, and no cap	55
3.29	The neutron absorption efficiency of stacked ^6LiF rod detectors with 100- μm perforation depth, 30- μm diameter rods, and no cap	55
3.30	The neutron absorption efficiency of stacked ^6LiF channel detectors with 100- μm perforation depth, 25- μm wide channels, and no cap	56
3.31	The neutron absorption efficiency of stacked ^6LiF chevron detectors with 100- μm perforation depth, 25- μm wide channels, and no cap	56

3.32	The ion-detection efficiency of a ^{10}B rod detector with 30- μm deep perforations, 6- μm diameter rods, and no cap	57
3.33	The ion-detection efficiency of a ^6LiF rod detector with 100- μm deep perforations, 30- μm diameter rods, and no cap	58
3.34	The ion-detection efficiency of a ^{10}B rod detector with 30- μm deep perforations, 6- μm diameter rods, and a 4- μm cap	59
3.35	The ion-detection efficiency of a ^{10}B channel detector with 30- μm deep perforations, 4- μm wide channels, and no cap	60
3.36	The ion-detection efficiency of a ^6LiF channel detector with 100- μm deep perforations, 20- μm wide channels, and no cap	60
3.37	The ion-detection efficiency of a ^{10}B chevron detector with 30- μm deep perforations, 4- μm wide channels, and no cap	61
3.38	The ion-detection efficiency of a ^6LiF chevron detector with 100- μm deep perforations, 20- μm wide channels, and no cap	61
3.39	The ion-detection efficiency of a ^{10}B sinusoid detector with 30- μm deep perforations, 4- μm wave period, 4- μm wave separation, 4- μm wave amplitude, and no cap	62
3.40	The ion-detection efficiency of a ^6LiF chevron detector with 100- μm deep perforations, 20- μm wave period, 20- μm wave separation, 20- μm wave amplitude, and no cap	63
3.41	The total detection efficiency of a ^{10}B rod perforated detector with 30- μm perforation depth, 6- μm diameter rods, and no cap	64
3.42	The total detection efficiency of a ^6LiF rod perforated detector with 100- μm perforation depth, 30- μm diameter rods, and no cap	64
3.43	The total detection efficiency of a ^{10}B channel perforated detector with 30- μm perforation depth, 4- μm wide channels, and no cap	65
3.44	The total detection efficiency of a ^6LiF channel perforated detector with 100- μm perforation depth, 20- μm wide channels, and no cap	66
3.45	The total detection efficiency of a ^{10}B chevron perforated detector with 30- μm perforation depth, 4- μm wide channels, and no cap	66
3.46	The total detection efficiency of a ^6LiF chevron perforated detector with 100- μm perforation depth, 20- μm wide channels, and no cap	67
3.47	The total detection efficiency of a ^{10}B sinusoid perforated detector with 10- μm perforation depth, 8- μm sine period, 1- μm sine amplitude, 0.5- μm sine wave separation, and no cap	67
3.48	The total detection efficiency of a ^6LiF sinusoid perforated detector with 100- μm perforation depth, 20- μm sine period, 20- μm sine amplitude, 20- μm sine wave separation, and no cap	68
3.49	The total detection efficiency of a ^6LiF sinusoid perforated detector with 100- μm perforation depth, 30- μm sine period, 40- μm sine amplitude, 30- μm sine wave separation, and no cap	68
3.50	The total detection efficiency of a ^6LiF sinusoid perforated detector with 100- μm perforation depth, 130- μm sine period, 40- μm sine amplitude, 35- μm sine wave separation, and no cap	69

3.51	Response variation as a function of channel widths for (a) ${}^6\text{LiF}$ and (b) ${}^{10}\text{B}{}^6\text{LiF}$	69
3.52	Chevron detector variable parameters	70
3.53	Finer view of response variation	71
3.54	Sinusoidal detector variable parameters	71
3.55	Response variation as a function of channel width and wave period for amplitudes Δ of (a) $20\ \mu\text{m}$, (b) $40\ \mu\text{m}$, and (c) $80\ \mu\text{m}$	72
4.1	Diagram of the cargo detector model	75
4.2	Detector response for end-on neutron incidence for varying radial polyethylene thicknesses	78
4.3	Composite plot showing the neutron absorption probability for end-on illumination for varying radial polyethylene thicknesses from 1 cm to 10 cm	79
4.4	Detector response for side neutron incidence for varying radial polyethylene thicknesses	81
4.5	Detector responses for end-on and side-on irradiation geometries	82
4.6	End-on detector response of a cargo-container detector with perforated detector radius of 2.5 cm, 5 cm front poly. thickness, 5 cm back poly. thickness, and 10 cm radial poly. thickness	83
4.7	k_{eff} as a function of the sphere radius and ${}^{240}\text{Pu}$ fraction	85
4.8	k_{eff} as a function of the sphere radius and ${}^{240}\text{Pu}$ fraction	86
4.9	The critical radius of a plutonium sphere as a function of the ${}^{240}\text{Pu}$ fractional content	86
4.10	Total neutron fluxes across sphere surface for both α -phase and δ -phase plutonium from spontaneous fissioning of ${}^{240}\text{Pu}$ alone (No Fission) and with secondary fissioning of ${}^{239}\text{Pu}$. The α and δ -phases produce almost exactly the same results.	87
4.11	Neutron energy flux crossing sphere surface for varying ${}^{240}\text{Pu}$ fractions	87
4.12	Equivalent point source strengths from plutonium spheres from both spontaneous fissions and neutron induced fissions	88
4.13	Neutron absorption rate in the detector	89
4.14	Estimated neutron count rate	90

List of Tables

3.1	MCNP materials and cross sections	28
4.1	MCNP material's and cross sections used	76
B.1	^{10}B rod detector with 30 μm deep perforations, 6 μm diameter rods, and no cap	134
B.2	^{10}B rod detector with 50 μm deep perforations, 6 μm diameter rods, and no cap	143
B.3	^{10}B rod detector with 30 μm deep perforations, 6 μm diameter rods, and 4 μm cap	152
B.4	^6LiF rod detector with 100 μm deep perforations, 30 μm diameter rods, and no cap	161
B.5	^6LiF rod detector with 300 μm deep perforations, 30 μm diameter rods, and no cap	170
B.6	^6LiF rod detector with 100 μm deep perforations, 30 μm diameter rods, and 20 μm cap	179
B.7	^{10}B channel detector with 30 μm deep perforations, 4 μm wide channels, and no cap	188
B.8	^{10}B channel detector with 50 μm deep perforations, 4 μm wide channels, and no cap	197
B.9	^6LiF channel detector with 100 μm deep perforations, 20 μm wide channels, and no cap	206
B.10	^{10}B chevron detector with 30 μm deep perforations, 4 μm wide channels, and no cap	215
B.11	^6LiF chevron detector with 100 μm deep perforations, 20 μm wide channels, and no cap	224
B.12	^{10}B sinusoid detector with 30 μm deep perforations, 4 μm wave separation, 4 μm wave period, 4 μm wave amplitude, and no cap	233
B.13	^{10}B sinusoid detector with 10 μm deep perforations, 0.5 μm wave separation, 8 μm wave period, 1 μm wave amplitude, and no cap	242
B.14	^6LiF sinusoid detector with 100 μm deep perforations, 20 μm wave separation, 20 μm wave period, 20 μm wave amplitude, and no cap	251
B.15	^6LiF sinusoid detector with 100 μm deep perforations, 30 μm wave separation, 30 μm wave period, 40 μm wave amplitude, and no cap	260

B.16 ${}^6\text{LiF}$ sinusoid detector with 100 μm deep perforations, 35 μm wave separation, 130 μm wave period, 40 μm wave amplitude, and no cap	269
D.1 End-on irradiation for 1 cm radial poly. thck.	296
D.2 End-on irradiation for 2 cm radial poly. thck.	300
D.3 End-on irradiation for 3 cm radial poly. thck.	304
D.4 End-on irradiation for 4 cm radial poly. thck.	308
D.5 End-on irradiation for 5 cm radial poly. thck.	312
D.6 End-on irradiation for 6 cm radial poly. thck.	316
D.7 End-on irradiation for 7 cm radial poly. thck.	320
D.8 End-on irradiation for 8 cm radial poly. thck.	324
D.9 End-on irradiation for 9 cm radial poly. thck.	328
D.10 End-on irradiation for 10 cm radial poly. thck.	332
D.11 Side irradiation for 1 cm radial poly. thck.	336
D.12 Side irradiation for 2 cm radial poly. thck.	340
D.13 Side irradiation for 3 cm radial poly. thck.	344
D.14 Side irradiation for 4 cm radial poly. thck.	348
D.15 Side irradiation for 5 cm radial poly. thck.	352
D.16 Side irradiation for 6 cm radial poly. thck.	356
D.17 Side irradiation for 7 cm radial poly. thck.	360
D.18 Side irradiation for 8 cm radial poly. thck.	364
D.19 Side irradiation for 9 cm radial poly. thck.	368
D.20 Side irradiation for 10 cm radial poly. thck.	372
D.21 α -phase criticality values	376
D.22 δ -phase criticality values	387
D.23 α -phase Pu sphere surface flux	398
D.24 δ -phase Pu sphere surface flux	399

Acknowledgments

I would like foremost to thank Dr. Ken Shultis for his mentoring and assistance with this research project. The guidance and instruction that he provided has been invaluable, not only for this project, but for my career goals and life aspirations as well.

I would like to acknowledge the assistance of many members of the KSU SMART Laboratory including Dr. Douglas McGregor, Walter McNeil, Steven Bellinger, Troy Unruh, Eric Patterson, former member Blake Rice, Beth Holste, Adam Streit, David Bruno, Brian Cooper, Melanie Elazegui, and Shawn Cowley.

I would also like to express my appreciation for the financial support of DTRA under contract number DTRA-01-03-C-0051, the National Science Foundation INR-MIP under grant number 0412208, and the U.S. Department of Energy under NEER grant number DE-FG07-04ID14599.

Special thanks goes to the U.S. Department of Energy's support through the DOE NE/HP Fellowship program sponsored by the U.S. Department of Energy's Office of Nuclear Energy, Science, and Technology.

Chapter 1

Introduction

The detection and quantification of neutron radiation fields is one of the more complicated topics in radiation-detection engineering and health physics. Much of the complexity arises from the fact that neutron interaction cross sections vary irregularly with neutron energy and are substantially different for each nuclide. By contrast, typical photon cross sections vary smoothly with photon energy, are mostly the same for all isotopes of an element, and change only slightly between neighboring elements. The neutrons also must typically be slowed from their high MeV-source energies over many decades of energy to around a few hundredths of an eV in order to be highly detectable. Thus, to analyze a neutron detector's response to a given source of neutrons, transport codes relying on highly accurate neutron cross sections and capability to calculate a neutron's change in energy as it interacts in the medium around the source and detector must be used.

As the science and technology of health physics, imaging, and radiation investigation of materials progresses, it is necessary to develop innovative radiation detectors with capabilities surpassing those available. One capability, always in demand, is a higher detection efficiency. Another demand is better spacial and angular resolution, i.e., smaller detectors. In general, a smaller detector has less neutron-absorbing material and, therefore, a lower efficiency. Thus, the two principal desired capabilities are generally contradictory.

Recently, detectors have been proposed by Shultis and McGregor [2004] that are small—giving high spatial resolution—and have efficiencies surpassing any solid state detectors available today. These detectors are called *perforated semiconductor detectors* because the semiconductor diodes have been perforated via plasma etching and backfilled with neutron absorbing materials, greatly increasing the probability an incident neutron is absorbed compared to a diode with only a film coating on one surface. In most cases there are three parts to the diode-detector, as shown in Fig. 1.1: the semiconductor diode, the perforations filled with neutron absorbing material, and a cap or film of neutron absorbing material.

In most applications, where the neutrons are normally incident to the detector, the proposed detectors perform well. However, when the angle of incidence to the detector is oblique the detectors do not perform as well because of streaming problems [Solomon et al., 2007]. Thus, in neutron scattering experiments or spallation experiments where the angles from which the neutrons originate is important these small detectors preferentially detect the neutrons traveling in a specific direction, which is undesirable.

The first part of this work focuses on Monte Carlo modeling the response of perforated

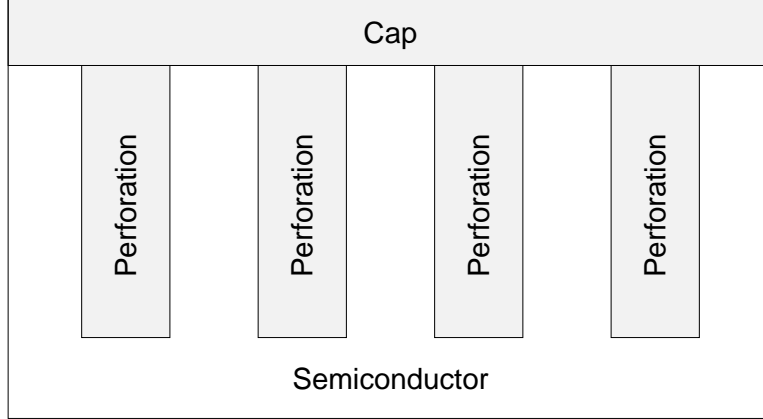


Fig. 1.1. A diagram of a perforated detector cross section

detectors having different shaped perforations. The efficiencies of such devices are investigated, and special attention is paid to the angular responses of the devices to minimize any streaming problems so as to maintain equal response regardless of the direction of neutron incidence. Both ^{10}B and ^6LiF are considered for the neutron-reactive materials with silicon as the diode material.

The second part of this work considers a special application of the perforated detectors in a situation where the direction of neutron incidence is unknown. The matter of national security is of particular interest to the United States and other nations across the world, particularly in response to the events of 9-11. Additional concern over the terrorist deployment of radiological and biological weapons has sparked research efforts to develop detectors and methods that can provide an early detection of threats. To this end, a cargo container detector design has been investigated to determine the feasibility of detecting a Pu-pit nuclear weapon that may, potentially, be transported in cargo transport containers.

This detector is constructed by placing a perforated detector at the center of a cylinder of polyethylene. The thickness of the polyethylene moderator producing the greatest response to spontaneous fission neutrons is investigated. Additionally, a nuclear-weapon pit is simulated and the detected response is calculated. It should be noted here that, for obvious reasons, information regarding the design of nuclear weapons is highly classified and the accuracy to which the weapon pit was simulated is unknown. In particular, the multiplication factor, k_{eff} , of a subcritical weapon pit is unknown to this investigator and is a highly important factor in determining the rate of spontaneous fission neutrons emitted from the pit. None the less, reasonable estimations are made and the neutron flux and detector response is estimated.

This thesis discusses the theory necessary to understand the computations for both the perforated-detector calculations and the cargo-container neutron detector calculations in Chapter 2. Chapter 3 focuses on the calculations associated with the perforated-detector angular efficiencies and describes how the calculations were performed, presents the results of the calculations, and gives concluding thoughts regarding these detectors. Lastly, the cargo-container detector calculations are discussed in Chapter 4 along with conclusions and suggestions of further study.

Chapter 2

Detector Modeling Theory

Modeling radiation detectors is a multi-faceted process requiring knowledge of both how the radiation to be detected interacts in the detector and the process through which an electrical signal is generated and recorded as a count. In general, ionizing radiation enters into the sensitive region of a detector, ionizes the detecting region, and the charge generated through the ionization is collected, and, if the collected charge is sufficient, a count is recorded. Multiple physical processes can be harnessed to produce ionization; in the case of high-energy photons the photoelectric effect, Compton scattering, and pair production cause excitation of electrons in the detection medium; thus, they are *indirectly ionizing*. Charged particles are *directly ionizing* in that their movement through the ambient medium alone generates charge along their paths of travel. Neutrons, as with photons, are indirectly ionizing and have many reactions that can be utilized to generate secondary ionizing effects. For example, the neutron-induced fission reactions are used in gaseous detectors because massive ions are emitted causing extreme ionization in the detector. Likewise, The ${}^3\text{He}(n,p){}^3\text{H}$ reaction is also utilized in gas detectors.

The most common of the neutrons reactions used for thermal-neutron detection is the ${}^{10}\text{B}(n,\alpha){}^7\text{Li}$ reaction. The perforated detectors are modeled using ${}^{10}\text{B}$ as the neutron absorbing material in a silicon substrate (diode). Calculations are also performed using ${}^6\text{LiF}$ as the absorbing medium in a silicon substrate.

2.1 Neutron Interaction in ${}^{10}\text{B}$, ${}^6\text{LiF}$, and Si

2.1.1 Basics of Neutron Interaction

The Macroscopic Cross Section

Consider a parallel beam of neutrons of intensity $I^\circ \text{ cm}^{-2} \text{ s}^{-1}$ incident on an infinite slab of some medium, as shown in Fig. 2.1. The probability, per differential distance of travel, that a neutron interacts (by scatter, absorption, etc.) is denoted by Σ , the *macroscopic cross section*. Thus, the probability the neutron interacts in dx about x is Σdx and the rate of change in the uncollided intensity with distance is given by

$$\frac{dI(x)}{dx} = -\Sigma I^\circ(x), \quad (2.1)$$

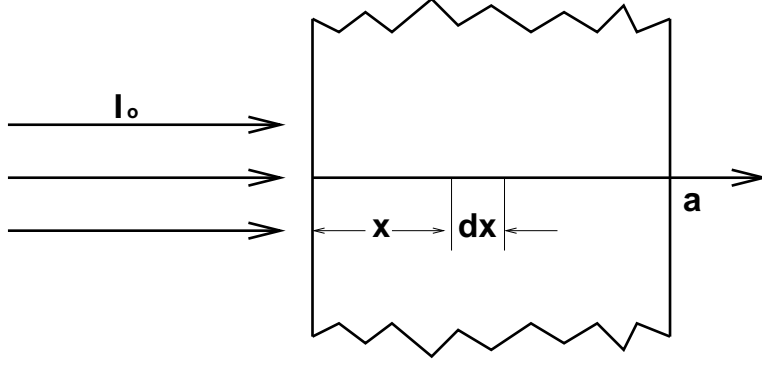


Fig. 2.1. A parallel neutron beam incident on a medium of thickness a

where $\Sigma I^\circ(x)$ is the interaction rate per unit volume. Solution of this differential equation yields the well-known interaction equation:

$$I^\circ(x) = I^\circ(0) \exp(-\Sigma x). \quad (2.2)$$

It follows that the reaction rate per unit volume, $F(x)$, occurring at distance x in the medium is

$$F(x) = \Sigma I^\circ(0) \exp(-\Sigma x), \quad (2.3)$$

which is termed *the reaction-rate density*. Any number of reaction types are possible depending on the elements composing the medium, so that if n types of reactions are possible the reaction-rate density of the i -th type is:

$$F_i(x) = \Sigma_i I^\circ \exp(-\Sigma x), \quad (2.4)$$

where the total Σ is:

$$\Sigma = \sum_{i=1}^n \Sigma_i. \quad (2.5)$$

The Microscopic Cross Section

The macroscopic cross section Σ is dependent on the isotopes composing the medium and their relative abundance. As the medium becomes more dense, the probability of interaction increases. Additionally, the macroscopic cross section varies with the isotope of the atom with which the neutron is interacting. Thus, the macroscopic cross section varies proportionally with the atomic density of the medium, i.e.,

$$\Sigma \propto N. \quad (2.6)$$

The constant of proportionality σ is the *microscopic cross section*. Thus,

$$\Sigma = N\sigma. \quad (2.7)$$

For media composed of m different nuclides, the i -th reaction type cross section Σ_i of the media is

$$\Sigma_i = \sum_{j=1}^m N_j \sigma_i^j. \quad (2.8)$$

The microscopic cross section is measured in barns (b) where $1 \text{ b} = 1 \times 10^{-24} \text{ cm}^2$ and is a strong function of the incident neutron's energy.

Thermal-Average Cross Sections

The continuous, non-resonant, low-energy tail of the cross section varies even for thermal neutrons—neutrons having kinetic energies equal to those of the Maxwellian distribution of the medium's kinetic energy in which they are traveling. Because neutron cross sections are typically tabulated at discrete energies, one must obtain a thermal-averaged cross section for calculations involving thermal fluxes of neutrons. Lamarsh [2002] showed that given the 0.0253-eV (the most probable thermal energy in a water moderated reactor) neutron cross section, Σ_o , the thermal-average cross section is given as

$$\bar{\Sigma} = \frac{\sqrt{\pi}}{2} \left(\frac{T_o}{T} \right)^{1/2} g(T) \Sigma_o, \quad (2.9)$$

where T_o is a reference temperature of the *2200-m/s neutrons* ($\sim 293 \text{ K}$), T is the temperature of the neutrons, and $g(T)$ is the non- $1/v$ factor—accounting for low-energy resonances in the cross section. For $1/v$ -absorbers (referring to the low-energy tail of the absorption cross section varying as one-over-neutron velocity) such as ^{10}B and ^6Li , the $g(T)$ factor is unity.

Thermal neutrons interacting with $1/v$ -absorber materials are “independent of the velocity distribution of either neutrons or nuclei” [Lamarsh, 2002]. The flux in the absence of diffusion cooling is given by a Maxwellian distribution shown by Lamarsh [2002] to be

$$\phi(E) = \frac{2\pi n}{(\pi kT)^{3/2}} \left(\frac{2}{m} \right)^{1/2} E \exp\left(-\frac{E}{kT}\right), \quad (2.10)$$

where n is the neutron density, T is the neutron temperature, k is Boltzmann's constant, and m is the neutron mass. The thermal flux $\bar{\phi}$ can be obtained by integrating the expression over thermal energies—up to $\sim 5kT$, but the Maxwellian dies off quickly so the upper energy bound can be considered to be ∞ —given by Lamarsh [2002] as

$$\begin{aligned} \bar{\phi} &= \int_0^\infty \phi(E) dE \\ \bar{\phi} &= \frac{2}{\sqrt{\pi}} n \left(\frac{2kT}{m} \right)^{1/2}. \end{aligned} \quad (2.11)$$

Because the thermal-neutron average velocity \bar{v} is given as $\bar{v} = \sqrt{\frac{2kT}{m}}$, Lamarsh [2002] shows the equation above can be expressed as

$$\bar{\phi} = \frac{2}{\sqrt{\pi}} n \bar{v}. \quad (2.12)$$

Lamarsh [2002] further shows that the relationship between \bar{v} and v_o is

$$\frac{\bar{v}}{v_o} = \left(\frac{T}{T_o}\right)^{1/2}, \quad (2.13)$$

so that the thermal flux can be expressed

$$\bar{\phi} = \frac{2}{\sqrt{\pi}} \left(\frac{T}{T_o}\right)^{1/2} \phi_o \quad (2.14)$$

where $\phi_o = nv_o$ and is the 2200-m/s flux. Multiplying Eq. (2.9) for $1/v$ -absorbers ($g(T) = 1$) by the expression above, one finds

$$\bar{\phi}\bar{\Sigma} = \phi_o\Sigma_o. \quad (2.15)$$

Thus, interaction rates may be calculated without the thermal-averaged cross section provided the 2200-m/s flux is known.

2.1.2 Thermal Neutron Interactions in ^{10}B

The microscopic cross section for ^{10}B is shown in Fig. 2.2. It is apparent the behavior of ^{10}B at energies below 10 eV is that of a $1/v$ absorber, and one observes the elastic-scattering cross section of ^{10}B is approximately four orders of magnitude lower than the absorption cross section in the thermal (10^{-8} MeV) region. The 2200-m/s absorption cross section for ^{10}B is $\sigma_o = 3840$ b, which corresponds to a thermal-averaged cross section of $\bar{\sigma} = 3403$ b (for $T = 293$ K).

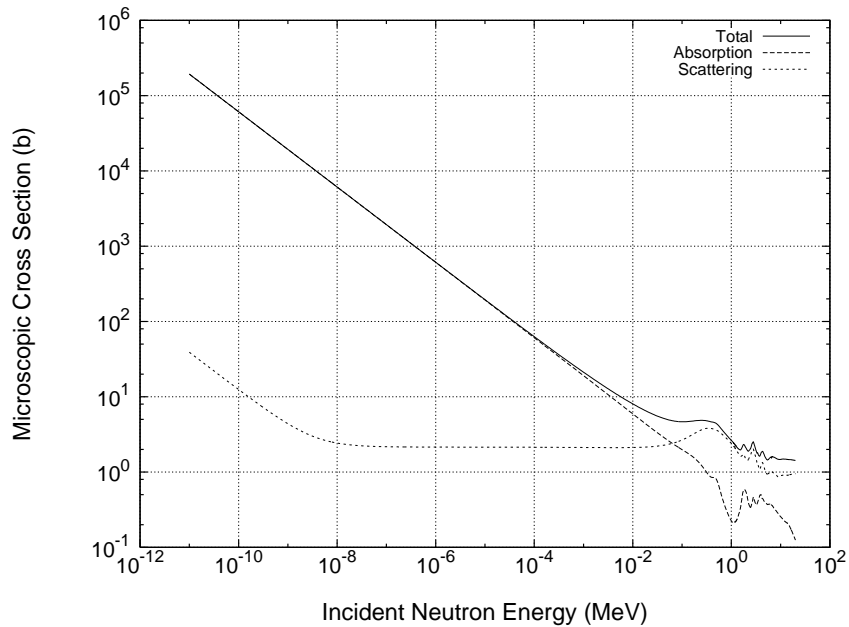


Fig. 2.2. Microscopic cross section for ^{10}B [X-5 Monte Carlo Team, 2003]

The macroscopic absorption cross section of pure ^{10}B is interesting to calculate because

the natural abundance of ^{10}B is about 20%. Because the addition or removal of a nucleon represents a much greater change in fractional mass for a light nuclide than a heavy nuclide, the density of ^{10}B is substantially less than that of naturally occurring boron (containing mostly ^{11}B). The density of ^{10}B $\rho(^{10}\text{B})$ is obtained from the ratio

$$\frac{M(^{10}\text{B})}{M(\text{B})} = \frac{\rho(^{10}\text{B})}{\rho(\text{B})}, \quad (2.16)$$

where $M(^{10}\text{B})$ represents the atomic mass of ^{10}B , $M(\text{B})$ represents the atomic mass of natural boron, and $\rho(\text{B})$ is the density of natural boron. One finds $\rho(^{10}\text{B}) = 2.176 \text{ g cm}^{-3}$. The thermal-averaged (n,α) cross section—practically equal to absorption cross section because almost all absorptions lead to an (n,α) reaction—for pure ^{10}B is $\bar{\Sigma}_{(n,\alpha)} \simeq \bar{\Sigma} = 443 \text{ cm}^{-1}$.

2.1.3 Thermal Neutron Interactions in ^6LiF

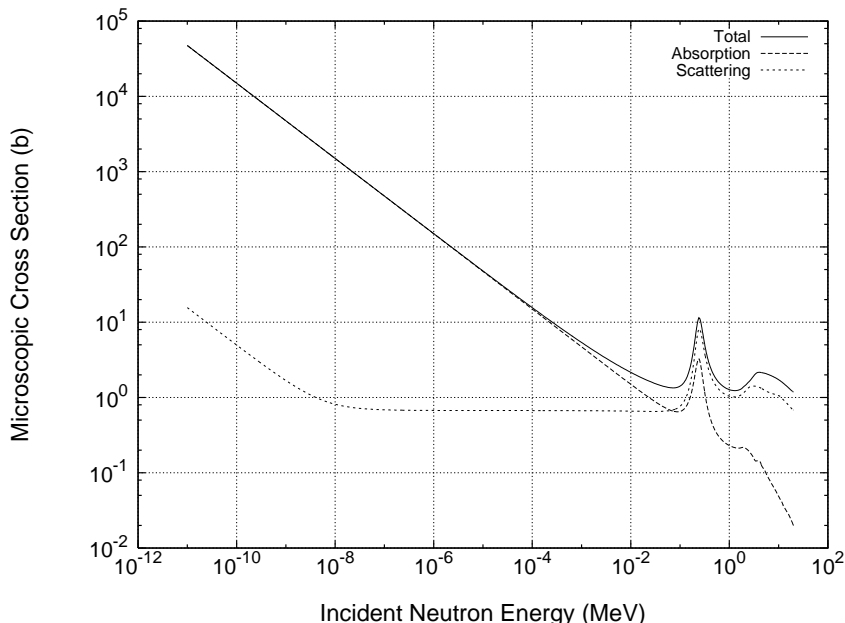


Fig. 2.3. Microscopic cross section for ^6Li [X-5 Monte Carlo Team, 2003]

The microscopic cross sections for ^6Li and ^{19}F are shown in Figs. 2.3 and 2.4, respectively. The cross sections show both nuclides are $1/v$ absorbers. The 2200-m/s microscopic absorption cross section for ^6Li is $\sigma_o = 940 \text{ b}$; the corresponding cross section for ^{19}F is $\sigma_o = 0.0091 \text{ b}$. Because ^{19}F has such a small absorption cross section, almost all the absorption occurs with the isotope ^6Li and seldom with ^{19}F . Additionally, all absorptions in ^{19}F are (n,γ) reactions, meaning the desired heavy ions are not produced, and, even if γ -rays are generated, they are unlikely to interact in the detector. Therefore, the absorption reactions in F are ignored in these computations.

To find the macroscopic absorption cross sections one solves the following equation for

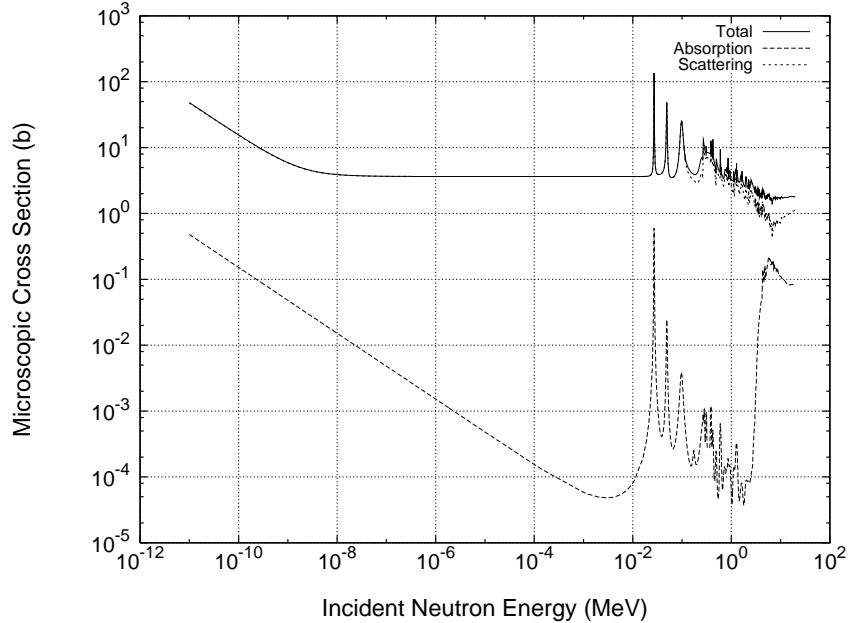


Fig. 2.4. Microscopic cross section for F [X-5 Monte Carlo Team, 2003]

the density of ${}^6\text{LiF}$:

$$\frac{M({}^6\text{LiF})}{M(\text{LiF})} = \frac{\rho({}^6\text{LiF})}{\rho(\text{LiF})}. \quad (2.17)$$

One finds that, given a density of 2.64 g cm^{-3} for natural LiF, the density of ${}^6\text{LiF}$ is 2.55 g cm^{-3} . From this density one finds, by Eq. (2.7), the 0.0253-eV macroscopic cross section of ${}^6\text{LiF}$ is $\Sigma_o = 57.6 \text{ cm}^{-1}$, thereby giving a thermal-averaged macroscopic cross section of $\bar{\Sigma} = 51.1 \text{ cm}^{-1}$, which again results almost exclusively from the (n,α) cross section.

The fluorine absorption cross section contribution is minuscule and is neglected in calculating the ${}^6\text{LiF}$ absorption cross sections. However, the scattering cross section of ${}^{19}\text{F}$ is slightly less negligible. The 0.0253-eV elastic scattering macroscopic cross section is $\Sigma_{so} = 0.229 \text{ cm}^{-1}$. The cross section, although not completely insignificant, is still only a fraction of the absorption cross section of the entire ${}^6\text{LiF}$ molecule, and thus is also neglected.

2.1.4 Neutron Interactions in Si

The microscopic cross section for Si (see Fig. 2.5) shows the thermal-neutron absorption interaction with Si is almost negligible when compared to ${}^{10}\text{B}$ or ${}^6\text{Li}$. In the thermal energy regime the absorption cross section is less than one-tenth of a barn indicating absorption is unlikely in the silicon; however, the scattering cross section for silicon in the thermal region is on the order of a few barns. For a silicon semiconductor $500 \mu\text{m}$ thick, the probability of normally incident thermal-neutron scattering interaction is $1 - \exp(-\Sigma_s x) = 0.002$, assuming a density of 2.33 g cm^{-3} . Absorption is even less likely, so both reactions are ignored in these calculations.

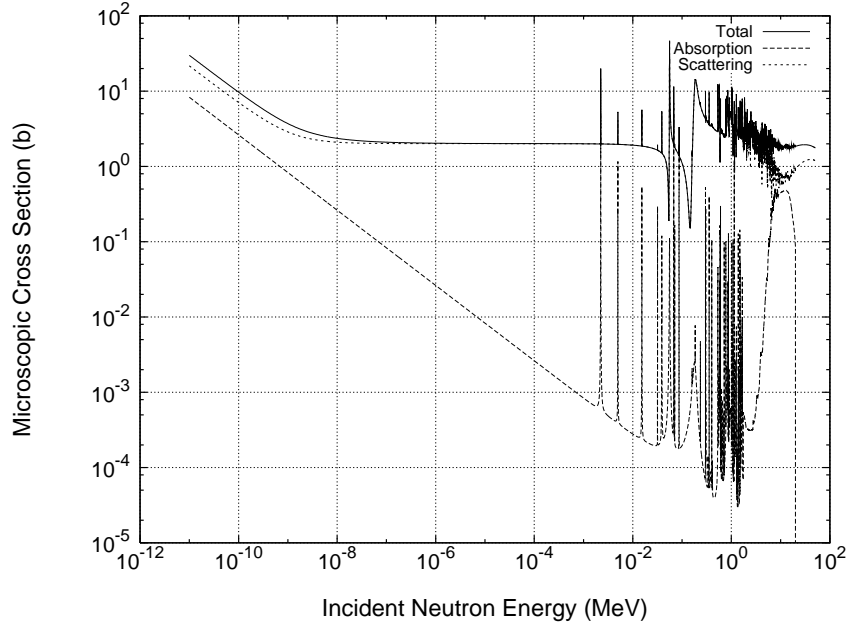


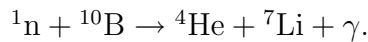
Fig. 2.5. Microscopic cross section for Si [X-5 Monte Carlo Team, 2003]

2.2 Ion Producing Reaction for ^{10}B and ^6LiF

2.2.1 The $^{10}\text{B}(n,\alpha)^7\text{Li}$ Reaction

The discussion of the ^{10}B cross section above shows the high cross section results primarily from absorption of neutrons, and it is this absorption that makes ^{10}B useful in radiation detectors. When a neutron is absorbed in ^{10}B , the nucleus is left in an excited and unstable state. To reach a point of stability, the nucleus splits into an α particle and a lithium ion.

The splitting of ^{10}B into an α particle and a lithium ion actually has two possible paths. The first possibility, occurring 94% of the time, goes as



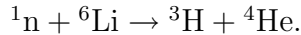
The Q-value for this reaction is 2.310 MeV, which, given the energy of the γ -ray is 0.48 MeV, means the kinetic energy of the emitted α particle is 1.47 MeV and the energy of the Li ion is 0.840 MeV.

The second branch of ^{10}B splitting upon neutron absorption occurs the remaining 6% of the time. In this reaction the gamma is not emitted and, as a result, the ions are ejected with greater energies. The Q-value for this reaction is 2.792 MeV, thereby giving an α energy of 1.777 MeV and a Li ion energy of 1.015 MeV.

2.2.2 The $^6\text{Li}(n,t)^4\text{He}$ Reaction

^6Li undergoes a similar process to that of ^{10}B when it absorbs a neutron. As noted above, the absorption reaction accounts for the majority of the cross section of ^6LiF , most of which

comes from neutron absorption by ${}^6\text{Li}$. The reaction is as follows:



The Q-value of the reaction is 4.78 MeV. The much higher Q-value for the ${}^6\text{Li}$ reaction as compared to the ${}^{10}\text{B}$ reaction produces secondary particles with substantially higher energies. The kinetic energy of the alpha particle emitted from the reaction is 2.05 MeV, and the energy of the triton is 2.73 MeV. The higher energies make ${}^6\text{LiF}$ preferable over ${}^{10}\text{B}$ because the higher-energy particles are more likely to escape the absorber material and enter the semiconductor with sufficient energy to be detected.

2.3 Ion Interactions

To properly model a neutron detector requires more than knowledge of how the neutron interacts in the detector, but is also dependent on understanding how the products of the ion-producing reactions interact, slow down, and deposit energy in the surrounding media. This section focuses on these mechanisms for the ions produced in the ${}^6\text{Li}(\text{n,t}){}^4\text{He}$ reaction and the ${}^{10}\text{B}(\text{n},\alpha){}^7\text{Li}$ reaction.

2.3.1 The Interaction and Energy Loss of Charged Particles

The interaction of fast charged particles is complicated by the Coulombic interactions as compared to neutral neutrons moving through a media. A neutron interacts only with the nucleus of an atom; however, charged particles interact continuously with the ambient electrons as well.

Charged particles, as they traverse a medium, interact with the ambient electrons and nuclei by both collision and emission of electro-magnetic radiation called bremsstrahlung. The collision of ions with atomic electrons dominates the rare interactions with the nuclei and comes in two “flavors”: (1) hard collisions where the energy transfer is great enough for the electron to be considered initially free, and (2) soft collisions in which binding effects of the electron must be considered.

Hard collisions are dependent, not only on the particle type, but also on the particle spin. The differential cross section Φ for spin 0 particles is shown by Evans [1955] to be

$$\Phi(Q)dQ = \frac{2\pi z^2 q^4}{m_o V^2} \frac{dQ}{Q^2} \left(1 - \beta^2 Q/Q_{max}\right), \quad (2.18)$$

where Q is the energy transferred, zq is the ion charge, m_o is the rest mass of an electron, and V is the velocity of the ion. Here, Q_{max} is the maximum possible energy transfer (see Evans [1955]). Of more interest than the cross section is the stopping power for hard collisions. An accurate expression for the stopping power resulting from a hard collision, regardless of spin, is given by [Evans, 1955]:

$$\frac{dT_H}{ds} = \frac{2\pi z^2 q^4}{m_o V^2} N Z \left(\ln \frac{Q_{max}}{H} - \beta^2\right). \quad (2.19)$$

The stopping power is of more practical importance because it describes the overall behavior of the ion in the slowing process by cumulatively considering many collisions. The stopping power is discussed in more depth in Section 2.3.2.

Soft collisions, however, are the dominant process in the slowing of ions. The stopping power for soft collisions in a medium can be expressed [Evans, 1955] as

$$\frac{dT_S}{ds} = \frac{4\pi z^2 q^4}{m_o V^2} N Z \ln \frac{2m_o V^2}{I}, \quad (2.20)$$

where I is the experimentally determined *mean ionization potential*. If one also considers relativistic effects of the ion then the expression for the stopping power becomes [Evans, 1955]

$$\left(\frac{dT_S}{ds}\right)_{Bethe} = \frac{4\pi z^2 q^4}{m_o V^2} N Z \left[\ln \frac{2m_o V^2 H}{I^2(1-\beta^2)} - \beta^2 \right], \quad (2.21)$$

where H is the minimum possible energy transfer.

The total stopping power of an ion is by the sum of the hard stopping power and soft stopping power, namely

$$\left(\frac{dT}{ds}\right)_{ion} = \frac{dT_H}{ds} + \frac{dT_S}{ds} = \frac{2\pi z^2 q^4}{m_o V^2} N Z \left[\ln \frac{2m_o V^2 Q_{max}}{I^2(1-\beta^2)} - \beta^2 \right]. \quad (2.22)$$

In the case that the kinetic energy of the particle is of an order of magnitude or less than the rest mass of the particle the stopping power simplifies to the well known Bethe-Bloch formula, shown by Evans [1955], to be

$$\left(\frac{dT}{ds}\right)_{ion} = \frac{4\pi z^2 q^4}{m_o V^2} N Z \left[\ln \frac{2m_o V^2}{I} - \ln(1-\beta^2) - \beta^2 \right]. \quad (2.23)$$

Although Eq. (2.23) gives a good approximation of the stopping power for high-energy particles, the formulations ceases to be effective for particles with energies less than about 1 MeV. A more rigorous treatment of the stopping powers at and below 1 MeV must be handled with higher order quantum mechanical calculations.

2.3.2 Stopping Power, Range, and Residual Energy of Ions

The stopping power is defined as the energy loss of a charged particle per unit differential path length of travel in a medium. It is a continuously varying function of the ion's kinetic energy. Figure 2.6, for example, presents the stopping power of an alpha particle in solid boron. The stopping power, in this example, is calculated using the Bethe-Bloch formula of Eq. (2.23). Immediately one notes some of the limitations of this formula; for example, one would expect the stopping power to go to zero at the origin because the particle has no velocity; however, the stopping power in the Bethe-Bloch formula goes to zero when the argument of the logarithm term is 1. Thus, by this model, the stopping power is zero at some finite energy.

The Bethe-Bloch formula is not the most rigorous treatment of the stopping power

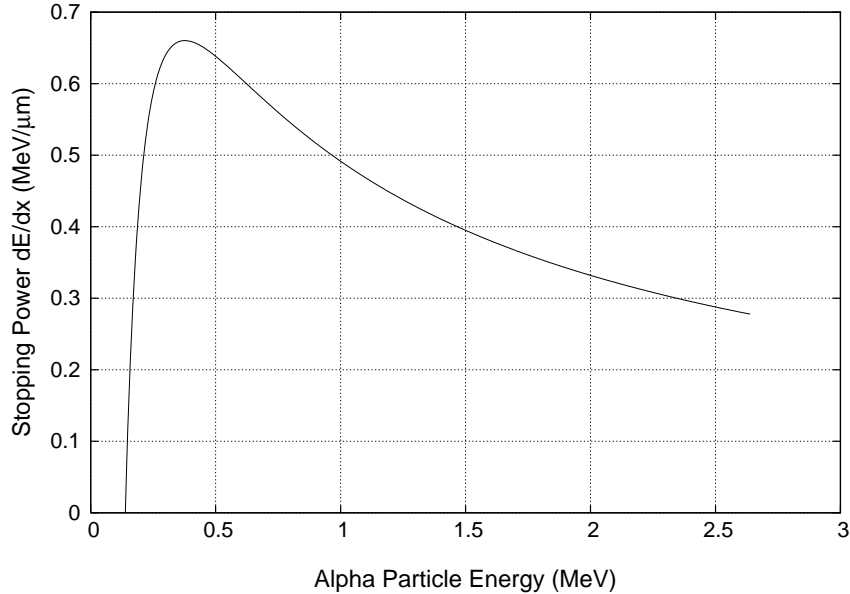


Fig. 2.6. The stopping power of an α particle in boron calculated from the Bethe-Bloche formula of Eq. (2.23)

available; however, for basic understanding of parametric variation of the stopping power it suffices. More extensive characterizations of the stopping power have been developed by Ziegler et al. [1985] where different quantum mechanical potentials are developed and applied. Lindhard et al. [1963] present another treatment of heavy ion slowing processes, but both treatments are not considered further in this work.

Given correct stopping powers for ions in a material, the average range of the particles can be calculated. The energy is related to the range. Specifically, given a heavy charged particle of some known energy, the average range of the particle is Gaussian distributed about some average range. The distribution results from the fact that not every particle undergoes the same interactions and therefore slows slightly differently, but the average behavior of many of the same type of particles is a distribution. For this reason, the range of heavy ions is often quoted to be the average range, but some of those particles exceed the average range and some terminate at a distance shorter than the average range.

The range of a particle can, in principle, be determined from the stopping power as given in Shultis and Faw [2000]:

$$\Lambda(E_o) = \int_0^{E_o} \frac{1}{dT/ds} dE. \quad (2.24)$$

Here Λ is the average range of the particle and E_o is the initial energy of the particle. The energy-range relationship is presented in Fig. 2.7 which shows the residual energy an alpha particle has after passing through a known distance of boron. The figure shows both the integrated Bethe-Bloche approximation and a more accurate range, calculated by Shultis and McGregor [2006] using the TRIM software package. One notes the Bethe-Bloche approximation is fairly accurate ($\pm 10\%$) to approximately 1 MeV. Lower than 1 MeV the approximation is poor and is a complete failure below energies at which the argument of the

logarithm term in Eq. (2.23) goes to 1.

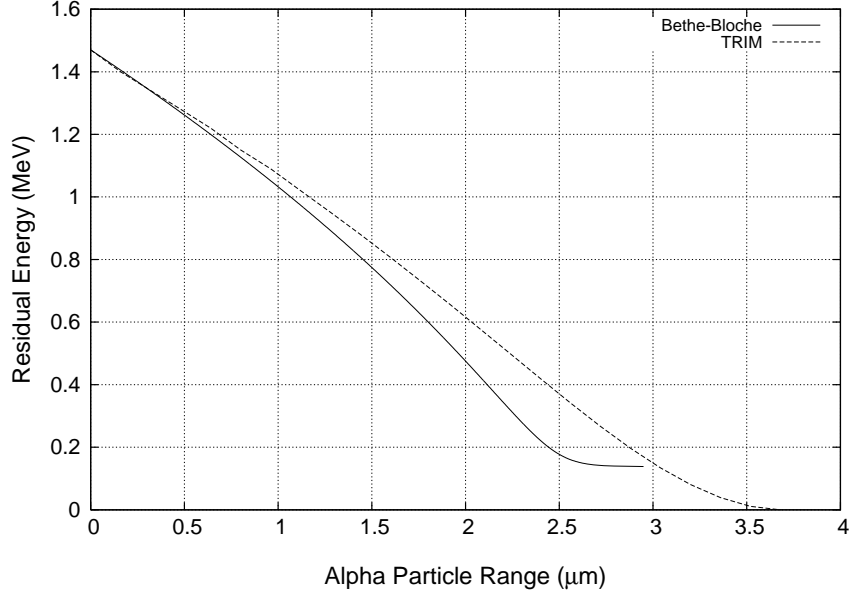


Fig. 2.7. Residual energy of a 1.47 MeV α particle in boron

2.3.3 Ion Straggling

Range Straggling

As previously mentioned, the range of a charged particle has a Gaussian distribution about the average range. A standard Gaussian distribution for the range is given by Evans [1955] as

$$\frac{dn}{n_o} = \frac{1}{\sqrt{2\pi}\sigma_R} \exp\left[-\frac{(x-R)^2}{2\sigma_R^2}\right] dx, \quad (2.25)$$

where R is the mean range, σ_R is the standard deviation, n is the number of particles traveling a specific range in the distribution, and n_o is the total number of particles. Alternatively, a parameter, α_o , is often defined as $\alpha_o \equiv \sqrt{2}\sigma_R$ and is called *the range-straggling parameter*. Substitution of this definition into the above expression yields

$$\frac{dn}{n_o} = \frac{1}{\sqrt{\pi}\alpha_o} \exp\left[-\left(\frac{(x-R)}{\alpha_o}\right)^2\right] dx. \quad (2.26)$$

Here, α_o is half the width of the distribution at a factor $1/e$ of the magnitude of the distribution at its mean [Evans, 1955].

Energy Straggling

It is also unlikely that any two ions slowing in the same medium undergo exactly the same number of collisions along every unit length of travel as they slow. Thus, the energy of heavy

charged particles, having traversed a given distance in a medium, has a distribution, and, because the slowing is stochastic, the distribution is a Gaussian distribution.

The variance in amount of energy lost ΔE by a charged particle over a distance Δx is given as [Evans, 1955]

$$\sigma_{\Delta E}^2 = 4\pi z^2 q^4 N Z \left(1 + \frac{kI}{m_o V^2} \ln \frac{2m_o V^2}{I} \right) \quad \text{ergs}^2/\text{cm}. \quad (2.27)$$

Here, k is a parameter approximately equal to $\frac{4}{3}$ for hydrogen like electrons. One notes the variance in the energy loss increases as target Z -number, ion Z -number, atom density, and mean ionization potential I increase, and the variance decreases as the velocity of the ion increases. These relationships are quite intuitive. As the Z -numbers and atom density increase the ion is more likely to collide causing more stochastic loss-of-energy collisions, thereby, increasing the variance of the energy loss. Likewise, as the mean ionization potential increases, the ion has a wider range of energy that can be transferred in a soft collision and, consequently, the variance of the energy loss increases. The energy-loss variance decreases with ion velocity because, as the ion moves faster, the time it spends in any unit length of a medium is smaller and the ion undergoes fewer interactions. The total variance of the energy σ_E^2 for a particle is then, in principle, given as

$$\sigma_E^2 = \int 4\pi z^2 q^4 N Z \left(1 + \frac{kI}{m_o V^2} \ln \frac{2m_o V^2}{I} \right) dx, \quad (2.28)$$

where the velocity itself is a continuously varying function of the distance obtained from stopping powers.

Combining the concepts of energy and range straggling, one notes a particle at any length along its path has a distribution of energies and ranges, unlike the relation shown in Fig. 2.7 where no straggling is shown. Truly, distributions exist in the values presented in Fig. 2.7, but the average behavior is plotted. Figure 2.8 on the other hand is a diagram depicting the energy and range straggle of some ion at a given point. Thus, at any given mean range and energy the ion can actually take on a value inside the rectangle marked out by the distributions.

2.3.4 Energy Deposition and Spectra

The amount of energy-deposited in the sensitive region of the neutron semiconductor detector, and therefore the resulting spectrum, is strangely dependent on the perforation design of the detector. The spectra produced by coated diodes dramatically differs from those produced by perforated detectors because of the ability for perforated detectors to collect both ions produced by the neutron absorption reaction. Both coated diode and perforated spectra are discussed below.

Coated Diode Detector Spectra

McGregor et al. [2003] showed ${}^6\text{LiF}$ coated diode detectors—semiconductor wafers coated with a neutron sensitive material—have maximum achievable efficiencies of less than 4%

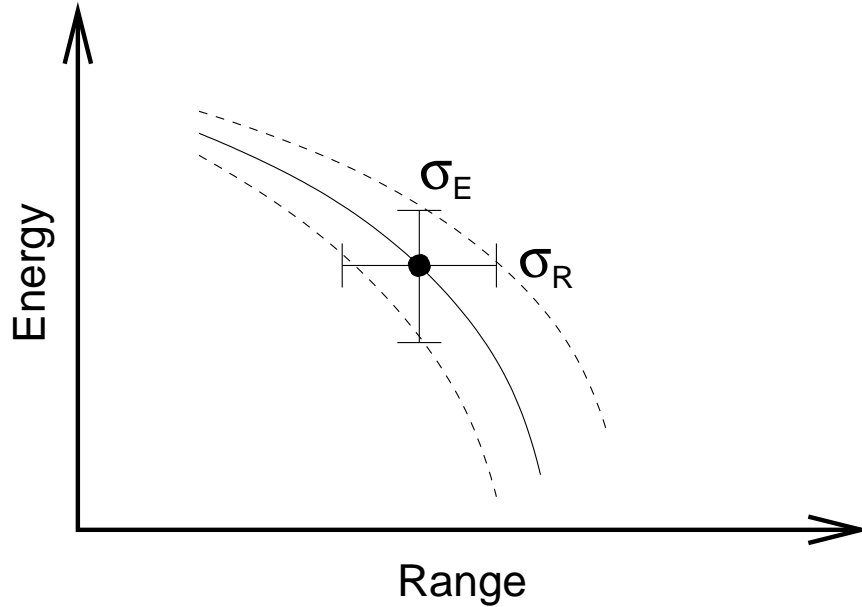


Fig. 2.8. Diagram of energy and range straggling. Adapted from Evans [1955]

depending on the absorber material used. The maximum efficiency is, among other factors, a function of the thickness of absorber. As the thickness of the absorption layer increases, the probability a neutron is absorbed increases proportionally. When the thickness reaches the range of the longer-range ion emitted from the neutron absorption reaction the efficiency reaches its maximum asymptotic value because any neutrons absorbed in an additional amount of absorber will not be able to penetrate the film and deposit energy in the detector. Thus, there is an intricate balance between how much absorber can be applied to the surface and the efficiency of the detector.

The energy-deposition spectra for coated detectors illustrates their dependence on the distance away from the semiconductor the absorption occurs. Fig. 2.9 presents a spectrum from a coated diode detector using ${}^6\text{LiF}$ as the absorbing material. One notes the maximum energy that can be deposited in the detector is that of the higher-energy ion, the 2.73 MeV triton. Another peak is evident at 2.05 MeV, the location of the energy of the alpha particle. The drop in counts at energies corresponding to the particles energies in Fig. 2.9 indicates, intuitively, only one particle, which must be born within range of the semiconductor, can contribute to the pulse formed in the detector.

Perforated Detector Spectra

Perforated detectors have more absorber material in which neutrons may be absorbed, and produce significantly different spectra. Neutrons may be absorbed in either the cap or the perforations. Ions produced from the absorption of neutrons in the cap may leave the cap and terminate in the semiconductor, leave the cap and terminate in the perforation, pass through the perforation to terminate in the semiconductor, or pass through the semiconductor and terminate in the perforation. Ions born in the perforation may enter directly

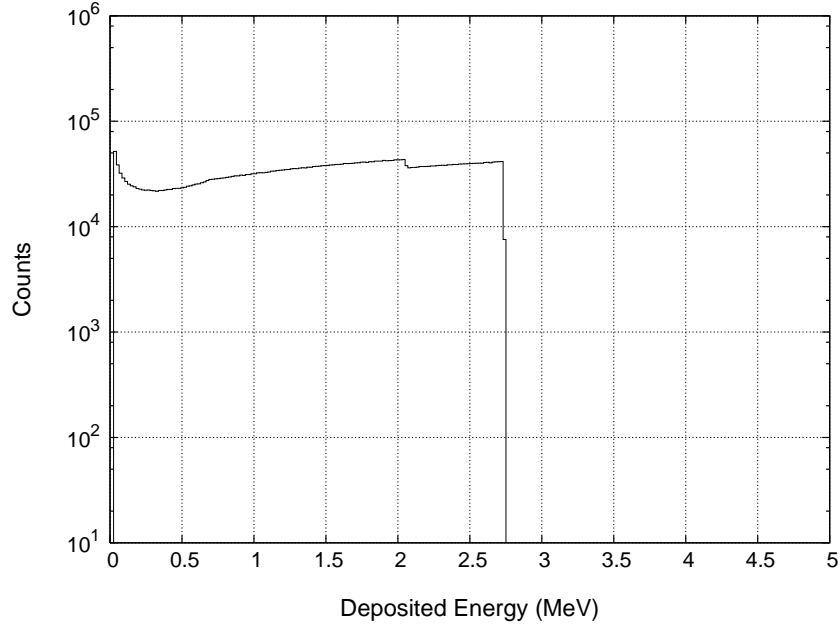


Fig. 2.9. Expected spectrum from a ${}^6\text{LiF}$ coated diode with a film thickness of $20\ \mu\text{m}$

into the semiconductor to deposit energy, pass through the semiconductor into the cap and terminate depositing some energy, or enter into the cap thereby depositing no energy. The possibility also exists that the ions travel along the direction of the perforation and deposit no energy at all.

If the detector is perforated then the spectrum changes dramatically from that of a coated diode, as shown in Fig. 2.10. Here one notes two additional “humps” at high-energy, resulting from both particles depositing energy in the detector at the same time. Because the two reaction ions travel in opposite directions, only neutrons absorbed in the perforations can have both ions depositing energy in the semiconductor. The lower-energy hump in the spectra results from neutrons being born close to the semiconductor material and the lower-energy particle depositing all of its energy in the the detector while the higher-energy particle deposits only some. The shape of the humps is an angular sensitive phenomenon in that if the low-energy particle leaves the semiconductor-absorber interface at a shallow angle then the high-energy particle is moving more in the direction of the perforation and is less likely to escape, thus explaining the sharp discontinuity between the humps. The second hump represents the case where the high-energy particle deposits most all of its energy and the low-energy particle only deposits some. This portion of the spectrum extends to the Q-value of the the reaction where both particles deposit all of their energy in the detector. As the size of the perforation decreases the first hump extends to higher and higher energies.

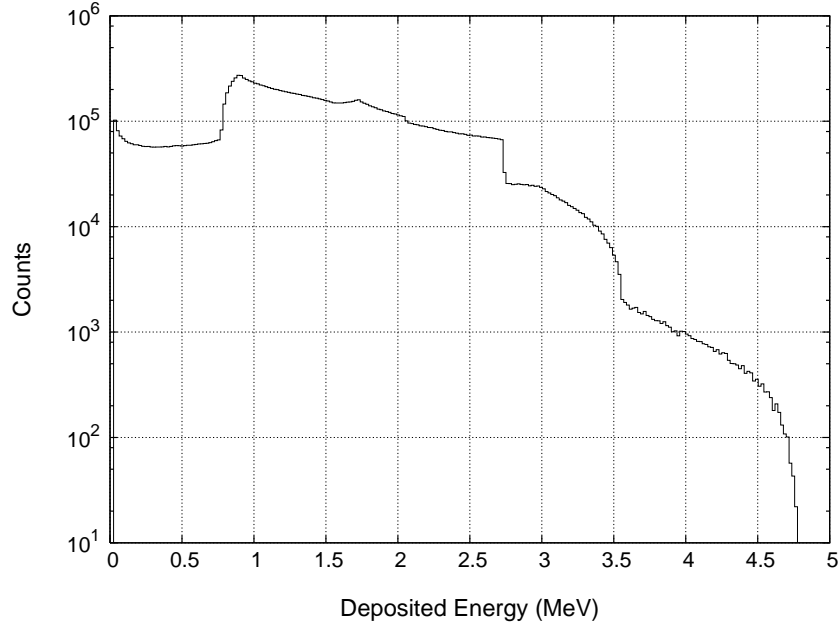


Fig. 2.10. Expected spectrum from a ${}^6\text{LiF}$ $20\ \mu\text{m}$ wide channel perforated detector with a $20\ \mu\text{m}$ cap

2.4 Detector Efficiency Considerations

The efficiency of a perforated neutron detector is dependent on two probabilities. The first is the probability a neutron is absorbed in the detector, herein designated p_n . The second probability is the probability the ions born by the absorption reaction reach the semiconductor material with sufficient energy to be detected, herein designated η . The total efficiency of the detector, ε , is then given by

$$\varepsilon = p_n \times \eta. \quad (2.29)$$

Interestingly, the two probabilities are independent of each other although the location where the neutrons are absorbed is also the birth location of the two reaction ions. Thus, the neutron absorptions can be calculated in one simulation, and, as long as the ion birth locations are recorded, the ion transport can be simulated in a completely different simulation. This fact is exploited in the calculation of detection efficiencies for rod-type perforations and is discussed in more detail in the next chapter.

2.4.1 Neutron Absorption Probability

The value of p_n is dependent on many factors. The probability a neutron is absorbed is dependent on the absorber material used and its distribution in the detector. As has been shown, the cross sections for the different absorbers differs substantially, with ${}^{10}\text{B}$ a much better neutron absorber than ${}^6\text{LiF}$.

Another factor directly affecting the probability a neutron is absorbed in the detector is

the thickness of the cap. As the thickness of the cap increases, the amount of absorption increases as well, thereby increasing p_n , albeit at the expense of more ions not being able to reach the semiconductor. However, the perforation depth can be increased indefinitely without detrimentally affecting the ability of the ions to be detected.

As the depth of the perforation increases, the probability a neutron is absorbed asymptotically approaches unity for neutrons not normally incident to the detector. For neutrons normally incident to the detector only neutrons entering at locations where they eventually enter the perforation are sure to be absorbed. Thus, the probability a normally incident neutron is absorbed by a detector with infinite perforation depth is the ratio of the detector's cross-sectional area covered by absorber to the total cross-sectional area of the detector. The detectors cannot, for obvious reasons, be made to a infinite depth, so the absorption probability is a strong function of the incident neutron angle.

The neutron's angle of incidence to the greatest extent determines its probability of being absorbed. Neutrons incident to the detector at nearly normal angles on average encounter less absorbing material than neutrons incident at nearly glancing angles. A neutron entering the detector at a glancing angle travels a longer distance through the cap and can quite possibly pass through more perforations than the normally incident neutron. Fig. 2.11 illustrates this phenomenon.

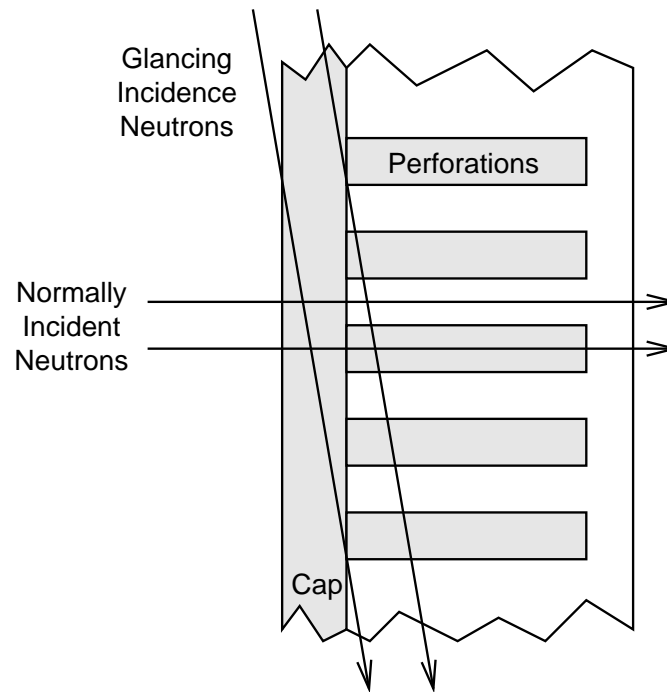


Fig. 2.11. Neutron incidence to perforated detector

2.4.2 Ion Detection Probability

Many factors also affect the probability an ion is detected. One important factor is the birth location of the ion; ions born close to the semiconductor material are more likely to travel in

a solid angle that passes into the semiconductor material, whereas ions born at the top of the cap or near the interior of the perforation are less likely to escape into the semiconductor.

Another important factor is the energy of the particles and the materials they are traversing. Ideally, the particle would lose little energy in the absorbing medium and most of its energy in the semiconductor, but this is not always the case. A selection of a low Z absorber material helps to ensure the energy lost by the ion is not significant enough to prevent the energy being deposited to produce a count; the minimum energy required is determined by the lower level discrimination.

The lower level discriminator (LLD) is the final factor affecting the probability an ion deposits sufficient energy to be detected, and, it, in fact, specifies what the sufficient energy is. The higher the lower level discriminator setting the more energy the particle must deposit in the semiconductor region to be counted. If the setting is too low, however, electrical noise and leakage become issues.

2.4.3 Normalizing the Efficiencies

There are two methods of normalizing the neutron detection efficiencies: (1) per unit fluence, and (2) per unit surface flow. The fluence and flow crossing the front plane of the detector, assumed to be perpendicular to the Cartesian z -axis, are related by [Shultis and Faw, 2000]

$$J_z(r, \hat{\Omega}) = \hat{\mathbf{k}} \cdot \hat{\Omega} \Phi(r, \hat{\Omega}), \quad (2.30)$$

where J_z is the flow in the z direction, $\hat{\Omega}$ is the direction of neutron travel, and Φ is the fluence. The value $\hat{\mathbf{k}} \cdot \hat{\Omega}$ is also $\cos \theta$, where θ is the cosine between the neutron's direction of travel and the surface normal vector $\hat{\mathbf{k}}$. Thus, the above equation may be equivalently written

$$J_z(r, \hat{\Omega}) = \cos \theta \Phi(r, \hat{\Omega}). \quad (2.31)$$

The fluence is represented by a beam of particles passing through a circle of area ΔA perpendicular to the direction of travel, as shown in Fig. 2.12. The same number of particles may pass through another circle perpendicular with the z - *axis*, but this circle must have a larger area given by $\Delta A \sec \theta$. The particles passing through the perpendicular circle is analogous to the fluence, while those passing through the circle normal to the z -axis are analogous to the flow.

In a simulation, if all of the neutrons are started at the detector surface and the number of detected particles is counted, then the ratio of the number detected to the number started is the efficiency normalized to the flow. If, however, the neutrons start away from the detector, allowing some to stream around the detector, then the ratio of those detected to the number of particles started is the efficiency normalized to the incident fluence. Normalization by unit fluence can easily be obtained from that by unit flow by multiplying by $\cos \theta$.

2.5 Monte Carlo Transport Simulation

The primary modeling method used in this work is the Monte Carlo technique. Monte Carlo involves the random sampling of probability distributions to obtain average behavior of a

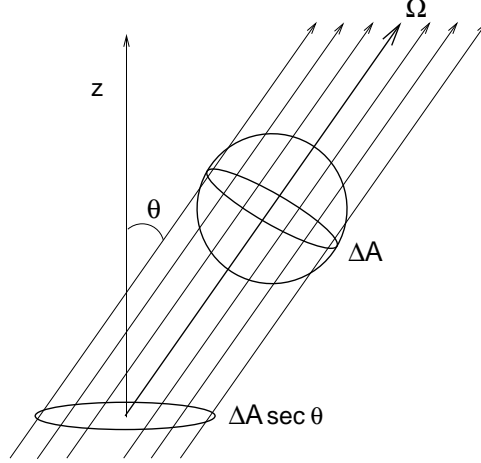


Fig. 2.12. Fluence and flow relation. Adapted from Shultis and Faw [2000].

modeled system. Both the general purpose Monte Carlo transport code MCNP and specially developed Monte Carlo codes are used for simulations.

2.5.1 Neutron Transport in Specialized Codes

The specialized codes avoid the issue of cross section energy dependence by assuming all neutrons are thermal at room temperature and transports them using the thermal-averaged cross section. From Eq. (2.4) one finds the probability a neutron interacts after traveling a distance x in a medium having cross section Σ is given as

$$p(x) = \frac{F}{I^0} = \Sigma \exp(-\Sigma x). \quad (2.32)$$

Because probabilities cumulatively sum to unity, the cumulative distribution function of the above distribution can be obtained by integrating from zero to an arbitrary value of x to obtain

$$P(x) = 1 - \exp(-\Sigma x). \quad (2.33)$$

When $x \rightarrow \infty$ in the above equation,signifying the fraction of neutrons interacting between a distance of zero and infinity, $P(x) \rightarrow 1$.

Random interaction locations are sampled from the cumulative distribution by equating it to a randomly sampled number ρ between zero and one. Random numbers sampled uniformly on the range (0,1) are themselves the cumulative distribution of the uniform probability density function. Thus, the equation of $P(x)$ and ρ is the equation of two cumulative distributions. Solution of such an equation for x , the randomly sampled distance, is

$$x = -\frac{\ln(1 - \rho)}{\Sigma} = -\frac{\ln(\rho)}{\Sigma}, \quad (2.34)$$

where the random values $1 - \rho$ and ρ are both uniformly distributed on the interval (0,1) and may be freely interchanged.

2.5.2 Neutron Transport in MCNP

MCNP samples neutron distances to collision in the same manner as described above for the specialized codes with the exception that MCNP keeps track of the energy of the particle; thus, depending on the neutron's energy, a different cross section is used. To obtain the desired thermal-neutron energy distributions the standard built in Maxwellian distributions are used. Two different Maxwellian distributions are available, one in velocity and the other in energy, respectively given by [X-5 Monte Carlo Team, 2003]

$$p(E) = C\sqrt{E}\exp\left(-\frac{E}{a}\right), \quad (2.35)$$

and

$$p(E) = CE\exp\left(-\frac{E}{a}\right). \quad (2.36)$$

Here a is a user specified parameter to determine where the distribution peaks, and C is a normalization constant. Because a thermal Maxwellian fluence distribution at room temperature has a most probable energy of 0.0253 eV, the later distribution, in terms of the energy, was used. However, the distribution that is actually used becomes inconsequential when one realizes the absorbers are $1/v$ absorbers and recalls absorption of thermal neutrons in $1/v$ absorbers is independent of neutron and target energy distributions [Lamarsh, 2002].

It is also necessary to quantify absorption of the neutrons in the sensitive material. MCNP records such information using Monte Carlo estimators called tallies; in this case the F4 tally, a volume fluence tally, is used. The F4 tally estimates

$$\bar{\Phi} = \frac{1}{V} \int_V \int_{4\pi} \int_0^\infty \int_0^\infty \Phi(\mathbf{r}, \hat{\Omega}, E, t) dt dE d\Omega d^3r, \quad (2.37)$$

which is more simply approximated in MCNP as

$$\bar{\Phi} \simeq \frac{1}{H} \sum_{h=1}^H \frac{W_h T_h}{V}. \quad (2.38)$$

In the above equation V represents the volume of the cell being tallied over, T_h is the track length of the h -th particle in the cell, and W_h is the weight of the h -th particle. H is the total number of histories simulated.

MCNP allows the user to adjust the tally by specific parameters so that the absorption efficiency can be estimated. Multiplying by the atom density of the medium, the microscopic cross section, and the volume one obtains the estimate of the fraction of neutrons absorbed:

$$p_n = \frac{1}{H} \sum_{h=1}^H \sigma_a(E) N W_h T_h. \quad (2.39)$$

2.5.3 Monte Carlo Simulation of Ion Energy Deposition

The ion transport method relies on knowing both the average residual energies of an ion after traveling a certain distance in a medium and the average range a particle has traveled given

its energy. To obtain the data for this information, the TRIM code was used to generate data for the ions' average range given an initial ion energy [Shultis and McGregor, 2004]. Figure 2.13 presents example plots of the residual energies of the alpha particle and triton emitted by the ${}^6\text{Li}$ neutron absorption reaction.

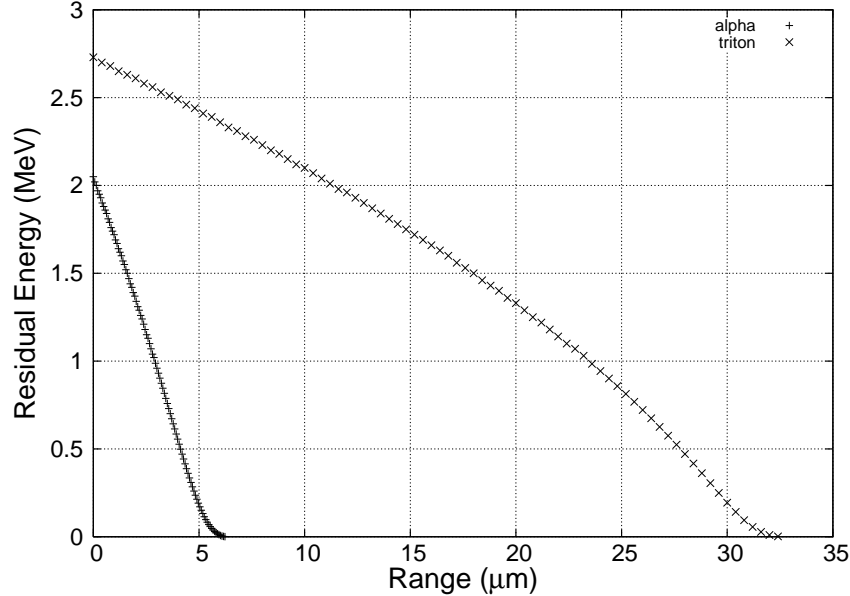


Fig. 2.13. Alpha and triton residual energies in LiF [Shultis and McGregor, 2004]

Shultis and McGregor [2004] generated curves such as those shown in Fig. 2.13 and fit them approximately with functions for the alpha and triton emitted from the ${}^6\text{Li}(n,t)\alpha$ reaction for both lithium fluoride and silicon and for the two alphas and lithium ions emitted from the ${}^{10}\text{B}(n,\alpha){}^7\text{Li}$ reaction for both boron and silicon. Additionally, approximating functions were developed to provide the range for each ion in the different media given the ion's energy. In this way, the energy deposited by the particle along its trajectory in a specified medium can be easily estimated.

Let $\Lambda_i(E)$ be the average distance an ion with initial energy E_o travels in medium i . Also, let $\xi_i(x)$ be the residual energy a ion has after traveling a distance x in medium i . Figure 2.14 represents a hypothetical $\text{X}(n,t){}^4\text{He}$ reaction in medium 1 where the alpha particle of initial energy E_o travels through mediums 1 and 2 and terminates in medium 3. Now, let d_1 , d_2 , and d_3 be the distances traveled by the alpha particle in each medium, respectively. The energy deposited in medium 1 E_1 is given as

$$E_1 = E_o - \xi_1(d_1), \quad (2.40)$$

where $E_{r1} = \xi_1(d_1)$ is the residual energy the ion has upon leaving medium 1. Then energy deposited in medium 2 is found by first calculating the equivalent distance the ion would have traveled if only in medium 2, which is given by $\Lambda_2(E_{r1})$. That equivalent distance is added to the actual distance traveled in medium 2, and the total energy deposited in medium

2 is then

$$E_2 = E_{r1} - \xi_2 (\Lambda_2(E_{r1}) + d_2). \quad (2.41)$$

The new residual energy is $E_{r2} = \xi_2 (\Lambda_2(E_r) + d_2)$. Similar to the energy deposition in medium 2, the energy deposited in medium 3 is given by

$$E_3 = E_{r2} - \xi_3 (\Lambda_3(E_{r2}) + d_3). \quad (2.42)$$

This process of finding the equivalent range traveled and computing the new residual energy continues until the particle has no average kinetic energy.

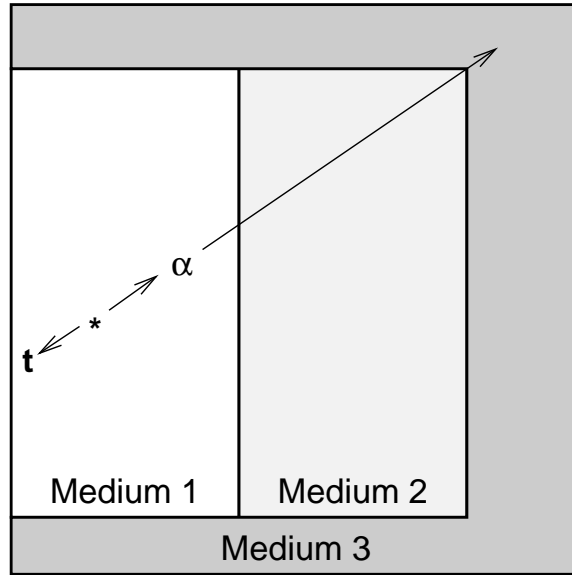


Fig. 2.14. Hypothetical ion transport situation

If the particle transport were done in full, at each step along the particle's path the stopping power would have to be computed for the particle's current energy. This computation would be time consuming and difficult to perform properly, so the approximation described above, which has been deemed the *back-tracking method*, is used.

This method for transporting ions assumes many things. First, the residual energy and range curves produced for each ion are specific to the density of the material such that a different density cannot realistically be used for the neutron transport without generation of new approximating functions. Second, the ions are assumed to travel only in straight line paths, which for heavy ions is generally a good approximation. Last, only the average behavior is being modeled and real ions will lose more or less energy along the same path.

Chapter 3

Directional Sensitivity of Perforated Neutron Detectors

3.1 Motivation

Solid state neutron detectors are revolutionizing the radiation-detection industry. Not only do solid state detectors now provide resolutions once thought to be impossible, but their compact size makes them portable and versatile in application. Present designs of solid state neutron detector have limitations however. To fabricate a solid state neutron detector two different methods can be used: (1) the semiconductor material can be a neutron absorber, or (2) a neutron absorber can coat the semiconductor. The first method is limited in that the semiconductor material must contain a neutron absorbing isotope. Additionally, it is desirable for the absorption reaction not to be a (n,γ) reaction, such as that with cadmium zinc telluride, so pulses from neutrons can be clearly distinguished from γ -ray backgrounds. Other materials, for instance boron carbide, have also been proposed as semiconductor material composed of a neutron absorber, but to-date it shows little promise.

The second method of coating the detector with a neutron sensitive material has the disadvantage that the thickness of the coating must be limited. As the thickness of the absorptive coating increases more neutrons are absorbed; however, particles emitted from the absorption reaction do not penetrate to the semiconductor material if the absorbing layer is too thick. Thus, a new concept has been proposed where perforations are etched into the semiconductor material and the perforations are backfilled with neutron absorbing material to increase the probability an absorbed neutron leads to an ion that can deposit energy in the semiconductor. The shape of the perforations affects the angular efficiency of the detector as demonstrated in this chapter.

Ideally one would like detectors whose response exhibits no angular dependence. An angular dependence implies that a neutron incident on the detector in a specific direction is more, or less, likely to be detected than a neutron incident from another direction. If the detectors are used in applications where angular resolution of the neutrons is important, then a dependence on the neutron's angle of incidence hinders or even prevents accurate measurement. For example, a neutron scattering experiment depending on the number of neutrons scattering in a specific direction would produce erroneous data if the detector's

response varied with incident direction.

In this chapter, different types of perforations are modeled to determine how to minimize the angular dependence of the detector. Specifically, four types of perforations have been investigated. The “rod-type” perforations are equally spaced cylinders of material oriented into the silicon semiconductor material. The “channel-type” detectors consist of etched alleys backfilled with absorbing material. “Chevron-type” perforations are channel type perforations with ninety-degree bends in them such that they zig-zag down the length of the detector. Finally, the “sinusoidal-type” perforations are etched alleys that have the curvature of sine waves.

3.2 Hybrid Method with MCNP and Specialized Ion Transport Code

The first detectors considered are the rod-type perforated detectors. Rod-type detectors represent the first generation of perforated detectors and are presently being fabricated at Kansas State University. The performance of these detectors were simulated using a hybridization of the MCNP code and a specialized ion-transport code described in Shultis and McGregor [2004]. MCNP is a general-purpose neutron, photon, and electron Monte Carlo transport code developed at Los Alamos National Laboratory (LANL) and distributed through the Radiation Safety Information Computational Center (RSICC). MCNP uses combinatorial geometry algorithms to perform ray tracing and transports neutrons with energies from 0 to 20 MeV, photons with energies from 0.001 MeV to 100000 MeV, and electrons from 0.001 MeV to 1000 MeV. MCNP includes many useful distributions, such as the Maxwellian distribution, built into it for sampling particle energies. Geometry is specified by defining the surfaces bounding a region and then using the “sense” of a surface to specify cells; for example, the negative sense of a spherical surface is the space inside the sphere.

Ion transport is performed using the method described in Chapter 2. The actual ion-transport code is an adapted version of that used in Shultis and McGregor [2004]. Because it is simply an adapted version, the restrictions of the original code must be considered, notably the restriction of transport in only rod-type perforated detectors. For this reason, the methodology is further developed in this study to utilize the same energy deposition routines from Shultis and McGregor [2004], but to uses a more general ray-tracing technique to allow analysis of different types of perforations.

3.2.1 The MCNP Model

The MCNP transport code is used to transport the neutrons from the source to the detector and to determine the expected number of absorptions in the detector. First, the geometry has to be established, and then, the absorption calculation must be performed. Hence, the geometry is considered first followed by a discussion of how neutron absorption is treated in the detector.

Geometry Specification

Because the perforations of the perforated detectors are multiple instances of the same pattern, hereafter called the *unit cell*, the detectors are most easily simulated using the repeated lattice structure of the MCNP geometry. Example cross sections of unit cells are pictured in Fig. 3.1. Sinusoidal-type perforations cannot be modeled in MCNP as MCNP only recognizes surfaces with a quadratic form. Custom codes were developed for these sinusoidal-type perforations and are discussed later.

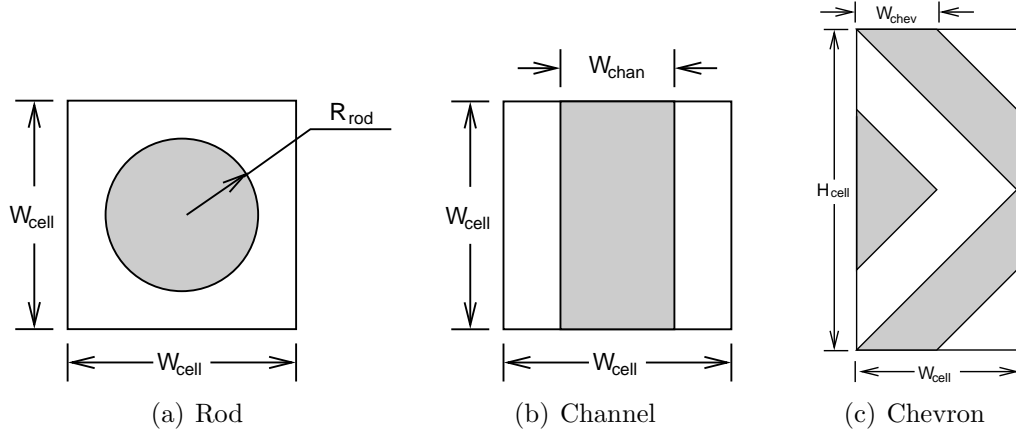


Fig. 3.1. Unit cell cross sections

The MCNP lattice structure works by first specifying a universe—a model where all of space is defined. In this case, one of the above unit-cell designs above fills a universe; then, the first universe is used to fill a lattice of repeated cells, thereby creating a second universe of lattice elements. The lattice universe of repeated cells then fills another cell creating the repeated structure of perforation elements. Figure 3.2 illustrates this process. In this example, universe one is created by defining all space, and universe two is specified as a lattice that is filled with universe one. Another cell, such as a right cylinder (not shown), would then be created and filled with universe two to model all the perforations of a circular detector.

When an universe exceeds the dimensions of the cell it is filling, the boundaries of the filled cell become the boundaries of the universe. Considering the example discussed in Fig. 3.2, universe one extends conceptually out to infinity in all directions; even the rod of neutron absorbing material extends along its axis to infinity. However, once a cell is filled with universe one, the boundaries of the cell bound the universe. For this reason, the unit cells created for this study are truly infinite in dimension, but, upon insertion into the lattice, become finite. The lattices filled with the perforations are bounded by a cylinder of 1-inch radius. A cap is optionally simulated by offsetting a plane from the top of the cylinder and modeling the material between it and the cylinder as neutron absorbing material.

Materials are modeled in MCNP by specifying the elemental cross sections to be used in a material along with either their mass or atom fractions. When a cell is defined, the density of the material is specified. In these models the ENDF B/VI cross section evaluation are used where possible; however, not all elements have ENDF B/VI evaluations and, in these

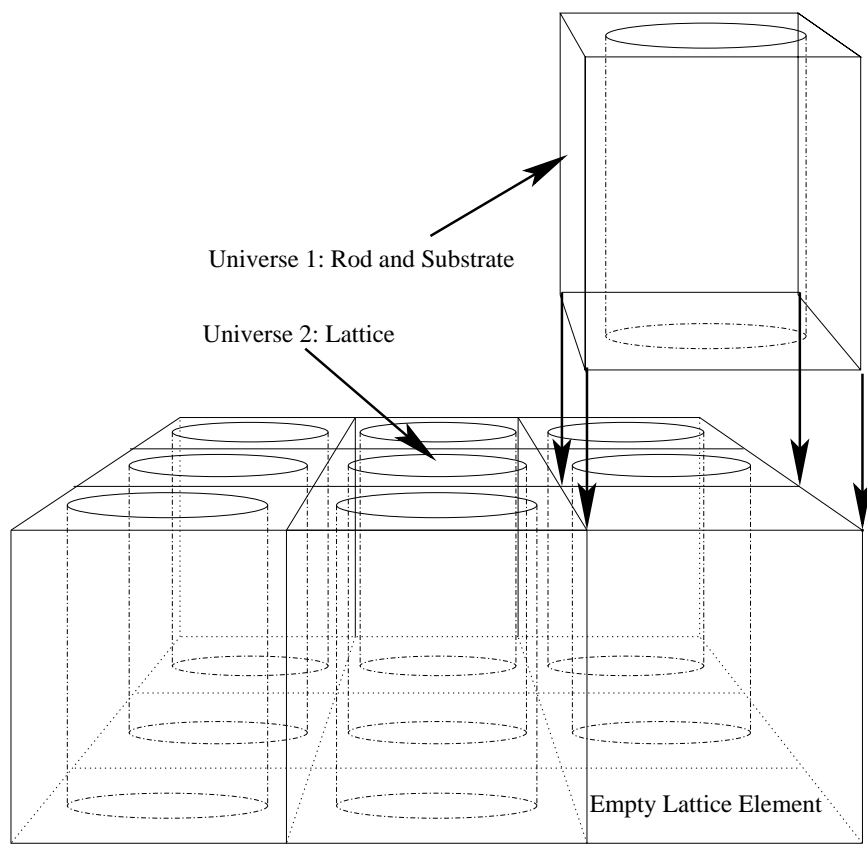


Fig. 3.2. Creating repeated structures in MCNP

cases, the most recently available cross section evaluation is used. Table 3.1 summarizes the applied cross sections. MCNP specifies cross sections using the ZAID number, that is, the concatenation of the three-digit Z number and the three digit A number followed by the cross section evaluation specifier. For example, the ENDF B/VI evaluation for ^{59}Fe is 26059.66c, where the 66c refers to the ENDF B/VI evaluation. ^6LiF is modeled using only lithium, because the cross section of fluorine is negligible compared to that of ^6Li . Silicon, despite its low cross section for thermal neutrons, is modeled.

Table 3.1. MCNP materials and cross sections

Material	Nuclide	Cross Section	Atom Fraction
Natural Silicon	^{28}Si	14028.66c	0.922297
	^{29}Si	14029.66c	0.046832
	^{30}Si	14030.66c	0.030872
Lithium-6 Fluoride	^6Li	3006.66c	1.000000
Boron-10	^{10}B	5010.66c	1.000000

Source Description

The neutron source is modeled as a disk source of radius 2.6 cm. The center of the disk source is always located a constant radius, 5 cm, from the center of the top plane of the detector. Neutrons are simulated to be emitted monodirectionally perpendicular out of the disk toward the detector. Figure 3.3 illustrates the geometry of the source about the detector.

The disk source is rotated about both the polar and azimuthal angles in discrete steps, and at each step a MCNP simulation is run to determine the number and coordinates of neutron absorptions in the detector’s perforation and, if present, the cap. The zero degree polar angle is considered to be coaxial with the detector. Because the solid angle of the detector decreases as the polar angle of the source increases, the number of absorptions appears to decrease with polar angle, but this decrease corresponds to the normalization of the data being per unit incident fluence (See Chapter 2). As the polar angle increases fewer particles actually pass through the detector and fewer counts are therefore registered.

Absorption Rate Tallying

As discussed briefly in Chapter 2, MCNP uses estimators (called tallies) to calculate the expected behavior of radiation in a system. The primary tally employed is the “F4” tally. The F4 tally computes the track length of the particle through the cell and divides this value by the volume of the cell to get an estimate of the fluence; however, a simple estimate of the fluence is only proportional to the absorption of interest.

The absorption is computed in MCNP by applying the “tally multiplier,” or FM, card. This card allows a tally to be multiplied by any numerical value, but, as a special case,

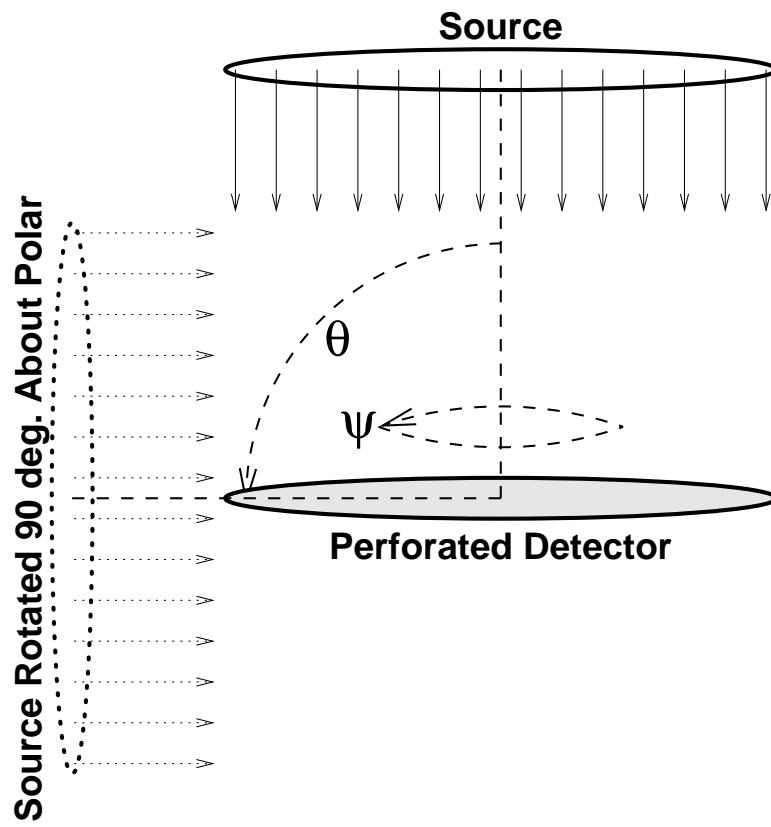


Fig. 3.3. Rotation of source about the perforated detector

multiplies the fluence by the atomic density of the medium the particle is traversing and a specific microscopic cross section of a specified material, consequently, it gives an estimate of the reaction density. The cross section of interest is specified using the ENDF/B MT reaction number. For example, corresponding MT numbers for the (n,α) and the (n,t) reactions are 107 and 105 [X-5 Monte Carlo Team, 2003].

The final step to producing the absorption fraction with MCNP is to multiply by the total volume. The F4 tally is divided by the volume of the cell(s) over which the tally is calculated; however, MCNP can be “tricked” into dividing by unity instead of the cell volume using the “segment divisor,” or SD, card. This card instructs MCNP to not use the default divisor and use the value specified on the SD card as the divisor. Therefore, instead of multiplying by the volume, the tally is never divided by the volume in the first place. The final result of all of the above tally modifications is that the tally directly yields efficiency or probability that neutrons cause the reaction specified on the MT portion of the FM card.

Physics Models and Implicit Capture

Variance reduction methods are often used in Monte Carlo programs to converge on the solution more rapidly. MCNP uses a default method of variance reduction called “implicit capture.” When a particle is absorbed in MCNP it is not terminated; rather, it continues to be tracked with a reduction in the weight—a variance reduction variable serving as the relative probability of a particle’s existence at its phase space.

MCNP determines the cross section for a particle and transports the particle through a medium using that cross section. When a collision occurs, the type of interaction is randomly selected, but weighted for the more probable reactions. If an absorption reaction is sampled, then the weight of the particle is multiplied by one minus the ratio of the absorption cross section to the total cross section and particle history continues. In this way, particles coming close to a highly improbable tally region are not terminated due to absorption, but may continue with a reduced weight.

In these calculations, implicit capture is turned off. As discussed later, the terminations points of the particles are of critical interest, so when a particle is absorbed it must be terminated. The MCNP `phys:n` card specifies how implicit capture of neutrons is handled; in the calculations the `phys` card is set to

```
phys:n 50 20
```

meaning neutrons are transported up to 50 MeV and the energy boundary above which implicit capture is used is 20 MeV, as opposed to the default of 0 MeV.

3.2.2 The Ion Code Model

The original ion-transport code described in Shultis and McGregor [2004] applies only to neutrons normally incident on the detector. In the problems being investigated here, the neutrons are incident at many varying angles and each angle produces a different distribution of where the reaction ions are produced in the detector. Without the correct distribution of neutron absorption sites the resulting ion-tracking and energy-depositions calculation would be erroneous.

A diagram of the unit cell used in the Shultis and McGregor [2006] rod-type perforation calculations is presented in Fig. 3.4. Their ion transport code records the energy deposited in the detector from particles born in both the perforation and, if present, the cap by the backtracking method described in Chapter 2. If the energy deposited exceeds the lower level energy discrimination value of 0.3 MeV, the event is deemed to have been detected. The fraction of ion product pairs being detected to the total number of pairs being tracked gives the ion capture efficiency. Because the simulation simply counts the number of energy depositions great enough to be detected, Poisson statistics are applied so the uncertainty in the number counted is simply the square-root of the number counted.

The 0.3 MeV discrimination energy is chosen because the majority of gammas interacting in the silicon are discriminated out of the response. Pair production is only possible for high energy gammas and has a threshold of 1.022 MeV but does not contribute significantly to the total cross section in silicon until above 2 MeV. If a pair production reaction occurs in the silicon, then the energy of the incident gamma is converted into a positron and an electron, and the energy in excess of 1.022 MeV the gamma has becomes kinetic energy of the two. The positron loses energy and annihilates with an electron. The annihilation photons produced are unlikely to be reabsorbed in such a small device, and are of little concern. The electron and positron together must have a minimum of 300 keV of kinetic energy and deposit all of that energy in the semiconductor, which is also unlikely, to produce a count with the LLD set at 0.3 MeV.

The photo-electric reaction dominates at low energies and the Compton scattering reaction at moderate energies. The Compton scattering cross section and the photo-electric absorption cross section cross at approximately 60 keV in silicon. Thus, the discrimination level is selected to be five times the cross over point so that only Compton scattering reactions, which do not allow the photon to deposit all of its energy in the silicon, are registered by the detector.

3.2.3 Marriage of the MCNP and Ion Transport Codes

MCNP and the ion-transport code are married using a script written in the Perl scripting language. Before the functionality of the script can be discussed however, a few other topics must be considered. First, the method by which absorption locations of neutrons in the MCNP simulation are recorded for use as ion birth locations must be considered. Second, modifications to MCNP for this specific application must be discussed. Finally, modifications to the ion-transport code itself are described.

The MCNP PTRAC File

The MCNP PTRAC file is a particle tracking file. It records user filtered events of the simulated particles; the filters are specified to MCNP by giving a keyword and then parameters associated with that keyword. The available keywords can be arranged into three categories: output control keywords, event filter keywords, and history filter keywords. While many keywords (12) are available, only those necessary for understanding the desired calculations are investigated. [X-5 Monte Carlo Team, 2003]

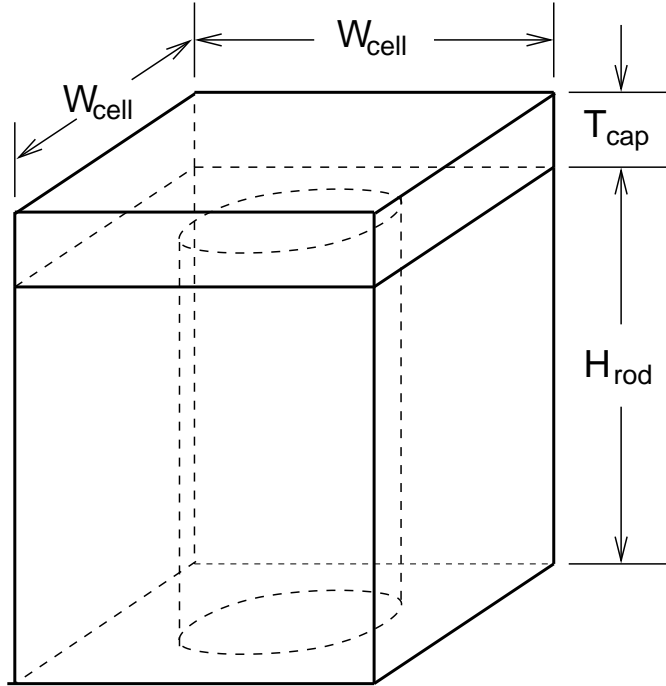


Fig. 3.4. 3D diagram of rod-type perforation unit cell

The `max` keyword specifies the number of total tracking events to record to the PTRAC file. Obviously, the default value of 10000 events is insufficient as many neutrons are going to be simulated and the absorption location for each is required. For this reason, the argument for the `max` keyword is specified to be the total number of histories, so, if every neutron is absorbed then every absorption location would be available.

By default the MCNP PTRAC file is written as a binary file, and binary files, although easy to access and read record by record, are difficult to match with regular expressions in Perl. To correct this issue the PTRAC file can be instructed to write the output to a ASCII file using the `file` keyword. The argument of the `file` keyword is either `bin` for binary or `asc` for ASCII. Here, `asc` is chosen.

The keyword filtering according to the particle is `type`. Type can be any particle MCNP can transport, i.e., `n` for neutron, `p` for photon, or `e` for electron. In addition, the `filter` keyword allows special filters to be placed on which particles are printed by selecting only particles of specific energies, in a certain cell, having specific x , y , or z coordinates, etc. There are many possibilities for the filter keyword that can greatly limit the number of particle events printed to the PTRAC file. Because only the absorption locations occurring in the cap or perforations of the model are of interest, a cell filtering scheme is used that only prints events occurring in the cap or perforation cells.

The most important keyword for this specific study is the `event` keyword, which specifies the types of events written to the the PTRAC file; there are five types of events and multiple types can be specified in unison if desired. The types are `src` for initial source events, `bnk` for banked events, `sur` for surface crossing events, `col` for collision events, and `ter` for termination events. For these calculations implicit capture is toggled off so that when

a particle is absorbed it is also terminated. In this way, the absorption locations of the neutrons, which can later be used as the starting position for ion-transport calculations, in cells specified by the cell filtering are written to the PTRAC file.

A Slight Modification to the MCNP PTRAC Routine

Dimensions in MCNP are given in units of centimeters, but the problem of interest deals with dimensions on the order of microns. The floating point output in the default PTRAC file does not offer precision to the micron range, and therefore, the output precision of the write statements are modified to include sub-micron precision.

Specifically, lines 418 and 450 of the MCNP source file “ptrak.F90” contain the write statements controlling output of the floating point quantities of interest. The FORTRAN output formatters given for the position is the “e13.5” designator, which does not provide micron precision if the output number is on the order of centimeters, as they are in MCNP. To obtain the desired level of precision, the output formatting is changed to the “e20.10” designator, which provides micron precision output to the PTRAC file.

Modification to the Ion Transport Code

The ion-transport code was modified to accept the ion birth locations, which are locations where neutron absorption occurred in the MCNP simulation, from an input file rather than randomly sampling the ion birth locations. Before modification, the program calculated the probability a neutron is absorbed in the cap and rod and then randomly sampled for the location of the absorption. All of this source code was removed, and, in its place, source code to read in the absorption locations from a temporary file, which is based on the PTRAC file, was inserted.

The code first reads in the number of absorptions present in the temporary file. Then, the program reads in triplets corresponding to the x , y , and z neutron absorption locations in the unit cell. The ion-transport algorithm remained unchanged, and the fraction of ions producing a count is output to the same output file as in the original ion-tracking program.

The Workings of the Control Script

The control script calculates the angular efficiencies of a specific dimension of a rod perforated detector by calling MCNP and, subsequently, the ion-transport code. The sequence of events produced by the control script are as follow:

1. Initialize parameters for the specific problem
2. Begin looping through polar and azimuthal angles
3. Create an MCNP input file
4. Run the newly created MCNP input file
5. Extract useful information from MCNP output and PTRAC files

6. Convert neutron absorption coordinates from the PTRAC file to equivalent unit-cell coordinates needed for the ion-transport calculations
7. Run the ion-transport code
8. Extract useful information from the ion-transport output file
9. Print processed data to file “datafile”
10. Repeat the entire procedure for all specified angles of neutron incidence

Each step of the control script is now discussed, and an example control script is provided in Appendix A.

Initialization: The initialization phase of the script sets parameters for the size of the detectors and fundamental constants such as π . The variables in the script governing the dimensions of the detector are `$rd`, the radius of the detector, `$tc`, the cap thickness, and `$hd`, the rod (hole) depth measured from below the cap. These three variables, along with some hard coded dimensions, entirely specify the dimensions of the detector. The unit-cell widths are hard coded into the program having values of $50 \mu\text{m}$ and $9 \mu\text{m}$ for ${}^6\text{LiF}$ and ${}^{10}\text{B}$, respectively. The variable `$r` defines the distance from the center of the top plane of the detector to the center of the source disk whose radius is `$rs`. The number of histories is specified by `$nps` and varies as one over the cosine of the polar angle, such that, as the detector fades out of the solid angle, the same number of particles are still crossing the front detector surface. `$pi` is simply the constant π , and the variables `$As` and `$Ad` correspond to the surface area of the source disk and the top plane surface area of the detector, respectively.

Angular Loops: Once the problem parameters have been initialized, the script initiates two loops: the first loops over the polar angle increasing in 5° increments, and the second over the azimuthal angle increasing by 3° increments. The detector remains fixed in all simulations, and the source is rotated about the polar and azimuth (see Fig. 3.3) Thus, the angles from the loops are used to establish the location of the center of the source disk and the direction of particles leaving the source. The angles in degrees are converted to radians and the coordinates of the center of the source disk are given as

$$\begin{aligned}
 x &= r \sin \theta \cos \psi \\
 y &= r \sin \theta \sin \psi \\
 z &= r \cos \theta,
 \end{aligned}
 \tag{3.1}$$

where r is the distance from the center of the top detector plane to the source and θ and ψ are the polar and azimuthal angles, respectively.

MCNP Input File: After calculating the angles for a specific case, the script prints an MCNP input file. The input file contains a model of a rod perforated detector with or without a cap; if the `$tc` variable is equal to zero then no cap is created, otherwise a cap of thickness `$tc` (in centimeters) is created. The disk source is constructed a distance `$r` away

from the center of the detector’s top plane in a direction specified by the angles calculated above. The source disk emits a Maxwellian distribution of neutrons toward the detector parallel to the source’s axis. The input file is named based on the polar and azimuthal angles, such that, the name of an input file with a polar angle of 10° and an azimuthal angle of 60° would be “10-60.i.”

Run MCNP: The next step calls MCNP and waits for execution of the MCNP run to complete. Both sequential and parallel versions of MCNP5 RSICC version 1.40 are available and used depending of the platform performing the calculations. The secondary files created by MCNP are named using the same scheme as the input file but with different extensions; namely, the output file had a “.o” extension, the run-tape file had a “.r” extension, and the PTRAC file had a “.p” extension.

Process MCNP Output: After MCNP completes the calculation, necessary information is extracted from the output and PTRAC files. The regular expression functionality of Perl is used to search for specific lines in the file and extract the values to variables in the script. For instance, the absorption efficiency and its relative error are extracted from the output file. The PTRAC file is read twice, once to count the number of absorptions, and the second to write the number of absorptions and the x , y , and z coordinates of all the absorptions to a temporary file.

Transform Absorption Site to Unit Cell: Once the absorption locations have been extracted to a temporary file, the ion transport begins; however, the absorption locations that have been specified are not relative to the unit-cell geometry required for the ion-transport code to work. To correct this problem, a FORTRAN code was written to calculate, given the unit-cell dimensions, the corresponding absorption locations in the unit-cell geometry. This FORTRAN code first determines in which lattice element each absorption occurs and subtracts the vector \mathbf{v}_c from the center of the unit cell to the center of the distant lattice from the vector \mathbf{v}_a from the center of the unit cell to the absorption location. Figure 3.5 illustrates this process. The difference of these two vectors gives the vector \mathbf{v}_u from the center of the distant lattice member to the absorption location that is also the vector from the center of the unit-cell member to the equivalent absorption location in the unit cell. The program reads in the absorption locations from the temporary file created in the previous step, performs the transformation on each point, and then prints the new unit cell absorption locations to another temporary file.

Ion Transport: Having all the absorption locations translated to the unit-cell geometry allows the ion-transport code to determine the probability that enough energy is deposited in the detector to produce a count per neutron absorption. The ion-transport program (see Appendix A) reads in absorption locations in the unit cell from the temporary file and counts the number of absorptions leading to sufficient energy being deposited in the detector. An output file is then created by the ion-transport program and the number of absorptions producing a count is extracted using Perl.

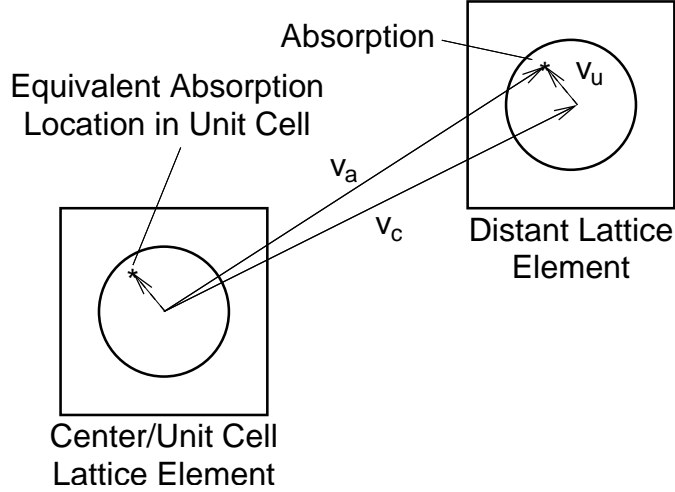


Fig. 3.5. Calculation of unit-cell absorption locations

Efficiency Calculation: The desired efficiency of the detector finally is calculated for the specific angular incidence defined by the polar and azimuthal angles. The efficiency is calculated by multiplying the values of the neutron absorption efficiency and the ion product detection efficiencies to obtain the total detector efficiency. Additionally, the total efficiency must be multiplied by the ratio of the detector area to the source area because the detector efficiency is normalized to unit fluence incident on the detector. To obtain the efficiency, normalized to the current crossing the surface of the detector, one simply divides by the cosine of the polar angle. Lastly, the polar angle, azimuthal angle, absorption efficiency, ion-detection efficiency, fluence-normalized total efficiency, and current-normalized total efficiency are printed to a data file. Then, the control script increments the inner loop over the azimuthal angles and repeats the entire process for the next angular iterate.

3.2.4 Verification and Validation of the Hybrid Model

To verify the model and simulations work together in the manner intended, many checks were performed. The first part of the process scrutinized was the conversion of the MCNP coordinate system into the unit-cell geometry. To check if the absorption locations are correctly mapped to the unit-cell locations, many plots of the unit-cell absorption locations were created. An example is presented in Fig. 3.6 for normal neutron incidence. From this figure, one can see the absorption in the cap and rod extending from 0 to 120 μm and that the unit cell is 50 μm by 50 μm .

Additionally, if the plot of Fig. 3.6 is taken and plotted in two dimensions using projection on to the x - y and y - z planes, then the two plots of Fig. 3.7 are obtained. In this case, Fig. 3.7(a) shows there is, in fact, absorption in the perforation and the perforation is circular in shape. This confirmation in combination with Fig. 3.7(b) indicates there is also absorption in the cap and the perforations must be cylindrical. Also, it is important to note there are no points outside the areas expected. Therefore, the transformation of the absorption locations to the unit cell worked correctly.

Fig. 3.8 presents a similar 2D mapping of absorption locations for the case of a glancing

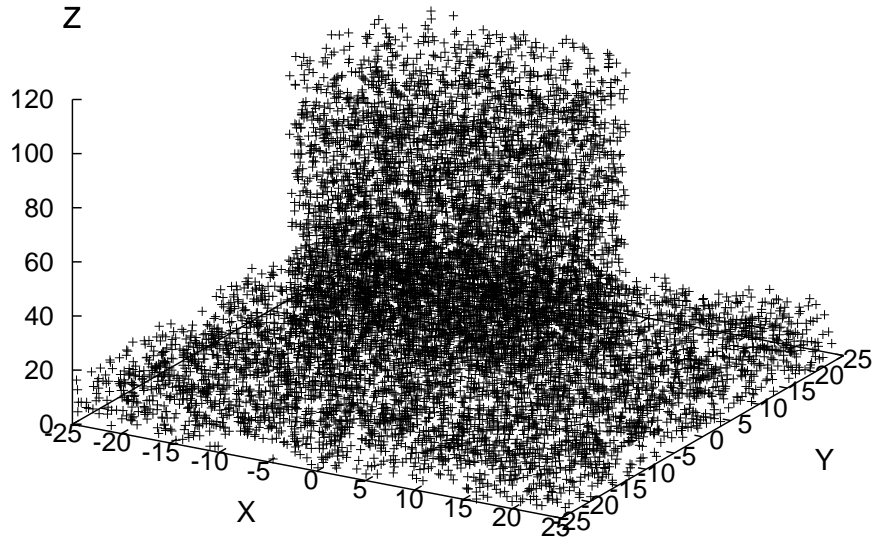


Fig. 3.6. 3D rod-type unit-cell absorption locations for a $50 \times 50 \times 120\text{-}\mu\text{m}^3$ unit cell with a $20\text{-}\mu\text{m}$ cap thickness and $30\text{-}\mu\text{m}$ diameter rods

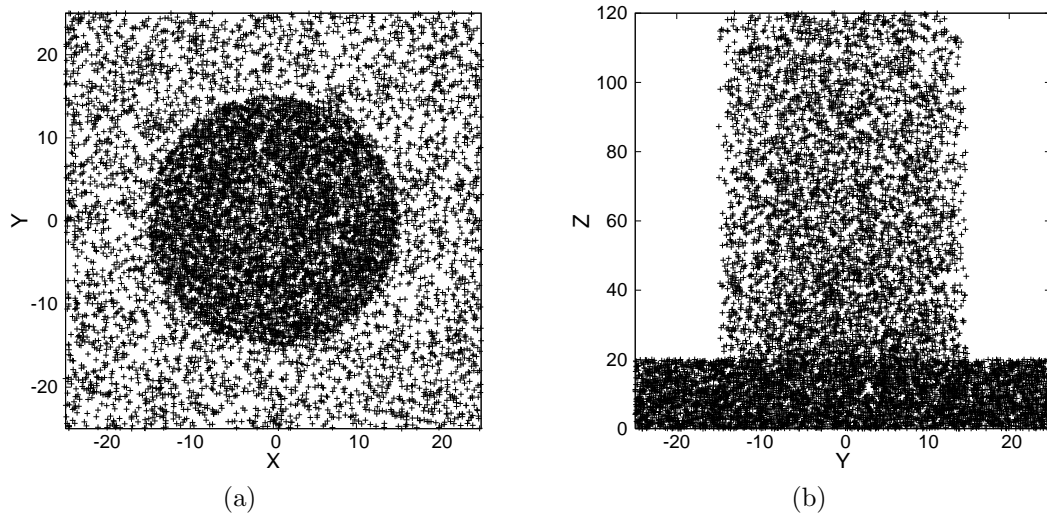


Fig. 3.7. 2D neutron absorption distributions for the normal incidence case. The data of Fig. 3.6 has been projected onto the (a) x - y and (b) y - z planes

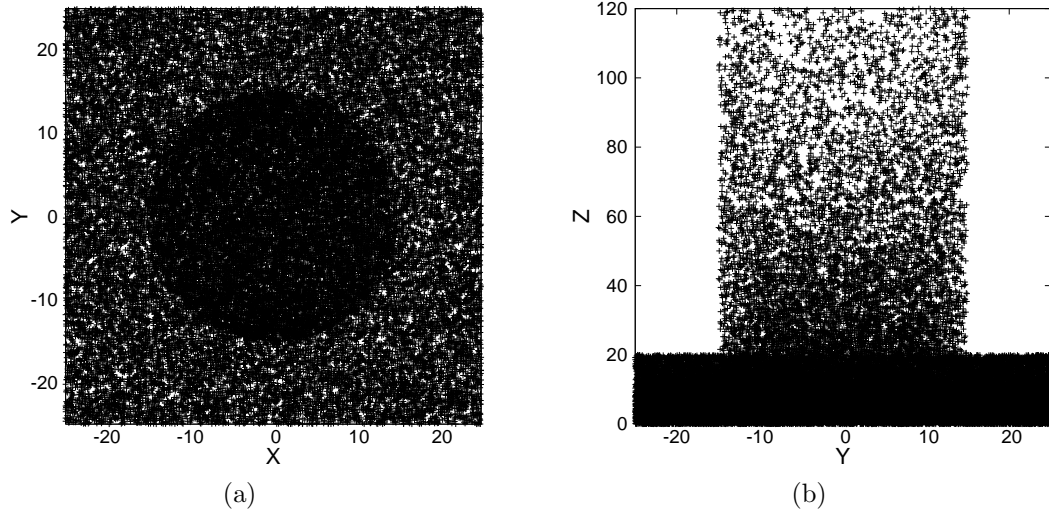


Fig. 3.8. 2D neutron absorption distributions for nearly glancing incidence

angle of incidence ($\theta = 85^\circ$). Because the angle is glancing, the neutrons that hit the detector, although few, are much more likely to be absorbed in the cap and the section of the rod nearest the cap. The rationale for this increase in absorbed particles hitting the detector is that, at a glancing angle, the distance through the absorber the neutron has to travel is much greater, or, rather, the neutron passes through many more lattice members increasing the likelihood of absorption. From the comparison of Fig. 3.7 and Fig. 3.8, one concludes that the extraction of the absorption locations from the MCNP PTRAC file and the subsequent translation of the absorption locations to the unit-cell geometry works correctly based on the densities of the absorptions in different sections of the cap and rod.

To test the overall correctness of the results produced, the script was modified to compute the efficiency for a coated diode detector, for which an analytical solution of the efficiency exists [McGregor et al., 2003]. Figure 3.9 compares the calculated efficiencies to the analytically determined efficiencies. One notes that, overall, the numerical prediction and the analytical result match quite closely. The discrepancies are a result of the fact that the analytical model only considers the 0.0253-eV cross section, while the MCNP simulation uses a Maxwellian thermal distribution of neutron energies for which the cross sections may be slightly different. Additionally, the analytical result assumes an infinite detector, while the hybrid numerical method does not. Because the detector used in the hybrid model is finite in radius, as the polar angle of incidence increases, this model under predicts the efficiency as compared to the analytical model because neutrons entering the detector close to the boundary of the finite detector are more likely to escape the detector.

3.3 Specialized Detector Efficiency Calculation Codes

The same methods were employed for estimating the angular absorption efficiencies of channel and chevron type perforations. However, the original ion-transport code could not be used in the hybrid technique because the ion-transport code specifically handles only the rod-

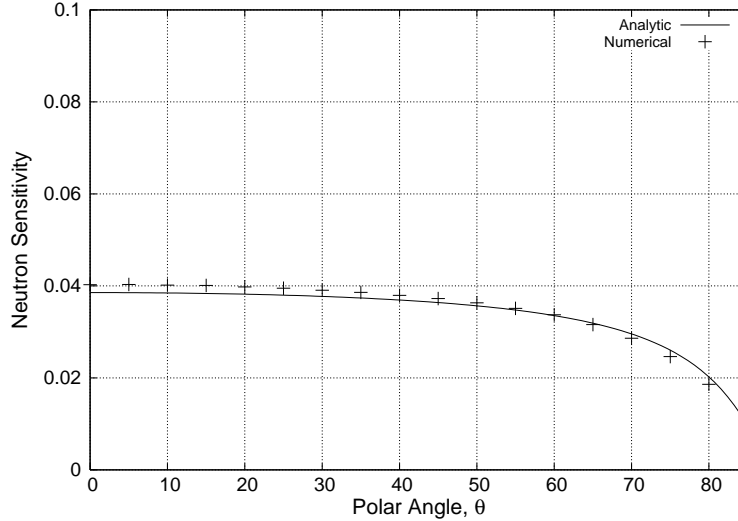


Fig. 3.9. Comparison of numerical calculation to analytical solution for a coated diode detector with a $3.54\text{-}\mu\text{m}$ thick film

type geometry. Instead, only the neutron absorption efficiencies are calculated. To quantify the total angular efficiencies of the channel, chevron, and sinusoidal detectors specialized codes for these geometries were written.

The customized codes to determine the total angular detector efficiencies for channel, chevron, and sinusoidal-perforated detectors were written in FORTRAN 90 using a modular programming style. The source code for the modules is given in Appendix A. In this section, the workings of the programs are explained and the special instance of ray-tracing sinusoidal geometries is discussed. Finally, some discussion of the validation of the code is presented.

3.3.1 General Description of the Customized Codes

Eight modules contain the necessary functions and variables to perform the calculations. The `parts_mod` module defines a new structured type for particles that stores their position, direction, and energy. The module `ions_mod` defines the ion-transport backtracking functions necessary to determine the energy deposition in the detector, and the `mca_mod` module provides a way of recording the energy deposition. `const_mod` is a module of fundamental constants used in the program, and `kind_mod` defines the precision of integer and real variables such that `real(dknd)` specifies a real double. Random numbers are seeded and generated using the source found in `random_mod`. The module `zero_mod` contains routines adapted from those given in Press et al. [1992] for finding the zeros of functions.

Geometry: The most intricate of the modules is `surf_mod`. This module specifies the geometry of the problem and is different for each type of perforated detector. Functions have been defined that, based on the initialization values of specific variables, calculate the distances to surfaces and determine in which cell a ion or neutron is. The geometry and ray-tracing in these programs is not, by any means, elegant, as the intent of the program is

not to make a general purpose code; rather, these programs are intended to be functional and to work repeatably and reliably.

The geometry considered is that of the unit cell as described above, and most of the boundary surfaces are planes. Three planes perpendicular to the z -axis bound the cap and detector body away from the rest of the universe. Two planes perpendicular to each of the x and y directions bound the unit cell in those respective directions. These planes are mirrored boundaries so particles leaving through one x or y plane enter through the x or y plane directly opposite, and, in this way, an infinite detector array (in the x and y) directions is simulated. The perforations are, in the case of the channel and chevron detectors, uniquely defined planes providing the desired perforation shape. Unless otherwise specified, the channel width of the absorber and the channel width of the silicon were equal for the channel, chevron, and sinusoidal geometries. The sinusoidal surfaces cannot be defined by standard means because they cannot be defined by quadratic surfaces. The method used to find intersections with sinusoidal surfaces is discussed below in a separate section. Each region bounded by the planes is given a unique cell number that is odd if the region is the neutron absorber and even if the region is the silicon semiconductor. Thus, by using the modulus operator on the cell number, the cell material can be obtained.

Code Operation: The program begins by initializing the variables defining the dimensions of the unit cell and perforations. Two loops begin cycling through the polar and azimuthal angles, as in the hybrid method, and then, the program loops over the number of specified histories. A logical variable defines the presence or not of a cap; if a cap is used an initial neutron birth location is sampled uniformly over the outer surface of the cap and it's direction is specified by the polar and azimuthal angles. If no cap is specified, the incident neutron location is sampled uniformly over the top surface of the perforated body of the detector.

The program determines in which cell the neutron is. If the neutron is in an odd cell, an absorber, the distance to collision is computed using the thermal-averaged cross section, as described in Chapter 2. The distance to the next surface is also computed, and, if the distance to collision is shorter, the distance to collision along the neutrons direction is added to the neutron's position and the neutron is terminated. If the distance to surface is less than the distance to collision, then, the neutron's position is updated by the distance to surface along its direction of travel. At this point, the program again determines which cell the neutron in is and repeats the process. If the neutron is in an even cell, silicon, the distance to collision is not computed, as the program assumes no interaction in the silicon.

When the neutron is terminated in the absorber, the reaction product ions are created at the point of absorption. The direction of one of the ions is sampled isotropically and the direction of the other ion is set directly opposite the former. Each ion is tracked independently by calculating it's distance to surface, updating it's position to the surface, determining the quantity of energy lost using the backtracking method, and repeating until all energy of the ion has been transferred to the media. If the total energy deposited in the silicon regions exceeds the cutoff of 0.3 MeV then a count is recorded. The process repeats with the initialization of a new neutron until all histories for a specified polar and azimuthal angle are complete, at which point the next angular iterate is considered.

3.3.2 Unit Cell for Sinusoidal Perforations

Because the planes defining the sinusoidal perforations cannot be expressed as quadratic surfaces, a different unit cell must be specified for the sinusoidal perforations. In this case, the perforations were modeled by creating three sinusoidal planes (defined below) and offsetting them from each other. The area between the first and second plane is the neutron absorber material, and the area between the second and third planes is the silicon. The sinusoidal planes are bounded in the z direction by normal quadratic planes. Thus, the entire unit cell has the shape of a sinusoid rather than a rectangular prism.

Similarly to the regular unit cell, if a particle leaves through a sinusoidal surface that bounds the unit cell, it enters through another sinusoidal plane mirroring the one it exited. In this manner, the neutrons cannot escape the detector in the x or y direction, rather they must be absorbed or exceed the z boundary of the unit cell, at which point they are terminated.

3.3.3 Ray Intersections with Sinusoidal Planes

Ray tracing is typically performed in general purpose Monte Carlo codes by solving for the intersection(s) of a line with a quadratic surface. The equation of a ray can be parameterized using the distance variable d as

$$x = x_o + \alpha d \quad y = y_o + \beta d \quad z = z_o + \gamma d, \quad (3.2)$$

where x_o , y_o , and z_o are the initial points in three-space and α , β , and γ are the *direction cosines*, i.e., the cosines of the angles formed between the line and the positive x , y , and z axes, respectively. Using these equations, the distance to a quadratic surface can be calculated by substitution into the surface equation. For example a plane perpendicular to the x -axis has an equation of

$$x = P, \quad (3.3)$$

where P is the x coordinate of the plane. Substitution of the expression for x from Eq. (3.2) into the equation above yields

$$x_o + \alpha d = P. \quad (3.4)$$

Solution for the distance to the plane gives

$$d = \frac{P - x_o}{\alpha}. \quad (3.5)$$

This process can be used to find a lines intersection with any surface expressed as a quadratic surface. However, sinusoidal forms cannot be expressed as a quadratic, so the distance cannot be solved explicitly and a numerical technique must be employed.

A sinusoidal plane is here defined to be a plane infinite in two dimensions and sinusoidally oscillating in the third dimension as a function of only one of the other variables. For example, the equation specifying a sinusoidal plane infinite in the x and z directions and oscillating

in the y direction as a function of the x variable would be

$$y = P_y + \Delta \sin\left(\frac{2\pi x}{w}\right). \quad (3.6)$$

Here, P_y represents the plane of the oscillation's offset from the y -axis, Δ is the magnitude of the sine wave, and w is the period (see Fig. 3.10). Substitution of the line equations from Eq. (3.2) yields

$$y_o + \beta d = P_y + \Delta \sin\left(\frac{2\pi(x_o + \alpha d)}{w}\right). \quad (3.7)$$

This transcendental equation cannot be solved explicitly for d . Moreover, multiple values of d may arise. However, in this particular application only the smallest positive value of d is needed. To find this smallest d , Eq. (3.7) is rearranged as

$$F(d) = P_y + \Delta \sin\left(\frac{2\pi(x_o + \alpha d)}{w}\right) - y_o - \beta d = 0. \quad (3.8)$$

and the smallest positive value of d is determined using the a zero-finding algorithm from Press et al. [1992].

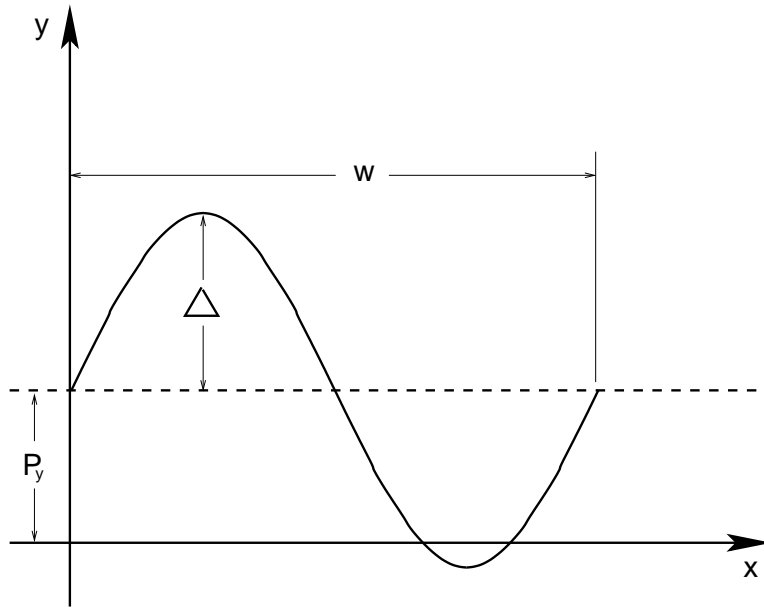


Fig. 3.10. A sinusoidal plane having a y offset of P_y , an amplitude of Δ , and a period of w

The process of finding the smallest positive distance begins by setting an upper bound, b_u , and lower bound (initially equal to zero), b_l , for the range over d where the zero is sought. The upper and lower bounds are incremented uniformly until either $F(b_l) > 0$ and $F(b_u) < 0$ or $F(b_l) < 0$ and $F(b_u) > 0$. Once the region encompassing the zero is bounded, a packaged zero-finding algorithm, namely the `zbrent` algorithm from Press et al. [1992], is employed to find the exact value. The d that is returned is the shortest distance to the sinusoidal plane

along the direction of particle motion. If no solution is found a large number, relative to the dimensions of the unit cell, is returned.

3.3.4 Verification and Validation of the Customized Codes

The specialized codes were also checked to ensure they functioned as expected. All of the perforation geometries are checked, but only the sinusoidal geometry is discussed as it is the most complicated. If the ray tracing and absorption works in the sinusoidal case it will work in the other much simpler cases, as well.

One of the checks performed starts source particles randomly positioned and isotropically throughout the detector and verifies the surface crossing locations are correct. Figure 3.11(a) illustrates the surface crossing locations in the sinusoidal detector for neutrons randomly positioned and isotropically directed. Particles leaving the unit cell through the largest y sinusoidal plane are reflected to enter through the lowest y sinusoidal plane. Similarly, particles leaving the left most x plane are reflected to enter through the right most x plane. One can see the map of the surface crossing clearly marks out the geometry of the unit cell. However, it appears that some of the crossing locations are incorrectly located inside the boundaries, i.e., between the sinusoidal planes. Upon inspection of Fig. 3.11(b) where the surface crossing have been projected onto the x - z plane, it is clear that the points that appear between the sinusoidal planes are the locations where neutrons are crossing planes perpendicular to the z -axis. Also, one notes that fewer crossing events occur at the peaks of the sinusoid than at other points.

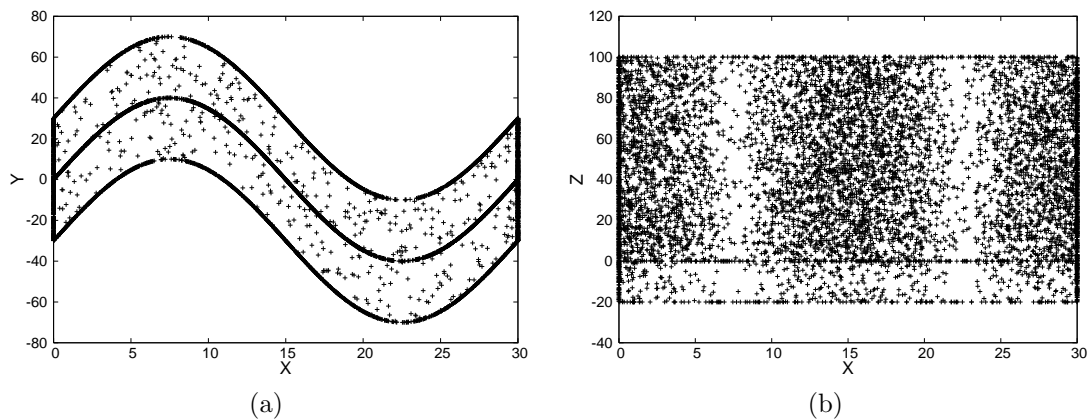


Fig. 3.11. Sinusoidal unit-cell surface crossing locations for neutrons randomly positioned and isotropically directed throughout the unit cell. (a) is the projection of the crossing locations on the x - y plane, and (b) is their projection on the x - z plane.

Another check is to verify the absorption locations fall in the expected regions. Figure 3.12 presents the three dimensional absorption locations in the sinusoidal unit cell resulting from normally incident neutrons. While it is difficult to ensure all of the absorption locations are in the proper regions in this figure, one can deduce that the approximate shape is correct and that the sinusoidal pattern is present.

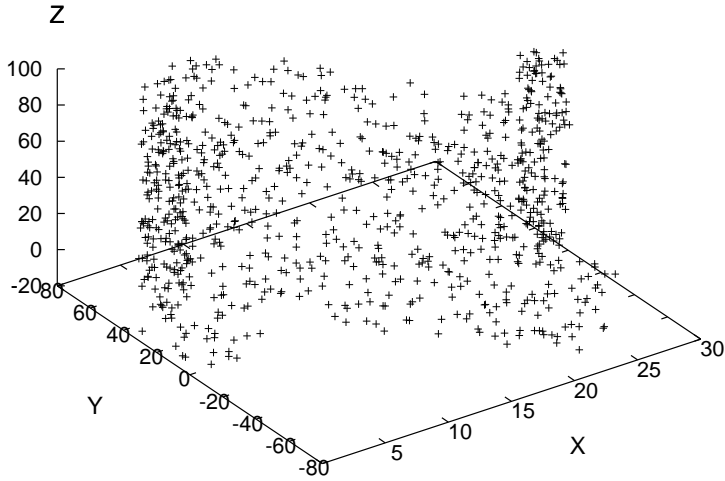


Fig. 3.12. 3D sinusoidal unit cell showing the absorption locations

A more distinct depiction of the absorption locations is presented in Fig. 3.13. Here, the first figure shows the x - y absorption locations, and the sinusoidal pattern can easily be seen. The region of higher density interactions represents the perforation and the lower density of interactions represents the cap. The second part of the figure presents the same absorption locations plotted on x - z axes. From this perspective the higher density of interactions occurs in the cap and not the perforation, so it is easy to distinguish the cap from the perforations.

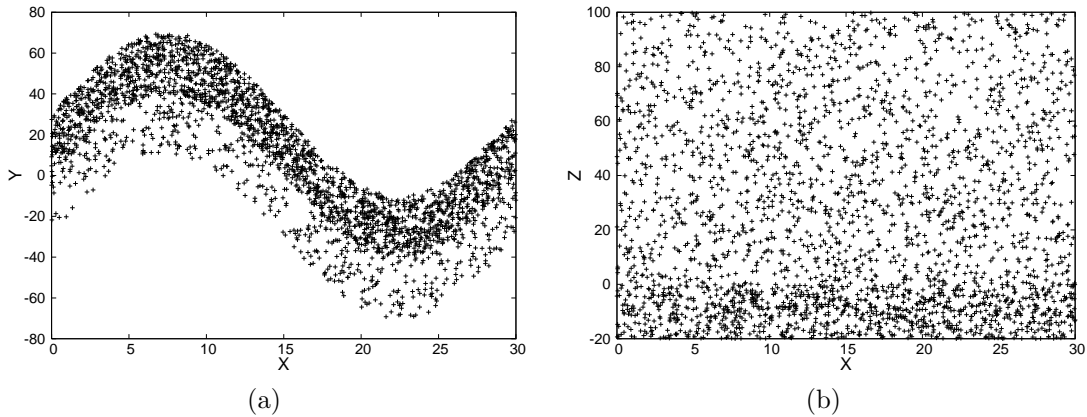


Fig. 3.13. 2D projections of the sinusoidal unit-cell absorption locations from Fig. 3.12 onto the (a) x - y plane and (b) x - z plane

It appears the absorptions and surface crossing interactions are occurring as expected. Many other trials with different dimensions were used to determine the cases that worked and the cases with problems. It was empirically discovered that an important factor affecting the proper simulation of the sinusoidal crossings is the stepping length used to find the zero

of Eq. (3.8). A smaller stepping length works better, but also increases the run time of the calculation. However, too large of a step in many cases produces incorrect crossing points. A good stepping length was determined empirically to be one-tenth of the width of the unit-cell being investigated.

In addition to verifying the geometric accuracy of the code, the accuracy of the efficiency calculation was compared to the analytical solution for the case of a coated diode. Coated diode detectors are simulated for both ${}^6\text{LiF}$ and ${}^{10}\text{B}$ detectors for cap thicknesses of $26.0\ \mu\text{m}$ and $2.4\ \mu\text{m}$, respectively. Figure 3.14 presents the comparison of the numerical results with the analytical solution from McGregor et al. [2003]. The correlation between the two methods is good and lends confidence to the numerical method used in the customized codes for the simulation of perforated detectors.

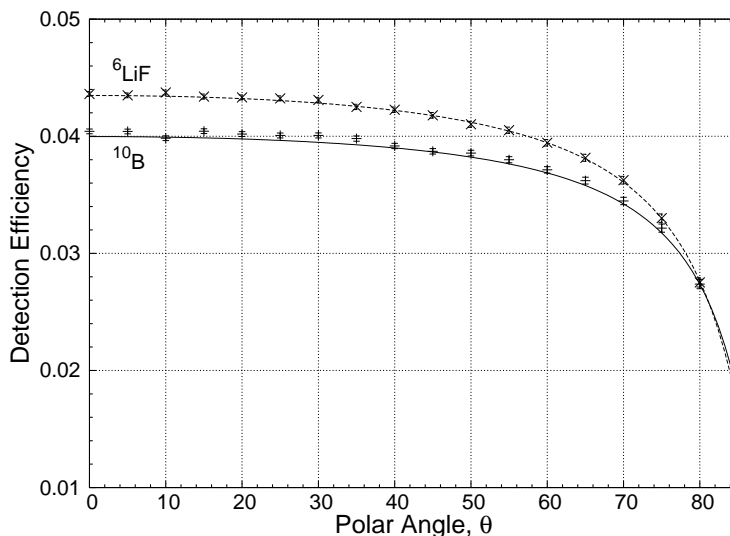


Fig. 3.14. Comparison of numerical and analytical solutions for coated diode detector efficiencies for a $26\text{-}\mu\text{m}$ ${}^6\text{LiF}$ film and a $2.4\text{-}\mu\text{m}$ ${}^{10}\text{B}$ film

3.4 Angular Efficiency Results

The angular detection efficiencies for rod, channel, chevron, and sinusoidal-shape perforations were calculated using the hybrid method for rod-type perforations and the customized codes for the other perforations. Unless otherwise specified, all channel-type, chevron-type, and sinusoidal-type models have equal widths of neutron absorber and semiconductor. Different perforation shapes give different neutron absorption efficiencies p_n , ion detection efficiencies η , and total detection efficiencies ε . Each of the efficiencies is discussed along with the effects the different perforations have on the respective efficiencies. Tabulated results of all calculations are given in Appendix B.

3.4.1 Neutron Absorption Efficiencies

Rod Perforations: The neutron absorption efficiency p_n varies with of the amount of absorber material the neutron passes through in its flight path. The more absorption material present, the more likely the neutron is to be absorbed. The rod perforated detectors have a fundamental problem in that the absorption efficiency decreases for incident directions that allow some of the neutrons to pass through the detector without encountering any absorber material. Figure 3.15 and Fig. 3.16 show the absorption efficiencies of a ^{10}B rod-type detector and a ^6LiF rod-type detector, respectively. One notes the absorption efficiency for the neutrons is much higher in boron than in lithium fluoride, a consequence of boron having a higher cross section.

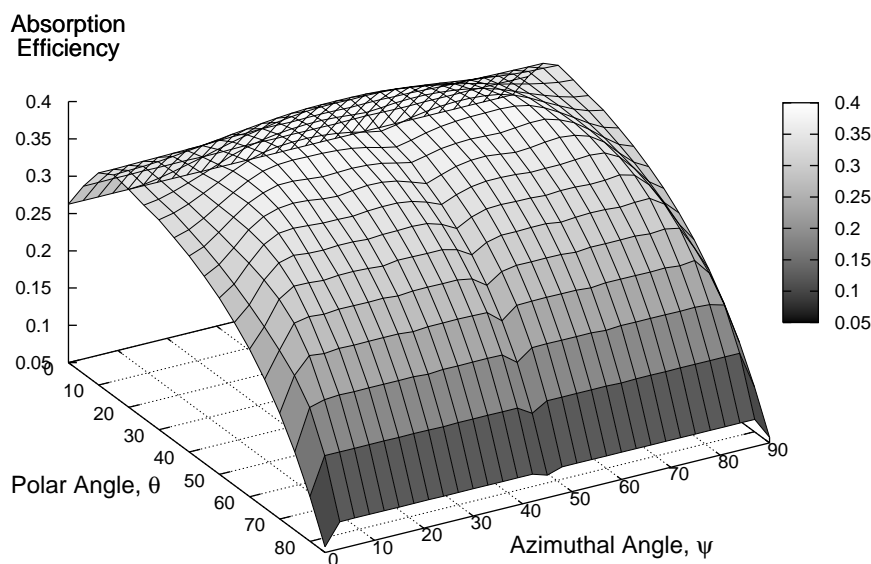


Fig. 3.15. The neutron absorption efficiency of a ^{10}B rod perforated detector with 30- μm perforation depth, 6- μm diameter rods, and no cap

One also observes from these figures that the detector absorption efficiency is not as uniform as is desired with respect to the azimuthal angle or even the polar angle. Recall, it is impossible to prevent the detector response from dropping to zero in the polar direction as the polar angle increases to 90° because the solid angle subtended by the detector fades to zero.

The increase in the absorption efficiency for increasing polar angles in the range of $(0, 20^\circ)$ is a result of many factors. One factor is that the projected perforation area, i.e. the area of a single perforation projected on a plane perpendicular to the incident neutrons, increases thereby giving neutrons more absorber area to pass through. Additionally, the average path length through the detector perforations is increased as the polar angle increases because, as the polar angle increases, the distance from the point the neutron enters the top of the perforation to where it leaves the bottom of the perforation is greater than the perfora-

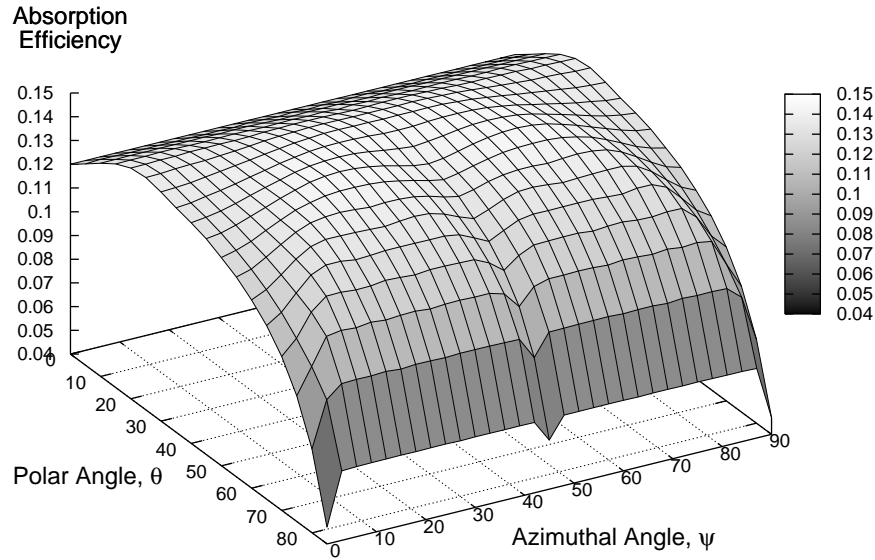


Fig. 3.16. The neutron absorption efficiency of a ${}^6\text{LiF}$ rod perforated detector with $100\text{-}\mu\text{m}$ perforation depth, $30\text{-}\mu\text{m}$ diameter rods, and no cap

tion depth—the depth the neutrons travel at normal incidence. This greater perforation travel path increases the probability the neutron is absorbed. The increasing travel distance through the perforation does not continue for all angles, but eventually begins to decrease for polar angles greater than $\sim 20^\circ$. Figure 3.17 presents the absorption probability for a ${}^6\text{LiF}$ perforated detector with three times the perforation depth of that shown in Fig. 3.16. Here, one notes that the increase in absorption probability at the low polar angles is more pronounced than the shallower perforations. Thus, if less variation is desired in the polar direction the depth of the perforations cannot exceed about $100\ \mu\text{m}$ for ${}^6\text{LiF}$ detectors and $10\ \mu\text{m}$ for ${}^{10}\text{B}$ detectors.

Noteworthy is the increase in efficiency at small polar angles is much greater for the ${}^{10}\text{B}$ detectors than for the ${}^6\text{LiF}$ detectors, again a result of the absorption cross section being higher for the boron, for which the additional distance through the perforations plays a much more significant role. As the distance through the perforations begins to decrease, the neutrons begin encountering multiple perforations, thereby alleviating some of the expected loss of efficiency. As the neutrons pass through more perforations they are more likely to be absorbed. But in the end, the increase in number of perforations neutrons pass through cannot compete with the loss of efficiency from fewer neutrons actually hitting the detector, and the efficiency drops dramatically for large polar angles.

The absorption efficiency across the azimuth varies as a function of the angles where neutrons are allowed to stream through the detector without encountering neutron absorbing material. Figure 3.18 illustrates the *streaming paths* in the rod perforated detectors. Neutrons incident at azimuthal angles ψ that are multiples of 45° “see” streaming paths that they may pass through without encountering any absorber material. Even multiples of

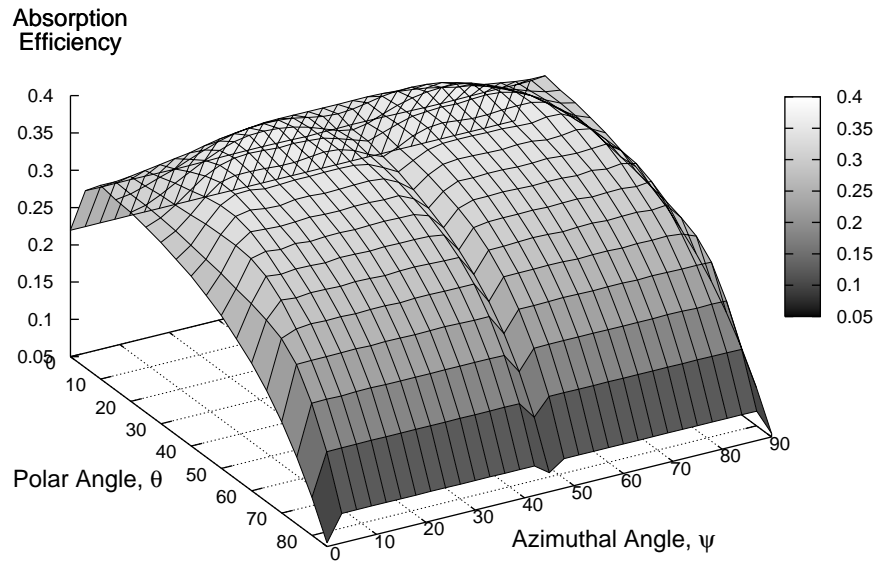


Fig. 3.17. The neutron absorption efficiency of a ${}^6\text{LiF}$ rod perforated detector with 300- μm perforation depth, 30- μm diameter rods, and no cap

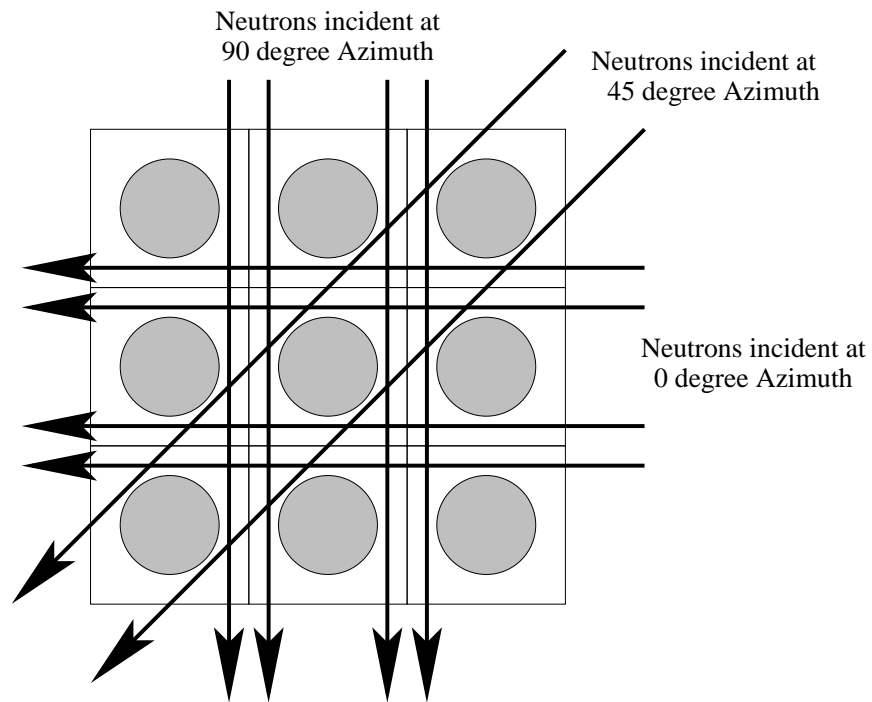


Fig. 3.18. Streaming in rod perforated detectors

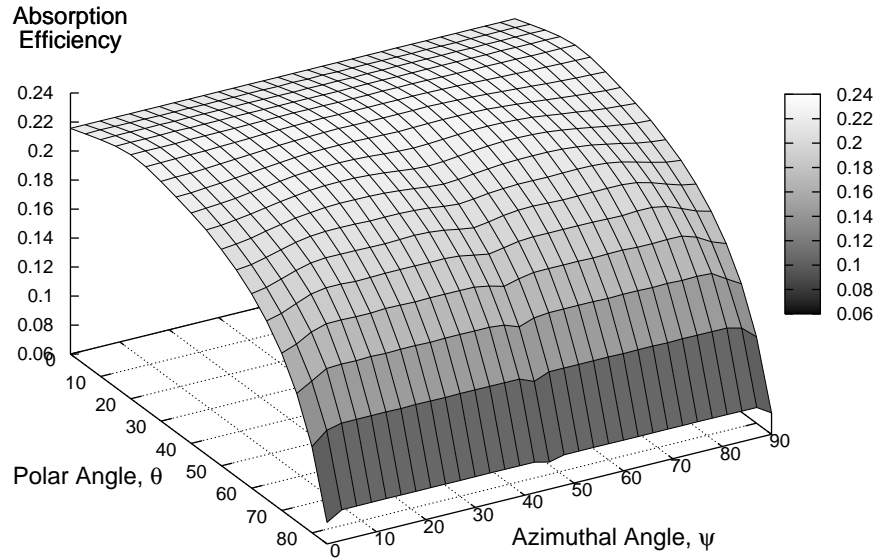


Fig. 3.19. The neutron absorption efficiency of a ${}^6\text{LiF}$ rod perforated detector with 100- μm perforation depth, 30- μm diameter rods, and a 20- μm cap

45°, i.e., 0°, 90°, etc., produce wider streaming paths than the odd multiples. At azimuthal angles for which streaming paths occur, the absorption efficiency dips as seen in Fig. 3.15 and Fig. 3.16. Ideally, one desires to be rid of such dips so the angular response of the detector is more uniform in the azimuthal direction.

The presence of a cap on the detector nearly doubles the absorption probability, but the ions born in the cap are less likely to deposit energy in the detector. The results from a ${}^6\text{LiF}$ detector having 100- μm deep perforations, 30- μm diameter rods, and a 20- μm cap are presented in Fig. 3.19. One notes that streaming seems to be slightly mitigated by presence of a cap, but the problem is not completely removed. Also, the cap absorbs a significant portion of neutrons incident to the detector, but the efficiency of the ion products to reach the semiconductor is no better than the case of a coated diode.

Channel Perforations: Because of the streaming problems with the rod perforated detectors, other perforation shapes were considered. The neutron absorption efficiencies for a ${}^{10}\text{B}$ and a ${}^6\text{LiF}$ channel-perforated detector are shown in Fig. 3.20 and Fig. 3.21, respectively. Again, one notes the increase in efficiency, especially for the boron detector, for increasing small polar angles. As before, the absorption efficiency drops to zero at high polar angle because the solid angle of the detector becomes small.

However, for the channel perforations, the azimuthal dependence of the absorption efficiency has greatly improved. No longer are dips present in the absorption efficiency for angles at all multiples of 45°, but, rather, a dip is only realized at 90°. The drop in efficiency is, again, a result of a streaming path at 90° as shown in Fig. 3.22. Source neutrons traveling in directions parallel to the channels can stream through the detector in over 50% of the

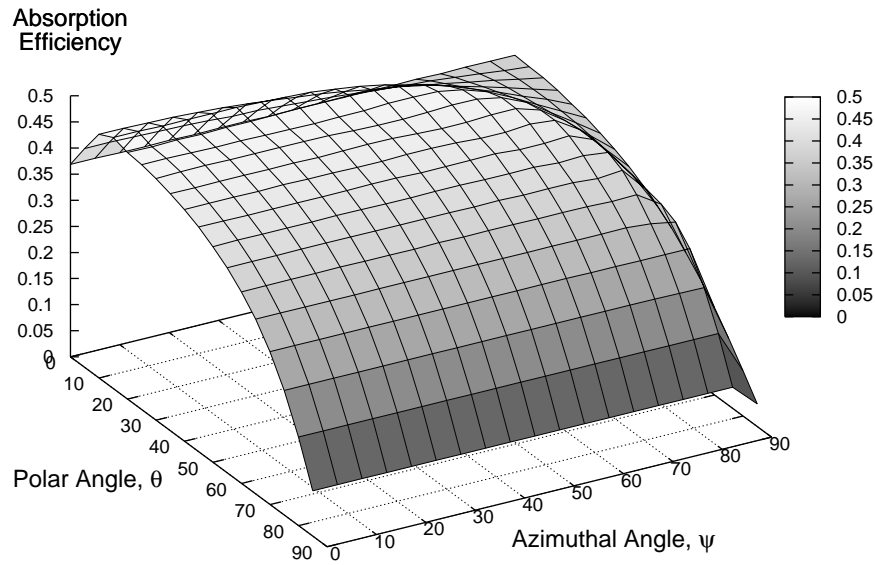


Fig. 3.20. The neutron absorption efficiency of a ^{10}B channel perforated detector with 30- μm perforation depth, 4- μm wide channels, and no cap

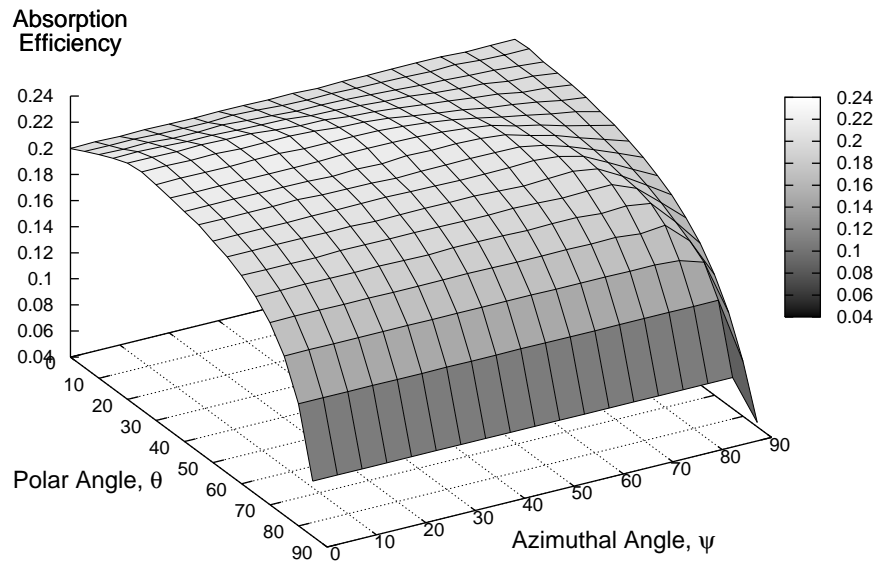


Fig. 3.21. The neutron absorption efficiency of a ^6LiF channel perforated detector with 100- μm perforation depth, 20- μm wide channels, and no cap

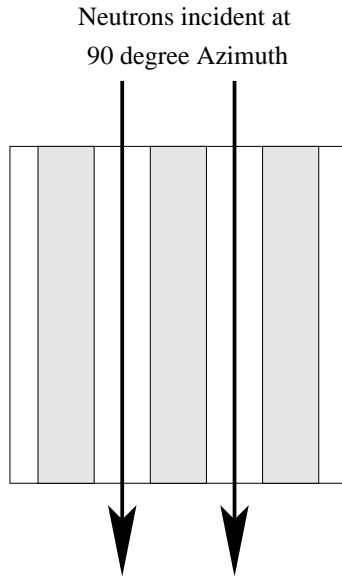


Fig. 3.22. Streaming in channel perforated detectors

coverage area.

Chevron Perforations: In an attempt to remove all direct streaming paths, the chevron perforations are investigated. The chevrons consist of a “zig-zag” of the channel pattern such that the bends in the chevron are at right angles to each other. The resulting neutron absorption efficiencies are plotted for the boron and lithium fluoride detectors in Fig. 3.23 and Fig. 3.24, respectively.

In the chevron-shaped perforations no direct streaming paths are possible; however, short paths, through which neutrons may stream, are created at $\pm 45^\circ$. The fact that the streaming paths are at 45° is a result of how the chevrons are created. If a different angle than 90° had been chosen for the chevron angle then the streaming would have been observed at half of that angle.

Sinusoidal Perforations: One final perforation design is considered to minimize the streaming problem of the neutron absorption efficiency. Sinusoidal patterns are modeled because they have no straight paths for neutrons to travel along, and eventually a neutron encounters some absorbing material. Interestingly, if a neutron does travel along one of the straighter parts of the sinusoid, it must then traverse the peak of the sinusoid, where a thicker amount of absorber is present. This phenomenon helps to flatten the azimuthal neutron absorption efficiency as shown in Fig. 3.25.

The sinusoidal perforations have more degrees of freedom than the other perforated detectors. The rod-type detectors can vary the rod’s diameter and spacing between rods. The channel and chevron detectors can vary channel thickness, but the sinusoid detectors can vary the spacing between sinusoids, the amplitude of the sine wave, and period of the sine wave. To remove one degree of freedom, the spacing between bounding sinusoidal planes for the silicon is set equal to the spacing between those for the absorber. It was discovered that

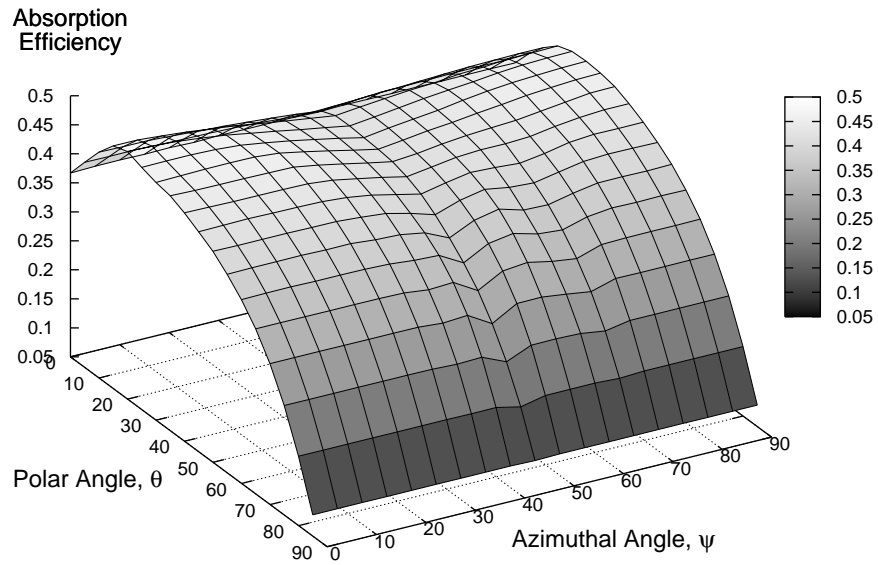


Fig. 3.23. The neutron absorption efficiency of a ^{10}B chevron perforated detector with 30- μm perforation depth, 4- μm wide channels, and no cap

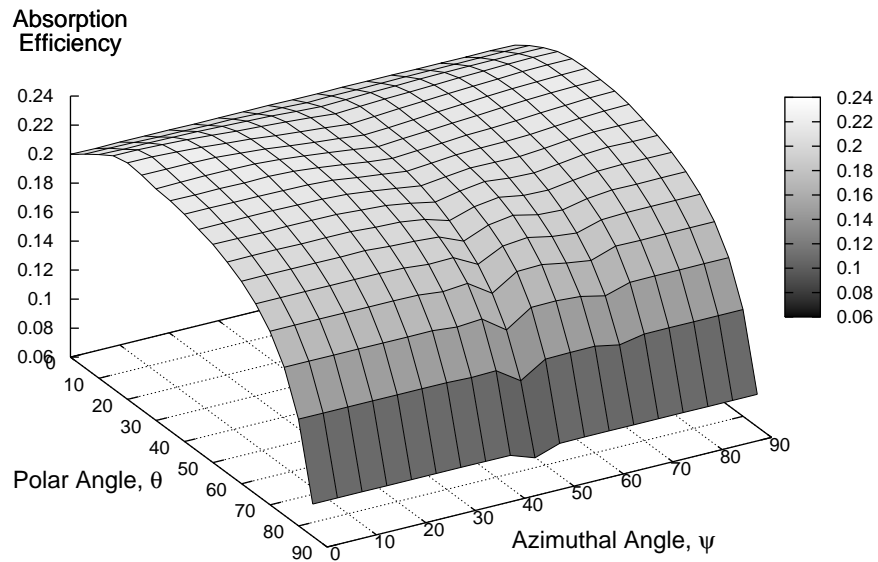


Fig. 3.24. The neutron absorption efficiency of a ^6LiF chevron perforated detector with 100- μm perforation depth, 20- μm wide channels, and no cap

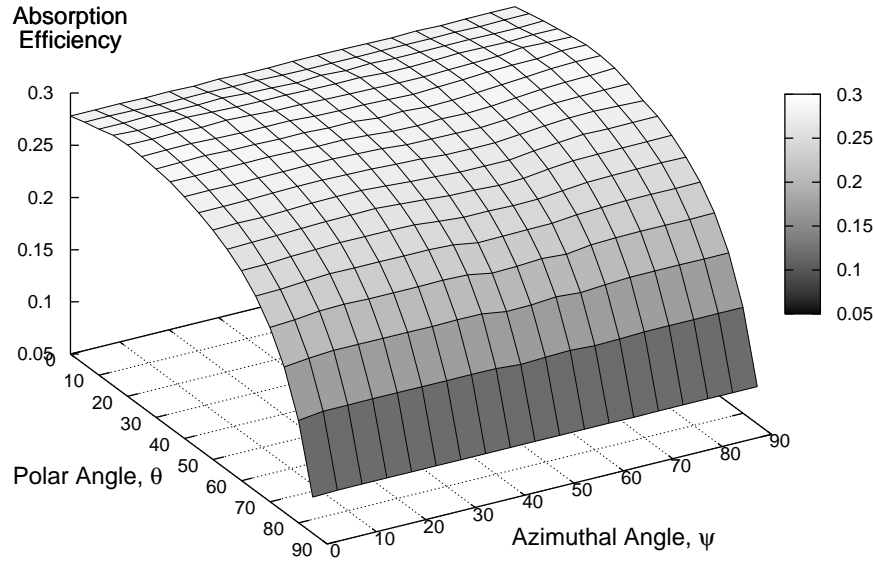


Fig. 3.25. The neutron absorption efficiency of a ${}^6\text{LiF}$ sinusoid perforated detector with $100\text{-}\mu\text{m}$ perforation depth, $130\text{-}\mu\text{m}$ sine period, $40\text{-}\mu\text{m}$ sine amplitude, $35\text{-}\mu\text{m}$ sine wave separation, and no cap

not all spacings, wave amplitudes, and wave periods produced the desired flat response in the azimuthal direction. Fig. 3.26 through Fig. 3.28 present neutron absorption efficiencies for sinusoidal-type detectors that do not have the desired flat response in the azimuthal direction.

The boron detectors exhibit this problem to a greater extent than the lithium fluoride detectors do. Moreover, it is seen that the absorption efficiencies are dropping at azimuthal angles just before 90° . Practically, the slight drop ($< 1\%$) with the ${}^6\text{LiF}$ detector is mostly inconsequential in application; however, because the drop is many percent for the ${}^{10}\text{B}$ detector, this detector could cause problems when the angular resolution is important.

Stacked Detectors In addition to examining the neutron absorption efficiencies of single detectors, the absorption efficiencies for two ${}^6\text{LiF}$ detectors stacked on top of each other are investigated with an MCNP model for the rod, channel, and chevron designs. The stacking is performed such that the absorbing perforations of one detector are placed over the silicon perforations of the other detector so that, at normal incidence, no matter where they enter the detector, neutrons pass through the same amount of absorber. Fig. 3.29 through Fig. 3.31 summarize the findings.

First, it is observed that these stacked or sandwich detectors have roughly twice the absorption efficiency as a single detector. One also notices that the stacked rods and channels create a greater problem with respect to the flatness of the response in the azimuthal direction. Interesting is the fact that the neutron absorption efficiency now drops rapidly for small increases in polar angle above 0° ; this drop is a result of the neutrons now being able

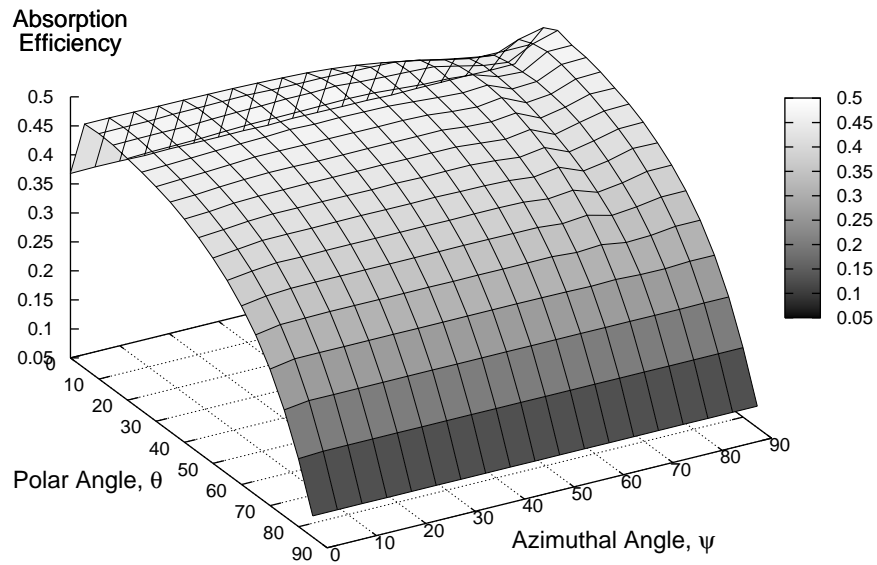


Fig. 3.26. The neutron absorption efficiency of a ^{10}B sinusoid perforated detector with $30\text{-}\mu\text{m}$ perforation depth, $4\text{-}\mu\text{m}$ sine period, $4\text{-}\mu\text{m}$ sine amplitude, $4\text{-}\mu\text{m}$ sine wave separation, and no cap

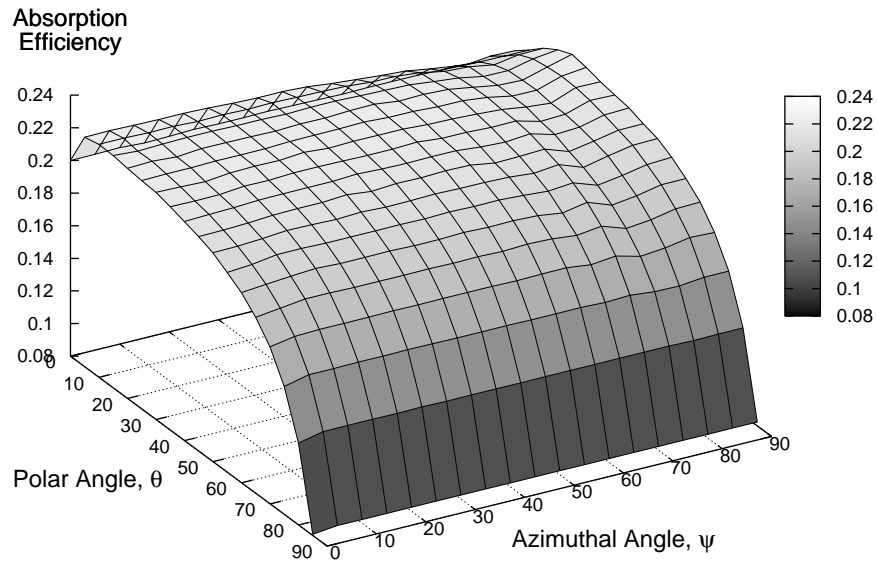


Fig. 3.27. The neutron absorption efficiency of a ^6LiF sinusoid perforated detector with $100\text{-}\mu\text{m}$ perforation depth, $20\text{-}\mu\text{m}$ sine period, $20\text{-}\mu\text{m}$ sine amplitude, $20\text{-}\mu\text{m}$ sine wave separation, and no cap

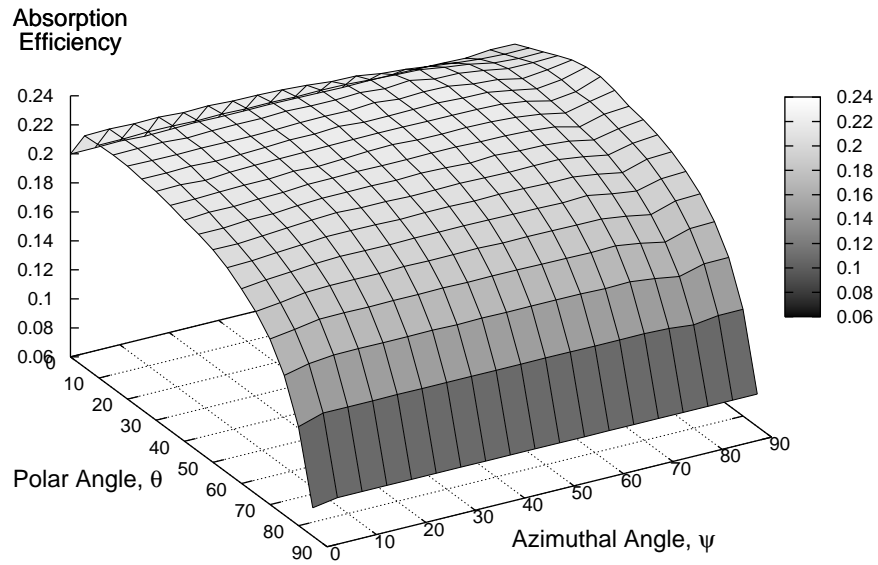


Fig. 3.28. The neutron absorption efficiency of a ${}^6\text{LiF}$ sinusoid perforated detector with $100\text{-}\mu\text{m}$ perforation depth, $30\text{-}\mu\text{m}$ sine period, $40\text{-}\mu\text{m}$ sine amplitude, $30\text{-}\mu\text{m}$ sine wave separation, and no cap

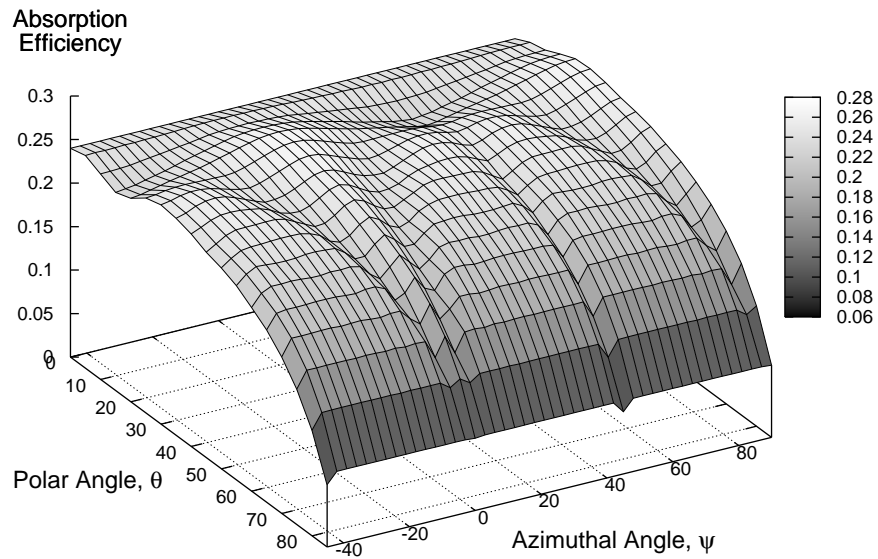


Fig. 3.29. The neutron absorption efficiency of stacked ${}^6\text{LiF}$ rod detectors with $100\text{-}\mu\text{m}$ perforation depth, $30\text{-}\mu\text{m}$ diameter rods, and no cap

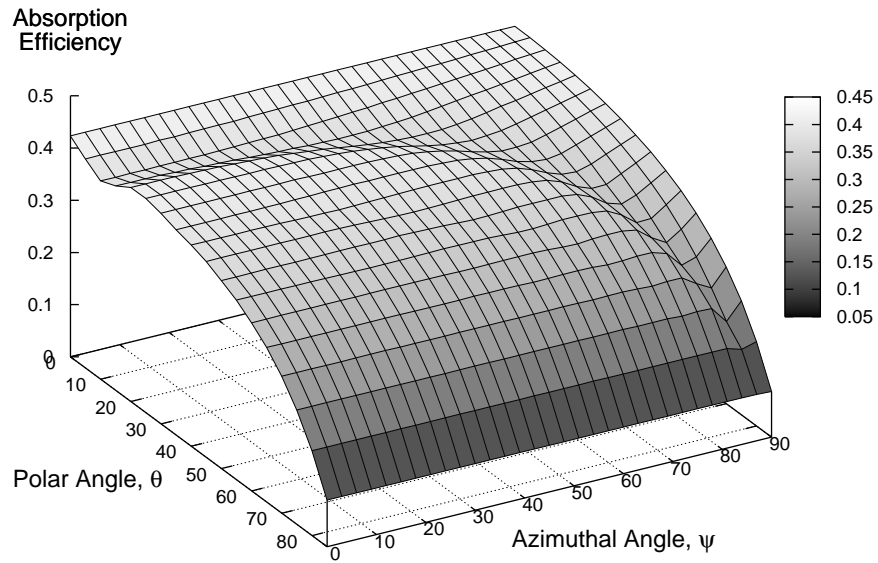


Fig. 3.30. The neutron absorption efficiency of stacked ${}^6\text{LiF}$ channel detectors with $100\text{-}\mu\text{m}$ perforation depth, $25\text{-}\mu\text{m}$ wide channels, and no cap

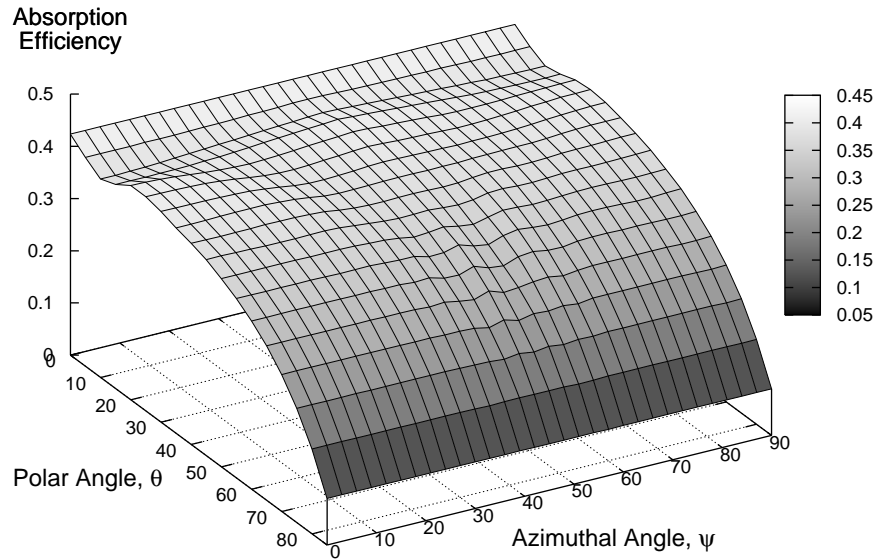


Fig. 3.31. The neutron absorption efficiency of stacked ${}^6\text{LiF}$ chevron detectors with $100\text{-}\mu\text{m}$ perforation depth, $25\text{-}\mu\text{m}$ wide channels, and no cap

to “cut” through the corners of adjoining perforations and encounter little or no absorber.

The chevron pattern, in contrast to the other two, is actually flat in the azimuthal direction. There is some fluctuation but it is slight. The larger problem in this case is the rapid 5% drop in efficiency as the polar angle increases from 0° , as a result would cause neutrons entering normally to the detector to have a higher probability of being detected.

3.4.2 Ion Detection Probabilities

The ion-detection probability η depends on where the neutrons are absorbed in the detector, but once the absorption locations are known, the probability the ions are detected can be determined independently. For reaction ions to be detected, it is assumed in this study they had to cumulatively deposit a minimum of 300 keV in the silicon portion of the detector. For values greater or less than 300 keV, η would be less or greater, respectively, than the following results.

The ion-detection efficiencies for the ^{10}B and ^6LiF rod detectors are shown, respectively, in Fig. 3.32 and Fig. 3.33. Immediately, it is obvious the lithium fluoride detector is detecting the ions in a much more favorable manner, i.e., regardless of the incident neutron angle and the absorption distribution produced at that angle, the response is fairly uniform. However, the boron detector’s ability to detect the ions is a strong function of the incident angle. Specifically, there is a strong increase in its ability to detect the ions for small polar angles. Also, the absorption distribution generated at the 25° azimuth for moderate to high polar angles indicates the ions are much less likely to be detected at this azimuthal direction of incidence.

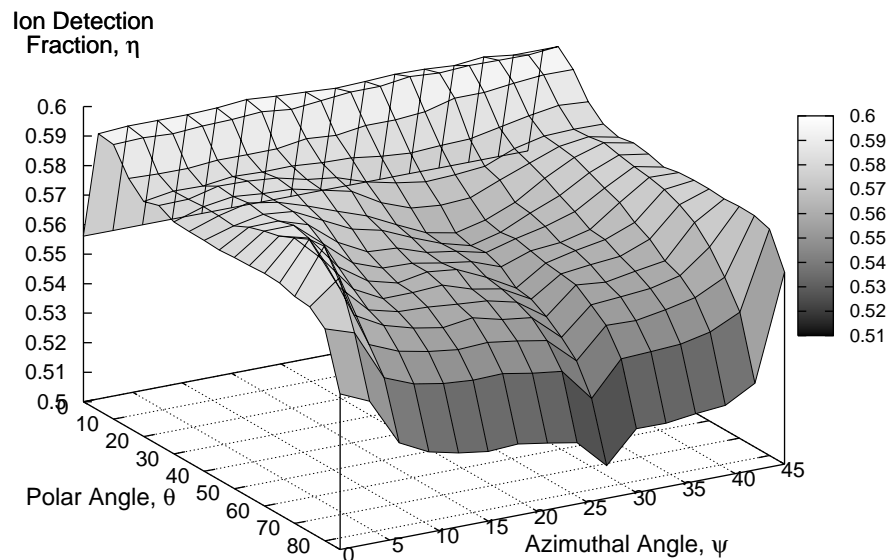


Fig. 3.32. The ion-detection efficiency of a ^{10}B rod detector with 30- μm deep perforations, 6- μm diameter rods, and no cap

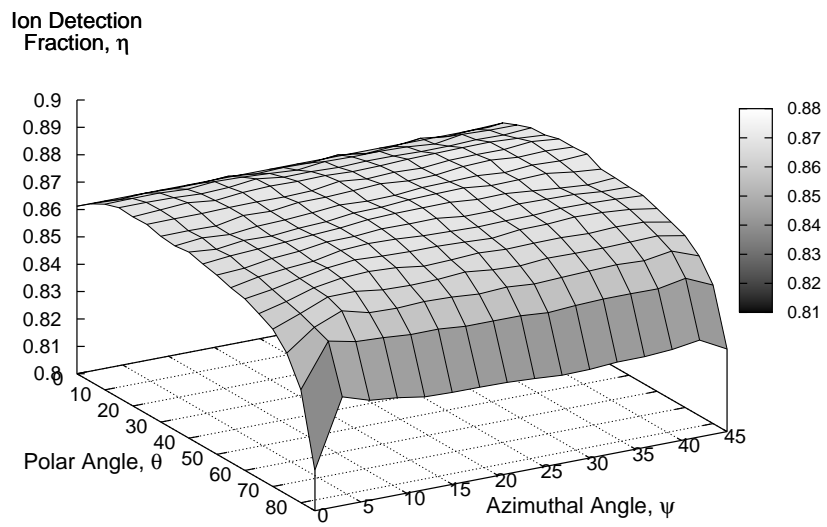


Fig. 3.33. The ion-detection efficiency of a ${}^6\text{LiF}$ rod detector with 100- μm deep perforations, 30- μm diameter rods, and no cap

If a cap is present on the detector, the absorption locations have a higher density in the cap. Ions born in the cap from a front irradiation have a lower probability of reaching the semiconductor because only one ion can travel toward the semiconductor, but there is less variation in the probability that they reach the semiconductor. If the detector is irradiated from the back rather than the front, a higher occurrence of absorptions occurs near the semiconductor and actually increases the probability the ions escape. This increase is not observed with front irradiation, and, for this reason, the ion detection probability of detectors with a cap is much smoother, but also much lower, as shown in Fig. 3.34.

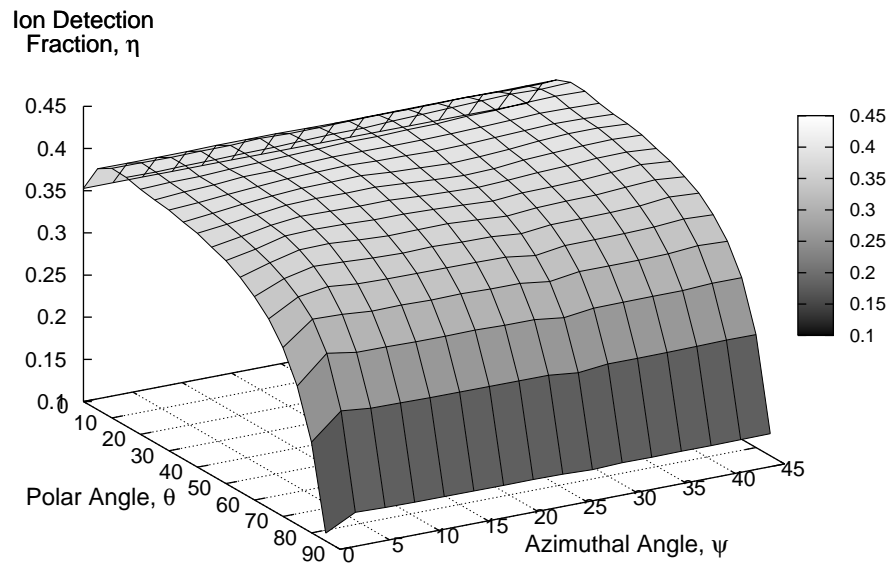


Fig. 3.34. The ion-detection efficiency of a ^{10}B rod detector with 30- μm deep perforations, 6- μm diameter rods, and a 4- μm cap

Similar types of problems arise for the channel and chevron ^{10}B detectors as shown in Figs. 3.35 through 3.37, respectively. Both the channel and chevron patterns exhibit the increased or decreased probability of detection as a function of the absorption distribution for the incident neutron angle. ^6LiF detectors (Fig. 3.36 and Fig. 3.38) are less susceptible to the problem of widely varying ion-detection efficiencies, the reason for which is rooted in the dimensions of the perforations and range of the ejected ions as well as the lower-level-discriminator (LLD) setting.

The lithium and alpha particle products from the $^{10}\text{B}(n,\alpha)^7\text{Li}$ reaction have respective ranges of 1.6 μm and 3.6 μm in boron, which are reduced to effective ranges of 0.81 and 2.65 μm for an LLD of 300 keV [McGregor et al., 2003]. If the perforation width of the channels or rods for the boron is 4-6 μm then reactions around the center of the rods or channel have only a slight probability of being detected, and reactions progressing further toward the side of the perforation are subject to the direction, either toward or away from the silicon, the longer range particle takes.

In the case of the $^6\text{Li}(n,t)^4\text{He}$ reaction the triton and alpha particles have respective

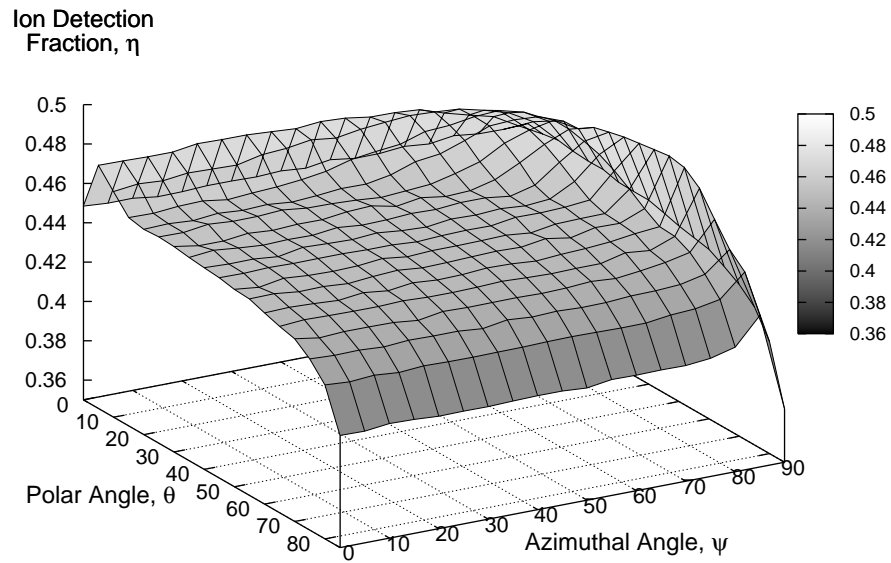


Fig. 3.35. The ion-detection efficiency of a ^{10}B channel detector with $30\text{-}\mu\text{m}$ deep perforations, $4\text{-}\mu\text{m}$ wide channels, and no cap

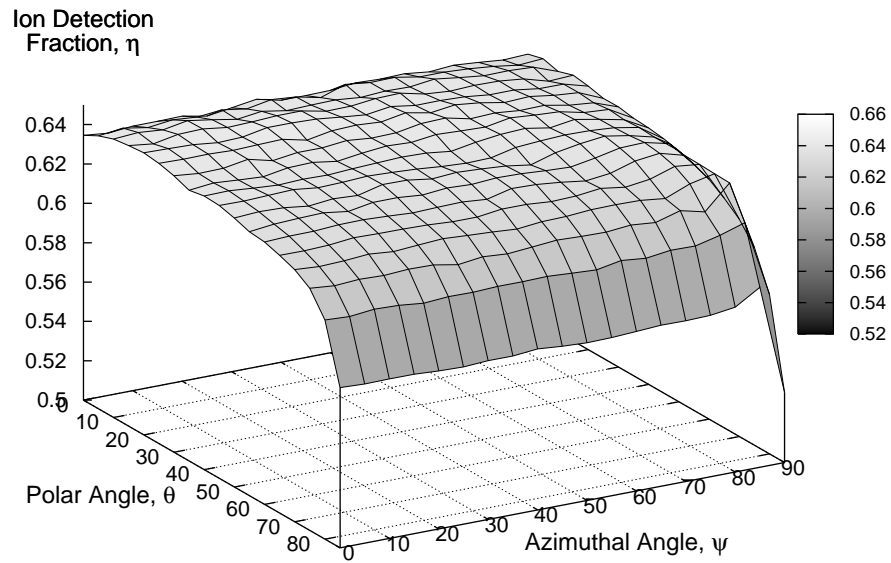


Fig. 3.36. The ion-detection efficiency of a ^6LiF channel detector with $100\text{-}\mu\text{m}$ deep perforations, $20\text{-}\mu\text{m}$ wide channels, and no cap

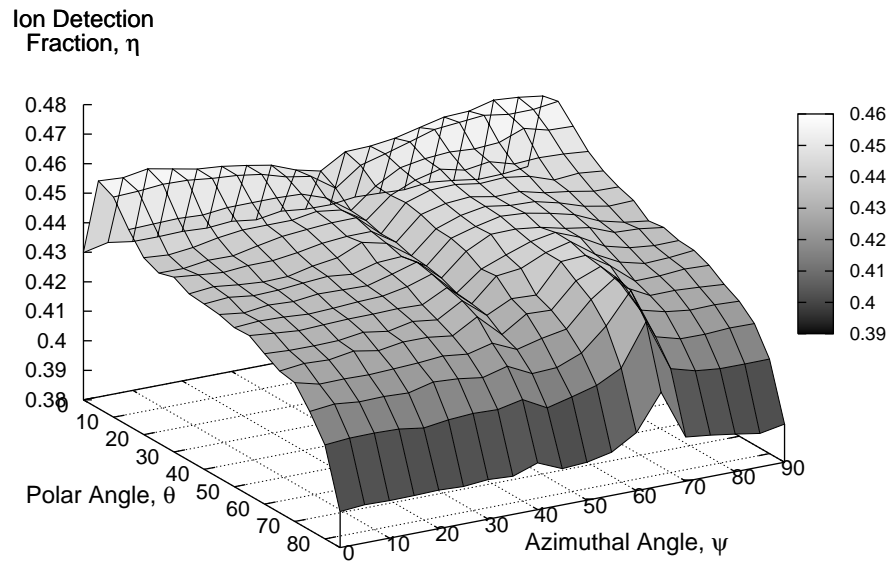


Fig. 3.37. The ion-detection efficiency of a ^{10}B chevron detector with $30\text{-}\mu\text{m}$ deep perforations, $4\text{-}\mu\text{m}$ wide channels, and no cap

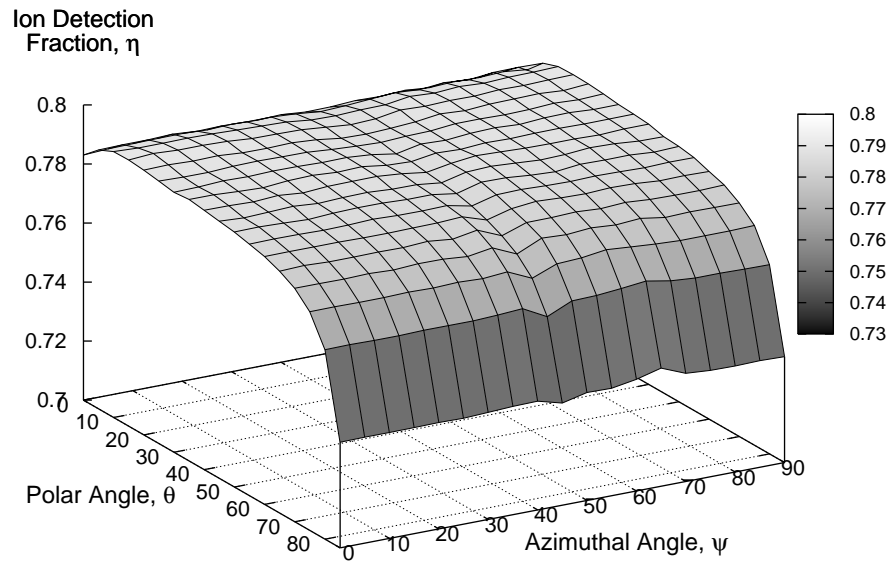


Fig. 3.38. The ion-detection efficiency of a ^6LiF chevron detector with $100\text{-}\mu\text{m}$ deep perforations, $20\text{-}\mu\text{m}$ wide channels, and no cap

ranges of $32.1 \mu\text{m}$ and $6.11 \mu\text{m}$ which gives an effective range of $29.25 \mu\text{m}$ and $4.64 \mu\text{m}$ [McGregor et al., 2003]. Because of the much higher range of the triton with respect to the perforation widths of $20\text{-}30 \mu\text{m}$ the triton has a much higher chance of escaping the absorber material and being detected. The dimensions of the boron detectors would have to be greatly reduced to obtain comparable performance, and doing so would make them increasingly difficult to fabricate.

The ion-detection probabilities of the sinusoidally perforated detectors are mostly flat for both the boron and lithium fluoride detectors. Figs. 3.39 and 3.40 present the ion-detection efficiencies for a ^{10}B and a ^6LiF detector, respectively, and it can be seen that both are relatively flat with respect to the azimuthal angle.

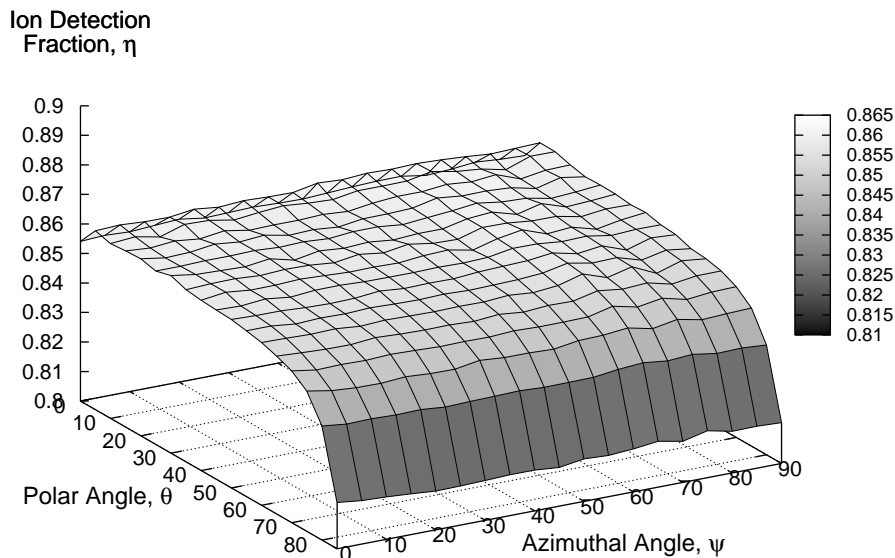


Fig. 3.39. The ion-detection efficiency of a ^{10}B sinusoid detector with $30\text{-}\mu\text{m}$ deep perforations, $4\text{-}\mu\text{m}$ wave period, $4\text{-}\mu\text{m}$ wave separation, $4\text{-}\mu\text{m}$ wave amplitude, and no cap

3.4.3 Total Neutron Detection Efficiencies

The total neutron detection efficiency ε is given by the product of the two previously discussed efficiencies, namely $\varepsilon = p_n \times \eta$. In general, the neutron absorption efficiency dominates the angular dependence of the total efficiency, but the effects of ion-detection efficiency can be seen in the rod-perforated ^{10}B detector efficiency presented in Fig. 3.41. While difficult to see because of the 3D representation of the data, the detection efficiency drops at 0° , 25° , 45° , 65° , and 90° . The drop in efficiency at 0° , 45° , and 90° are shown above to result from neutron streaming paths in the detector. The drops at 25° and 65° originate from the lack of ion-detection for the neutron absorption distribution produced. Because the ion-detection efficiency is much flatter with the lithium fluoride detectors, the total detection efficiency

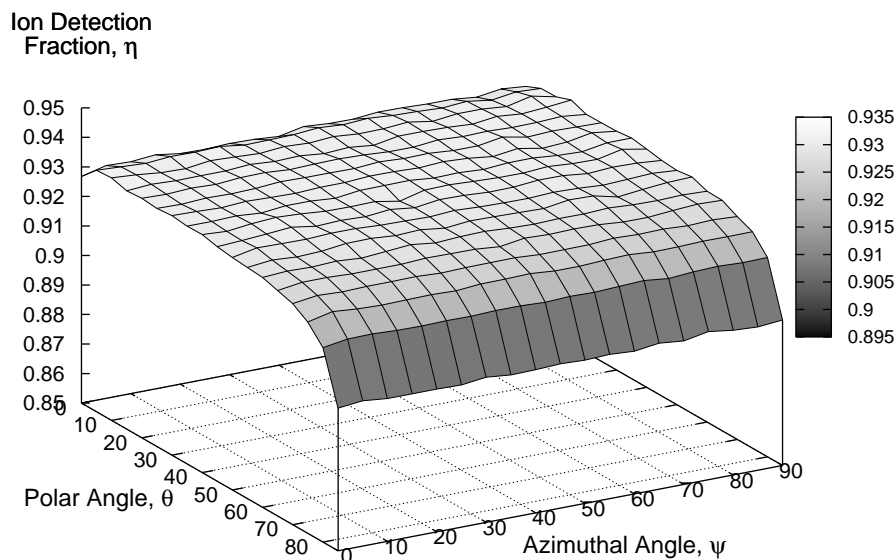


Fig. 3.40. The ion-detection efficiency of a ${}^6\text{LiF}$ chevron detector with 100- μm deep perforations, 20- μm wave period, 20- μm wave separation, 20- μm wave amplitude, and no cap

only suffers when neutrons are able to stream through gaps in the detector, namely at $\psi = 0^\circ$, 45° , and 90° (see Fig 3.42).

The channel-type detectors are most affected by the neutron-absorption efficiencies. The ion-detection efficiencies do not fluctuate enough, in the case of the channel perforations, to greatly affect the total efficiencies. Thus, the drops in efficiency result from the streaming of the neutrons through channels of silicon. Figure 3.43 and Fig. 3.44 present the total detection efficiencies for a boron and a lithium fluoride detector, respectively.

The boron chevron perforations are only slightly affected by the ion-detection efficiencies. Recall, the ion-detection efficiency for the boron increased for small polar angles and for an azimuthal angle of 60° , so the total efficiency replicates this behavior as shown in Fig. 3.45. Also both the ${}^{10}\text{B}$ and ${}^6\text{LiF}$ (Fig. 3.46) lose efficiency at the 45° azimuthal angle because neutrons are able to stream along short paths without encountering absorbing material.

Lastly, the sinusoidal-perforated detectors maintain a relatively flat profile in the azimuthal direction. The sinusoid perforations are still subject to streaming problems, but because the degrees of freedom are much greater, the proper choice of dimensions alleviates most of these problems. Figs. 3.47 through 3.50 present a series of angular sinusoidal detector efficiencies for various dimensions of ${}^{10}\text{B}$ and ${}^6\text{LiF}$ detectors. The boron detector requires the dimensions of the sinusoid are reduced to sub-micron measures to ensure an azimuthally flat response; this requirement makes them more difficult to fabricate. The first two ${}^6\text{LiF}$ figures show some effect of lost efficiency due to lack of neutron absorption, as discussed in the section on neutron absorption efficiency, but Fig. 3.50 presents a detector where the response has been flattened along the azimuthal direction. Also notable about

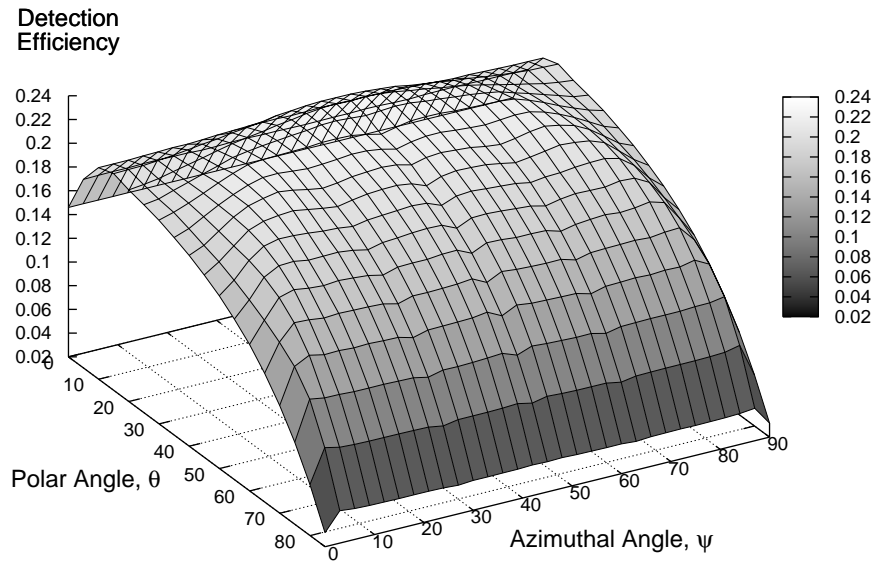


Fig. 3.41. The total detection efficiency of a ^{10}B rod perforated detector with 30- μm perforation depth, 6- μm diameter rods, and no cap

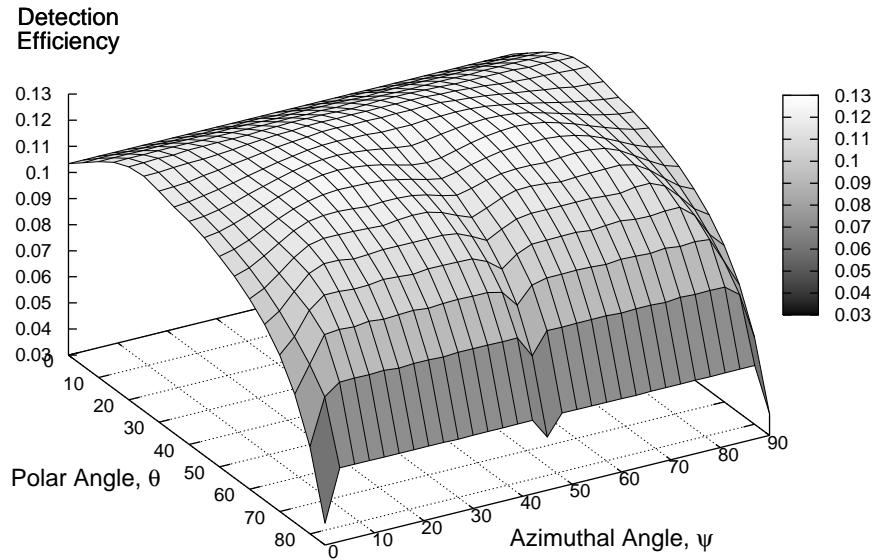


Fig. 3.42. The total detection efficiency of a ^6LiF rod perforated detector with 100- μm perforation depth, 30- μm diameter rods, and no cap

this simulated detector is that the efficiency is approximately 15% with a $\pm 1\%$ variation over the polar angles of 0° to 60° . A detector such as this one is well-suited for applications where the efficiency needs to be the same, regardless of the incident neutron's direction.

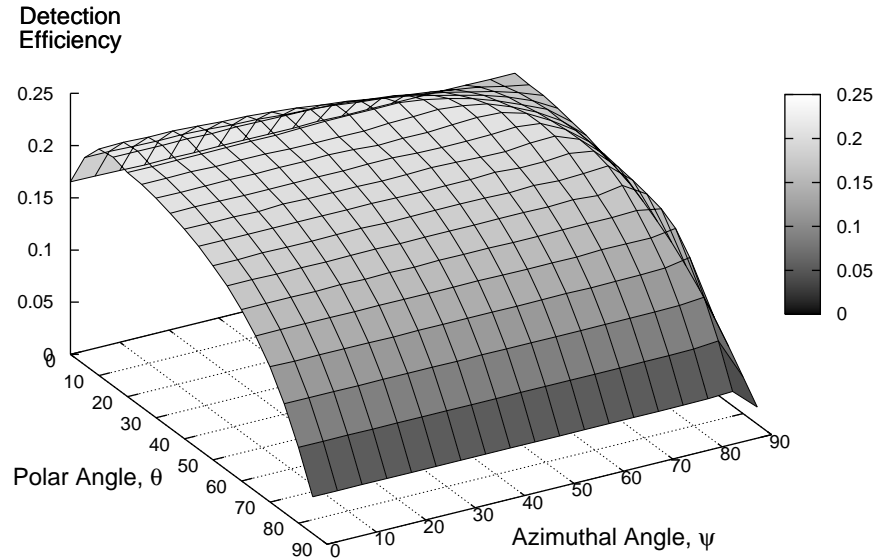


Fig. 3.43. The total detection efficiency of a ^{10}B channel perforated detector with $30\text{-}\mu\text{m}$ perforation depth, $4\text{-}\mu\text{m}$ wide channels, and no cap

3.5 Normal Incidence Optimization

Once the perforation design giving the most desired angular response is determined, the detectors are modeled to determine the dimensions that produce the greatest normal-incidence detection efficiencies. Only chevron and sinusoidal perforations are considered because optimization of the other two perforation schemes were considered previously by Shultis and McGregor [2006].

3.5.1 Chevron Detector Optimization

Figure 3.52 illustrates the parameters that may be varied to increase the response of the detector. The parameters δ_a , the absorber width, and δ_{Si} , the silicon width, are both considered variable. Both widths are varied incrementally from 5 to $50\ \mu\text{m}$ by $2.5\text{-}\mu\text{m}$ increments for ^6LiF , and 0.5 to $10\ \mu\text{m}$ by $0.5\text{-}\mu\text{m}$ increments for ^{10}B . The results are shown in Fig. 3.51.

From the results one observes that, as both channels are made smaller, the probability the neutron is detected increases. As the width of the absorber channel increases, the response flattens out and approaches an asymptotic value because only the ions born within a certain proximity to the silicon channels have a probability of escaping the absorber material into

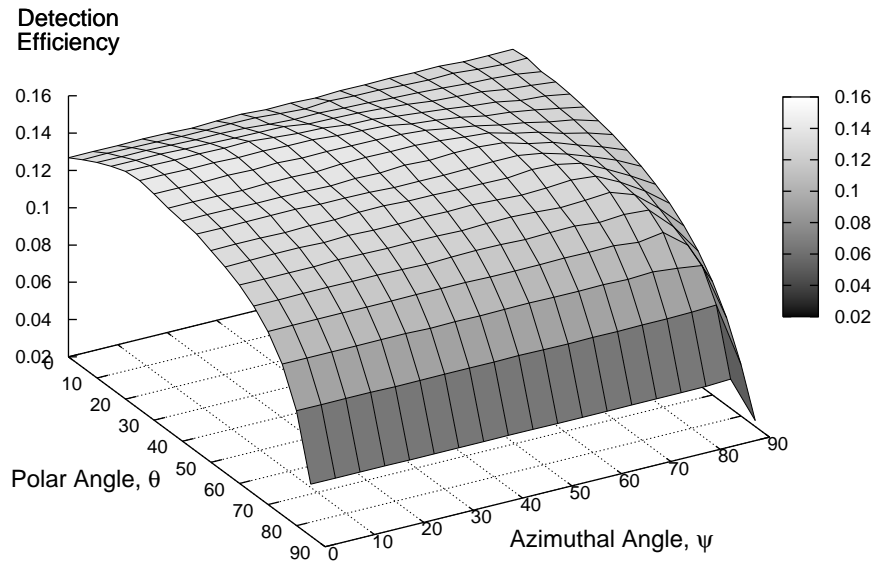


Fig. 3.44. The total detection efficiency of a ${}^6\text{LiF}$ channel perforated detector with 100- μm perforation depth, 20- μm wide channels, and no cap

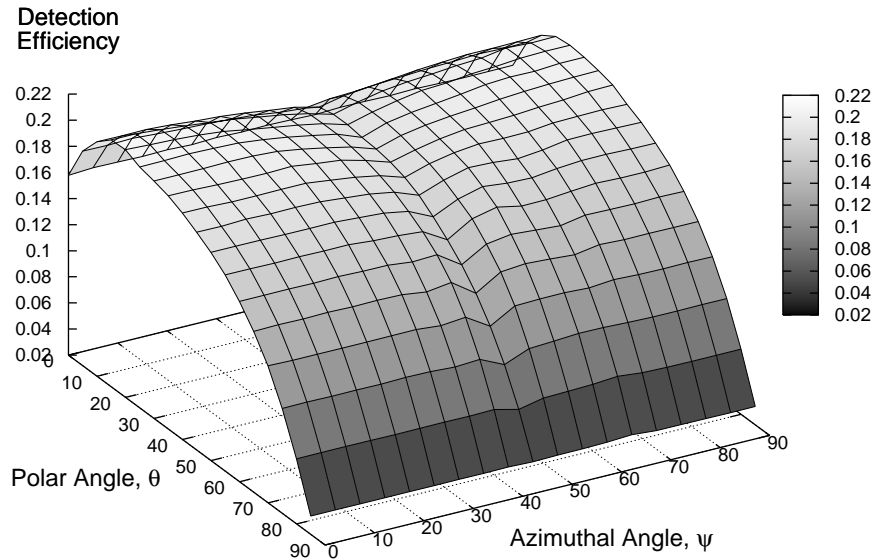


Fig. 3.45. The total detection efficiency of a ${}^{10}\text{B}$ chevron perforated detector with 30- μm perforation depth, 4- μm wide channels, and no cap

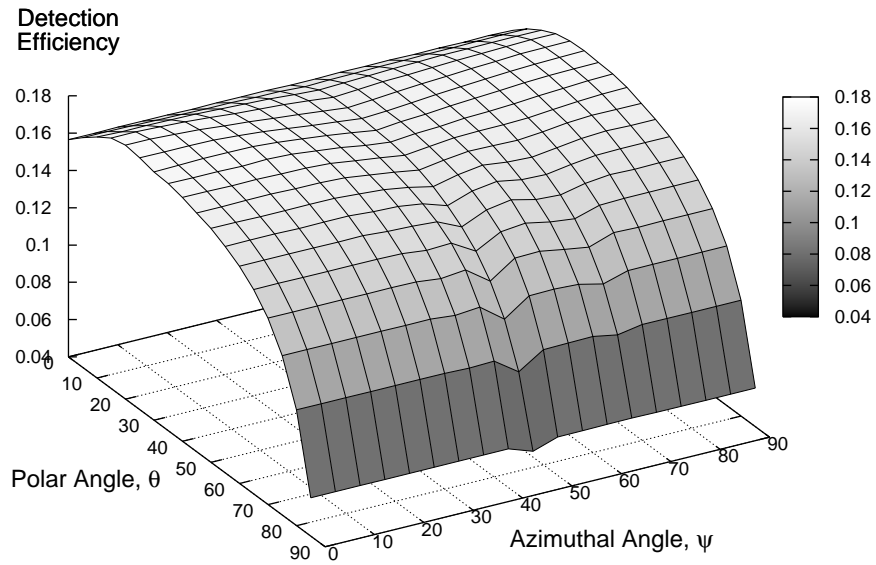


Fig. 3.46. The total detection efficiency of a ${}^6\text{LiF}$ chevron perforated detector with $100\text{-}\mu\text{m}$ perforation depth, $20\text{-}\mu\text{m}$ wide channels, and no cap

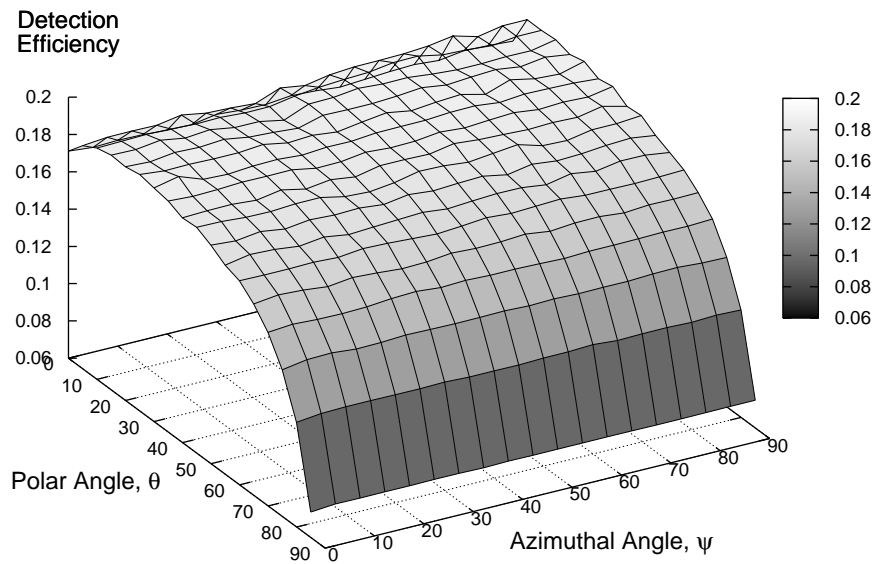


Fig. 3.47. The total detection efficiency of a ${}^{10}\text{B}$ sinusoid perforated detector with $10\text{-}\mu\text{m}$ perforation depth, $8\text{-}\mu\text{m}$ sine period, $1\text{-}\mu\text{m}$ sine amplitude, $0.5\text{-}\mu\text{m}$ sine wave separation, and no cap

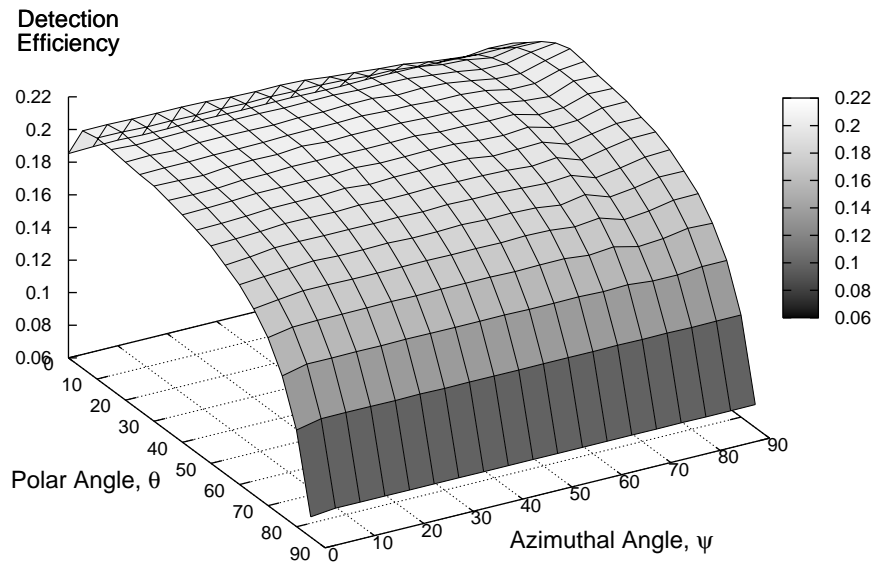


Fig. 3.48. The total detection efficiency of a ${}^6\text{LiF}$ sinusoid perforated detector with $100\text{-}\mu\text{m}$ perforation depth, $20\text{-}\mu\text{m}$ sine period, $20\text{-}\mu\text{m}$ sine amplitude, $20\text{-}\mu\text{m}$ sine wave separation, and no cap

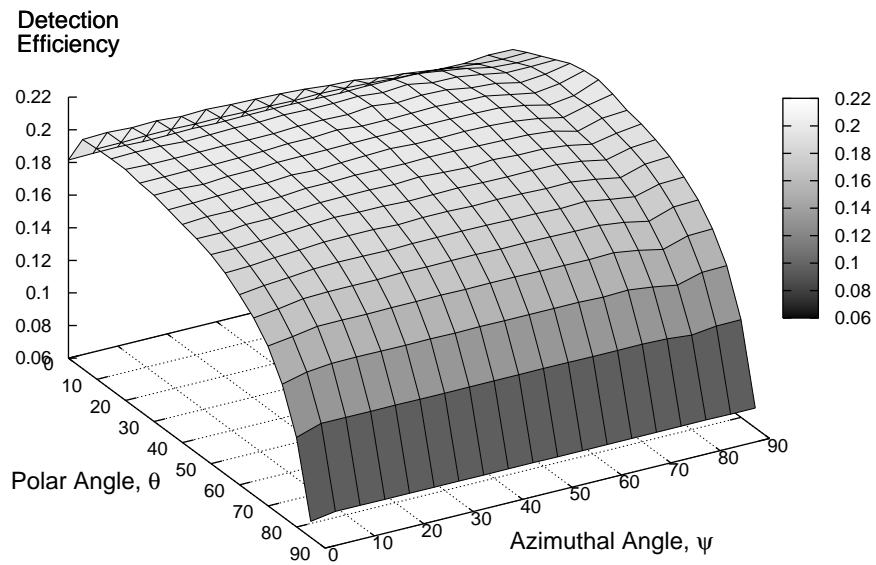


Fig. 3.49. The total detection efficiency of a ${}^6\text{LiF}$ sinusoid perforated detector with $100\text{-}\mu\text{m}$ perforation depth, $30\text{-}\mu\text{m}$ sine period, $40\text{-}\mu\text{m}$ sine amplitude, $30\text{-}\mu\text{m}$ sine wave separation, and no cap

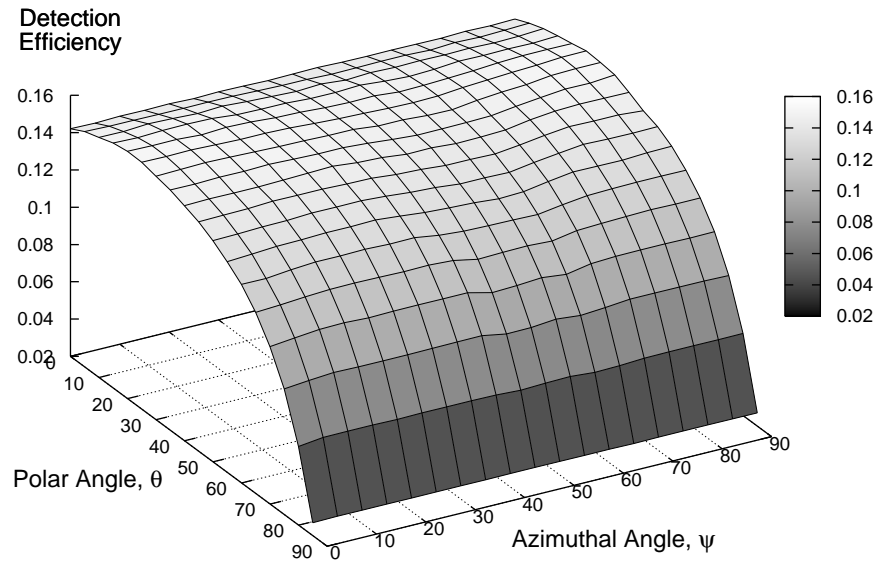


Fig. 3.50. The total detection efficiency of a ${}^6\text{LiF}$ sinusoid perforated detector with $100\text{-}\mu\text{m}$ perforation depth, $130\text{-}\mu\text{m}$ sine period, $40\text{-}\mu\text{m}$ sine amplitude, $35\text{-}\mu\text{m}$ sine wave separation, and no cap

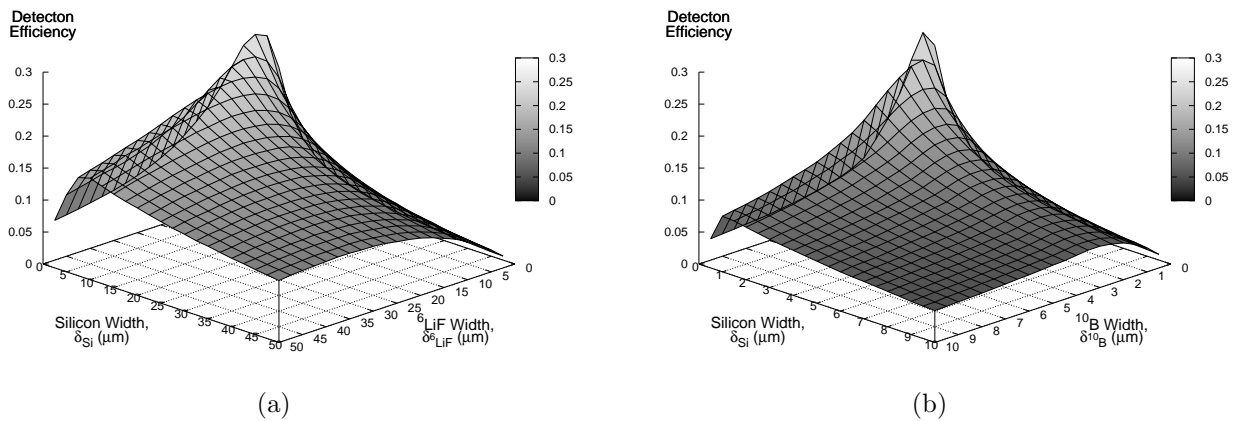


Fig. 3.51. Response variation as a function of channel widths for (a) ${}^6\text{LiF}$ and (b) ${}^{10}\text{B}$ ${}^6\text{LiF}$

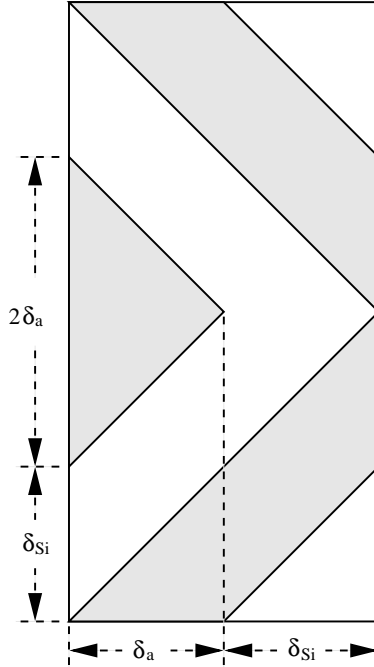


Fig. 3.52. Chevron detector variable parameters

the silicon, provided there is sufficient silicon to absorb the ion energy. On the other hand, as the thickness of the silicon decreases it reaches a point where the silicon thickness is insufficient to absorb enough energy for the incident neutron to be detected. As a result, the efficiency decreases dramatically for small silicon thicknesses.

As a further investigation of the behavior, the region of the ${}^6\text{LiF}$ detector is expanded in the range from 0 to 5 μm . Figure 3.53 presents the efficiency, and again the same basic shape as described above is realized. Noteworthy is that the efficiency can still be increased by shrinking the dimensions to smaller and smaller values because the ions become more and more easily detected if a neutron is absorbed. The limit of this increased detection efficiency is simply the absorption probability. That is, as the channel widths become smaller and smaller the detector more closely approximates a mixture of the media that can both absorb neutrons and collect charge produced by the ions.

3.5.2 Sinusoidal Detector Optimization

The sinusoidal detectors have, in addition to the channel widths, two alternate parameters that may be varied to increase the detector efficiency. The two new parameters are functions of the sine wave, namely, the amplitude Δ and period w . Figure 3.54 illustrates these parameters.

Data were generated only for the ${}^6\text{LiF}$ detectors because of the long run-times of the ${}^{10}\text{B}$ detector codes. The general behavior of the ${}^{10}\text{B}$ detector is expected to be the same but on a smaller dimensional scale. To reduce the problem to a manageable number of degrees of freedom, it is assumed the silicon width δ_{Si} is equal to the absorber width δ_a . The amplitude of the sine wave is held fixed as the wave period and the widths are varied.

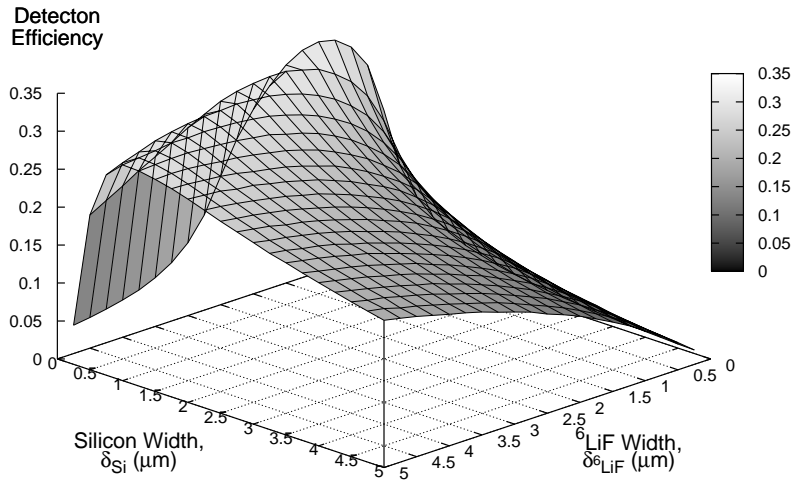


Fig. 3.53. Finer view of response variation

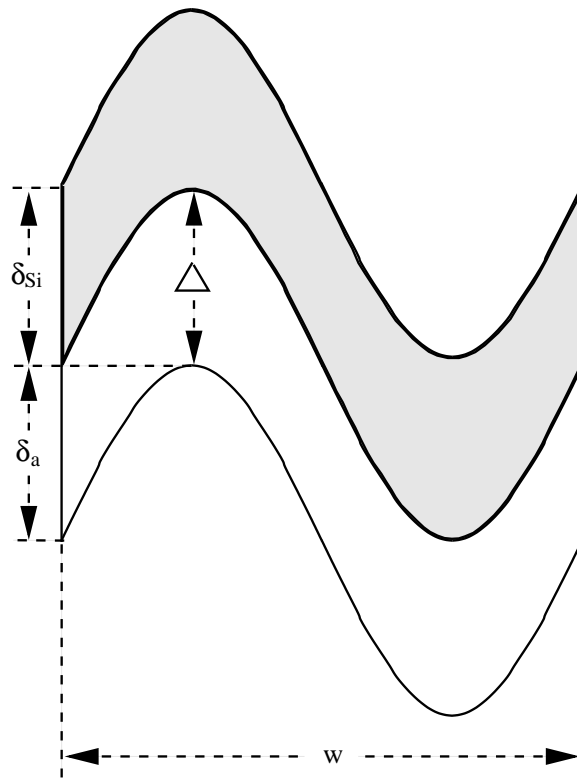


Fig. 3.54. Sinusoidal detector variable parameters

Figure 3.55 illustrates the variation in the efficiency for changing period and channel width for 3 different wave amplitudes.

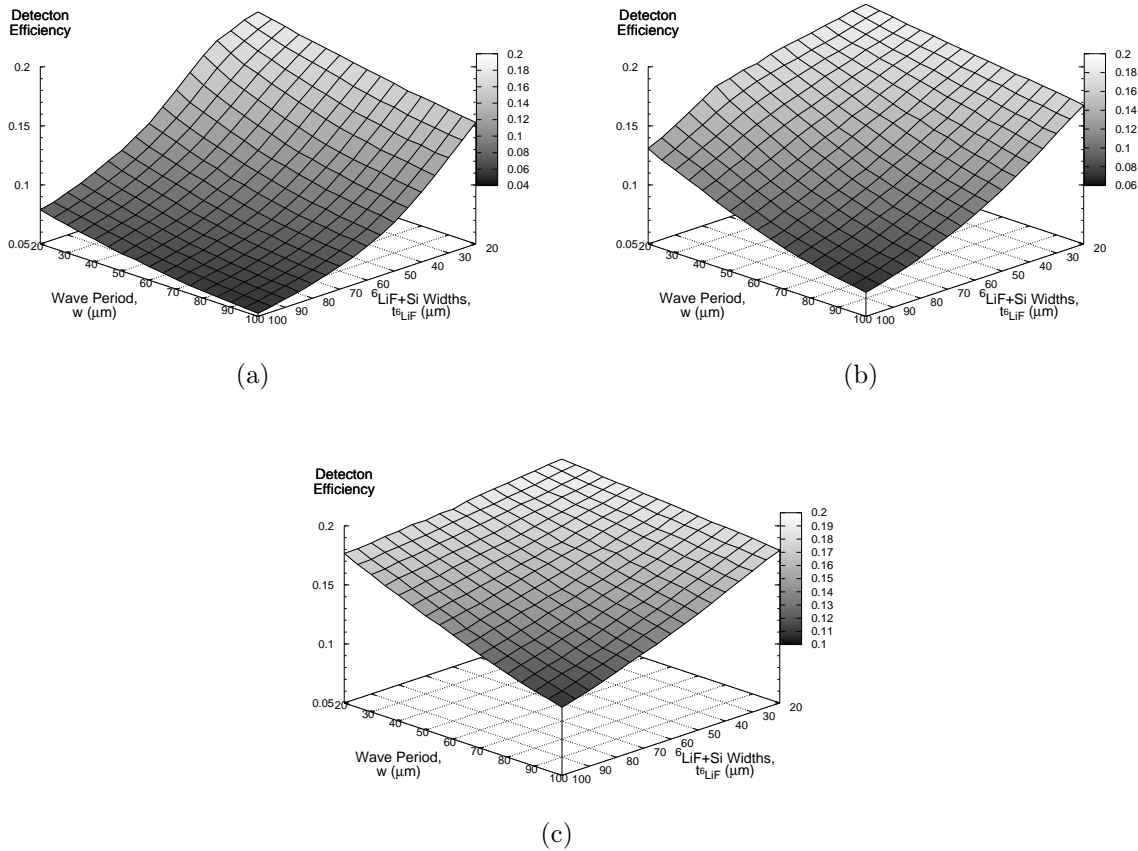


Fig. 3.55. Response variation as a function of channel width and wave period for amplitudes Δ of (a) $20 \mu\text{m}$, (b) $40 \mu\text{m}$, and (c) $80 \mu\text{m}$

From the plots in Fig. 3.55 one sees that, as the channels and wave period get smaller, the efficiency increases. Interestingly, altering the wave amplitude does not seem to increase the maximum efficiency of the detector, but a greater wave amplitude produces less of a drop in efficiency for greater channel widths and wave periods. Increasing the channel width decreases the efficiency in a much more linear manner than increasing the wave period. This drop most likely results from the fact that as the wave period increases, the shortest distance between the sine waves is varying nonlinearly; thus, there is more shape to the curve along increasing wave period.

3.6 Conclusions and Recommendations

Different perforated detectors lend themselves to different applications. It has been shown that the directional dependence of the detector can be greatly improved by using sinusoidal

type perforations, albeit, at some loss of efficiency. The sinusoidal detectors, although excellent for neutron scattering, dosimetry, and other experiments of the kind where the angle of incidence is important, are not suited to applications where a higher efficiency detector is more desired, the topic discussed in Chapter 4. High efficiency perforated detectors using channel or chevron type perforations are more suited to total, normally incident or directionally independent, neutron counting.

Channel and chevron type detectors are shown to be more efficient than the rod perforated detectors. This results primarily from the fact that a greater fraction of the area of the semiconductor is etched away and filled with absorbing material. Also, in fabrication of these detectors ${}^6\text{LiF}$ has demonstrated itself to be superior to ${}^{10}\text{B}$ as an absorber for two reasons. The first is that the triton emitted from the absorption of a neutron by ${}^6\text{Li}$ has a much greater range than any of the He or Li ions emitted by either absorber. The greater range leads to a greater probability of leaving the absorber and depositing energy in the silicon. Second, the perforations must be much smaller in the case of the ${}^{10}\text{B}$, because of the previous reason, and this restriction makes the detector more difficult, though not impossible, to fabricate.

Chapter 4

A Feasibility Study of a Cargo Detector for Smuggled Nuclear Weapons

4.1 Motivation

In the wake of 11 Sept. 2001, the United States finds itself in a position of having to enhance security structures and defenses to better protect the country from possible future terrorist attacks. To this end, the United States began funding many projects developing new techniques and devices to detect and, hopefully, to prevent impending threats. The work discussed in this chapter is a feasibility study of a device that may aid in the detection of nuclear devices and, more generally, in the transport and shipment of neutron-emitting materials.

In this chapter, the modeling and simulation of a cargo-container detector is considered for the large freight containers transported generally by land and sea. Cargo containers come in all sizes and varieties, having heights ranging from 5 ft to 10 ft and lengths ranging from 10 ft to over 80 ft. Detection of neutrons over these distances is difficult, and simulation of effective detectors is difficult as well.

In addition to modeling and optimizing the design of a cargo-container detector, nuclear weapons pits were simulated, and the response of the cargo-container detector to the neutrons emitted from the weapon pit was determined. Because of the high classification level of the details of nuclear-weapon pits, approximations and estimations had to be made.

4.2 Cargo-container Detector Optimization

The first goal of this study is to determine an optimal thickness of a polyethylene moderator on the front, back, and radially around the detector that generates the largest count rate from a source of high-energy fission neutrons. A model is constructed using MCNP that alters the dimensions of the polyethylene around the detector and determines the number of expected absorptions in the neutron detector.

4.2.1 Detector Model

The cargo detector is modeled as a single 6.3-mm diameter ${}^6\text{LiF}$ rod-perforated detector having 100- μm deep perforations, 30- μm diameter rods, and a 20- μm cap thickness surrounded on the front, back, and radially with a polyethylene moderator. For the purpose of optimization, the detector itself is maintained at a constant diameter while the radius, front, and back polyethylene thicknesses are varied between 1 and 10 cm. The amount of neutron absorption, per source neutron, in the detector is tallied using the MCNP code. Figure 4.1 shows a diagram of the simple detector design.

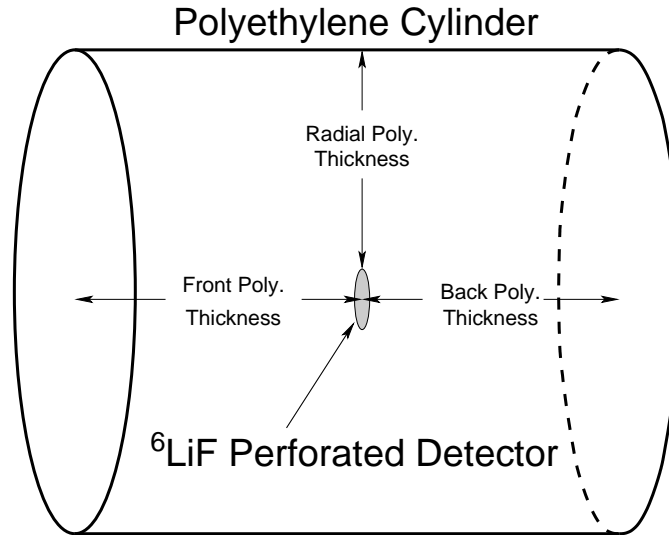


Fig. 4.1. Diagram of the cargo detector model

The neutron source is modeled as a point source of ${}^{252}\text{Cf}$, simulated in MCNP using a Watt fission distribution. The source is placed 300 cm from the front of the perforated detector (not the front of the polyethylene) on the detector’s axis, called “end-on illumination.” To increase the efficiency of the Monte Carlo calculations, the emission of the source neutron is biased into a cone toward the detector rather than using an isotropic emission. Such source biasing ensures most of the particles head toward and interact in at least the polyethylene and, hopefully, the detector.

The materials used in this analysis are summarized in Table 4.1. The perforated detector is constructed from ${}^6\text{LiF}$ and natural silicon, as described in Chapter 3. Polyethylene is simply modeled as a compound of hydrogen and carbon with the atomic ratio of 2:1, which is essentially the definition of the polyethylene hydrocarbon chain, and having a density of 0.92 g cm^{-3} .

A Perl script was written to automatically generate the MCNP input files and run the files for differing front, back, and radial polyethylene thicknesses. The script first initializes values such as the detector radius, the cap thickness, the perforation depth, the incremental increase in polyethylene thicknesses, the number of histories to run, and the incremental number of histories to increase for a continuation run if not all of MCNP’s statistical checks are passed. The MCNP statistical checks are a measure of the reliability of the solution

Table 4.1. MCNP material's and cross sections used

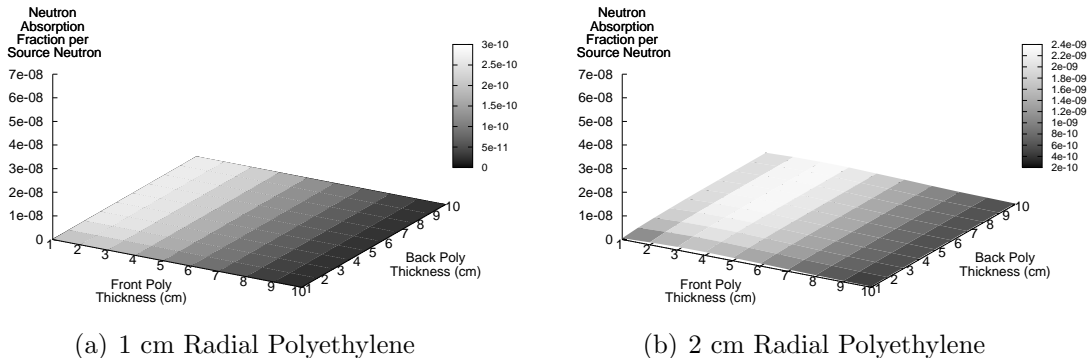
Material	Nuclide	Cross Section	Atom Fraction
Natural Silicon	^{28}Si	14028.66c	0.922297
	^{29}Si	14029.66c	0.046832
	^{30}Si	14030.66c	0.030872
Lithium-6 Fluoride	^6Li	3006.66c	1.000000
Polyethylene	^1H	1001.66c	0.666667
	^{12}C	6012.66c	0.333333

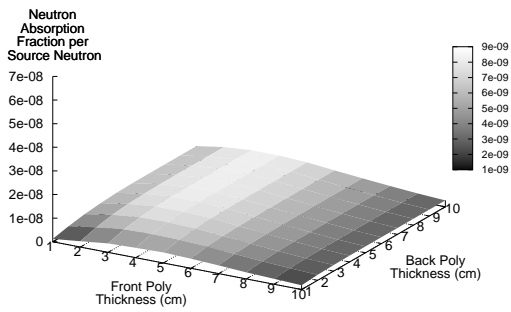
probability distribution function MCNP generates, and in most cases the checks should be passed.

After the script initializes the variables necessary to generate the MCNP input file, the input file is created. Depending on the iteration through which the script is running, the thicknesses of the front, back, and radial polyethylene are set. The source is positioned, and the fractional solid angles are set, based on the radial thickness of the detector, for biasing the source particle emission. The script then calls MCNP to run the input file, and, once complete, the script checks to see if all statistical checks are passed. If so, the script extracts the probability of neutron absorption in the detector and its relative error from the output file; otherwise, a continuation run of MCNP is called and more histories are executed. This process repeats until all statistical checks are passed, at which point the next iteration begins. Iterations continue until all values of front, back, and radial polyethylene are analyzed. The Perl script is listed in Appendix D.

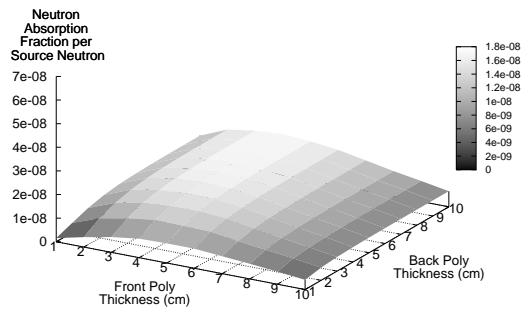
4.2.2 Results of Cargo-Detector Simulations

The script discussed above is used to calculate the expected neutron absorption in the detector. The results are summarized in Fig. 4.2.

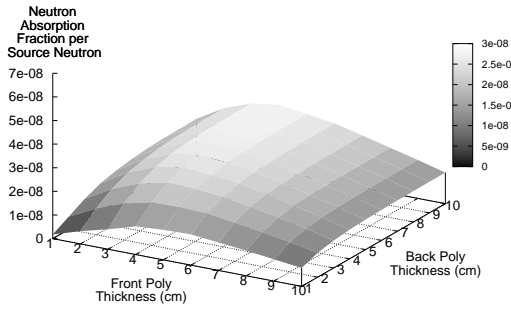




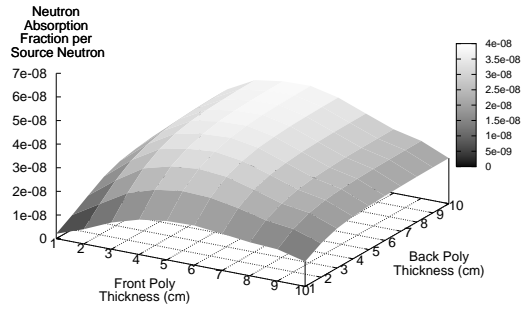
(c) 3 cm Radial Polyethylene



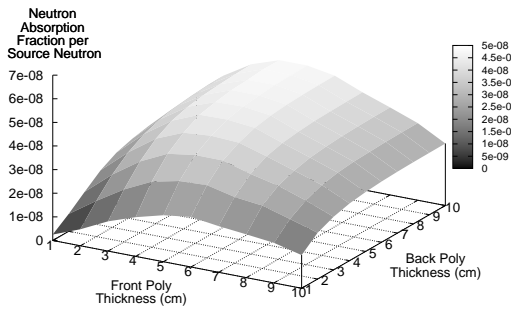
(d) 4 cm Radial Polyethylene



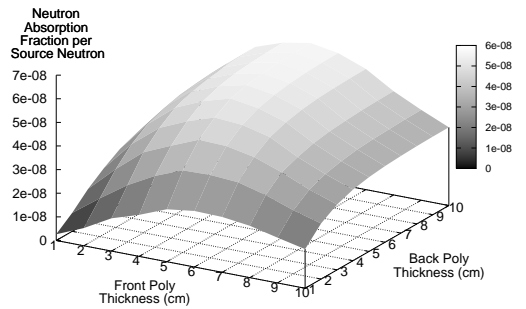
(e) 5 cm Radial Polyethylene



(f) 6 cm Radial Polyethylene



(g) 7 cm Radial Polyethylene



(h) 8 cm Radial Polyethylene

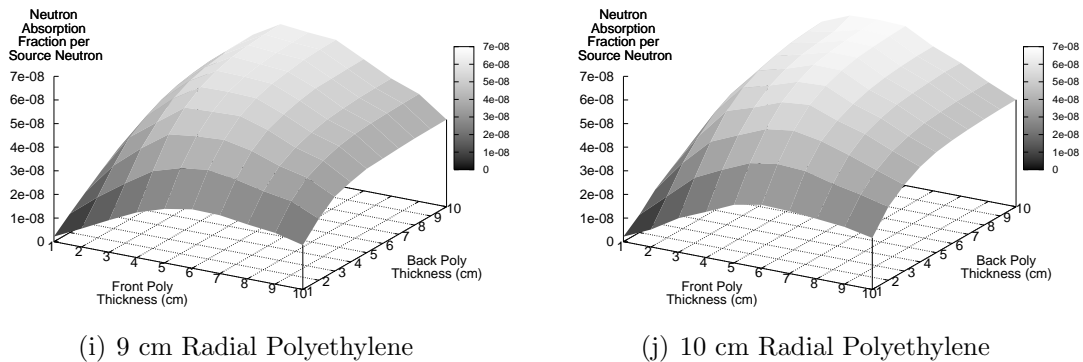


Fig. 4.2. Detector response for end-on neutron incidence for varying radial polyethylene thicknesses

In all of the figures one sees a general trend in the optimum front-polyethylene thickness. In all cases the response increases until the front-polyethylene thickness reaches approximately 5 cm. Beyond 5 cm, however, the front polyethylene begins shielding the detector from the thermalized neutrons rather than constructively thermalizing the neutrons. An exception exists for the lower thicknesses of radial polyethylene, where it is observed that the optimum front and back-polyethylene thicknesses are smaller, but so are the responses and this situation is less desirable.

The behavior of the detector response to a varying back-polyethylene thickness is significantly different than that of the front-polyethylene thickness. No thickness of back polyethylene exists such that the detector’s absorption begins to decrease; rather, increasing the back-polyethylene thickness up to about 5 cm increases the probability a neutron is backscattered toward the detector. At a thickness of 5 cm the increase in absorption plateaus and little is gained by increasing the thickness beyond this point.

The radial-polyethylene thickness, as with the back-polyethylene thickness, has no optimum value. In the case of the radial-polyethylene thickness, it is more difficult to determine what the practical optimum is; Fig. 4.3 presents a composite of the plots shown in Fig. 4.2(a) through Fig. 4.2(j). Even at 10 cm of radial polyethylene the neutron absorption probability is still increasing. The plot does show, that with increasing radial-polyethylene thickness, the separation between plots is narrowing, indicating the optimum is being approached but has not yet been achieved.

Irradiation was also considered for the case the point isotropic neutron source was placed 300 cm away from the detector in the radial direction (“side-on illumination”). In this case the source illuminates the detector from the side rather than the top or bottom of the cylinder. Fig 4.4 presents the expected responses of the detector per source particle for such irradiation.

The response obtained from side-on irradiation exhibits a behavior similar to the end-on irradiation. In this case, as both the front and back-polyethylene thicknesses increase the response also increases. This increase results from the fact the larger polyethylene dimensions allow fewer neutrons to escape and increases the probability neutrons are scattered toward

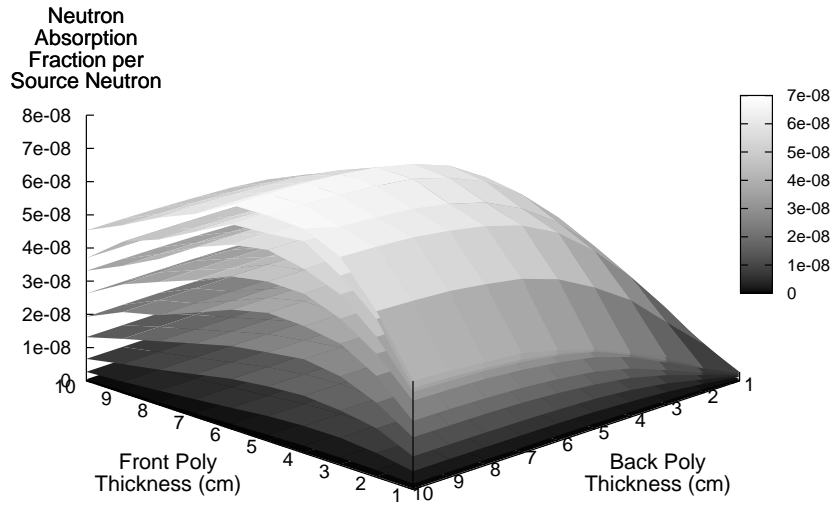
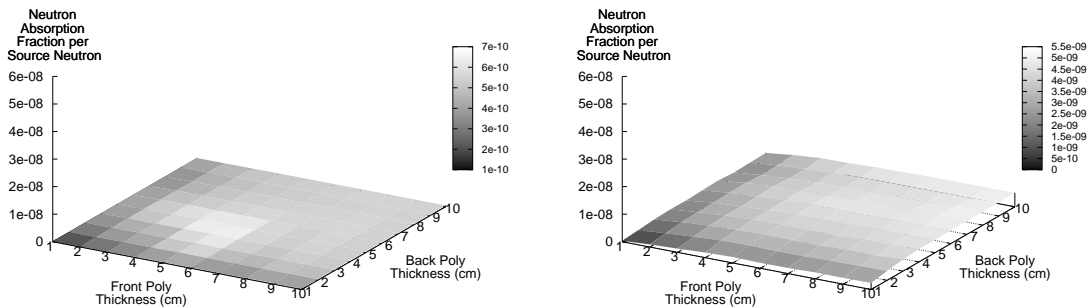


Fig. 4.3. Composite plot showing the neutron absorption probability for end-on illumination for varying radial polyethylene thicknesses from 1 cm to 10 cm

the detector.

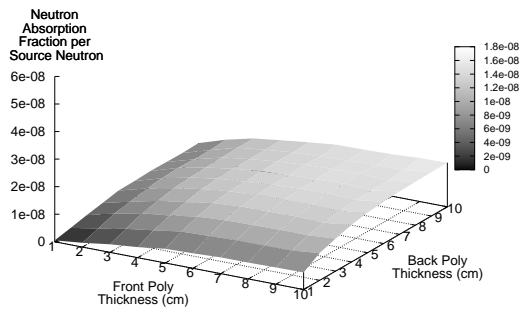
As the radial thickness increases it is observed that an optimum dimension producing the greatest response exists. Depending on the front and back-thicknesses, the optimum radial polyethylene thicknesses is between 6 and 8 cm. This is seen by closely observing the differences between Figs. 4.4(f) through 4.4(i), where the response is generally increasing with radial polyethylene thickness and then begins to drop beyond a thickness of 8 cm.

For the end-on irradiation case, little is gained by increasing the front and back polyethylene thicknesses beyond 5 cm. For this reason, the responses of both detectors were compared as a function of varying radial thicknesses with front and back thicknesses maintained at 5 cm; the results are presented in Fig. 4.5(a). Interestingly, the response of the detector is greater for side-on irradiation up to a radial thickness of about 5.5 cm, beyond which, the

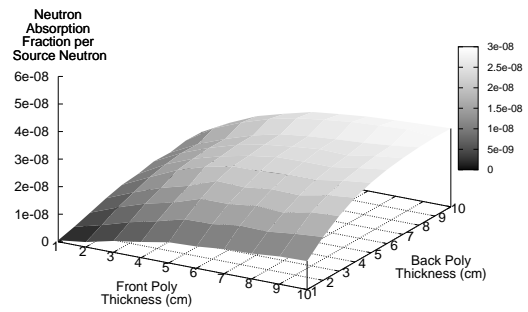


(a) 1 cm Radial Polyethylene

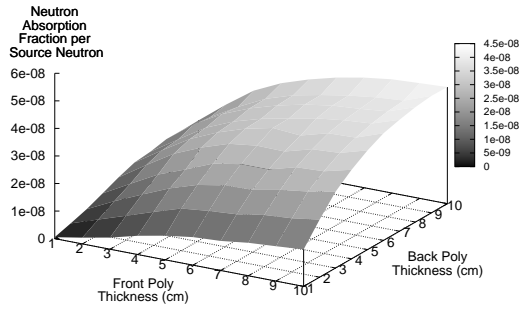
(b) 2 cm Radial Polyethylene



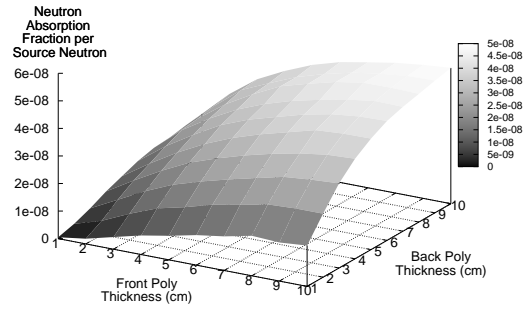
(c) 3 cm Radial Polyethylene



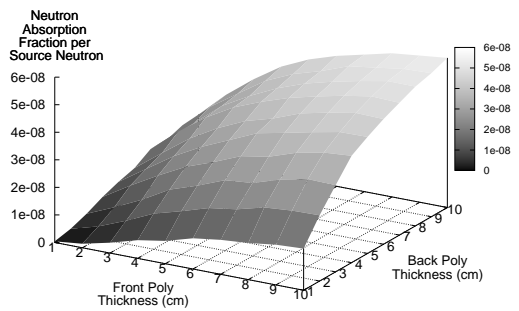
(d) 4 cm Radial Polyethylene



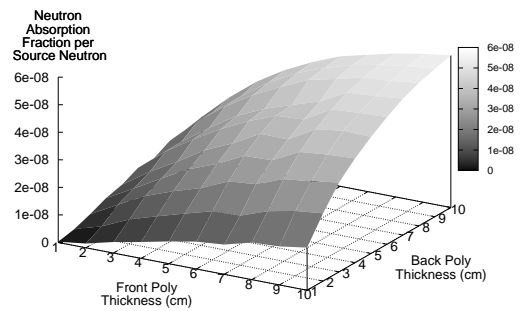
(e) 5 cm Radial Polyethylene



(f) 6 cm Radial Polyethylene



(g) 7 cm Radial Polyethylene



(h) 8 cm Radial Polyethylene

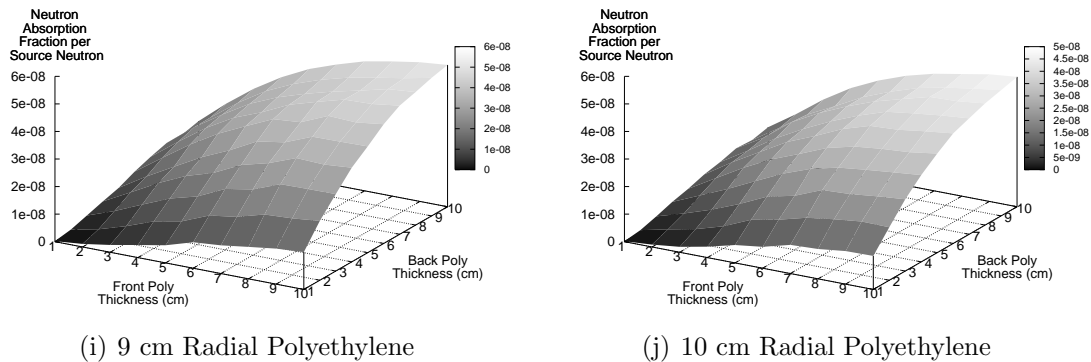


Fig. 4.4. Detector response for side neutron incidence for varying radial polyethylene thicknesses

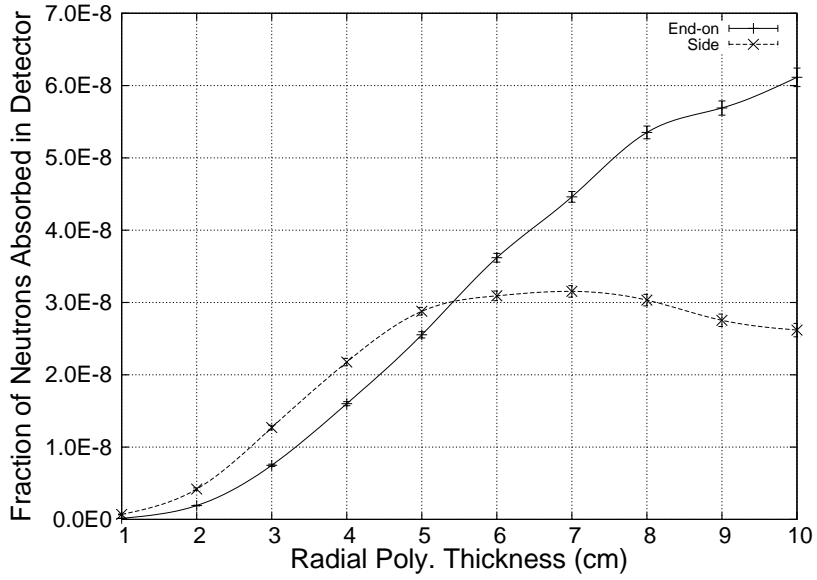
response is higher for end-on irradiation. This result arises because the end-on irradiation is much more optimized for the front and back-polyethylene thicknesses; however, as the front and back polyethylene thicknesses increase to optimum values for side-on irradiation, the detector responses cross the end-on response at higher radial thicknesses.

The results presented in Fig. 4.5(b) indicate a neutron absorption response of approximately $5.5E-8$ per source neutron can be obtained using either irradiation geometry. If a higher response is desired, the detector’s deployment must be optimized for end-on irradiation. In essence, two detector designs are possible: (1) a long tubular detector, or (2) a flatter “hockey-puck” shaped detector. A longer tube design could be made to extend the length of a cargo container and contain multiple perforated detector devices, all of which could be connected to a single readout system. Such devices might fit nicely in the upper corners of a cargo container. On the other hand, the hockey-puck shaped devices might be constructed to be affixed to the ceiling of the cargo containers, and although the spacing could not be as close as the tube detectors, the efficiency should be higher.

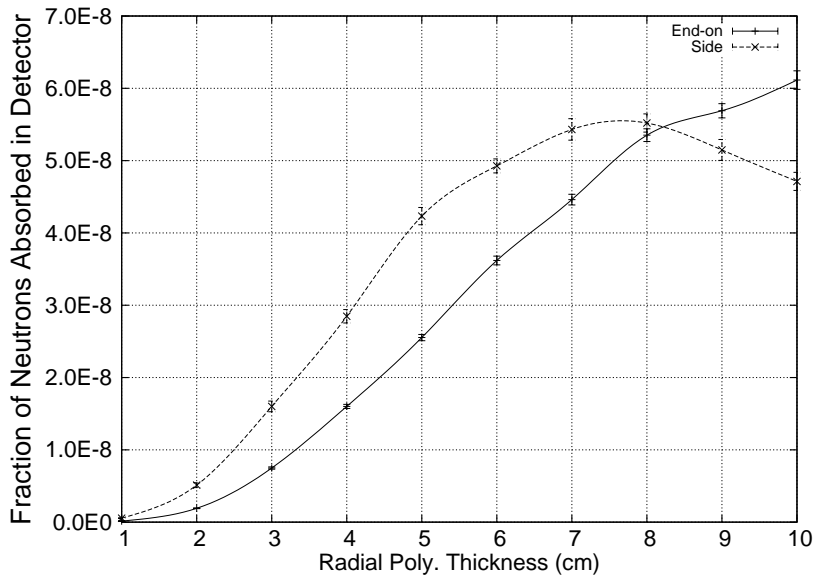
If the perforated detector size were increased, the efficiency of the detectors would also increase. Figure 4.6 presents the results for a 2.5 cm diameter detector, having approximately 16 times the effective surface area of the previous detector. The figure shows the absorption probability is increased by approximately an order of magnitude as would be expected.

4.3 Nuclear Weapon Pit Modeling

To estimate how responsive the cargo detector would be to a Pu nuclear weapon, it is necessary to determine the expected neutron flux emitted from a Pu weapon pit. Information about nuclear weapon pits is, for obvious reasons, highly classified. Thus, a “best guess,” yet conservative, model was developed. This model and the fluxes obtained from the model are discussed below. Also, much of the estimation has been made from the viewpoint of one trying to develop an improvised nuclear explosive, that is, without access to the highest quality materials.



(a) 5 cm front, 5 cm back, and varying radial thicknesses



(b) Optimum dimensions for both

Fig. 4.5. Detector responses for end-on and side-on irradiation geometries

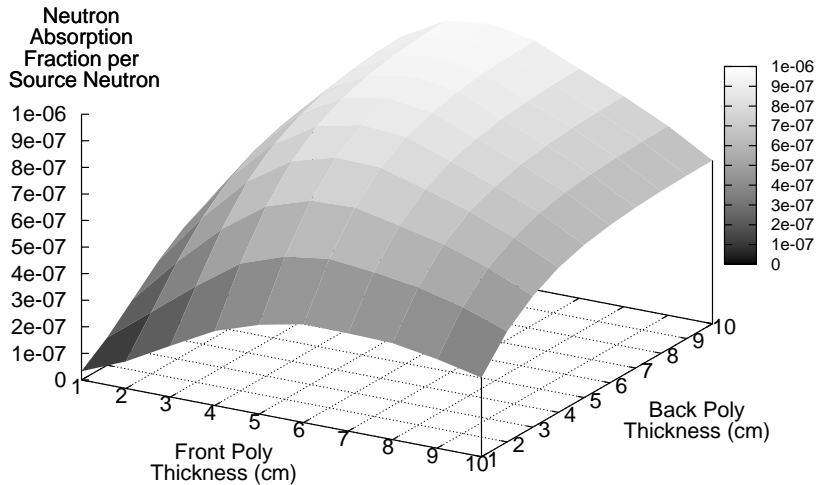


Fig. 4.6. End-on detector response of a cargo-container detector with perforated detector radius of 2.5 cm, 5 cm front poly. thickness, 5 cm back poly. thickness, and 10 cm radial poly. thickness

4.3.1 Nuclear Weapon Pit Model

MCNP5 is used to model the nuclear weapon pits using its `kcode` functionality. Calculations using `kcode` estimate the effective multiplication factor k_{eff} of a system. In this case the nuclear pit is modeled as a sphere. The radius of the sphere is varied as one of the two model parameters investigated; the other model parameter investigated was the ^{240}Pu content.

Ideally, weapons-grade plutonium is composed of only ^{239}Pu , but in reality, it is impossible to completely separate all of the ^{240}Pu from the ^{239}Pu . For this reason, weapon-grade plutonium is defined as plutonium having less than 7% ^{240}Pu . For the purposes of this study, the amount of ^{240}Pu is varied from 0 to 20% because someone developing an improvised nuclear device would not generally possess the highest quality plutonium. [Cochran et al., 1984]

A Perl script was written to calculate the multiplication factor k_{eff} for a sphere of plutonium while varying the radius of the sphere and the ^{240}Pu content. The script initializes values such as the minimum and maximum radius of the sphere, the minimum and maximum fraction of ^{240}Pu , and the increment to be taken with each iteration. The minimum and maximum radii investigated were 1 and 10 cm, respectively, and the minimum and maximum fractions of ^{240}Pu were 0 and 20%, respectively.

Once the necessary variables are initialized, the script begins looping through the radius and fraction of ^{240}Pu variables. For each combination of radius and ^{240}Pu fraction, an MCNP `kcode` input file is created with the appropriate radius of pit and proper fractions of ^{239}Pu and ^{240}Pu . The initial source is taken to be a spherically distributed source emitting a Watt fission distribution of ^{240}Pu neutrons. Thirty cycles of the `kcode` are ignored so that the proper source distribution may be developed, and eight hundred and seventy cycles are used

to determine the criticality of the sphere. Each cycle consists of 1500 histories.

Once the criticality for each combination of radius and ^{240}Pu fraction is determined, the radius at which the sphere is subcritical with k_{eff} equal to 0.9 is extracted from the data for fixed values of the ^{240}Pu fraction. In general, it is difficult to believe k_{eff} would be as low as, and almost inconceivably less than, 0.9, so it is a conservative estimate of k_{eff} . If the multiplication is greater than 0.9, then, more source neutrons are emitted and more counts are registered. A program was written to fit the criticality data with a cubic spline and then a spline interpolation procedure was used to determine the pit radius of to achieve $k_{eff} = 0.9$ for a given ^{240}Pu fraction. Thus, the 1-to-1 correlation between radius and fraction of ^{240}Pu is determined for a fixed $k_{eff} = 0.9$.

The neutron flux leaving the surface of the subcritical plutonium sphere is calculated using another script. The values obtained for the radii and fractions of ^{240}Pu obtained from the criticality runs are used, and the fluxes leaving the sphere for each case are tallied. Realistically, no flux exists without a source of neutrons; this source in weapon pits results from the spontaneous fission of both ^{239}Pu and ^{240}Pu , of which ^{240}Pu greatly dominates. ^{239}Pu emits 0.0022 neutrons per gram per second where ^{240}Pu emits 920 neutrons per gram per second [Shultis and Faw, 2000]. Because ^{240}Pu dominates, the modeled source is uniformly distributed throughout the sphere as a Watt fission spectrum of ^{240}Pu simply to calculate the steady-state flux across the sphere's surface. When the steady state-flux is determined, it is multiplied by the properly weighted number of neutrons, S , emitted inside the sphere, namely

$$S = \frac{4}{3}\pi r^3 \rho [920f + 0.0022(1 - f)], \quad (4.1)$$

where r is the radius of the sphere, ρ is the density of plutonium, and f is the fraction of the plutonium that is ^{240}Pu .

Another important consideration is the density of the modeled plutonium. Plutonium has six different crystal structures it transforms into as it is heated to the melting point, the so called α , β , γ , δ , δ' , and ϵ structures. Each crystal structure varies significantly in properties such as the thermal expansion coefficient and density, which varies between 16.00 and 19.83 g cm^{-3} . Two of the plutonium structures lend themselves most readily to nuclear weapons: α -phase and δ -phase. α -phase plutonium has a density of 19.2 g cm^{-3} and δ -phase has a density of 16.9 g cm^{-3} . One would initially think, because of its higher density and therefore greater fission rate, α -phase plutonium is the best candidate for a nuclear weapons. However, α -phase plutonium is brittle and difficult to machine into the desired shape of the pit, whereas the δ -phase variety is malleable and more easily machined, but it too has limitations. δ -phase plutonium is not stable as such at room temperature, so it must be alloyed (typically with 3% gallium by atomic content) to prevent it from transitioning to another phase. This so called δ -phase stabilization also helps prevent the shrinkage and distortion of the plutonium during casting and hot working. Interestingly, δ -phase plutonium transition to α -phase at relatively low (tens of kilobars) pressures, as compared to the megabar pressures generated by an implosive shock wave, so that the greater change in density leads to a much larger reactivity insertion and yield than can be achieved with the α -phase. Both α -phase and δ -phase plutonium were considered as candidates for an improvised nuclear weapon in this work. [GlobalSecurity.org, 2005]

4.3.2 Results of Nuclear Pit Modeling

The scripts and programs discussed above are run for both α and δ -phase plutonium to obtain k_{eff} as a function of the radius and ^{240}Pu fraction. Figure 4.7 and Fig. 4.8 present the calculated values of k_{eff} for α and δ -phase plutonium, respectively.

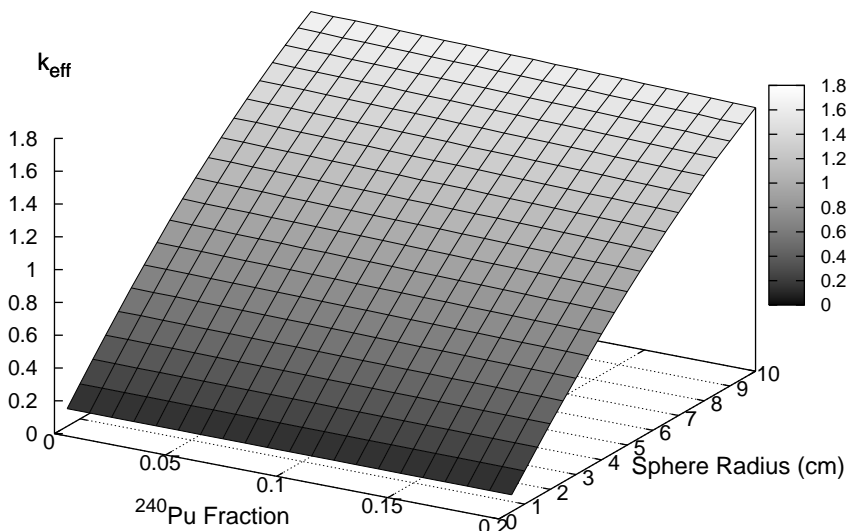


Fig. 4.7. k_{eff} as a function of the sphere radius and ^{240}Pu fraction

Fig. 4.7 and Fig. 4.8 confirm the intuitive idea that the same radius sphere with a higher density has a higher k_{eff} . Also one notes, as the radius increases, so does k_{eff} , which is also to be expected because more reactive material is present. However, as the ratio of ^{240}Pu to ^{239}Pu increases k_{eff} decreases because the ^{240}Pu has a lower fission absorption cross section. This effect appears slight in the three-dimensional plots, but does in fact increase the subcritical radius by more than half a centimeter. Fig. 4.9 presents the subcritical radius with $k_{eff} = 0.9$ as a function of the ^{240}Pu fraction present in the sample for both α and δ -phase plutonium. Both the α -phase and δ -phase plutonium radii are increased as the ^{240}Pu fraction increases and the multiplication factor remains constant.

The surface flux across the sphere is calculated for the varying ^{240}Pu fractions in the nuclear pit. Almost all of the neutrons leaving the surface are, as expected, high energy neutrons distributed in energy as shown in Fig. 4.11. Because ^{240}Pu spontaneously fissions more frequently than ^{239}Pu , the flux of neutrons crossing the surface is much higher as the ^{240}Pu fraction increases. The total flux, which results almost exclusively from spontaneous fission neutrons, across the surface of the sphere as a function of the ^{240}Pu fraction is shown in Fig. 4.10, and a contour plot of the energies is shown in Fig. 4.11

In Fig. 4.10 four lines are shown, of which, two pairs are almost exactly on top of each other. From the figure one notes that the flux is independent of the phase of the plutonium. The radii and density of the α -phase and δ -phase spheres differ for the same values of k_{eff} .

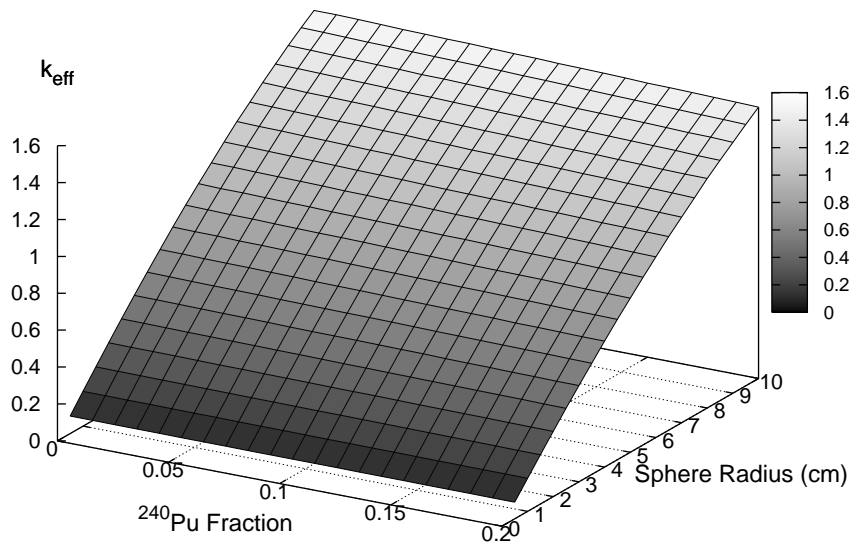


Fig. 4.8. k_{eff} as a function of the sphere radius and ^{240}Pu fraction

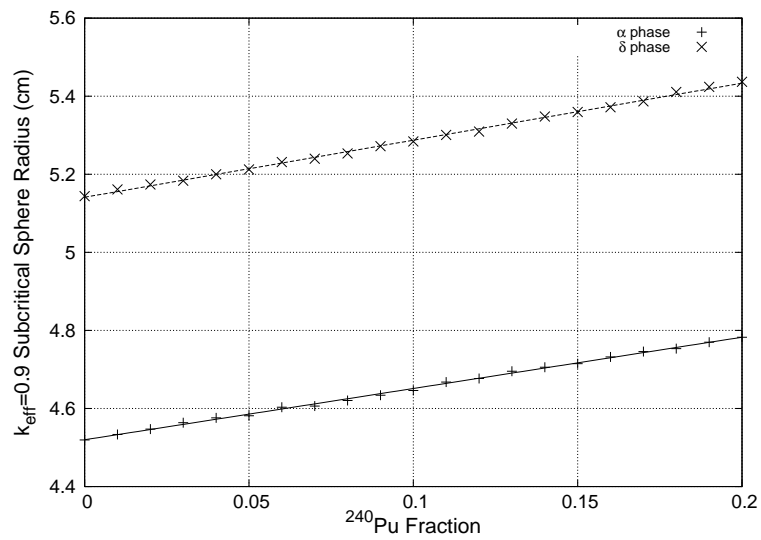


Fig. 4.9. The critical radius of a plutonium sphere as a function of the ^{240}Pu fractional content

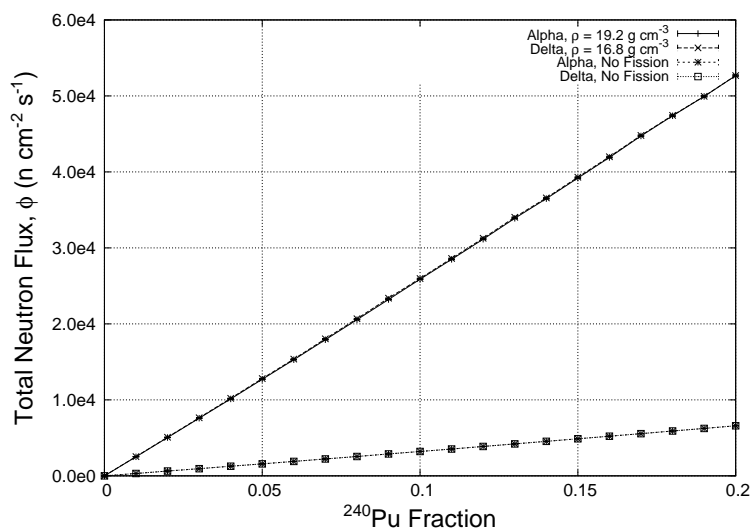


Fig. 4.10. Total neutron fluxes across sphere surface for both α -phase and δ -phase plutonium from spontaneous fissioning of ^{240}Pu alone (No Fission) and with secondary fissioning of ^{239}Pu . The α and δ -phases produce almost exactly the same results.

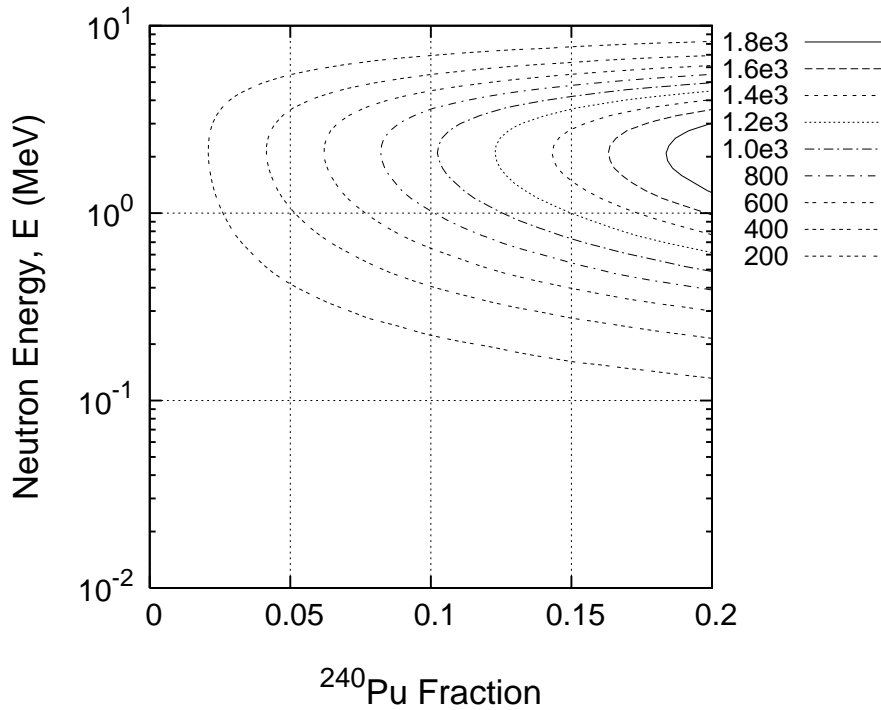


Fig. 4.11. Neutron energy flux crossing sphere surface for varying ^{240}Pu fractions

This results in the surface flux, but not the source strength, to be the same in both instances. Figure 4.10 also shows the flux with fission neutron production deactivated in the code and one sees that the substantial difference the multiplication, in conjunction with the greater fraction of ^{240}Pu , makes. For weapon-grade plutonium with a ^{240}Pu fraction of 7% the resulting output flux is about $18000 \text{ n cm}^{-2} \text{ s}^{-1}$. At ^{240}Pu fractions of 10%, 15%, and 20% the fluxes become 26000, 40000, and 53000 $\text{n cm}^{-2} \text{ s}^{-1}$, thereby making the pit more easily detected.

The surface fluxes were reduced to equivalent point source strengths by multiplying the fluxes by the surface areas of the plutonium spheres. Because the radii required for α -phase and δ -phase plutonium to be subcritical with k_{eff} equal to 0.9 are different, the equivalent point source strength is different. In this case the radii of the δ -phase plutonium is greater, so the equivalent point source strength is greater as well. Fig. 4.12 presents the source strengths as a function of the ^{240}Pu fraction. Here, the parabolic upward trend is a function of the sphere's surface area being proportional to r^2 .

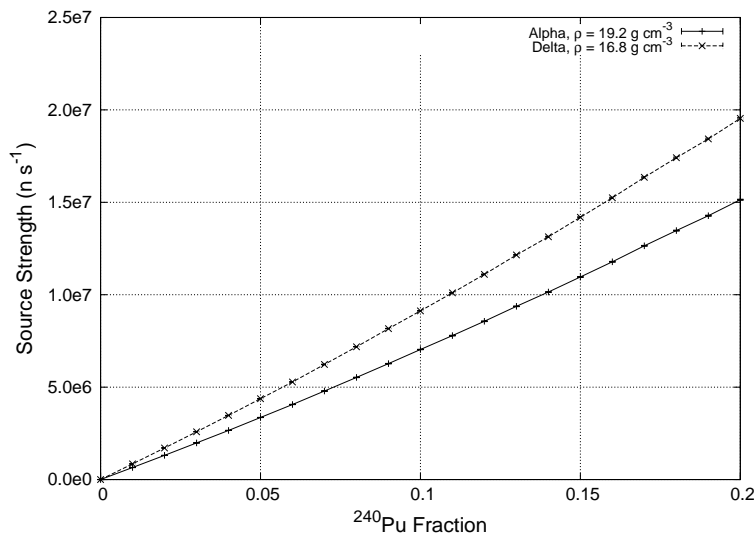


Fig. 4.12. Equivalent point source strengths from plutonium spheres from both spontaneous fissions and neutron induced fissions

Weapons-grade plutonium yields a equivalent source strength of $6.2\text{E}+06$ neutrons per second for the δ -phase and $4.8\text{E}+06$ neutrons per second for the α phase. At a 10% ^{240}Pu concentration, the source strengths increase to $9.1\text{E}+06$ and $7.0\text{E}+06$ for δ and α -phase, respectively. Finally, at the maximum ^{240}Pu fraction considered, the equivalent source strengths are $1.95\text{E}+07$ neutrons per second for the δ -phase and $1.51\text{E}+07$ for the α -phase.

4.4 Feasibility of Pit Detection

To determine whether or not a Pu pit would be detectable, it is necessary only to multiply the equivalent source strengths (Fig. 4.12) by the optimized responses of the detectors

(Fig. 4.5(b)). If one assumes an average neutron absorption probability of $5.5E-8$ neutrons per source particle (the cross over point shown in Fig. 4.5(b)), then the neutron absorption rate in the detector, as a function of the ^{240}Pu content, is obtained. Results are shown in Fig. 4.13.

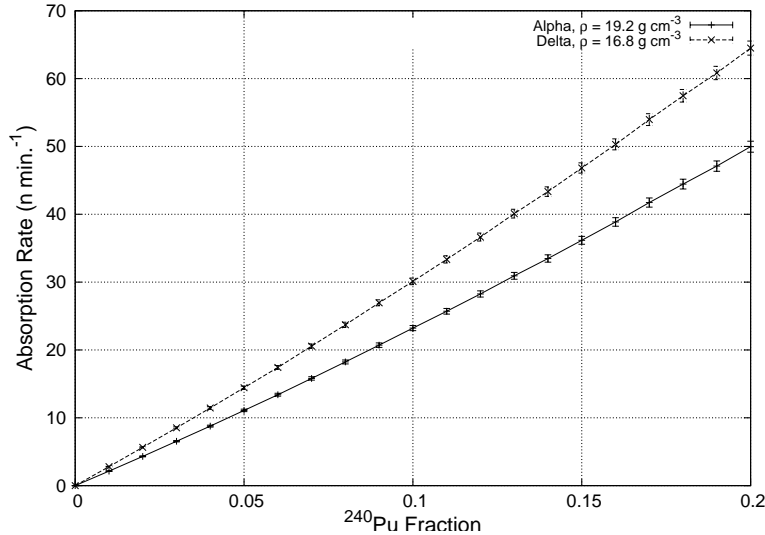


Fig. 4.13. Neutron absorption rate in the detector

In Chapter 2 the probabilities an absorbed neutron leads to a count for various directions of incidence are calculated for perforated detectors like that simulated in the present model of the cargo-container detector. Table B.6 shows the probability a neutron leads to a count ranges from 40% to 60%. Thus, if one assumes 50% for the neutrons absorbed in the detector lead to a count, the estimated count rate (Fig. 4.14) is obtained by multiplying the values in Fig. 4.12 by 0.5.

One observes that, even for a ^{240}Pu fraction of 7% (weapon-grade), there is a predicted count rate of 7 and 10 cpm for α and δ -phase plutonium, respectively. As already discussed, a terrorist nuclear device is likely to contain a much higher content of ^{240}Pu , which increases the expected count rates. With 10% ^{240}Pu an expected count rate of 11 and 15 cpm was calculated and for 20% ^{240}Pu this rate increases to 25 and 32 cpm, respectively, for α and δ -phases.

Typical reports of fast-neutron background fluxes at sea level do not exceed $0.01 \text{ cm}^{-2} \text{ s}^{-1}$, and are typically given in the range of 0.005 to $0.0083 \text{ cm}^{-2} \text{ s}^{-1}$ [Faw and Shultis, 1999] [Nakamura et al., 2005]. Thermal neutron fluxes are on the order of 0.001 to $0.0025 \text{ cm}^{-2} \text{ s}^{-1}$ [Faw and Shultis, 1999] [Dirk et al., 2003]. For the cargo-container detector design presented, thermal neutrons are much more likely to be absorbed in the polyethylene than to reach the detector and are almost inconsequential. For background fluxes of $0.01 \text{ cm}^{-2} \text{ s}^{-1}$, background contributions to counts are going to be substantially less than the count rates predicted above for the Pu pit.

It is, therefore, shown that such detectors, as described here, possess the capability of detecting a bare Pu nuclear-weapon pit. Additionally, it has been assumed that the predictions are conservative in that k_{eff} for a terrorist device is likely to be closer to 1,

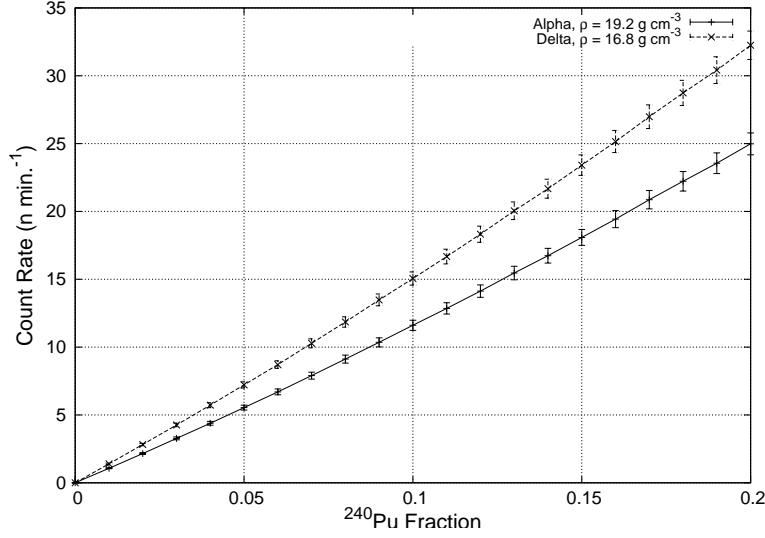


Fig. 4.14. Estimated neutron count rate

to ensure detonation, than the value of 0.9 assumed for the present calculations. Given a source of strength S_o neutrons per generation in a subcritical configuration of material, the number of neutrons created in the zeroth generation is S_o . In the first generation it is $S_1 = S_o + k_{eff}S_o$, and in the second is $S_2 = S_o + k_{eff}S_o + k_{eff}^2S_o$. The N th generation can be expressed as

$$S_N = S_o + k_{eff}S_o + \dots + k_{eff}^N S_o = S_o \sum_{n=1}^N k_{eff}^n, \quad (4.2)$$

which is a geometric series summing to

$$S_N = S_o \frac{1 + k_{eff}^N}{1 - k_{eff}}. \quad (4.3)$$

As $N \rightarrow \infty$ the term $k_{eff}^N \rightarrow 0$ because $k_{eff} < 1$. After a sufficient number of generations, the effective source strength, S_∞ , is given as

$$S_\infty = \frac{S_o}{1 - k_{eff}}, \quad (4.4)$$

where $M = \frac{1}{1 - k_{eff}}$ is defined as the subcritical multiplication factor. [US DOE, 1993]

Using this simple calculation and the fact the detector response scales linearly with source strength, then, as k_{eff} increases so does the multiplication factor. Because the count rate C is proportional to the multiplied source strength one obtains (as shown in [US DOE, 1993])

$$C \propto S_\infty = S_o M, \quad (4.5)$$

from which one can determine

$$\frac{C_1}{M_1} = \frac{C_2}{M_2}. \quad (4.6)$$

Thus, given the count rates calculated here, if a terrorist device has a k_{eff} equal to 0.98 rather than the cautionary 0.9, then estimates of the count rates are going to be a factor of 5 greater:

$$\frac{M_2}{M_1} = \frac{\frac{1}{1-k_2}}{\frac{1}{1-k_1}} = \frac{1 - .9}{1 - .98} = 5 \quad (4.7)$$

Increasing the effective multiplication factor of the subcritical pit increases the likelihood the pit is detected. Even if the ^{240}Pu content is 7% when k_{eff} is 0.95 or 0.98 the resulting count rates are predicted to be 16 and 40 cpm for α -phase plutonium and 20 and 50 cpm for δ -phase. These count rates greatly exceed the neutron background making this detector a feasible device for the application.

4.5 Conclusions, Recommendations, and Suggested Future Work

Even though the count rates for the detectors are low, the calculated responses exceed background by sufficient statistical margins to be a feasible instrument for detecting nuclear weapons pits in cargo containers. In reality, however, a nuclear weapon pit is shielded and not left bare. Thus, although this present analysis demonstrates feasibility, if the pit is shielded to prevent detection, then the detector must be much closer to the device to be practical. Future work should consider how a terrorist may conceal a nuclear weapon pit and what additional measures could be taken to circumvent the concealment—possibly investigating the capture gamma emitted from the $^1\text{H}(n,\gamma)^2\text{H}$ reaction.

Because of the low cost to make a detector such as the ones proposed herein, it is reasonable to conceive of implementing many detectors in a single cargo container. If the density of detectors is sufficient that the pits, although shielded, are much closer to a detector, then there is a much higher probability a neutron is detected because the source is not as far away as has been simulated herein. It is even possible to consider lining the walls of the cargo containers with polyethylene impregnated with the detectors so that a smooth surface, filled with detectors, exists along the entire container.

Bibliography

- T. Cochran, et al. (1984). *Nuclear Weapons Databook Volume 1: U.S. Nuclear Forces and Capabilities*. Ballinger Publishing Co., Cambridge.
- J. Dirk, et al. (2003). ‘Terrestrial Thermal Neutrons’. *IEEE Trans. Nuc. Sci.* **50**(6):2060–2064.
- R. Evans (1955). *The Atomic Nucleus*. McGraw-Hill Book Co., Inc., New York.
- R. Faw and J. Shultis (1999). *Radiological Assessment: Sources and Doses*. American Nuclear Society, La Grange Park.
- GlobalSecurity.org (2005). ‘Plutonium Crystal Phase Transitions’. World Wide Web, <http://www.globalsecurity.org/wmd/intro/pu-phase.htm>.
- J. Lamarsh (2002). *Introduction to Nuclear Reactor Theory*. American Nuclear Society, LaGrange Park.
- J. Lindhard, et al. (1963). ‘Range Concepts and Heavy Ion Ranges’. *Matematisk-Fysiske Meddelelser* **33**(14).
- D. McGregor, et al. (2003). ‘Design Considerations for Thin Film Coated Semiconductor Thermal Neutron Detectors—I. Basics Regarding Alpha Particle Emitting Neutron Reactive Films’. *Nucl. Instr. and Meth. A* **500**:272–308.
- T. Nakamura, et al. (2005). ‘Sequential Measurement of Cosmic-Ray Neutron Spectrum and Dose Rate at Sea Level in Sendai, Japan’. *J. of Nuc. Sci. and Tech.* **42**(10):843–853.
- S. Park and K. Miller (1988). ‘Random Number Generators: Good Ones are Hard to Find’. *Communications of the ACM* **31**:1192–1201.
- W. Press, et al. (1992). *Numerical Recipes in Fortran*. Cambridge University Press, Cambridge, 2nd edn.
- J. Shultis and R. Faw (2000). *Radiation Shielding*. American Nuclear Society, LaGrange Park.
- J. Shultis and D. McGregor (2004). ‘Calculation of Ion Energy-Deposition Spectra in Silicon, Lithium-fluoride, Boron, and Boron Carbide’. Tech. Rep. 299, Engineering Experiment Station Kansas State University.

- J. Shultis and D. McGregor (2006). ‘Efficiencies of Coated and Perforated Semiconductor Neutron Detectors’. *IEEE Trans. on Nucl. Sci.* **53**:1659–1665.
- C. Solomon, et al. (2007). ‘A Hybrid Method for Coupled Neutron-Ion Transport Calculations for ^{10}B and ^6LiF Coated and Peforated Detector Efficiencies’. *Nucl. Instr. and Meth. A* (In Press).
- US DOE (1993). *DOE Fundamentals Handbook: Nuclear Physics and Reactor Theory, Vol. 2*. U.S. Department of Energy, Springfield.
- X-5 Monte Carlo Team (2003). *MCNP— A General Monte Carlo N-Particle Transport Code, Version 5*. Los Alamos National Lab.
- J. Ziegler, et al. (1985). *The Stopping and Range of Ions in Solids*, vol. 1. Pergamon Press.

Appendix A

Perforated Detector Efficiency Calculation Scripts and Codes

File Name	Description	Page
runli6.pl	Control Script for Running ${}^6\text{LiF}$ Rod Perforated Detector Simulations	95
coord.f90	Program that converts all extracted absorption locations from the MCNP PTRAC file to a unit cell geometry	98
ion_tran.Li.f90	Ion transport code for lithium fluoride rod perforated detectors	99
li6_sindet.f90	The specialized transport code written to calculate the efficiencies of lithium fluoride sinusoidal perforated detectors, The channel and chevron codes are similar	113
const_mod.f90	A Fortran module containing fundamental constants used in the specialized transport codes	116
ions_mod.f90	A Fortran module containing the algorithms used for the ion transport	117
kind_mod.f90	A Fortran module containing special declarations for variable kinds	120
mca_mod.f90	A module that simulates a multi channel analyzer for producing energy deposition spectra	121
arts_mod.f90	A module that creates a new structure variable type called particle	123
random_mod.f90	A module for the generation of pseudo random numbers using a linear congruential generator Park and Miller [1988]	124
surf_mod.f90	A module for surface and cell geometry specification and ray tracing	125
zero_mod.f90	A module finding zeros of a function using routines adapted from Press et al. [1992]	129

runli6.pl: Angular Rod Efficiency Control Script

```
#!/usr/bin/perl
$r = 5.0000;      #distance from source to detector
$rs = 2.6;       #radius of source (cm)
$rd = 2.54;      #radius of detector (cm)
$tc = 0.0020;    #cap thickness (cm)
$hd = 0.0100;    #hole depth (cm)
$nps = 2500000;  #number of particles to run
$pi = 3.141592653; #pi
$As = $pi*$rs*$rs; #Area of source plane
$Ad = $pi*$rd*$rd; #Area of detector

open(DATA,">datafile");
print DATA "#Polar      Azimuth      Fna      Fion      Eff      Eff/n-incident\n\n";

for($pol=85; $pol<=85; $pol=$pol+5){ for($azm=0; $azm<=0; $azm=$azm+3){

    #create MCNP input file
    open(RUNFIL,">$pol-$azm.i");

    $x = -$r*sin($pol*$pi/180)*cos($azm*$pi/180);
    $y = -$r*sin($pol*$pi/180)*sin($azm*$pi/180);
    $z = -$r*cos($pol*$pi/180);

    $u = sin($pol*$pi/180)*cos($azm*$pi/180);
    $v = sin($pol*$pi/180)*sin($azm*$pi/180);
    $w = cos($pol*$pi/180);

    $npart = int($nps/cos($pol*$pi/180));

    print RUNFIL "This is a input file that models B-10 coated Si detectors\n";
    print RUNFIL "c 34567890123456789012345678901234567890123456789012345678901234567890\n";
    print RUNFIL "c      1      2      3      4      5      6      7      8\n";
    print RUNFIL "c *****\n";
    print RUNFIL "c                                  Cell Cards\n";
    print RUNFIL "c *****\n";
    print RUNFIL "1100 1 5.73e-2 -110                                u=1\n";
    print RUNFIL "1200 2 -2.33 110                                u=1\n";
    print RUNFIL "c \n";
    print RUNFIL "2000 0          -210 211 -212 213          lat=1 u=2 fill=1\n";
    print RUNFIL "c \n";
    if($tc != 0.0){
    print RUNFIL "3100 1 5.73e-2 -310 311 -312\n";
    print RUNFIL "3200 0          -310 312 -313          fill=2\n";
    print RUNFIL "3300 0          (310:-311:313) -999\n";
    }
    else{
    print RUNFIL "3100 0          -310 311 -312          fill=2\n";
    print RUNFIL "3200 0          (310:-311:312) -999\n";
    }
    print RUNFIL "9999 0          999\n";
    print RUNFIL "\n";
    print RUNFIL "c *****\n";
    print RUNFIL "c                                  Surface Cards\n";
    print RUNFIL "c *****\n";
    print RUNFIL "110 cz 0.0015\n";
    print RUNFIL "c \n";
    print RUNFIL "210 px 0.0025\n";
    print RUNFIL "211 px -0.0025\n";
    print RUNFIL "212 py 0.0025\n";
    print RUNFIL "213 py -0.0025\n";
    print RUNFIL "c \n";
    print RUNFIL "310 cz $rd\n";
    if($tc != 0.0){
    print RUNFIL "311 pz 0.0000\n";
    print RUNFIL "312 pz $tc\n";
    }
    }
}
```

```

print RUNFIL "313 pz ",$tc+$hd,"\n";
}
else{
print RUNFIL "311 pz 0.0000\n";
print RUNFIL "312 pz $hd\n";
}
print RUNFIL "c \n";
print RUNFIL "999 so 10\n";
print RUNFIL "\n";
print RUNFIL "c *****\n";
print RUNFIL "c                               Data Cards\n";
print RUNFIL "c *****\n";
if($tc != 0.0){
print RUNFIL "imp:n 1 1 1 1 1 0\n";
}
else{
print RUNFIL "imp:n 1 1 1 1 1 0\n";
}
print RUNFIL "mode n\n";
print RUNFIL "phys:n 50 20\n";
print RUNFIL "c \n";
print RUNFIL "nps $npart\n";
print RUNFIL "c \n";
print RUNFIL "sdef pos=$x $y $z\n";
print RUNFIL "   axs=$u $v $w\n";
print RUNFIL "   vec=$u $v $w\n";
print RUNFIL "   rad=d1 ext=0 erg=d2 dir=1 par=1\n";
print RUNFIL "si1 0  $rs\n";
print RUNFIL "sp1 -21  1\n";
print RUNFIL "sp2 -2  2.53e-8\n";
print RUNFIL "c \n";
if($tc != 0.0){
print RUNFIL "f4:n (1100 3100)\n";
}
else{
print RUNFIL "f4:n 1100\n";
}
print RUNFIL "fm4 -1  1  105\n";
print RUNFIL "sd4 1\n";
print RUNFIL "c \n";
if($tc != 0.0){
print RUNFIL "ptrac file=asc event=ter max=$npart type=n filter=1100,3100,icl\n";
}
else{
print RUNFIL "ptrac file=asc event=ter max=$npart type=n filter=1100,icl\n";
}
print RUNFIL "c \n";
print RUNFIL "m1  3006.66c 1.000\n";
print RUNFIL "c \n";
print RUNFIL "m2  14028.66c 0.922297\n";
print RUNFIL "   14029.66c 0.046832\n";
print RUNFIL "   14030.66c 0.030872\n";
print RUNFIL "\n";

close(RUNFIL);

#run MCNP
print "MCNP file $pol-$azm.i created...starting MCNP...\n";
system "mcnp5 i=$pol-$azm.i o=$pol-$azm.o r=$pol-$azm.r ptrac=$pol-$azm.p\n";
system "rm $pol-$azm.r\n";

#read neutron interaction value from MCNP output
open(INFILE,"<$pol-$azm.o");
while($line = <INFILE>){ if($line =~ /\^scell\s+1100/ ||
    $line =~ /\^scell\s+(1100\s3100)/){ $line = <INFILE>; $line = <INFILE>; if($line =~
    /\^s+(\.d\.d+E[+-]\d+)\s(\.d\.d+)/){
        $nu_int = $1; }
} } close(INFILE);

```

```

#extract pertinent particle terminations from ptrac file
print "Extracting particle termination positions from $pol-$azm.p...\n";

open(PFILE,"<$pol-$azm.p");
open(INTFIL,">temp1");
$num_na = 0;
while($line = <PFILE>){ if ($line =~ /\s+9000\s+\d+\s+12\s+1\s+1100\s+1\s+/ ||
    $line =~ /\s+9000\s+\d+\s+12\s+1\s+3100\s+1\s+/){
    $line = <PFILE>;
    $num_na += 1; }
}
close(PFILE);
open(PFILE,"<$pol-$azm.p");
print INTFIL $num_na, "\n";
while($line = <PFILE>){ if ($line =~ /\s+9000\s+\d+\s+12\s+1\s+1100\s+1\s+/ ||
    $line =~ /\s+9000\s+\d+\s+12\s+1\s+3100\s+1\s+/){
    $line = <PFILE>;
    print INTFIL $line; }
}
close(PFILE);
close(INTFIL);

#delete ptrac file
system "rm $pol-$azm.p";

print "MCNP interaction positions extracted...\n";

#change coordinate system for Ion Transport
print "Calculating positions for Ion Transport...\n";
system "./coord.exe > temp2\n";
print "Ion Transport positions calculated...\n";

#run the ion code
print "Running Ion Transport...\n";
system "./ion_tran_Li.exe > temp3\n";

#Extract fraction of Ions Contributing to a Count
open(INPUT,"<temp3");

while($line = <INPUT>){ if ($line =~ /^#\s*Fraction\s*of\s*ions\s*recorded\s*=\s*(\d+\.\d+)/){
$num_ion = $1; }
}

print DATA $pol," ",$azm," ",$nu_int," ",$nu_int*$As/($Ad*cos($pol*$pi/180))," ",$num_ion,"
    ",$nu_int*$num_ion," ",$nu_int*$num_ion*$As/($Ad*cos($pol*$pi/180)),"\n";

#remove temporary files # system "rm temp*\n";

#rename RodD1.out to correspond with the other file names
system "mv Rod1L.out $pol-$azm.dat\n"; } print DATA "\n";
}
print "\nDone!\n";

```

coord.f90: Coordinate trasformatoin to unit cell code

```
program coord
  implicit none

  real(kind=8), parameter :: cw = 0.0050, hr = 0.0015, tc=.0020, floattol=0.0000001
  real(kind=8) :: xxx,yyy,zzz,uuu,vvv,www

  integer :: ylat, xlat, nlines, cnt

  open(unit=10,file="temp1",status="old")

  read(10,*) nlines
  print *, nlines
  do cnt=1,nlines
    read(10,*)xxx,yyy,zzz

    xlat = nint(xxx/cw)
    ylat = nint(yyy/cw)

    uuu = cw * xlat
    vvv = cw * ylat
    www = 0.000

    xxx = xxx - uuu
    yyy = yyy - vvv
    zzz = zzz - www

    if (xxx < 0.0) xxx = xxx + floattol
    if (xxx > 0.0) xxx = xxx - floattol
    if (yyy < 0.0) yyy = yyy + floattol
    if (yyy > 0.0) yyy = yyy - floattol
!   if (zzz < 0.0) zzz = zzz + floattol
!   if (zzz > 0.0) zzz = zzz - floattol

    if (zzz > tc .AND. xxx*xxx+yyy*yyy > hr*hr) &
      & print *, "Error calculating absorpton location: rod"
    if (zzz < tc .AND. (abs(xxx) > cw/2.0 .OR. abs(yyy) > cw/2.0) ) &
      & print *, "Error calculating absorpton location: cap"

    print *, xxx*10000, yyy*10000, zzz*10000

  end do
end program coord
```

ion_tran_Li.f90: Modified Ion Transport Code from J.K. Shultis

```

!C***** Rod1L *****
!C***** Rod1L is a Monte Carlo simulation of energy deposition spectra
!C***** produced by H-3 and He-4 ions from Li-6(n,t)He-4 reaction in a Si
!C***** rectangular parallelepiped. One end of the Si block is coated
!C***** by a thin layer of LiF and there is a cylindrical void filled
!C***** with LiF extending perpendicularly from the coated surface
!C***** into the Si block.
!C***** Thermal neutrons are normally incident on the coated surface.
!C*****
      INTEGER seed
      DIMENSION RmaxSi(2),RmaxLF(2)
      DIMENSION Nions(2)
      DOUBLE PRECISION Gint,ddel,ans
      DIMENSION e(256),eup(256),spec(0:6,256),specr(0:6,256)
      DIMENSION vsprd(20),vsprd2(20)
      COMMON/RANCOM/SEED
      COMMON/SPEC/eup,spec,Ecut,nmax,Nnorec,Nrec
      COMMON del,sig,kk
      EXTERNAL Gint
      DATA RmaxLF/6.13d0,32.4d0/
      DATA RmaxSi/7.37,42.1/
      DATA Nions/2*0/

!C
!C
!C***** Open output file
      OPEN (10,FILE='Rod1L.out',STATUS='UNKNOWN')
!C***** Open input file
      OPEN (11,FILE='temp2',status='old')
!C
!C***** Initial Data for Problem
      seed = 73907
      pi = 3.141592654
      twopi=6.2831853d0
!C-- stnd deviation of resolution Guassian (MeV)
      sig=0.020

!C***** Obtain problem parameters:
!C      nhist = 100
      READ(11,*)nhist
      idir=1
      Xcap = 50.0
      Tcap = 20.0
      Rrod = 15.0
      Rrod2 = Rrod*Rrod
      Hrsi = 100.0
      Ecut = 0.300
      Hrod = Hrsi + Tcap
      WRITE(*,50) Xcap,Tcap,Rrod,Hrsi,Ecut,nhist
      WRITE(10,50) Xcap,Tcap,Rrod,Hrsi,Ecut,nhist
50  FORMAT('# MC Simulation of E-deposition Spectrum in a Square',/
& '# LiF Coated Si Cell with a Central LiF Rod',/
& '# Width of the square cell (um) = ',F9.2,/
& '# Thickness of the LiF cap (um) = ',F9.2,/
& '# Radius of central LiF rod (um) = ',F9.2,/
& '# Rod depth in the silicon (um) = ',F9.2,/
& '# MCA spectrum energy cutoff(MeV) =',F9.4,/
& '# No. of requested ion histories =',I9)
!      IF (idir.EQ.1) THEN
!          WRITE(*,53)
!          WRITE(10,53)
!      ELSE
!          WRITE(*,54)

```

```

!          WRITE(10,54)
!          ENDIF
!53  FORMAT (' NOTE: Neutrons normally incident on cap ',/)
!54  FORMAT (' NOTE: Neutrons normally incident on rod end ',/)

!C***** find transmission and efficiency of LiF-layer
!C***** Li-6 sigma (um)^-1
!      sigLF = 0.0051
!C      sigLF = 0.005753
!      Rrod2 = Rrod*Rrod
!      Arod = pi*Rrod2
!      Acap = Xcap*Xcap - Arod
!C      WRITE(*,*) ' Xcap*Xcap, Arod and Acap =',Xcap*Xcap,Arod,Acap
!
!      Pcap = 1 - EXP(-sigLF*Tcap)
!      Prod = 1 - EXP(-sigLF*Hrod)
!C      WRITE(*,*) 'Pcap and Prod =',Prod,Pcap
!
!      Pionr = Arod*Prod/(Arod*Prod+Acap*Pcap)
!      Pionc = Acap*Pcap/(Arod*Prod+Acap*Pcap)
!      Pion = (Acap*Pcap+Arod*Prod)/(Acap+Arod)
!      trans = 1-Pion
!C      WRITE(*,51) Pion,trans,Pionc,Pionr
!      WRITE(10,51) Pion,trans,Pionc,Pionr
!51  FORMAT(' Prob. neut interacts in detector = ',F9.5,/          &
!      &      ' Prob. neut. passes thru detector = ',F9.5,/          &
!      &      ' Fract. of ions produced reduced cap =',F9.5,/          &
!      &      ' Fract. of ions produced in rod = ',F9.5,/)

!C***** Setup the MCA energy grid
      nmax = 256
      Emax = 5.0
      del = 0.5*Emax/nmax
      DO 11 n = 1,nmax
          e(n) = (2*n-1)*del
          eup(n) = 2*n*del
          DO 12 j=0,6
              spec(j,n) = 0
              specr(j,n) = 0.0
12      CONTINUE
11      CONTINUE

!C***** Begin Simulation
      Nnrec=0
      Nrec=0
      DO 10 nalpha=1,nhist
!          IF (MOD(nalpha,1000000).EQ.0) WRITE(*,*)'nions =',nalpha

!C===== Select xo,yo,Omega_o (downwards),ipart
!C-- Pick xo,yo depending on prob ions are created cell or rod
!      rion = FLTRN()
!C-- ion in rod (use 100% eff disk sampling method)
!      IF (rion.LE.Pionr) THEN
!          Ro = Rrod*SQRT(FLTRN())
!          ango=twopi*FLTRN()
!          xo = Ro*COS(ang)
!          yo = Ro*SIN(ang)
!          ro2 = xo*xo+yo*yo
!C-- ion in reduced cap (use rejection method)
!      ELSE
!31      xo = Xcap*(0.5-FLTRN())

```

```

!          yo = Xcap*(0.5-FLTRN())
!          ro2=xo*xo+yo*yo
!          IF(ro2.LT.Rrod2) GOTO 31
!          ENDDIF

!C-- Select depth zo (positive z) for ion in cap or rod
!          IF (ro2.LT.Rrod*Rrod) THEN
!              Cnorm=Prod
!          ELSE
!              Cnorm=Pcap
!          ENDDIF
!          zo = -LOG(1.-Cnorm*FLTRN())/sigLF
!C-- Flip zo if detector irradiated from below
!          IF (idir.EQ.-1) THEN
!              IF (ro2.LT.Rrod*Rrod) THEN
!                  zo = Hrod - zo
!              ELSE
!                  zo = Tcap - zo
!              ENDDIF
!          ENDDIF

!C-- Get initial positions from input file
!          READ(11,*)xo,yo,zo
!          ro2 = xo*xo+yo*yo
!C-- Get initial direction cosines (force w>0)
!          CALL GTISO(u,v,w)
!          IF (w.LT.0.0) w=-w
!C-- Get downward ion type
!          ipart=1
!          rion = FLTRN()
!          IF (rion.GT.0.5) ipart=2
!          Nions(ipart)=Nions(ipart)+1

!C*****
!C***** ION BORN IN CAP
!C*****
!          IF (ro2.GT.Rrod2) THEN
!C-- Calc dist to cap base and energy at base
!C-- kill ion if it does not escape the cap
!          CALL IntPZ(xo,yo,zo,u,v,w,Tcap,x1,y1,z1,s1)
!          IF (s1.GE.RmaxLF(ipart)) THEN
!              Nnorec=Nnorec+1
!              GOTO 10
!          ENDDIF
!          E1 = EresLF(s1,ipart)

!C--
!C-- Cap escape point is outside rod
!C--
!          IF ((x1*x1+y1*y1).GT.Rrod2) THEN
!C-- see if ion trajectory intersects rod
!          CALL IntCZ(x1,y1,z1,u,v,w,Rrod,x3,y3,z3,x2,y2,z2,s3,s2)

!C-- case: ion does not intersect rod
!          IF (s2.LE.0.0) THEN
!              CALL SpcAdd(E1,1)
!              GOTO 10

!C---- case: ion does intersect rod (4 subcases!)
!C          energy deposited before hitting rod
!          ELSE

!C-- subcase: ion shoots below rod
!          IF (z2.GT.Hrod) THEN
!              CALL SpcAdd(E1,1)

!C-- subcase: ion shoots thru cylinder in the cap
!          ELSEIF (z3.LT.Tcap) THEN

```



```

                CALL SpcAdd(E1,1)
!C--   subcases: ion hits rod and emerges on cyl surface and on rod base
        ELSE
!C     check if ion hits rod base
            IF (z3.GT.Hrod)
                CALL IntPZ(x1,y1,z1,u,v,w,Hrod,x3,y3,z3,s3)
                Ed = Edep(E1,s2,1,ipart)
!C     energy at rod surface
                E2=E1-Ed
!C     energy lost in rod
                Edrod=Edep(E2,s3-s2,2,ipart)
!C     energy deposited in Si after rod
                E4 = E2-Edrod
                IF (Edrod.LT.0.) Edrod=0.0
                CALL SpcAdd(E4+Ed,2)
            ENDIF
            GOTO 10
        ENDIF

!C-- Cap escape point is inside rod
        ELSE
!C--   find escape point and energy on rod surface
            CALL IntCZ(xo,yo,zo,u,v,w,Rrod,x2,y2,z2,x1,y1,z1,s2,s1)
            IF (z2.GT.Hrod)
                CALL IntPZ(xo,yo,zo,u,v,w,Hrod,x2,y2,z2,s2)
                Ed = EresLF(s2,ipart)
                CALL SpcAdd(Ed,3)
                GOTO 10
            ENDIF

!C*****
!C***** ION BORN IN ROD
!C*****
        ELSE

!C---- CASE ion born in rod below cap--find escape pt on surface/bottom
            IF (zo.GT.Tcap) THEN
                CALL IntCZ(xo,yo,zo,u,v,w,Rrod,x1,y1,z1,x2,y2,z2,s1,s2)
                IF (z1.GT.Hrod) CALL IntPZ(xo,yo,zo,u,v,w,Hrod,x1,y1,z1,s1)
!C--   down ion resid energy
                Ed1 = EresLF(s1,ipart)
!C--   up-ion lost in cap
                IF(z2.LT.Tcap) THEN
                    CALL SpcAdd(Ed1,4)
                    GOTO 10
                ENDIF
!C--   up ion enters Si: find up-ion type
                IF (ipart.EQ.2) THEN
                    ionup=1
                ELSE
                    ionup=2
                ENDIF
!C--   find distances to cap base and energy deposited in Si
                CALL IntPZ(x2,y2,z2,u,v,w,Tcap,x3,y3,z3,s3)
                E2=EresLF(-s2,ionup)
                Ed2=Edep(E2,-s3,1,ionup)
                CALL SpcAdd(Ed1+Ed2,5)
                GOTO 10

!C---- CASE ion born in rod above cap bottom
        ELSE
            CALL IntCZ(xo,yo,zo,u,v,w,Rrod,x1,y1,z1,x2,y2,z2,s1,s2)
            IF (z1.LT.Tcap) CALL IntPZ(xo,yo,zo,u,v,w,Tcap,x1,y1,z1,s1)
            IF (z1.GT.Hrod) CALL IntPZ(xo,yo,zo,u,v,w,Hrod,x1,y1,z1,s1)
            E1 = EresLF(s1,ipart)

```



```

      WRITE(*,89) (n,e(n),spec(0,n),specr(0,n),n=1,nmax)
89  FORMAT(//'ch.no.      Emid(MeV)      Total-0      Total-0r  ',      &
&      (I5,G16.5,2G12.4))

      WRITE(10,90) (n,e(n),spec(0,n),(specr(k,n),k=0,6),n=1,nmax)
90  FORMAT(//'#ch.no.      Emid(MeV)      Total-0      Total-0r  ',      &
&' Component1 Component2 Component3 Component4',      &
&' Component5 Component6',/      &
&      (I5,G16.5,8G12.4))

      Ntot=Nnorec+Nrec
      Fion = Nrec/(FLOAT(Ntot))
      Fneut = Fion*Pion
      WRITE(*,91) Nnorec,Nrec,Ntot,Fion,Fneut
      WRITE(10,91) Nnorec,Nrec,Ntot,Fion,Fneut
91  FORMAT(//'# No. ions depositing no energy = ',I9,/      &
&      '# No. ions depositing energy = ',I9,/      &
&      '# Total no. of ions tracked = ',I9,/      &
&      '# Fraction of ions recorded = ',F9.4,/      &
&      '# Fraction of neutrons recorded = ',F9.4)

!C      WRITE(*,92) (Nions(i),i=1,4)
!C92    FORMAT (' no. ions 1-4 =',4I8)

```

END

```

!C=====
!C===== Specialized Subroutines =====
!C=====
!C=====

```

```

      SUBROUTINE SpcAdd(E,mode)
!C-----
!C Add count to MCA spectrum in energy channel containing E
!C Also add count to the component spectra (MODE)
!C-----
      COMMON/SPEC/Eup(256),spec(0:6,256),Ecut,nmax,Nnorec,Nrec

      IF (E.GT.Ecut) THEN
        DO 15 n=2,nmax
          IF (E.LT.Eup(n)) THEN
            spec(0,n)=spec(0,n)+1
            spec(mode,n)=spec(mode,n)+1
            Nrec=Nrec+1
            RETURN
          ENDF
15      CONTINUE
        ELSE
          Nnorec=Nnorec+1
        ENDF
      RETURN
      END

```

```

      SUBROUTINE IntPZ(xo,yo,zo,uo,vo,wo,Zplane,x,y,z,s)
!C-----
!C Calculates intersection point r(x,y,z) on plane z=Zplane
!C from a specified point ro(xo.yo.zo) in a given direction
!C (uo,vo,wo). Distane from ro to r is returned as d. If d>0
!C intersection is in the specified direction; if s<0 intersection
!C is opposite of the given direction.
!C-----
!C      d = (Zplane - zo)/wo
!C      s = (Zplane - zo)/wo
!C      s = SQRT(uo*uo + vo*vo + wo*wo)*d
!C      x = xo+uo*s

```

```

y = yo+vo*s
z = Zplane
RETURN
END

```

```

SUBROUTINE IntCZ(xo,yo,zo,uo,vo,wo,R,x1,y1,z1,x2,y2,z2,s1,s2)

```

```

!C-----
!C Calculates intersection points r1(x1,y1,z1) and r2(x2,y2,z2) and
!C corresponding distances s1 and s2 to a cylinder of radius R about
!C the z-axis from a point ro(xo,yo,zo) in direction (uo,vo,wo)
!C If no intersection s1=s2=0, if 1 interesection (point ro is inside
!C cylinder) s1>0 and s2<0, if 2 interesections (ro outside cylinder)
!C s1>s2>0.
!C-----

```

```

      dd2 = uo*uo+vo*vo
      ddd = SQRT(dd2 + wo*wo)
      fact = uo*xo + vo*yo
      fact1 = xo*xo+yo*yo - R*R
      det = fact*fact - dd2*fact1

```

```

!C-- case of no intersection or near tangent

```

```

      IF (det.LE.1E-6) THEN
        s1=0.0
        s2=0.0
        RETURN

```

```

!C-- case of two intersections

```

```

      ELSE
        sdet=SQRT(det)
        s1 = (-fact + sdet)/dd2
        s2 = (-fact - sdet)/dd2
        x1 = xo+s1*uo
        y1 = yo+s1*vo
        z1 = zo+s1*wo
        x2 = xo+s2*uo
        y2 = yo+s2*vo
        z2 = zo+s2*wo
      ENDIF
      RETURN
      END

```

```

!C%%%%%%%%%%%%%%%%%%%%%%%%%%%%%%%%%%%%%%%%%%%%%%%%%%%%%%%%%%%%%%%%%%%%%%%%%%
!C%%%%%%%%%%%%%%%%%%%%%%%%%%%%%%%%%%%%%%%%%%%%%%%%%%%%%%%%%%%%%%%%%%%%%%%%%%
!C%%%%%%%%%%%%%%%%%%%%%%%%%%%%%%%%%%%%%%%%%%%%%%%%%%%%%%%%%%%%%%%%%%%%%%%%%%  Routines for Li-6 Ions %%%%%%%%%%%%%%%%%%%%%%%%%%%%%%%%%%%%%%%%%%%%%%%%%%%%%%%%%%%%%%%%%%%%%%%%%%%
!C%%%%%%%%%%%%%%%%%%%%%%%%%%%%%%%%%%%%%%%%%%%%%%%%%%%%%%%%%%%%%%%%%%%%%%%%%%
!C%%%%%%%%%%%%%%%%%%%%%%%%%%%%%%%%%%%%%%%%%%%%%%%%%%%%%%%%%%%%%%%%%%%%%%%%%%

```

```

FUNCTION Edep(Eo,s,imat,ipart)

```

```

!C-----
!C Calculates the energy deposited (Edep) along a path length s in
!C material IMAT for a Li-6 ion (of type IPART) that initially has
!C energy Eo (<Emax) at the start of the path
!C      ipart =1 alpha, =2 tiriton
!C      imat = 1 silicon, =2 LiF
!C-----

```

```

      EXTERNAL XSi,XLiF,EresSi,EresLF
      IF (imat.EQ.1) THEN
        so = XSi(Eo,ipart)
        E1 = EresSi(s+so,ipart)
!C      WRITE(10,*)'Si: E1,s,s1,Edep=',E1,s,s1,Edep
      ELSE
        so = XLiF(Eo,ipart)
        E1 = EresLF(s+so,ipart)
!C      WRITE(10,*)'LiF: E1,s,s1,Edep=',E1,s,s1,Edep
      ENDIF
      Edep = Eo-E1

```

```

RETURN
END

FUNCTION EresLF(xx,ipart)
!C-----
!C Residual energy (MeV) for Li-6(n,t)He-4 ions in LiF
!C xx = path length (um)
!C ipart = 1 alpha; =2 triton
!C-----
DOUBLE PRECISION x,y,range(2)
DATA range/6.13d0,32.4d0/

x=xx
IF (x.GT.range(ipart)) THEN
  EresLF=0.0d0
  RETURN
ENDIF

!C-- case of alpha particle in LiF
IF (ipart.EQ.1) THEN
  EresLF = (2.045795872242105D0+x*(-0.6656803951074236D0+
& x*(0.05419252954318524D0)))/
& (1.0+x*(-0.1618681522606121D0+x*(-0.0004073163152857422D0+
& x*(0.001694213790128516D0))))
!C-- case of triton in LiF
ELSE
  y = (1.002503409342673D0+x*(-0.06518537556264785D0+
& x*(0.0009570698188079860D0)))/
& (1.0+x*(-0.04378737038158115D0+x*(0.0004104515518016601D0)))
  EresLF = DEXP(y)
ENDIF

RETURN
END

FUNCTION EresSi(xx,ipart)
!C-----
!C Residual energy (MeV) for Li-6(n,t)He-4 ions in Si
!C xx = path length (um)
!C ipart = 1 alpha; =2 triton
!C-----
DOUBLE PRECISION x,y,range(2)
DATA range/7.37d0,42.1d0/

x=xx
IF (x.GT.range(ipart)) THEN
  EresSi=0.0d0
  RETURN
ENDIF

!C-- case of alpha particle in silicon
IF (ipart.EQ.1) THEN
  EresSi = (2.054968416876924D0+x*(-0.5570727177716902D0+
& x*(0.03778001355325864D0)))/
& (1.0+x*(-0.1483764307642617D0
& +x*(-0.0005753511256927519D0+
& x*(0.0007588407797898662D0))))
!C-- case of triton in silicon
ELSE
  y = (0.9984993786783298D0+x*(-0.04902551060382791D0+
& x*(0.0005428269966035989D0)))/
& (1.0+x*(-0.03278510294862023D0+x*(0.0002214134270311182D0)))
  EresSi = DEXP(y)

ENDIF
RETURN
END

```

```

FUNCTION XSi(EE,ipart)
!C-----
!C Path length in Si to reduce the original energy of the alpha
!C (ipart=1) and the triton (ipart=2) from the Li-6(n,t)He-4 reaction
!C to an energy EE
!C-----
DOUBLE PRECISION e,Rmax(2),emax(2)
DOUBLE PRECISION x1,x2,x3,x4,DLG
DATA Rmax/7.37d0,42.1d0/,Emax/2.05d0,2.73d0/

e=EE
IF (e.LE.0.0d0) THEN
  Xsi=Rmax(ipart)
  RETURN
ELSEIF (e.GE.Emax(ipart)) THEN
  Xsi = 0.0d0
  RETURN
ENDIF

!C-- alpha in silicon (TC 7904)
IF(ipart.EQ.1) THEN
  x=DSQRT(e)
  XSi = 7.650654782456231D0+x*(-2.951907906029242D0+
& x*(-3.226254043595208D0+x*(12.90757367270686D0+
& x*(-19.00554784825017D0+x*(10.85346324881674D0+
& x*(-2.337319132539310D0))))))
!C-- triton in silicon (TC 4328)
ELSE
  x1=e
  x2=e*e
  DLG = DLOG(e)
  x3=x2*DLG
  x4=DSQRT(e)*DLG
  XSi = 42.55432730826800D0-6.126822912741065D0*x1
& -5.405288206496186D0*x2+1.274522449649497D0*x3
& +2.744516841023055D0*x4
ENDIF
XSi = MAX(0.0,XSi)

RETURN
END

FUNCTION XLiF(EE,ipart)
!C-----
!C Path length in LiF to reduce the original energy of the alpha
!C (ipart=1) and the triton (ipart=2) from the Li-6(n,t)He-4 reaction
!C to an energy EE
!C-----
DOUBLE PRECISION e,Emax(2),Rmax(2)
DOUBLE PRECISION x1,x2,x3,x4,DLG
DATA Rmax/6.13d0,32.4d0/,Emax/2.05d0,2.73d0/

e=EE
IF (e.LE.0.0d0) THEN
  XLiF=Rmax(ipart)
  RETURN
ELSEIF (e.GE.Emax(ipart)) THEN
  XLiF = 0.0d0
  RETURN
ENDIF

!C-- alpha in silicon (TC 7904)
IF(ipart.EQ.1) THEN
  x=DSQRT(e)
  XLiF=6.312636231356213D0+x*(-3.594256350143011D0+
&

```

```

&      x*(1.968648983630100D0+x*(-1.822537261104411D0+
&      x*(0.1363849426609869D0+x*(-0.1283915688540728D0+
&      x*(0.03773779891639750D0))))))
!C-- triton in silicon (TC 4328)
  ELSE
    x1=e
    x2=e*e
    DLG = DLOG(e)
    x3=x2*DLG
    x4=DSQRT(e)*DLG

    XLiF=33.05498950931498D0-6.885172032726404D0*x1
&      -2.727479733376275D0*x2+0.3125211180119474D0*x3
&      +2.194886238812784D0*x4
  ENDIF
  XLiF = MAX(0.0, XLiF)

  RETURN
  END

```

```

!C=====
!C=====
!C===== Utility Subroutines =====
!C=====
!C=====

```

```

      FUNCTION erf(x)
!C-----
!C The erf(x) function -- from Numerical Recipes
!C-----
      REAL erfcc,x
      REAL t,z
      z=ABS(x)
      t=1./(1.+0.5*z)
      erfcc=t*EXP(-z*z-1.26551223+t*(1.00002368+t*(.37409196+t*
&      (.09678418+t*(-.18628806+t*(.27886807+t*(-1.13520398+t*
&      (1.48851587+t*(-.82215223+t*.17087277))))))))))
      if (x.lt.0.) erfcc=2.-erfcc
      erf = 1.-erfcc
      RETURN
      END

```

```

      REAL FUNCTION FLTRN()
!C-----
!C**** PURPOSE: RETURNS A SINGLE PRECISION FLOATING POINT RANDOM
!C****          NUMBER IN THE OPEN INTERVAL (0,1).
!C****          WORKS ON ANY SYSTEM FOR WHICH THE MAXIMUM VALUE
!C****          OF AN INTEGER VARIABLE IS 2**31-1 OR LARGER.
!C
!C**** ARGUMENTS: (NONE)
!C****          SEED NUMBER IS KEPT IN COMMON
!C
!C**** SUBPROGRAMS CALLED:
!C**** MOD      - FORTRAN INTRINSIC FUNCTION TO RETURN REMAINDER
!C**** REAL     - FORTRAN INTRINSIC FUNCTION TO CONVERT TO SINGLE PRECISION
!C
!C**** METHOD:   MINIMAL STANDARD GENERATOR SPECIFIED IN THE ARTICLE
!C****          S. K. PARK AND K. W. MILLER, "RANDOM NUMBER GENERATORS:
!C****          GOOD ONES ARE HARD TO FIND", COMM. ACM, VOL. 31, NO. 10,
!C****          OCTOBER 1988.
!C
!C**** AUTHOR:  J. C. RYMAN
!C****          NUCLEAR ENGINEERING APPLICATIONS
!C****          COMPUTING & TELECOMMUNICATIONS DIVISION

```

```

!C****          OAK RIDGE NATIONAL LABORATORY
!C****          P. O. BOX 2008
!C****          OAK RIDGE, TN  37831
!C-----
!C
      INTEGER SEED
      COMMON/RANCOM/ SEED
      INTEGER A,M,Q,R,LO,HI,TEST
      REAL MINV
      PARAMETER(A=16807,M=2147483647,Q=127773,R=2836)
      PARAMETER(MINV=4.6566129E-10)
!C
      HI=SEED/Q
      LO=MOD(SEED,Q)
      TEST=A*LO-R*HI
!C
      IF(TEST.GT.0) THEN
          SEED=TEST
      ELSE
          SEED=TEST+M
      ENDIF
!C
      FLTRN = MINV*REAL(SEED)
      RETURN
      END
!C
!C
!C
      REAL FUNCTION EXPRN()
!C-----
!C**** PURPOSE:  RETURNS A SINGLE PRECISION EXPONENTIALLY DISTRIBUTED
!C****          RANDOM NUMBER
!C
!C**** ARGUMENTS: (NONE)
!C
!C**** SUBPROGRAMS CALLED:
!C**** FLTRN  - RETURNS SINGLE PRECISION UNIFORMLY DISTRIBUTED RANDOM
!C****          NUMBER IN THE OPEN INTERVAL (0,1)
!C**** LOG    - GENERIC NAME FOR NATURAL LOGARITHM INTRINSIC FUNCTION
!C-----
      REAL FLTRN
      EXTERNAL FLTRN
!C
      EXPRN = -LOG(FLTRN())
      RETURN
      END
!C
!C
!C
      SUBROUTINE GTISO(U,V,W)
!C-----
!C**** PURPOSE:  RETURNS SINGLE PRECISION DIRECTION COSINES FOR A
!C****          RANDOM DIRECTION UNIFORMLY SELECTED FROM 4*PI
!C****          STERADIANS
!C
!C**** ARGUMENTS:
!C**** U      = DIRECTION COSINE WITH RESPECT TO X-AXIS
!C**** V      = DIRECTION COSINE WITH RESPECT TO Y-AXIS
!C**** W      = DIRECTION COSINE WITH RESPECT TO Z-AXIS
!C
!C**** SUBPROGRAMS CALLED:
!C**** FLTRN  - RETURNS SINGLE PRECISION UNIFORMLY DISTRIBUTED RANDOM
!C****          NUMBER IN THE OPEN INTERVAL (0,1)
!C**** SIN    - GENERIC NAME FOR SINE INTRINSIC FUNCTION
!C**** COS    - GENERIC NAME FOR COSINE INTRINSIC FUNCTION
!C**** SQRT   - GENERIC NAME FOR SQUARE ROOT INTRINSIC FUNCTION
!C-----
!C

```



```

REAL U,V,W
REAL TWOPI,THETA,FLTRN,SN,CS,UV
PARAMETER (TWOPI=6.2831853EO)
!C
W = -1.E0+2.E0*FLTRN()
THETA = TWOPI*FLTRN()
SN = SIN(THETA)
CS = COS(THETA)
UV = SQRT(1.E0-W**2)
U = CS*UV
V = SN*UV
RETURN
END

DOUBLE PRECISION FUNCTION Gint(x)
!C-----
!C -- integrand for evaluating the Guassian smoothing vector
!C-----
DOUBLE PRECISION x
COMMON del,sig,kk
Gint = DEXP(-(2*kk*del-x)**2/(2*sig*sig))
RETURN
END

SUBROUTINE GAUS8(FUN,A,B,ERR,ANS,IERR)
!C-----
!C****
!C**** PURPOSE
!C**** GAUS8 INTEGRATES REAL FUNCTIONS OF ONE VARIABLE OVER FINITE
!C**** INTERVALS, USING AN ADAPTIVE 8-POINT GAUSS-LEGENDRE ALGORITHM.
!C**** GAUS8 IS INTENDED PRIMARILY FOR HIGH ACCURACY INTEGRATION OR
!C**** INTEGRATION OF SMOOTH FUNCTIONS. FOR LOWER ACCURACY
!C**** INTEGRATION OF FUNCTIONS WHICH ARE NOT VERY SMOOTH, EITHER
!C**** QNC3 OR QNC7 MAY BE MORE EFFICIENT.
!C****
!C**** USAGE
!C**** CALL GAUS8(FUN,A,B,ERR,ANS,IERR)
!C****
!C**** FUN - NAME OF EXTERNAL FUNCTION TO BE INTEGRATED. THIS NAME
!C**** MUST BE IN AN EXTERNAL STATEMENT IN THE CALLING PROGRAM.
!C**** FUN MUST BE A FUNCTION OF ONE REAL ARGUMENT (THE
!C**** VARIABLE OF INTEGRATION).
!C**** A - LOWER LIMIT OF INTEGRAL.
!C**** B - UPPER LIMIT OF INTEGRAL (MAY BE LESS THAN A).
!C**** ERR - USER-SUPPLIED ERROR PARAMETER. ANS WILL NORMALLY HAVE
!C**** NO MORE ERROR THAN ERR TIMES THE INTEGRAL OF THE
!C**** ABSOLUTE VALUE OF FUN(X).
!C**** ANS - COMPUTED VALUE OF INTEGRAL.
!C**** IERR - ERROR PARAMETER SET BY GAUS8:
!C**** IERR = 1 IS NORMAL.
!C**** IERR = 2 MEANS ANS IS PROBABLY INSUFFICIENTLY ACCURATE.
!C****
!C**** SUBROUTINES AND FUNCTION SUBPROGRAMS REQUIRED
!C**** THE EXTERNAL FUNCTION FUN(X) MUST BE SUPPLIED BY THE USER.
!C****
!C**** METHOD
!C**** AN ADAPTIVE 8-POINT GAUSS-LEGENDRE ALGORITHM WITH INTERVAL
!C**** BISECTION, COMBINED RELATIVE/ABSOLUTE ERROR CONTROL, AND
!C**** COMPUTED MAXIMUM REFINEMENT LEVEL WHEN A IS CLOSE TO B.
!C****
!C**** .....
!C****
IMPLICIT DOUBLE PRECISION (A-H,O-Z)
DIMENSION AA(30),HH(30),LR(30),VL(30),GR(30)

```

```

!C**** 8-POINT GAUSS-LEGEGNDRE QUADRATURE DATA.
  DATA X1,X2,X3,X4/0.183434642495650D0,0.525532409916329D0,      &
    & 0.796666477413627D0,0.960289856497536D0/
  DATA W1,W2,W3,W4/0.362683783378362D0,0.313706645877887D0,      &
    & 0.222381034453374D0,0.101228536290376D0/
!C**** MISCELLANEOUS PARAMETERS.
  DATA SQ2/1.414213562373095D0/
  DATA LMN,NLMX,KMX,KML,NBITS/1,30,5000,6,64/
!C**** 8-POINT GAUSS-LEGENDRE INTEGRATION FUNCTION.
  G8(X,H)=H*((W1*(FUN(X-X1*H)+FUN(X+X1*H))+W2*(FUN(X-X2*H)+FUN(X+X2*H)
    &H)))+(W3*(FUN(X-X3*H)+FUN(X+X3*H))+W4*(FUN(X-X4*H)+FUN(X+X4*H)))
!C**** INITIALIZE.
  ANS=0.D0
  IERR=1
  IF(A.EQ.B) RETURN
  LMX=NLMX
  IF(B.EQ.0.D0) GO TO 3
  IF(DSIGN(1.D0,B)*A.LE.0.D0) GO TO 3
  C=DABS(1.D0-A/B)
  IF(C.GT.0.1D0) GO TO 3
  NIB=-IDINT(DLOG(C)/DLOG(2.D0))
  LMX=MINO(NLMX,NBITS-NIB-6)
  LMX=MAXO(LMX,LMN)
3  TOL=DMAX1(ERR,2.D0**(5-NBITS))/2.D0
  IF(ERR.LT.0.D0) TOL=0.5D-6
  EPS=TOL
  HH(1)=(B-A)/4.D0
  AA(1)=A
  LR(1)=1
  L=1
  EST=G8(AA(L)+2.D0*HH(L),2.D0*HH(L))
  K=8
  AREA=DABS(EST)
  EF=0.5D0
  MXL=0
!C**** COMPUTE REFINED ESTIMATES, ESTIMATE THE ERROR, ETC.
  4  GL=G8(AA(L)+HH(L),HH(L))
  GR(L)=G8(AA(L)+3.D0*HH(L),HH(L))
  K=K+16
  AREA=AREA+(DABS(GL)+DABS(GR(L))-DABS(EST))
!C  IF(L.LT.LMN) GO TO 11
  GLR=GL+GR(L)
  EE=EF*DABS(EST-GLR)
  AE=DMAX1(EPS*AREA,TOL*DABS(GLR))
  IF(EE-AE) 6,6,7
  5  MXL=1
  6  IF(LR(L)) 8,8,10
!C**** CONSIDER THE LEFT HALF OF THIS LEVEL.
  7  IF(K.GT.KMX) LMX=KML
  IF(L.GE.LMX) GO TO 5
  L=L+1
  EPS=EPS/2.D0
  EF=EF/SQ2
  HH(L)=HH(L-1)/2.D0
  LR(L)=-1
  AA(L)=AA(L-1)
  EST=GL
  GO TO 4
!C**** PROCEED TO RIGHT HALF AT THIS LEVEL.
  8  VL(L)=GLR
  9  EST=GR(L-1)
  LR(L)=1
  AA(L)=AA(L)+4.D0*HH(L)
  GO TO 4
!C**** RETURN ONE LEVEL.
  10 VR=GLR
  11 IF(L.LE.1) GO TO 14
  L=L-1

```

```
EPS=EPS*2.DO
EF=EF*SQ2
IF(LR(L).GT.0) GO TO 13
VL(L)=VL(L+1)+VR
GO TO 9
13 VR=VL(L+1)+VR
GO TO 11
!C*** EXIT.
14 ANS=VR
IF(MXL.GT.0) IERR=2
RETURN
END
```

li6_sindet.f90: Specialized Detector Efficiency Calculation Code for Sinusoidal Perforations

```
program sindet
  use const_mod
  use kind_mod
  use ions_mod
  use mca_mod
  use parts_mod
  use random_mod
  use surf_mod
  implicit none

  character(len=20) :: arg1, arg2
  real(dknd) :: omega, costheta, phi, d2s, d2c, rand, naeff, naefferr, ed, el, &
    & toteff, totefferr
  real(dknd), parameter :: sigma = 0.0051, ep = 1e-3
  integer :: i, nabs, ndet, theta, psi

  integer, parameter :: NHIST = 1000000
  logical, parameter :: WITH_CAP = .false.
  real(dknd), parameter :: lld = 0.0, uld = 5.0
  integer, parameter :: mcabins = 256

  type (particle_type) :: neut, he, h3

!  open(unit=1,status='unknown',file='coll.dat')
!  open(unit=2,status='unknown',file='surf.dat')
  open(unit=3,status='unknown',file='li6_sin_100-30-30-40.dat')

  delta = 40.0
  width = 30.0
  Adelta = 30.0
  Sidelta = Adelta
  capt = 20.0
  dett = 100.0

!  call init_mca(lld,uld,mcabins)

do theta=0,85,5
  do psi=0,90,5

    write(*,*) "Starting simulation for ", theta, ",", psi

    nabs = 0
    ndet = 0
    do i=1, NHIST

      neut%alive = .true.

      ! SAMPLE FOR NEUTRON INITIAL POSITION
      neut%x = width*fltrnf()
      neut%y = delta*sin(2.0*pi*neut%x/width)-Sidelta + (Adelta+Sidelta)*fltrnf()
      if(WITH_CAP)then
        neut%z = -capt + ep
      else
        neut%z = 0 + ep
      endif
!      neut%z = -capt + (dett+capt)*fltrnf()

      ! SAMPLE FOR NEUTRON INITIAL DIRECTION
      costheta = cos(theta*pi/180.0)
      neut%w = costheta
      neut%u = sqrt(1-costheta*costheta)*cos(psi*pi/180.0)
      neut%v = sqrt(1-costheta*costheta)*sin(psi*pi/180.0)
    enddo
  enddo
```

```

!      costheta = -1.0 + 2.0*fltrnf()
!      phi = 2.0*pi*fltrnf()
!      neut%w = costheta
!      neut%u = sqrt(1.0-costheta*costheta)*cos(phi)
!      neut%v = sqrt(1.0-costheta*costheta)*sin(phi)

do while( neut%alive )

    call getcell(neut)

    if( mod(neut%mycell,2) == 0 )then
        d2c = 0.0
    else
        d2c = -log( fltrnf() ) / sigma
    endif

    d2s = dist2surf(neut)

    if(d2c < d2s .and. d2c /= 0.0)then
        neut%x = neut%x+neut%u*d2c
        neut%y = neut%y+neut%v*d2c
        neut%z = neut%z+neut%w*d2c
        neut%alive = .false.
        nabs = nabs + 1
!      write(1,*) neut%x, neut%y, neut%z

        !set deposited enery to zero
        ed = 0.0

        !make ions alive
        he%alive = .true.
        h3%alive = .true.

        !set he and h3 initial positions
        he%x = neut%x
        he%y = neut%y
        he%z = neut%z
        h3%x = neut%x
        h3%y = neut%y
        h3%z = neut%z

        !set initial energies

        he%e = EresLF(real(0.0,dknd),1)
        h3%e = EresLF(real(0.0,dknd),2)

        !sample he direction and set h3's opposite
        omega = -1+2*fltrnf()
        phi = 2.0*pi*fltrnf()
        he%w = omega
        he%u = sqrt(1-omega*omega) * cos(phi)
        he%v = sqrt(1-omega*omega) * sin(phi)

        h3%u = -he%u
        h3%v = -he%v
        h3%w = -he%w

    do while (he%alive)
        call getcell(he)
        d2s = dist2surf(he)
        if(mod(he%mycell,2)==0)then
            e1 = Edep(he%e,d2s,1,1)
            ed = ed + e1
            he%e = he%e - e1
        else
            he%e = he%e - Edep(he%e,d2s,2,1)
        endif
        if(he%e <= 0.0) he%alive = .false.
    enddo

```

```

    he%x = he%x+he%u*(d2s+ep)
    he%y = he%y+he%v*(d2s+ep)
    he%z = he%z+he%w*(d2s+ep)
    call checkreflect(he)
    if(he%z < -capt) he%alive = .false.
    if(he%z > dett)then
        ed = ed + he%e
        he%alive = .false.
    endif
enddo

do while (h3%alive)
    call getcell(h3)
    d2s = dist2surf(h3)
    if(mod(h3%mycell,2)==0)then
        e1 = Edep(h3%e,d2s,1,2)
        ed = ed + e1
        h3%e = h3%e - e1
    else
        h3%e = h3%e - Edep(h3%e,d2s,2,2)
    endif
    if(h3%e <= 0.0) h3%alive = .false.
    h3%x = h3%x+h3%u*(d2s+ep)
    h3%y = h3%y+h3%v*(d2s+ep)
    h3%z = h3%z+h3%w*(d2s+ep)
    call checkreflect(h3)
    if(h3%z < -capt) h3%alive = .false.
    if(h3%z > dett)then
        ed = ed + h3%e
        h3%alive = .false.
    endif
enddo

if(ed>0.300)ndet = ndet + 1
!   call mca_cnt(ed)

else
    neut%x = neut%x+neut%u*(d2s+ep)
    neut%y = neut%y+neut%v*(d2s+ep)
    neut%z = neut%z+neut%w*(d2s+ep)
    call checkreflect(neut)
    if(neut%z < -capt) neut%alive = .false.
    if(neut%z > dett) neut%alive = .false.
!   write(2,*) neut%x, neut%y, neut%z
endif

enddo
if (mod(i,NHIST/10)==0) write(*,'(2x,i9,a)') i, " histories done..."

enddo

naeff = real(nabs, dknd)/real(NHIST,dknd)
naefferr = sqrt(real(nabs, dknd))/real(NHIST,dknd)
toteff = real(ndet,dknd)/real(NHIST,dknd)
totefferr = sqrt(real(ndet,dknd))/real(NHIST,dknd)

write(3,'(1x,2(i4),6(2x,es12.5))') theta, psi, &
    & naeff, naeff*costheta, naefferr, toteff, toteff*costheta, totefferr

enddo

write(3,*)

enddo

! call deinit_mca()

end program sindet

```

const_mod.f90: A Module of Fundamental Constants

```
module const_mod
  use kind_mod
  implicit none

  real(dknd), parameter :: pi = 3.14159265359
  real(dknd), parameter :: big = 1.0e30

end module const_mod
```

ions_mod.f90: The Ion Transport Algorithms

```
module ions_mod
  use kind_mod
  implicit none

contains

!C%%%%%%%%%%%%%%%%%%%%%%%%%%%%%%%%%%%%%%%%%%%%%%%%%%%%%%%%%%%%%%%%%%%%%%%%
!C%%%%%%%%%%%%%%%%%%%%%%%%%%%%%%%%%%%%%%%%%%%%%%%%%%%%%%%%%%%%%%%%%%%%%%%%
!C%%%%%%%%%%%%%%%%%%%%%%%%%%%%%%%%%%%%%%%%%%%%%%%%%%%%%%%%%%%%%%%%%%%%%%%% Routines for Li-6 Ions %%%%%%%%%
!C%%%%%%%%%%%%%%%%%%%%%%%%%%%%%%%%%%%%%%%%%%%%%%%%%%%%%%%%%%%%%%%%%%%%%%%%
!C%%%%%%%%%%%%%%%%%%%%%%%%%%%%%%%%%%%%%%%%%%%%%%%%%%%%%%%%%%%%%%%%%%%%%%%%

real(dknd) FUNCTION Edep(Eo,s,imat,ipart)
  implicit none
  real(dknd) :: Eo, s, so, E1
  integer :: imat, ipart
!C-----
!C Calculates the energy deposited (Edep) along a path length s in
!C material IMAT for a Li-6 ion (of type IPART) that initially has
!C energy Eo (<Emax) at the start of the path
!C   ipart =1 alpha, =2 triton
!C   imat = 1 silicon, =2 LiF
!C-----
  IF (imat.EQ.1) THEN
    so = XSi(Eo,ipart)
    E1 = EresSi(s+so,ipart)
  ELSE
    so = XLiF(Eo,ipart)
    E1 = EresLF(s+so,ipart)
  ENDIF
  Edep = Eo-E1
  RETURN
END function Edep

real(dknd) FUNCTION EresLF(xx,ipart)
!C-----
!C Residual energy (MeV) for Li-6(n,t)He-4 ions in LiF
!C   xx = path length (um)
!C   ipart = 1 alpha; =2 triton
!C-----
  real(dknd) :: x,xx,y
  real(dknd), dimension(2), parameter :: range = (/6.13d0,32.4d0/)
  integer :: ipart

  x=xx
  IF (x.GT.range(ipart)) THEN
    EresLF=0.0d0
    RETURN
  ENDIF

!C-- case of alpha particle in LiF
  IF (ipart.EQ.1) THEN
    EresLF = (2.045795872242105D0+x*(-0.6656803951074236D0+
& x*(0.05419252954318524D0)))/
& (1.0+x*(-0.1618681522606121D0+x*(-0.0004073163152857422D0+
& x*(0.001694213790128516D0))))
!C-- case of triton in LiF
  ELSE
    y = (1.002503409342673D0+x*(-0.06518537556264785D0+
& x*(0.0009570698188079860D0)))/
& (1.0+x*(-0.04378737038158115D0+x*(0.0004104515518016601D0)))
    EresLF = DEXP(y)
  ENDIF

```



```

RETURN
END function EresLF

```

```

real(dknd) FUNCTION EresSi(xx,ipart)
  implicit none
!C-----
!C Residual energy (MeV) for Li-6(n,t)He-4 ions in Si
!C   xx   = path length (um)
!C   ipart = 1 alpha; =2 triton
!C-----
  real(dknd) :: x,xx,y
  real(dknd), dimension(2), parameter :: range = (/7.37d0,42.1d0/)
  integer :: ipart

  x=xx
  IF (x.GT.range(ipart)) THEN
    EresSi=0.0d0
    RETURN
  ENDIF
!C-- case of alpha particle in silicon
  IF (ipart.EQ.1) THEN
    EresSi = (2.054968416876924D0+x*(-0.5570727177716902D0+
&      x*(0.03778001355325864D0)))/
&      (1.0+x*(-0.1483764307642617D0
&      +x*(-0.0005753511256927519D0+
&      x*(0.0007588407797898662D0))))
!C-- case of triton in silicon
  ELSE
    y = (0.9984993786783298D0+x*(-0.04902551060382791D0+
&      x*(0.0005428269966035989D0)))/
&      (1.0+x*(-0.03278510294862023D0+x*(0.0002214134270311182D0)))
    EresSi = DEXP(y)

  ENDIF
  RETURN
END function EresSi

```

```

real(dknd) FUNCTION XSi(EE,ipart)
  implicit none
!C-----
!C Path length in Si to reduce the original energy of the alpha
!C (ipart=1) and the triton (ipart=2) from the Li-6(n,t)He-4 reaction
!C to an energy EE
!C-----
  real(dknd) :: e, EE
  real(dknd) :: x,x1,x2,x3,x4,DLG
  real(dknd), dimension(2), parameter :: Rmax=(/7.37d0,42.1d0/),
&      Emax=(/2.05d0,2.73d0/)
  integer :: ipart

  e=EE
  IF (e.LE.0.0d0) THEN
    Xsi=Rmax(ipart)
    RETURN
  ELSEIF (e.GE.Emax(ipart)) THEN
    Xsi = 0.0d0
    RETURN
  ENDIF
!C-- alpha in silicon (TC 7904)
  IF(ipart.EQ.1) THEN
    x=DSQRT(e)
    XSi = 7.650654782456231D0+x*(-2.951907906029242D0+
&      x*(-3.226254043595208D0+x*(12.90757367270686D0+
&      x*(-19.00554784825017D0+x*(10.85346324881674D0+
&      x*(-2.337319132539310D0))))))

```

```

!C-- triton in silicon (TC 4328)
ELSE
  x1=e
  x2=e*e
  DLG = DLOG(e)
  x3=x2*DLG
  x4=DSQRT(e)*DLG
  XSi = 42.55432730826800D0-6.126822912741065D0*x1          &
&      -5.405288206496186D0*x2+1.274522449649497D0*x3      &
&      +2.744516841023055D0*x4
ENDIF
XSi = MAX(0.0,XSi)

RETURN
END function XSi

real(dknd) FUNCTION XLiF(EE,ipart)
  implicit none
!C-----
!C  Path length in LiF to reduce the original energy of the alpha
!C  (ipart=1) and the triton (ipart=2) from the Li-6(n,t)He-4 reaction
!C  to an energy EE
!C-----
  real(dknd) :: e, EE
  real(dknd) :: x,x1,x2,x3,x4,DLG
  real(dknd), dimension(2), parameter :: Rmax=(/6.13d0,32.4d0/), &
    & Emax=(/2.05d0,2.73d0/)
  integer :: ipart

  e=EE
  IF (e.LE.0.0d0) THEN
    XLiF=Rmax(ipart)
    RETURN
  ELSEIF (e.GE.Emax(ipart)) THEN
    XLiF = 0.0d0
    RETURN
  ENDIF

!C-- alpha in silicon (TC 7904)
  IF(ipart.EQ.1) THEN
    x=DSQRT(e)
    XLiF=6.312636231356213D0+x*(-3.594256350143011D0+
&      x*(1.968648983630100D0+x*(-1.822537261104411D0+
&      x*(0.1363849426609869D0+x*(-0.1283915688540728D0+
&      x*(0.03773779891639750D0))))))
!C-- triton in silicon (TC 4328)
  ELSE
    x1=e
    x2=e*e
    DLG = DLOG(e)
    x3=x2*DLG
    x4=DSQRT(e)*DLG

    XLiF=33.05498950931498D0-6.885172032726404D0*x1          &
&      -2.727479733376275D0*x2+0.3125211180119474D0*x3      &
&      +2.194886238812784D0*x4
  ENDIF
  XLiF = MAX(0.0,XLiF)

RETURN
END function XLiF

end module ions_mod

```

kind_mod.f90: A Module of Fortran Kinds

```
module kind_mod
  implicit none

  integer,parameter :: i4knd = selected_int_kind( 9)      != 4-byte integer kind
  integer,parameter :: i8knd = selected_int_kind(18)      != 8-byte integer kind
  integer,parameter :: rknd  = selected_real_kind( 6, 37) != real kind
  integer,parameter :: dknd  = selected_real_kind(15,307) != 8-byte real kind

end module kind_mod
```

mca_mod.f90: A Module for Energy Depositon Spectra

```
module mca_mod
  use kind_mod
  implicit none

  real(dknd) :: mca_max_e, mca_min_e, mca_de
  integer :: mca_nbin

  integer, dimension(:), pointer :: mca_bin_cnts
  real, dimension(:), pointer :: mca_e_bins

contains

subroutine init_mca(mine, maxe, nbin)
  implicit none

  real(dknd) :: mine, maxe
  integer :: i, nbin

  mca_min_e = mine
  mca_max_e = maxe
  mca_nbin = nbin

  mca_de = (mca_max_e - mca_min_e)/real(mca_nbin, dknd)

  allocate(mca_bin_cnts(mca_nbin))
  mca_bin_cnts = 0.0

  allocate(mca_e_bins(mca_nbin))
  do i=1, mca_nbin
    mca_e_bins(i) = mca_min_e + i * mca_de
  enddo

end subroutine init_mca

subroutine mca_cnt(energy)
  implicit none

  real(dknd) :: energy
  integer :: i

  if (energy < mca_min_e .or. energy > mca_max_e) return

  do i=1,mca_nbin
    if(energy < mca_e_bins(i))then
      mca_bin_cnts(i) = mca_bin_cnts(i) + 1
      return
    endif
  enddo
end subroutine mca_cnt

subroutine deinit_mca()
  implicit none
  integer :: i

  open(unit=4,status='unknown',file='mca.dat')

  do i=1, mca_nbin
    write(4,'(2x,es12.5,2x,i9)')mca_e_bins(i), mca_bin_cnts(i)
  enddo

  if(associated(mca_bin_cnts))deallocate(mca_bin_cnts)
  if(associated(mca_e_bins))deallocate(mca_e_bins)

  close(4)
```

```
end subroutine deinit_mca
end module mca_mod
```

parts_mod.f90: A Module for a Particle Type

```
module parts_mod
  use kind_mod
  implicit none

  type particle_type
    real(dknd) :: x,y,z
    real(dknd) :: u,v,w
    real(dknd) :: e

    integer :: mycell

    logical :: alive
  end type particle_type
end module parts_mod
```

random_mod.f90: A Module for a Pseudo Random Number Generation

```
module random_mod
  use kind_mod
  implicit none
  real(dknd) :: dseed = 12473

  contains

  real(kind=8) function fltrnf()
    implicit none
    real(dknd), parameter :: &
      & A = 16807.0, &
      & M = 2147483647.0, &
      & B = 0.465661287524579692e-9
    real(dknd) :: temp

    temp = dseed*A
    dseed = temp-M*int(temp*B)
    fltrnf = dseed*B

    return
  end function fltrnf
end module random_mod
```

surf_mod.f90: A Module for Geometry Specification

```
module surf_mod
  use const_mod
  use kind_mod
  use parts_mod
  use zero_mod
  implicit none

  real(dknd) :: delta, Adelta, Sdelta, capt, dett
  real(dknd) :: xo, yo, zo, alfa, beta, gama, width

contains

#####

real(dknd) function s1zero(d)
  implicit none
  real(dknd) :: d
  s1zero = delta*sin( 2.0*pi*(xo+d*alfa)/width ) + Adelta - yo - d*beta
  return
end function s1zero

#####

real(dknd) function s2zero(d)
  implicit none
  real(dknd) :: d
  s2zero = delta*sin( 2.0*pi*(xo+d*alfa)/width ) - yo - d*beta
  return
end function s2zero

#####

real(dknd) function s3zero(d)
  implicit none
  real(dknd) :: d
  s3zero = delta*sin( 2.0*pi*(xo+d*alfa)/width ) - Sdelta - yo - d*beta
  return
end function s3zero

#####

real(dknd) function dist2s1()
  implicit none
  real(dknd) :: lb, ub
  real(dknd) :: step

  step = nint(width/10)

  lb = 0.0
  do while (lb < 300.0)
    ub = lb + step
    if ( (s1zero(lb) < 0.0 .and. s1zero(ub) > 0.0) .or. &
        & (s1zero(lb) > 0.0 .and. s1zero(ub) < 0.0) ) exit
    lb = ub
  enddo

  dist2s1 = zbrent(s1zero,lb,ub,real(1e-6, dknd))

  return
end function dist2s1

#####

real(dknd) function dist2s2()
  implicit none
```



```

real(dknd) :: lb, ub
real(dknd) :: step

step = nint(width/10)

lb = 0.0
do while (lb < 300.0)
  ub = lb + step
  if ( (s2zero(lb) < 0.0 .and. s2zero(ub) > 0.0) .or. &
    & (s2zero(lb) > 0.0 .and. s2zero(ub) < 0.0) ) exit
  lb = ub
enddo

dist2s2 = zbrent(s2zero,lb,ub,real(1e-6, dknd))

return
end function dist2s2

!#####

real(dknd) function dist2s3()
  implicit none
  real(dknd) :: lb, ub
  real(dknd) :: step

  step = nint(width/10)

  lb = 0.0
  do while (lb < 300.0)
    ub = lb + step
    if ( (s3zero(lb) < 0.0 .and. s3zero(ub) > 0.0) .or. &
      & (s3zero(lb) > 0.0 .and. s3zero(ub) < 0.0) ) exit
    lb = ub
  enddo

  dist2s3 = zbrent(s3zero,lb,ub,real(1e-6, dknd))

  return
end function dist2s3

!#####

real(dknd) function dist2s4()
  implicit none

  dist2s4 = -xo / alfa

  return
end function dist2s4

!#####

real(dknd) function dist2s5()
  implicit none

  dist2s5 = (width-xo) / alfa

  return
end function dist2s5

!#####

real(dknd) function dist2s6()
  implicit none

  dist2s6 = (-capt - zo) / gama

  return

```

```

end function dist2s6

!#####

real(dknd) function dist2s7()
  implicit none

  dist2s7 = -zo / gama

  return
end function dist2s7

!#####

real(dknd) function dist2s8()
  implicit none

  dist2s8 = (dett - zo) / gama

  return
end function dist2s8

!#####

real(dknd) function dist2surf(part)
  implicit none

  type (particle_type) :: part

  real(dknd) :: d, dtemp

  xo = part%x
  yo = part%y
  zo = part%z
  alfa = part%u
  beta = part%v
  gama = part%w

  d = big

  select case (part%mycell)

  case(1)
    dtemp = dist2s1()
    if(dtemp > 0.0 .and. dtemp < d)d=dtemp
    dtemp = dist2s3()
    if(dtemp > 0.0 .and. dtemp < d)d=dtemp
    dtemp = dist2s4()
    if(dtemp > 0.0 .and. dtemp < d)d=dtemp
    dtemp = dist2s5()
    if(dtemp > 0.0 .and. dtemp < d)d=dtemp
    dtemp = dist2s6()
    if(dtemp > 0.0 .and. dtemp < d)d=dtemp
    dtemp = dist2s7()
    if(dtemp > 0.0 .and. dtemp < d)d=dtemp

  case(2)
    dtemp = dist2s2()
    if(dtemp > 0.0 .and. dtemp < d)d=dtemp
    dtemp = dist2s3()
    if(dtemp > 0.0 .and. dtemp < d)d=dtemp
    dtemp = dist2s4()
    if(dtemp > 0.0 .and. dtemp < d)d=dtemp
    dtemp = dist2s5()
    if(dtemp > 0.0 .and. dtemp < d)d=dtemp
    dtemp = dist2s7()
    if(dtemp > 0.0 .and. dtemp < d)d=dtemp
    dtemp = dist2s8()

```

```

        if(dtemp > 0.0 .and. dtemp < d)d=dtemp

case(3)
    dtemp = dist2s1()
    if(dtemp > 0.0 .and. dtemp < d)d=dtemp
    dtemp = dist2s2()
    if(dtemp > 0.0 .and. dtemp < d)d=dtemp
    dtemp = dist2s4()
    if(dtemp > 0.0 .and. dtemp < d)d=dtemp
    dtemp = dist2s5()
    if(dtemp > 0.0 .and. dtemp < d)d=dtemp
    dtemp = dist2s7()
    if(dtemp > 0.0 .and. dtemp < d)d=dtemp
    dtemp = dist2s8()
    if(dtemp > 0.0 .and. dtemp < d)d=dtemp
end select

dist2surf = d

return
end function dist2surf

!#####

subroutine getcell(part)
    implicit none

    type (particle_type) :: part

    xo = part%x
    yo = part%y
    zo = part%z

    if( zo < 0.0 )then
        part%mycell = 1
        return
    else
        if((yo > delta*sin(2.0*pi*xo/width) - Sidelta) .and. (yo < delta*sin(2.0*pi*xo/width)) )then
            part%mycell = 2
            return
        endif

        if((yo > delta*sin(2.0*pi*xo/width)) .and. (yo < delta*sin(2.0*pi*xo/width) + Adelta))then
            part%mycell = 3
            return
        endif
    endif

end subroutine getcell

!#####

subroutine checkreflect(part)
    implicit none

    type (particle_type) :: part

    if(part%x > width) part%x = part%x - width
    if(part%x < 0.0) part%x = part%x + width
    if(part%y > delta*sin(2.0*pi*part%x/width)+Adelta) part%y = part%y - Adelta - Sidelta
    if(part%y < delta*sin(2.0*pi*part%x/width)-Sidelta) part%y = part%y + Adelta + Sidelta

end subroutine checkreflect

end module surf_mod

```

zero_mod.f90: A Module for Finding Zeros of a Function

```
module zero_mod
  use kind_mod
  implicit none

  interface
    real(dknd) function func(x)
      use kind_mod
      implicit none
      real(dknd) :: x
    end function func
  end interface

contains

real(dknd) function zridders(func, x1, x2, xacc)
  integer, parameter :: MAXIT = 60
  real(dknd) x1,x2,xacc, func
  real(dknd) , parameter :: UNUSED=-1.11e30
  integer j
  real(dknd) fh,f1,fm,fnew,s,xh,xl,xm,xnew
  f1=func(x1)
  fh=func(x2)
  if((f1>0..and.fh<0.)..or.(f1<0..and.fh>0.))then
    xl=x1
    xh=x2
    zridders=UNUSED
    do j=1,MAXIT
      xm=0.5*(x1+xh)
      fm=func(xm)
      s=sqrt(fm**2-f1*fh)
      if(s==0.)return
      xnew=xm+(xm-xl)*(sign(1.,real(f1-fh, rknd))*fm/s)
      if (abs(xnew-zridders)<=xacc) return
      zridders=xnew
      fnew=func(zridders)
      if (fnew==0.) return
      if (sign(real(fm,rknd),real(fnew,rknd))/=fm) then
        xl=xm
        fl=fm
        xh=zridders
        fh=fnew
      else if (sign(real(fl, rknd),real(fnew,rknd))/=fl) then
        xh=zridders
        fh=fnew
      else if (sign(real(fh, rknd),real(fnew, rknd))/=fh) then
        xl=zridders
        fl=fnew
      else
        pause 'never get here in zriddr'
      endif
      if(abs(xh-xl)<=xacc) return
    enddo
    pause 'zriddr exceed maximum iterations'
  else if (f1==0.) then
    zridders=x1
  else if (fh==0.) then
    zridders=x2
  else
    pause 'root must be bracketed in zriddr'
  endif
  return
end function zridders
```

```

real(dknd) function zbrent(func,x1,x2,tol)
  integer, parameter :: ITMAX = 100
  real(dknd) :: tol,x1,x2,func
  real(dknd) , parameter :: EPS = 3.0e-8
  integer :: iter
  real(dknd) :: a,b,c,d,e,fa,fb,fc,p,q,r,s,tol1,xm
  a=x1
  b=x2
  fa=func(a)
  fb=func(b)
! if((fa>0..and.fb>0.)..or.(fa<0..and.fb<0.))
  c=b
  fc=fb
  do iter=1,ITMAX
    if((fb>0..and.fc>0.)..or.(fb<0..and.fc<0.))then
      c=a
      fc=fa
      d=b-a
      e=d
    endif

    if(abs(fc)<abs(fb)) then
      a=b
      b=c
      c=a
      fa=fb
      fb=fc
      fc=fa
    endif
    tol1=2.*EPS*abs(b)+0.5*tol
    xm=.5*(c-b)
    if(abs(xm)<=tol1 .or. fb==0.)then
      zbrent=b
      return
    endif
    if(abs(e)>=tol1 .and. abs(fa)>abs(fb)) then
      s=fb/fa
      if(a==c) then
        p=2.*xm*s
        q=1.-s
      else
        q=fa/fc
        r=fb/fc
        p=s*(2.*xm*q*(q-r)-(b-a)*(r-1.))
        q=(q-1.)*(r-1.)*(s-1.)
      endif
      if(p>0.) q=-q
      p=abs(p)
      if(2.*p < min(3.*xm*q-abs(tol1*q),abs(e*q))) then
        e=d
        d=p/q
      else
        d=xm
        e=d
      endif
    else
      d=xm
      e=d
    endif
    a=b
    fa=fb
    if(abs(d) > tol1) then
      b=b+d
    else
      b=b+sign(real(tol1,rknd),real(xm,rknd))
    endif
    fb=func(b)

```

```
    enddo
    pause 'zbrent exceeding maximum iterations'
    zbrent=b
    return
end function zbrent

end module zero_mod
```

Appendix B

Perforated Detector Efficiency Tabulated Data

Absorber	Perforation Type	Description	Page
^{10}B	Rod	30 μm Perforation Depth, 6 μm Diameter Rods, and no cap	134
^{10}B	Rod	50 μm Perforation Depth, 6 μm Diameter Rods, and no cap	143
^{10}B	Rod	30 μm Perforation Depth, 6 μm Diameter Rods, and 4 μm cap	152
^6LiF	Rod	100 μm Perforation Depth, 30 μm Diameter Rods, and no cap	161
^6LiF	Rod	300 μm Perforation Depth, 30 μm Diameter Rods, and no cap	170
^6LiF	Rod	100 μm Perforation Depth, 30 μm Diameter Rods, and 20 μm cap	179
^{10}B	Channel	30 μm Perforation Depth, 4 μm Channel Width, and no cap	188
^{10}B	Channel	50 μm Perforation Depth, 4 μm Channel Width, and no cap	197
^6LiF	Channel	100 μm Perforation Depth, 20 μm Channel Width, and no cap	206
^{10}B	Chevron	30 μm Perforation Depth, 4 μm Channel Width, and no cap	215
^6LiF	Chevron	100 μm Perforation Depth, 20 μm Channel Width, and no cap	224
^{10}B	Sinusoidal	30 μm Perforation Depth, 4 μm Cell Width, 4 μm Pitch, 4 μm Wave Amplitude, and no cap	233
^{10}B	Sinusoidal	10 μm Perforation Depth, 8 μm Cell Width, 0.5 μm Pitch, 1 μm Wave Amplitude, and no cap	242

Absorber	Perforation Type	Description	Page
${}^6\text{LiF}$	Sinusoidal	100 μm Perforation Depth, 20 μm Cell Width, 20 μm Pitch, 20 μm Wave Amplitude, and no cap	251
${}^6\text{LiF}$	Sinusoidal	100 μm Perforation Depth, 30 μm Cell Width, 30 μm Pitch, 40 μm Wave Amplitude, and no cap	260
${}^6\text{LiF}$	Sinusoidal	100 μm Perforation Depth, 130 μm Cell Width, 35 μm Pitch, 40 μm Wave Amplitude, and no cap	269

Table B.1. ^{10}B rod detector with 30 μm deep perforations, 6 μm diameter rods, and no cap

ψ	p_n	η	ε
$\theta = 0$			
0	2.62378E-01	5.56098E-01	1.45908E-01
3	2.62378E-01	5.56098E-01	1.45908E-01
6	2.62378E-01	5.56098E-01	1.45908E-01
9	2.62378E-01	5.56098E-01	1.45908E-01
12	2.62378E-01	5.56098E-01	1.45908E-01
15	2.62378E-01	5.56098E-01	1.45908E-01
18	2.62378E-01	5.56098E-01	1.45908E-01
21	2.62378E-01	5.56098E-01	1.45908E-01
24	2.62378E-01	5.56098E-01	1.45908E-01
27	2.62378E-01	5.56098E-01	1.45908E-01
30	2.62378E-01	5.56098E-01	1.45908E-01
33	2.62378E-01	5.56098E-01	1.45908E-01
36	2.62378E-01	5.56098E-01	1.45908E-01
39	2.62378E-01	5.56098E-01	1.45908E-01
42	2.62378E-01	5.56098E-01	1.45908E-01
45	2.62378E-01	5.56098E-01	1.45908E-01
$\theta = 5$			
0	3.01552E-01	5.93702E-01	1.79032E-01
3	3.01700E-01	5.94398E-01	1.79330E-01
6	3.01936E-01	5.94401E-01	1.79471E-01
9	3.01897E-01	5.94401E-01	1.79448E-01
12	3.02228E-01	5.94799E-01	1.79765E-01
15	3.01896E-01	5.95699E-01	1.79839E-01
18	3.02007E-01	5.94900E-01	1.79664E-01
21	3.02015E-01	5.94401E-01	1.79518E-01
24	3.01456E-01	5.93699E-01	1.78974E-01
27	3.01619E-01	5.94101E-01	1.79192E-01
30	3.02100E-01	5.94601E-01	1.79629E-01
33	3.02464E-01	5.94398E-01	1.79784E-01
36	3.02241E-01	5.93698E-01	1.79440E-01
39	3.01788E-01	5.94699E-01	1.79473E-01
42	3.02045E-01	5.93398E-01	1.79233E-01
45	3.01886E-01	5.93399E-01	1.79139E-01

ψ	p_n	η	ε
$\theta = 10$			
0	3.34282E-01	5.92999E-01	1.98229E-01
3	3.34330E-01	5.93399E-01	1.98391E-01
6	3.34781E-01	5.92799E-01	1.98458E-01
9	3.35106E-01	5.93499E-01	1.98885E-01
12	3.35532E-01	5.93800E-01	1.99239E-01
15	3.35979E-01	5.94498E-01	1.99739E-01
18	3.36317E-01	5.93401E-01	1.99571E-01
21	3.36798E-01	5.94401E-01	2.00193E-01
24	3.37752E-01	5.95398E-01	2.01097E-01
27	3.38522E-01	5.95400E-01	2.01556E-01
30	3.38699E-01	5.96798E-01	2.02135E-01
33	3.39362E-01	5.96101E-01	2.02294E-01
36	3.39362E-01	5.96699E-01	2.02497E-01
39	3.38829E-01	5.96499E-01	2.02111E-01
42	3.39344E-01	5.96401E-01	2.02385E-01
45	3.39664E-01	5.97299E-01	2.02881E-01
$\theta = 15$			
0	3.46661E-01	5.84499E-01	2.02623E-01
3	3.47588E-01	5.84100E-01	2.03026E-01
6	3.48237E-01	5.83999E-01	2.03370E-01
9	3.49543E-01	5.84898E-01	2.04447E-01
12	3.51730E-01	5.84801E-01	2.05692E-01
15	3.54241E-01	5.84901E-01	2.07196E-01
18	3.56436E-01	5.86400E-01	2.09014E-01
21	3.59104E-01	5.85599E-01	2.10291E-01
24	3.61856E-01	5.87001E-01	2.12410E-01
27	3.64258E-01	5.86999E-01	2.13819E-01
30	3.66531E-01	5.87800E-01	2.15447E-01
33	3.68664E-01	5.90500E-01	2.17696E-01
36	3.70449E-01	5.90500E-01	2.18750E-01
39	3.71588E-01	5.91701E-01	2.19869E-01
42	3.72041E-01	5.92599E-01	2.20471E-01
45	3.72114E-01	5.92501E-01	2.20478E-01

ψ	p_n	η	ε
$\theta = 20$			
0	3.42093E-01	5.79600E-01	1.98277E-01
3	3.43656E-01	5.81200E-01	1.99733E-01
6	3.47041E-01	5.81001E-01	2.01631E-01
9	3.51241E-01	5.82301E-01	2.04528E-01
12	3.56071E-01	5.81901E-01	2.07198E-01
15	3.60770E-01	5.82000E-01	2.09968E-01
18	3.66394E-01	5.81199E-01	2.12948E-01
21	3.71406E-01	5.80901E-01	2.15750E-01
24	3.75952E-01	5.79500E-01	2.17864E-01
27	3.79552E-01	5.78701E-01	2.19647E-01
30	3.83008E-01	5.79301E-01	2.21877E-01
33	3.85702E-01	5.79600E-01	2.23553E-01
36	3.88049E-01	5.81599E-01	2.25689E-01
39	3.89192E-01	5.83601E-01	2.27133E-01
42	3.89473E-01	5.85201E-01	2.27920E-01
45	3.89072E-01	5.84501E-01	2.27413E-01
$\theta = 25$			
0	3.35986E-01	5.81200E-01	1.95275E-01
3	3.38889E-01	5.81400E-01	1.97030E-01
6	3.44408E-01	5.83900E-01	2.01100E-01
9	3.51063E-01	5.83699E-01	2.04915E-01
12	3.58407E-01	5.82801E-01	2.08880E-01
15	3.66198E-01	5.80402E-01	2.12542E-01
18	3.73965E-01	5.79100E-01	2.16563E-01
21	3.79731E-01	5.75700E-01	2.18611E-01
24	3.84188E-01	5.73500E-01	2.20332E-01
27	3.87377E-01	5.71900E-01	2.21541E-01
30	3.89433E-01	5.72401E-01	2.22912E-01
33	3.90631E-01	5.73301E-01	2.23949E-01
36	3.90812E-01	5.77400E-01	2.25655E-01
39	3.89890E-01	5.79699E-01	2.26019E-01
42	3.88125E-01	5.80099E-01	2.25151E-01
45	3.86720E-01	5.79900E-01	2.24259E-01

ψ	p_n	η	ε
$\theta = 30$			
0	3.31309E-01	5.78599E-01	1.91695E-01
3	3.35511E-01	5.81802E-01	1.95201E-01
6	3.42710E-01	5.83301E-01	1.99903E-01
9	3.52099E-01	5.82402E-01	2.05063E-01
12	3.61926E-01	5.82000E-01	2.10641E-01
15	3.72122E-01	5.79700E-01	2.15719E-01
18	3.80783E-01	5.77400E-01	2.19864E-01
21	3.86846E-01	5.71600E-01	2.21121E-01
24	3.89975E-01	5.67901E-01	2.21467E-01
27	3.91333E-01	5.66901E-01	2.21847E-01
30	3.91605E-01	5.67500E-01	2.22236E-01
33	3.90511E-01	5.71600E-01	2.23216E-01
36	3.88219E-01	5.75399E-01	2.23381E-01
39	3.84992E-01	5.79100E-01	2.22949E-01
42	3.80225E-01	5.80501E-01	2.20721E-01
45	3.76713E-01	5.78401E-01	2.17891E-01
$\theta = 35$			
0	3.22400E-01	5.78300E-01	1.86444E-01
3	3.28212E-01	5.81700E-01	1.90921E-01
6	3.38667E-01	5.84102E-01	1.97816E-01
9	3.51133E-01	5.82400E-01	2.04500E-01
12	3.63111E-01	5.79200E-01	2.10314E-01
15	3.73864E-01	5.75501E-01	2.15159E-01
18	3.82056E-01	5.72000E-01	2.18536E-01
21	3.85959E-01	5.67099E-01	2.18877E-01
24	3.87149E-01	5.62499E-01	2.17771E-01
27	3.86713E-01	5.60501E-01	2.16753E-01
30	3.86374E-01	5.62900E-01	2.17490E-01
33	3.85221E-01	5.66999E-01	2.18420E-01
36	3.83256E-01	5.73199E-01	2.19682E-01
39	3.79547E-01	5.78300E-01	2.19492E-01
42	3.74554E-01	5.81398E-01	2.17765E-01
45	3.70550E-01	5.79401E-01	2.14697E-01

ψ	p_n	η	ε
$\theta = 40$			
0	3.12832E-01	5.78199E-01	1.80879E-01
3	3.20347E-01	5.81198E-01	1.86185E-01
6	3.34574E-01	5.83198E-01	1.95123E-01
9	3.50113E-01	5.82201E-01	2.03836E-01
12	3.64000E-01	5.77299E-01	2.10137E-01
15	3.72869E-01	5.72399E-01	2.13430E-01
18	3.78520E-01	5.70099E-01	2.15794E-01
21	3.78686E-01	5.65701E-01	2.14223E-01
24	3.76736E-01	5.61799E-01	2.11650E-01
27	3.74952E-01	5.59101E-01	2.09636E-01
30	3.75737E-01	5.61699E-01	2.11051E-01
33	3.76507E-01	5.66300E-01	2.13216E-01
36	3.75543E-01	5.70300E-01	2.14172E-01
39	3.73311E-01	5.76099E-01	2.15064E-01
42	3.68848E-01	5.80201E-01	2.14006E-01
45	3.64538E-01	5.78601E-01	2.10922E-01
$\theta = 45$			
0	3.00592E-01	5.77900E-01	1.73712E-01
3	3.11328E-01	5.83700E-01	1.81722E-01
6	3.28846E-01	5.83899E-01	1.92013E-01
9	3.48101E-01	5.80699E-01	2.02142E-01
12	3.60857E-01	5.72800E-01	2.06699E-01
15	3.67087E-01	5.67699E-01	2.08395E-01
18	3.69225E-01	5.66998E-01	2.09350E-01
21	3.67771E-01	5.63601E-01	2.07276E-01
24	3.65131E-01	5.62100E-01	2.05240E-01
27	3.63783E-01	5.59699E-01	2.03609E-01
30	3.66271E-01	5.62499E-01	2.06027E-01
33	3.68478E-01	5.64701E-01	2.08080E-01
36	3.67882E-01	5.67802E-01	2.08884E-01
39	3.64581E-01	5.73798E-01	2.09196E-01
42	3.58202E-01	5.79198E-01	2.07470E-01
45	3.51276E-01	5.77099E-01	2.02721E-01

ψ	p_n	η	ε
$\theta = 50$			
0	2.86445E-01	5.78299E-01	1.65651E-01
3	3.00203E-01	5.85301E-01	1.75709E-01
6	3.23300E-01	5.85401E-01	1.89260E-01
9	3.43276E-01	5.77200E-01	1.98139E-01
12	3.53603E-01	5.68799E-01	2.01129E-01
15	3.55446E-01	5.65098E-01	2.00862E-01
18	3.54036E-01	5.64798E-01	1.99959E-01
21	3.52547E-01	5.63000E-01	1.98484E-01
24	3.52484E-01	5.61501E-01	1.97920E-01
27	3.51958E-01	5.57800E-01	1.96322E-01
30	3.53938E-01	5.61299E-01	1.98665E-01
33	3.54942E-01	5.62199E-01	1.99548E-01
36	3.54846E-01	5.64698E-01	2.00381E-01
39	3.52241E-01	5.71898E-01	2.01446E-01
42	3.46442E-01	5.78501E-01	2.00417E-01
45	3.38303E-01	5.78201E-01	1.95607E-01
$\theta = 55$			
0	2.68637E-01	5.78498E-01	1.55406E-01
3	2.87347E-01	5.86601E-01	1.68558E-01
6	3.15849E-01	5.84001E-01	1.84456E-01
9	3.33776E-01	5.72300E-01	1.91020E-01
12	3.38950E-01	5.65600E-01	1.91710E-01
15	3.36732E-01	5.63000E-01	1.89580E-01
18	3.36169E-01	5.64802E-01	1.89869E-01
21	3.37497E-01	5.63700E-01	1.90247E-01
24	3.37537E-01	5.59100E-01	1.88717E-01
27	3.36053E-01	5.53600E-01	1.86039E-01
30	3.37545E-01	5.60100E-01	1.89059E-01
33	3.37723E-01	5.62402E-01	1.89936E-01
36	3.38596E-01	5.64200E-01	1.91036E-01
39	3.37493E-01	5.68101E-01	1.91730E-01
42	3.31474E-01	5.77300E-01	1.91360E-01
45	3.21162E-01	5.78499E-01	1.85792E-01

ψ	p_n	η	ε
$\theta = 60$			
0	2.47755E-01	5.78802E-01	1.43401E-01
3	2.72961E-01	5.88901E-01	1.60747E-01
6	3.05064E-01	5.79400E-01	1.76754E-01
9	3.17688E-01	5.67702E-01	1.80352E-01
12	3.17204E-01	5.62600E-01	1.78459E-01
15	3.15583E-01	5.62701E-01	1.77579E-01
18	3.17424E-01	5.63300E-01	1.78805E-01
21	3.17741E-01	5.60000E-01	1.77935E-01
24	3.16762E-01	5.58201E-01	1.76817E-01
27	3.15051E-01	5.52799E-01	1.74160E-01
30	3.17913E-01	5.59398E-01	1.77840E-01
33	3.17821E-01	5.60602E-01	1.78171E-01
36	3.17283E-01	5.61499E-01	1.78154E-01
39	3.17347E-01	5.65400E-01	1.79428E-01
42	3.12500E-01	5.75101E-01	1.79719E-01
45	3.00931E-01	5.78501E-01	1.74089E-01
$\theta = 65$			
0	2.22381E-01	5.78503E-01	1.28648E-01
3	2.56515E-01	5.91400E-01	1.51703E-01
6	2.87736E-01	5.73300E-01	1.64959E-01
9	2.91623E-01	5.63601E-01	1.64359E-01
12	2.90013E-01	5.61099E-01	1.62726E-01
15	2.91860E-01	5.60700E-01	1.63646E-01
18	2.91580E-01	5.59802E-01	1.63227E-01
21	2.91439E-01	5.58999E-01	1.62914E-01
24	2.91771E-01	5.56601E-01	1.62400E-01
27	2.89920E-01	5.49800E-01	1.59398E-01
30	2.91750E-01	5.58602E-01	1.62972E-01
33	2.91981E-01	5.57598E-01	1.62808E-01
36	2.91661E-01	5.59399E-01	1.63155E-01
39	2.91863E-01	5.61000E-01	1.63735E-01
42	2.88427E-01	5.71999E-01	1.64980E-01
45	2.74961E-01	5.78100E-01	1.58955E-01

ψ	p_n	η	ε
$\theta = 70$			
0	1.92065E-01	5.76898E-01	1.10802E-01
3	2.37566E-01	5.92000E-01	1.40639E-01
6	2.59415E-01	5.66698E-01	1.47010E-01
9	2.57192E-01	5.61301E-01	1.44362E-01
12	2.59191E-01	5.58499E-01	1.44758E-01
15	2.58538E-01	5.56700E-01	1.43928E-01
18	2.58905E-01	5.58100E-01	1.44495E-01
21	2.58957E-01	5.55598E-01	1.43876E-01
24	2.58967E-01	5.54302E-01	1.43546E-01
27	2.57079E-01	5.45700E-01	1.40288E-01
30	2.58765E-01	5.54801E-01	1.43563E-01
33	2.58909E-01	5.55601E-01	1.43850E-01
36	2.59168E-01	5.56500E-01	1.44227E-01
39	2.58745E-01	5.58902E-01	1.44613E-01
42	2.58173E-01	5.66701E-01	1.46307E-01
45	2.42422E-01	5.78499E-01	1.40241E-01
$\theta = 75$			
0	1.55141E-01	5.76299E-01	8.94076E-02
3	2.09808E-01	5.84201E-01	1.22570E-01
6	2.15293E-01	5.59698E-01	1.20499E-01
9	2.16669E-01	5.55497E-01	1.20359E-01
12	2.16152E-01	5.53499E-01	1.19640E-01
15	2.16427E-01	5.52200E-01	1.19511E-01
18	2.16399E-01	5.52701E-01	1.19604E-01
21	2.16344E-01	5.51298E-01	1.19270E-01
24	2.16553E-01	5.49501E-01	1.18996E-01
27	2.15134E-01	5.40700E-01	1.16323E-01
30	2.16624E-01	5.50798E-01	1.19316E-01
33	2.16406E-01	5.50498E-01	1.19131E-01
36	2.16580E-01	5.52198E-01	1.19595E-01
39	2.16754E-01	5.54398E-01	1.20168E-01
42	2.16367E-01	5.59401E-01	1.21036E-01
45	2.01543E-01	5.78298E-01	1.16552E-01

ψ	p_n	η	ε
$\theta = 80$			
0	1.10307E-01	5.71802E-01	6.30738E-02
3	1.60233E-01	5.68500E-01	9.10925E-02
6	1.60160E-01	5.51399E-01	8.83121E-02
9	1.60115E-01	5.47399E-01	8.76468E-02
12	1.60147E-01	5.45601E-01	8.73763E-02
15	1.60305E-01	5.44801E-01	8.73343E-02
18	1.60076E-01	5.45100E-01	8.72574E-02
21	1.60293E-01	5.43299E-01	8.70871E-02
24	1.60149E-01	5.42001E-01	8.68009E-02
27	1.59576E-01	5.30900E-01	8.47189E-02
30	1.60350E-01	5.42402E-01	8.69741E-02
33	1.60239E-01	5.42901E-01	8.69939E-02
36	1.60269E-01	5.43499E-01	8.71060E-02
39	1.60153E-01	5.45701E-01	8.73957E-02
42	1.60161E-01	5.50499E-01	8.81685E-02
45	1.48347E-01	5.76699E-01	8.55516E-02
$\theta = 85$			
0	5.77854E-02	5.52700E-01	3.19380E-02
3	8.64926E-02	5.48300E-01	4.74239E-02
6	8.66883E-02	5.32300E-01	4.61442E-02
9	8.65968E-02	5.27300E-01	4.56625E-02
12	8.65645E-02	5.25000E-01	4.54464E-02
15	8.65525E-02	5.23600E-01	4.53189E-02
18	8.65898E-02	5.24200E-01	4.53904E-02
21	8.67074E-02	5.22600E-01	4.53133E-02
24	8.65377E-02	5.20800E-01	4.50688E-02
27	8.65203E-02	5.11100E-01	4.42205E-02
30	8.66513E-02	5.21700E-01	4.52060E-02
33	8.65696E-02	5.21600E-01	4.51547E-02
36	8.66081E-02	5.22900E-01	4.52874E-02
39	8.66234E-02	5.23800E-01	4.53733E-02
42	8.66374E-02	5.29400E-01	4.58658E-02
45	8.04884E-02	5.65100E-01	4.54840E-02

Table B.2. ^{10}B rod detector with 50 μm deep perforations, 6 μm diameter rods, and no cap

ψ	p_n	η	ε
$\theta = 0$			
0	3.09090E-01	5.54101E-01	1.71267E-01
3	3.09090E-01	5.54101E-01	1.71267E-01
6	3.09090E-01	5.54101E-01	1.71267E-01
9	3.09090E-01	5.54101E-01	1.71267E-01
12	3.09090E-01	5.54101E-01	1.71267E-01
15	3.09090E-01	5.54101E-01	1.71267E-01
18	3.09090E-01	5.54101E-01	1.71267E-01
21	3.09090E-01	5.54101E-01	1.71267E-01
24	3.09090E-01	5.54101E-01	1.71267E-01
27	3.09090E-01	5.54101E-01	1.71267E-01
30	3.09090E-01	5.54101E-01	1.71267E-01
33	3.09090E-01	5.54101E-01	1.71267E-01
36	3.09090E-01	5.54101E-01	1.71267E-01
39	3.09090E-01	5.54101E-01	1.71267E-01
42	3.09090E-01	5.54101E-01	1.71267E-01
45	3.09090E-01	5.54101E-01	1.71267E-01
$\theta = 5$			
0	4.17432E-01	6.11901E-01	2.55427E-01
3	4.17558E-01	6.11000E-01	2.55128E-01
6	4.17954E-01	6.12299E-01	2.55913E-01
9	4.18352E-01	6.12099E-01	2.56073E-01
12	4.19055E-01	6.12900E-01	2.56839E-01
15	4.18950E-01	6.12601E-01	2.56649E-01
18	4.19623E-01	6.13501E-01	2.57439E-01
21	4.19891E-01	6.13500E-01	2.57603E-01
24	4.19694E-01	6.13299E-01	2.57398E-01
27	4.20222E-01	6.14701E-01	2.58311E-01
30	4.21134E-01	6.14299E-01	2.58702E-01
33	4.21222E-01	6.13700E-01	2.58504E-01
36	4.20832E-01	6.13701E-01	2.58265E-01
39	4.20998E-01	6.14001E-01	2.58493E-01
42	4.21222E-01	6.13999E-01	2.58630E-01
45	4.20991E-01	6.14101E-01	2.58531E-01

ψ	p_n	η	ε
$\theta = 10$			
0	4.55356E-01	5.92400E-01	2.69753E-01
3	4.56423E-01	5.91999E-01	2.70202E-01
6	4.59255E-01	5.93400E-01	2.72522E-01
9	4.63379E-01	5.93499E-01	2.75015E-01
12	4.68434E-01	5.94199E-01	2.78343E-01
15	4.74286E-01	5.93899E-01	2.81678E-01
18	4.79841E-01	5.93301E-01	2.84690E-01
21	4.86370E-01	5.93700E-01	2.88758E-01
24	4.92300E-01	5.94400E-01	2.92623E-01
27	4.98510E-01	5.94399E-01	2.96314E-01
30	5.03813E-01	5.96199E-01	3.00373E-01
33	5.08132E-01	5.97699E-01	3.03710E-01
36	5.12043E-01	5.99500E-01	3.06970E-01
39	5.14484E-01	6.01200E-01	3.09308E-01
42	5.15836E-01	6.01701E-01	3.10379E-01
45	5.15997E-01	6.02000E-01	3.10630E-01
$\theta = 15$			
0	4.46575E-01	5.86600E-01	2.61961E-01
3	4.52471E-01	5.89401E-01	2.66687E-01
6	4.61478E-01	5.91701E-01	2.73057E-01
9	4.72696E-01	5.91700E-01	2.79694E-01
12	4.85658E-01	5.90500E-01	2.86781E-01
15	4.98825E-01	5.87501E-01	2.93060E-01
18	5.11843E-01	5.86301E-01	3.00094E-01
21	5.21676E-01	5.82099E-01	3.03667E-01
24	5.29646E-01	5.78600E-01	3.06453E-01
27	5.35445E-01	5.77099E-01	3.09005E-01
30	5.39597E-01	5.77199E-01	3.11455E-01
33	5.42235E-01	5.79201E-01	3.14063E-01
36	5.43939E-01	5.83100E-01	3.17171E-01
39	5.43366E-01	5.86901E-01	3.18902E-01
42	5.41064E-01	5.87799E-01	3.18037E-01
45	5.38338E-01	5.88199E-01	3.16650E-01

ψ	p_n	η	ε
$\theta = 20$			
0	4.43513E-01	5.84199E-01	2.59100E-01
3	4.51280E-01	5.88300E-01	2.65488E-01
6	4.66728E-01	5.90899E-01	2.75789E-01
9	4.84397E-01	5.89900E-01	2.85746E-01
12	5.04009E-01	5.87799E-01	2.96256E-01
15	5.21732E-01	5.83200E-01	3.04274E-01
18	5.38891E-01	5.79100E-01	3.12072E-01
21	5.47881E-01	5.71701E-01	3.13224E-01
24	5.52236E-01	5.66200E-01	3.12676E-01
27	5.53979E-01	5.64500E-01	3.12721E-01
30	5.53847E-01	5.66301E-01	3.13644E-01
33	5.51605E-01	5.70800E-01	3.14856E-01
36	5.47635E-01	5.78299E-01	3.16697E-01
39	5.40725E-01	5.85200E-01	3.16432E-01
42	5.31791E-01	5.87500E-01	3.12427E-01
45	5.24159E-01	5.85000E-01	3.06633E-01
$\theta = 25$			
0	4.33173E-01	5.84000E-01	2.52973E-01
3	4.45869E-01	5.89301E-01	2.62751E-01
6	4.68291E-01	5.91700E-01	2.77088E-01
9	4.93901E-01	5.88300E-01	2.90562E-01
12	5.16155E-01	5.82600E-01	3.00712E-01
15	5.32596E-01	5.75999E-01	3.06775E-01
18	5.44334E-01	5.72801E-01	3.11795E-01
21	5.46932E-01	5.66100E-01	3.09618E-01
24	5.45935E-01	5.61900E-01	3.06761E-01
27	5.44066E-01	5.58701E-01	3.03970E-01
30	5.44377E-01	5.61400E-01	3.05613E-01
33	5.44268E-01	5.67101E-01	3.08655E-01
36	5.41984E-01	5.73799E-01	3.10990E-01
39	5.37166E-01	5.81701E-01	3.12470E-01
42	5.29464E-01	5.85299E-01	3.09895E-01
45	5.21797E-01	5.83800E-01	3.04625E-01

ψ	p_n	η	ε
$\theta = 30$			
0	4.22130E-01	5.83500E-01	2.46313E-01
3	4.40386E-01	5.91100E-01	2.60312E-01
6	4.69766E-01	5.91401E-01	2.77820E-01
9	5.01459E-01	5.85801E-01	2.93755E-01
12	5.23885E-01	5.76000E-01	3.01758E-01
15	5.35536E-01	5.69400E-01	3.04934E-01
18	5.39876E-01	5.67701E-01	3.06488E-01
21	5.37536E-01	5.64799E-01	3.03600E-01
24	5.32879E-01	5.61099E-01	2.98998E-01
27	5.29886E-01	5.59100E-01	2.96259E-01
30	5.33593E-01	5.62101E-01	2.99933E-01
33	5.37037E-01	5.66000E-01	3.03963E-01
36	5.35976E-01	5.69901E-01	3.05453E-01
39	5.31375E-01	5.76900E-01	3.06550E-01
42	5.21468E-01	5.83700E-01	3.04381E-01
45	5.09693E-01	5.81399E-01	2.96335E-01
$\theta = 35$			
0	4.08300E-01	5.83399E-01	2.38202E-01
3	4.32223E-01	5.92199E-01	2.55962E-01
6	4.70529E-01	5.91300E-01	2.78224E-01
9	5.04010E-01	5.81000E-01	2.92830E-01
12	5.20967E-01	5.70700E-01	2.97316E-01
15	5.24587E-01	5.66200E-01	2.97021E-01
18	5.23133E-01	5.66500E-01	2.96355E-01
21	5.21049E-01	5.63899E-01	2.93819E-01
24	5.19989E-01	5.60500E-01	2.91454E-01
27	5.18718E-01	5.57000E-01	2.88926E-01
30	5.22679E-01	5.61201E-01	2.93328E-01
33	5.24695E-01	5.63701E-01	2.95771E-01
36	5.24433E-01	5.66200E-01	2.96934E-01
39	5.19975E-01	5.73001E-01	2.97946E-01
42	5.10285E-01	5.82900E-01	2.97445E-01
45	4.96182E-01	5.82500E-01	2.89026E-01

ψ	p_n	η	ε
$\theta = 40$			
0	3.91288E-01	5.84401E-01	2.28669E-01
3	4.22625E-01	5.93100E-01	2.50659E-01
6	4.69530E-01	5.89300E-01	2.76694E-01
9	4.98737E-01	5.75700E-01	2.87123E-01
12	5.08080E-01	5.67600E-01	2.88386E-01
15	5.05395E-01	5.64699E-01	2.85396E-01
18	5.04238E-01	5.65501E-01	2.85147E-01
21	5.05993E-01	5.63800E-01	2.85279E-01
24	5.06752E-01	5.58200E-01	2.82869E-01
27	5.04670E-01	5.54099E-01	2.79637E-01
30	5.06517E-01	5.59900E-01	2.83599E-01
33	5.06510E-01	5.63401E-01	2.85368E-01
36	5.07659E-01	5.64999E-01	2.86827E-01
39	5.06098E-01	5.70200E-01	2.88577E-01
42	4.96458E-01	5.81300E-01	2.88591E-01
45	4.79577E-01	5.81500E-01	2.78874E-01
$\theta = 45$			
0	3.71568E-01	5.83901E-01	2.16959E-01
3	4.12056E-01	5.95599E-01	2.45420E-01
6	4.63532E-01	5.84799E-01	2.71073E-01
9	4.86287E-01	5.70001E-01	2.77184E-01
12	4.86406E-01	5.65001E-01	2.74820E-01
15	4.83368E-01	5.64601E-01	2.72910E-01
18	4.86035E-01	5.65099E-01	2.74658E-01
21	4.88075E-01	5.62100E-01	2.74347E-01
24	4.86197E-01	5.58399E-01	2.71492E-01
27	4.82734E-01	5.53800E-01	2.67338E-01
30	4.87060E-01	5.60600E-01	2.73046E-01
33	4.86977E-01	5.61199E-01	2.73291E-01
36	4.87008E-01	5.63301E-01	2.74332E-01
39	4.86887E-01	5.67300E-01	2.76211E-01
42	4.78301E-01	5.78600E-01	2.76745E-01
45	4.59519E-01	5.82601E-01	2.67716E-01

ψ	p_n	η	ε
$\theta = 50$			
0	3.48435E-01	5.84100E-01	2.03521E-01
3	3.99860E-01	5.97399E-01	2.38876E-01
6	4.51860E-01	5.80100E-01	2.62124E-01
9	4.63346E-01	5.66801E-01	2.62625E-01
12	4.60009E-01	5.64100E-01	2.59491E-01
15	4.61525E-01	5.63300E-01	2.59977E-01
18	4.63217E-01	5.62600E-01	2.60606E-01
21	4.61591E-01	5.60700E-01	2.58814E-01
24	4.62249E-01	5.58500E-01	2.58166E-01
27	4.59945E-01	5.51601E-01	2.53706E-01
30	4.62287E-01	5.59799E-01	2.58788E-01
33	4.62424E-01	5.60700E-01	2.59281E-01
36	4.62814E-01	5.63300E-01	2.60703E-01
39	4.63402E-01	5.64499E-01	2.61590E-01
42	4.56909E-01	5.76500E-01	2.63408E-01
45	4.34444E-01	5.83000E-01	2.53281E-01
$\theta = 55$			
0	3.21300E-01	5.85201E-01	1.88025E-01
3	3.86088E-01	5.98299E-01	2.30996E-01
6	4.31202E-01	5.74000E-01	2.47510E-01
9	4.31371E-01	5.65400E-01	2.43897E-01
12	4.31922E-01	5.63301E-01	2.43302E-01
15	4.33246E-01	5.61399E-01	2.43224E-01
18	4.32255E-01	5.61701E-01	2.42798E-01
21	4.33343E-01	5.59799E-01	2.42585E-01
24	4.33040E-01	5.57500E-01	2.41420E-01
27	4.29678E-01	5.50000E-01	2.36323E-01
30	4.33703E-01	5.59401E-01	2.42614E-01
33	4.33285E-01	5.59200E-01	2.42293E-01
36	4.33050E-01	5.62000E-01	2.43374E-01
39	4.33343E-01	5.63501E-01	2.44189E-01
42	4.29985E-01	5.74101E-01	2.46855E-01
45	4.05925E-01	5.83699E-01	2.36938E-01

ψ	p_n	η	ε
$\theta = 60$			
0	2.89945E-01	5.85801E-01	1.69850E-01
3	3.68287E-01	5.97800E-01	2.20162E-01
6	3.98168E-01	5.68901E-01	2.26518E-01
9	3.95384E-01	5.64201E-01	2.23076E-01
12	3.98543E-01	5.60800E-01	2.23503E-01
15	3.97190E-01	5.59400E-01	2.22188E-01
18	3.98182E-01	5.60400E-01	2.23141E-01
21	3.97562E-01	5.58102E-01	2.21880E-01
24	3.98015E-01	5.57600E-01	2.21933E-01
27	3.95129E-01	5.47601E-01	2.16373E-01
30	3.97869E-01	5.57900E-01	2.21971E-01
33	3.98203E-01	5.58100E-01	2.22237E-01
36	3.97784E-01	5.59402E-01	2.22521E-01
39	3.97293E-01	5.62499E-01	2.23477E-01
42	3.96445E-01	5.69802E-01	2.25895E-01
45	3.71761E-01	5.84002E-01	2.17109E-01
$\theta = 65$			
0	2.53811E-01	5.86401E-01	1.48835E-01
3	3.42180E-01	5.91800E-01	2.02502E-01
6	3.53924E-01	5.66000E-01	2.00321E-01
9	3.55363E-01	5.61299E-01	1.99465E-01
12	3.54821E-01	5.58800E-01	1.98274E-01
15	3.55742E-01	5.57702E-01	1.98398E-01
18	3.54995E-01	5.58101E-01	1.98123E-01
21	3.55624E-01	5.56700E-01	1.97976E-01
24	3.55604E-01	5.55101E-01	1.97396E-01
27	3.53468E-01	5.44901E-01	1.92605E-01
30	3.55478E-01	5.55801E-01	1.97575E-01
33	3.55315E-01	5.56199E-01	1.97626E-01
36	3.55458E-01	5.57301E-01	1.98097E-01
39	3.55222E-01	5.60100E-01	1.98960E-01
42	3.55288E-01	5.66000E-01	2.01093E-01
45	3.30677E-01	5.83999E-01	1.93115E-01

ψ	p_n	η	ε
$\theta = 70$			
0	2.12892E-01	5.85203E-01	1.24585E-01
3	3.02148E-01	5.82602E-01	1.76032E-01
6	3.03330E-01	5.63601E-01	1.70957E-01
9	3.04065E-01	5.58700E-01	1.69881E-01
12	3.04561E-01	5.55701E-01	1.69245E-01
15	3.04836E-01	5.55299E-01	1.69275E-01
18	3.04366E-01	5.55200E-01	1.68984E-01
21	3.04486E-01	5.54101E-01	1.68716E-01
24	3.04499E-01	5.52898E-01	1.68357E-01
27	3.02816E-01	5.41900E-01	1.64096E-01
30	3.04442E-01	5.52999E-01	1.68356E-01
33	3.04491E-01	5.53599E-01	1.68566E-01
36	3.04760E-01	5.55099E-01	1.69172E-01
39	3.04402E-01	5.56202E-01	1.69309E-01
42	3.04877E-01	5.62200E-01	1.71402E-01
45	2.82494E-01	5.86101E-01	1.65570E-01
$\theta = 75$			
0	1.66441E-01	5.83901E-01	9.71851E-02
3	2.43479E-01	5.74201E-01	1.39806E-01
6	2.43331E-01	5.57899E-01	1.35754E-01
9	2.43511E-01	5.53901E-01	1.34881E-01
12	2.43405E-01	5.51402E-01	1.34214E-01
15	2.43377E-01	5.51001E-01	1.34101E-01
18	2.43365E-01	5.51201E-01	1.34143E-01
21	2.43405E-01	5.50001E-01	1.33873E-01
24	2.43522E-01	5.48599E-01	1.33596E-01
27	2.42733E-01	5.37599E-01	1.30493E-01
30	2.43686E-01	5.49100E-01	1.33808E-01
33	2.43413E-01	5.49198E-01	1.33682E-01
36	2.43565E-01	5.50900E-01	1.34180E-01
39	2.43815E-01	5.52501E-01	1.34708E-01
42	2.43105E-01	5.57401E-01	1.35507E-01
45	2.25512E-01	5.85902E-01	1.32128E-01

ψ	p_n	η	ε
$\theta = 80$			
0	1.14456E-01	5.78298E-01	6.61897E-02
3	1.70366E-01	5.67001E-01	9.65977E-02
6	1.70600E-01	5.50600E-01	9.39324E-02
9	1.70603E-01	5.46200E-01	9.31834E-02
12	1.70603E-01	5.44900E-01	9.29616E-02
15	1.70834E-01	5.43599E-01	9.28652E-02
18	1.70630E-01	5.44201E-01	9.28571E-02
21	1.70871E-01	5.42501E-01	9.26977E-02
24	1.70662E-01	5.40900E-01	9.23110E-02
27	1.70610E-01	5.30202E-01	9.04577E-02
30	1.70891E-01	5.42401E-01	9.26914E-02
33	1.70746E-01	5.41899E-01	9.25271E-02
36	1.70757E-01	5.43100E-01	9.27382E-02
39	1.70654E-01	5.44702E-01	9.29555E-02
42	1.70839E-01	5.49200E-01	9.38247E-02
45	1.58367E-01	5.83800E-01	9.24546E-02
$\theta = 85$			
0	5.86210E-02	5.56299E-01	3.26108E-02
3	8.78585E-02	5.48300E-01	4.81728E-02
6	8.80520E-02	5.32500E-01	4.68877E-02
9	8.79651E-02	5.27400E-01	4.63928E-02
12	8.79197E-02	5.25000E-01	4.61578E-02
15	8.79269E-02	5.23600E-01	4.60385E-02
18	8.79674E-02	5.24000E-01	4.60949E-02
21	8.80824E-02	5.22800E-01	4.60495E-02
24	8.78999E-02	5.21300E-01	4.58222E-02
27	8.79066E-02	5.11100E-01	4.49291E-02
30	8.80173E-02	5.21500E-01	4.59010E-02
33	8.79431E-02	5.22300E-01	4.59327E-02
36	8.79705E-02	5.23000E-01	4.60086E-02
39	8.79779E-02	5.23800E-01	4.60828E-02
42	8.80077E-02	5.29200E-01	4.65737E-02
45	8.23168E-02	5.69400E-01	4.68712E-02

Table B.3. ^{10}B rod detector with 30 μm deep perforations, 6 μm diameter rods, and 4 μm cap

ψ	p_n	η	ε
$\theta = 0$			
0	4.02039E-01	3.52700E-01	1.41799E-01
3	4.02039E-01	3.52700E-01	1.41799E-01
6	4.02039E-01	3.52700E-01	1.41799E-01
9	4.02039E-01	3.52700E-01	1.41799E-01
12	4.02039E-01	3.52700E-01	1.41799E-01
15	4.02039E-01	3.52700E-01	1.41799E-01
18	4.02039E-01	3.52700E-01	1.41799E-01
21	4.02039E-01	3.52700E-01	1.41799E-01
24	4.02039E-01	3.52700E-01	1.41799E-01
27	4.02039E-01	3.52700E-01	1.41799E-01
30	4.02039E-01	3.52700E-01	1.41799E-01
33	4.02039E-01	3.52700E-01	1.41799E-01
36	4.02039E-01	3.52700E-01	1.41799E-01
39	4.02039E-01	3.52700E-01	1.41799E-01
42	4.02039E-01	3.52700E-01	1.41799E-01
45	4.02039E-01	3.52700E-01	1.41799E-01
$\theta = 5$			
0	4.30561E-01	3.85699E-01	1.66067E-01
3	4.31314E-01	3.85501E-01	1.66272E-01
6	4.31211E-01	3.85500E-01	1.66232E-01
9	4.30844E-01	3.85699E-01	1.66176E-01
12	4.31314E-01	3.86500E-01	1.66703E-01
15	4.30988E-01	3.86500E-01	1.66577E-01
18	4.31048E-01	3.86699E-01	1.66686E-01
21	4.30785E-01	3.86100E-01	1.66326E-01
24	4.30834E-01	3.85801E-01	1.66216E-01
27	4.30861E-01	3.86002E-01	1.66313E-01
30	4.31011E-01	3.86099E-01	1.66413E-01
33	4.30988E-01	3.86401E-01	1.66534E-01
36	4.31251E-01	3.86601E-01	1.66722E-01
39	4.30938E-01	3.86000E-01	1.66342E-01
42	4.31202E-01	3.85200E-01	1.66099E-01
45	4.30938E-01	3.85501E-01	1.66127E-01

ψ	p_n	η	ε
$\theta = 10$			
0	4.54088E-01	3.95899E-01	1.79773E-01
3	4.54414E-01	3.95800E-01	1.79857E-01
6	4.54865E-01	3.95500E-01	1.79899E-01
9	4.54602E-01	3.96100E-01	1.80068E-01
12	4.55156E-01	3.96200E-01	1.80333E-01
15	4.55317E-01	3.97800E-01	1.81125E-01
18	4.55688E-01	3.96699E-01	1.80771E-01
21	4.56120E-01	3.97200E-01	1.81171E-01
24	4.56838E-01	3.97999E-01	1.81821E-01
27	4.57536E-01	3.98500E-01	1.82328E-01
30	4.57087E-01	3.98399E-01	1.82103E-01
33	4.57496E-01	3.98799E-01	1.82449E-01
36	4.57743E-01	3.99700E-01	1.82960E-01
39	4.57270E-01	3.99300E-01	1.82588E-01
42	4.57652E-01	3.99400E-01	1.82786E-01
45	4.58272E-01	3.99699E-01	1.83171E-01
$\theta = 15$			
0	4.61908E-01	3.94899E-01	1.82407E-01
3	4.62669E-01	3.94500E-01	1.82523E-01
6	4.63130E-01	3.95399E-01	1.83121E-01
9	4.63908E-01	3.95800E-01	1.83615E-01
12	4.65370E-01	3.96500E-01	1.84519E-01
15	4.67501E-01	3.96900E-01	1.85551E-01
18	4.69173E-01	3.98201E-01	1.86825E-01
21	4.70342E-01	3.99299E-01	1.87807E-01
24	4.72987E-01	3.99400E-01	1.88911E-01
27	4.74275E-01	4.01101E-01	1.90232E-01
30	4.76266E-01	4.02300E-01	1.91602E-01
33	4.77875E-01	4.03599E-01	1.92870E-01
36	4.78922E-01	4.04999E-01	1.93963E-01
39	4.79846E-01	4.06101E-01	1.94866E-01
42	4.80253E-01	4.04999E-01	1.94502E-01
45	4.79987E-01	4.06501E-01	1.95115E-01

ψ	p_n	η	ε
$\theta = 20$			
0	4.55837E-01	3.90600E-01	1.78050E-01
3	4.56931E-01	3.92000E-01	1.79117E-01
6	4.59770E-01	3.92300E-01	1.80368E-01
9	4.62720E-01	3.94100E-01	1.82358E-01
12	4.65937E-01	3.95300E-01	1.84185E-01
15	4.69320E-01	3.96699E-01	1.86179E-01
18	4.73413E-01	3.97900E-01	1.88371E-01
21	4.76989E-01	3.99500E-01	1.90557E-01
24	4.80168E-01	3.99300E-01	1.91731E-01
27	4.82595E-01	4.00499E-01	1.93279E-01
30	4.85328E-01	4.00801E-01	1.94520E-01
33	4.87224E-01	4.02899E-01	1.96302E-01
36	4.89136E-01	4.03399E-01	1.97317E-01
39	4.89729E-01	4.05500E-01	1.98585E-01
42	4.90003E-01	4.06600E-01	1.99235E-01
45	4.89523E-01	4.05599E-01	1.98550E-01
$\theta = 25$			
0	4.48013E-01	3.87600E-01	1.73650E-01
3	4.50218E-01	3.90400E-01	1.75765E-01
6	4.53952E-01	3.92000E-01	1.77949E-01
9	4.58535E-01	3.94899E-01	1.81075E-01
12	4.63904E-01	3.95200E-01	1.83335E-01
15	4.69608E-01	3.96801E-01	1.86341E-01
18	4.74718E-01	3.98100E-01	1.88985E-01
21	4.79196E-01	3.98000E-01	1.90720E-01
24	4.82451E-01	3.97700E-01	1.91871E-01
27	4.84581E-01	3.98000E-01	1.92863E-01
30	4.86352E-01	3.98701E-01	1.93909E-01
33	4.87198E-01	3.99800E-01	1.94782E-01
36	4.87154E-01	4.01200E-01	1.95446E-01
39	4.86390E-01	4.02800E-01	1.95918E-01
42	4.85394E-01	4.02201E-01	1.95226E-01
45	4.83997E-01	4.01100E-01	1.94131E-01

ψ	p_n	η	ε
$\theta = 30$			
0	4.40619E-01	3.85399E-01	1.69814E-01
3	4.43668E-01	3.87499E-01	1.71921E-01
6	4.48221E-01	3.90600E-01	1.75075E-01
9	4.54771E-01	3.93101E-01	1.78771E-01
12	4.61968E-01	3.95499E-01	1.82708E-01
15	4.68892E-01	3.96801E-01	1.86057E-01
18	4.75057E-01	3.97801E-01	1.88978E-01
21	4.79467E-01	3.96401E-01	1.90061E-01
24	4.81805E-01	3.95899E-01	1.90746E-01
27	4.82706E-01	3.94899E-01	1.90620E-01
30	4.82829E-01	3.95600E-01	1.91007E-01
33	4.82105E-01	3.97200E-01	1.91492E-01
36	4.80594E-01	3.98700E-01	1.91613E-01
39	4.78070E-01	4.00201E-01	1.91324E-01
42	4.74787E-01	3.99400E-01	1.89630E-01
45	4.72457E-01	3.98000E-01	1.88038E-01
$\theta = 35$			
0	4.28988E-01	3.80901E-01	1.63402E-01
3	4.32687E-01	3.84599E-01	1.66411E-01
6	4.39745E-01	3.88600E-01	1.70885E-01
9	4.48601E-01	3.91700E-01	1.75717E-01
12	4.56733E-01	3.94000E-01	1.79953E-01
15	4.64457E-01	3.94601E-01	1.83275E-01
18	4.69947E-01	3.95500E-01	1.85864E-01
21	4.72994E-01	3.92899E-01	1.85839E-01
24	4.73730E-01	3.91301E-01	1.85371E-01
27	4.73613E-01	3.89601E-01	1.84520E-01
30	4.73433E-01	3.90900E-01	1.85065E-01
33	4.72491E-01	3.93100E-01	1.85736E-01
36	4.70948E-01	3.96101E-01	1.86543E-01
39	4.68517E-01	3.98101E-01	1.86517E-01
42	4.64830E-01	3.98100E-01	1.85049E-01
45	4.62283E-01	3.96099E-01	1.83110E-01

ψ	p_n	η	ε
$\theta = 40$			
0	4.15563E-01	3.77300E-01	1.56792E-01
3	4.20622E-01	3.81399E-01	1.60425E-01
6	4.30129E-01	3.86000E-01	1.66030E-01
9	4.40612E-01	3.90500E-01	1.72059E-01
12	4.50197E-01	3.91700E-01	1.76342E-01
15	4.56465E-01	3.91099E-01	1.78523E-01
18	4.60187E-01	3.91600E-01	1.80209E-01
21	4.60551E-01	3.89299E-01	1.79292E-01
24	4.59043E-01	3.87001E-01	1.77650E-01
27	4.57877E-01	3.85300E-01	1.76420E-01
30	4.58544E-01	3.86401E-01	1.77182E-01
33	4.58977E-01	3.89900E-01	1.78955E-01
36	4.58555E-01	3.91800E-01	1.79662E-01
39	4.56729E-01	3.93400E-01	1.79677E-01
42	4.53750E-01	3.94199E-01	1.78868E-01
45	4.50707E-01	3.92801E-01	1.77038E-01
$\theta = 45$			
0	3.99135E-01	3.70699E-01	1.47959E-01
3	4.06073E-01	3.76600E-01	1.52927E-01
6	4.17574E-01	3.83101E-01	1.59973E-01
9	4.30247E-01	3.86901E-01	1.66463E-01
12	4.39454E-01	3.86300E-01	1.69761E-01
15	4.43548E-01	3.85600E-01	1.71032E-01
18	4.45029E-01	3.85901E-01	1.71737E-01
21	4.43972E-01	3.83700E-01	1.70352E-01
24	4.41953E-01	3.82301E-01	1.68959E-01
27	4.40997E-01	3.80901E-01	1.67976E-01
30	4.43030E-01	3.82599E-01	1.69503E-01
33	4.44353E-01	3.84899E-01	1.71031E-01
36	4.43855E-01	3.86101E-01	1.71373E-01
39	4.41569E-01	3.88399E-01	1.71505E-01
42	4.37508E-01	3.88999E-01	1.70190E-01
45	4.32885E-01	3.86500E-01	1.67310E-01

ψ	p_n	η	ε
$\theta = 50$			
0	3.79936E-01	3.64401E-01	1.38449E-01
3	3.88724E-01	3.71199E-01	1.44294E-01
6	4.03348E-01	3.80101E-01	1.53313E-01
9	4.16358E-01	3.81299E-01	1.58757E-01
12	4.23412E-01	3.80599E-01	1.61150E-01
15	4.24521E-01	3.79100E-01	1.60936E-01
18	4.23779E-01	3.79101E-01	1.60655E-01
21	4.22851E-01	3.77899E-01	1.59795E-01
24	4.22695E-01	3.76399E-01	1.59102E-01
27	4.22253E-01	3.74399E-01	1.58091E-01
30	4.23720E-01	3.77299E-01	1.59869E-01
33	4.24443E-01	3.77900E-01	1.60397E-01
36	4.24078E-01	3.79001E-01	1.60726E-01
39	4.22484E-01	3.81200E-01	1.61051E-01
42	4.18424E-01	3.83800E-01	1.60591E-01
45	4.13500E-01	3.80900E-01	1.57502E-01
$\theta = 55$			
0	3.56507E-01	3.54302E-01	1.26311E-01
3	3.67889E-01	3.64901E-01	1.34243E-01
6	3.85364E-01	3.73499E-01	1.43933E-01
9	3.96959E-01	3.74099E-01	1.48502E-01
12	4.00341E-01	3.71701E-01	1.48807E-01
15	3.98939E-01	3.69801E-01	1.47528E-01
18	3.98475E-01	3.70400E-01	1.47595E-01
21	3.99279E-01	3.70701E-01	1.48013E-01
24	3.99466E-01	3.68499E-01	1.47203E-01
27	3.98550E-01	3.66200E-01	1.45949E-01
30	3.99520E-01	3.69301E-01	1.47543E-01
33	3.99609E-01	3.70500E-01	1.48055E-01
36	4.00266E-01	3.71001E-01	1.48499E-01
39	3.99417E-01	3.73499E-01	1.49182E-01
42	3.95351E-01	3.75600E-01	1.48494E-01
45	3.89102E-01	3.72501E-01	1.44941E-01

ψ	p_n	η	ε
$\theta = 60$			
0	3.28523E-01	3.41200E-01	1.12092E-01
3	3.43092E-01	3.55800E-01	1.22072E-01
6	3.62379E-01	3.63600E-01	1.31761E-01
9	3.70245E-01	3.62101E-01	1.34066E-01
12	3.69656E-01	3.60100E-01	1.33113E-01
15	3.68813E-01	3.59000E-01	1.32404E-01
18	3.69891E-01	3.60001E-01	1.33161E-01
21	3.70413E-01	3.58700E-01	1.32867E-01
24	3.69691E-01	3.58199E-01	1.32423E-01
27	3.68394E-01	3.55101E-01	1.30817E-01
30	3.70702E-01	3.58900E-01	1.33045E-01
33	3.70317E-01	3.59300E-01	1.33055E-01
36	3.70048E-01	3.59899E-01	1.33180E-01
39	3.70135E-01	3.61001E-01	1.33619E-01
42	3.66931E-01	3.64900E-01	1.33893E-01
45	3.60207E-01	3.62700E-01	1.30647E-01
$\theta = 65$			
0	2.95845E-01	3.24500E-01	9.60016E-02
3	3.13910E-01	3.43901E-01	1.07954E-01
6	3.31727E-01	3.49200E-01	1.15839E-01
9	3.34095E-01	3.45800E-01	1.15530E-01
12	3.33221E-01	3.44900E-01	1.14928E-01
15	3.34204E-01	3.44700E-01	1.15200E-01
18	3.34176E-01	3.44600E-01	1.15157E-01
21	3.33907E-01	3.44401E-01	1.14998E-01
24	3.33982E-01	3.43701E-01	1.14790E-01
27	3.32795E-01	3.38998E-01	1.12817E-01
30	3.34145E-01	3.44099E-01	1.14979E-01
33	3.34226E-01	3.44201E-01	1.15041E-01
36	3.34155E-01	3.44798E-01	1.15216E-01
39	3.34235E-01	3.45802E-01	1.15579E-01
42	3.32278E-01	3.48500E-01	1.15799E-01
45	3.24682E-01	3.46801E-01	1.12600E-01

ψ	p_n	η	ε
$\theta = 70$			
0	2.56406E-01	3.00300E-01	7.69986E-02
3	2.78570E-01	3.27200E-01	9.11480E-02
6	2.90046E-01	3.26100E-01	9.45841E-02
9	2.88906E-01	3.23200E-01	9.33745E-02
12	2.90115E-01	3.23801E-01	9.39394E-02
15	2.89674E-01	3.22900E-01	9.35358E-02
18	2.90023E-01	3.23500E-01	9.38225E-02
21	2.89872E-01	3.22400E-01	9.34548E-02
24	2.90101E-01	3.22300E-01	9.34995E-02
27	2.89006E-01	3.17900E-01	9.18750E-02
30	2.89912E-01	3.22900E-01	9.36126E-02
33	2.89972E-01	3.22900E-01	9.36319E-02
36	2.90103E-01	3.23000E-01	9.37032E-02
39	2.89939E-01	3.23701E-01	9.38534E-02
42	2.89366E-01	3.26700E-01	9.45360E-02
45	2.81559E-01	3.25200E-01	9.15630E-02
$\theta = 75$			
0	2.09148E-01	2.64299E-01	5.52777E-02
3	2.32158E-01	2.96501E-01	6.88350E-02
6	2.34621E-01	2.90900E-01	6.82512E-02
9	2.35338E-01	2.90601E-01	6.83894E-02
12	2.35123E-01	2.89799E-01	6.81385E-02
15	2.35337E-01	2.89801E-01	6.82008E-02
18	2.35303E-01	2.90300E-01	6.83084E-02
21	2.35352E-01	2.89200E-01	6.80638E-02
24	2.35275E-01	2.89100E-01	6.80179E-02
27	2.34469E-01	2.84700E-01	6.67533E-02
30	2.35193E-01	2.89300E-01	6.80413E-02
33	2.35242E-01	2.89600E-01	6.81261E-02
36	2.35317E-01	2.89900E-01	6.82185E-02
39	2.35370E-01	2.89900E-01	6.82337E-02
42	2.35293E-01	2.91900E-01	6.86821E-02
45	2.28825E-01	2.91700E-01	6.67483E-02

ψ	p_n	η	ε
$\theta = 80$			
0	1.52182E-01	2.07500E-01	3.15777E-02
3	1.67815E-01	2.38000E-01	3.99400E-02
6	1.67879E-01	2.34400E-01	3.93508E-02
9	1.67884E-01	2.33900E-01	3.92681E-02
12	1.67931E-01	2.33401E-01	3.91952E-02
15	1.67835E-01	2.33300E-01	3.91559E-02
18	1.67862E-01	2.33100E-01	3.91287E-02
21	1.67869E-01	2.33001E-01	3.91136E-02
24	1.67865E-01	2.33000E-01	3.91126E-02
27	1.67599E-01	2.29300E-01	3.84305E-02
30	1.67825E-01	2.33000E-01	3.91033E-02
33	1.67791E-01	2.32900E-01	3.90785E-02
36	1.67870E-01	2.33101E-01	3.91306E-02
39	1.67870E-01	2.33600E-01	3.92145E-02
42	1.67804E-01	2.34201E-01	3.92998E-02
45	1.63993E-01	2.34000E-01	3.83743E-02
$\theta = 85$			
0	8.35255E-02	1.09500E-01	9.14605E-03
3	8.74207E-02	1.27400E-01	1.11374E-02
6	8.74639E-02	1.26300E-01	1.10467E-02
9	8.74402E-02	1.26000E-01	1.10175E-02
12	8.74255E-02	1.25800E-01	1.09981E-02
15	8.74737E-02	1.25800E-01	1.10042E-02
18	8.74288E-02	1.25700E-01	1.09898E-02
21	8.74434E-02	1.25900E-01	1.10091E-02
24	8.74647E-02	1.25400E-01	1.09681E-02
27	8.74214E-02	1.24100E-01	1.08490E-02
30	8.74336E-02	1.25500E-01	1.09729E-02
33	8.74313E-02	1.25300E-01	1.09551E-02
36	8.74612E-02	1.25700E-01	1.09939E-02
39	8.74404E-02	1.25600E-01	1.09825E-02
42	8.74362E-02	1.25900E-01	1.10082E-02
45	8.65839E-02	1.26299E-01	1.09355E-02

Table B.4. ${}^6\text{LiF}$ rod detector with 100 μm deep perforations, 30 μm diameter rods, and no cap

ψ	p_n	η	ε
$\theta = 0$			
0	1.20002E-01	8.61194E-01	1.03345E-01
3	1.20002E-01	8.61194E-01	1.03345E-01
6	1.20002E-01	8.61194E-01	1.03345E-01
9	1.20002E-01	8.61194E-01	1.03345E-01
12	1.20002E-01	8.61194E-01	1.03345E-01
15	1.20002E-01	8.61194E-01	1.03345E-01
18	1.20002E-01	8.61194E-01	1.03345E-01
21	1.20002E-01	8.61194E-01	1.03345E-01
24	1.20002E-01	8.61194E-01	1.03345E-01
27	1.20002E-01	8.61194E-01	1.03345E-01
30	1.20002E-01	8.61194E-01	1.03345E-01
33	1.20002E-01	8.61194E-01	1.03345E-01
36	1.20002E-01	8.61194E-01	1.03345E-01
39	1.20002E-01	8.61194E-01	1.03345E-01
42	1.20002E-01	8.61194E-01	1.03345E-01
45	1.20002E-01	8.61194E-01	1.03345E-01
$\theta = 5$			
0	1.24841E-01	8.65004E-01	1.07988E-01
3	1.25190E-01	8.64606E-01	1.08240E-01
6	1.25118E-01	8.65103E-01	1.08240E-01
9	1.24995E-01	8.64803E-01	1.08096E-01
12	1.24946E-01	8.64902E-01	1.08066E-01
15	1.24968E-01	8.65502E-01	1.08160E-01
18	1.24898E-01	8.64401E-01	1.07962E-01
21	1.24981E-01	8.64795E-01	1.08083E-01
24	1.24794E-01	8.64601E-01	1.07897E-01
27	1.24936E-01	8.65595E-01	1.08144E-01
30	1.24765E-01	8.64097E-01	1.07809E-01
33	1.25188E-01	8.64803E-01	1.08263E-01
36	1.24992E-01	8.65903E-01	1.08231E-01
39	1.24706E-01	8.64602E-01	1.07821E-01
42	1.25078E-01	8.65300E-01	1.08230E-01
45	1.24701E-01	8.65703E-01	1.07954E-01

ψ	p_n	η	ε
$\theta = 10$			
0	1.29804E-01	8.67801E-01	1.12644E-01
3	1.29874E-01	8.68003E-01	1.12731E-01
6	1.29964E-01	8.68102E-01	1.12822E-01
9	1.29904E-01	8.67502E-01	1.12692E-01
12	1.30023E-01	8.68400E-01	1.12912E-01
15	1.29965E-01	8.68103E-01	1.12823E-01
18	1.29971E-01	8.67501E-01	1.12750E-01
21	1.30042E-01	8.66797E-01	1.12720E-01
24	1.29851E-01	8.68003E-01	1.12711E-01
27	1.30027E-01	8.67797E-01	1.12837E-01
30	1.30005E-01	8.67897E-01	1.12831E-01
33	1.29858E-01	8.67602E-01	1.12665E-01
36	1.29656E-01	8.66701E-01	1.12373E-01
39	1.29722E-01	8.68303E-01	1.12638E-01
42	1.29931E-01	8.67899E-01	1.12767E-01
45	1.29877E-01	8.67898E-01	1.12720E-01
$\theta = 15$			
0	1.34207E-01	8.69500E-01	1.16693E-01
3	1.34332E-01	8.69502E-01	1.16802E-01
6	1.34365E-01	8.69296E-01	1.16803E-01
9	1.34577E-01	8.68796E-01	1.16920E-01
12	1.34538E-01	8.69197E-01	1.16940E-01
15	1.34342E-01	8.70398E-01	1.16931E-01
18	1.34301E-01	8.69100E-01	1.16721E-01
21	1.34482E-01	8.69202E-01	1.16892E-01
24	1.34546E-01	8.68803E-01	1.16894E-01
27	1.34412E-01	8.69201E-01	1.16831E-01
30	1.34300E-01	8.69099E-01	1.16720E-01
33	1.34432E-01	8.68796E-01	1.16794E-01
36	1.34587E-01	8.68903E-01	1.16943E-01
39	1.34344E-01	8.69298E-01	1.16785E-01
42	1.34569E-01	8.69101E-01	1.16954E-01
45	1.34142E-01	8.69795E-01	1.16676E-01

ψ	p_n	η	ε
$\theta = 20$			
0	1.37191E-01	8.69102E-01	1.19233E-01
3	1.37305E-01	8.69699E-01	1.19414E-01
6	1.37538E-01	8.70399E-01	1.19713E-01
9	1.37502E-01	8.69304E-01	1.19531E-01
12	1.37876E-01	8.70304E-01	1.19994E-01
15	1.37934E-01	8.70699E-01	1.20099E-01
18	1.38058E-01	8.70504E-01	1.20180E-01
21	1.38008E-01	8.70703E-01	1.20164E-01
24	1.38137E-01	8.70201E-01	1.20207E-01
27	1.38490E-01	8.70402E-01	1.20542E-01
30	1.38591E-01	8.70901E-01	1.20699E-01
33	1.38805E-01	8.71100E-01	1.20913E-01
36	1.38789E-01	8.71301E-01	1.20927E-01
39	1.38764E-01	8.71400E-01	1.20919E-01
42	1.38550E-01	8.70798E-01	1.20649E-01
45	1.38448E-01	8.70103E-01	1.20464E-01
$\theta = 25$			
0	1.37933E-01	8.69299E-01	1.19905E-01
3	1.38059E-01	8.69404E-01	1.20029E-01
6	1.38527E-01	8.69397E-01	1.20435E-01
9	1.38801E-01	8.69698E-01	1.20715E-01
12	1.38967E-01	8.69796E-01	1.20873E-01
15	1.39405E-01	8.69696E-01	1.21240E-01
18	1.39870E-01	8.70001E-01	1.21687E-01
21	1.40397E-01	8.71500E-01	1.22356E-01
24	1.41017E-01	8.70505E-01	1.22756E-01
27	1.41489E-01	8.71001E-01	1.23237E-01
30	1.41697E-01	8.70604E-01	1.23362E-01
33	1.42020E-01	8.71504E-01	1.23771E-01
36	1.42140E-01	8.71697E-01	1.23903E-01
39	1.42025E-01	8.71600E-01	1.23789E-01
42	1.41961E-01	8.72606E-01	1.23876E-01
45	1.42030E-01	8.71598E-01	1.23793E-01

ψ	p_n	η	ε
$\theta = 30$			
0	1.36522E-01	8.67904E-01	1.18488E-01
3	1.36859E-01	8.67996E-01	1.18793E-01
6	1.37360E-01	8.67800E-01	1.19201E-01
9	1.38219E-01	8.69700E-01	1.20209E-01
12	1.39060E-01	8.69301E-01	1.20885E-01
15	1.39923E-01	8.70600E-01	1.21817E-01
18	1.40737E-01	8.70596E-01	1.22525E-01
21	1.41681E-01	8.71098E-01	1.23418E-01
24	1.42478E-01	8.71699E-01	1.24198E-01
27	1.43309E-01	8.70797E-01	1.24793E-01
30	1.43780E-01	8.71004E-01	1.25233E-01
33	1.44285E-01	8.72204E-01	1.25846E-01
36	1.44341E-01	8.72600E-01	1.25952E-01
39	1.44247E-01	8.71699E-01	1.25740E-01
42	1.44254E-01	8.72101E-01	1.25804E-01
45	1.44134E-01	8.71599E-01	1.25627E-01
$\theta = 35$			
0	1.34558E-01	8.67299E-01	1.16702E-01
3	1.35090E-01	8.68303E-01	1.17299E-01
6	1.36250E-01	8.67596E-01	1.18210E-01
9	1.37231E-01	8.68696E-01	1.19212E-01
12	1.38457E-01	8.69100E-01	1.20333E-01
15	1.39842E-01	8.69796E-01	1.21634E-01
18	1.41109E-01	8.70696E-01	1.22863E-01
21	1.42513E-01	8.70194E-01	1.24014E-01
24	1.43565E-01	8.70400E-01	1.24959E-01
27	1.44457E-01	8.71304E-01	1.25866E-01
30	1.44934E-01	8.71500E-01	1.26310E-01
33	1.45105E-01	8.71796E-01	1.26502E-01
36	1.45037E-01	8.70998E-01	1.26327E-01
39	1.44788E-01	8.71806E-01	1.26227E-01
42	1.44291E-01	8.71399E-01	1.25735E-01
45	1.44206E-01	8.72003E-01	1.25748E-01

ψ	p_n	η	ε
$\theta = 40$			
0	1.33013E-01	8.67998E-01	1.15455E-01
3	1.33757E-01	8.67102E-01	1.15981E-01
6	1.34853E-01	8.68397E-01	1.17106E-01
9	1.36465E-01	8.68098E-01	1.18465E-01
12	1.38328E-01	8.69000E-01	1.20207E-01
15	1.40094E-01	8.69502E-01	1.21812E-01
18	1.41781E-01	8.70702E-01	1.23449E-01
21	1.43429E-01	8.70905E-01	1.24913E-01
24	1.44536E-01	8.71700E-01	1.25992E-01
27	1.45129E-01	8.71997E-01	1.26552E-01
30	1.45347E-01	8.72202E-01	1.26772E-01
33	1.45134E-01	8.71098E-01	1.26426E-01
36	1.44442E-01	8.71298E-01	1.25852E-01
39	1.43457E-01	8.71697E-01	1.25051E-01
42	1.42662E-01	8.70302E-01	1.24159E-01
45	1.42013E-01	8.69399E-01	1.23466E-01
$\theta = 45$			
0	1.30970E-01	8.66603E-01	1.13499E-01
3	1.31817E-01	8.67597E-01	1.14364E-01
6	1.33623E-01	8.68204E-01	1.16012E-01
9	1.35782E-01	8.68797E-01	1.17967E-01
12	1.37986E-01	8.69501E-01	1.19979E-01
15	1.40269E-01	8.70100E-01	1.22048E-01
18	1.42205E-01	8.71200E-01	1.23889E-01
21	1.43959E-01	8.71595E-01	1.25474E-01
24	1.44939E-01	8.71705E-01	1.26344E-01
27	1.45359E-01	8.71800E-01	1.26724E-01
30	1.45118E-01	8.70905E-01	1.26384E-01
33	1.44319E-01	8.71098E-01	1.25716E-01
36	1.43196E-01	8.70199E-01	1.24609E-01
39	1.41643E-01	8.69298E-01	1.23130E-01
42	1.40191E-01	8.68501E-01	1.21756E-01
45	1.39414E-01	8.69203E-01	1.21179E-01

ψ	p_n	η	ε
$\theta = 50$			
0	1.27747E-01	8.65500E-01	1.10565E-01
3	1.29240E-01	8.66102E-01	1.11935E-01
6	1.31451E-01	8.67700E-01	1.14060E-01
9	1.34492E-01	8.68401E-01	1.16793E-01
12	1.37343E-01	8.69895E-01	1.19474E-01
15	1.39948E-01	8.69995E-01	1.21754E-01
18	1.41647E-01	8.70799E-01	1.23346E-01
21	1.42887E-01	8.70695E-01	1.24411E-01
24	1.43464E-01	8.70797E-01	1.24928E-01
27	1.43498E-01	8.69594E-01	1.24785E-01
30	1.43294E-01	8.69604E-01	1.24609E-01
33	1.42722E-01	8.70300E-01	1.24211E-01
36	1.41574E-01	8.70096E-01	1.23183E-01
39	1.40199E-01	8.69899E-01	1.21959E-01
42	1.38611E-01	8.69000E-01	1.20453E-01
45	1.37423E-01	8.68799E-01	1.19393E-01
$\theta = 55$			
0	1.24242E-01	8.63798E-01	1.07320E-01
3	1.26030E-01	8.65794E-01	1.09116E-01
6	1.29517E-01	8.66898E-01	1.12278E-01
9	1.33331E-01	8.67698E-01	1.15691E-01
12	1.36882E-01	8.69698E-01	1.19046E-01
15	1.39334E-01	8.70297E-01	1.21262E-01
18	1.40351E-01	8.69997E-01	1.22105E-01
21	1.40683E-01	8.69302E-01	1.22296E-01
24	1.40332E-01	8.69004E-01	1.21949E-01
27	1.39755E-01	8.68699E-01	1.21405E-01
30	1.40157E-01	8.69004E-01	1.21797E-01
33	1.40128E-01	8.69098E-01	1.21785E-01
36	1.39553E-01	8.69698E-01	1.21369E-01
39	1.38260E-01	8.69601E-01	1.20231E-01
42	1.36391E-01	8.69200E-01	1.18551E-01
45	1.35070E-01	8.68601E-01	1.17322E-01

ψ	p_n	η	ε
$\theta = 60$			
0	1.19305E-01	8.62696E-01	1.02924E-01
3	1.22149E-01	8.64199E-01	1.05561E-01
6	1.26822E-01	8.66301E-01	1.09866E-01
9	1.31828E-01	8.68199E-01	1.14453E-01
12	1.35601E-01	8.69205E-01	1.17865E-01
15	1.37102E-01	8.68696E-01	1.19100E-01
18	1.37078E-01	8.68396E-01	1.19038E-01
21	1.36949E-01	8.68396E-01	1.18926E-01
24	1.36693E-01	8.68003E-01	1.18650E-01
27	1.36391E-01	8.67499E-01	1.18319E-01
30	1.37084E-01	8.68701E-01	1.19085E-01
33	1.37572E-01	8.68803E-01	1.19523E-01
36	1.37214E-01	8.69496E-01	1.19307E-01
39	1.35428E-01	8.69200E-01	1.17714E-01
42	1.32733E-01	8.68405E-01	1.15266E-01
45	1.30455E-01	8.66797E-01	1.13078E-01
$\theta = 65$			
0	1.13243E-01	8.60202E-01	9.74119E-02
3	1.17218E-01	8.62700E-01	1.01124E-01
6	1.23818E-01	8.65795E-01	1.07201E-01
9	1.29877E-01	8.67398E-01	1.12655E-01
12	1.32551E-01	8.67900E-01	1.15041E-01
15	1.32577E-01	8.67405E-01	1.14998E-01
18	1.31668E-01	8.65996E-01	1.14024E-01
21	1.32000E-01	8.66402E-01	1.14365E-01
24	1.32465E-01	8.66999E-01	1.14847E-01
27	1.32501E-01	8.66401E-01	1.14799E-01
30	1.32453E-01	8.66700E-01	1.14797E-01
33	1.32371E-01	8.66799E-01	1.14739E-01
36	1.32435E-01	8.66402E-01	1.14742E-01
39	1.31470E-01	8.66897E-01	1.13971E-01
42	1.28626E-01	8.66699E-01	1.11480E-01
45	1.25540E-01	8.64800E-01	1.08567E-01

ψ	p_n	η	ε
$\theta = 70$			
0	1.04891E-01	8.57503E-01	8.99443E-02
3	1.11009E-01	8.61303E-01	9.56124E-02
6	1.20504E-01	8.65399E-01	1.04284E-01
9	1.25652E-01	8.65502E-01	1.08752E-01
12	1.25825E-01	8.64200E-01	1.08738E-01
15	1.25217E-01	8.63900E-01	1.08175E-01
18	1.25384E-01	8.64097E-01	1.08344E-01
21	1.26175E-01	8.64902E-01	1.09129E-01
24	1.25893E-01	8.63805E-01	1.08747E-01
27	1.25377E-01	8.63300E-01	1.08238E-01
30	1.26065E-01	8.64205E-01	1.08946E-01
33	1.26014E-01	8.63999E-01	1.08876E-01
36	1.25847E-01	8.64002E-01	1.08732E-01
39	1.25648E-01	8.64303E-01	1.08598E-01
42	1.22791E-01	8.64599E-01	1.06165E-01
45	1.18105E-01	8.62800E-01	1.01901E-01
$\theta = 75$			
0	9.30330E-02	8.51700E-01	7.92362E-02
3	1.03856E-01	8.59196E-01	8.92327E-02
6	1.14984E-01	8.63298E-01	9.92654E-02
9	1.15993E-01	8.60698E-01	9.98350E-02
12	1.15540E-01	8.60401E-01	9.94107E-02
15	1.16329E-01	8.60903E-01	1.00148E-01
18	1.15670E-01	8.60600E-01	9.95456E-02
21	1.16166E-01	8.59797E-01	9.98792E-02
24	1.16367E-01	8.60399E-01	1.00122E-01
27	1.15761E-01	8.59601E-01	9.95083E-02
30	1.16215E-01	8.60099E-01	9.99564E-02
33	1.16345E-01	8.60501E-01	1.00115E-01
36	1.16139E-01	8.60903E-01	9.99844E-02
39	1.16177E-01	8.60401E-01	9.99588E-02
42	1.14414E-01	8.61998E-01	9.86246E-02
45	1.07581E-01	8.58300E-01	9.23368E-02

ψ	p_n	η	ε
$\theta = 80$			
0	7.53522E-02	8.41300E-01	6.33938E-02
3	9.45977E-02	8.57100E-01	8.10797E-02
6	9.97741E-02	8.55000E-01	8.53069E-02
9	1.00025E-01	8.54501E-01	8.54715E-02
12	9.99704E-02	8.53700E-01	8.53447E-02
15	1.00292E-01	8.53803E-01	8.56296E-02
18	9.97339E-02	8.52900E-01	8.50630E-02
21	1.00192E-01	8.52902E-01	8.54540E-02
24	1.00149E-01	8.52896E-01	8.54167E-02
27	9.99568E-02	8.52100E-01	8.51732E-02
30	1.00288E-01	8.52801E-01	8.55257E-02
33	1.00219E-01	8.53201E-01	8.55070E-02
36	1.00194E-01	8.53203E-01	8.54858E-02
39	1.00062E-01	8.53101E-01	8.53630E-02
42	9.99580E-02	8.55000E-01	8.54641E-02
45	9.07821E-02	8.50601E-01	7.72193E-02
$\theta = 85$			
0	4.70707E-02	8.14800E-01	3.83532E-02
3	6.93198E-02	8.39699E-01	5.82078E-02
6	6.95830E-02	8.36500E-01	5.82062E-02
9	6.96209E-02	8.35501E-01	5.81683E-02
12	6.96820E-02	8.33900E-01	5.81078E-02
15	6.97687E-02	8.33600E-01	5.81592E-02
18	6.96929E-02	8.33600E-01	5.80960E-02
21	6.97601E-02	8.33400E-01	5.81381E-02
24	6.97858E-02	8.32900E-01	5.81246E-02
27	6.96493E-02	8.32199E-01	5.79621E-02
30	6.97540E-02	8.32400E-01	5.80632E-02
33	6.97676E-02	8.33100E-01	5.81234E-02
36	6.97431E-02	8.33199E-01	5.81099E-02
39	6.97369E-02	8.33900E-01	5.81536E-02
42	6.97003E-02	8.35400E-01	5.82276E-02
45	6.07216E-02	8.30200E-01	5.04111E-02

Table B.5. ${}^6\text{LiF}$ rod detector with 300 μm deep perforations, 30 μm diameter rods, and no cap

ψ	p_n	η	ε
$\theta = 0$			
0	2.19566E-01	8.68199E-01	1.90627E-01
3	2.19566E-01	8.68199E-01	1.90627E-01
6	2.19566E-01	8.68199E-01	1.90627E-01
9	2.19566E-01	8.68199E-01	1.90627E-01
12	2.19566E-01	8.68199E-01	1.90627E-01
15	2.19566E-01	8.68199E-01	1.90627E-01
18	2.19566E-01	8.68199E-01	1.90627E-01
21	2.19566E-01	8.68199E-01	1.90627E-01
24	2.19566E-01	8.68199E-01	1.90627E-01
27	2.19566E-01	8.68199E-01	1.90627E-01
30	2.19566E-01	8.68199E-01	1.90627E-01
33	2.19566E-01	8.68199E-01	1.90627E-01
36	2.19566E-01	8.68199E-01	1.90627E-01
39	2.19566E-01	8.68199E-01	1.90627E-01
42	2.19566E-01	8.68199E-01	1.90627E-01
45	2.19566E-01	8.68199E-01	1.90627E-01
$\theta = 5$			
0	2.87580E-01	8.82499E-01	2.53789E-01
3	2.87062E-01	8.82301E-01	2.53275E-01
6	2.87519E-01	8.82401E-01	2.53707E-01
9	2.87554E-01	8.82899E-01	2.53881E-01
12	2.87285E-01	8.84101E-01	2.53989E-01
15	2.87021E-01	8.82301E-01	2.53239E-01
18	2.86809E-01	8.83497E-01	2.53395E-01
21	2.86811E-01	8.83401E-01	2.53369E-01
24	2.87196E-01	8.82700E-01	2.53508E-01
27	2.87570E-01	8.83201E-01	2.53982E-01
30	2.87865E-01	8.83299E-01	2.54271E-01
33	2.87992E-01	8.82400E-01	2.54124E-01
36	2.88181E-01	8.82799E-01	2.54406E-01
39	2.87839E-01	8.83900E-01	2.54421E-01
42	2.87707E-01	8.83600E-01	2.54218E-01
45	2.87078E-01	8.82401E-01	2.53318E-01

ψ	p_n	η	ε
$\theta = 10$			
0	3.09635E-01	8.81299E-01	2.72881E-01
3	3.09651E-01	8.81098E-01	2.72833E-01
6	3.11808E-01	8.81000E-01	2.74703E-01
9	3.14811E-01	8.82101E-01	2.77695E-01
12	3.17804E-01	8.81399E-01	2.80112E-01
15	3.20945E-01	8.82201E-01	2.83138E-01
18	3.23628E-01	8.81401E-01	2.85246E-01
21	3.28254E-01	8.82402E-01	2.89652E-01
24	3.32342E-01	8.82501E-01	2.93292E-01
27	3.35125E-01	8.81901E-01	2.95547E-01
30	3.37386E-01	8.82301E-01	2.97676E-01
33	3.39583E-01	8.83301E-01	2.99954E-01
36	3.40126E-01	8.84499E-01	3.00841E-01
39	3.40076E-01	8.84699E-01	3.00865E-01
42	3.39840E-01	8.84001E-01	3.00419E-01
45	3.39907E-01	8.83801E-01	3.00410E-01
$\theta = 15$			
0	3.05339E-01	8.81898E-01	2.69278E-01
3	3.08051E-01	8.81500E-01	2.71547E-01
6	3.13884E-01	8.80000E-01	2.76218E-01
9	3.20926E-01	8.81702E-01	2.82961E-01
12	3.27065E-01	8.80999E-01	2.88144E-01
15	3.34923E-01	8.82600E-01	2.95603E-01
18	3.42623E-01	8.81701E-01	3.02091E-01
21	3.49680E-01	8.81700E-01	3.08313E-01
24	3.54589E-01	8.81200E-01	3.12464E-01
27	3.57320E-01	8.81901E-01	3.15121E-01
30	3.58354E-01	8.82200E-01	3.16140E-01
33	3.58115E-01	8.81700E-01	3.15750E-01
36	3.55849E-01	8.81601E-01	3.13717E-01
39	3.51927E-01	8.82200E-01	3.10470E-01
42	3.48431E-01	8.82100E-01	3.07351E-01
45	3.46869E-01	8.80799E-01	3.05522E-01

ψ	p_n	η	ε
$\theta = 20$			
0	3.03325E-01	8.80201E-01	2.66987E-01
3	3.07878E-01	8.80300E-01	2.71025E-01
6	3.16930E-01	8.80298E-01	2.78993E-01
9	3.27848E-01	8.80899E-01	2.88801E-01
12	3.38000E-01	8.82101E-01	2.98150E-01
15	3.48517E-01	8.82298E-01	3.07496E-01
18	3.57008E-01	8.81801E-01	3.14810E-01
21	3.63990E-01	8.81098E-01	3.20711E-01
24	3.67480E-01	8.81300E-01	3.23860E-01
27	3.68174E-01	8.79698E-01	3.23882E-01
30	3.66953E-01	8.80399E-01	3.23065E-01
33	3.63800E-01	8.81600E-01	3.20726E-01
36	3.58736E-01	8.83301E-01	3.16872E-01
39	3.51706E-01	8.82501E-01	3.10381E-01
42	3.44327E-01	8.79600E-01	3.02870E-01
45	3.40587E-01	8.81099E-01	3.00091E-01
$\theta = 25$			
0	2.98449E-01	8.79299E-01	2.62426E-01
3	3.06102E-01	8.80399E-01	2.69492E-01
6	3.18323E-01	8.80002E-01	2.80125E-01
9	3.33102E-01	8.81598E-01	2.93662E-01
12	3.47432E-01	8.82302E-01	3.06540E-01
15	3.56893E-01	8.81301E-01	3.14530E-01
18	3.61817E-01	8.80998E-01	3.18760E-01
21	3.63369E-01	8.80601E-01	3.19983E-01
24	3.62381E-01	8.80501E-01	3.19077E-01
27	3.60968E-01	8.79499E-01	3.17471E-01
30	3.61800E-01	8.79599E-01	3.18239E-01
33	3.60755E-01	8.81900E-01	3.18150E-01
36	3.59137E-01	8.83201E-01	3.17190E-01
39	3.53496E-01	8.82101E-01	3.11819E-01
42	3.46945E-01	8.82301E-01	3.06110E-01
45	3.40461E-01	8.81199E-01	3.00014E-01

ψ	p_n	η	ε
$\theta = 30$			
0	2.93112E-01	8.78200E-01	2.57411E-01
3	3.03566E-01	8.80000E-01	2.67138E-01
6	3.20342E-01	8.80702E-01	2.82126E-01
9	3.39093E-01	8.80599E-01	2.98605E-01
12	3.53803E-01	8.81799E-01	3.11983E-01
15	3.58195E-01	8.80601E-01	3.15427E-01
18	3.58558E-01	8.80600E-01	3.15746E-01
21	3.57815E-01	8.80301E-01	3.14985E-01
24	3.56347E-01	8.79901E-01	3.13550E-01
27	3.56146E-01	8.80201E-01	3.13480E-01
30	3.58262E-01	8.81701E-01	3.15880E-01
33	3.60345E-01	8.80101E-01	3.17140E-01
36	3.58630E-01	8.82801E-01	3.16599E-01
39	3.52614E-01	8.81000E-01	3.10653E-01
42	3.42534E-01	8.81799E-01	3.02046E-01
45	3.34430E-01	8.81201E-01	2.94700E-01
$\theta = 35$			
0	2.85343E-01	8.79198E-01	2.50873E-01
3	2.99357E-01	8.80701E-01	2.63644E-01
6	3.22926E-01	8.82202E-01	2.84886E-01
9	3.43023E-01	8.81200E-01	3.02272E-01
12	3.52932E-01	8.80501E-01	3.10757E-01
15	3.53713E-01	8.80199E-01	3.11338E-01
18	3.50486E-01	8.79998E-01	3.08427E-01
21	3.51265E-01	8.80700E-01	3.09359E-01
24	3.52554E-01	8.79899E-01	3.10212E-01
27	3.52398E-01	8.79801E-01	3.10040E-01
30	3.52994E-01	8.79800E-01	3.10564E-01
33	3.53155E-01	8.79801E-01	3.10706E-01
36	3.52612E-01	8.80699E-01	3.10545E-01
39	3.48976E-01	8.80298E-01	3.07203E-01
42	3.39629E-01	8.82301E-01	2.99655E-01
45	3.29116E-01	8.82200E-01	2.90346E-01

ψ	p_n	η	ε
$\theta = 40$			
0	2.77857E-01	8.78902E-01	2.44209E-01
3	2.95469E-01	8.81199E-01	2.60367E-01
6	3.23677E-01	8.81400E-01	2.85289E-01
9	3.43172E-01	8.80299E-01	3.02094E-01
12	3.46749E-01	8.80700E-01	3.05382E-01
15	3.43902E-01	8.79599E-01	3.02496E-01
18	3.42871E-01	8.80002E-01	3.01727E-01
21	3.46060E-01	8.80399E-01	3.04671E-01
24	3.46258E-01	8.79700E-01	3.04603E-01
27	3.44767E-01	8.79200E-01	3.03119E-01
30	3.45388E-01	8.78901E-01	3.03562E-01
33	3.46179E-01	8.80299E-01	3.04741E-01
36	3.46549E-01	8.80701E-01	3.05206E-01
39	3.44480E-01	8.80698E-01	3.03383E-01
42	3.35046E-01	8.81900E-01	2.95477E-01
45	3.20227E-01	8.80500E-01	2.81960E-01
$\theta = 45$			
0	2.66964E-01	8.77901E-01	2.34368E-01
3	2.91627E-01	8.80903E-01	2.56895E-01
6	3.24062E-01	8.81300E-01	2.85596E-01
9	3.37603E-01	8.80099E-01	2.97124E-01
12	3.36225E-01	8.79899E-01	2.95844E-01
15	3.35085E-01	8.78899E-01	2.94506E-01
18	3.36057E-01	8.79702E-01	2.95630E-01
21	3.37646E-01	8.79501E-01	2.96960E-01
24	3.36486E-01	8.78301E-01	2.95536E-01
27	3.36311E-01	8.78499E-01	2.95449E-01
30	3.37478E-01	8.79302E-01	2.96745E-01
33	3.37560E-01	8.78300E-01	2.96479E-01
36	3.36421E-01	8.79199E-01	2.95781E-01
39	3.36982E-01	8.79599E-01	2.96409E-01
42	3.28024E-01	8.80701E-01	2.88891E-01
45	3.10559E-01	8.79701E-01	2.73199E-01

ψ	p_n	η	ε
$\theta = 50$			
0	2.55002E-01	8.76499E-01	2.23509E-01
3	2.85873E-01	8.80499E-01	2.51711E-01
6	3.21528E-01	8.79898E-01	2.82912E-01
9	3.26291E-01	8.77698E-01	2.86385E-01
12	3.23909E-01	8.78602E-01	2.84587E-01
15	3.26957E-01	8.79100E-01	2.87428E-01
18	3.24861E-01	8.78400E-01	2.85358E-01
21	3.26422E-01	8.78201E-01	2.86664E-01
24	3.26732E-01	8.78500E-01	2.87034E-01
27	3.25957E-01	8.78398E-01	2.86320E-01
30	3.26820E-01	8.78000E-01	2.86948E-01
33	3.27556E-01	8.79898E-01	2.88216E-01
36	3.26802E-01	8.78299E-01	2.87030E-01
39	3.26660E-01	8.79199E-01	2.87199E-01
42	3.20068E-01	8.80100E-01	2.81692E-01
45	2.99336E-01	8.79099E-01	2.63146E-01
$\theta = 55$			
0	2.38750E-01	8.76699E-01	2.09312E-01
3	2.80943E-01	8.81300E-01	2.47595E-01
6	3.12740E-01	8.78298E-01	2.74679E-01
9	3.10491E-01	8.76802E-01	2.72239E-01
12	3.12735E-01	8.78300E-01	2.74675E-01
15	3.12372E-01	8.77201E-01	2.74013E-01
18	3.11249E-01	8.76999E-01	2.72965E-01
21	3.13513E-01	8.78101E-01	2.75296E-01
24	3.13010E-01	8.76799E-01	2.74447E-01
27	3.12209E-01	8.76503E-01	2.73652E-01
30	3.13230E-01	8.76800E-01	2.74640E-01
33	3.12723E-01	8.77399E-01	2.74383E-01
36	3.12858E-01	8.77999E-01	2.74689E-01
39	3.12323E-01	8.77198E-01	2.73969E-01
42	3.09355E-01	8.78799E-01	2.71861E-01
45	2.84429E-01	8.78599E-01	2.49899E-01

ψ	p_n	η	ε
$\theta = 60$			
0	2.21181E-01	8.74700E-01	1.93467E-01
3	2.73944E-01	8.79399E-01	2.40906E-01
6	2.95831E-01	8.77102E-01	2.59474E-01
9	2.93945E-01	8.76402E-01	2.57614E-01
12	2.95943E-01	8.77402E-01	2.59661E-01
15	2.95419E-01	8.76301E-01	2.58876E-01
18	2.94683E-01	8.77601E-01	2.58614E-01
21	2.96128E-01	8.76800E-01	2.59645E-01
24	2.95458E-01	8.76801E-01	2.59058E-01
27	2.94396E-01	8.75698E-01	2.57802E-01
30	2.95675E-01	8.75701E-01	2.58923E-01
33	2.96228E-01	8.76700E-01	2.59703E-01
36	2.95416E-01	8.77400E-01	2.59198E-01
39	2.94538E-01	8.76400E-01	2.58133E-01
42	2.94186E-01	8.78101E-01	2.58325E-01
45	2.66757E-01	8.77398E-01	2.34052E-01
$\theta = 65$			
0	1.99340E-01	8.72103E-01	1.73845E-01
3	2.64236E-01	8.78098E-01	2.32025E-01
6	2.72020E-01	8.75300E-01	2.38099E-01
9	2.74082E-01	8.75701E-01	2.40014E-01
12	2.73427E-01	8.76000E-01	2.39522E-01
15	2.73777E-01	8.76001E-01	2.39829E-01
18	2.72836E-01	8.75299E-01	2.38813E-01
21	2.73753E-01	8.76001E-01	2.39808E-01
24	2.73732E-01	8.75002E-01	2.39516E-01
27	2.72782E-01	8.74200E-01	2.38466E-01
30	2.74038E-01	8.75601E-01	2.39948E-01
33	2.74199E-01	8.75302E-01	2.40007E-01
36	2.73736E-01	8.76100E-01	2.39820E-01
39	2.73640E-01	8.75201E-01	2.39490E-01
42	2.73481E-01	8.75999E-01	2.39569E-01
45	2.45191E-01	8.77100E-01	2.15057E-01

ψ	p_n	η	ε
$\theta = 70$			
0	1.72549E-01	8.69602E-01	1.50049E-01
3	2.44439E-01	8.74398E-01	2.13737E-01
6	2.44912E-01	8.73902E-01	2.14029E-01
9	2.44944E-01	8.72297E-01	2.13664E-01
12	2.45267E-01	8.73102E-01	2.14143E-01
15	2.45692E-01	8.72698E-01	2.14415E-01
18	2.44955E-01	8.74001E-01	2.14091E-01
21	2.45778E-01	8.73199E-01	2.14613E-01
24	2.45615E-01	8.72601E-01	2.14324E-01
27	2.45169E-01	8.71501E-01	2.13665E-01
30	2.45569E-01	8.72199E-01	2.14185E-01
33	2.46025E-01	8.72700E-01	2.14706E-01
36	2.45405E-01	8.73699E-01	2.14410E-01
39	2.44914E-01	8.73200E-01	2.13859E-01
42	2.44981E-01	8.72602E-01	2.13771E-01
45	2.17289E-01	8.74402E-01	1.89998E-01
$\theta = 75$			
0	1.40172E-01	8.63696E-01	1.21066E-01
3	2.07407E-01	8.70501E-01	1.80548E-01
6	2.07905E-01	8.69700E-01	1.80815E-01
9	2.07361E-01	8.68900E-01	1.80176E-01
12	2.08281E-01	8.69700E-01	1.81142E-01
15	2.08618E-01	8.68703E-01	1.81227E-01
18	2.07996E-01	8.69098E-01	1.80769E-01
21	2.07921E-01	8.69099E-01	1.80704E-01
24	2.07954E-01	8.68601E-01	1.80629E-01
27	2.07987E-01	8.68198E-01	1.80574E-01
30	2.08196E-01	8.68499E-01	1.80818E-01
33	2.08174E-01	8.69403E-01	1.80987E-01
36	2.08245E-01	8.69802E-01	1.81132E-01
39	2.08131E-01	8.68602E-01	1.80783E-01
42	2.07659E-01	8.69098E-01	1.80476E-01
45	1.81282E-01	8.70599E-01	1.57824E-01

ψ	p_n	η	ε
$\theta = 80$			
0	1.01097E-01	8.53102E-01	8.62461E-02
3	1.57453E-01	8.64702E-01	1.36150E-01
6	1.57663E-01	8.62897E-01	1.36047E-01
9	1.57735E-01	8.61901E-01	1.35952E-01
12	1.58035E-01	8.61898E-01	1.36210E-01
15	1.57784E-01	8.62001E-01	1.36010E-01
18	1.57954E-01	8.61301E-01	1.36046E-01
21	1.57969E-01	8.60795E-01	1.35979E-01
24	1.58028E-01	8.61202E-01	1.36094E-01
27	1.57842E-01	8.60601E-01	1.35839E-01
30	1.58113E-01	8.61700E-01	1.36246E-01
33	1.57937E-01	8.61901E-01	1.36126E-01
36	1.57970E-01	8.61600E-01	1.36107E-01
39	1.58204E-01	8.61704E-01	1.36325E-01
42	1.58089E-01	8.62002E-01	1.36273E-01
45	1.35137E-01	8.63302E-01	1.16664E-01
$\theta = 85$			
0	5.50491E-02	8.26800E-01	4.55146E-02
3	8.96576E-02	8.45900E-01	7.58414E-02
6	8.98001E-02	8.44200E-01	7.58092E-02
9	8.98048E-02	8.42900E-01	7.56965E-02
12	8.97943E-02	8.41700E-01	7.55799E-02
15	8.96658E-02	8.41499E-01	7.54537E-02
18	8.96866E-02	8.40900E-01	7.54175E-02
21	8.99234E-02	8.40700E-01	7.55986E-02
24	8.97648E-02	8.40600E-01	7.54563E-02
27	8.96398E-02	8.40000E-01	7.52974E-02
30	8.97729E-02	8.40699E-01	7.54720E-02
33	8.97202E-02	8.40399E-01	7.54008E-02
36	8.96004E-02	8.40699E-01	7.53270E-02
39	8.96797E-02	8.41600E-01	7.54744E-02
42	8.96611E-02	8.42499E-01	7.55394E-02
45	7.57505E-02	8.42301E-01	6.38047E-02

Table B.6. ${}^6\text{LiF}$ rod detector with 100 μm deep perforations, 30 μm diameter rods, and 20 μm cap

ψ	p_n	η	ε
$\theta = 0$			
0	2.15613E-01	5.69298E-01	1.22748E-01
3	2.15613E-01	5.69298E-01	1.22748E-01
6	2.15613E-01	5.69298E-01	1.22748E-01
9	2.15613E-01	5.69298E-01	1.22748E-01
12	2.15613E-01	5.69298E-01	1.22748E-01
15	2.15613E-01	5.69298E-01	1.22748E-01
18	2.15613E-01	5.69298E-01	1.22748E-01
21	2.15613E-01	5.69298E-01	1.22748E-01
24	2.15613E-01	5.69298E-01	1.22748E-01
27	2.15613E-01	5.69298E-01	1.22748E-01
30	2.15613E-01	5.69298E-01	1.22748E-01
33	2.15613E-01	5.69298E-01	1.22748E-01
36	2.15613E-01	5.69298E-01	1.22748E-01
39	2.15613E-01	5.69298E-01	1.22748E-01
42	2.15613E-01	5.69298E-01	1.22748E-01
45	2.15613E-01	5.69298E-01	1.22748E-01
$\theta = 5$			
0	2.19435E-01	5.75701E-01	1.26329E-01
3	2.19764E-01	5.75399E-01	1.26452E-01
6	2.19691E-01	5.74898E-01	1.26300E-01
9	2.19651E-01	5.76100E-01	1.26541E-01
12	2.19702E-01	5.75998E-01	1.26548E-01
15	2.19491E-01	5.75901E-01	1.26405E-01
18	2.19551E-01	5.76199E-01	1.26505E-01
21	2.19692E-01	5.75401E-01	1.26411E-01
24	2.19451E-01	5.75801E-01	1.26360E-01
27	2.19637E-01	5.75800E-01	1.26467E-01
30	2.19609E-01	5.75500E-01	1.26385E-01
33	2.19681E-01	5.75899E-01	1.26514E-01
36	2.19640E-01	5.76102E-01	1.26535E-01
39	2.19454E-01	5.76198E-01	1.26449E-01
42	2.19764E-01	5.77301E-01	1.26870E-01
45	2.19442E-01	5.76900E-01	1.26596E-01

ψ	p_n	η	ε
$\theta = 10$			
0	2.23224E-01	5.81801E-01	1.29872E-01
3	2.23433E-01	5.80599E-01	1.29725E-01
6	2.23499E-01	5.81801E-01	1.30032E-01
9	2.23408E-01	5.82002E-01	1.30024E-01
12	2.23488E-01	5.81499E-01	1.29958E-01
15	2.23335E-01	5.81602E-01	1.29892E-01
18	2.23491E-01	5.81401E-01	1.29938E-01
21	2.23381E-01	5.81898E-01	1.29985E-01
24	2.23377E-01	5.81501E-01	1.29894E-01
27	2.23439E-01	5.81698E-01	1.29974E-01
30	2.23533E-01	5.82898E-01	1.30297E-01
33	2.23375E-01	5.81699E-01	1.29937E-01
36	2.23340E-01	5.82802E-01	1.30163E-01
39	2.23158E-01	5.81400E-01	1.29744E-01
42	2.23373E-01	5.82801E-01	1.30182E-01
45	2.23219E-01	5.81599E-01	1.29824E-01
$\theta = 15$			
0	2.26445E-01	5.85599E-01	1.32606E-01
3	2.26557E-01	5.85601E-01	1.32672E-01
6	2.26445E-01	5.86398E-01	1.32787E-01
9	2.26481E-01	5.86800E-01	1.32899E-01
12	2.26739E-01	5.86101E-01	1.32892E-01
15	2.26533E-01	5.86299E-01	1.32816E-01
18	2.26596E-01	5.86899E-01	1.32989E-01
21	2.26650E-01	5.86901E-01	1.33021E-01
24	2.26665E-01	5.86098E-01	1.32848E-01
27	2.26631E-01	5.86901E-01	1.33010E-01
30	2.26569E-01	5.86201E-01	1.32815E-01
33	2.26560E-01	5.86498E-01	1.32877E-01
36	2.26643E-01	5.86098E-01	1.32835E-01
39	2.26613E-01	5.86802E-01	1.32977E-01
42	2.26543E-01	5.85602E-01	1.32664E-01
45	2.26405E-01	5.86100E-01	1.32696E-01

ψ	p_n	η	ε
$\theta = 20$			
0	2.28188E-01	5.89102E-01	1.34426E-01
3	2.28340E-01	5.88600E-01	1.34401E-01
6	2.28280E-01	5.89500E-01	1.34571E-01
9	2.28313E-01	5.89200E-01	1.34522E-01
12	2.28613E-01	5.89000E-01	1.34653E-01
15	2.28700E-01	5.88999E-01	1.34704E-01
18	2.28782E-01	5.89400E-01	1.34844E-01
21	2.28791E-01	5.89499E-01	1.34872E-01
24	2.28916E-01	5.89701E-01	1.34992E-01
27	2.29050E-01	5.90701E-01	1.35300E-01
30	2.29214E-01	5.89899E-01	1.35213E-01
33	2.29345E-01	5.89200E-01	1.35130E-01
36	2.29225E-01	5.90398E-01	1.35334E-01
39	2.29345E-01	5.89902E-01	1.35291E-01
42	2.29078E-01	5.91100E-01	1.35408E-01
45	2.29147E-01	5.90900E-01	1.35403E-01
$\theta = 25$			
0	2.27670E-01	5.90201E-01	1.34371E-01
3	2.27855E-01	5.89502E-01	1.34321E-01
6	2.28110E-01	5.89799E-01	1.34539E-01
9	2.28407E-01	5.89203E-01	1.34578E-01
12	2.28511E-01	5.90698E-01	1.34981E-01
15	2.28924E-01	5.90799E-01	1.35248E-01
18	2.29231E-01	5.91198E-01	1.35521E-01
21	2.29631E-01	5.92699E-01	1.36102E-01
24	2.30075E-01	5.91703E-01	1.36136E-01
27	2.30472E-01	5.92701E-01	1.36601E-01
30	2.30679E-01	5.92499E-01	1.36677E-01
33	2.30910E-01	5.92300E-01	1.36768E-01
36	2.31049E-01	5.93298E-01	1.37081E-01
39	2.30865E-01	5.93403E-01	1.36996E-01
42	2.30943E-01	5.93402E-01	1.37042E-01
45	2.30910E-01	5.94002E-01	1.37161E-01

ψ	p_n	η	ε
$\theta = 30$			
0	2.25280E-01	5.87398E-01	1.32329E-01
3	2.25623E-01	5.87001E-01	1.32441E-01
6	2.25930E-01	5.87501E-01	1.32734E-01
9	2.26532E-01	5.88398E-01	1.33291E-01
12	2.27171E-01	5.89001E-01	1.33804E-01
15	2.27916E-01	5.90498E-01	1.34584E-01
18	2.28604E-01	5.91801E-01	1.35288E-01
21	2.29258E-01	5.92001E-01	1.35721E-01
24	2.29977E-01	5.93699E-01	1.36537E-01
27	2.30533E-01	5.94301E-01	1.37006E-01
30	2.30906E-01	5.93999E-01	1.37158E-01
33	2.31242E-01	5.94399E-01	1.37450E-01
36	2.31549E-01	5.94699E-01	1.37702E-01
39	2.31278E-01	5.94099E-01	1.37402E-01
42	2.31284E-01	5.94403E-01	1.37476E-01
45	2.31221E-01	5.94699E-01	1.37507E-01
$\theta = 35$			
0	2.22154E-01	5.83501E-01	1.29627E-01
3	2.22520E-01	5.84199E-01	1.29996E-01
6	2.23396E-01	5.86300E-01	1.30977E-01
9	2.24150E-01	5.87401E-01	1.31666E-01
12	2.25143E-01	5.88799E-01	1.32564E-01
15	2.26227E-01	5.90098E-01	1.33496E-01
18	2.27244E-01	5.90801E-01	1.34256E-01
21	2.28224E-01	5.92300E-01	1.35177E-01
24	2.29122E-01	5.93500E-01	1.35984E-01
27	2.29819E-01	5.94098E-01	1.36535E-01
30	2.30153E-01	5.94100E-01	1.36734E-01
33	2.30256E-01	5.95198E-01	1.37048E-01
36	2.30267E-01	5.95500E-01	1.37124E-01
39	2.30005E-01	5.95000E-01	1.36853E-01
42	2.29745E-01	5.94603E-01	1.36607E-01
45	2.29468E-01	5.94697E-01	1.36464E-01

ψ	p_n	η	ε
$\theta = 40$			
0	2.18837E-01	5.81200E-01	1.27188E-01
3	2.19620E-01	5.82702E-01	1.27973E-01
6	2.20416E-01	5.83397E-01	1.28590E-01
9	2.21452E-01	5.84998E-01	1.29549E-01
12	2.22951E-01	5.86900E-01	1.30850E-01
15	2.24153E-01	5.88701E-01	1.31959E-01
18	2.25600E-01	5.90399E-01	1.33194E-01
21	2.26930E-01	5.91901E-01	1.34320E-01
24	2.27664E-01	5.93199E-01	1.35050E-01
27	2.28198E-01	5.93599E-01	1.35458E-01
30	2.28278E-01	5.94100E-01	1.35620E-01
33	2.28132E-01	5.93801E-01	1.35465E-01
36	2.27578E-01	5.93203E-01	1.35000E-01
39	2.26825E-01	5.92902E-01	1.34485E-01
42	2.26252E-01	5.91800E-01	1.33896E-01
45	2.25818E-01	5.90701E-01	1.33391E-01
$\theta = 45$			
0	2.14886E-01	5.79303E-01	1.24484E-01
3	2.15503E-01	5.78897E-01	1.24754E-01
6	2.16884E-01	5.80997E-01	1.26009E-01
9	2.18297E-01	5.83998E-01	1.27485E-01
12	2.20045E-01	5.85198E-01	1.28770E-01
15	2.21765E-01	5.88100E-01	1.30420E-01
18	2.23245E-01	5.90199E-01	1.31759E-01
21	2.24521E-01	5.90399E-01	1.32557E-01
24	2.25223E-01	5.92502E-01	1.33445E-01
27	2.25535E-01	5.92099E-01	1.33539E-01
30	2.25411E-01	5.92101E-01	1.33466E-01
33	2.24829E-01	5.91899E-01	1.33076E-01
36	2.23962E-01	5.90203E-01	1.32183E-01
39	2.22850E-01	5.89199E-01	1.31303E-01
42	2.21696E-01	5.86898E-01	1.30113E-01
45	2.21259E-01	5.86900E-01	1.29857E-01

ψ	p_n	η	ε
$\theta = 50$			
0	2.09287E-01	5.72802E-01	1.19880E-01
3	2.10298E-01	5.75602E-01	1.21048E-01
6	2.11903E-01	5.77500E-01	1.22374E-01
9	2.14235E-01	5.79901E-01	1.24235E-01
12	2.16178E-01	5.83302E-01	1.26097E-01
15	2.18162E-01	5.85602E-01	1.27756E-01
18	2.19365E-01	5.87099E-01	1.28789E-01
21	2.20386E-01	5.88300E-01	1.29653E-01
24	2.20789E-01	5.88200E-01	1.29868E-01
27	2.20772E-01	5.88399E-01	1.29902E-01
30	2.20619E-01	5.89002E-01	1.29945E-01
33	2.20230E-01	5.88598E-01	1.29627E-01
36	2.19366E-01	5.87798E-01	1.28943E-01
39	2.18315E-01	5.85498E-01	1.27823E-01
42	2.17120E-01	5.84700E-01	1.26950E-01
45	2.16429E-01	5.82500E-01	1.26070E-01
$\theta = 55$			
0	2.02695E-01	5.66102E-01	1.14746E-01
3	2.03915E-01	5.69198E-01	1.16068E-01
6	2.06335E-01	5.72802E-01	1.18189E-01
9	2.09071E-01	5.76000E-01	1.20425E-01
12	2.11673E-01	5.80499E-01	1.22876E-01
15	2.13397E-01	5.82501E-01	1.24304E-01
18	2.14128E-01	5.83501E-01	1.24944E-01
21	2.14299E-01	5.83997E-01	1.25150E-01
24	2.14164E-01	5.83301E-01	1.24922E-01
27	2.13821E-01	5.82801E-01	1.24615E-01
30	2.13960E-01	5.83399E-01	1.24824E-01
33	2.13933E-01	5.83000E-01	1.24723E-01
36	2.13478E-01	5.83503E-01	1.24565E-01
39	2.12670E-01	5.82099E-01	1.23795E-01
42	2.11292E-01	5.79899E-01	1.22528E-01
45	2.10370E-01	5.78799E-01	1.21762E-01

ψ	p_n	η	ε
$\theta = 60$			
0	1.94049E-01	5.57900E-01	1.08260E-01
3	1.95913E-01	5.61601E-01	1.10025E-01
6	1.99130E-01	5.67097E-01	1.12926E-01
9	2.02528E-01	5.72701E-01	1.15988E-01
12	2.05168E-01	5.75499E-01	1.18074E-01
15	2.06167E-01	5.76799E-01	1.18917E-01
18	2.06194E-01	5.76801E-01	1.18933E-01
21	2.06104E-01	5.77301E-01	1.18984E-01
24	2.05912E-01	5.77101E-01	1.18832E-01
27	2.05762E-01	5.76501E-01	1.18622E-01
30	2.06197E-01	5.77598E-01	1.19099E-01
33	2.06634E-01	5.77398E-01	1.19310E-01
36	2.06245E-01	5.78099E-01	1.19230E-01
39	2.05082E-01	5.75799E-01	1.18086E-01
42	2.03223E-01	5.73803E-01	1.16610E-01
45	2.01703E-01	5.71201E-01	1.15213E-01
$\theta = 65$			
0	1.82995E-01	5.47201E-01	1.00135E-01
3	1.85694E-01	5.51897E-01	1.02484E-01
6	1.89934E-01	5.59400E-01	1.06249E-01
9	1.93899E-01	5.65800E-01	1.09708E-01
12	1.95772E-01	5.67502E-01	1.11101E-01
15	1.95808E-01	5.68899E-01	1.11395E-01
18	1.95120E-01	5.67697E-01	1.10769E-01
21	1.95307E-01	5.67302E-01	1.10798E-01
24	1.95658E-01	5.67899E-01	1.11114E-01
27	1.95688E-01	5.68400E-01	1.11229E-01
30	1.95695E-01	5.68599E-01	1.11272E-01
33	1.95600E-01	5.67899E-01	1.11081E-01
36	1.95699E-01	5.67898E-01	1.11137E-01
39	1.94945E-01	5.67298E-01	1.10592E-01
42	1.93083E-01	5.65099E-01	1.09111E-01
45	1.91269E-01	5.61502E-01	1.07398E-01

ψ	p_n	η	ε
$\theta = 70$			
0	1.68492E-01	5.30400E-01	8.93681E-02
3	1.72224E-01	5.39400E-01	9.28977E-02
6	1.77921E-01	5.50000E-01	9.78565E-02
9	1.81177E-01	5.55700E-01	1.00680E-01
12	1.81336E-01	5.55698E-01	1.00768E-01
15	1.80940E-01	5.54101E-01	1.00259E-01
18	1.80971E-01	5.54901E-01	1.00421E-01
21	1.81600E-01	5.55600E-01	1.00897E-01
24	1.81451E-01	5.55599E-01	1.00814E-01
27	1.81085E-01	5.54601E-01	1.00430E-01
30	1.81434E-01	5.55701E-01	1.00823E-01
33	1.81403E-01	5.55300E-01	1.00733E-01
36	1.81389E-01	5.55199E-01	1.00707E-01
39	1.81263E-01	5.55000E-01	1.00601E-01
42	1.79412E-01	5.51600E-01	9.89637E-02
45	1.76736E-01	5.46700E-01	9.66215E-02
$\theta = 75$			
0	1.48441E-01	5.04900E-01	7.49479E-02
3	1.54373E-01	5.19999E-01	8.02738E-02
6	1.60504E-01	5.33301E-01	8.55970E-02
9	1.61083E-01	5.34500E-01	8.60988E-02
12	1.60838E-01	5.34199E-01	8.59195E-02
15	1.61263E-01	5.34500E-01	8.61951E-02
18	1.60921E-01	5.33502E-01	8.58516E-02
21	1.61232E-01	5.33898E-01	8.60815E-02
24	1.61319E-01	5.34299E-01	8.61925E-02
27	1.61001E-01	5.34100E-01	8.59907E-02
30	1.61275E-01	5.34698E-01	8.62335E-02
33	1.61315E-01	5.34102E-01	8.61586E-02
36	1.61235E-01	5.34299E-01	8.61477E-02
39	1.61249E-01	5.34501E-01	8.61878E-02
42	1.60184E-01	5.32599E-01	8.53139E-02
45	1.56542E-01	5.24798E-01	8.21530E-02

ψ	p_n	η	ε
$\theta = 80$			
0	1.19519E-01	4.61199E-01	5.51220E-02
3	1.28158E-01	4.89399E-01	6.27204E-02
6	1.30634E-01	4.96299E-01	6.48335E-02
9	1.30656E-01	4.96599E-01	6.48836E-02
12	1.30690E-01	4.96801E-01	6.49269E-02
15	1.30821E-01	4.96701E-01	6.49789E-02
18	1.30550E-01	4.96699E-01	6.48441E-02
21	1.30859E-01	4.96600E-01	6.49846E-02
24	1.30797E-01	4.96300E-01	6.49146E-02
27	1.30660E-01	4.96400E-01	6.48596E-02
30	1.30836E-01	4.96300E-01	6.49339E-02
33	1.30823E-01	4.96301E-01	6.49276E-02
36	1.30777E-01	4.96901E-01	6.49832E-02
39	1.30758E-01	4.96302E-01	6.48954E-02
42	1.30703E-01	4.96800E-01	6.49332E-02
45	1.26636E-01	4.84501E-01	6.13553E-02
$\theta = 85$			
0	7.49173E-02	3.69301E-01	2.76670E-02
3	8.11148E-02	4.07800E-01	3.30786E-02
6	8.11712E-02	4.07300E-01	3.30610E-02
9	8.12382E-02	4.07600E-01	3.31127E-02
12	8.12692E-02	4.07500E-01	3.31172E-02
15	8.12896E-02	4.07400E-01	3.31174E-02
18	8.12405E-02	4.07100E-01	3.30730E-02
21	8.12870E-02	4.07300E-01	3.31082E-02
24	8.12466E-02	4.07000E-01	3.30674E-02
27	8.12284E-02	4.07401E-01	3.30925E-02
30	8.12622E-02	4.06800E-01	3.30575E-02
33	8.12550E-02	4.07600E-01	3.31195E-02
36	8.12690E-02	4.07500E-01	3.31171E-02
39	8.12515E-02	4.07300E-01	3.30937E-02
42	8.12090E-02	4.07600E-01	3.31008E-02
45	7.87590E-02	3.93900E-01	3.10232E-02

Table B.7. ^{10}B channel detector with $30\ \mu\text{m}$ deep perforations, $4\ \mu\text{m}$ wide channels, and no cap

ψ	p_n	η	ε	$\sigma(\varepsilon)$
$\theta = 0$				
0	3.68482E-01	4.48451E-01	1.65246E-01	4.06505E-04
5	3.68641E-01	4.47533E-01	1.64979E-01	4.06176E-04
10	3.67414E-01	4.47672E-01	1.64481E-01	4.05563E-04
15	3.67279E-01	4.46007E-01	1.63809E-01	4.04733E-04
20	3.68211E-01	4.46146E-01	1.64276E-01	4.05310E-04
25	3.66958E-01	4.46784E-01	1.63951E-01	4.04909E-04
30	3.67749E-01	4.46764E-01	1.64297E-01	4.05336E-04
35	3.68091E-01	4.46460E-01	1.64338E-01	4.05386E-04
40	3.66887E-01	4.47061E-01	1.64021E-01	4.04995E-04
45	3.67750E-01	4.46064E-01	1.64040E-01	4.05019E-04
50	3.67890E-01	4.47965E-01	1.64802E-01	4.05958E-04
55	3.67628E-01	4.46234E-01	1.64048E-01	4.05028E-04
60	3.68085E-01	4.46364E-01	1.64300E-01	4.05339E-04
65	3.67275E-01	4.47493E-01	1.64353E-01	4.05405E-04
70	3.68435E-01	4.46361E-01	1.64455E-01	4.05531E-04
75	3.67266E-01	4.48155E-01	1.64592E-01	4.05699E-04
80	3.68350E-01	4.46638E-01	1.64519E-01	4.05609E-04
85	3.67851E-01	4.46480E-01	1.64238E-01	4.05263E-04
90	3.67810E-01	4.47011E-01	1.64415E-01	4.05481E-04
$\theta = 5$				
0	4.19187E-01	4.73567E-01	1.98513E-01	4.46398E-04
5	4.19432E-01	4.73426E-01	1.98570E-01	4.46463E-04
10	4.18161E-01	4.73083E-01	1.97825E-01	4.45624E-04
15	4.16980E-01	4.73095E-01	1.97271E-01	4.45000E-04
20	4.16135E-01	4.74940E-01	1.97639E-01	4.45414E-04
25	4.14197E-01	4.74598E-01	1.96577E-01	4.44216E-04
30	4.10920E-01	4.74567E-01	1.95009E-01	4.42441E-04
35	4.10371E-01	4.73815E-01	1.94440E-01	4.41795E-04
40	4.07148E-01	4.72943E-01	1.92558E-01	4.39652E-04
45	4.04078E-01	4.74134E-01	1.91587E-01	4.38542E-04
50	4.01164E-01	4.73497E-01	1.89950E-01	4.36665E-04
55	3.96771E-01	4.71612E-01	1.87122E-01	4.33402E-04
60	3.92445E-01	4.71472E-01	1.85027E-01	4.30969E-04
65	3.88207E-01	4.70563E-01	1.82676E-01	4.28222E-04
70	3.85497E-01	4.66468E-01	1.79822E-01	4.24864E-04
75	3.80606E-01	4.63012E-01	1.76225E-01	4.20592E-04
80	3.75888E-01	4.59839E-01	1.72848E-01	4.16543E-04
85	3.70118E-01	4.52804E-01	1.67591E-01	4.10160E-04
90	3.66092E-01	4.46104E-01	1.63315E-01	4.04894E-04

ψ	p_n	η	ε	$\sigma(\varepsilon)$
$\theta = 10$				
0	4.66675E-01	4.64645E-01	2.16838E-01	4.69237E-04
5	4.66499E-01	4.66153E-01	2.17460E-01	4.69910E-04
10	4.65185E-01	4.65348E-01	2.16473E-01	4.68841E-04
15	4.64165E-01	4.66866E-01	2.16703E-01	4.69091E-04
20	4.61799E-01	4.66482E-01	2.15421E-01	4.67701E-04
25	4.59034E-01	4.66079E-01	2.13946E-01	4.66097E-04
30	4.54831E-01	4.68888E-01	2.13265E-01	4.65355E-04
35	4.50165E-01	4.69766E-01	2.11472E-01	4.63394E-04
40	4.44288E-01	4.71672E-01	2.09558E-01	4.61293E-04
45	4.39141E-01	4.70159E-01	2.06466E-01	4.57877E-04
50	4.32298E-01	4.72195E-01	2.04129E-01	4.55278E-04
55	4.23778E-01	4.73399E-01	2.00616E-01	4.51344E-04
60	4.17392E-01	4.74389E-01	1.98006E-01	4.48398E-04
65	4.08320E-01	4.73844E-01	1.93480E-01	4.43244E-04
70	4.00748E-01	4.72891E-01	1.89510E-01	4.38673E-04
75	3.91646E-01	4.69861E-01	1.84019E-01	4.32271E-04
80	3.83361E-01	4.66198E-01	1.78722E-01	4.26004E-04
85	3.73851E-01	4.59244E-01	1.71689E-01	4.17538E-04
90	3.64887E-01	4.47421E-01	1.63258E-01	4.07157E-04
$\theta = 15$				
0	4.80622E-01	4.55897E-01	2.19114E-01	4.76281E-04
5	4.80845E-01	4.55604E-01	2.19075E-01	4.76238E-04
10	4.79228E-01	4.56724E-01	2.18875E-01	4.76021E-04
15	4.79799E-01	4.57104E-01	2.19318E-01	4.76503E-04
20	4.79640E-01	4.55294E-01	2.18377E-01	4.75479E-04
25	4.80074E-01	4.56303E-01	2.19059E-01	4.76222E-04
30	4.78360E-01	4.57022E-01	2.18621E-01	4.75745E-04
35	4.76285E-01	4.58228E-01	2.18247E-01	4.75338E-04
40	4.74136E-01	4.60142E-01	2.18170E-01	4.75254E-04
45	4.68489E-01	4.63590E-01	2.17187E-01	4.74182E-04
50	4.61991E-01	4.65360E-01	2.14992E-01	4.71780E-04
55	4.53229E-01	4.66660E-01	2.11504E-01	4.67937E-04
60	4.41685E-01	4.70668E-01	2.07887E-01	4.63918E-04
65	4.29315E-01	4.71449E-01	2.02400E-01	4.57755E-04
70	4.15482E-01	4.73426E-01	1.96700E-01	4.51264E-04
75	4.02711E-01	4.74134E-01	1.90939E-01	4.44607E-04
80	3.89455E-01	4.70927E-01	1.83405E-01	4.35746E-04
85	3.75232E-01	4.63924E-01	1.74079E-01	4.24523E-04
90	3.61095E-01	4.46193E-01	1.61118E-01	4.08414E-04

ψ	p_n	η	ε	$\sigma(\varepsilon)$
$\theta = 20$				
0	4.72144E-01	4.54342E-01	2.14515E-01	4.77789E-04
5	4.71403E-01	4.54738E-01	2.14365E-01	4.77622E-04
10	4.72978E-01	4.53903E-01	2.14686E-01	4.77979E-04
15	4.71911E-01	4.55249E-01	2.14837E-01	4.78147E-04
20	4.73489E-01	4.54283E-01	2.15098E-01	4.78437E-04
25	4.73495E-01	4.54907E-01	2.15396E-01	4.78769E-04
30	4.74412E-01	4.53709E-01	2.15245E-01	4.78601E-04
35	4.75584E-01	4.54553E-01	2.16178E-01	4.79637E-04
40	4.76012E-01	4.55768E-01	2.16951E-01	4.80493E-04
45	4.76526E-01	4.55631E-01	2.17120E-01	4.80681E-04
50	4.73996E-01	4.57867E-01	2.17027E-01	4.80578E-04
55	4.70237E-01	4.62175E-01	2.17332E-01	4.80916E-04
60	4.62118E-01	4.63765E-01	2.14314E-01	4.77565E-04
65	4.47755E-01	4.68173E-01	2.09627E-01	4.72313E-04
70	4.30543E-01	4.73123E-01	2.03700E-01	4.65589E-04
75	4.13038E-01	4.73838E-01	1.95713E-01	4.56369E-04
80	3.93403E-01	4.73080E-01	1.86111E-01	4.45034E-04
85	3.75782E-01	4.68314E-01	1.75984E-01	4.32756E-04
90	3.54633E-01	4.45635E-01	1.58037E-01	4.10096E-04
$\theta = 25$				
0	4.68937E-01	4.54882E-01	2.13311E-01	4.85142E-04
5	4.69178E-01	4.54708E-01	2.13339E-01	4.85173E-04
10	4.68424E-01	4.56482E-01	2.13827E-01	4.85728E-04
15	4.67385E-01	4.55571E-01	2.12927E-01	4.84705E-04
20	4.68057E-01	4.55667E-01	2.13278E-01	4.85104E-04
25	4.67058E-01	4.56556E-01	2.13238E-01	4.85059E-04
30	4.66549E-01	4.55039E-01	2.12298E-01	4.83989E-04
35	4.66051E-01	4.54924E-01	2.12018E-01	4.83669E-04
40	4.66971E-01	4.54292E-01	2.12141E-01	4.83810E-04
45	4.67481E-01	4.53276E-01	2.11898E-01	4.83533E-04
50	4.70026E-01	4.54162E-01	2.13468E-01	4.85321E-04
55	4.70234E-01	4.55137E-01	2.14021E-01	4.85949E-04
60	4.69307E-01	4.58176E-01	2.15025E-01	4.87087E-04
65	4.60813E-01	4.61766E-01	2.12788E-01	4.84547E-04
70	4.45445E-01	4.68765E-01	2.08809E-01	4.79995E-04
75	4.22891E-01	4.73112E-01	2.00075E-01	4.69849E-04
80	3.97712E-01	4.75653E-01	1.89173E-01	4.56869E-04
85	3.73475E-01	4.68800E-01	1.75085E-01	4.39528E-04
90	3.48648E-01	4.45796E-01	1.55426E-01	4.14118E-04

ψ	p_n	η	ε	$\sigma(\varepsilon)$
$\theta = 30$				
0	4.62630E-01	4.54441E-01	2.10238E-01	4.92709E-04
5	4.63846E-01	4.52443E-01	2.09864E-01	4.92270E-04
10	4.64622E-01	4.52383E-01	2.10187E-01	4.92649E-04
15	4.63698E-01	4.53890E-01	2.10468E-01	4.92979E-04
20	4.63820E-01	4.52980E-01	2.10101E-01	4.92548E-04
25	4.63817E-01	4.53681E-01	2.10425E-01	4.92928E-04
30	4.63582E-01	4.53572E-01	2.10268E-01	4.92743E-04
35	4.63294E-01	4.55173E-01	2.10879E-01	4.93459E-04
40	4.60903E-01	4.55818E-01	2.10088E-01	4.92533E-04
45	4.59796E-01	4.53155E-01	2.08359E-01	4.90502E-04
50	4.59724E-01	4.55160E-01	2.09248E-01	4.91548E-04
55	4.61165E-01	4.53371E-01	2.09079E-01	4.91349E-04
60	4.63675E-01	4.53893E-01	2.10459E-01	4.92968E-04
65	4.63268E-01	4.57081E-01	2.11751E-01	4.94479E-04
70	4.54451E-01	4.63282E-01	2.10539E-01	4.93062E-04
75	4.33874E-01	4.70164E-01	2.03992E-01	4.85335E-04
80	4.02283E-01	4.75518E-01	1.91293E-01	4.69985E-04
85	3.71355E-01	4.74015E-01	1.76028E-01	4.50844E-04
90	3.39357E-01	4.43727E-01	1.50582E-01	4.16986E-04
$\theta = 35$				
0	4.54083E-01	4.53281E-01	2.05827E-01	5.01266E-04
5	4.53640E-01	4.54515E-01	2.06186E-01	5.01704E-04
10	4.54224E-01	4.53285E-01	2.05893E-01	5.01347E-04
15	4.54107E-01	4.52272E-01	2.05380E-01	5.00722E-04
20	4.53687E-01	4.52735E-01	2.05400E-01	5.00746E-04
25	4.54359E-01	4.52488E-01	2.05592E-01	5.00981E-04
30	4.53271E-01	4.53982E-01	2.05777E-01	5.01206E-04
35	4.54167E-01	4.52794E-01	2.05644E-01	5.01044E-04
40	4.55091E-01	4.53125E-01	2.06213E-01	5.01736E-04
45	4.54666E-01	4.53973E-01	2.06406E-01	5.01971E-04
50	4.52333E-01	4.53613E-01	2.05184E-01	5.00484E-04
55	4.50376E-01	4.54698E-01	2.04785E-01	4.99996E-04
60	4.50584E-01	4.54677E-01	2.04870E-01	5.00100E-04
65	4.53302E-01	4.53106E-01	2.05394E-01	5.00739E-04
70	4.53510E-01	4.56321E-01	2.06946E-01	5.02627E-04
75	4.39098E-01	4.65507E-01	2.04403E-01	4.99530E-04
80	4.07157E-01	4.73763E-01	1.92896E-01	4.85265E-04
85	3.67223E-01	4.76057E-01	1.74819E-01	4.61969E-04
90	3.28818E-01	4.43492E-01	1.45828E-01	4.21928E-04

ψ	p_n	η	ε	$\sigma(\varepsilon)$
$\theta = 40$				
0	4.43790E-01	4.52459E-01	2.00797E-01	5.11979E-04
5	4.44009E-01	4.51930E-01	2.00661E-01	5.11805E-04
10	4.44137E-01	4.52068E-01	2.00780E-01	5.11957E-04
15	4.43632E-01	4.50865E-01	2.00018E-01	5.10984E-04
20	4.44751E-01	4.53204E-01	2.01563E-01	5.12954E-04
25	4.43598E-01	4.52673E-01	2.00805E-01	5.11988E-04
30	4.43688E-01	4.52340E-01	2.00698E-01	5.11853E-04
35	4.42915E-01	4.53306E-01	2.00776E-01	5.11951E-04
40	4.42728E-01	4.52065E-01	2.00142E-01	5.11143E-04
45	4.44390E-01	4.51446E-01	2.00618E-01	5.11750E-04
50	4.44438E-01	4.53094E-01	2.01372E-01	5.12711E-04
55	4.43134E-01	4.52764E-01	2.00635E-01	5.11772E-04
60	4.40250E-01	4.53624E-01	1.99708E-01	5.10588E-04
65	4.40125E-01	4.52631E-01	1.99214E-01	5.09957E-04
70	4.44260E-01	4.53653E-01	2.01540E-01	5.12925E-04
75	4.39748E-01	4.60189E-01	2.02367E-01	5.13976E-04
80	4.10432E-01	4.71457E-01	1.93501E-01	5.02590E-04
85	3.62900E-01	4.77925E-01	1.73439E-01	4.75825E-04
90	3.16061E-01	4.43506E-01	1.40175E-01	4.27767E-04
$\theta = 45$				
0	4.30437E-01	4.51834E-01	1.94486E-01	5.24447E-04
5	4.30428E-01	4.51660E-01	1.94407E-01	5.24341E-04
10	4.29776E-01	4.52159E-01	1.94327E-01	5.24233E-04
15	4.29968E-01	4.51862E-01	1.94286E-01	5.24177E-04
20	4.30065E-01	4.51897E-01	1.94345E-01	5.24258E-04
25	4.30064E-01	4.51989E-01	1.94384E-01	5.24309E-04
30	4.30343E-01	4.51589E-01	1.94338E-01	5.24247E-04
35	4.31039E-01	4.51600E-01	1.94657E-01	5.24678E-04
40	4.30863E-01	4.50800E-01	1.94233E-01	5.24106E-04
45	4.29363E-01	4.51464E-01	1.93842E-01	5.23578E-04
50	4.29492E-01	4.51869E-01	1.94074E-01	5.23891E-04
55	4.29849E-01	4.51710E-01	1.94167E-01	5.24017E-04
60	4.30682E-01	4.53604E-01	1.95359E-01	5.25623E-04
65	4.27040E-01	4.53407E-01	1.93623E-01	5.23282E-04
70	4.27307E-01	4.53910E-01	1.93959E-01	5.23737E-04
75	4.30377E-01	4.55206E-01	1.95910E-01	5.26364E-04
80	4.11297E-01	4.67628E-01	1.92334E-01	5.21538E-04
85	3.56878E-01	4.79183E-01	1.71010E-01	4.91776E-04
90	2.99873E-01	4.41444E-01	1.32377E-01	4.32677E-04

ψ	p_n	η	ε	$\sigma(\varepsilon)$
$\theta = 50$				
0	4.12938E-01	4.50327E-01	1.85957E-01	5.37864E-04
5	4.14102E-01	4.48933E-01	1.85904E-01	5.37788E-04
10	4.13732E-01	4.51111E-01	1.86639E-01	5.38849E-04
15	4.13676E-01	4.50116E-01	1.86202E-01	5.38218E-04
20	4.13634E-01	4.49859E-01	1.86077E-01	5.38037E-04
25	4.14358E-01	4.50190E-01	1.86540E-01	5.38707E-04
30	4.13913E-01	4.51506E-01	1.86884E-01	5.39203E-04
35	4.13294E-01	4.50026E-01	1.85993E-01	5.37916E-04
40	4.13179E-01	4.50730E-01	1.86232E-01	5.38262E-04
45	4.13994E-01	4.50731E-01	1.86600E-01	5.38793E-04
50	4.14022E-01	4.50974E-01	1.86713E-01	5.38956E-04
55	4.13119E-01	4.51383E-01	1.86475E-01	5.38612E-04
60	4.12952E-01	4.50093E-01	1.85867E-01	5.37733E-04
65	4.13613E-01	4.52128E-01	1.87006E-01	5.39378E-04
70	4.10237E-01	4.52558E-01	1.85656E-01	5.37429E-04
75	4.12499E-01	4.52726E-01	1.86749E-01	5.39008E-04
80	4.06789E-01	4.62707E-01	1.88224E-01	5.41132E-04
85	3.50988E-01	4.80358E-01	1.68600E-01	5.12147E-04
90	2.80466E-01	4.39272E-01	1.23201E-01	4.37798E-04
$\theta = 55$				
0	3.92950E-01	4.49833E-01	1.76762E-01	5.55136E-04
5	3.93166E-01	4.50120E-01	1.76972E-01	5.55466E-04
10	3.92906E-01	4.48685E-01	1.76291E-01	5.54395E-04
15	3.93539E-01	4.48952E-01	1.76680E-01	5.55006E-04
20	3.93553E-01	4.48029E-01	1.76323E-01	5.54445E-04
25	3.93464E-01	4.49180E-01	1.76736E-01	5.55095E-04
30	3.93259E-01	4.49983E-01	1.76960E-01	5.55447E-04
35	3.93118E-01	4.48817E-01	1.76438E-01	5.54627E-04
40	3.93356E-01	4.49105E-01	1.76658E-01	5.54972E-04
45	3.93297E-01	4.49589E-01	1.76822E-01	5.55230E-04
50	3.92582E-01	4.50077E-01	1.76692E-01	5.55025E-04
55	3.93459E-01	4.49691E-01	1.76935E-01	5.55406E-04
60	3.91951E-01	4.51615E-01	1.77011E-01	5.55526E-04
65	3.92704E-01	4.49580E-01	1.76552E-01	5.54805E-04
70	3.92487E-01	4.52430E-01	1.77573E-01	5.56407E-04
75	3.88807E-01	4.52150E-01	1.75799E-01	5.53621E-04
80	3.92884E-01	4.57178E-01	1.79618E-01	5.59603E-04
85	3.43696E-01	4.81539E-01	1.65503E-01	5.37164E-04
90	2.58887E-01	4.37666E-01	1.13306E-01	4.44458E-04

ψ	p_n	η	ε	$\sigma(\varepsilon)$
$\theta = 60$				
0	3.66963E-01	4.47189E-01	1.64102E-01	5.72892E-04
5	3.67134E-01	4.47594E-01	1.64327E-01	5.73284E-04
10	3.67579E-01	4.47069E-01	1.64333E-01	5.73294E-04
15	3.67436E-01	4.46339E-01	1.64001E-01	5.72715E-04
20	3.67824E-01	4.47807E-01	1.64714E-01	5.73959E-04
25	3.67315E-01	4.46391E-01	1.63966E-01	5.72654E-04
30	3.67454E-01	4.48015E-01	1.64625E-01	5.73803E-04
35	3.66844E-01	4.47032E-01	1.63991E-01	5.72697E-04
40	3.68132E-01	4.47369E-01	1.64691E-01	5.73918E-04
45	3.66948E-01	4.48336E-01	1.64516E-01	5.73613E-04
50	3.67576E-01	4.48033E-01	1.64686E-01	5.73909E-04
55	3.67390E-01	4.47070E-01	1.64249E-01	5.73147E-04
60	3.66703E-01	4.48000E-01	1.64283E-01	5.73207E-04
65	3.67044E-01	4.48595E-01	1.64654E-01	5.73855E-04
70	3.66707E-01	4.49539E-01	1.64849E-01	5.74193E-04
75	3.65084E-01	4.51307E-01	1.64765E-01	5.74048E-04
80	3.66329E-01	4.52451E-01	1.65746E-01	5.75753E-04
85	3.36609E-01	4.80050E-01	1.61589E-01	5.68487E-04
90	2.31901E-01	4.36078E-01	1.01127E-01	4.49727E-04
$\theta = 65$				
0	3.34910E-01	4.44743E-01	1.48949E-01	5.93669E-04
5	3.35018E-01	4.45681E-01	1.49311E-01	5.94391E-04
10	3.34908E-01	4.45415E-01	1.49173E-01	5.94115E-04
15	3.34801E-01	4.45259E-01	1.49073E-01	5.93917E-04
20	3.34469E-01	4.45222E-01	1.48913E-01	5.93598E-04
25	3.34764E-01	4.45714E-01	1.49209E-01	5.94187E-04
30	3.34900E-01	4.45148E-01	1.49080E-01	5.93931E-04
35	3.34755E-01	4.45084E-01	1.48994E-01	5.93760E-04
40	3.34769E-01	4.45376E-01	1.49098E-01	5.93965E-04
45	3.34813E-01	4.45986E-01	1.49322E-01	5.94412E-04
50	3.34628E-01	4.45369E-01	1.49033E-01	5.93838E-04
55	3.34454E-01	4.45021E-01	1.48839E-01	5.93451E-04
60	3.34666E-01	4.45331E-01	1.49037E-01	5.93845E-04
65	3.34152E-01	4.45336E-01	1.48810E-01	5.93392E-04
70	3.34358E-01	4.48441E-01	1.49940E-01	5.95642E-04
75	3.34879E-01	4.47197E-01	1.49757E-01	5.95278E-04
80	3.30853E-01	4.51965E-01	1.49534E-01	5.94834E-04
85	3.22680E-01	4.73974E-01	1.52942E-01	6.01575E-04
90	2.02199E-01	4.31861E-01	8.73218E-02	4.54556E-04

ψ	p_n	η	ε	$\sigma(\varepsilon)$
$\theta = 70$				
0	2.93012E-01	4.42852E-01	1.29761E-01	6.15951E-04
5	2.92944E-01	4.40951E-01	1.29174E-01	6.14556E-04
10	2.92921E-01	4.41679E-01	1.29377E-01	6.15039E-04
15	2.92817E-01	4.41638E-01	1.29319E-01	6.14902E-04
20	2.92904E-01	4.41489E-01	1.29314E-01	6.14890E-04
25	2.92884E-01	4.40185E-01	1.28923E-01	6.13958E-04
30	2.92846E-01	4.42273E-01	1.29518E-01	6.15373E-04
35	2.92910E-01	4.41921E-01	1.29443E-01	6.15196E-04
40	2.92848E-01	4.42004E-01	1.29440E-01	6.15188E-04
45	2.92881E-01	4.42125E-01	1.29490E-01	6.15307E-04
50	2.92685E-01	4.41796E-01	1.29307E-01	6.14872E-04
55	2.93058E-01	4.42199E-01	1.29590E-01	6.15546E-04
60	2.93025E-01	4.43126E-01	1.29847E-01	6.16154E-04
65	2.92534E-01	4.42174E-01	1.29351E-01	6.14976E-04
70	2.92494E-01	4.43602E-01	1.29751E-01	6.15928E-04
75	2.92013E-01	4.45484E-01	1.30087E-01	6.16724E-04
80	2.92113E-01	4.48214E-01	1.30929E-01	6.18717E-04
85	2.92022E-01	4.62650E-01	1.35104E-01	6.28505E-04
90	1.67514E-01	4.27097E-01	7.15448E-02	4.57365E-04
$\theta = 75$				
0	2.38841E-01	4.37015E-01	1.04377E-01	6.35044E-04
5	2.38798E-01	4.36478E-01	1.04230E-01	6.34596E-04
10	2.38975E-01	4.36669E-01	1.04353E-01	6.34972E-04
15	2.38825E-01	4.35922E-01	1.04109E-01	6.34230E-04
20	2.38954E-01	4.36921E-01	1.04404E-01	6.35127E-04
25	2.38953E-01	4.36655E-01	1.04340E-01	6.34933E-04
30	2.39006E-01	4.36671E-01	1.04367E-01	6.35015E-04
35	2.38944E-01	4.35592E-01	1.04082E-01	6.34147E-04
40	2.38974E-01	4.37604E-01	1.04576E-01	6.35650E-04
45	2.39040E-01	4.36642E-01	1.04375E-01	6.35038E-04
50	2.38893E-01	4.37238E-01	1.04453E-01	6.35277E-04
55	2.38890E-01	4.36674E-01	1.04317E-01	6.34863E-04
60	2.38949E-01	4.36842E-01	1.04383E-01	6.35064E-04
65	2.38837E-01	4.37742E-01	1.04549E-01	6.35567E-04
70	2.38859E-01	4.37986E-01	1.04617E-01	6.35775E-04
75	2.38695E-01	4.38740E-01	1.04725E-01	6.36101E-04
80	2.38031E-01	4.41564E-01	1.05106E-01	6.37259E-04
85	2.37352E-01	4.51721E-01	1.07217E-01	6.43627E-04
90	1.28608E-01	4.20158E-01	5.40357E-02	4.56922E-04

ψ	p_n	η	ε	$\sigma(\varepsilon)$
$\theta = 80$				
0	1.69876E-01	4.28266E-01	7.27521E-02	6.47274E-04
5	1.69855E-01	4.27430E-01	7.26011E-02	6.46601E-04
10	1.69887E-01	4.28346E-01	7.27704E-02	6.47355E-04
15	1.69847E-01	4.27323E-01	7.25795E-02	6.46505E-04
20	1.69866E-01	4.28338E-01	7.27601E-02	6.47309E-04
25	1.69835E-01	4.28030E-01	7.26945E-02	6.47017E-04
30	1.69826E-01	4.27885E-01	7.26660E-02	6.46890E-04
35	1.69821E-01	4.28053E-01	7.26924E-02	6.47008E-04
40	1.69865E-01	4.28146E-01	7.27271E-02	6.47162E-04
45	1.69905E-01	4.28509E-01	7.28058E-02	6.47512E-04
50	1.69852E-01	4.28695E-01	7.28147E-02	6.47552E-04
55	1.69842E-01	4.28557E-01	7.27869E-02	6.47428E-04
60	1.69822E-01	4.28323E-01	7.27386E-02	6.47213E-04
65	1.69875E-01	4.28412E-01	7.27765E-02	6.47382E-04
70	1.69857E-01	4.30014E-01	7.30409E-02	6.48557E-04
75	1.69793E-01	4.30803E-01	7.31474E-02	6.49029E-04
80	1.69775E-01	4.33159E-01	7.35395E-02	6.50766E-04
85	1.69730E-01	4.44684E-01	7.54762E-02	6.59280E-04
90	8.69600E-02	4.07049E-01	3.53970E-02	4.51490E-04
$\theta = 85$				
0	8.71151E-02	4.07025E-01	3.54580E-02	6.37836E-04
5	8.71148E-02	4.06724E-01	3.54317E-02	6.37599E-04
10	8.71138E-02	4.08227E-01	3.55622E-02	6.38773E-04
15	8.71117E-02	4.07895E-01	3.55324E-02	6.38505E-04
20	8.71117E-02	4.07135E-01	3.54662E-02	6.37910E-04
25	8.71133E-02	4.07319E-01	3.54829E-02	6.38060E-04
30	8.71134E-02	4.07186E-01	3.54714E-02	6.37957E-04
35	8.71123E-02	4.07646E-01	3.55110E-02	6.38313E-04
40	8.71142E-02	4.07933E-01	3.55368E-02	6.38544E-04
45	8.71148E-02	4.07896E-01	3.55338E-02	6.38518E-04
50	8.71113E-02	4.07069E-01	3.54603E-02	6.37857E-04
55	8.71097E-02	4.08933E-01	3.56220E-02	6.39310E-04
60	8.71112E-02	4.08729E-01	3.56049E-02	6.39156E-04
65	8.71170E-02	4.08948E-01	3.56263E-02	6.39348E-04
70	8.71130E-02	4.08825E-01	3.56140E-02	6.39238E-04
75	8.71124E-02	4.10055E-01	3.57209E-02	6.40197E-04
80	8.71119E-02	4.13329E-01	3.60059E-02	6.42746E-04
85	8.71092E-02	4.27044E-01	3.71995E-02	6.53312E-04
90	4.36108E-02	3.77150E-01	1.64478E-02	4.34416E-04

Table B.8. ^{10}B channel detector with 50 μm deep perforations, 4 μm wide channels, and no cap

ψ	p_n	η	ε	$\sigma(\varepsilon)$
$\theta = 0$				
0	4.45872E-01	4.44002E-01	1.97968E-01	4.44936E-04
5	4.45787E-01	4.43241E-01	1.97591E-01	4.44512E-04
10	4.45295E-01	4.43079E-01	1.97301E-01	4.44186E-04
15	4.45423E-01	4.42018E-01	1.96885E-01	4.43717E-04
20	4.45730E-01	4.42907E-01	1.97417E-01	4.44316E-04
25	4.44808E-01	4.43036E-01	1.97066E-01	4.43921E-04
30	4.45659E-01	4.42958E-01	1.97408E-01	4.44306E-04
35	4.45870E-01	4.43481E-01	1.97735E-01	4.44674E-04
40	4.44941E-01	4.43717E-01	1.97428E-01	4.44329E-04
45	4.45928E-01	4.42816E-01	1.97464E-01	4.44369E-04
50	4.45188E-01	4.43035E-01	1.97234E-01	4.44110E-04
55	4.45218E-01	4.42287E-01	1.96914E-01	4.43750E-04
60	4.44362E-01	4.43204E-01	1.96943E-01	4.43783E-04
65	4.45922E-01	4.42400E-01	1.97276E-01	4.44158E-04
70	4.44817E-01	4.43571E-01	1.97308E-01	4.44194E-04
75	4.45525E-01	4.43010E-01	1.97372E-01	4.44266E-04
80	4.45293E-01	4.43358E-01	1.97424E-01	4.44324E-04
85	4.45776E-01	4.41574E-01	1.96843E-01	4.43670E-04
90	4.46269E-01	4.42462E-01	1.97457E-01	4.44361E-04
$\theta = 5$				
0	6.10902E-01	4.75613E-01	2.90553E-01	5.40058E-04
5	6.10019E-01	4.76413E-01	2.90621E-01	5.40121E-04
10	6.07773E-01	4.77422E-01	2.90164E-01	5.39696E-04
15	6.05385E-01	4.78420E-01	2.89628E-01	5.39198E-04
20	6.00313E-01	4.76335E-01	2.85950E-01	5.35763E-04
25	5.95364E-01	4.78252E-01	2.84734E-01	5.34623E-04
30	5.88580E-01	4.79870E-01	2.82442E-01	5.32467E-04
35	5.81303E-01	4.80386E-01	2.79250E-01	5.29450E-04
40	5.71734E-01	4.81913E-01	2.75526E-01	5.25907E-04
45	5.61705E-01	4.83020E-01	2.71315E-01	5.21873E-04
50	5.51160E-01	4.84592E-01	2.67088E-01	5.17791E-04
55	5.39401E-01	4.84254E-01	2.61207E-01	5.12060E-04
60	5.27523E-01	4.85660E-01	2.56197E-01	5.07125E-04
65	5.14528E-01	4.85002E-01	2.49547E-01	5.00500E-04
70	5.00376E-01	4.81490E-01	2.40926E-01	4.91778E-04
75	4.86869E-01	4.77761E-01	2.32607E-01	4.83214E-04
80	4.73037E-01	4.70291E-01	2.22465E-01	4.72562E-04
85	4.58564E-01	4.58710E-01	2.10348E-01	4.59512E-04
90	4.44553E-01	4.43835E-01	1.97308E-01	4.45042E-04

ψ	p_n	η	ε	$\sigma(\varepsilon)$
$\theta = 10$				
0	6.63236E-01	4.53003E-01	3.00448E-01	5.52343E-04
5	6.63168E-01	4.52544E-01	3.00113E-01	5.52035E-04
10	6.63774E-01	4.53556E-01	3.01059E-01	5.52904E-04
15	6.64630E-01	4.53935E-01	3.01699E-01	5.53492E-04
20	6.65117E-01	4.53723E-01	3.01779E-01	5.53565E-04
25	6.64612E-01	4.53633E-01	3.01490E-01	5.53300E-04
30	6.64816E-01	4.55242E-01	3.02652E-01	5.54365E-04
35	6.62687E-01	4.57749E-01	3.03344E-01	5.54999E-04
40	6.58362E-01	4.59149E-01	3.02286E-01	5.54030E-04
45	6.53911E-01	4.61445E-01	3.01744E-01	5.53533E-04
50	6.43626E-01	4.65628E-01	2.99690E-01	5.51646E-04
55	6.29746E-01	4.71338E-01	2.96823E-01	5.49001E-04
60	6.08228E-01	4.76708E-01	2.89947E-01	5.42605E-04
65	5.82644E-01	4.80206E-01	2.79789E-01	5.33015E-04
70	5.55086E-01	4.83349E-01	2.68300E-01	5.21957E-04
75	5.27145E-01	4.85430E-01	2.55892E-01	5.09745E-04
80	4.98404E-01	4.83780E-01	2.41118E-01	4.94811E-04
85	4.69815E-01	4.69340E-01	2.20503E-01	4.73186E-04
90	4.40311E-01	4.43191E-01	1.95142E-01	4.45143E-04
$\theta = 15$				
0	6.54207E-01	4.51169E-01	2.95158E-01	5.52784E-04
5	6.54654E-01	4.52146E-01	2.95999E-01	5.53571E-04
10	6.53704E-01	4.52599E-01	2.95866E-01	5.53446E-04
15	6.53778E-01	4.51058E-01	2.94892E-01	5.52535E-04
20	6.52465E-01	4.51727E-01	2.94736E-01	5.52388E-04
25	6.51211E-01	4.51425E-01	2.93973E-01	5.51673E-04
30	6.50940E-01	4.52017E-01	2.94236E-01	5.51920E-04
35	6.51491E-01	4.53368E-01	2.95365E-01	5.52977E-04
40	6.53982E-01	4.52282E-01	2.95784E-01	5.53370E-04
45	6.55409E-01	4.51736E-01	2.96072E-01	5.53639E-04
50	6.57607E-01	4.52500E-01	2.97567E-01	5.55035E-04
55	6.58373E-01	4.54586E-01	2.99287E-01	5.56637E-04
60	6.52755E-01	4.59437E-01	2.99900E-01	5.57206E-04
65	6.37384E-01	4.66890E-01	2.97588E-01	5.55055E-04
70	6.09037E-01	4.76163E-01	2.90001E-01	5.47933E-04
75	5.66756E-01	4.80971E-01	2.72593E-01	5.31233E-04
80	5.22650E-01	4.85072E-01	2.53523E-01	5.12314E-04
85	4.79166E-01	4.79283E-01	2.29656E-01	4.87603E-04
90	4.33605E-01	4.43355E-01	1.92241E-01	4.46120E-04

ψ	p_n	η	ε	$\sigma(\varepsilon)$
$\theta = 20$				
0	6.48389E-01	4.49727E-01	2.91598E-01	5.57057E-04
5	6.48962E-01	4.49418E-01	2.91655E-01	5.57111E-04
10	6.48663E-01	4.49927E-01	2.91851E-01	5.57298E-04
15	6.49609E-01	4.49911E-01	2.92266E-01	5.57694E-04
20	6.49657E-01	4.50122E-01	2.92425E-01	5.57846E-04
25	6.49860E-01	4.50282E-01	2.92620E-01	5.58032E-04
30	6.51402E-01	4.50418E-01	2.93403E-01	5.58778E-04
35	6.49459E-01	4.51496E-01	2.93228E-01	5.58612E-04
40	6.47372E-01	4.51354E-01	2.92194E-01	5.57625E-04
45	6.44799E-01	4.52713E-01	2.91909E-01	5.57354E-04
50	6.41923E-01	4.52765E-01	2.90640E-01	5.56141E-04
55	6.43934E-01	4.51590E-01	2.90794E-01	5.56288E-04
60	6.47795E-01	4.52702E-01	2.93258E-01	5.58640E-04
65	6.49910E-01	4.55772E-01	2.96211E-01	5.61445E-04
70	6.39113E-01	4.62364E-01	2.95503E-01	5.60774E-04
75	6.03920E-01	4.74257E-01	2.86413E-01	5.52082E-04
80	5.46365E-01	4.84211E-01	2.64556E-01	5.30599E-04
85	4.86442E-01	4.84827E-01	2.35840E-01	5.00975E-04
90	4.24831E-01	4.41773E-01	1.87679E-01	4.46905E-04
$\theta = 25$				
0	6.38211E-01	4.48801E-01	2.86430E-01	5.62175E-04
5	6.39190E-01	4.48766E-01	2.86847E-01	5.62584E-04
10	6.39475E-01	4.49603E-01	2.87510E-01	5.63234E-04
15	6.38169E-01	4.50139E-01	2.87265E-01	5.62994E-04
20	6.38109E-01	4.50492E-01	2.87463E-01	5.63187E-04
25	6.37545E-01	4.50028E-01	2.86913E-01	5.62649E-04
30	6.36948E-01	4.50421E-01	2.86895E-01	5.62631E-04
35	6.37104E-01	4.49286E-01	2.86242E-01	5.61990E-04
40	6.37906E-01	4.49022E-01	2.86434E-01	5.62179E-04
45	6.39561E-01	4.49305E-01	2.87358E-01	5.63085E-04
50	6.38258E-01	4.50567E-01	2.87578E-01	5.63300E-04
55	6.34550E-01	4.51388E-01	2.86428E-01	5.62173E-04
60	6.31979E-01	4.51805E-01	2.85531E-01	5.61292E-04
65	6.34732E-01	4.51702E-01	2.86710E-01	5.62449E-04
70	6.38899E-01	4.54820E-01	2.90584E-01	5.66237E-04
75	6.25415E-01	4.64693E-01	2.90626E-01	5.66277E-04
80	5.69917E-01	4.80428E-01	2.73804E-01	5.49644E-04
85	4.92086E-01	4.87970E-01	2.40123E-01	5.14729E-04
90	4.14102E-01	4.41280E-01	1.82735E-01	4.49028E-04

ψ	p_n	η	ε	$\sigma(\varepsilon)$
$\theta = 30$				
0	6.23902E-01	4.48909E-01	2.80075E-01	5.68685E-04
5	6.23789E-01	4.49508E-01	2.80398E-01	5.69013E-04
10	6.23845E-01	4.48979E-01	2.80093E-01	5.68703E-04
15	6.23546E-01	4.48515E-01	2.79670E-01	5.68274E-04
20	6.23647E-01	4.49099E-01	2.80079E-01	5.68689E-04
25	6.23846E-01	4.47806E-01	2.79362E-01	5.67960E-04
30	6.24553E-01	4.47642E-01	2.79576E-01	5.68178E-04
35	6.24408E-01	4.49495E-01	2.80668E-01	5.69286E-04
40	6.23773E-01	4.49726E-01	2.80527E-01	5.69144E-04
45	6.21782E-01	4.49540E-01	2.79516E-01	5.68117E-04
50	6.23420E-01	4.49206E-01	2.80044E-01	5.68654E-04
55	6.24307E-01	4.50270E-01	2.81107E-01	5.69732E-04
60	6.22843E-01	4.52116E-01	2.81597E-01	5.70228E-04
65	6.18269E-01	4.51156E-01	2.78936E-01	5.67527E-04
70	6.19307E-01	4.52714E-01	2.80369E-01	5.68983E-04
75	6.23592E-01	4.56154E-01	2.84454E-01	5.73113E-04
80	5.87913E-01	4.74795E-01	2.79138E-01	5.67733E-04
85	4.95751E-01	4.89562E-01	2.42701E-01	5.29384E-04
90	4.00359E-01	4.41246E-01	1.76657E-01	4.51648E-04
$\theta = 35$				
0	6.06539E-01	4.48205E-01	2.71854E-01	5.76084E-04
5	6.06364E-01	4.47706E-01	2.71473E-01	5.75680E-04
10	6.06243E-01	4.48812E-01	2.72089E-01	5.76332E-04
15	6.06385E-01	4.47006E-01	2.71058E-01	5.75240E-04
20	6.07078E-01	4.47664E-01	2.71767E-01	5.75991E-04
25	6.07188E-01	4.48008E-01	2.72025E-01	5.76265E-04
30	6.06682E-01	4.48269E-01	2.71957E-01	5.76193E-04
35	6.06394E-01	4.48164E-01	2.71764E-01	5.75989E-04
40	6.05910E-01	4.47832E-01	2.71346E-01	5.75545E-04
45	6.07744E-01	4.47958E-01	2.72244E-01	5.76497E-04
50	6.06223E-01	4.49674E-01	2.72603E-01	5.76877E-04
55	6.04256E-01	4.49336E-01	2.71514E-01	5.75724E-04
60	6.06692E-01	4.48877E-01	2.72330E-01	5.76588E-04
65	6.06465E-01	4.50156E-01	2.73004E-01	5.77301E-04
70	5.99957E-01	4.52994E-01	2.71777E-01	5.76003E-04
75	6.05415E-01	4.52049E-01	2.73677E-01	5.78012E-04
80	5.93677E-01	4.66136E-01	2.76734E-01	5.81231E-04
85	5.00953E-01	4.89772E-01	2.45353E-01	5.47285E-04
90	3.81559E-01	4.40781E-01	1.68184E-01	4.53117E-04

ψ	p_n	η	ε	$\sigma(\varepsilon)$
$\theta = 40$				
0	5.85200E-01	4.46972E-01	2.61568E-01	5.84340E-04
5	5.85516E-01	4.46978E-01	2.61713E-01	5.84501E-04
10	5.85702E-01	4.47560E-01	2.62137E-01	5.84975E-04
15	5.85247E-01	4.47493E-01	2.61894E-01	5.84703E-04
20	5.85697E-01	4.47827E-01	2.62291E-01	5.85147E-04
25	5.85057E-01	4.47394E-01	2.61751E-01	5.84544E-04
30	5.85247E-01	4.47098E-01	2.61663E-01	5.84446E-04
35	5.85092E-01	4.46485E-01	2.61235E-01	5.83967E-04
40	5.85209E-01	4.47334E-01	2.61784E-01	5.84581E-04
45	5.84736E-01	4.47609E-01	2.61733E-01	5.84524E-04
50	5.84572E-01	4.49110E-01	2.62537E-01	5.85421E-04
55	5.85265E-01	4.48769E-01	2.62649E-01	5.85546E-04
60	5.83475E-01	4.48413E-01	2.61638E-01	5.84418E-04
65	5.83971E-01	4.48003E-01	2.61621E-01	5.84399E-04
70	5.83415E-01	4.50391E-01	2.62765E-01	5.85676E-04
75	5.78921E-01	4.51571E-01	2.61424E-01	5.84179E-04
80	5.84277E-01	4.58240E-01	2.67739E-01	5.91193E-04
85	5.02903E-01	4.88653E-01	2.45745E-01	5.66389E-04
90	3.61895E-01	4.39017E-01	1.58878E-01	4.55412E-04
$\theta = 45$				
0	5.58971E-01	4.47018E-01	2.49870E-01	5.94449E-04
5	5.59243E-01	4.46913E-01	2.49933E-01	5.94524E-04
10	5.59425E-01	4.46669E-01	2.49878E-01	5.94459E-04
15	5.59819E-01	4.46564E-01	2.49995E-01	5.94597E-04
20	5.59404E-01	4.46913E-01	2.50005E-01	5.94609E-04
25	5.59568E-01	4.47742E-01	2.50542E-01	5.95248E-04
30	5.58331E-01	4.47249E-01	2.49713E-01	5.94262E-04
35	5.60335E-01	4.46513E-01	2.50197E-01	5.94838E-04
40	5.59336E-01	4.47355E-01	2.50222E-01	5.94867E-04
45	5.58879E-01	4.48310E-01	2.50551E-01	5.95259E-04
50	5.59525E-01	4.46845E-01	2.50021E-01	5.94628E-04
55	5.59171E-01	4.47276E-01	2.50104E-01	5.94727E-04
60	5.59270E-01	4.45913E-01	2.49386E-01	5.93873E-04
65	5.57687E-01	4.48866E-01	2.50327E-01	5.94992E-04
70	5.58824E-01	4.48784E-01	2.50791E-01	5.95543E-04
75	5.54249E-01	4.52465E-01	2.50778E-01	5.95527E-04
80	5.58499E-01	4.53193E-01	2.53108E-01	5.98288E-04
85	5.04196E-01	4.87120E-01	2.45604E-01	5.89352E-04
90	3.38544E-01	4.38416E-01	1.48423E-01	4.58151E-04

ψ	p_n	η	ε	$\sigma(\varepsilon)$
$\theta = 50$				
0	5.27815E-01	4.46463E-01	2.35650E-01	6.05481E-04
5	5.27673E-01	4.46032E-01	2.35359E-01	6.05106E-04
10	5.27729E-01	4.46337E-01	2.35545E-01	6.05345E-04
15	5.27749E-01	4.45920E-01	2.35334E-01	6.05074E-04
20	5.28034E-01	4.46166E-01	2.35591E-01	6.05405E-04
25	5.27905E-01	4.46317E-01	2.35613E-01	6.05433E-04
30	5.27700E-01	4.46333E-01	2.35530E-01	6.05326E-04
35	5.28138E-01	4.45073E-01	2.35060E-01	6.04722E-04
40	5.27149E-01	4.46246E-01	2.35238E-01	6.04951E-04
45	5.27776E-01	4.45735E-01	2.35248E-01	6.04964E-04
50	5.27725E-01	4.46958E-01	2.35871E-01	6.05764E-04
55	5.27753E-01	4.46385E-01	2.35581E-01	6.05392E-04
60	5.27065E-01	4.46387E-01	2.35275E-01	6.04998E-04
65	5.27567E-01	4.46887E-01	2.35763E-01	6.05625E-04
70	5.25737E-01	4.48220E-01	2.35646E-01	6.05475E-04
75	5.27462E-01	4.47985E-01	2.36295E-01	6.06308E-04
80	5.23145E-01	4.52685E-01	2.36820E-01	6.06982E-04
85	4.99736E-01	4.80772E-01	2.40259E-01	6.11372E-04
90	3.10930E-01	4.37446E-01	1.36015E-01	4.60002E-04
$\theta = 55$				
0	4.90470E-01	4.46700E-01	2.19093E-01	6.18043E-04
5	4.90197E-01	4.44307E-01	2.17798E-01	6.16214E-04
10	4.90425E-01	4.44357E-01	2.17924E-01	6.16392E-04
15	4.89920E-01	4.44477E-01	2.17758E-01	6.16157E-04
20	4.90099E-01	4.44663E-01	2.17929E-01	6.16398E-04
25	4.90445E-01	4.45084E-01	2.18289E-01	6.16908E-04
30	4.90458E-01	4.43467E-01	2.17502E-01	6.15795E-04
35	4.90179E-01	4.44895E-01	2.18078E-01	6.16609E-04
40	4.90648E-01	4.45821E-01	2.18741E-01	6.17547E-04
45	4.89788E-01	4.45027E-01	2.17969E-01	6.16456E-04
50	4.90065E-01	4.45665E-01	2.18405E-01	6.17072E-04
55	4.90147E-01	4.44726E-01	2.17981E-01	6.16473E-04
60	4.89826E-01	4.45452E-01	2.18194E-01	6.16774E-04
65	4.89779E-01	4.46473E-01	2.18673E-01	6.17450E-04
70	4.90601E-01	4.45409E-01	2.18518E-01	6.17231E-04
75	4.88523E-01	4.47258E-01	2.18496E-01	6.17201E-04
80	4.84916E-01	4.51218E-01	2.18803E-01	6.17634E-04
85	4.80939E-01	4.71544E-01	2.26784E-01	6.28797E-04
90	2.81143E-01	4.34715E-01	1.22217E-01	4.61605E-04

ψ	p_n	η	ε	$\sigma(\varepsilon)$
$\theta = 60$				
0	4.45430E-01	4.43122E-01	1.97380E-01	6.28299E-04
5	4.45055E-01	4.43154E-01	1.97228E-01	6.28057E-04
10	4.45233E-01	4.43828E-01	1.97607E-01	6.28661E-04
15	4.45175E-01	4.42810E-01	1.97128E-01	6.27899E-04
20	4.45418E-01	4.42077E-01	1.96909E-01	6.27549E-04
25	4.45303E-01	4.43202E-01	1.97359E-01	6.28267E-04
30	4.45354E-01	4.43119E-01	1.97345E-01	6.28244E-04
35	4.45337E-01	4.42970E-01	1.97271E-01	6.28127E-04
40	4.45761E-01	4.43635E-01	1.97755E-01	6.28897E-04
45	4.45329E-01	4.43636E-01	1.97564E-01	6.28592E-04
50	4.45438E-01	4.44681E-01	1.98078E-01	6.29409E-04
55	4.45401E-01	4.42561E-01	1.97117E-01	6.27881E-04
60	4.45248E-01	4.44101E-01	1.97735E-01	6.28864E-04
65	4.44668E-01	4.44199E-01	1.97521E-01	6.28524E-04
70	4.45019E-01	4.44826E-01	1.97956E-01	6.29216E-04
75	4.45047E-01	4.46378E-01	1.98659E-01	6.30332E-04
80	4.44993E-01	4.48585E-01	1.99617E-01	6.31850E-04
85	4.44724E-01	4.64729E-01	2.06676E-01	6.42925E-04
90	2.47148E-01	4.32356E-01	1.06856E-01	4.62291E-04
$\theta = 65$				
0	3.91711E-01	4.41050E-01	1.72764E-01	6.39370E-04
5	3.91863E-01	4.41073E-01	1.72840E-01	6.39512E-04
10	3.91975E-01	4.40600E-01	1.72704E-01	6.39260E-04
15	3.91916E-01	4.41069E-01	1.72862E-01	6.39551E-04
20	3.91707E-01	4.41294E-01	1.72858E-01	6.39545E-04
25	3.91942E-01	4.41313E-01	1.72969E-01	6.39750E-04
30	3.91811E-01	4.41065E-01	1.72814E-01	6.39463E-04
35	3.91898E-01	4.41725E-01	1.73111E-01	6.40012E-04
40	3.91976E-01	4.40986E-01	1.72856E-01	6.39541E-04
45	3.91661E-01	4.40692E-01	1.72602E-01	6.39071E-04
50	3.91721E-01	4.42537E-01	1.73351E-01	6.40456E-04
55	3.91879E-01	4.41458E-01	1.72998E-01	6.39802E-04
60	3.91691E-01	4.41912E-01	1.73093E-01	6.39979E-04
65	3.91645E-01	4.42385E-01	1.73258E-01	6.40284E-04
70	3.91343E-01	4.43038E-01	1.73380E-01	6.40508E-04
75	3.90994E-01	4.44153E-01	1.73661E-01	6.41029E-04
80	3.90652E-01	4.47175E-01	1.74690E-01	6.42925E-04
85	3.90230E-01	4.58758E-01	1.79021E-01	6.50845E-04
90	2.09810E-01	4.30389E-01	9.03000E-02	4.62242E-04

ψ	p_n	η	ε	$\sigma(\varepsilon)$
$\theta = 70$				
0	3.28655E-01	4.39622E-01	1.44484E-01	6.49956E-04
5	3.28606E-01	4.37670E-01	1.43821E-01	6.48464E-04
10	3.28619E-01	4.38757E-01	1.44184E-01	6.49281E-04
15	3.28511E-01	4.38363E-01	1.44007E-01	6.48882E-04
20	3.28621E-01	4.38581E-01	1.44127E-01	6.49153E-04
25	3.28571E-01	4.36928E-01	1.43562E-01	6.47879E-04
30	3.28507E-01	4.39123E-01	1.44255E-01	6.49440E-04
35	3.28628E-01	4.38185E-01	1.44000E-01	6.48867E-04
40	3.28523E-01	4.38246E-01	1.43974E-01	6.48809E-04
45	3.28536E-01	4.38573E-01	1.44087E-01	6.49063E-04
50	3.28615E-01	4.38866E-01	1.44218E-01	6.49358E-04
55	3.28570E-01	4.38738E-01	1.44156E-01	6.49217E-04
60	3.28598E-01	4.39631E-01	1.44462E-01	6.49908E-04
65	3.28569E-01	4.39774E-01	1.44496E-01	6.49984E-04
70	3.28520E-01	4.40065E-01	1.44570E-01	6.50148E-04
75	3.28258E-01	4.40800E-01	1.44696E-01	6.50433E-04
80	3.28622E-01	4.43360E-01	1.45698E-01	6.52681E-04
85	3.25850E-01	4.56919E-01	1.48887E-01	6.59785E-04
90	1.70789E-01	4.26527E-01	7.28462E-02	4.61506E-04
$\theta = 75$				
0	2.55250E-01	4.33982E-01	1.10774E-01	6.54216E-04
5	2.55246E-01	4.33319E-01	1.10603E-01	6.53710E-04
10	2.55176E-01	4.33579E-01	1.10639E-01	6.53817E-04
15	2.55200E-01	4.34111E-01	1.10785E-01	6.54247E-04
20	2.55252E-01	4.33775E-01	1.10722E-01	6.54061E-04
25	2.55255E-01	4.33261E-01	1.10592E-01	6.53677E-04
30	2.55212E-01	4.34643E-01	1.10926E-01	6.54666E-04
35	2.55213E-01	4.34923E-01	1.10998E-01	6.54876E-04
40	2.55287E-01	4.34558E-01	1.10937E-01	6.54698E-04
45	2.55185E-01	4.33689E-01	1.10671E-01	6.53912E-04
50	2.55212E-01	4.34141E-01	1.10798E-01	6.54287E-04
55	2.55210E-01	4.34376E-01	1.10857E-01	6.54459E-04
60	2.55203E-01	4.34685E-01	1.10933E-01	6.54685E-04
65	2.55254E-01	4.34489E-01	1.10905E-01	6.54601E-04
70	2.55221E-01	4.35297E-01	1.11097E-01	6.55168E-04
75	2.55279E-01	4.36879E-01	1.11526E-01	6.56433E-04
80	2.55256E-01	4.39672E-01	1.12229E-01	6.58499E-04
85	2.55253E-01	4.52136E-01	1.15409E-01	6.67761E-04
90	1.29375E-01	4.20244E-01	5.43691E-02	4.58330E-04

ψ	p_n	η	ε	$\sigma(\varepsilon)$
$\theta = 80$				
0	1.73359E-01	4.27038E-01	7.40309E-02	6.52937E-04
5	1.73348E-01	4.26269E-01	7.38928E-02	6.52328E-04
10	1.73359E-01	4.26315E-01	7.39055E-02	6.52384E-04
15	1.73351E-01	4.27276E-01	7.40687E-02	6.53104E-04
20	1.73352E-01	4.26462E-01	7.39281E-02	6.52484E-04
25	1.73346E-01	4.26981E-01	7.40154E-02	6.52869E-04
30	1.73357E-01	4.26186E-01	7.38824E-02	6.52282E-04
35	1.73358E-01	4.26150E-01	7.38765E-02	6.52256E-04
40	1.73350E-01	4.27678E-01	7.41379E-02	6.53409E-04
45	1.73361E-01	4.27710E-01	7.41483E-02	6.53455E-04
50	1.73342E-01	4.26052E-01	7.38527E-02	6.52151E-04
55	1.73348E-01	4.27209E-01	7.40559E-02	6.53047E-04
60	1.73342E-01	4.28350E-01	7.42511E-02	6.53907E-04
65	1.73360E-01	4.27919E-01	7.41840E-02	6.53612E-04
70	1.73358E-01	4.28387E-01	7.42643E-02	6.53966E-04
75	1.73344E-01	4.30571E-01	7.46369E-02	6.55604E-04
80	1.73348E-01	4.31482E-01	7.47965E-02	6.56305E-04
85	1.73356E-01	4.44658E-01	7.70841E-02	6.66266E-04
90	8.66596E-02	4.06837E-01	3.52563E-02	4.50592E-04
$\theta = 85$				
0	8.71556E-02	4.07857E-01	3.55470E-02	6.38636E-04
5	8.71554E-02	4.07898E-01	3.55505E-02	6.38667E-04
10	8.71552E-02	4.07822E-01	3.55438E-02	6.38607E-04
15	8.71554E-02	4.06925E-01	3.54657E-02	6.37906E-04
20	8.71554E-02	4.07206E-01	3.54902E-02	6.38125E-04
25	8.71553E-02	4.07280E-01	3.54966E-02	6.38183E-04
30	8.71555E-02	4.07791E-01	3.55412E-02	6.38584E-04
35	8.71554E-02	4.07614E-01	3.55258E-02	6.38446E-04
40	8.71554E-02	4.06653E-01	3.54420E-02	6.37693E-04
45	8.71553E-02	4.07755E-01	3.55380E-02	6.38555E-04
50	8.71554E-02	4.07734E-01	3.55362E-02	6.38539E-04
55	8.71555E-02	4.07946E-01	3.55547E-02	6.38706E-04
60	8.71554E-02	4.07535E-01	3.55189E-02	6.38384E-04
65	8.71555E-02	4.09231E-01	3.56667E-02	6.39711E-04
70	8.71552E-02	4.08824E-01	3.56311E-02	6.39391E-04
75	8.71555E-02	4.08959E-01	3.56430E-02	6.39498E-04
80	8.71553E-02	4.14453E-01	3.61218E-02	6.43779E-04
85	8.71552E-02	4.27052E-01	3.72198E-02	6.53490E-04
90	4.35690E-02	3.77569E-01	1.64503E-02	4.34449E-04

Table B.9. ${}^6\text{LiF}$ channel detector with 100 μm deep perforations, 20 μm wide channels, and no cap

ψ	p_n	η	ε	$\sigma(\varepsilon)$
$\theta = 0$				
0	1.99769E-01	6.34533E-01	1.26760E-01	3.56034E-04
5	2.00331E-01	6.33207E-01	1.26851E-01	3.56161E-04
10	1.99750E-01	6.34418E-01	1.26725E-01	3.55985E-04
15	2.00252E-01	6.34456E-01	1.27051E-01	3.56442E-04
20	1.99892E-01	6.34663E-01	1.26864E-01	3.56180E-04
25	1.99719E-01	6.32303E-01	1.26283E-01	3.55363E-04
30	2.00127E-01	6.34067E-01	1.26894E-01	3.56222E-04
35	2.00116E-01	6.35961E-01	1.27266E-01	3.56744E-04
40	1.99690E-01	6.33106E-01	1.26425E-01	3.55563E-04
45	2.00092E-01	6.33084E-01	1.26675E-01	3.55914E-04
50	1.99155E-01	6.33301E-01	1.26125E-01	3.55141E-04
55	1.99823E-01	6.34672E-01	1.26822E-01	3.56121E-04
60	1.99734E-01	6.34158E-01	1.26663E-01	3.55897E-04
65	2.00015E-01	6.34532E-01	1.26916E-01	3.56253E-04
70	2.00081E-01	6.33109E-01	1.26673E-01	3.55912E-04
75	2.00040E-01	6.34053E-01	1.26836E-01	3.56140E-04
80	1.99043E-01	6.33089E-01	1.26012E-01	3.54982E-04
85	1.99427E-01	6.31920E-01	1.26022E-01	3.54996E-04
90	1.99529E-01	6.32510E-01	1.26204E-01	3.55252E-04
$\theta = 5$				
0	2.05671E-01	6.38670E-01	1.31356E-01	3.63123E-04
5	2.05510E-01	6.40227E-01	1.31573E-01	3.63423E-04
10	2.05774E-01	6.38084E-01	1.31301E-01	3.63047E-04
15	2.05018E-01	6.39607E-01	1.31131E-01	3.62811E-04
20	2.04751E-01	6.38634E-01	1.30761E-01	3.62298E-04
25	2.04570E-01	6.39879E-01	1.30900E-01	3.62491E-04
30	2.05495E-01	6.37933E-01	1.31092E-01	3.62757E-04
35	2.04658E-01	6.40239E-01	1.31030E-01	3.62672E-04
40	2.03478E-01	6.39214E-01	1.30066E-01	3.61335E-04
45	2.03004E-01	6.36470E-01	1.29206E-01	3.60139E-04
50	2.03386E-01	6.40777E-01	1.30325E-01	3.61695E-04
55	2.02818E-01	6.39283E-01	1.29658E-01	3.60767E-04
60	2.02532E-01	6.39553E-01	1.29530E-01	3.60590E-04
65	2.02162E-01	6.37330E-01	1.28844E-01	3.59633E-04
70	2.01455E-01	6.37378E-01	1.28403E-01	3.59017E-04
75	2.02237E-01	6.36659E-01	1.28756E-01	3.59511E-04
80	2.00831E-01	6.35504E-01	1.27629E-01	3.57934E-04
85	2.00246E-01	6.33671E-01	1.26890E-01	3.56896E-04
90	2.00351E-01	6.34606E-01	1.27144E-01	3.57253E-04

ψ	p_n	η	ε	$\sigma(\varepsilon)$
$\theta = 10$				
0	2.11328E-01	6.41472E-01	1.35561E-01	3.71015E-04
5	2.10768E-01	6.42384E-01	1.35394E-01	3.70787E-04
10	2.11280E-01	6.41324E-01	1.35499E-01	3.70930E-04
15	2.09833E-01	6.43593E-01	1.35047E-01	3.70311E-04
20	2.09842E-01	6.41683E-01	1.34652E-01	3.69769E-04
25	2.10761E-01	6.39445E-01	1.34770E-01	3.69931E-04
30	2.09478E-01	6.41151E-01	1.34307E-01	3.69295E-04
35	2.08479E-01	6.39067E-01	1.33232E-01	3.67814E-04
40	2.07286E-01	6.39513E-01	1.32562E-01	3.66888E-04
45	2.07378E-01	6.39759E-01	1.32672E-01	3.67041E-04
50	2.06900E-01	6.38565E-01	1.32119E-01	3.66274E-04
55	2.05895E-01	6.39418E-01	1.31653E-01	3.65628E-04
60	2.04926E-01	6.39104E-01	1.30969E-01	3.64677E-04
65	2.03724E-01	6.40676E-01	1.30521E-01	3.64052E-04
70	2.03075E-01	6.38986E-01	1.29762E-01	3.62993E-04
75	2.02048E-01	6.37576E-01	1.28821E-01	3.61674E-04
80	2.01297E-01	6.37700E-01	1.28367E-01	3.61036E-04
85	1.99911E-01	6.37073E-01	1.27358E-01	3.59615E-04
90	1.98341E-01	6.32512E-01	1.25453E-01	3.56915E-04
$\theta = 15$				
0	2.16522E-01	6.42581E-01	1.39133E-01	3.79527E-04
5	2.16968E-01	6.41071E-01	1.39092E-01	3.79472E-04
10	2.16284E-01	6.43423E-01	1.39162E-01	3.79567E-04
15	2.15379E-01	6.43791E-01	1.38659E-01	3.78880E-04
20	2.15506E-01	6.42145E-01	1.38386E-01	3.78508E-04
25	2.14732E-01	6.42601E-01	1.37987E-01	3.77962E-04
30	2.14172E-01	6.43324E-01	1.37782E-01	3.77680E-04
35	2.13841E-01	6.43338E-01	1.37572E-01	3.77392E-04
40	2.11886E-01	6.40816E-01	1.35780E-01	3.74927E-04
45	2.11458E-01	6.40931E-01	1.35530E-01	3.74581E-04
50	2.10323E-01	6.42402E-01	1.35112E-01	3.74003E-04
55	2.08927E-01	6.42717E-01	1.34281E-01	3.72851E-04
60	2.08118E-01	6.39930E-01	1.33181E-01	3.71321E-04
65	2.06037E-01	6.38914E-01	1.31640E-01	3.69167E-04
70	2.04690E-01	6.39479E-01	1.30895E-01	3.68120E-04
75	2.03619E-01	6.39263E-01	1.30166E-01	3.67094E-04
80	2.00922E-01	6.37929E-01	1.28174E-01	3.64275E-04
85	2.00284E-01	6.34354E-01	1.27051E-01	3.62675E-04
90	1.97853E-01	6.35017E-01	1.25640E-01	3.60655E-04

ψ	p_n	η	ε	$\sigma(\varepsilon)$
$\theta = 20$				
0	2.20908E-01	6.43336E-01	1.42118E-01	3.88895E-04
5	2.20725E-01	6.42995E-01	1.41925E-01	3.88630E-04
10	2.20397E-01	6.42613E-01	1.41630E-01	3.88227E-04
15	2.21014E-01	6.41244E-01	1.41724E-01	3.88354E-04
20	2.20477E-01	6.41722E-01	1.41485E-01	3.88027E-04
25	2.20222E-01	6.44068E-01	1.41838E-01	3.88511E-04
30	2.18410E-01	6.44068E-01	1.40671E-01	3.86910E-04
35	2.16937E-01	6.43625E-01	1.39626E-01	3.85470E-04
40	2.16795E-01	6.42206E-01	1.39227E-01	3.84918E-04
45	2.14722E-01	6.40950E-01	1.37626E-01	3.82700E-04
50	2.13688E-01	6.42783E-01	1.37355E-01	3.82322E-04
55	2.11889E-01	6.40887E-01	1.35797E-01	3.80147E-04
60	2.09765E-01	6.40984E-01	1.34456E-01	3.78266E-04
65	2.07858E-01	6.40476E-01	1.33128E-01	3.76393E-04
70	2.05729E-01	6.39117E-01	1.31485E-01	3.74063E-04
75	2.03903E-01	6.39123E-01	1.30319E-01	3.72402E-04
80	2.00591E-01	6.37396E-01	1.27856E-01	3.68866E-04
85	1.99372E-01	6.37266E-01	1.27053E-01	3.67705E-04
90	1.96892E-01	6.33850E-01	1.24800E-01	3.64430E-04
$\theta = 25$				
0	2.22260E-01	6.42396E-01	1.42779E-01	3.96912E-04
5	2.22363E-01	6.42067E-01	1.42772E-01	3.96903E-04
10	2.21817E-01	6.42228E-01	1.42457E-01	3.96464E-04
15	2.22228E-01	6.41728E-01	1.42610E-01	3.96677E-04
20	2.21317E-01	6.42160E-01	1.42121E-01	3.95996E-04
25	2.21556E-01	6.42537E-01	1.42358E-01	3.96327E-04
30	2.21756E-01	6.39744E-01	1.41867E-01	3.95643E-04
35	2.20855E-01	6.42041E-01	1.41798E-01	3.95546E-04
40	2.19073E-01	6.42571E-01	1.40770E-01	3.94110E-04
45	2.18484E-01	6.41708E-01	1.40203E-01	3.93315E-04
50	2.16760E-01	6.44026E-01	1.39599E-01	3.92467E-04
55	2.13973E-01	6.41581E-01	1.37281E-01	3.89195E-04
60	2.11485E-01	6.43251E-01	1.36038E-01	3.87429E-04
65	2.09231E-01	6.41831E-01	1.34291E-01	3.84934E-04
70	2.06016E-01	6.39601E-01	1.31768E-01	3.81300E-04
75	2.03864E-01	6.40216E-01	1.30517E-01	3.79486E-04
80	2.01188E-01	6.38443E-01	1.28447E-01	3.76465E-04
85	1.97755E-01	6.37354E-01	1.26040E-01	3.72921E-04
90	1.95394E-01	6.32092E-01	1.23507E-01	3.69154E-04

ψ	p_n	η	ε	$\sigma(\varepsilon)$
$\theta = 30$				
0	2.20604E-01	6.40519E-01	1.41301E-01	4.03931E-04
5	2.21007E-01	6.39220E-01	1.41272E-01	4.03890E-04
10	2.20759E-01	6.39458E-01	1.41166E-01	4.03738E-04
15	2.20533E-01	6.41609E-01	1.41496E-01	4.04210E-04
20	2.21056E-01	6.38526E-01	1.41150E-01	4.03715E-04
25	2.21231E-01	6.40258E-01	1.41645E-01	4.04423E-04
30	2.20135E-01	6.40225E-01	1.40936E-01	4.03409E-04
35	2.20135E-01	6.41547E-01	1.41227E-01	4.03825E-04
40	2.20231E-01	6.40378E-01	1.41031E-01	4.03546E-04
45	2.19964E-01	6.40623E-01	1.40914E-01	4.03378E-04
50	2.18630E-01	6.42936E-01	1.40565E-01	4.02877E-04
55	2.16817E-01	6.43331E-01	1.39485E-01	4.01327E-04
60	2.14312E-01	6.40547E-01	1.37277E-01	3.98138E-04
65	2.11032E-01	6.41116E-01	1.35296E-01	3.95254E-04
70	2.07119E-01	6.39961E-01	1.32548E-01	3.91220E-04
75	2.03826E-01	6.40183E-01	1.30486E-01	3.88165E-04
80	2.00210E-01	6.37820E-01	1.27698E-01	3.83996E-04
85	1.97258E-01	6.36633E-01	1.25581E-01	3.80800E-04
90	1.92593E-01	6.32147E-01	1.21747E-01	3.74941E-04
$\theta = 35$				
0	2.18506E-01	6.37516E-01	1.39301E-01	4.12377E-04
5	2.18282E-01	6.38862E-01	1.39452E-01	4.12602E-04
10	2.18369E-01	6.37948E-01	1.39308E-01	4.12388E-04
15	2.18272E-01	6.37127E-01	1.39067E-01	4.12030E-04
20	2.18266E-01	6.39261E-01	1.39529E-01	4.12714E-04
25	2.18274E-01	6.39687E-01	1.39627E-01	4.12860E-04
30	2.18389E-01	6.37770E-01	1.39282E-01	4.12349E-04
35	2.19122E-01	6.39484E-01	1.40125E-01	4.13595E-04
40	2.19181E-01	6.40790E-01	1.40449E-01	4.14074E-04
45	2.19048E-01	6.40207E-01	1.40236E-01	4.13758E-04
50	2.18637E-01	6.41808E-01	1.40323E-01	4.13888E-04
55	2.17704E-01	6.41178E-01	1.39587E-01	4.12800E-04
60	2.15910E-01	6.40776E-01	1.38350E-01	4.10967E-04
65	2.13492E-01	6.43003E-01	1.37276E-01	4.09369E-04
70	2.08398E-01	6.42036E-01	1.33799E-01	4.04152E-04
75	2.04388E-01	6.41310E-01	1.31076E-01	4.00017E-04
80	1.99143E-01	6.38536E-01	1.27160E-01	3.93997E-04
85	1.94677E-01	6.37651E-01	1.24136E-01	3.89284E-04
90	1.90249E-01	6.30763E-01	1.20002E-01	3.82747E-04

ψ	p_n	η	ε	$\sigma(\varepsilon)$
$\theta = 40$				
0	2.16162E-01	6.39053E-01	1.38139E-01	4.24650E-04
5	2.16299E-01	6.39277E-01	1.38275E-01	4.24859E-04
10	2.16463E-01	6.38248E-01	1.38157E-01	4.24678E-04
15	2.16208E-01	6.37340E-01	1.37798E-01	4.24125E-04
20	2.16179E-01	6.37939E-01	1.37909E-01	4.24297E-04
25	2.16045E-01	6.37622E-01	1.37755E-01	4.24059E-04
30	2.15134E-01	6.38407E-01	1.37343E-01	4.23425E-04
35	2.16109E-01	6.38974E-01	1.38088E-01	4.24572E-04
40	2.15391E-01	6.39586E-01	1.37761E-01	4.24068E-04
45	2.16979E-01	6.39214E-01	1.38696E-01	4.25506E-04
50	2.16398E-01	6.37631E-01	1.37982E-01	4.24409E-04
55	2.16825E-01	6.39852E-01	1.38736E-01	4.25567E-04
60	2.16185E-01	6.41432E-01	1.38668E-01	4.25462E-04
65	2.14363E-01	6.42056E-01	1.37633E-01	4.23871E-04
70	2.09138E-01	6.39936E-01	1.33835E-01	4.17982E-04
75	2.04543E-01	6.41845E-01	1.31285E-01	4.13982E-04
80	1.98002E-01	6.39483E-01	1.26619E-01	4.06559E-04
85	1.92122E-01	6.36851E-01	1.22353E-01	3.99650E-04
90	1.86128E-01	6.30271E-01	1.17311E-01	3.91329E-04
$\theta = 45$				
0	2.14171E-01	6.38663E-01	1.36783E-01	4.39819E-04
5	2.14033E-01	6.38476E-01	1.36655E-01	4.39613E-04
10	2.14109E-01	6.38969E-01	1.36809E-01	4.39860E-04
15	2.14120E-01	6.39492E-01	1.36928E-01	4.40052E-04
20	2.14691E-01	6.38005E-01	1.36974E-01	4.40126E-04
25	2.13690E-01	6.38401E-01	1.36420E-01	4.39235E-04
30	2.13534E-01	6.39102E-01	1.36470E-01	4.39315E-04
35	2.13379E-01	6.38568E-01	1.36257E-01	4.38973E-04
40	2.12524E-01	6.37881E-01	1.35565E-01	4.37856E-04
45	2.13111E-01	6.36762E-01	1.35701E-01	4.38075E-04
50	2.13268E-01	6.36073E-01	1.35654E-01	4.38000E-04
55	2.13611E-01	6.36330E-01	1.35927E-01	4.38440E-04
60	2.13443E-01	6.39220E-01	1.36437E-01	4.39262E-04
65	2.13133E-01	6.40154E-01	1.36438E-01	4.39263E-04
70	2.09739E-01	6.40806E-01	1.34402E-01	4.35974E-04
75	2.04000E-01	6.40549E-01	1.30672E-01	4.29881E-04
80	1.96991E-01	6.39654E-01	1.26006E-01	4.22137E-04
85	1.89595E-01	6.37359E-01	1.20840E-01	4.13392E-04
90	1.81740E-01	6.29174E-01	1.14346E-01	4.02132E-04

ψ	p_n	η	ε	$\sigma(\varepsilon)$
$\theta = 50$				
0	2.09724E-01	6.36699E-01	1.33531E-01	4.55783E-04
5	2.09913E-01	6.37464E-01	1.33812E-01	4.56262E-04
10	2.09979E-01	6.37073E-01	1.33772E-01	4.56194E-04
15	2.09900E-01	6.35522E-01	1.33396E-01	4.55551E-04
20	2.10181E-01	6.36794E-01	1.33842E-01	4.56312E-04
25	2.10272E-01	6.36090E-01	1.33752E-01	4.56159E-04
30	2.10537E-01	6.39275E-01	1.34591E-01	4.57587E-04
35	2.10775E-01	6.39084E-01	1.34703E-01	4.57777E-04
40	2.10272E-01	6.37279E-01	1.34002E-01	4.56585E-04
45	2.09959E-01	6.38182E-01	1.33992E-01	4.56569E-04
50	2.09568E-01	6.37554E-01	1.33611E-01	4.55919E-04
55	2.09713E-01	6.36646E-01	1.33513E-01	4.55751E-04
60	2.09988E-01	6.34765E-01	1.33293E-01	4.55376E-04
65	2.10775E-01	6.38543E-01	1.34589E-01	4.57585E-04
70	2.09228E-01	6.40703E-01	1.34053E-01	4.56673E-04
75	2.04656E-01	6.42175E-01	1.31425E-01	4.52174E-04
80	1.95357E-01	6.40044E-01	1.25037E-01	4.41048E-04
85	1.85455E-01	6.36866E-01	1.18110E-01	4.28657E-04
90	1.75865E-01	6.27493E-01	1.10354E-01	4.14343E-04
$\theta = 55$				
0	2.05668E-01	6.34109E-01	1.30416E-01	4.76836E-04
5	2.05704E-01	6.35598E-01	1.30745E-01	4.77438E-04
10	2.05836E-01	6.36167E-01	1.30946E-01	4.77804E-04
15	2.05824E-01	6.36486E-01	1.31004E-01	4.77911E-04
20	2.05512E-01	6.34780E-01	1.30455E-01	4.76908E-04
25	2.05738E-01	6.37009E-01	1.31057E-01	4.78007E-04
30	2.04970E-01	6.37049E-01	1.30576E-01	4.77130E-04
35	2.05368E-01	6.35898E-01	1.30593E-01	4.77160E-04
40	2.05561E-01	6.37086E-01	1.30960E-01	4.77829E-04
45	2.05376E-01	6.36496E-01	1.30721E-01	4.77394E-04
50	2.05652E-01	6.37412E-01	1.31085E-01	4.78058E-04
55	2.04814E-01	6.37080E-01	1.30483E-01	4.76959E-04
60	2.03920E-01	6.36259E-01	1.29746E-01	4.75610E-04
65	2.05028E-01	6.35669E-01	1.30330E-01	4.76680E-04
70	2.05923E-01	6.37884E-01	1.31355E-01	4.78550E-04
75	2.03140E-01	6.40588E-01	1.30129E-01	4.76312E-04
80	1.92935E-01	6.40910E-01	1.23654E-01	4.64311E-04
85	1.81312E-01	6.37978E-01	1.15673E-01	4.49077E-04
90	1.69274E-01	6.24999E-01	1.05796E-01	4.29476E-04

ψ	p_n	η	ε	$\sigma(\varepsilon)$
$\theta = 60$				
0	1.99598E-01	6.33313E-01	1.26408E-01	5.02809E-04
5	1.99278E-01	6.33918E-01	1.26326E-01	5.02645E-04
10	1.99372E-01	6.34021E-01	1.26406E-01	5.02805E-04
15	1.99088E-01	6.34845E-01	1.26390E-01	5.02772E-04
20	1.99964E-01	6.35019E-01	1.26981E-01	5.03947E-04
25	1.99773E-01	6.34430E-01	1.26742E-01	5.03473E-04
30	1.99589E-01	6.33672E-01	1.26474E-01	5.02940E-04
35	1.99714E-01	6.34087E-01	1.26636E-01	5.03262E-04
40	1.99463E-01	6.34418E-01	1.26543E-01	5.03078E-04
45	1.99179E-01	6.33310E-01	1.26142E-01	5.02279E-04
50	1.99152E-01	6.36403E-01	1.26741E-01	5.03471E-04
55	1.99644E-01	6.36042E-01	1.26982E-01	5.03948E-04
60	1.99060E-01	6.34753E-01	1.26354E-01	5.02701E-04
65	1.98158E-01	6.33045E-01	1.25443E-01	5.00885E-04
70	1.98808E-01	6.34522E-01	1.26148E-01	5.02292E-04
75	1.99155E-01	6.38357E-01	1.27132E-01	5.04246E-04
80	1.91624E-01	6.39842E-01	1.22609E-01	4.95196E-04
85	1.75954E-01	6.36416E-01	1.11980E-01	4.73244E-04
90	1.59811E-01	6.21863E-01	9.93805E-02	4.45826E-04
$\theta = 65$				
0	1.91438E-01	6.30982E-01	1.20794E-01	5.34624E-04
5	1.91511E-01	6.30878E-01	1.20820E-01	5.34681E-04
10	1.91743E-01	6.31387E-01	1.21064E-01	5.35222E-04
15	1.91416E-01	6.32680E-01	1.21105E-01	5.35311E-04
20	1.91290E-01	6.32344E-01	1.20961E-01	5.34993E-04
25	1.91513E-01	6.32270E-01	1.21088E-01	5.35274E-04
30	1.91088E-01	6.31992E-01	1.20766E-01	5.34562E-04
35	1.90772E-01	6.31198E-01	1.20415E-01	5.33785E-04
40	1.91563E-01	6.31140E-01	1.20903E-01	5.34864E-04
45	1.91556E-01	6.32818E-01	1.21220E-01	5.35567E-04
50	1.91373E-01	6.32790E-01	1.21099E-01	5.35299E-04
55	1.90826E-01	6.31806E-01	1.20565E-01	5.34118E-04
60	1.91366E-01	6.32249E-01	1.20991E-01	5.35059E-04
65	1.91339E-01	6.33676E-01	1.21247E-01	5.35625E-04
70	1.89753E-01	6.31864E-01	1.19898E-01	5.32637E-04
75	1.90908E-01	6.33536E-01	1.20947E-01	5.34964E-04
80	1.88239E-01	6.37647E-01	1.20030E-01	5.32931E-04
85	1.69423E-01	6.36277E-01	1.07800E-01	5.05050E-04
90	1.48338E-01	6.16699E-01	9.14799E-02	4.65253E-04

ψ	p_n	η	ε	$\sigma(\varepsilon)$
$\theta = 70$				
0	1.79619E-01	6.28102E-01	1.12819E-01	5.74335E-04
5	1.79928E-01	6.27306E-01	1.12870E-01	5.74465E-04
10	1.79833E-01	6.27810E-01	1.12901E-01	5.74544E-04
15	1.79658E-01	6.28772E-01	1.12964E-01	5.74705E-04
20	1.79730E-01	6.27614E-01	1.12801E-01	5.74288E-04
25	1.79498E-01	6.28586E-01	1.12830E-01	5.74364E-04
30	1.79535E-01	6.29376E-01	1.12995E-01	5.74783E-04
35	1.79686E-01	6.28602E-01	1.12951E-01	5.74670E-04
40	1.79887E-01	6.28000E-01	1.12969E-01	5.74717E-04
45	1.79605E-01	6.27076E-01	1.12626E-01	5.73844E-04
50	1.79236E-01	6.28389E-01	1.12630E-01	5.73855E-04
55	1.79301E-01	6.28664E-01	1.12720E-01	5.74083E-04
60	1.79527E-01	6.29655E-01	1.13040E-01	5.74898E-04
65	1.79113E-01	6.29815E-01	1.12808E-01	5.74307E-04
70	1.79534E-01	6.29585E-01	1.13032E-01	5.74877E-04
75	1.77705E-01	6.28142E-01	1.11624E-01	5.71285E-04
80	1.79551E-01	6.33191E-01	1.13690E-01	5.76547E-04
85	1.62921E-01	6.35903E-01	1.03602E-01	5.50374E-04
90	1.32443E-01	6.10496E-01	8.08559E-02	4.86217E-04
$\theta = 75$				
0	1.62095E-01	6.23085E-01	1.00999E-01	6.24686E-04
5	1.62324E-01	6.21954E-01	1.00958E-01	6.24557E-04
10	1.62130E-01	6.22815E-01	1.00977E-01	6.24615E-04
15	1.62209E-01	6.22376E-01	1.00955E-01	6.24549E-04
20	1.62175E-01	6.23148E-01	1.01059E-01	6.24869E-04
25	1.62231E-01	6.22853E-01	1.01046E-01	6.24829E-04
30	1.62036E-01	6.20615E-01	1.00562E-01	6.23330E-04
35	1.62215E-01	6.22180E-01	1.00927E-01	6.24461E-04
40	1.62127E-01	6.21297E-01	1.00729E-01	6.23849E-04
45	1.62191E-01	6.22353E-01	1.00940E-01	6.24501E-04
50	1.62209E-01	6.23480E-01	1.01134E-01	6.25101E-04
55	1.61948E-01	6.22928E-01	1.00882E-01	6.24321E-04
60	1.61956E-01	6.22700E-01	1.00850E-01	6.24222E-04
65	1.62020E-01	6.23886E-01	1.01082E-01	6.24941E-04
70	1.61702E-01	6.22775E-01	1.00704E-01	6.23770E-04
75	1.61891E-01	6.26391E-01	1.01407E-01	6.25944E-04
80	1.60548E-01	6.23353E-01	1.00078E-01	6.21830E-04
85	1.54707E-01	6.35645E-01	9.83388E-02	6.16402E-04
90	1.11423E-01	6.00452E-01	6.69042E-02	5.08427E-04

ψ	p_n	η	ε	$\sigma(\varepsilon)$
$\theta = 80$				
0	1.33588E-01	6.11339E-01	8.16676E-02	6.85788E-04
5	1.33636E-01	6.10727E-01	8.16151E-02	6.85568E-04
10	1.33558E-01	6.12033E-01	8.17419E-02	6.86100E-04
15	1.33704E-01	6.11570E-01	8.17693E-02	6.86215E-04
20	1.33509E-01	6.10234E-01	8.14717E-02	6.84965E-04
25	1.33510E-01	6.11156E-01	8.15954E-02	6.85485E-04
30	1.33680E-01	6.10986E-01	8.16766E-02	6.85826E-04
35	1.33580E-01	6.11546E-01	8.16903E-02	6.85883E-04
40	1.33520E-01	6.11564E-01	8.16560E-02	6.85739E-04
45	1.33770E-01	6.11860E-01	8.18485E-02	6.86547E-04
50	1.33635E-01	6.11089E-01	8.16629E-02	6.85768E-04
55	1.33590E-01	6.10329E-01	8.15339E-02	6.85226E-04
60	1.33513E-01	6.12702E-01	8.18037E-02	6.86359E-04
65	1.33639E-01	6.11399E-01	8.17068E-02	6.85953E-04
70	1.33682E-01	6.13058E-01	8.19548E-02	6.86993E-04
75	1.33649E-01	6.12860E-01	8.19081E-02	6.86797E-04
80	1.33568E-01	6.15873E-01	8.22609E-02	6.88275E-04
85	1.33634E-01	6.19893E-01	8.28388E-02	6.90688E-04
90	8.21719E-02	5.81056E-01	4.77465E-02	5.24367E-04
$\theta = 85$				
0	8.24907E-02	5.81464E-01	4.79654E-02	7.41850E-04
5	8.24713E-02	5.80869E-01	4.79050E-02	7.41382E-04
10	8.24717E-02	5.81039E-01	4.79193E-02	7.41494E-04
15	8.24873E-02	5.80962E-01	4.79220E-02	7.41514E-04
20	8.24693E-02	5.80290E-01	4.78561E-02	7.41004E-04
25	8.25099E-02	5.79915E-01	4.78487E-02	7.40947E-04
30	8.24672E-02	5.80668E-01	4.78861E-02	7.41237E-04
35	8.24862E-02	5.80640E-01	4.78948E-02	7.41304E-04
40	8.24729E-02	5.81811E-01	4.79836E-02	7.41991E-04
45	8.25029E-02	5.80767E-01	4.79150E-02	7.41460E-04
50	8.24649E-02	5.80121E-01	4.78396E-02	7.40877E-04
55	8.24801E-02	5.80397E-01	4.78712E-02	7.41121E-04
60	8.24325E-02	5.81079E-01	4.78998E-02	7.41343E-04
65	8.24898E-02	5.81868E-01	4.79982E-02	7.42104E-04
70	8.24545E-02	5.81661E-01	4.79606E-02	7.41813E-04
75	8.24627E-02	5.82049E-01	4.79973E-02	7.42097E-04
80	8.24669E-02	5.83780E-01	4.81425E-02	7.43218E-04
85	8.25144E-02	5.91487E-01	4.88062E-02	7.48324E-04
90	4.34535E-02	5.35685E-01	2.32774E-02	5.16796E-04

Table B.10. ^{10}B chevron detector with 30 μm deep perforations, 4 μm wide channels, and no cap

ψ	p_n	η	ε	$\sigma(\varepsilon)$
$\theta = 0$				
0	3.66797E-01	4.29892E-01	1.57683E-01	3.97093E-04
5	3.67929E-01	4.31727E-01	1.58845E-01	3.98554E-04
10	3.68394E-01	4.30417E-01	1.58563E-01	3.98200E-04
15	3.67614E-01	4.30408E-01	1.58224E-01	3.97774E-04
20	3.68553E-01	4.30641E-01	1.58714E-01	3.98389E-04
25	3.67098E-01	4.30174E-01	1.57916E-01	3.97386E-04
30	3.68353E-01	4.30891E-01	1.58720E-01	3.98397E-04
35	3.67924E-01	4.29746E-01	1.58114E-01	3.97636E-04
40	3.67950E-01	4.31094E-01	1.58621E-01	3.98273E-04
45	3.67823E-01	4.30177E-01	1.58229E-01	3.97780E-04
50	3.66515E-01	4.30032E-01	1.57613E-01	3.97005E-04
55	3.67720E-01	4.31064E-01	1.58511E-01	3.98134E-04
60	3.67681E-01	4.30784E-01	1.58391E-01	3.97984E-04
65	3.67307E-01	4.30343E-01	1.58068E-01	3.97578E-04
70	3.67706E-01	4.31279E-01	1.58584E-01	3.98226E-04
75	3.67416E-01	4.30311E-01	1.58103E-01	3.97622E-04
80	3.67951E-01	4.29073E-01	1.57878E-01	3.97339E-04
85	3.67958E-01	4.29291E-01	1.57961E-01	3.97443E-04
90	3.67636E-01	4.30162E-01	1.58143E-01	3.97672E-04
$\theta = 5$				
0	4.03424E-01	4.57107E-01	1.84408E-01	4.30246E-04
5	4.03107E-01	4.56579E-01	1.84050E-01	4.29829E-04
10	4.03346E-01	4.58004E-01	1.84734E-01	4.30627E-04
15	4.02155E-01	4.56374E-01	1.83533E-01	4.29225E-04
20	4.01396E-01	4.54721E-01	1.82523E-01	4.28042E-04
25	4.00633E-01	4.54007E-01	1.81890E-01	4.27300E-04
30	3.99327E-01	4.52709E-01	1.80779E-01	4.25993E-04
35	3.97656E-01	4.51204E-01	1.79424E-01	4.24393E-04
40	3.94573E-01	4.47975E-01	1.76759E-01	4.21229E-04
45	3.92993E-01	4.46018E-01	1.75282E-01	4.19466E-04
50	3.94281E-01	4.50937E-01	1.77796E-01	4.22463E-04
55	3.95923E-01	4.51239E-01	1.78656E-01	4.23483E-04
60	3.98409E-01	4.52297E-01	1.80199E-01	4.25308E-04
65	3.98901E-01	4.54306E-01	1.81223E-01	4.26515E-04
70	3.99654E-01	4.56272E-01	1.82351E-01	4.27841E-04
75	4.00715E-01	4.56676E-01	1.82997E-01	4.28598E-04
80	4.01166E-01	4.58828E-01	1.84066E-01	4.29848E-04
85	4.00545E-01	4.58146E-01	1.83508E-01	4.29196E-04
90	4.02190E-01	4.57013E-01	1.83806E-01	4.29544E-04

ψ	p_n	η	ε	$\sigma(\varepsilon)$
$\theta = 10$				
0	4.39054E-01	4.54598E-01	1.99593E-01	4.50191E-04
5	4.38314E-01	4.54989E-01	1.99428E-01	4.50004E-04
10	4.38168E-01	4.55729E-01	1.99686E-01	4.50295E-04
15	4.35867E-01	4.55455E-01	1.98518E-01	4.48977E-04
20	4.33142E-01	4.54500E-01	1.96863E-01	4.47102E-04
25	4.31040E-01	4.53881E-01	1.95641E-01	4.45712E-04
30	4.27870E-01	4.52642E-01	1.93672E-01	4.43464E-04
35	4.24418E-01	4.50174E-01	1.91062E-01	4.40465E-04
40	4.20625E-01	4.48737E-01	1.88750E-01	4.37792E-04
45	4.15668E-01	4.43120E-01	1.84191E-01	4.32472E-04
50	4.18834E-01	4.49316E-01	1.88189E-01	4.37141E-04
55	4.21307E-01	4.51576E-01	1.90252E-01	4.39530E-04
60	4.23137E-01	4.54042E-01	1.92122E-01	4.41685E-04
65	4.25091E-01	4.56608E-01	1.94100E-01	4.43953E-04
70	4.27213E-01	4.57409E-01	1.95411E-01	4.45450E-04
75	4.28826E-01	4.58193E-01	1.96485E-01	4.46672E-04
80	4.29837E-01	4.56922E-01	1.96402E-01	4.46578E-04
85	4.30627E-01	4.56962E-01	1.96780E-01	4.47008E-04
90	4.30509E-01	4.58132E-01	1.97230E-01	4.47519E-04
$\theta = 15$				
0	4.68214E-01	4.46499E-01	2.09057E-01	4.65223E-04
5	4.68033E-01	4.46795E-01	2.09115E-01	4.65287E-04
10	4.64560E-01	4.47034E-01	2.07674E-01	4.63681E-04
15	4.60782E-01	4.46606E-01	2.05788E-01	4.61570E-04
20	4.55516E-01	4.47541E-01	2.03862E-01	4.59405E-04
25	4.50659E-01	4.47605E-01	2.01717E-01	4.56982E-04
30	4.43830E-01	4.47633E-01	1.98673E-01	4.53521E-04
35	4.37711E-01	4.47302E-01	1.95789E-01	4.50218E-04
40	4.31817E-01	4.44401E-01	1.91900E-01	4.45723E-04
45	4.25788E-01	4.38559E-01	1.86733E-01	4.39682E-04
50	4.30390E-01	4.45212E-01	1.91615E-01	4.45392E-04
55	4.34244E-01	4.49821E-01	1.95332E-01	4.49692E-04
60	4.37973E-01	4.51295E-01	1.97655E-01	4.52358E-04
65	4.40323E-01	4.51955E-01	1.99006E-01	4.53901E-04
70	4.44851E-01	4.51383E-01	2.00798E-01	4.55940E-04
75	4.46565E-01	4.51954E-01	2.01827E-01	4.57107E-04
80	4.50237E-01	4.55131E-01	2.04917E-01	4.60593E-04
85	4.50547E-01	4.52934E-01	2.04068E-01	4.59638E-04
90	4.51494E-01	4.52653E-01	2.04370E-01	4.59977E-04

ψ	p_n	η	ε	$\sigma(\varepsilon)$
$\theta = 20$				
0	4.76725E-01	4.39935E-01	2.09728E-01	4.72428E-04
5	4.75398E-01	4.39278E-01	2.08832E-01	4.71417E-04
10	4.72903E-01	4.40215E-01	2.08179E-01	4.70679E-04
15	4.68288E-01	4.41858E-01	2.06917E-01	4.69252E-04
20	4.63019E-01	4.42926E-01	2.05083E-01	4.67167E-04
25	4.55651E-01	4.42988E-01	2.01848E-01	4.63467E-04
30	4.48661E-01	4.43012E-01	1.98762E-01	4.59911E-04
35	4.40791E-01	4.44381E-01	1.95879E-01	4.56563E-04
40	4.33826E-01	4.43247E-01	1.92292E-01	4.52364E-04
45	4.26412E-01	4.38093E-01	1.86808E-01	4.45867E-04
50	4.31281E-01	4.45014E-01	1.91926E-01	4.51933E-04
55	4.36658E-01	4.48562E-01	1.95868E-01	4.56550E-04
60	4.41875E-01	4.50641E-01	1.99127E-01	4.60332E-04
65	4.46056E-01	4.48726E-01	2.00157E-01	4.61522E-04
70	4.49977E-01	4.49963E-01	2.02473E-01	4.64184E-04
75	4.54643E-01	4.47624E-01	2.03509E-01	4.65371E-04
80	4.57881E-01	4.48136E-01	2.05193E-01	4.67292E-04
85	4.59599E-01	4.47797E-01	2.05807E-01	4.67990E-04
90	4.60206E-01	4.47035E-01	2.05728E-01	4.67901E-04
$\theta = 25$				
0	4.67395E-01	4.37664E-01	2.04562E-01	4.75088E-04
5	4.67940E-01	4.37627E-01	2.04783E-01	4.75345E-04
10	4.67974E-01	4.38791E-01	2.05343E-01	4.75995E-04
15	4.66816E-01	4.38693E-01	2.04789E-01	4.75353E-04
20	4.63716E-01	4.40481E-01	2.04258E-01	4.74736E-04
25	4.57248E-01	4.42093E-01	2.02146E-01	4.72274E-04
30	4.50275E-01	4.42843E-01	1.99401E-01	4.69058E-04
35	4.41985E-01	4.43479E-01	1.96011E-01	4.65053E-04
40	4.33584E-01	4.43605E-01	1.92340E-01	4.60678E-04
45	4.24260E-01	4.36522E-01	1.85199E-01	4.52045E-04
50	4.30235E-01	4.45477E-01	1.91660E-01	4.59862E-04
55	4.35121E-01	4.48147E-01	1.94998E-01	4.63849E-04
60	4.39918E-01	4.48397E-01	1.97258E-01	4.66530E-04
65	4.46541E-01	4.47128E-01	1.99661E-01	4.69363E-04
70	4.51981E-01	4.47590E-01	2.02302E-01	4.72457E-04
75	4.55955E-01	4.46395E-01	2.03536E-01	4.73896E-04
80	4.58253E-01	4.43552E-01	2.03259E-01	4.73574E-04
85	4.60494E-01	4.44210E-01	2.04556E-01	4.75082E-04
90	4.61445E-01	4.43372E-01	2.04592E-01	4.75123E-04

ψ	p_n	η	ε	$\sigma(\varepsilon)$
$\theta = 30$				
0	4.59723E-01	4.39219E-01	2.01919E-01	4.82862E-04
5	4.60587E-01	4.38373E-01	2.01909E-01	4.82850E-04
10	4.61739E-01	4.37663E-01	2.02086E-01	4.83062E-04
15	4.61870E-01	4.38327E-01	2.02450E-01	4.83497E-04
20	4.61601E-01	4.38402E-01	2.02367E-01	4.83397E-04
25	4.57774E-01	4.39501E-01	2.01192E-01	4.81992E-04
30	4.49587E-01	4.41054E-01	1.98292E-01	4.78506E-04
35	4.40618E-01	4.41795E-01	1.94663E-01	4.74108E-04
40	4.31371E-01	4.41875E-01	1.90612E-01	4.69148E-04
45	4.22440E-01	4.36637E-01	1.84453E-01	4.61506E-04
50	4.27662E-01	4.44407E-01	1.90056E-01	4.68463E-04
55	4.33088E-01	4.46537E-01	1.93390E-01	4.72555E-04
60	4.37237E-01	4.47211E-01	1.95537E-01	4.75170E-04
65	4.42491E-01	4.45634E-01	1.97189E-01	4.77173E-04
70	4.46846E-01	4.45807E-01	1.99207E-01	4.79609E-04
75	4.51991E-01	4.43757E-01	2.00574E-01	4.81251E-04
80	4.55270E-01	4.42579E-01	2.01493E-01	4.82353E-04
85	4.58200E-01	4.41087E-01	2.02106E-01	4.83086E-04
90	4.59200E-01	4.40926E-01	2.02473E-01	4.83525E-04
$\theta = 35$				
0	4.54998E-01	4.36538E-01	1.98624E-01	4.92418E-04
5	4.53682E-01	4.37377E-01	1.98430E-01	4.92177E-04
10	4.53161E-01	4.36386E-01	1.97753E-01	4.91337E-04
15	4.53121E-01	4.35751E-01	1.97448E-01	4.90958E-04
20	4.52391E-01	4.35983E-01	1.97235E-01	4.90692E-04
25	4.51780E-01	4.37886E-01	1.97828E-01	4.91431E-04
30	4.44890E-01	4.39082E-01	1.95343E-01	4.88334E-04
35	4.36377E-01	4.42725E-01	1.93195E-01	4.85642E-04
40	4.27393E-01	4.40810E-01	1.88399E-01	4.79576E-04
45	4.19294E-01	4.34995E-01	1.82391E-01	4.71867E-04
50	4.22835E-01	4.42496E-01	1.87103E-01	4.77923E-04
55	4.28650E-01	4.45431E-01	1.90934E-01	4.82791E-04
60	4.32715E-01	4.46904E-01	1.93382E-01	4.85877E-04
65	4.35745E-01	4.45605E-01	1.94170E-01	4.86865E-04
70	4.38033E-01	4.45302E-01	1.95057E-01	4.87976E-04
75	4.43242E-01	4.43273E-01	1.96477E-01	4.89749E-04
80	4.48213E-01	4.40541E-01	1.97456E-01	4.90967E-04
85	4.53421E-01	4.38972E-01	1.99039E-01	4.92932E-04
90	4.54239E-01	4.39251E-01	1.99525E-01	4.93533E-04

ψ	p_n	η	ε	$\sigma(\varepsilon)$
$\theta = 40$				
0	4.43775E-01	4.36048E-01	1.93507E-01	5.02598E-04
5	4.43037E-01	4.36670E-01	1.93461E-01	5.02539E-04
10	4.42248E-01	4.35604E-01	1.92645E-01	5.01478E-04
15	4.42024E-01	4.35938E-01	1.92695E-01	5.01544E-04
20	4.41845E-01	4.36701E-01	1.92954E-01	5.01879E-04
25	4.41371E-01	4.37342E-01	1.93030E-01	5.01979E-04
30	4.36914E-01	4.36482E-01	1.90705E-01	4.98947E-04
35	4.28920E-01	4.38788E-01	1.88205E-01	4.95665E-04
40	4.20761E-01	4.39278E-01	1.84831E-01	4.91203E-04
45	4.11490E-01	4.34472E-01	1.78781E-01	4.83096E-04
50	4.17581E-01	4.42230E-01	1.84667E-01	4.90984E-04
55	4.23711E-01	4.44605E-01	1.88384E-01	4.95901E-04
60	4.26511E-01	4.46486E-01	1.90431E-01	4.98588E-04
65	4.26310E-01	4.45910E-01	1.90096E-01	4.98150E-04
70	4.28508E-01	4.44281E-01	1.90378E-01	4.98519E-04
75	4.35223E-01	4.42210E-01	1.92460E-01	5.01237E-04
80	4.40106E-01	4.38510E-01	1.92991E-01	5.01928E-04
85	4.42895E-01	4.36424E-01	1.93290E-01	5.02317E-04
90	4.42933E-01	4.35287E-01	1.92803E-01	5.01683E-04
$\theta = 45$				
0	4.29287E-01	4.35406E-01	1.86914E-01	5.14136E-04
5	4.29917E-01	4.34326E-01	1.86724E-01	5.13875E-04
10	4.30828E-01	4.35396E-01	1.87581E-01	5.15053E-04
15	4.30005E-01	4.34960E-01	1.87035E-01	5.14303E-04
20	4.29422E-01	4.35939E-01	1.87202E-01	5.14532E-04
25	4.28757E-01	4.35734E-01	1.86824E-01	5.14013E-04
30	4.25231E-01	4.35523E-01	1.85198E-01	5.11771E-04
35	4.18988E-01	4.37841E-01	1.83450E-01	5.09350E-04
40	4.09363E-01	4.40360E-01	1.80267E-01	5.04912E-04
45	3.99710E-01	4.33347E-01	1.73213E-01	4.94934E-04
50	4.08678E-01	4.40782E-01	1.80138E-01	5.04731E-04
55	4.15924E-01	4.44951E-01	1.85066E-01	5.11589E-04
60	4.14128E-01	4.45118E-01	1.84336E-01	5.10579E-04
65	4.10942E-01	4.44099E-01	1.82499E-01	5.08029E-04
70	4.17253E-01	4.42111E-01	1.84472E-01	5.10767E-04
75	4.25638E-01	4.40785E-01	1.87615E-01	5.15099E-04
80	4.29336E-01	4.37576E-01	1.87867E-01	5.15445E-04
85	4.28884E-01	4.37179E-01	1.87499E-01	5.14941E-04
90	4.29141E-01	4.36015E-01	1.87112E-01	5.14409E-04

ψ	p_n	η	ε	$\sigma(\varepsilon)$
$\theta = 50$				
0	4.13818E-01	4.33911E-01	1.79560E-01	5.28532E-04
5	4.13206E-01	4.34544E-01	1.79556E-01	5.28525E-04
10	4.13398E-01	4.34298E-01	1.79538E-01	5.28500E-04
15	4.13363E-01	4.33665E-01	1.79261E-01	5.28092E-04
20	4.12895E-01	4.34079E-01	1.79229E-01	5.28045E-04
25	4.12582E-01	4.34614E-01	1.79314E-01	5.28169E-04
30	4.09427E-01	4.34979E-01	1.78092E-01	5.26367E-04
35	4.05332E-01	4.36543E-01	1.76945E-01	5.24668E-04
40	3.95228E-01	4.39238E-01	1.73599E-01	5.19685E-04
45	3.82304E-01	4.31173E-01	1.64839E-01	5.06403E-04
50	3.96682E-01	4.37723E-01	1.73637E-01	5.19742E-04
55	4.05070E-01	4.40865E-01	1.78581E-01	5.27088E-04
60	3.97970E-01	4.43782E-01	1.76612E-01	5.24175E-04
65	3.95226E-01	4.45315E-01	1.76000E-01	5.23267E-04
70	4.03486E-01	4.42040E-01	1.78357E-01	5.26759E-04
75	4.11051E-01	4.37457E-01	1.79817E-01	5.28910E-04
80	4.13478E-01	4.35324E-01	1.79997E-01	5.29174E-04
85	4.12981E-01	4.34436E-01	1.79414E-01	5.28317E-04
90	4.12421E-01	4.34532E-01	1.79210E-01	5.28017E-04
$\theta = 55$				
0	3.92396E-01	4.34138E-01	1.70354E-01	5.44981E-04
5	3.92956E-01	4.33354E-01	1.70289E-01	5.44875E-04
10	3.93192E-01	4.32623E-01	1.70104E-01	5.44581E-04
15	3.93332E-01	4.32996E-01	1.70311E-01	5.44911E-04
20	3.92349E-01	4.33354E-01	1.70026E-01	5.44455E-04
25	3.92602E-01	4.33421E-01	1.70162E-01	5.44672E-04
30	3.88786E-01	4.33655E-01	1.68599E-01	5.42166E-04
35	3.87119E-01	4.33345E-01	1.67756E-01	5.40808E-04
40	3.79767E-01	4.37576E-01	1.66177E-01	5.38257E-04
45	3.60652E-01	4.30498E-01	1.55260E-01	5.20276E-04
50	3.80401E-01	4.38311E-01	1.66734E-01	5.39159E-04
55	3.89123E-01	4.39285E-01	1.70936E-01	5.45910E-04
60	3.77179E-01	4.42997E-01	1.67089E-01	5.39732E-04
65	3.75907E-01	4.45123E-01	1.67325E-01	5.40114E-04
70	3.85017E-01	4.39225E-01	1.69109E-01	5.42985E-04
75	3.92240E-01	4.34971E-01	1.70613E-01	5.45393E-04
80	3.92582E-01	4.32916E-01	1.69955E-01	5.44341E-04
85	3.91970E-01	4.33311E-01	1.69845E-01	5.44165E-04
90	3.93032E-01	4.34133E-01	1.70628E-01	5.45418E-04

ψ	p_n	η	ε	$\sigma(\varepsilon)$
$\theta = 60$				
0	3.66943E-01	4.30952E-01	1.58135E-01	5.62379E-04
5	3.67598E-01	4.30484E-01	1.58245E-01	5.62574E-04
10	3.67917E-01	4.30412E-01	1.58356E-01	5.62772E-04
15	3.66977E-01	4.30599E-01	1.58020E-01	5.62174E-04
20	3.67055E-01	4.31818E-01	1.58501E-01	5.63029E-04
25	3.66730E-01	4.30507E-01	1.57880E-01	5.61926E-04
30	3.65124E-01	4.32256E-01	1.57827E-01	5.61831E-04
35	3.61098E-01	4.31213E-01	1.55710E-01	5.58050E-04
40	3.59080E-01	4.36081E-01	1.56588E-01	5.59622E-04
45	3.35825E-01	4.29515E-01	1.44242E-01	5.37108E-04
50	3.58572E-01	4.33584E-01	1.55471E-01	5.57623E-04
55	3.65353E-01	4.33165E-01	1.58258E-01	5.62598E-04
60	3.54187E-01	4.42910E-01	1.56873E-01	5.60130E-04
65	3.50685E-01	4.43424E-01	1.55502E-01	5.57678E-04
70	3.62602E-01	4.38263E-01	1.58915E-01	5.63764E-04
75	3.67445E-01	4.31556E-01	1.58573E-01	5.63157E-04
80	3.66742E-01	4.31649E-01	1.58304E-01	5.62680E-04
85	3.67317E-01	4.32357E-01	1.58812E-01	5.63581E-04
90	3.66859E-01	4.32043E-01	1.58499E-01	5.63026E-04
$\theta = 65$				
0	3.34643E-01	4.28041E-01	1.43241E-01	5.82183E-04
5	3.34894E-01	4.28986E-01	1.43665E-01	5.83044E-04
10	3.34592E-01	4.28603E-01	1.43407E-01	5.82520E-04
15	3.34519E-01	4.29999E-01	1.43843E-01	5.83405E-04
20	3.34616E-01	4.28548E-01	1.43399E-01	5.82503E-04
25	3.34352E-01	4.29867E-01	1.43727E-01	5.83171E-04
30	3.33633E-01	4.29847E-01	1.43411E-01	5.82529E-04
35	3.28539E-01	4.28731E-01	1.40855E-01	5.77314E-04
40	3.30731E-01	4.33582E-01	1.43399E-01	5.82505E-04
45	3.06257E-01	4.25976E-01	1.30458E-01	5.55600E-04
50	3.29564E-01	4.31343E-01	1.42155E-01	5.79972E-04
55	3.33762E-01	4.31026E-01	1.43860E-01	5.83439E-04
60	3.24937E-01	4.39359E-01	1.42764E-01	5.81213E-04
65	3.19397E-01	4.42606E-01	1.41367E-01	5.78362E-04
70	3.32890E-01	4.33888E-01	1.44437E-01	5.84608E-04
75	3.34157E-01	4.29594E-01	1.43552E-01	5.82815E-04
80	3.34549E-01	4.29689E-01	1.43752E-01	5.83221E-04
85	3.34376E-01	4.29158E-01	1.43500E-01	5.82710E-04
90	3.34849E-01	4.28501E-01	1.43483E-01	5.82674E-04

ψ	p_n	η	ε	$\sigma(\varepsilon)$
$\theta = 70$				
0	2.92851E-01	4.27029E-01	1.25056E-01	6.04681E-04
5	2.93051E-01	4.24950E-01	1.24532E-01	6.03414E-04
10	2.93106E-01	4.25102E-01	1.24600E-01	6.03577E-04
15	2.93013E-01	4.24909E-01	1.24504E-01	6.03345E-04
20	2.92806E-01	4.25275E-01	1.24523E-01	6.03392E-04
25	2.92801E-01	4.25719E-01	1.24651E-01	6.03700E-04
30	2.92613E-01	4.26440E-01	1.24782E-01	6.04019E-04
35	2.89216E-01	4.25471E-01	1.23053E-01	5.99818E-04
40	2.92106E-01	4.27588E-01	1.24901E-01	6.04306E-04
45	2.67504E-01	4.23855E-01	1.13383E-01	5.75768E-04
50	2.91583E-01	4.25999E-01	1.24214E-01	6.02642E-04
55	2.92164E-01	4.27544E-01	1.24913E-01	6.04335E-04
60	2.86814E-01	4.35986E-01	1.25047E-01	6.04659E-04
65	2.80574E-01	4.41916E-01	1.23990E-01	6.02098E-04
70	2.92909E-01	4.29140E-01	1.25699E-01	6.06233E-04
75	2.92433E-01	4.27021E-01	1.24875E-01	6.04243E-04
80	2.92518E-01	4.25946E-01	1.24597E-01	6.03569E-04
85	2.92894E-01	4.26137E-01	1.24813E-01	6.04093E-04
90	2.92741E-01	4.25752E-01	1.24635E-01	6.03661E-04
$\theta = 75$				
0	2.38898E-01	4.20246E-01	1.00396E-01	6.22816E-04
5	2.38913E-01	4.21170E-01	1.00623E-01	6.23521E-04
10	2.38986E-01	4.20271E-01	1.00439E-01	6.22950E-04
15	2.38988E-01	4.20465E-01	1.00486E-01	6.23095E-04
20	2.38863E-01	4.20107E-01	1.00348E-01	6.22667E-04
25	2.38877E-01	4.22180E-01	1.00849E-01	6.24220E-04
30	2.38641E-01	4.21671E-01	1.00628E-01	6.23534E-04
35	2.36741E-01	4.20490E-01	9.95472E-02	6.20178E-04
40	2.38261E-01	4.22700E-01	1.00713E-01	6.23799E-04
45	2.19879E-01	4.18604E-01	9.20423E-02	5.96342E-04
50	2.37847E-01	4.19034E-01	9.96660E-02	6.20548E-04
55	2.38382E-01	4.22389E-01	1.00690E-01	6.23727E-04
60	2.37069E-01	4.29934E-01	1.01924E-01	6.27538E-04
65	2.31115E-01	4.40339E-01	1.01769E-01	6.27062E-04
70	2.38691E-01	4.23062E-01	1.00981E-01	6.24629E-04
75	2.38840E-01	4.20780E-01	1.00499E-01	6.23137E-04
80	2.38870E-01	4.20693E-01	1.00491E-01	6.23112E-04
85	2.38970E-01	4.21245E-01	1.00665E-01	6.23649E-04
90	2.38978E-01	4.21097E-01	1.00633E-01	6.23551E-04

ψ	p_n	η	ε	$\sigma(\varepsilon)$
$\theta = 80$				
0	1.69888E-01	4.11860E-01	6.99700E-02	6.34776E-04
5	1.69832E-01	4.12547E-01	7.00637E-02	6.35202E-04
10	1.69886E-01	4.12646E-01	7.01028E-02	6.35379E-04
15	1.69806E-01	4.12431E-01	7.00332E-02	6.35063E-04
20	1.69815E-01	4.11167E-01	6.98224E-02	6.34106E-04
25	1.69851E-01	4.12311E-01	7.00314E-02	6.35055E-04
30	1.69833E-01	4.12901E-01	7.01243E-02	6.35476E-04
35	1.69489E-01	4.12585E-01	6.99286E-02	6.34589E-04
40	1.69801E-01	4.14376E-01	7.03614E-02	6.36549E-04
45	1.60535E-01	4.09972E-01	6.58149E-02	6.15640E-04
50	1.69514E-01	4.12083E-01	6.98538E-02	6.34249E-04
55	1.69784E-01	4.14363E-01	7.03522E-02	6.36508E-04
60	1.69803E-01	4.18599E-01	7.10794E-02	6.39789E-04
65	1.67682E-01	4.32646E-01	7.25469E-02	6.46360E-04
70	1.69880E-01	4.15237E-01	7.05404E-02	6.37359E-04
75	1.69851E-01	4.12890E-01	7.01297E-02	6.35501E-04
80	1.69850E-01	4.12022E-01	6.99819E-02	6.34831E-04
85	1.69850E-01	4.11984E-01	6.99755E-02	6.34802E-04
90	1.69836E-01	4.12053E-01	6.99814E-02	6.34828E-04
$\theta = 85$				
0	8.71147E-02	3.92229E-01	3.41689E-02	6.26134E-04
5	8.71158E-02	3.92928E-01	3.42302E-02	6.26696E-04
10	8.71157E-02	3.92704E-01	3.42107E-02	6.26517E-04
15	8.71139E-02	3.92836E-01	3.42215E-02	6.26616E-04
20	8.71100E-02	3.93075E-01	3.42408E-02	6.26793E-04
25	8.71150E-02	3.92681E-01	3.42084E-02	6.26497E-04
30	8.71133E-02	3.93429E-01	3.42729E-02	6.27087E-04
35	8.71072E-02	3.92978E-01	3.42312E-02	6.26705E-04
40	8.71113E-02	3.95884E-01	3.44860E-02	6.29033E-04
45	8.61810E-02	3.92325E-01	3.38110E-02	6.22847E-04
50	8.71018E-02	3.92895E-01	3.42219E-02	6.26620E-04
55	8.71124E-02	3.94682E-01	3.43817E-02	6.28081E-04
60	8.71097E-02	3.99719E-01	3.48194E-02	6.32066E-04
65	8.71095E-02	4.11765E-01	3.58686E-02	6.41519E-04
70	8.71104E-02	3.95023E-01	3.44106E-02	6.28345E-04
75	8.71128E-02	3.94030E-01	3.43251E-02	6.27564E-04
80	8.71115E-02	3.92798E-01	3.42172E-02	6.26577E-04
85	8.71152E-02	3.91425E-01	3.40991E-02	6.25494E-04
90	8.71123E-02	3.92972E-01	3.42327E-02	6.26718E-04

Table B.11. ${}^6\text{LiF}$ chevron detector with 100 μm deep perforations, 20 μm wide channels, and no cap

ψ	p_n	η	ε	$\sigma(\varepsilon)$
$\theta = 0$				
0	1.99838E-01	7.83039E-01	1.56481E-01	1.25092E-04
5	1.99615E-01	7.83498E-01	1.56398E-01	1.25059E-04
10	1.99878E-01	7.83653E-01	1.56635E-01	1.25154E-04
15	1.99815E-01	7.83810E-01	1.56617E-01	1.25147E-04
20	1.99851E-01	7.83889E-01	1.56661E-01	1.25164E-04
25	1.99638E-01	7.83463E-01	1.56409E-01	1.25064E-04
30	1.99776E-01	7.83813E-01	1.56587E-01	1.25135E-04
35	1.99813E-01	7.83548E-01	1.56563E-01	1.25125E-04
40	1.99872E-01	7.83847E-01	1.56669E-01	1.25167E-04
45	1.99643E-01	7.83173E-01	1.56355E-01	1.25042E-04
50	1.99605E-01	7.83297E-01	1.56350E-01	1.25040E-04
55	1.99886E-01	7.83807E-01	1.56672E-01	1.25169E-04
60	1.99789E-01	7.83602E-01	1.56555E-01	1.25122E-04
65	1.99864E-01	7.84043E-01	1.56702E-01	1.25181E-04
70	1.99714E-01	7.83365E-01	1.56449E-01	1.25080E-04
75	1.99772E-01	7.83804E-01	1.56582E-01	1.25133E-04
80	1.99646E-01	7.83557E-01	1.56434E-01	1.25073E-04
85	1.99936E-01	7.83956E-01	1.56741E-01	1.25196E-04
90	1.99597E-01	7.83073E-01	1.56299E-01	1.25020E-04
$\theta = 5$				
0	2.07219E-01	7.87684E-01	1.63223E-01	1.28003E-04
5	2.07152E-01	7.87876E-01	1.63210E-01	1.27998E-04
10	2.06927E-01	7.87887E-01	1.63035E-01	1.27929E-04
15	2.06463E-01	7.88248E-01	1.62744E-01	1.27815E-04
20	2.06405E-01	7.87617E-01	1.62568E-01	1.27745E-04
25	2.06068E-01	7.87827E-01	1.62346E-01	1.27658E-04
30	2.06142E-01	7.87554E-01	1.62348E-01	1.27659E-04
35	2.05608E-01	7.87601E-01	1.61937E-01	1.27497E-04
40	2.05678E-01	7.87094E-01	1.61888E-01	1.27478E-04
45	2.04907E-01	7.86259E-01	1.61110E-01	1.27171E-04
50	2.05412E-01	7.86624E-01	1.61582E-01	1.27357E-04
55	2.05418E-01	7.87239E-01	1.61713E-01	1.27409E-04
60	2.05690E-01	7.87860E-01	1.62055E-01	1.27544E-04
65	2.06000E-01	7.87238E-01	1.62171E-01	1.27589E-04
70	2.06169E-01	7.88009E-01	1.62463E-01	1.27704E-04
75	2.06315E-01	7.87393E-01	1.62451E-01	1.27699E-04
80	2.06467E-01	7.88276E-01	1.62753E-01	1.27818E-04
85	2.06596E-01	7.88408E-01	1.62882E-01	1.27869E-04
90	2.06539E-01	7.88200E-01	1.62794E-01	1.27834E-04

ψ	p_n	η	ε	$\sigma(\varepsilon)$
$\theta = 10$				
0	2.14188E-01	7.90058E-01	1.69221E-01	1.31084E-04
5	2.13664E-01	7.89688E-01	1.68728E-01	1.30894E-04
10	2.13770E-01	7.89709E-01	1.68816E-01	1.30928E-04
15	2.13520E-01	7.89828E-01	1.68644E-01	1.30861E-04
20	2.13283E-01	7.89664E-01	1.68422E-01	1.30775E-04
25	2.12685E-01	7.89346E-01	1.67882E-01	1.30565E-04
30	2.12118E-01	7.89113E-01	1.67385E-01	1.30372E-04
35	2.11423E-01	7.88850E-01	1.66781E-01	1.30136E-04
40	2.10428E-01	7.87946E-01	1.65806E-01	1.29755E-04
45	2.09536E-01	7.87793E-01	1.65071E-01	1.29467E-04
50	2.10097E-01	7.88145E-01	1.65587E-01	1.29669E-04
55	2.10710E-01	7.88263E-01	1.66095E-01	1.29868E-04
60	2.11121E-01	7.89533E-01	1.66687E-01	1.30099E-04
65	2.11694E-01	7.89045E-01	1.67036E-01	1.30235E-04
70	2.12044E-01	7.89638E-01	1.67438E-01	1.30392E-04
75	2.12258E-01	7.89191E-01	1.67512E-01	1.30421E-04
80	2.12328E-01	7.89613E-01	1.67657E-01	1.30477E-04
85	2.12380E-01	7.89712E-01	1.67719E-01	1.30502E-04
90	2.12304E-01	7.89985E-01	1.67717E-01	1.30501E-04
$\theta = 15$				
0	2.20594E-01	7.90167E-01	1.74306E-01	1.34333E-04
5	2.20554E-01	7.90790E-01	1.74412E-01	1.34374E-04
10	2.19954E-01	7.90320E-01	1.73834E-01	1.34151E-04
15	2.19149E-01	7.90325E-01	1.73199E-01	1.33906E-04
20	2.18029E-01	7.90092E-01	1.72263E-01	1.33544E-04
25	2.16678E-01	7.89406E-01	1.71047E-01	1.33072E-04
30	2.15682E-01	7.89343E-01	1.70247E-01	1.32760E-04
35	2.14596E-01	7.89199E-01	1.69359E-01	1.32414E-04
40	2.13314E-01	7.88434E-01	1.68184E-01	1.31953E-04
45	2.11774E-01	7.87679E-01	1.66810E-01	1.31413E-04
50	2.12788E-01	7.88071E-01	1.67692E-01	1.31760E-04
55	2.13575E-01	7.89470E-01	1.68611E-01	1.32121E-04
60	2.14185E-01	7.89122E-01	1.69018E-01	1.32280E-04
65	2.14878E-01	7.89457E-01	1.69637E-01	1.32522E-04
70	2.15670E-01	7.89340E-01	1.70237E-01	1.32756E-04
75	2.16076E-01	7.89884E-01	1.70675E-01	1.32927E-04
80	2.16677E-01	7.89738E-01	1.71118E-01	1.33099E-04
85	2.17112E-01	7.90048E-01	1.71529E-01	1.33259E-04
90	2.16990E-01	7.90193E-01	1.71464E-01	1.33234E-04

ψ	p_n	η	ε	$\sigma(\varepsilon)$
$\theta = 20$				
0	2.23058E-01	7.89669E-01	1.76142E-01	1.36911E-04
5	2.22957E-01	7.89861E-01	1.76105E-01	1.36897E-04
10	2.22214E-01	7.89523E-01	1.75443E-01	1.36639E-04
15	2.21190E-01	7.89751E-01	1.74685E-01	1.36344E-04
20	2.19746E-01	7.89120E-01	1.73406E-01	1.35843E-04
25	2.18460E-01	7.89074E-01	1.72381E-01	1.35441E-04
30	2.16565E-01	7.89324E-01	1.70940E-01	1.34874E-04
35	2.15101E-01	7.88755E-01	1.69662E-01	1.34369E-04
40	2.13630E-01	7.87661E-01	1.68268E-01	1.33816E-04
45	2.11908E-01	7.87441E-01	1.66865E-01	1.33257E-04
50	2.13052E-01	7.87826E-01	1.67848E-01	1.33649E-04
55	2.14283E-01	7.88401E-01	1.68941E-01	1.34083E-04
60	2.15185E-01	7.89493E-01	1.69887E-01	1.34458E-04
65	2.16218E-01	7.88944E-01	1.70584E-01	1.34734E-04
70	2.17155E-01	7.89570E-01	1.71459E-01	1.35079E-04
75	2.17921E-01	7.89731E-01	1.72099E-01	1.35331E-04
80	2.18831E-01	7.89934E-01	1.72862E-01	1.35630E-04
85	2.19203E-01	7.89369E-01	1.73032E-01	1.35697E-04
90	2.19269E-01	7.90007E-01	1.73224E-01	1.35772E-04
$\theta = 25$				
0	2.21844E-01	7.88942E-01	1.75022E-01	1.38966E-04
5	2.21804E-01	7.88665E-01	1.74929E-01	1.38929E-04
10	2.21818E-01	7.88642E-01	1.74935E-01	1.38932E-04
15	2.21465E-01	7.89113E-01	1.74761E-01	1.38862E-04
20	2.20251E-01	7.89268E-01	1.73837E-01	1.38495E-04
25	2.18903E-01	7.89139E-01	1.72745E-01	1.38059E-04
30	2.16883E-01	7.89034E-01	1.71128E-01	1.37411E-04
35	2.15062E-01	7.88415E-01	1.69558E-01	1.36780E-04
40	2.13528E-01	7.87915E-01	1.68242E-01	1.36248E-04
45	2.11698E-01	7.87570E-01	1.66727E-01	1.35633E-04
50	2.12551E-01	7.88065E-01	1.67504E-01	1.35949E-04
55	2.13826E-01	7.88262E-01	1.68551E-01	1.36373E-04
60	2.15104E-01	7.89107E-01	1.69740E-01	1.36853E-04
65	2.16290E-01	7.89116E-01	1.70678E-01	1.37231E-04
70	2.17512E-01	7.88890E-01	1.71593E-01	1.37598E-04
75	2.18441E-01	7.89101E-01	1.72372E-01	1.37910E-04
80	2.19034E-01	7.89603E-01	1.72950E-01	1.38141E-04
85	2.19630E-01	7.89191E-01	1.73330E-01	1.38293E-04
90	2.19923E-01	7.89558E-01	1.73642E-01	1.38417E-04

ψ	p_n	η	ε	$\sigma(\varepsilon)$
$\theta = 30$				
0	2.19689E-01	7.88055E-01	1.73127E-01	1.41390E-04
5	2.20009E-01	7.88259E-01	1.73424E-01	1.41511E-04
10	2.20318E-01	7.88724E-01	1.73770E-01	1.41652E-04
15	2.20328E-01	7.88538E-01	1.73737E-01	1.41638E-04
20	2.20090E-01	7.88841E-01	1.73616E-01	1.41589E-04
25	2.18912E-01	7.88764E-01	1.72670E-01	1.41203E-04
30	2.17207E-01	7.88529E-01	1.71274E-01	1.40631E-04
35	2.15295E-01	7.88616E-01	1.69785E-01	1.40018E-04
40	2.13179E-01	7.87953E-01	1.67975E-01	1.39270E-04
45	2.11050E-01	7.86619E-01	1.66016E-01	1.38455E-04
50	2.12345E-01	7.88368E-01	1.67406E-01	1.39034E-04
55	2.13397E-01	7.88038E-01	1.68165E-01	1.39349E-04
60	2.14629E-01	7.88766E-01	1.69292E-01	1.39815E-04
65	2.15669E-01	7.89047E-01	1.70173E-01	1.40178E-04
70	2.16815E-01	7.88594E-01	1.70979E-01	1.40510E-04
75	2.17916E-01	7.89208E-01	1.71981E-01	1.40921E-04
80	2.18620E-01	7.89347E-01	1.72567E-01	1.41161E-04
85	2.19144E-01	7.88819E-01	1.72865E-01	1.41282E-04
90	2.19355E-01	7.88927E-01	1.73055E-01	1.41360E-04
$\theta = 35$				
0	2.18783E-01	7.88590E-01	1.72530E-01	1.45127E-04
5	2.18523E-01	7.88562E-01	1.72319E-01	1.45039E-04
10	2.18730E-01	7.88090E-01	1.72379E-01	1.45064E-04
15	2.18417E-01	7.87745E-01	1.72057E-01	1.44929E-04
20	2.18744E-01	7.88488E-01	1.72477E-01	1.45105E-04
25	2.18049E-01	7.88708E-01	1.71977E-01	1.44895E-04
30	2.16324E-01	7.88165E-01	1.70499E-01	1.44271E-04
35	2.14312E-01	7.88453E-01	1.68975E-01	1.43625E-04
40	2.11949E-01	7.87312E-01	1.66870E-01	1.42727E-04
45	2.10185E-01	7.86940E-01	1.65403E-01	1.42098E-04
50	2.11361E-01	7.88234E-01	1.66602E-01	1.42613E-04
55	2.12265E-01	7.87907E-01	1.67245E-01	1.42887E-04
60	2.13585E-01	7.88492E-01	1.68410E-01	1.43384E-04
65	2.14201E-01	7.88311E-01	1.68857E-01	1.43575E-04
70	2.15089E-01	7.88557E-01	1.69610E-01	1.43894E-04
75	2.16301E-01	7.88605E-01	1.70576E-01	1.44303E-04
80	2.17282E-01	7.88478E-01	1.71322E-01	1.44619E-04
85	2.18347E-01	7.88538E-01	1.72175E-01	1.44978E-04
90	2.18741E-01	7.88595E-01	1.72498E-01	1.45114E-04

ψ	p_n	η	ε	$\sigma(\varepsilon)$
$\theta = 40$				
0	2.16766E-01	7.87845E-01	1.70778E-01	1.49310E-04
5	2.16744E-01	7.87787E-01	1.70748E-01	1.49297E-04
10	2.16474E-01	7.87489E-01	1.70471E-01	1.49176E-04
15	2.16463E-01	7.88047E-01	1.70583E-01	1.49225E-04
20	2.16243E-01	7.87295E-01	1.70247E-01	1.49078E-04
25	2.15928E-01	7.87929E-01	1.70136E-01	1.49029E-04
30	2.14997E-01	7.88044E-01	1.69427E-01	1.48718E-04
35	2.12638E-01	7.88086E-01	1.67577E-01	1.47904E-04
40	2.10619E-01	7.87408E-01	1.65843E-01	1.47137E-04
45	2.08571E-01	7.86236E-01	1.63986E-01	1.46311E-04
50	2.09968E-01	7.87725E-01	1.65397E-01	1.46939E-04
55	2.11461E-01	7.88675E-01	1.66774E-01	1.47549E-04
60	2.12084E-01	7.88367E-01	1.67200E-01	1.47738E-04
65	2.12296E-01	7.88027E-01	1.67295E-01	1.47780E-04
70	2.12897E-01	7.87940E-01	1.67750E-01	1.47981E-04
75	2.14316E-01	7.87953E-01	1.68871E-01	1.48474E-04
80	2.15669E-01	7.87707E-01	1.69884E-01	1.48919E-04
85	2.16540E-01	7.88136E-01	1.70663E-01	1.49260E-04
90	2.16882E-01	7.88134E-01	1.70932E-01	1.49377E-04
$\theta = 45$				
0	2.13539E-01	7.87079E-01	1.68072E-01	1.54172E-04
5	2.13680E-01	7.86606E-01	1.68082E-01	1.54176E-04
10	2.13895E-01	7.86947E-01	1.68324E-01	1.54288E-04
15	2.13879E-01	7.87356E-01	1.68399E-01	1.54322E-04
20	2.13537E-01	7.86665E-01	1.67982E-01	1.54131E-04
25	2.13412E-01	7.87088E-01	1.67974E-01	1.54127E-04
30	2.12522E-01	7.87236E-01	1.67305E-01	1.53820E-04
35	2.10483E-01	7.86686E-01	1.65584E-01	1.53027E-04
40	2.08253E-01	7.86635E-01	1.63819E-01	1.52209E-04
45	2.05826E-01	7.85649E-01	1.61707E-01	1.51224E-04
50	2.07883E-01	7.87650E-01	1.63739E-01	1.52171E-04
55	2.09678E-01	7.88037E-01	1.65234E-01	1.52865E-04
60	2.09511E-01	7.87548E-01	1.65000E-01	1.52756E-04
65	2.09194E-01	7.86954E-01	1.64626E-01	1.52583E-04
70	2.10601E-01	7.87195E-01	1.65784E-01	1.53119E-04
75	2.12422E-01	7.87908E-01	1.67369E-01	1.53849E-04
80	2.13544E-01	7.87660E-01	1.68200E-01	1.54231E-04
85	2.13612E-01	7.86974E-01	1.68107E-01	1.54188E-04
90	2.13611E-01	7.86842E-01	1.68078E-01	1.54175E-04

ψ	p_n	η	ε	$\sigma(\varepsilon)$
$\theta = 50$				
0	2.10477E-01	7.86404E-01	1.65520E-01	1.60469E-04
5	2.10348E-01	7.86482E-01	1.65435E-01	1.60428E-04
10	2.10091E-01	7.86183E-01	1.65170E-01	1.60299E-04
15	2.10274E-01	7.85803E-01	1.65234E-01	1.60330E-04
20	2.10237E-01	7.86351E-01	1.65320E-01	1.60372E-04
25	2.10060E-01	7.86599E-01	1.65233E-01	1.60330E-04
30	2.08944E-01	7.86546E-01	1.64344E-01	1.59898E-04
35	2.07840E-01	7.86167E-01	1.63397E-01	1.59437E-04
40	2.05214E-01	7.86213E-01	1.61342E-01	1.58431E-04
45	2.01858E-01	7.84968E-01	1.58452E-01	1.57006E-04
50	2.05252E-01	7.87223E-01	1.61579E-01	1.58547E-04
55	2.07645E-01	7.87122E-01	1.63442E-01	1.59459E-04
60	2.05825E-01	7.86372E-01	1.61855E-01	1.58682E-04
65	2.05156E-01	7.85929E-01	1.61238E-01	1.58380E-04
70	2.07148E-01	7.86843E-01	1.62993E-01	1.59239E-04
75	2.09369E-01	7.86683E-01	1.64707E-01	1.60075E-04
80	2.10404E-01	7.86748E-01	1.65535E-01	1.60476E-04
85	2.10019E-01	7.86153E-01	1.65107E-01	1.60269E-04
90	2.09988E-01	7.86488E-01	1.65153E-01	1.60291E-04
$\theta = 55$				
0	2.05570E-01	7.85231E-01	1.61420E-01	1.67758E-04
5	2.05766E-01	7.85363E-01	1.61601E-01	1.67852E-04
10	2.05812E-01	7.85285E-01	1.61621E-01	1.67862E-04
15	2.05466E-01	7.85103E-01	1.61312E-01	1.67702E-04
20	2.05575E-01	7.85261E-01	1.61430E-01	1.67763E-04
25	2.05542E-01	7.85659E-01	1.61486E-01	1.67792E-04
30	2.04385E-01	7.85307E-01	1.60505E-01	1.67282E-04
35	2.03788E-01	7.85238E-01	1.60022E-01	1.67030E-04
40	2.01393E-01	7.85429E-01	1.58180E-01	1.66066E-04
45	1.96397E-01	7.83714E-01	1.53919E-01	1.63814E-04
50	2.01739E-01	7.85877E-01	1.58542E-01	1.66256E-04
55	2.04057E-01	7.86060E-01	1.60401E-01	1.67228E-04
60	2.01147E-01	7.85724E-01	1.58046E-01	1.65995E-04
65	2.00634E-01	7.85570E-01	1.57612E-01	1.65767E-04
70	2.03168E-01	7.85813E-01	1.59652E-01	1.66837E-04
75	2.05307E-01	7.85677E-01	1.61305E-01	1.67698E-04
80	2.05741E-01	7.85405E-01	1.61590E-01	1.67846E-04
85	2.05668E-01	7.85698E-01	1.61593E-01	1.67848E-04
90	2.05613E-01	7.85631E-01	1.61536E-01	1.67818E-04

ψ	p_n	η	ε	$\sigma(\varepsilon)$
$\theta = 60$				
0	1.99596E-01	7.83939E-01	1.56471E-01	1.76902E-04
5	1.99681E-01	7.84026E-01	1.56555E-01	1.76949E-04
10	1.99642E-01	7.84018E-01	1.56523E-01	1.76931E-04
15	1.99610E-01	7.84044E-01	1.56503E-01	1.76920E-04
20	1.99465E-01	7.83847E-01	1.56350E-01	1.76833E-04
25	1.99743E-01	7.83862E-01	1.56571E-01	1.76958E-04
30	1.98470E-01	7.84008E-01	1.55602E-01	1.76410E-04
35	1.97776E-01	7.84119E-01	1.55080E-01	1.76113E-04
40	1.96490E-01	7.84559E-01	1.54158E-01	1.75589E-04
45	1.89521E-01	7.81882E-01	1.48183E-01	1.72153E-04
50	1.96421E-01	7.84137E-01	1.54021E-01	1.75511E-04
55	1.98923E-01	7.85027E-01	1.56160E-01	1.76726E-04
60	1.95061E-01	7.84560E-01	1.53037E-01	1.74950E-04
65	1.94156E-01	7.84385E-01	1.52293E-01	1.74524E-04
70	1.97765E-01	7.84780E-01	1.55202E-01	1.76183E-04
75	1.99611E-01	7.84601E-01	1.56615E-01	1.76983E-04
80	1.99302E-01	7.83956E-01	1.56244E-01	1.76774E-04
85	1.99524E-01	7.84076E-01	1.56442E-01	1.76885E-04
90	1.99550E-01	7.83884E-01	1.56424E-01	1.76875E-04
$\theta = 65$				
0	1.91352E-01	7.81936E-01	1.49625E-01	1.88161E-04
5	1.91388E-01	7.82254E-01	1.49714E-01	1.88216E-04
10	1.91370E-01	7.81878E-01	1.49628E-01	1.88162E-04
15	1.91255E-01	7.81925E-01	1.49547E-01	1.88111E-04
20	1.91300E-01	7.82002E-01	1.49597E-01	1.88143E-04
25	1.91236E-01	7.81924E-01	1.49532E-01	1.88101E-04
30	1.90820E-01	7.82402E-01	1.49298E-01	1.87955E-04
35	1.89175E-01	7.81520E-01	1.47844E-01	1.87037E-04
40	1.89522E-01	7.83028E-01	1.48401E-01	1.87389E-04
45	1.80737E-01	7.79514E-01	1.40887E-01	1.82584E-04
50	1.89129E-01	7.82387E-01	1.47972E-01	1.87118E-04
55	1.90879E-01	7.82449E-01	1.49353E-01	1.87989E-04
60	1.87396E-01	7.82760E-01	1.46686E-01	1.86303E-04
65	1.85598E-01	7.82271E-01	1.45188E-01	1.85349E-04
70	1.90458E-01	7.82792E-01	1.49089E-01	1.87823E-04
75	1.91191E-01	7.82155E-01	1.49541E-01	1.88108E-04
80	1.91257E-01	7.81990E-01	1.49561E-01	1.88120E-04
85	1.91334E-01	7.81983E-01	1.49620E-01	1.88157E-04
90	1.91285E-01	7.82278E-01	1.49638E-01	1.88169E-04

ψ	p_n	η	ε	$\sigma(\varepsilon)$
$\theta = 70$				
0	1.79717E-01	7.79080E-01	1.40014E-01	2.02330E-04
5	1.79674E-01	7.79083E-01	1.39981E-01	2.02306E-04
10	1.79727E-01	7.79020E-01	1.40011E-01	2.02327E-04
15	1.79686E-01	7.79243E-01	1.40019E-01	2.02333E-04
20	1.79628E-01	7.78865E-01	1.39906E-01	2.02252E-04
25	1.79650E-01	7.79399E-01	1.40019E-01	2.02333E-04
30	1.79425E-01	7.79334E-01	1.39832E-01	2.02198E-04
35	1.77634E-01	7.78601E-01	1.38306E-01	2.01092E-04
40	1.79079E-01	7.79957E-01	1.39674E-01	2.02084E-04
45	1.68060E-01	7.76276E-01	1.30461E-01	1.95305E-04
50	1.78852E-01	7.80019E-01	1.39508E-01	2.01964E-04
55	1.79458E-01	7.79614E-01	1.39908E-01	2.02253E-04
60	1.76385E-01	7.80287E-01	1.37631E-01	2.00600E-04
65	1.73877E-01	7.79678E-01	1.35568E-01	1.99092E-04
70	1.79595E-01	7.80283E-01	1.40135E-01	2.02417E-04
75	1.79389E-01	7.79028E-01	1.39749E-01	2.02139E-04
80	1.79607E-01	7.79318E-01	1.39971E-01	2.02299E-04
85	1.79593E-01	7.79167E-01	1.39933E-01	2.02271E-04
90	1.79630E-01	7.79135E-01	1.39956E-01	2.02288E-04
$\theta = 75$				
0	1.62136E-01	7.74085E-01	1.25507E-01	2.20210E-04
5	1.62140E-01	7.74170E-01	1.25524E-01	2.20225E-04
10	1.62139E-01	7.74064E-01	1.25506E-01	2.20209E-04
15	1.62112E-01	7.74070E-01	1.25486E-01	2.20191E-04
20	1.62111E-01	7.74315E-01	1.25525E-01	2.20226E-04
25	1.62042E-01	7.74089E-01	1.25435E-01	2.20146E-04
30	1.62117E-01	7.74447E-01	1.25551E-01	2.20248E-04
35	1.60532E-01	7.74070E-01	1.24263E-01	2.19115E-04
40	1.61846E-01	7.74780E-01	1.25395E-01	2.20111E-04
45	1.50103E-01	7.70984E-01	1.15727E-01	2.11455E-04
50	1.61427E-01	7.74282E-01	1.24990E-01	2.19756E-04
55	1.61726E-01	7.74705E-01	1.25290E-01	2.20019E-04
60	1.60568E-01	7.75821E-01	1.24572E-01	2.19387E-04
65	1.56818E-01	7.75166E-01	1.21560E-01	2.16719E-04
70	1.61952E-01	7.74575E-01	1.25444E-01	2.20154E-04
75	1.62131E-01	7.74146E-01	1.25513E-01	2.20215E-04
80	1.62079E-01	7.74147E-01	1.25473E-01	2.20179E-04
85	1.62156E-01	7.74199E-01	1.25541E-01	2.20240E-04
90	1.62132E-01	7.74418E-01	1.25558E-01	2.20254E-04

ψ	p_n	η	ε	$\sigma(\varepsilon)$
$\theta = 80$				
0	1.33662E-01	7.64174E-01	1.02141E-01	2.42530E-04
5	1.33625E-01	7.64266E-01	1.02125E-01	2.42511E-04
10	1.33638E-01	7.64124E-01	1.02116E-01	2.42500E-04
15	1.33658E-01	7.64077E-01	1.02125E-01	2.42511E-04
20	1.33630E-01	7.64349E-01	1.02140E-01	2.42529E-04
25	1.33640E-01	7.64337E-01	1.02146E-01	2.42535E-04
30	1.33549E-01	7.64289E-01	1.02070E-01	2.42445E-04
35	1.32961E-01	7.64698E-01	1.01675E-01	2.41976E-04
40	1.33440E-01	7.65250E-01	1.02115E-01	2.42499E-04
45	1.22389E-01	7.60934E-01	9.31300E-02	2.31585E-04
50	1.33040E-01	7.64650E-01	1.01729E-01	2.42040E-04
55	1.33476E-01	7.64902E-01	1.02096E-01	2.42476E-04
60	1.33615E-01	7.65648E-01	1.02302E-01	2.42720E-04
65	1.30312E-01	7.66572E-01	9.98935E-02	2.39847E-04
70	1.33569E-01	7.65073E-01	1.02190E-01	2.42588E-04
75	1.33641E-01	7.64399E-01	1.02155E-01	2.42546E-04
80	1.33582E-01	7.64399E-01	1.02110E-01	2.42493E-04
85	1.33633E-01	7.64227E-01	1.02126E-01	2.42512E-04
90	1.33653E-01	7.64106E-01	1.02125E-01	2.42511E-04
$\theta = 85$				
0	8.24727E-02	7.35766E-01	6.06806E-02	2.63862E-04
5	8.24762E-02	7.35873E-01	6.06920E-02	2.63887E-04
10	8.24771E-02	7.35882E-01	6.06934E-02	2.63890E-04
15	8.24753E-02	7.35933E-01	6.06963E-02	2.63896E-04
20	8.24768E-02	7.36045E-01	6.07066E-02	2.63919E-04
25	8.24742E-02	7.35876E-01	6.06908E-02	2.63884E-04
30	8.24797E-02	7.36265E-01	6.07269E-02	2.63963E-04
35	8.24685E-02	7.36719E-01	6.07561E-02	2.64026E-04
40	8.24421E-02	7.36864E-01	6.07486E-02	2.64010E-04
45	7.65242E-02	7.34624E-01	5.62165E-02	2.53971E-04
50	8.23059E-02	7.36586E-01	6.06254E-02	2.63742E-04
55	8.24580E-02	7.36412E-01	6.07231E-02	2.63955E-04
60	8.24735E-02	7.37833E-01	6.08517E-02	2.64234E-04
65	8.24215E-02	7.40042E-01	6.09954E-02	2.64546E-04
70	8.24628E-02	7.36661E-01	6.07471E-02	2.64007E-04
75	8.24777E-02	7.36077E-01	6.07099E-02	2.63926E-04
80	8.24744E-02	7.35930E-01	6.06954E-02	2.63894E-04
85	8.24776E-02	7.36134E-01	6.07146E-02	2.63936E-04
90	8.24840E-02	7.35899E-01	6.06999E-02	2.63904E-04

Table B.12. ^{10}B sinusoid detector with 30 μm deep perforations, 4 μm wave separation, 4 μm wave period, 4 μm wave amplitude, and no cap

ψ	p_n	η	ε	$\sigma(\varepsilon)$
$\theta = 0$				
0	3.67852E-01	8.54064E-01	3.14169E-01	5.60508E-04
5	3.68573E-01	8.54534E-01	3.14958E-01	5.61211E-04
10	3.68189E-01	8.54105E-01	3.14472E-01	5.60778E-04
15	3.67242E-01	8.54695E-01	3.13880E-01	5.60250E-04
20	3.68126E-01	8.55194E-01	3.14819E-01	5.61087E-04
25	3.67742E-01	8.53955E-01	3.14035E-01	5.60388E-04
30	3.67772E-01	8.54225E-01	3.14160E-01	5.60500E-04
35	3.68121E-01	8.54491E-01	3.14556E-01	5.60853E-04
40	3.67042E-01	8.54161E-01	3.13513E-01	5.59922E-04
45	3.68512E-01	8.53994E-01	3.14707E-01	5.60988E-04
50	3.68139E-01	8.54446E-01	3.14555E-01	5.60852E-04
55	3.67883E-01	8.54924E-01	3.14512E-01	5.60814E-04
60	3.67933E-01	8.55224E-01	3.14665E-01	5.60950E-04
65	3.66502E-01	8.55297E-01	3.13468E-01	5.59882E-04
70	3.67406E-01	8.53976E-01	3.13756E-01	5.60139E-04
75	3.67491E-01	8.54440E-01	3.13999E-01	5.60356E-04
80	3.67896E-01	8.55274E-01	3.14652E-01	5.60938E-04
85	3.67265E-01	8.54647E-01	3.13882E-01	5.60252E-04
90	3.67785E-01	8.54268E-01	3.14187E-01	5.60524E-04
$\theta = 5$				
0	4.71386E-01	8.60641E-01	4.05694E-01	6.38157E-04
5	4.71298E-01	8.61033E-01	4.05803E-01	6.38242E-04
10	4.71005E-01	8.60486E-01	4.05293E-01	6.37841E-04
15	4.70551E-01	8.60436E-01	4.04879E-01	6.37515E-04
20	4.70494E-01	8.61550E-01	4.05354E-01	6.37889E-04
25	4.70091E-01	8.60623E-01	4.04571E-01	6.37272E-04
30	4.69498E-01	8.61194E-01	4.04329E-01	6.37082E-04
35	4.68368E-01	8.60883E-01	4.03210E-01	6.36200E-04
40	4.66852E-01	8.60767E-01	4.01851E-01	6.35127E-04
45	4.65036E-01	8.62365E-01	4.01031E-01	6.34479E-04
50	4.61634E-01	8.61891E-01	3.97878E-01	6.31979E-04
55	4.57269E-01	8.62490E-01	3.94390E-01	6.29203E-04
60	4.50707E-01	8.62234E-01	3.88615E-01	6.24579E-04
65	4.43296E-01	8.62532E-01	3.82357E-01	6.19530E-04
70	4.34744E-01	8.62202E-01	3.74837E-01	6.13408E-04
75	4.26402E-01	8.61685E-01	3.67424E-01	6.07311E-04
80	4.19209E-01	8.60991E-01	3.60935E-01	6.01925E-04
85	4.18573E-01	8.61269E-01	3.60504E-01	6.01565E-04
90	4.18836E-01	8.61540E-01	3.60844E-01	6.01849E-04

ψ	p_n	η	ε	$\sigma(\varepsilon)$
$\theta = 10$				
0	4.72847E-01	8.59227E-01	4.06283E-01	6.42301E-04
5	4.73129E-01	8.59920E-01	4.06853E-01	6.42751E-04
10	4.73380E-01	8.58296E-01	4.06300E-01	6.42315E-04
15	4.74784E-01	8.60916E-01	4.08749E-01	6.44248E-04
20	4.75139E-01	8.60660E-01	4.08933E-01	6.44392E-04
25	4.75838E-01	8.59223E-01	4.08851E-01	6.44328E-04
30	4.76267E-01	8.60156E-01	4.09664E-01	6.44968E-04
35	4.74783E-01	8.60854E-01	4.08719E-01	6.44224E-04
40	4.74225E-01	8.60088E-01	4.07875E-01	6.43558E-04
45	4.74156E-01	8.59690E-01	4.07627E-01	6.43362E-04
50	4.72727E-01	8.61070E-01	4.07051E-01	6.42907E-04
55	4.71998E-01	8.61044E-01	4.06411E-01	6.42403E-04
60	4.70347E-01	8.61171E-01	4.05049E-01	6.41325E-04
65	4.63370E-01	8.62762E-01	3.99778E-01	6.37138E-04
70	4.53317E-01	8.61219E-01	3.90405E-01	6.29625E-04
75	4.44913E-01	8.60438E-01	3.82820E-01	6.23479E-04
80	4.40075E-01	8.58576E-01	3.77838E-01	6.19409E-04
85	4.56907E-01	8.61539E-01	3.93643E-01	6.32231E-04
90	4.66591E-01	8.61463E-01	4.01951E-01	6.38868E-04
$\theta = 15$				
0	4.71372E-01	8.59693E-01	4.05235E-01	6.47711E-04
5	4.72175E-01	8.59078E-01	4.05635E-01	6.48031E-04
10	4.72393E-01	8.59884E-01	4.06203E-01	6.48484E-04
15	4.72137E-01	8.58963E-01	4.05548E-01	6.47961E-04
20	4.74153E-01	8.60117E-01	4.07827E-01	6.49780E-04
25	4.75406E-01	8.58698E-01	4.08230E-01	6.50101E-04
30	4.75825E-01	8.58879E-01	4.08676E-01	6.50456E-04
35	4.77396E-01	8.58845E-01	4.10009E-01	6.51516E-04
40	4.77316E-01	8.59257E-01	4.10137E-01	6.51617E-04
45	4.78613E-01	8.58612E-01	4.10943E-01	6.52258E-04
50	4.75416E-01	8.59836E-01	4.08780E-01	6.50538E-04
55	4.73607E-01	8.60517E-01	4.07547E-01	6.49557E-04
60	4.72011E-01	8.60501E-01	4.06166E-01	6.48455E-04
65	4.69997E-01	8.61365E-01	4.04839E-01	6.47395E-04
70	4.60671E-01	8.60640E-01	3.96472E-01	6.40670E-04
75	4.51188E-01	8.61461E-01	3.88681E-01	6.34344E-04
80	4.46117E-01	8.58430E-01	3.82960E-01	6.29658E-04
85	4.67529E-01	8.59739E-01	4.01953E-01	6.45083E-04
90	4.80083E-01	8.59945E-01	4.12845E-01	6.53765E-04

ψ	p_n	η	ε	$\sigma(\varepsilon)$
$\theta = 20$				
0	4.66260E-01	8.59962E-01	4.00966E-01	6.53222E-04
5	4.68061E-01	8.58674E-01	4.01912E-01	6.53992E-04
10	4.68753E-01	8.58964E-01	4.02642E-01	6.54586E-04
15	4.69718E-01	8.60148E-01	4.04027E-01	6.55711E-04
20	4.71791E-01	8.59239E-01	4.05381E-01	6.56808E-04
25	4.73235E-01	8.59947E-01	4.06957E-01	6.58084E-04
30	4.73674E-01	8.58303E-01	4.06556E-01	6.57760E-04
35	4.74269E-01	8.58635E-01	4.07224E-01	6.58300E-04
40	4.75008E-01	8.57882E-01	4.07501E-01	6.58523E-04
45	4.75788E-01	8.59107E-01	4.08753E-01	6.59535E-04
50	4.74525E-01	8.59150E-01	4.07688E-01	6.58674E-04
55	4.71396E-01	8.59496E-01	4.05163E-01	6.56632E-04
60	4.68420E-01	8.61323E-01	4.03461E-01	6.55251E-04
65	4.67563E-01	8.60370E-01	4.02277E-01	6.54289E-04
70	4.63855E-01	8.60487E-01	3.99141E-01	6.51734E-04
75	4.50071E-01	8.60000E-01	3.87061E-01	6.41796E-04
80	4.47860E-01	8.58105E-01	3.84311E-01	6.39512E-04
85	4.72134E-01	8.60184E-01	4.06122E-01	6.57409E-04
90	4.72794E-01	8.58892E-01	4.06079E-01	6.57374E-04
$\theta = 25$				
0	4.61080E-01	8.58751E-01	3.95953E-01	6.60974E-04
5	4.62512E-01	8.58808E-01	3.97209E-01	6.62021E-04
10	4.64340E-01	8.59090E-01	3.98910E-01	6.63437E-04
15	4.66368E-01	8.59049E-01	4.00633E-01	6.64868E-04
20	4.67910E-01	8.59311E-01	4.02080E-01	6.66068E-04
25	4.69157E-01	8.58764E-01	4.02895E-01	6.66743E-04
30	4.71615E-01	8.59091E-01	4.05160E-01	6.68614E-04
35	4.70373E-01	8.58512E-01	4.03821E-01	6.67508E-04
40	4.71082E-01	8.59281E-01	4.04792E-01	6.68311E-04
45	4.70336E-01	8.59313E-01	4.04166E-01	6.67793E-04
50	4.69795E-01	8.58453E-01	4.03297E-01	6.67075E-04
55	4.66999E-01	8.59233E-01	4.01261E-01	6.65389E-04
60	4.63667E-01	8.59915E-01	3.98714E-01	6.63274E-04
65	4.61270E-01	8.60908E-01	3.97111E-01	6.61939E-04
70	4.64061E-01	8.59676E-01	3.98942E-01	6.63464E-04
75	4.46917E-01	8.59352E-01	3.84059E-01	6.50970E-04
80	4.49462E-01	8.57699E-01	3.85503E-01	6.52192E-04
85	4.68248E-01	8.58289E-01	4.01892E-01	6.65912E-04
90	4.69651E-01	8.59031E-01	4.03445E-01	6.67197E-04

ψ	p_n	η	ε	$\sigma(\varepsilon)$
$\theta = 30$				
0	4.54238E-01	8.60164E-01	3.90719E-01	6.71687E-04
5	4.56254E-01	8.58921E-01	3.91886E-01	6.72689E-04
10	4.58205E-01	8.58638E-01	3.93432E-01	6.74015E-04
15	4.60562E-01	8.58349E-01	3.95323E-01	6.75633E-04
20	4.63330E-01	8.59441E-01	3.98205E-01	6.78091E-04
25	4.63472E-01	8.57370E-01	3.97367E-01	6.77377E-04
30	4.63037E-01	8.58908E-01	3.97706E-01	6.77666E-04
35	4.63356E-01	8.58195E-01	3.97650E-01	6.77619E-04
40	4.63324E-01	8.58669E-01	3.97842E-01	6.77782E-04
45	4.63182E-01	8.57779E-01	3.97308E-01	6.77327E-04
50	4.63420E-01	8.58362E-01	3.97782E-01	6.77731E-04
55	4.62154E-01	8.58335E-01	3.96683E-01	6.76794E-04
60	4.57797E-01	8.60159E-01	3.93778E-01	6.74312E-04
65	4.55213E-01	8.60808E-01	3.91851E-01	6.72660E-04
70	4.60820E-01	8.58433E-01	3.95583E-01	6.75855E-04
75	4.41412E-01	8.60511E-01	3.79840E-01	6.62270E-04
80	4.45962E-01	8.57757E-01	3.82527E-01	6.64608E-04
85	4.61379E-01	8.58234E-01	3.95971E-01	6.76186E-04
90	4.63114E-01	8.58905E-01	3.97771E-01	6.77721E-04
$\theta = 35$				
0	4.45923E-01	8.58323E-01	3.82746E-01	6.83555E-04
5	4.47657E-01	8.58740E-01	3.84421E-01	6.85049E-04
10	4.50939E-01	8.58859E-01	3.87293E-01	6.87603E-04
15	4.53357E-01	8.58324E-01	3.89127E-01	6.89229E-04
20	4.54757E-01	8.58797E-01	3.90544E-01	6.90482E-04
25	4.54630E-01	8.58599E-01	3.90345E-01	6.90306E-04
30	4.53832E-01	8.57842E-01	3.89316E-01	6.89396E-04
35	4.53796E-01	8.59071E-01	3.89843E-01	6.89863E-04
40	4.54222E-01	8.57951E-01	3.89700E-01	6.89736E-04
45	4.54154E-01	8.59310E-01	3.90259E-01	6.90230E-04
50	4.54066E-01	8.58003E-01	3.89590E-01	6.89639E-04
55	4.54395E-01	8.57741E-01	3.89753E-01	6.89783E-04
60	4.49906E-01	8.60171E-01	3.86996E-01	6.87339E-04
65	4.47823E-01	8.60038E-01	3.85145E-01	6.85693E-04
70	4.52590E-01	8.59166E-01	3.88850E-01	6.88983E-04
75	4.33299E-01	8.59120E-01	3.72256E-01	6.74122E-04
80	4.41735E-01	8.57426E-01	3.78755E-01	6.79981E-04
85	4.53576E-01	8.58436E-01	3.89366E-01	6.89440E-04
90	4.53449E-01	8.58275E-01	3.89184E-01	6.89279E-04

ψ	p_n	η	ε	$\sigma(\varepsilon)$
$\theta = 40$				
0	4.34794E-01	8.57700E-01	3.72923E-01	6.97722E-04
5	4.37030E-01	8.58795E-01	3.75319E-01	6.99960E-04
10	4.41363E-01	8.57933E-01	3.78660E-01	7.03068E-04
15	4.42805E-01	8.58014E-01	3.79933E-01	7.04249E-04
20	4.43387E-01	8.58433E-01	3.80618E-01	7.04884E-04
25	4.43806E-01	8.58037E-01	3.80802E-01	7.05055E-04
30	4.43726E-01	8.57604E-01	3.80541E-01	7.04813E-04
35	4.43806E-01	8.57715E-01	3.80659E-01	7.04922E-04
40	4.44130E-01	8.57503E-01	3.80843E-01	7.05092E-04
45	4.43648E-01	8.58334E-01	3.80798E-01	7.05050E-04
50	4.43632E-01	8.58676E-01	3.80936E-01	7.05178E-04
55	4.43583E-01	8.57053E-01	3.80174E-01	7.04473E-04
60	4.39651E-01	8.59295E-01	3.77790E-01	7.02261E-04
65	4.36023E-01	8.60668E-01	3.75271E-01	6.99916E-04
70	4.42190E-01	8.57720E-01	3.79275E-01	7.03640E-04
75	4.23218E-01	8.58392E-01	3.63287E-01	6.88649E-04
80	4.33367E-01	8.56099E-01	3.71005E-01	6.95925E-04
85	4.42742E-01	8.57628E-01	3.79708E-01	7.04040E-04
90	4.44183E-01	8.58522E-01	3.81341E-01	7.05553E-04
$\theta = 45$				
0	4.20848E-01	8.57350E-01	3.60814E-01	7.14330E-04
5	4.24345E-01	8.57081E-01	3.63698E-01	7.17180E-04
10	4.28312E-01	8.57891E-01	3.67445E-01	7.20865E-04
15	4.30286E-01	8.56891E-01	3.68708E-01	7.22102E-04
20	4.30101E-01	8.57610E-01	3.68859E-01	7.22250E-04
25	4.30538E-01	8.57662E-01	3.69256E-01	7.22639E-04
30	4.30433E-01	8.57302E-01	3.69011E-01	7.22399E-04
35	4.29864E-01	8.57225E-01	3.68490E-01	7.21889E-04
40	4.30644E-01	8.57198E-01	3.69147E-01	7.22532E-04
45	4.29857E-01	8.57427E-01	3.68571E-01	7.21968E-04
50	4.30436E-01	8.57212E-01	3.68975E-01	7.22364E-04
55	4.30491E-01	8.57535E-01	3.69161E-01	7.22546E-04
60	4.27499E-01	8.58966E-01	3.67207E-01	7.20631E-04
65	4.23023E-01	8.58889E-01	3.63330E-01	7.16817E-04
70	4.29314E-01	8.58064E-01	3.68379E-01	7.21780E-04
75	4.11227E-01	8.58312E-01	3.52961E-01	7.06514E-04
80	4.19936E-01	8.56921E-01	3.59852E-01	7.13378E-04
85	4.29944E-01	8.57384E-01	3.68627E-01	7.22024E-04
90	4.31014E-01	8.57316E-01	3.69515E-01	7.22892E-04

ψ	p_n	η	ε	$\sigma(\varepsilon)$
$\theta = 50$				
0	4.03987E-01	8.57092E-01	3.46254E-01	7.33946E-04
5	4.08540E-01	8.56785E-01	3.50031E-01	7.37937E-04
10	4.13304E-01	8.56752E-01	3.54099E-01	7.42213E-04
15	4.13654E-01	8.56291E-01	3.54208E-01	7.42327E-04
20	4.13405E-01	8.56030E-01	3.53887E-01	7.41991E-04
25	4.13998E-01	8.56243E-01	3.54483E-01	7.42615E-04
30	4.14257E-01	8.57086E-01	3.55054E-01	7.43213E-04
35	4.13859E-01	8.56342E-01	3.54405E-01	7.42534E-04
40	4.13877E-01	8.56547E-01	3.54505E-01	7.42639E-04
45	4.14202E-01	8.56415E-01	3.54729E-01	7.42873E-04
50	4.13415E-01	8.57112E-01	3.54343E-01	7.42469E-04
55	4.13003E-01	8.57478E-01	3.54141E-01	7.42257E-04
60	4.11610E-01	8.57732E-01	3.53051E-01	7.41114E-04
65	4.07247E-01	8.58774E-01	3.49733E-01	7.37623E-04
70	4.13438E-01	8.56900E-01	3.54275E-01	7.42397E-04
75	3.96527E-01	8.57964E-01	3.40206E-01	7.27507E-04
80	4.03641E-01	8.54945E-01	3.45091E-01	7.32711E-04
85	4.14547E-01	8.57452E-01	3.55454E-01	7.43632E-04
90	4.13530E-01	8.56934E-01	3.54368E-01	7.42495E-04
$\theta = 55$				
0	3.83564E-01	8.56173E-01	3.28397E-01	7.56665E-04
5	3.89189E-01	8.56198E-01	3.33223E-01	7.62205E-04
10	3.93114E-01	8.55299E-01	3.36230E-01	7.65636E-04
15	3.92522E-01	8.55702E-01	3.35882E-01	7.65240E-04
20	3.93187E-01	8.55524E-01	3.36381E-01	7.65808E-04
25	3.93280E-01	8.55945E-01	3.36626E-01	7.66087E-04
30	3.93321E-01	8.55619E-01	3.36533E-01	7.65982E-04
35	3.93081E-01	8.55475E-01	3.36271E-01	7.65683E-04
40	3.93166E-01	8.55786E-01	3.36466E-01	7.65905E-04
45	3.92766E-01	8.55446E-01	3.35990E-01	7.65363E-04
50	3.93276E-01	8.55654E-01	3.36508E-01	7.65953E-04
55	3.93463E-01	8.55864E-01	3.36751E-01	7.66230E-04
60	3.92570E-01	8.56477E-01	3.36227E-01	7.65633E-04
65	3.87696E-01	8.58206E-01	3.32723E-01	7.61632E-04
70	3.92257E-01	8.56678E-01	3.36038E-01	7.65418E-04
75	3.78113E-01	8.56924E-01	3.24014E-01	7.51599E-04
80	3.83962E-01	8.54444E-01	3.28074E-01	7.56294E-04
85	3.93095E-01	8.56246E-01	3.36586E-01	7.66042E-04
90	3.93478E-01	8.55128E-01	3.36474E-01	7.65914E-04

ψ	p_n	η	ε	$\sigma(\varepsilon)$
$\theta = 60$				
0	3.57892E-01	8.55177E-01	3.06061E-01	7.82382E-04
5	3.64468E-01	8.54983E-01	3.11614E-01	7.89449E-04
10	3.67255E-01	8.54763E-01	3.13916E-01	7.92359E-04
15	3.67575E-01	8.54982E-01	3.14270E-01	7.92805E-04
20	3.67248E-01	8.54251E-01	3.13722E-01	7.92114E-04
25	3.67551E-01	8.54733E-01	3.14158E-01	7.92664E-04
30	3.67269E-01	8.54513E-01	3.13836E-01	7.92258E-04
35	3.67380E-01	8.54382E-01	3.13883E-01	7.92317E-04
40	3.67335E-01	8.54555E-01	3.13908E-01	7.92348E-04
45	3.67789E-01	8.54430E-01	3.14250E-01	7.92780E-04
50	3.67570E-01	8.55116E-01	3.14315E-01	7.92863E-04
55	3.67232E-01	8.54419E-01	3.13770E-01	7.92174E-04
60	3.66992E-01	8.55190E-01	3.13848E-01	7.92273E-04
65	3.63190E-01	8.57521E-01	3.11443E-01	7.89232E-04
70	3.67150E-01	8.54711E-01	3.13807E-01	7.92221E-04
75	3.56370E-01	8.56764E-01	3.05325E-01	7.81442E-04
80	3.60734E-01	8.52947E-01	3.07687E-01	7.84458E-04
85	3.67261E-01	8.55560E-01	3.14214E-01	7.92735E-04
90	3.67507E-01	8.54631E-01	3.14083E-01	7.92570E-04
$\theta = 65$				
0	3.26108E-01	8.53499E-01	2.78333E-01	8.11537E-04
5	3.33341E-01	8.53006E-01	2.84342E-01	8.20250E-04
10	3.34274E-01	8.52639E-01	2.85015E-01	8.21221E-04
15	3.34938E-01	8.52570E-01	2.85558E-01	8.22002E-04
20	3.34774E-01	8.53337E-01	2.85675E-01	8.22170E-04
25	3.34543E-01	8.52943E-01	2.85346E-01	8.21698E-04
30	3.34760E-01	8.52733E-01	2.85461E-01	8.21863E-04
35	3.34699E-01	8.52847E-01	2.85447E-01	8.21842E-04
40	3.34468E-01	8.52437E-01	2.85113E-01	8.21362E-04
45	3.34701E-01	8.53200E-01	2.85567E-01	8.22015E-04
50	3.34604E-01	8.52360E-01	2.85203E-01	8.21491E-04
55	3.34672E-01	8.52993E-01	2.85473E-01	8.21880E-04
60	3.34834E-01	8.52829E-01	2.85556E-01	8.22000E-04
65	3.31728E-01	8.54751E-01	2.83545E-01	8.19100E-04
70	3.34640E-01	8.53720E-01	2.85689E-01	8.22190E-04
75	3.27952E-01	8.54229E-01	2.80146E-01	8.14175E-04
80	3.29690E-01	8.52204E-01	2.80963E-01	8.15362E-04
85	3.34917E-01	8.53397E-01	2.85817E-01	8.22375E-04
90	3.34963E-01	8.53458E-01	2.85877E-01	8.22462E-04

ψ	p_n	η	ε	$\sigma(\varepsilon)$
$\theta = 70$				
0	2.85308E-01	8.51445E-01	2.42924E-01	8.42770E-04
5	2.92634E-01	8.50154E-01	2.48784E-01	8.52876E-04
10	2.92971E-01	8.50405E-01	2.49144E-01	8.53492E-04
15	2.92667E-01	8.50161E-01	2.48814E-01	8.52927E-04
20	2.92848E-01	8.50615E-01	2.49101E-01	8.53418E-04
25	2.92792E-01	8.50344E-01	2.48974E-01	8.53200E-04
30	2.92764E-01	8.49999E-01	2.48849E-01	8.52987E-04
35	2.92742E-01	8.50185E-01	2.48885E-01	8.53047E-04
40	2.92933E-01	8.50065E-01	2.49012E-01	8.53265E-04
45	2.92966E-01	8.50600E-01	2.49197E-01	8.53583E-04
50	2.93064E-01	8.50265E-01	2.49182E-01	8.53557E-04
55	2.92863E-01	8.50288E-01	2.49018E-01	8.53276E-04
60	2.92492E-01	8.50447E-01	2.48749E-01	8.52815E-04
65	2.91543E-01	8.52464E-01	2.48530E-01	8.52439E-04
70	2.92792E-01	8.50577E-01	2.49042E-01	8.53318E-04
75	2.90927E-01	8.51970E-01	2.47861E-01	8.51291E-04
80	2.90402E-01	8.49977E-01	2.46835E-01	8.49528E-04
85	2.92875E-01	8.50854E-01	2.49194E-01	8.53577E-04
90	2.92768E-01	8.51097E-01	2.49174E-01	8.53544E-04
$\theta = 75$				
0	2.33332E-01	8.47548E-01	1.97760E-01	8.74120E-04
5	2.38835E-01	8.46078E-01	2.02073E-01	8.83602E-04
10	2.38747E-01	8.45456E-01	2.01850E-01	8.83112E-04
15	2.38860E-01	8.45345E-01	2.01919E-01	8.83264E-04
20	2.38855E-01	8.45978E-01	2.02066E-01	8.83586E-04
25	2.38969E-01	8.45432E-01	2.02032E-01	8.83511E-04
30	2.38931E-01	8.45332E-01	2.01976E-01	8.83388E-04
35	2.38896E-01	8.46724E-01	2.02279E-01	8.84052E-04
40	2.38924E-01	8.46039E-01	2.02139E-01	8.83745E-04
45	2.38939E-01	8.46015E-01	2.02146E-01	8.83761E-04
50	2.38857E-01	8.45678E-01	2.01996E-01	8.83433E-04
55	2.38934E-01	8.46954E-01	2.02366E-01	8.84242E-04
60	2.38880E-01	8.47241E-01	2.02389E-01	8.84291E-04
65	2.38827E-01	8.48049E-01	2.02537E-01	8.84615E-04
70	2.38857E-01	8.46222E-01	2.02126E-01	8.83717E-04
75	2.38856E-01	8.47749E-01	2.02490E-01	8.84512E-04
80	2.38559E-01	8.46030E-01	2.01828E-01	8.83066E-04
85	2.39050E-01	8.46455E-01	2.02345E-01	8.84196E-04
90	2.38996E-01	8.46809E-01	2.02384E-01	8.84280E-04

ψ	p_n	η	ε	$\sigma(\varepsilon)$
$\theta = 80$				
0	1.67411E-01	8.38649E-01	1.40399E-01	8.99180E-04
5	1.69837E-01	8.37686E-01	1.42270E-01	9.05152E-04
10	1.69839E-01	8.37876E-01	1.42304E-01	9.05260E-04
15	1.69835E-01	8.37595E-01	1.42253E-01	9.05097E-04
20	1.69868E-01	8.37798E-01	1.42315E-01	9.05296E-04
25	1.69840E-01	8.37064E-01	1.42167E-01	9.04823E-04
30	1.69860E-01	8.37331E-01	1.42229E-01	9.05023E-04
35	1.69855E-01	8.37520E-01	1.42257E-01	9.05110E-04
40	1.69838E-01	8.37757E-01	1.42283E-01	9.05195E-04
45	1.69896E-01	8.37312E-01	1.42256E-01	9.05107E-04
50	1.69840E-01	8.37382E-01	1.42221E-01	9.04997E-04
55	1.69854E-01	8.37513E-01	1.42255E-01	9.05105E-04
60	1.69853E-01	8.38560E-01	1.42432E-01	9.05669E-04
65	1.69730E-01	8.39203E-01	1.42438E-01	9.05686E-04
70	1.69844E-01	8.38234E-01	1.42369E-01	9.05467E-04
75	1.69630E-01	8.38867E-01	1.42297E-01	9.05239E-04
80	1.69738E-01	8.37579E-01	1.42169E-01	9.04832E-04
85	1.69844E-01	8.37810E-01	1.42297E-01	9.05238E-04
90	1.69891E-01	8.37219E-01	1.42236E-01	9.05043E-04
$\theta = 85$				
0	8.69562E-02	8.15680E-01	7.09284E-02	9.02115E-04
5	8.71134E-02	8.14737E-01	7.09745E-02	9.02409E-04
10	8.71132E-02	8.14379E-01	7.09432E-02	9.02210E-04
15	8.71118E-02	8.13833E-01	7.08945E-02	9.01900E-04
20	8.71081E-02	8.13151E-01	7.08320E-02	9.01503E-04
25	8.71140E-02	8.13295E-01	7.08494E-02	9.01613E-04
30	8.71107E-02	8.13520E-01	7.08663E-02	9.01721E-04
35	8.71122E-02	8.13847E-01	7.08960E-02	9.01910E-04
40	8.71120E-02	8.13834E-01	7.08947E-02	9.01901E-04
45	8.71125E-02	8.13144E-01	7.08350E-02	9.01521E-04
50	8.71162E-02	8.14437E-01	7.09507E-02	9.02257E-04
55	8.71168E-02	8.13989E-01	7.09121E-02	9.02012E-04
60	8.71122E-02	8.14603E-01	7.09619E-02	9.02329E-04
65	8.71113E-02	8.15574E-01	7.10457E-02	9.02861E-04
70	8.71126E-02	8.13944E-01	7.09048E-02	9.01966E-04
75	8.71150E-02	8.15927E-01	7.10795E-02	9.03076E-04
80	8.71071E-02	8.14162E-01	7.09193E-02	9.02058E-04
85	8.71105E-02	8.14266E-01	7.09311E-02	9.02133E-04
90	8.71113E-02	8.13879E-01	7.08981E-02	9.01923E-04

Table B.13. ^{10}B sinusoid detector with 10 μm deep perforations, 0.5 μm wave separation, 8 μm wave period, 1 μm wave amplitude, and no cap

ψ	p_n	η	ε	$\sigma(\varepsilon)$
$\theta = 0$				
0	1.79980E-01	9.50439E-01	1.71060E-01	1.30790E-03
5	1.78810E-01	9.49444E-01	1.69770E-01	1.30296E-03
10	1.79190E-01	9.50444E-01	1.70310E-01	1.30503E-03
15	1.78670E-01	9.51587E-01	1.70020E-01	1.30392E-03
20	1.77620E-01	9.52821E-01	1.69240E-01	1.30092E-03
25	1.77900E-01	9.49635E-01	1.68940E-01	1.29977E-03
30	1.79460E-01	9.54029E-01	1.71210E-01	1.30847E-03
35	1.78640E-01	9.52978E-01	1.70240E-01	1.30476E-03
40	1.78620E-01	9.51293E-01	1.69920E-01	1.30353E-03
45	1.80210E-01	9.50835E-01	1.71350E-01	1.30901E-03
50	1.79400E-01	9.51616E-01	1.70720E-01	1.30660E-03
55	1.78670E-01	9.48452E-01	1.69460E-01	1.30177E-03
60	1.79400E-01	9.49387E-01	1.70320E-01	1.30507E-03
65	1.80000E-01	9.51167E-01	1.71210E-01	1.30847E-03
70	1.80590E-01	9.50772E-01	1.71700E-01	1.31034E-03
75	1.79970E-01	9.48547E-01	1.70710E-01	1.30656E-03
80	1.81630E-01	9.50173E-01	1.72580E-01	1.31370E-03
85	1.81170E-01	9.50157E-01	1.72140E-01	1.31202E-03
90	1.79830E-01	9.52177E-01	1.71230E-01	1.30855E-03
$\theta = 5$				
0	1.88769E-01	9.51449E-01	1.79604E-01	1.34272E-03
5	1.90363E-01	9.50074E-01	1.80859E-01	1.34740E-03
10	1.90383E-01	9.50552E-01	1.80969E-01	1.34781E-03
15	1.89805E-01	9.52499E-01	1.80789E-01	1.34715E-03
20	1.91678E-01	9.54731E-01	1.83001E-01	1.35536E-03
25	1.90074E-01	9.51045E-01	1.80769E-01	1.34707E-03
30	1.89516E-01	9.51112E-01	1.80251E-01	1.34514E-03
35	1.88470E-01	9.51637E-01	1.79355E-01	1.34179E-03
40	1.94029E-01	9.50760E-01	1.84475E-01	1.36081E-03
45	1.91150E-01	9.54816E-01	1.82513E-01	1.35355E-03
50	1.94158E-01	9.52595E-01	1.84954E-01	1.36257E-03
55	1.94905E-01	9.54055E-01	1.85950E-01	1.36624E-03
60	1.95503E-01	9.52001E-01	1.86119E-01	1.36686E-03
65	1.95712E-01	9.52716E-01	1.86458E-01	1.36810E-03
70	1.96370E-01	9.54443E-01	1.87424E-01	1.37164E-03
75	1.99319E-01	9.50517E-01	1.89456E-01	1.37906E-03
80	1.95284E-01	9.51793E-01	1.85870E-01	1.36594E-03
85	1.97784E-01	9.52453E-01	1.88380E-01	1.37514E-03
90	1.98014E-01	9.51397E-01	1.88390E-01	1.37517E-03

ψ	p_n	η	ε	$\sigma(\varepsilon)$
$\theta = 10$				
0	1.93613E-01	9.50406E-01	1.84011E-01	1.36693E-03
5	1.93515E-01	9.52670E-01	1.84356E-01	1.36821E-03
10	1.94411E-01	9.50255E-01	1.84740E-01	1.36963E-03
15	1.93928E-01	9.51049E-01	1.84435E-01	1.36850E-03
20	1.93534E-01	9.49730E-01	1.83805E-01	1.36616E-03
25	1.93702E-01	9.50630E-01	1.84139E-01	1.36741E-03
30	1.92589E-01	9.51778E-01	1.83302E-01	1.36429E-03
35	1.92559E-01	9.52186E-01	1.83352E-01	1.36448E-03
40	1.95061E-01	9.52036E-01	1.85705E-01	1.37321E-03
45	1.96696E-01	9.51834E-01	1.87222E-01	1.37880E-03
50	1.97434E-01	9.52815E-01	1.88118E-01	1.38210E-03
55	1.98281E-01	9.51523E-01	1.88669E-01	1.38412E-03
60	2.00783E-01	9.49577E-01	1.90659E-01	1.39140E-03
65	2.00034E-01	9.54118E-01	1.90856E-01	1.39212E-03
70	1.98025E-01	9.50668E-01	1.88256E-01	1.38261E-03
75	1.97385E-01	9.51303E-01	1.87773E-01	1.38083E-03
80	1.96449E-01	9.50272E-01	1.86680E-01	1.37681E-03
85	1.97759E-01	9.52144E-01	1.88295E-01	1.38275E-03
90	1.97090E-01	9.55528E-01	1.88325E-01	1.38286E-03
$\theta = 15$				
0	1.94991E-01	9.53188E-01	1.85863E-01	1.38716E-03
5	1.94924E-01	9.52079E-01	1.85583E-01	1.38611E-03
10	1.96846E-01	9.51861E-01	1.87370E-01	1.39277E-03
15	1.94431E-01	9.52508E-01	1.85197E-01	1.38467E-03
20	1.95590E-01	9.53137E-01	1.86424E-01	1.38924E-03
25	1.93629E-01	9.51913E-01	1.84318E-01	1.38138E-03
30	1.93388E-01	9.53001E-01	1.84299E-01	1.38130E-03
35	1.91543E-01	9.48868E-01	1.81749E-01	1.37171E-03
40	1.96218E-01	9.53725E-01	1.87138E-01	1.39191E-03
45	1.96749E-01	9.52528E-01	1.87409E-01	1.39291E-03
50	1.98469E-01	9.52597E-01	1.89061E-01	1.39904E-03
55	1.97619E-01	9.52100E-01	1.88153E-01	1.39567E-03
60	1.98024E-01	9.50930E-01	1.88307E-01	1.39624E-03
65	1.96518E-01	9.51094E-01	1.86907E-01	1.39104E-03
70	1.95523E-01	9.50845E-01	1.85912E-01	1.38734E-03
75	1.95735E-01	9.49861E-01	1.85921E-01	1.38737E-03
80	1.95957E-01	9.51398E-01	1.86433E-01	1.38928E-03
85	1.96180E-01	9.49924E-01	1.86356E-01	1.38899E-03
90	1.98276E-01	9.53181E-01	1.88993E-01	1.39879E-03

ψ	p_n	η	ε	$\sigma(\varepsilon)$
$\theta = 20$				
0	1.94657E-01	9.51967E-01	1.85307E-01	1.40428E-03
5	1.94009E-01	9.51760E-01	1.84650E-01	1.40178E-03
10	1.95315E-01	9.54489E-01	1.86426E-01	1.40851E-03
15	1.95315E-01	9.51985E-01	1.85937E-01	1.40666E-03
20	1.95973E-01	9.53871E-01	1.86933E-01	1.41043E-03
25	1.94216E-01	9.51806E-01	1.84856E-01	1.40257E-03
30	1.93708E-01	9.50859E-01	1.84189E-01	1.40004E-03
35	1.92205E-01	9.52478E-01	1.83071E-01	1.39578E-03
40	1.96161E-01	9.51999E-01	1.86745E-01	1.40972E-03
45	1.95644E-01	9.53456E-01	1.86538E-01	1.40894E-03
50	1.96151E-01	9.50992E-01	1.86538E-01	1.40894E-03
55	1.96612E-01	9.52348E-01	1.87243E-01	1.41159E-03
60	1.97223E-01	9.55639E-01	1.88474E-01	1.41623E-03
65	1.96330E-01	9.50843E-01	1.86679E-01	1.40947E-03
70	1.96828E-01	9.53452E-01	1.87666E-01	1.41319E-03
75	1.98341E-01	9.50066E-01	1.88437E-01	1.41609E-03
80	1.96001E-01	9.52393E-01	1.86670E-01	1.40943E-03
85	1.98266E-01	9.51086E-01	1.88568E-01	1.41658E-03
90	1.96612E-01	9.49866E-01	1.86755E-01	1.40975E-03
$\theta = 25$				
0	1.95554E-01	9.55276E-01	1.86808E-01	1.43569E-03
5	1.94602E-01	9.52919E-01	1.85440E-01	1.43042E-03
10	1.94557E-01	9.54538E-01	1.85712E-01	1.43147E-03
15	1.94276E-01	9.54096E-01	1.85358E-01	1.43010E-03
20	1.94466E-01	9.53395E-01	1.85403E-01	1.43028E-03
25	1.95472E-01	9.54566E-01	1.86591E-01	1.43485E-03
30	1.93732E-01	9.50648E-01	1.84171E-01	1.42552E-03
35	1.94231E-01	9.52454E-01	1.84996E-01	1.42871E-03
40	1.93116E-01	9.50020E-01	1.83464E-01	1.42278E-03
45	1.94865E-01	9.52003E-01	1.85512E-01	1.43070E-03
50	1.96261E-01	9.53959E-01	1.87225E-01	1.43729E-03
55	1.95046E-01	9.48704E-01	1.85041E-01	1.42888E-03
60	1.95826E-01	9.51774E-01	1.86382E-01	1.43405E-03
65	1.96379E-01	9.53661E-01	1.87279E-01	1.43750E-03
70	1.93497E-01	9.51240E-01	1.84062E-01	1.42510E-03
75	1.97838E-01	9.53179E-01	1.88575E-01	1.44246E-03
80	1.95636E-01	9.50244E-01	1.85902E-01	1.43220E-03
85	1.94738E-01	9.50718E-01	1.85141E-01	1.42927E-03
90	1.97620E-01	9.54554E-01	1.88639E-01	1.44271E-03

ψ	p_n	η	ε	$\sigma(\varepsilon)$
$\theta = 30$				
0	1.94631E-01	9.51765E-01	1.85243E-01	1.46253E-03
5	1.98025E-01	9.49971E-01	1.88118E-01	1.47384E-03
10	1.92491E-01	9.52491E-01	1.83346E-01	1.45503E-03
15	1.92465E-01	9.49877E-01	1.82818E-01	1.45293E-03
20	1.93332E-01	9.51394E-01	1.83935E-01	1.45736E-03
25	1.93080E-01	9.54252E-01	1.84247E-01	1.45860E-03
30	1.93115E-01	9.49010E-01	1.83268E-01	1.45472E-03
35	1.93496E-01	9.52381E-01	1.84282E-01	1.45873E-03
40	1.93531E-01	9.51403E-01	1.84126E-01	1.45812E-03
45	1.95289E-01	9.49265E-01	1.85381E-01	1.46308E-03
50	1.95012E-01	9.51413E-01	1.85537E-01	1.46369E-03
55	1.94968E-01	9.52161E-01	1.85641E-01	1.46410E-03
60	1.96172E-01	9.51308E-01	1.86620E-01	1.46796E-03
65	1.96363E-01	9.51350E-01	1.86810E-01	1.46871E-03
70	1.94795E-01	9.51498E-01	1.85347E-01	1.46294E-03
75	1.96276E-01	9.50845E-01	1.86628E-01	1.46799E-03
80	1.95514E-01	9.53093E-01	1.86343E-01	1.46687E-03
85	1.95479E-01	9.51488E-01	1.85996E-01	1.46550E-03
90	1.94423E-01	9.51492E-01	1.84992E-01	1.46154E-03
$\theta = 35$				
0	1.93377E-01	9.51116E-01	1.83924E-01	1.49843E-03
5	1.92214E-01	9.52610E-01	1.83105E-01	1.49509E-03
10	1.92902E-01	9.51208E-01	1.83490E-01	1.49666E-03
15	1.93172E-01	9.53736E-01	1.84235E-01	1.49970E-03
20	1.93459E-01	9.51902E-01	1.84154E-01	1.49937E-03
25	1.93574E-01	9.51967E-01	1.84276E-01	1.49987E-03
30	1.91247E-01	9.50959E-01	1.81868E-01	1.49003E-03
35	1.91501E-01	9.50893E-01	1.82097E-01	1.49097E-03
40	1.93172E-01	9.52214E-01	1.83941E-01	1.49850E-03
45	1.92083E-01	9.52875E-01	1.83031E-01	1.49479E-03
50	1.92624E-01	9.51730E-01	1.83326E-01	1.49599E-03
55	1.94475E-01	9.51012E-01	1.84948E-01	1.50260E-03
60	1.93459E-01	9.50501E-01	1.83883E-01	1.49827E-03
65	1.94827E-01	9.48873E-01	1.84866E-01	1.50226E-03
70	1.94827E-01	9.52491E-01	1.85571E-01	1.50512E-03
75	1.93402E-01	9.51293E-01	1.83982E-01	1.49867E-03
80	1.93901E-01	9.52476E-01	1.84686E-01	1.50153E-03
85	1.93951E-01	9.49611E-01	1.84178E-01	1.49947E-03
90	1.96801E-01	9.47932E-01	1.86554E-01	1.50911E-03

ψ	p_n	η	ε	$\sigma(\varepsilon)$
$\theta = 40$				
0	1.89941E-01	9.50674E-01	1.80572E-01	1.53532E-03
5	1.90063E-01	9.52726E-01	1.81078E-01	1.53747E-03
10	1.90699E-01	9.50230E-01	1.81208E-01	1.53802E-03
15	1.89351E-01	9.51777E-01	1.80220E-01	1.53382E-03
20	1.91366E-01	9.53283E-01	1.82426E-01	1.54318E-03
25	1.89236E-01	9.49397E-01	1.79660E-01	1.53144E-03
30	1.90109E-01	9.54063E-01	1.81376E-01	1.53873E-03
35	1.88968E-01	9.50584E-01	1.79630E-01	1.53131E-03
40	1.91833E-01	9.50681E-01	1.82372E-01	1.54295E-03
45	1.91994E-01	9.50082E-01	1.82410E-01	1.54311E-03
50	1.91450E-01	9.51063E-01	1.82081E-01	1.54172E-03
55	1.93694E-01	9.52306E-01	1.84456E-01	1.55174E-03
60	1.92913E-01	9.49806E-01	1.83230E-01	1.54658E-03
65	1.92101E-01	9.51552E-01	1.82794E-01	1.54473E-03
70	1.91335E-01	9.52157E-01	1.82181E-01	1.54214E-03
75	1.91856E-01	9.52006E-01	1.82648E-01	1.54412E-03
80	1.91136E-01	9.53107E-01	1.82173E-01	1.54211E-03
85	1.94652E-01	9.49310E-01	1.84785E-01	1.55313E-03
90	1.90783E-01	9.51578E-01	1.81545E-01	1.53945E-03
$\theta = 45$				
0	1.90452E-01	9.50917E-01	1.81104E-01	1.60037E-03
5	1.90049E-01	9.52118E-01	1.80949E-01	1.59969E-03
10	1.88720E-01	9.53540E-01	1.79952E-01	1.59527E-03
15	1.89151E-01	9.50241E-01	1.79739E-01	1.59433E-03
20	1.89809E-01	9.51678E-01	1.80637E-01	1.59831E-03
25	1.89894E-01	9.51963E-01	1.80772E-01	1.59891E-03
30	1.87214E-01	9.50634E-01	1.77972E-01	1.58647E-03
35	1.86542E-01	9.50419E-01	1.77293E-01	1.58345E-03
40	1.87843E-01	9.52455E-01	1.78912E-01	1.59066E-03
45	1.90650E-01	9.53491E-01	1.81783E-01	1.60337E-03
50	1.90806E-01	9.50819E-01	1.81422E-01	1.60178E-03
55	1.89731E-01	9.49276E-01	1.80107E-01	1.59596E-03
60	1.90940E-01	9.50786E-01	1.81543E-01	1.60231E-03
65	1.92036E-01	9.52868E-01	1.82985E-01	1.60866E-03
70	1.88083E-01	9.52670E-01	1.79181E-01	1.59185E-03
75	1.88331E-01	9.48898E-01	1.78707E-01	1.58975E-03
80	1.90438E-01	9.51323E-01	1.81168E-01	1.60066E-03
85	1.90777E-01	9.49706E-01	1.81182E-01	1.60072E-03
90	1.91336E-01	9.52440E-01	1.82236E-01	1.60537E-03

ψ	p_n	η	ε	$\sigma(\varepsilon)$
$\theta = 50$				
0	1.87045E-01	9.47521E-01	1.77229E-01	1.66048E-03
5	1.86081E-01	9.47217E-01	1.76259E-01	1.65593E-03
10	1.87148E-01	9.51055E-01	1.77988E-01	1.66403E-03
15	1.84994E-01	9.51707E-01	1.76060E-01	1.65499E-03
20	1.86968E-01	9.50387E-01	1.77692E-01	1.66265E-03
25	1.86074E-01	9.51326E-01	1.77017E-01	1.65949E-03
30	1.86235E-01	9.53027E-01	1.77487E-01	1.66169E-03
35	1.85412E-01	9.50046E-01	1.76150E-01	1.65542E-03
40	1.87636E-01	9.49573E-01	1.78174E-01	1.66490E-03
45	1.85946E-01	9.51394E-01	1.76908E-01	1.65898E-03
50	1.86788E-01	9.51442E-01	1.77718E-01	1.66277E-03
55	1.87469E-01	9.50829E-01	1.78251E-01	1.66526E-03
60	1.85277E-01	9.48725E-01	1.75777E-01	1.65366E-03
65	1.87193E-01	9.51750E-01	1.78161E-01	1.66484E-03
70	1.86196E-01	9.48667E-01	1.76638E-01	1.65771E-03
75	1.85907E-01	9.52976E-01	1.77165E-01	1.66018E-03
80	1.87932E-01	9.49381E-01	1.78419E-01	1.66604E-03
85	1.88530E-01	9.49812E-01	1.79068E-01	1.66907E-03
90	1.87058E-01	9.47765E-01	1.77287E-01	1.66075E-03
$\theta = 55$				
0	1.81348E-01	9.49142E-01	1.72125E-01	1.73231E-03
5	1.83499E-01	9.51455E-01	1.74591E-01	1.74468E-03
10	1.82730E-01	9.52318E-01	1.74017E-01	1.74181E-03
15	1.81428E-01	9.50807E-01	1.72503E-01	1.73421E-03
20	1.83413E-01	9.49366E-01	1.74126E-01	1.74235E-03
25	1.81376E-01	9.49117E-01	1.72147E-01	1.73243E-03
30	1.81818E-01	9.51259E-01	1.72956E-01	1.73649E-03
35	1.82501E-01	9.51535E-01	1.73656E-01	1.74000E-03
40	1.83596E-01	9.49547E-01	1.74333E-01	1.74339E-03
45	1.81990E-01	9.50014E-01	1.72893E-01	1.73617E-03
50	1.82713E-01	9.51558E-01	1.73862E-01	1.74103E-03
55	1.83447E-01	9.51632E-01	1.74574E-01	1.74459E-03
60	1.83923E-01	9.48701E-01	1.74488E-01	1.74416E-03
65	1.81262E-01	9.53167E-01	1.72773E-01	1.73557E-03
70	1.84634E-01	9.50329E-01	1.75463E-01	1.74903E-03
75	1.82690E-01	9.49483E-01	1.73461E-01	1.73902E-03
80	1.84720E-01	9.51191E-01	1.75704E-01	1.75023E-03
85	1.84973E-01	9.49549E-01	1.75641E-01	1.74991E-03
90	1.82994E-01	9.49507E-01	1.73754E-01	1.74049E-03

ψ	p_n	η	ε	$\sigma(\varepsilon)$
$\theta = 60$				
0	1.78220E-01	9.50875E-01	1.69465E-01	1.84101E-03
5	1.78095E-01	9.50111E-01	1.69210E-01	1.83962E-03
10	1.77790E-01	9.52022E-01	1.69260E-01	1.83989E-03
15	1.78190E-01	9.51737E-01	1.69590E-01	1.84168E-03
20	1.77900E-01	9.49213E-01	1.68865E-01	1.83774E-03
25	1.79350E-01	9.49679E-01	1.70325E-01	1.84567E-03
30	1.78750E-01	9.50517E-01	1.69905E-01	1.84339E-03
35	1.78065E-01	9.50131E-01	1.69185E-01	1.83948E-03
40	1.77370E-01	9.49315E-01	1.68380E-01	1.83510E-03
45	1.77955E-01	9.51645E-01	1.69350E-01	1.84038E-03
50	1.79615E-01	9.49949E-01	1.70625E-01	1.84730E-03
55	1.78995E-01	9.47680E-01	1.69630E-01	1.84190E-03
60	1.79455E-01	9.48678E-01	1.70245E-01	1.84524E-03
65	1.80020E-01	9.48978E-01	1.70835E-01	1.84843E-03
70	1.78105E-01	9.51742E-01	1.69510E-01	1.84125E-03
75	1.78620E-01	9.48830E-01	1.69480E-01	1.84109E-03
80	1.78425E-01	9.48830E-01	1.69295E-01	1.84008E-03
85	1.78435E-01	9.50514E-01	1.69605E-01	1.84177E-03
90	1.78795E-01	9.51061E-01	1.70045E-01	1.84415E-03
$\theta = 65$				
0	1.71427E-01	9.48643E-01	1.62623E-01	1.96163E-03
5	1.72648E-01	9.51410E-01	1.64259E-01	1.97147E-03
10	1.72179E-01	9.50023E-01	1.63574E-01	1.96736E-03
15	1.70539E-01	9.50909E-01	1.62167E-01	1.95888E-03
20	1.72365E-01	9.49856E-01	1.63722E-01	1.96825E-03
25	1.72061E-01	9.47164E-01	1.62970E-01	1.96372E-03
30	1.70873E-01	9.47838E-01	1.61960E-01	1.95763E-03
35	1.71000E-01	9.49386E-01	1.62345E-01	1.95995E-03
40	1.72306E-01	9.50304E-01	1.63743E-01	1.96837E-03
45	1.71456E-01	9.51002E-01	1.63055E-01	1.96423E-03
50	1.71731E-01	9.50929E-01	1.63304E-01	1.96573E-03
55	1.72826E-01	9.49892E-01	1.64166E-01	1.97091E-03
60	1.71190E-01	9.48946E-01	1.62450E-01	1.96059E-03
65	1.72314E-01	9.49528E-01	1.63617E-01	1.96761E-03
70	1.72204E-01	9.51163E-01	1.63794E-01	1.96868E-03
75	1.71224E-01	9.48979E-01	1.62488E-01	1.96082E-03
80	1.72356E-01	9.48804E-01	1.63532E-01	1.96710E-03
85	1.71862E-01	9.50373E-01	1.63333E-01	1.96591E-03
90	1.72276E-01	9.49540E-01	1.63583E-01	1.96741E-03

ψ	p_n	η	ε	$\sigma(\varepsilon)$
$\theta = 70$				
0	1.61269E-01	9.49209E-01	1.53078E-01	2.11559E-03
5	1.62583E-01	9.48162E-01	1.54155E-01	2.12302E-03
10	1.61947E-01	9.47915E-01	1.53512E-01	2.11858E-03
15	1.61567E-01	9.48981E-01	1.53324E-01	2.11729E-03
20	1.62193E-01	9.47513E-01	1.53680E-01	2.11974E-03
25	1.63133E-01	9.49121E-01	1.54833E-01	2.12767E-03
30	1.63588E-01	9.50119E-01	1.55428E-01	2.13176E-03
35	1.63041E-01	9.45922E-01	1.54224E-01	2.12349E-03
40	1.63048E-01	9.49843E-01	1.54870E-01	2.12793E-03
45	1.62620E-01	9.48770E-01	1.54289E-01	2.12394E-03
50	1.62713E-01	9.48498E-01	1.54333E-01	2.12424E-03
55	1.62333E-01	9.48464E-01	1.53967E-01	2.12172E-03
60	1.61721E-01	9.49308E-01	1.53523E-01	2.11866E-03
65	1.62340E-01	9.49205E-01	1.54094E-01	2.12259E-03
70	1.62730E-01	9.47139E-01	1.54128E-01	2.12283E-03
75	1.62778E-01	9.47745E-01	1.54272E-01	2.12382E-03
80	1.62921E-01	9.48988E-01	1.54610E-01	2.12615E-03
85	1.62531E-01	9.50256E-01	1.54446E-01	2.12502E-03
90	1.63472E-01	9.48511E-01	1.55055E-01	2.12920E-03
$\theta = 75$				
0	1.46429E-01	9.46766E-01	1.38634E-01	2.31439E-03
5	1.48567E-01	9.47774E-01	1.40808E-01	2.33247E-03
10	1.49064E-01	9.47217E-01	1.41196E-01	2.33568E-03
15	1.47951E-01	9.46597E-01	1.40050E-01	2.32618E-03
20	1.48402E-01	9.45075E-01	1.40251E-01	2.32785E-03
25	1.49018E-01	9.46154E-01	1.40994E-01	2.33401E-03
30	1.48500E-01	9.47785E-01	1.40746E-01	2.33195E-03
35	1.48733E-01	9.45116E-01	1.40570E-01	2.33049E-03
40	1.48606E-01	9.46483E-01	1.40653E-01	2.33118E-03
45	1.48904E-01	9.45992E-01	1.40862E-01	2.33292E-03
50	1.48386E-01	9.45898E-01	1.40358E-01	2.32873E-03
55	1.48860E-01	9.45922E-01	1.40810E-01	2.33249E-03
60	1.48076E-01	9.47230E-01	1.40262E-01	2.32794E-03
65	1.48645E-01	9.45118E-01	1.40487E-01	2.32981E-03
70	1.48407E-01	9.45986E-01	1.40391E-01	2.32901E-03
75	1.48782E-01	9.48300E-01	1.41090E-01	2.33480E-03
80	1.49235E-01	9.46983E-01	1.41323E-01	2.33673E-03
85	1.48497E-01	9.45743E-01	1.40440E-01	2.32942E-03
90	1.47995E-01	9.47079E-01	1.40163E-01	2.32712E-03

ψ	p_n	η	ε	$\sigma(\varepsilon)$
$\theta = 80$				
0	1.23349E-01	9.41815E-01	1.16172E-01	2.58652E-03
5	1.24912E-01	9.41711E-01	1.17631E-01	2.60271E-03
10	1.25424E-01	9.41048E-01	1.18030E-01	2.60712E-03
15	1.25096E-01	9.43603E-01	1.18041E-01	2.60724E-03
20	1.25145E-01	9.42035E-01	1.17891E-01	2.60559E-03
25	1.24922E-01	9.43653E-01	1.17883E-01	2.60549E-03
30	1.25412E-01	9.42398E-01	1.18188E-01	2.60887E-03
35	1.24540E-01	9.44283E-01	1.17601E-01	2.60238E-03
40	1.24789E-01	9.42679E-01	1.17636E-01	2.60277E-03
45	1.24606E-01	9.43020E-01	1.17506E-01	2.60133E-03
50	1.25086E-01	9.42815E-01	1.17933E-01	2.60605E-03
55	1.25350E-01	9.42090E-01	1.18091E-01	2.60780E-03
60	1.25530E-01	9.45184E-01	1.18649E-01	2.61394E-03
65	1.24867E-01	9.42026E-01	1.17628E-01	2.60267E-03
70	1.25001E-01	9.43456E-01	1.17933E-01	2.60605E-03
75	1.25089E-01	9.43488E-01	1.18020E-01	2.60701E-03
80	1.24671E-01	9.42601E-01	1.17515E-01	2.60142E-03
85	1.25075E-01	9.44673E-01	1.18155E-01	2.60851E-03
90	1.24811E-01	9.42818E-01	1.17674E-01	2.60319E-03
$\theta = 85$				
0	7.93570E-02	9.29326E-01	7.37485E-02	2.90890E-03
5	8.02094E-02	9.32696E-01	7.48110E-02	2.92978E-03
10	8.02103E-02	9.31599E-01	7.47238E-02	2.92807E-03
15	8.02931E-02	9.31192E-01	7.47683E-02	2.92894E-03
20	8.02660E-02	9.31495E-01	7.47674E-02	2.92892E-03
25	8.03471E-02	9.32692E-01	7.49391E-02	2.93229E-03
30	8.04046E-02	9.31179E-01	7.48711E-02	2.93096E-03
35	8.01161E-02	9.31649E-01	7.46401E-02	2.92643E-03
40	8.03340E-02	9.32985E-01	7.49504E-02	2.93251E-03
45	8.02913E-02	9.31929E-01	7.48258E-02	2.93007E-03
50	8.02556E-02	9.32300E-01	7.48223E-02	2.93000E-03
55	8.01981E-02	9.32980E-01	7.48232E-02	2.93002E-03
60	8.02146E-02	9.33330E-01	7.48667E-02	2.93087E-03
65	8.02573E-02	9.32682E-01	7.48545E-02	2.93063E-03
70	8.01763E-02	9.31482E-01	7.46828E-02	2.92727E-03
75	8.01989E-02	9.31938E-01	7.47404E-02	2.92840E-03
80	8.01275E-02	9.33747E-01	7.48188E-02	2.92993E-03
85	8.03375E-02	9.32359E-01	7.49034E-02	2.93159E-03
90	8.03898E-02	9.31850E-01	7.49112E-02	2.93174E-03

Table B.14. ${}^6\text{LiF}$ sinusoid detector with 100 μm deep perforations, 20 μm wave separation, 20 μm wave period, 20 μm wave amplitude, and no cap

ψ	p_n	η	ε	$\sigma(\varepsilon)$
$\theta = 0$				
0	1.99886E-01	9.26728E-01	1.85240E-01	4.30395E-04
5	1.99986E-01	9.28855E-01	1.85758E-01	4.30997E-04
10	2.00325E-01	9.28526E-01	1.86007E-01	4.31285E-04
15	1.99507E-01	9.29311E-01	1.85404E-01	4.30586E-04
20	1.99865E-01	9.28081E-01	1.85491E-01	4.30687E-04
25	2.00330E-01	9.27939E-01	1.85894E-01	4.31154E-04
30	1.99995E-01	9.28293E-01	1.85654E-01	4.30876E-04
35	2.00032E-01	9.28092E-01	1.85648E-01	4.30869E-04
40	2.00256E-01	9.27478E-01	1.85733E-01	4.30968E-04
45	1.99980E-01	9.29238E-01	1.85829E-01	4.31079E-04
50	1.99751E-01	9.28606E-01	1.85490E-01	4.30686E-04
55	1.99473E-01	9.28532E-01	1.85217E-01	4.30368E-04
60	1.99736E-01	9.29297E-01	1.85614E-01	4.30829E-04
65	1.99759E-01	9.29205E-01	1.85617E-01	4.30833E-04
70	1.99660E-01	9.28854E-01	1.85455E-01	4.30645E-04
75	1.99309E-01	9.28824E-01	1.85123E-01	4.30259E-04
80	1.98784E-01	9.27952E-01	1.84462E-01	4.29490E-04
85	2.00391E-01	9.29144E-01	1.86192E-01	4.31500E-04
90	2.00082E-01	9.28409E-01	1.85758E-01	4.30997E-04
$\theta = 5$				
0	2.20679E-01	9.31797E-01	2.05628E-01	4.54327E-04
5	2.20908E-01	9.31370E-01	2.05747E-01	4.54459E-04
10	2.20550E-01	9.30959E-01	2.05323E-01	4.53990E-04
15	2.20279E-01	9.31628E-01	2.05218E-01	4.53874E-04
20	2.20357E-01	9.31525E-01	2.05268E-01	4.53930E-04
25	2.19875E-01	9.31884E-01	2.04898E-01	4.53521E-04
30	2.19108E-01	9.30728E-01	2.03930E-01	4.52448E-04
35	2.18603E-01	9.30879E-01	2.03493E-01	4.51962E-04
40	2.18773E-01	9.31052E-01	2.03689E-01	4.52180E-04
45	2.17954E-01	9.31756E-01	2.03080E-01	4.51504E-04
50	2.16245E-01	9.31212E-01	2.01370E-01	4.49599E-04
55	2.14981E-01	9.31766E-01	2.00312E-01	4.48416E-04
60	2.13673E-01	9.31124E-01	1.98956E-01	4.46896E-04
65	2.12707E-01	9.30853E-01	1.97999E-01	4.45819E-04
70	2.10312E-01	9.30427E-01	1.95680E-01	4.43201E-04
75	2.08336E-01	9.31097E-01	1.93981E-01	4.41273E-04
80	2.07145E-01	9.29909E-01	1.92626E-01	4.39729E-04
85	2.07005E-01	9.31103E-01	1.92743E-01	4.39862E-04
90	2.06901E-01	9.30662E-01	1.92555E-01	4.39649E-04

ψ	p_n	η	ε	$\sigma(\varepsilon)$
$\theta = 10$				
0	2.22813E-01	9.32154E-01	2.07696E-01	4.59239E-04
5	2.22777E-01	9.31627E-01	2.07545E-01	4.59072E-04
10	2.22319E-01	9.30721E-01	2.06917E-01	4.58376E-04
15	2.22523E-01	9.30488E-01	2.07055E-01	4.58529E-04
20	2.21843E-01	9.31578E-01	2.06664E-01	4.58096E-04
25	2.22186E-01	9.31233E-01	2.06907E-01	4.58366E-04
30	2.21728E-01	9.30812E-01	2.06387E-01	4.57789E-04
35	2.22034E-01	9.31538E-01	2.06833E-01	4.58284E-04
40	2.21701E-01	9.31128E-01	2.06432E-01	4.57839E-04
45	2.21489E-01	9.31739E-01	2.06370E-01	4.57771E-04
50	2.20974E-01	9.31051E-01	2.05738E-01	4.57069E-04
55	2.19689E-01	9.31125E-01	2.04558E-01	4.55757E-04
60	2.19546E-01	9.31782E-01	2.04569E-01	4.55769E-04
65	2.18153E-01	9.30480E-01	2.02987E-01	4.54002E-04
70	2.15245E-01	9.31427E-01	2.00485E-01	4.51196E-04
75	2.14379E-01	9.31397E-01	1.99672E-01	4.50280E-04
80	2.11805E-01	9.30686E-01	1.97124E-01	4.47398E-04
85	2.14236E-01	9.32565E-01	1.99789E-01	4.50412E-04
90	2.14480E-01	9.30753E-01	1.99628E-01	4.50231E-04
$\theta = 15$				
0	2.22407E-01	9.30753E-01	2.07006E-01	4.62934E-04
5	2.21325E-01	9.31354E-01	2.06132E-01	4.61957E-04
10	2.21932E-01	9.30979E-01	2.06614E-01	4.62496E-04
15	2.22260E-01	9.31036E-01	2.06932E-01	4.62852E-04
20	2.22277E-01	9.31041E-01	2.06949E-01	4.62870E-04
25	2.22034E-01	9.31673E-01	2.06863E-01	4.62774E-04
30	2.22076E-01	9.31042E-01	2.06762E-01	4.62662E-04
35	2.21575E-01	9.31337E-01	2.06361E-01	4.62213E-04
40	2.22095E-01	9.30516E-01	2.06663E-01	4.62551E-04
45	2.22189E-01	9.31032E-01	2.06865E-01	4.62776E-04
50	2.21689E-01	9.30069E-01	2.06186E-01	4.62016E-04
55	2.21315E-01	9.31600E-01	2.06177E-01	4.62006E-04
60	2.20904E-01	9.31577E-01	2.05789E-01	4.61571E-04
65	2.19238E-01	9.31367E-01	2.04191E-01	4.59776E-04
70	2.17669E-01	9.30845E-01	2.02616E-01	4.58000E-04
75	2.14862E-01	9.31854E-01	2.00220E-01	4.55283E-04
80	2.14727E-01	9.31127E-01	1.99938E-01	4.54963E-04
85	2.18198E-01	9.31787E-01	2.03314E-01	4.58788E-04
90	2.20025E-01	9.32612E-01	2.05198E-01	4.60909E-04

ψ	p_n	η	ε	$\sigma(\varepsilon)$
$\theta = 20$				
0	2.21030E-01	9.31141E-01	2.05810E-01	4.67994E-04
5	2.21558E-01	9.30903E-01	2.06249E-01	4.68493E-04
10	2.20566E-01	9.31386E-01	2.05432E-01	4.67564E-04
15	2.21894E-01	9.31048E-01	2.06594E-01	4.68885E-04
20	2.21875E-01	9.31741E-01	2.06730E-01	4.69039E-04
25	2.21660E-01	9.31851E-01	2.06554E-01	4.68839E-04
30	2.21417E-01	9.31238E-01	2.06192E-01	4.68428E-04
35	2.22111E-01	9.31525E-01	2.06902E-01	4.69234E-04
40	2.21962E-01	9.31664E-01	2.06794E-01	4.69112E-04
45	2.22734E-01	9.31389E-01	2.07452E-01	4.69857E-04
50	2.22972E-01	9.30857E-01	2.07555E-01	4.69973E-04
55	2.21150E-01	9.30794E-01	2.05845E-01	4.68034E-04
60	2.21546E-01	9.31698E-01	2.06414E-01	4.68680E-04
65	2.20835E-01	9.31216E-01	2.05645E-01	4.67807E-04
70	2.18455E-01	9.31418E-01	2.03473E-01	4.65329E-04
75	2.15873E-01	9.31057E-01	2.00990E-01	4.62481E-04
80	2.15267E-01	9.31165E-01	2.00449E-01	4.61858E-04
85	2.19643E-01	9.31607E-01	2.04621E-01	4.66640E-04
90	2.23641E-01	9.30697E-01	2.08142E-01	4.70638E-04
$\theta = 25$				
0	2.19965E-01	9.30648E-01	2.04710E-01	4.75261E-04
5	2.20327E-01	9.30435E-01	2.05000E-01	4.75596E-04
10	2.20303E-01	9.30981E-01	2.05098E-01	4.75711E-04
15	2.20747E-01	9.30790E-01	2.05469E-01	4.76141E-04
20	2.20707E-01	9.31013E-01	2.05481E-01	4.76154E-04
25	2.20834E-01	9.31655E-01	2.05741E-01	4.76456E-04
30	2.21471E-01	9.31454E-01	2.06290E-01	4.77091E-04
35	2.21702E-01	9.31435E-01	2.06501E-01	4.77335E-04
40	2.21779E-01	9.31337E-01	2.06551E-01	4.77393E-04
45	2.22196E-01	9.31974E-01	2.07081E-01	4.78005E-04
50	2.21376E-01	9.31524E-01	2.06217E-01	4.77006E-04
55	2.21266E-01	9.31666E-01	2.06146E-01	4.76925E-04
60	2.20389E-01	9.30999E-01	2.05182E-01	4.75808E-04
65	2.20400E-01	9.30998E-01	2.05192E-01	4.75819E-04
70	2.18663E-01	9.32353E-01	2.03871E-01	4.74286E-04
75	2.15774E-01	9.30770E-01	2.00836E-01	4.70742E-04
80	2.15645E-01	9.31169E-01	2.00802E-01	4.70703E-04
85	2.20478E-01	9.30955E-01	2.05255E-01	4.75893E-04
90	2.22154E-01	9.30773E-01	2.06775E-01	4.77652E-04

ψ	p_n	η	ε	$\sigma(\varepsilon)$
$\theta = 30$				
0	2.19179E-01	9.31143E-01	2.04087E-01	4.85447E-04
5	2.18803E-01	9.30947E-01	2.03694E-01	4.84980E-04
10	2.18328E-01	9.30600E-01	2.03176E-01	4.84362E-04
15	2.19832E-01	9.31197E-01	2.04707E-01	4.86184E-04
20	2.20329E-01	9.30890E-01	2.05102E-01	4.86653E-04
25	2.20103E-01	9.30682E-01	2.04846E-01	4.86350E-04
30	2.21366E-01	9.31110E-01	2.06116E-01	4.87854E-04
35	2.20163E-01	9.31137E-01	2.05002E-01	4.86535E-04
40	2.20629E-01	9.31677E-01	2.05555E-01	4.87190E-04
45	2.20564E-01	9.31643E-01	2.05487E-01	4.87110E-04
50	2.20627E-01	9.31278E-01	2.05465E-01	4.87083E-04
55	2.19706E-01	9.31813E-01	2.04725E-01	4.86206E-04
60	2.19389E-01	9.31346E-01	2.04327E-01	4.85732E-04
65	2.18640E-01	9.30328E-01	2.03407E-01	4.84638E-04
70	2.17692E-01	9.31403E-01	2.02759E-01	4.83866E-04
75	2.15574E-01	9.29890E-01	2.00460E-01	4.81114E-04
80	2.14133E-01	9.30417E-01	1.99233E-01	4.79640E-04
85	2.20035E-01	9.31911E-01	2.05053E-01	4.86595E-04
90	2.19757E-01	9.30892E-01	2.04570E-01	4.86022E-04
$\theta = 35$				
0	2.16825E-01	9.30543E-01	2.01765E-01	4.96295E-04
5	2.16610E-01	9.30520E-01	2.01560E-01	4.96043E-04
10	2.16823E-01	9.30801E-01	2.01819E-01	4.96362E-04
15	2.18217E-01	9.30166E-01	2.02978E-01	4.97785E-04
20	2.18107E-01	9.31048E-01	2.03068E-01	4.97896E-04
25	2.18959E-01	9.31010E-01	2.03853E-01	4.98858E-04
30	2.19004E-01	9.30344E-01	2.03749E-01	4.98729E-04
35	2.18785E-01	9.31389E-01	2.03774E-01	4.98760E-04
40	2.18469E-01	9.31473E-01	2.03498E-01	4.98423E-04
45	2.18587E-01	9.31574E-01	2.03630E-01	4.98584E-04
50	2.19149E-01	9.30782E-01	2.03980E-01	4.99012E-04
55	2.17740E-01	9.31019E-01	2.02720E-01	4.97469E-04
60	2.17690E-01	9.30484E-01	2.02557E-01	4.97269E-04
65	2.16981E-01	9.31123E-01	2.02036E-01	4.96629E-04
70	2.17146E-01	9.31134E-01	2.02192E-01	4.96821E-04
75	2.13153E-01	9.30402E-01	1.98318E-01	4.92038E-04
80	2.13832E-01	9.30067E-01	1.98878E-01	4.92732E-04
85	2.18550E-01	9.31471E-01	2.03573E-01	4.98515E-04
90	2.18189E-01	9.31514E-01	2.03246E-01	4.98114E-04

ψ	p_n	η	ε	$\sigma(\varepsilon)$
$\theta = 40$				
0	2.14273E-01	9.30621E-01	1.99407E-01	5.10204E-04
5	2.14829E-01	9.30098E-01	1.99812E-01	5.10721E-04
10	2.15254E-01	9.31100E-01	2.00423E-01	5.11501E-04
15	2.16118E-01	9.31639E-01	2.01344E-01	5.12675E-04
20	2.16302E-01	9.31207E-01	2.01422E-01	5.12775E-04
25	2.16451E-01	9.30502E-01	2.01408E-01	5.12756E-04
30	2.16444E-01	9.30384E-01	2.01376E-01	5.12716E-04
35	2.17282E-01	9.30537E-01	2.02189E-01	5.13750E-04
40	2.16562E-01	9.29092E-01	2.01206E-01	5.12500E-04
45	2.16336E-01	9.31246E-01	2.01462E-01	5.12826E-04
50	2.16672E-01	9.31422E-01	2.01813E-01	5.13272E-04
55	2.16585E-01	9.31006E-01	2.01642E-01	5.13055E-04
60	2.15124E-01	9.30645E-01	2.00204E-01	5.11222E-04
65	2.14469E-01	9.30615E-01	1.99588E-01	5.10435E-04
70	2.15738E-01	9.31222E-01	2.00900E-01	5.12109E-04
75	2.11585E-01	9.30609E-01	1.96903E-01	5.06990E-04
80	2.12413E-01	9.30447E-01	1.97639E-01	5.07937E-04
85	2.16123E-01	9.32205E-01	2.01471E-01	5.12837E-04
90	2.16670E-01	9.30687E-01	2.01652E-01	5.13067E-04
$\theta = 45$				
0	2.11494E-01	9.29483E-01	1.96580E-01	5.27263E-04
5	2.11718E-01	9.29949E-01	1.96887E-01	5.27674E-04
10	2.12372E-01	9.30528E-01	1.97618E-01	5.28653E-04
15	2.13368E-01	9.31246E-01	1.98698E-01	5.30095E-04
20	2.13741E-01	9.29939E-01	1.98766E-01	5.30187E-04
25	2.13758E-01	9.30342E-01	1.98868E-01	5.30323E-04
30	2.14787E-01	9.30005E-01	1.99753E-01	5.31501E-04
35	2.13069E-01	9.30849E-01	1.98335E-01	5.29611E-04
40	2.14135E-01	9.29829E-01	1.99109E-01	5.30644E-04
45	2.13967E-01	9.30985E-01	1.99200E-01	5.30765E-04
50	2.14523E-01	9.30814E-01	1.99681E-01	5.31406E-04
55	2.14212E-01	9.30293E-01	1.99280E-01	5.30871E-04
60	2.11843E-01	9.30415E-01	1.97102E-01	5.27963E-04
65	2.12129E-01	9.31165E-01	1.97527E-01	5.28532E-04
70	2.12846E-01	9.31068E-01	1.98174E-01	5.29396E-04
75	2.07656E-01	9.30159E-01	1.93153E-01	5.22647E-04
80	2.10299E-01	9.30703E-01	1.95726E-01	5.26116E-04
85	2.13232E-01	9.30517E-01	1.98416E-01	5.29720E-04
90	2.13413E-01	9.29812E-01	1.98434E-01	5.29743E-04

ψ	p_n	η	ε	$\sigma(\varepsilon)$
$\theta = 50$				
0	2.08106E-01	9.28733E-01	1.93275E-01	5.48346E-04
5	2.08371E-01	9.30393E-01	1.93867E-01	5.49184E-04
10	2.09232E-01	9.30259E-01	1.94640E-01	5.50278E-04
15	2.10500E-01	9.30105E-01	1.95787E-01	5.51897E-04
20	2.10289E-01	9.30553E-01	1.95685E-01	5.51754E-04
25	2.09870E-01	9.30514E-01	1.95287E-01	5.51192E-04
30	2.10625E-01	9.30075E-01	1.95897E-01	5.52052E-04
35	2.09882E-01	9.29913E-01	1.95172E-01	5.51030E-04
40	2.10041E-01	9.29714E-01	1.95278E-01	5.51180E-04
45	2.10507E-01	9.30264E-01	1.95827E-01	5.51954E-04
50	2.10157E-01	9.29819E-01	1.95408E-01	5.51363E-04
55	2.10084E-01	9.29642E-01	1.95303E-01	5.51214E-04
60	2.09571E-01	9.29547E-01	1.94806E-01	5.50513E-04
65	2.08247E-01	9.29982E-01	1.93666E-01	5.48900E-04
70	2.09852E-01	9.29750E-01	1.95110E-01	5.50943E-04
75	2.04423E-01	9.29147E-01	1.89939E-01	5.43592E-04
80	2.07680E-01	9.29531E-01	1.93045E-01	5.48018E-04
85	2.10485E-01	9.29967E-01	1.95744E-01	5.51837E-04
90	2.10859E-01	9.29351E-01	1.95962E-01	5.52143E-04
$\theta = 55$				
0	2.02437E-01	9.28328E-01	1.87928E-01	5.72400E-04
5	2.03632E-01	9.29255E-01	1.89226E-01	5.74374E-04
10	2.05853E-01	9.28672E-01	1.91170E-01	5.77316E-04
15	2.05971E-01	9.29000E-01	1.91347E-01	5.77584E-04
20	2.05487E-01	9.30005E-01	1.91104E-01	5.77217E-04
25	2.05538E-01	9.30149E-01	1.91181E-01	5.77334E-04
30	2.05519E-01	9.29491E-01	1.91028E-01	5.77103E-04
35	2.05620E-01	9.29875E-01	1.91201E-01	5.77363E-04
40	2.05464E-01	9.28810E-01	1.90837E-01	5.76815E-04
45	2.05963E-01	9.29652E-01	1.91474E-01	5.77775E-04
50	2.05582E-01	9.29473E-01	1.91083E-01	5.77185E-04
55	2.05717E-01	9.29277E-01	1.91168E-01	5.77314E-04
60	2.04880E-01	9.29017E-01	1.90337E-01	5.76057E-04
65	2.03742E-01	9.30284E-01	1.89538E-01	5.74848E-04
70	2.05106E-01	9.30080E-01	1.90765E-01	5.76704E-04
75	1.99876E-01	9.28155E-01	1.85516E-01	5.68716E-04
80	2.02181E-01	9.29064E-01	1.87839E-01	5.72265E-04
85	2.05134E-01	9.29817E-01	1.90737E-01	5.76662E-04
90	2.05881E-01	9.30081E-01	1.91486E-01	5.77793E-04

ψ	p_n	η	ε	$\sigma(\varepsilon)$
$\theta = 60$				
0	1.96598E-01	9.27858E-01	1.82415E-01	6.04012E-04
5	1.97866E-01	9.28411E-01	1.83701E-01	6.06137E-04
10	1.99166E-01	9.28175E-01	1.84861E-01	6.08049E-04
15	2.00202E-01	9.28592E-01	1.85906E-01	6.09764E-04
20	1.99494E-01	9.27998E-01	1.85130E-01	6.08490E-04
25	1.99442E-01	9.28631E-01	1.85208E-01	6.08618E-04
30	1.99644E-01	9.29369E-01	1.85543E-01	6.09169E-04
35	1.99170E-01	9.28323E-01	1.84894E-01	6.08102E-04
40	1.99235E-01	9.28863E-01	1.85062E-01	6.08378E-04
45	1.99819E-01	9.29031E-01	1.85638E-01	6.09324E-04
50	1.99279E-01	9.28522E-01	1.85035E-01	6.08335E-04
55	1.99593E-01	9.28259E-01	1.85274E-01	6.08727E-04
60	1.98966E-01	9.28561E-01	1.84752E-01	6.07869E-04
65	1.96805E-01	9.28483E-01	1.82730E-01	6.04533E-04
70	1.99633E-01	9.28925E-01	1.85444E-01	6.09007E-04
75	1.94171E-01	9.28414E-01	1.80271E-01	6.00451E-04
80	1.96188E-01	9.28247E-01	1.82111E-01	6.03508E-04
85	1.99251E-01	9.28562E-01	1.85017E-01	6.08305E-04
90	1.99215E-01	9.28183E-01	1.84908E-01	6.08126E-04
$\theta = 65$				
0	1.87955E-01	9.26360E-01	1.74114E-01	6.41864E-04
5	1.89769E-01	9.27586E-01	1.76027E-01	6.45380E-04
10	1.91662E-01	9.27586E-01	1.77783E-01	6.48591E-04
15	1.91647E-01	9.27194E-01	1.77694E-01	6.48429E-04
20	1.91315E-01	9.27251E-01	1.77397E-01	6.47887E-04
25	1.91287E-01	9.27277E-01	1.77376E-01	6.47848E-04
30	1.91294E-01	9.27750E-01	1.77473E-01	6.48025E-04
35	1.91435E-01	9.27636E-01	1.77582E-01	6.48225E-04
40	1.91183E-01	9.27546E-01	1.77331E-01	6.47765E-04
45	1.91463E-01	9.26811E-01	1.77450E-01	6.47984E-04
50	1.90960E-01	9.28074E-01	1.77225E-01	6.47572E-04
55	1.91702E-01	9.27726E-01	1.77847E-01	6.48708E-04
60	1.91219E-01	9.27978E-01	1.77447E-01	6.47978E-04
65	1.89574E-01	9.27838E-01	1.75894E-01	6.45136E-04
70	1.91473E-01	9.27133E-01	1.77521E-01	6.48113E-04
75	1.86397E-01	9.27086E-01	1.72806E-01	6.39449E-04
80	1.87943E-01	9.27813E-01	1.74376E-01	6.42346E-04
85	1.90928E-01	9.28355E-01	1.77249E-01	6.47616E-04
90	1.91310E-01	9.28091E-01	1.77553E-01	6.48171E-04

ψ	p_n	η	ε	$\sigma(\varepsilon)$
$\theta = 70$				
0	1.76220E-01	9.24878E-01	1.62982E-01	6.90310E-04
5	1.78910E-01	9.26041E-01	1.65678E-01	6.95996E-04
10	1.79468E-01	9.25680E-01	1.66130E-01	6.96945E-04
15	1.79419E-01	9.25894E-01	1.66123E-01	6.96929E-04
20	1.79515E-01	9.25945E-01	1.66221E-01	6.97135E-04
25	1.79707E-01	9.26046E-01	1.66417E-01	6.97546E-04
30	1.79620E-01	9.25593E-01	1.66255E-01	6.97207E-04
35	1.79818E-01	9.25869E-01	1.66488E-01	6.97694E-04
40	1.79734E-01	9.25918E-01	1.66419E-01	6.97551E-04
45	1.79730E-01	9.26000E-01	1.66430E-01	6.97574E-04
50	1.79486E-01	9.25459E-01	1.66107E-01	6.96895E-04
55	1.79804E-01	9.25519E-01	1.66412E-01	6.97536E-04
60	1.79896E-01	9.25613E-01	1.66514E-01	6.97750E-04
65	1.78090E-01	9.26211E-01	1.64949E-01	6.94463E-04
70	1.79636E-01	9.25867E-01	1.66319E-01	6.97341E-04
75	1.75781E-01	9.26090E-01	1.62789E-01	6.89901E-04
80	1.77158E-01	9.25592E-01	1.63976E-01	6.92411E-04
85	1.79785E-01	9.26001E-01	1.66481E-01	6.97680E-04
90	1.79218E-01	9.25487E-01	1.65864E-01	6.96386E-04
$\theta = 75$				
0	1.58435E-01	9.21615E-01	1.46016E-01	7.51107E-04
5	1.61906E-01	9.23542E-01	1.49527E-01	7.60085E-04
10	1.61988E-01	9.22840E-01	1.49489E-01	7.59987E-04
15	1.62247E-01	9.22544E-01	1.49680E-01	7.60474E-04
20	1.62067E-01	9.22680E-01	1.49536E-01	7.60106E-04
25	1.62342E-01	9.22830E-01	1.49814E-01	7.60814E-04
30	1.62208E-01	9.22550E-01	1.49645E-01	7.60385E-04
35	1.62056E-01	9.23230E-01	1.49615E-01	7.60308E-04
40	1.62028E-01	9.23310E-01	1.49602E-01	7.60274E-04
45	1.62137E-01	9.23546E-01	1.49741E-01	7.60627E-04
50	1.61927E-01	9.22866E-01	1.49437E-01	7.59855E-04
55	1.61980E-01	9.22855E-01	1.49484E-01	7.59975E-04
60	1.62043E-01	9.23267E-01	1.49609E-01	7.60293E-04
65	1.61403E-01	9.23570E-01	1.49067E-01	7.58914E-04
70	1.62138E-01	9.22899E-01	1.49637E-01	7.60364E-04
75	1.60565E-01	9.23016E-01	1.48204E-01	7.56714E-04
80	1.60394E-01	9.23295E-01	1.48091E-01	7.56426E-04
85	1.61966E-01	9.23225E-01	1.49531E-01	7.60095E-04
90	1.61974E-01	9.23315E-01	1.49553E-01	7.60151E-04

ψ	p_n	η	ε	$\sigma(\varepsilon)$
$\theta = 80$				
0	1.30259E-01	9.15875E-01	1.19301E-01	8.28870E-04
5	1.33520E-01	9.17166E-01	1.22460E-01	8.39775E-04
10	1.33631E-01	9.17340E-01	1.22585E-01	8.40201E-04
15	1.33635E-01	9.16915E-01	1.22532E-01	8.40021E-04
20	1.33539E-01	9.16803E-01	1.22429E-01	8.39668E-04
25	1.33773E-01	9.16986E-01	1.22668E-01	8.40486E-04
30	1.33493E-01	9.16872E-01	1.22396E-01	8.39553E-04
35	1.33652E-01	9.17203E-01	1.22586E-01	8.40206E-04
40	1.33606E-01	9.17167E-01	1.22539E-01	8.40043E-04
45	1.33543E-01	9.16798E-01	1.22432E-01	8.39678E-04
50	1.33657E-01	9.17161E-01	1.22585E-01	8.40201E-04
55	1.33681E-01	9.16967E-01	1.22581E-01	8.40187E-04
60	1.33627E-01	9.17352E-01	1.22583E-01	8.40193E-04
65	1.33718E-01	9.17722E-01	1.22716E-01	8.40651E-04
70	1.33668E-01	9.16816E-01	1.22549E-01	8.40079E-04
75	1.33710E-01	9.17463E-01	1.22674E-01	8.40506E-04
80	1.33353E-01	9.17752E-01	1.22385E-01	8.39517E-04
85	1.33639E-01	9.17374E-01	1.22597E-01	8.40242E-04
90	1.33647E-01	9.17529E-01	1.22625E-01	8.40339E-04
$\theta = 85$				
0	8.08149E-02	8.98333E-01	7.25987E-02	9.12676E-04
5	8.24931E-02	8.99199E-01	7.41777E-02	9.22548E-04
10	8.24680E-02	8.98381E-01	7.40877E-02	9.21988E-04
15	8.24898E-02	8.98358E-01	7.41054E-02	9.22098E-04
20	8.24966E-02	8.98353E-01	7.41111E-02	9.22133E-04
25	8.25071E-02	8.98149E-01	7.41037E-02	9.22087E-04
30	8.24550E-02	8.99187E-01	7.41425E-02	9.22329E-04
35	8.24944E-02	8.98364E-01	7.41100E-02	9.22126E-04
40	8.24641E-02	8.98500E-01	7.40940E-02	9.22027E-04
45	8.24517E-02	8.98879E-01	7.41141E-02	9.22152E-04
50	8.24692E-02	8.98529E-01	7.41010E-02	9.22070E-04
55	8.24571E-02	8.98863E-01	7.41176E-02	9.22174E-04
60	8.24891E-02	8.98378E-01	7.41064E-02	9.22104E-04
65	8.24572E-02	8.99480E-01	7.41686E-02	9.22491E-04
70	8.24517E-02	8.98613E-01	7.40922E-02	9.22016E-04
75	8.24876E-02	9.00168E-01	7.42527E-02	9.23014E-04
80	8.24063E-02	8.99023E-01	7.40852E-02	9.21972E-04
85	8.24858E-02	8.98570E-01	7.41193E-02	9.22184E-04
90	8.24788E-02	8.99316E-01	7.41745E-02	9.22528E-04

Table B.15. ${}^6\text{LiF}$ sinusoid detector with 100 μm deep perforations, 30 μm wave separation, 30 μm wave period, 40 μm wave amplitude, and no cap

ψ	p_n	η	ε	$\sigma(\varepsilon)$
$\theta = 0$				
0	1.99886E-01	9.07712E-01	1.81439E-01	4.25957E-04
5	1.99986E-01	9.09204E-01	1.81828E-01	4.26413E-04
10	2.00325E-01	9.08474E-01	1.81990E-01	4.26603E-04
15	1.99507E-01	9.09597E-01	1.81471E-01	4.25994E-04
20	1.99865E-01	9.08663E-01	1.81610E-01	4.26157E-04
25	2.00330E-01	9.08466E-01	1.81993E-01	4.26606E-04
30	1.99995E-01	9.08123E-01	1.81620E-01	4.26169E-04
35	2.00032E-01	9.09305E-01	1.81890E-01	4.26486E-04
40	2.00256E-01	9.08917E-01	1.82016E-01	4.26633E-04
45	1.99980E-01	9.09571E-01	1.81896E-01	4.26493E-04
50	1.99751E-01	9.09157E-01	1.81605E-01	4.26151E-04
55	1.99473E-01	9.09146E-01	1.81350E-01	4.25852E-04
60	1.99736E-01	9.10051E-01	1.81770E-01	4.26345E-04
65	1.99759E-01	9.09846E-01	1.81750E-01	4.26321E-04
70	1.99660E-01	9.09772E-01	1.81645E-01	4.26198E-04
75	1.99309E-01	9.08358E-01	1.81044E-01	4.25493E-04
80	1.98784E-01	9.09560E-01	1.80806E-01	4.25213E-04
85	2.00391E-01	9.09816E-01	1.82319E-01	4.26988E-04
90	2.00082E-01	9.09687E-01	1.82012E-01	4.26629E-04
$\theta = 5$				
0	2.19673E-01	9.12693E-01	2.00494E-01	4.48620E-04
5	2.20219E-01	9.13009E-01	2.01062E-01	4.49255E-04
10	2.19612E-01	9.11940E-01	2.00273E-01	4.48373E-04
15	2.19922E-01	9.13046E-01	2.00799E-01	4.48961E-04
20	2.18877E-01	9.12503E-01	1.99726E-01	4.47760E-04
25	2.19397E-01	9.12902E-01	2.00288E-01	4.48389E-04
30	2.18488E-01	9.12993E-01	1.99478E-01	4.47482E-04
35	2.18295E-01	9.12142E-01	1.99116E-01	4.47076E-04
40	2.17828E-01	9.12064E-01	1.98673E-01	4.46578E-04
45	2.16765E-01	9.12569E-01	1.97813E-01	4.45611E-04
50	2.15143E-01	9.12542E-01	1.96327E-01	4.43934E-04
55	2.14765E-01	9.11713E-01	1.95804E-01	4.43342E-04
60	2.12222E-01	9.12271E-01	1.93604E-01	4.40845E-04
65	2.11026E-01	9.11395E-01	1.92328E-01	4.39389E-04
70	2.08930E-01	9.11363E-01	1.90411E-01	4.37193E-04
75	2.06946E-01	9.10672E-01	1.88460E-01	4.34948E-04
80	2.05423E-01	9.10779E-01	1.87095E-01	4.33371E-04
85	2.04576E-01	9.10200E-01	1.86205E-01	4.32338E-04
90	2.04685E-01	9.12045E-01	1.86682E-01	4.32891E-04

ψ	p_n	η	ε	$\sigma(\varepsilon)$
$\theta = 10$				
0	2.20537E-01	9.12423E-01	2.01223E-01	4.52025E-04
5	2.20614E-01	9.12558E-01	2.01323E-01	4.52138E-04
10	2.21319E-01	9.12082E-01	2.01861E-01	4.52742E-04
15	2.21205E-01	9.12895E-01	2.01937E-01	4.52827E-04
20	2.20675E-01	9.13570E-01	2.01602E-01	4.52451E-04
25	2.21056E-01	9.12746E-01	2.01768E-01	4.52638E-04
30	2.20484E-01	9.13332E-01	2.01375E-01	4.52197E-04
35	2.20715E-01	9.12249E-01	2.01347E-01	4.52165E-04
40	2.20291E-01	9.12044E-01	2.00915E-01	4.51679E-04
45	2.20606E-01	9.12749E-01	2.01358E-01	4.52177E-04
50	2.20354E-01	9.12014E-01	2.00966E-01	4.51737E-04
55	2.19367E-01	9.12959E-01	2.00273E-01	4.50958E-04
60	2.18589E-01	9.12452E-01	1.99452E-01	4.50032E-04
65	2.17999E-01	9.12367E-01	1.98895E-01	4.49403E-04
70	2.15464E-01	9.13336E-01	1.96791E-01	4.47020E-04
75	2.13330E-01	9.11635E-01	1.94479E-01	4.44386E-04
80	2.10112E-01	9.10952E-01	1.91402E-01	4.40857E-04
85	2.08900E-01	9.11819E-01	1.90479E-01	4.39792E-04
90	2.09248E-01	9.11942E-01	1.90822E-01	4.40189E-04
$\theta = 15$				
0	2.21005E-01	9.11871E-01	2.01528E-01	4.56768E-04
5	2.21258E-01	9.12939E-01	2.01995E-01	4.57297E-04
10	2.21295E-01	9.12456E-01	2.01922E-01	4.57214E-04
15	2.20172E-01	9.12895E-01	2.00994E-01	4.56162E-04
20	2.20954E-01	9.11669E-01	2.01437E-01	4.56665E-04
25	2.21161E-01	9.12810E-01	2.01878E-01	4.57165E-04
30	2.21007E-01	9.12691E-01	2.01711E-01	4.56976E-04
35	2.21852E-01	9.12257E-01	2.02386E-01	4.57739E-04
40	2.21214E-01	9.12890E-01	2.01944E-01	4.57240E-04
45	2.21162E-01	9.13172E-01	2.01959E-01	4.57256E-04
50	2.22040E-01	9.12241E-01	2.02554E-01	4.57929E-04
55	2.20461E-01	9.12365E-01	2.01141E-01	4.56329E-04
60	2.21983E-01	9.11655E-01	2.02372E-01	4.57724E-04
65	2.18835E-01	9.12551E-01	1.99698E-01	4.54690E-04
70	2.18614E-01	9.12636E-01	1.99515E-01	4.54481E-04
75	2.16327E-01	9.11980E-01	1.97286E-01	4.51935E-04
80	2.13377E-01	9.12141E-01	1.94630E-01	4.48883E-04
85	2.13310E-01	9.12428E-01	1.94630E-01	4.48883E-04
90	2.13903E-01	9.12217E-01	1.95126E-01	4.49454E-04

ψ	p_n	η	ε	$\sigma(\varepsilon)$
$\theta = 20$				
0	2.20616E-01	9.13669E-01	2.01570E-01	4.63148E-04
5	2.20279E-01	9.12316E-01	2.00964E-01	4.62451E-04
10	2.20108E-01	9.12811E-01	2.00917E-01	4.62397E-04
15	2.20457E-01	9.11706E-01	2.00992E-01	4.62484E-04
20	2.20343E-01	9.13113E-01	2.01198E-01	4.62720E-04
25	2.20149E-01	9.12741E-01	2.00939E-01	4.62423E-04
30	2.20544E-01	9.11791E-01	2.01090E-01	4.62597E-04
35	2.21212E-01	9.12622E-01	2.01883E-01	4.63507E-04
40	2.21443E-01	9.12321E-01	2.02027E-01	4.63673E-04
45	2.21109E-01	9.11677E-01	2.01580E-01	4.63160E-04
50	2.22415E-01	9.13369E-01	2.03147E-01	4.64956E-04
55	2.20636E-01	9.12811E-01	2.01399E-01	4.62951E-04
60	2.21494E-01	9.13271E-01	2.02284E-01	4.63968E-04
65	2.21109E-01	9.12844E-01	2.01838E-01	4.63457E-04
70	2.18455E-01	9.12591E-01	1.99360E-01	4.60602E-04
75	2.17321E-01	9.12254E-01	1.98252E-01	4.59320E-04
80	2.13787E-01	9.12226E-01	1.95022E-01	4.55563E-04
85	2.15621E-01	9.11354E-01	1.96507E-01	4.57294E-04
90	2.18241E-01	9.13449E-01	1.99352E-01	4.60593E-04
$\theta = 25$				
0	2.18954E-01	9.11749E-01	1.99631E-01	4.69327E-04
5	2.18917E-01	9.12213E-01	1.99699E-01	4.69407E-04
10	2.19510E-01	9.10801E-01	1.99930E-01	4.69679E-04
15	2.18751E-01	9.13358E-01	1.99798E-01	4.69524E-04
20	2.19133E-01	9.13372E-01	2.00150E-01	4.69937E-04
25	2.19781E-01	9.12163E-01	2.00476E-01	4.70320E-04
30	2.20746E-01	9.12456E-01	2.01421E-01	4.71427E-04
35	2.20629E-01	9.12514E-01	2.01327E-01	4.71317E-04
40	2.21713E-01	9.12689E-01	2.02355E-01	4.72519E-04
45	2.20371E-01	9.11935E-01	2.00964E-01	4.70892E-04
50	2.20520E-01	9.11759E-01	2.01061E-01	4.71005E-04
55	2.20840E-01	9.11828E-01	2.01368E-01	4.71365E-04
60	2.21121E-01	9.12654E-01	2.01807E-01	4.71878E-04
65	2.20257E-01	9.12579E-01	2.01002E-01	4.70936E-04
70	2.19937E-01	9.12502E-01	2.00693E-01	4.70574E-04
75	2.17131E-01	9.11565E-01	1.97929E-01	4.67323E-04
80	2.14027E-01	9.11955E-01	1.95183E-01	4.64070E-04
85	2.16115E-01	9.12315E-01	1.97165E-01	4.66419E-04
90	2.20657E-01	9.12706E-01	2.01395E-01	4.71397E-04

ψ	p_n	η	ε	$\sigma(\varepsilon)$
$\theta = 30$				
0	2.17727E-01	9.12188E-01	1.98608E-01	4.78887E-04
5	2.18107E-01	9.11603E-01	1.98827E-01	4.79151E-04
10	2.16962E-01	9.12049E-01	1.97880E-01	4.78008E-04
15	2.18379E-01	9.11676E-01	1.99091E-01	4.79469E-04
20	2.18937E-01	9.10148E-01	1.99265E-01	4.79678E-04
25	2.19220E-01	9.12982E-01	2.00144E-01	4.80735E-04
30	2.19438E-01	9.12846E-01	2.00313E-01	4.80939E-04
35	2.19757E-01	9.11875E-01	2.00391E-01	4.81032E-04
40	2.19990E-01	9.12010E-01	2.00633E-01	4.81322E-04
45	2.20232E-01	9.12102E-01	2.00874E-01	4.81611E-04
50	2.20125E-01	9.12050E-01	2.00765E-01	4.81481E-04
55	2.19873E-01	9.12540E-01	2.00643E-01	4.81335E-04
60	2.19828E-01	9.12623E-01	2.00620E-01	4.81307E-04
65	2.19663E-01	9.12334E-01	2.00406E-01	4.81050E-04
70	2.19181E-01	9.12410E-01	1.99983E-01	4.80542E-04
75	2.16842E-01	9.11945E-01	1.97748E-01	4.77849E-04
80	2.13005E-01	9.12044E-01	1.94270E-01	4.73629E-04
85	2.15103E-01	9.12358E-01	1.96251E-01	4.76037E-04
90	2.21315E-01	9.13725E-01	2.02221E-01	4.83224E-04
$\theta = 35$				
0	2.15314E-01	9.11246E-01	1.96204E-01	4.89409E-04
5	2.15512E-01	9.12139E-01	1.96577E-01	4.89873E-04
10	2.16232E-01	9.12044E-01	1.97213E-01	4.90666E-04
15	2.16751E-01	9.12397E-01	1.97763E-01	4.91349E-04
20	2.16755E-01	9.11910E-01	1.97661E-01	4.91223E-04
25	2.17995E-01	9.12131E-01	1.98840E-01	4.92685E-04
30	2.17083E-01	9.12480E-01	1.98084E-01	4.91748E-04
35	2.17942E-01	9.12665E-01	1.98908E-01	4.92770E-04
40	2.19004E-01	9.11002E-01	1.99513E-01	4.93519E-04
45	2.19471E-01	9.11956E-01	2.00148E-01	4.94304E-04
50	2.18463E-01	9.11939E-01	1.99225E-01	4.93162E-04
55	2.18300E-01	9.12034E-01	1.99097E-01	4.93003E-04
60	2.18714E-01	9.12150E-01	1.99500E-01	4.93502E-04
65	2.18403E-01	9.11805E-01	1.99141E-01	4.93058E-04
70	2.17284E-01	9.12258E-01	1.98219E-01	4.91916E-04
75	2.15202E-01	9.11632E-01	1.96185E-01	4.89385E-04
80	2.11838E-01	9.11413E-01	1.93072E-01	4.85487E-04
85	2.15697E-01	9.12368E-01	1.96795E-01	4.90145E-04
90	2.19085E-01	9.12755E-01	1.99971E-01	4.94084E-04

ψ	p_n	η	ε	$\sigma(\varepsilon)$
$\theta = 40$				
0	2.12423E-01	9.11620E-01	1.93649E-01	5.02783E-04
5	2.13733E-01	9.11394E-01	1.94795E-01	5.04269E-04
10	2.13468E-01	9.11846E-01	1.94650E-01	5.04081E-04
15	2.14467E-01	9.11371E-01	1.95459E-01	5.05128E-04
20	2.14875E-01	9.11507E-01	1.95860E-01	5.05645E-04
25	2.16141E-01	9.12057E-01	1.97133E-01	5.07286E-04
30	2.16281E-01	9.11703E-01	1.97184E-01	5.07352E-04
35	2.16653E-01	9.12856E-01	1.97773E-01	5.08108E-04
40	2.16451E-01	9.12437E-01	1.97498E-01	5.07755E-04
45	2.16472E-01	9.11305E-01	1.97272E-01	5.07464E-04
50	2.16719E-01	9.12301E-01	1.97713E-01	5.08031E-04
55	2.16743E-01	9.11587E-01	1.97580E-01	5.07860E-04
60	2.16190E-01	9.11707E-01	1.97102E-01	5.07246E-04
65	2.15975E-01	9.10953E-01	1.96743E-01	5.06784E-04
70	2.15350E-01	9.11586E-01	1.96310E-01	5.06226E-04
75	2.13736E-01	9.11746E-01	1.94873E-01	5.04369E-04
80	2.09572E-01	9.11835E-01	1.91095E-01	4.99457E-04
85	2.14101E-01	9.12378E-01	1.95341E-01	5.04975E-04
90	2.15435E-01	9.12001E-01	1.96477E-01	5.06442E-04
$\theta = 45$				
0	2.10070E-01	9.11053E-01	1.91385E-01	5.20249E-04
5	2.10090E-01	9.10833E-01	1.91357E-01	5.20211E-04
10	2.11348E-01	9.11610E-01	1.92667E-01	5.21989E-04
15	2.11491E-01	9.11268E-01	1.92725E-01	5.22068E-04
20	2.12889E-01	9.10456E-01	1.93826E-01	5.23556E-04
25	2.13852E-01	9.11233E-01	1.94869E-01	5.24963E-04
30	2.13920E-01	9.11860E-01	1.95065E-01	5.25227E-04
35	2.13986E-01	9.12158E-01	1.95189E-01	5.25394E-04
40	2.13700E-01	9.11759E-01	1.94843E-01	5.24929E-04
45	2.14379E-01	9.12468E-01	1.95614E-01	5.25966E-04
50	2.13798E-01	9.11131E-01	1.94798E-01	5.24868E-04
55	2.12971E-01	9.11068E-01	1.94031E-01	5.23833E-04
60	2.14047E-01	9.11501E-01	1.95104E-01	5.25280E-04
65	2.12986E-01	9.11426E-01	1.94121E-01	5.23955E-04
70	2.12642E-01	9.12510E-01	1.94038E-01	5.23843E-04
75	2.11195E-01	9.11778E-01	1.92563E-01	5.21848E-04
80	2.07864E-01	9.12092E-01	1.89591E-01	5.17805E-04
85	2.11371E-01	9.11038E-01	1.92567E-01	5.21853E-04
90	2.13448E-01	9.11758E-01	1.94613E-01	5.24619E-04

ψ	p_n	η	ε	$\sigma(\varepsilon)$
$\theta = 50$				
0	2.06622E-01	9.10750E-01	1.88181E-01	5.41071E-04
5	2.06499E-01	9.11554E-01	1.88235E-01	5.41148E-04
10	2.07753E-01	9.10312E-01	1.89120E-01	5.42420E-04
15	2.09015E-01	9.10394E-01	1.90286E-01	5.44089E-04
20	2.10253E-01	9.09989E-01	1.91328E-01	5.45576E-04
25	2.11175E-01	9.10411E-01	1.92256E-01	5.46899E-04
30	2.10437E-01	9.11603E-01	1.91835E-01	5.46298E-04
35	2.10422E-01	9.11183E-01	1.91733E-01	5.46153E-04
40	2.09848E-01	9.10459E-01	1.91058E-01	5.45191E-04
45	2.10066E-01	9.10780E-01	1.91324E-01	5.45570E-04
50	2.10404E-01	9.10819E-01	1.91640E-01	5.46021E-04
55	2.09985E-01	9.10651E-01	1.91223E-01	5.45426E-04
60	2.09668E-01	9.10773E-01	1.90960E-01	5.45051E-04
65	2.09965E-01	9.10614E-01	1.91197E-01	5.45389E-04
70	2.09978E-01	9.10033E-01	1.91087E-01	5.45233E-04
75	2.07736E-01	9.11657E-01	1.89384E-01	5.42797E-04
80	2.04722E-01	9.10659E-01	1.86432E-01	5.38550E-04
85	2.08655E-01	9.11370E-01	1.90162E-01	5.43912E-04
90	2.10231E-01	9.10594E-01	1.91435E-01	5.45729E-04
$\theta = 55$				
0	2.01525E-01	9.09609E-01	1.83309E-01	5.65322E-04
5	2.02078E-01	9.10158E-01	1.83923E-01	5.66268E-04
10	2.03537E-01	9.10070E-01	1.85233E-01	5.68282E-04
15	2.04610E-01	9.10131E-01	1.86222E-01	5.69797E-04
20	2.05998E-01	9.09455E-01	1.87346E-01	5.71513E-04
25	2.06046E-01	9.10433E-01	1.87591E-01	5.71887E-04
30	2.05912E-01	9.10875E-01	1.87560E-01	5.71840E-04
35	2.05369E-01	9.09465E-01	1.86776E-01	5.70643E-04
40	2.05923E-01	9.10515E-01	1.87496E-01	5.71743E-04
45	2.05954E-01	9.10490E-01	1.87519E-01	5.71778E-04
50	2.05460E-01	9.09895E-01	1.86947E-01	5.70905E-04
55	2.05858E-01	9.09948E-01	1.87320E-01	5.71474E-04
60	2.05630E-01	9.09663E-01	1.87054E-01	5.71067E-04
65	2.05102E-01	9.09621E-01	1.86565E-01	5.70322E-04
70	2.05273E-01	9.10125E-01	1.86824E-01	5.70717E-04
75	2.02976E-01	9.10364E-01	1.84782E-01	5.67590E-04
80	1.99890E-01	9.10766E-01	1.82053E-01	5.63383E-04
85	2.04965E-01	9.10272E-01	1.86574E-01	5.70335E-04
90	2.05807E-01	9.11028E-01	1.87496E-01	5.71743E-04

ψ	p_n	η	ε	$\sigma(\varepsilon)$
$\theta = 60$				
0	1.94290E-01	9.08467E-01	1.76506E-01	5.94149E-04
5	1.96191E-01	9.09165E-01	1.78370E-01	5.97277E-04
10	1.97548E-01	9.08994E-01	1.79570E-01	5.99283E-04
15	1.99086E-01	9.09295E-01	1.81028E-01	6.01711E-04
20	1.99816E-01	9.08746E-01	1.81582E-01	6.02632E-04
25	1.99523E-01	9.09544E-01	1.81475E-01	6.02454E-04
30	1.99433E-01	9.08786E-01	1.81242E-01	6.02066E-04
35	1.99831E-01	9.09298E-01	1.81706E-01	6.02837E-04
40	1.99699E-01	9.10015E-01	1.81729E-01	6.02875E-04
45	1.99903E-01	9.09671E-01	1.81846E-01	6.03070E-04
50	1.99693E-01	9.10082E-01	1.81737E-01	6.02889E-04
55	1.99461E-01	9.09566E-01	1.81423E-01	6.02368E-04
60	1.99308E-01	9.10069E-01	1.81384E-01	6.02302E-04
65	1.98874E-01	9.08711E-01	1.80719E-01	6.01197E-04
70	1.99731E-01	9.08242E-01	1.81404E-01	6.02335E-04
75	1.96753E-01	9.09607E-01	1.78968E-01	5.98278E-04
80	1.94434E-01	9.09460E-01	1.76830E-01	5.94694E-04
85	1.98761E-01	9.10093E-01	1.80891E-01	6.01484E-04
90	1.99542E-01	9.09428E-01	1.81469E-01	6.02444E-04
$\theta = 65$				
0	1.85824E-01	9.07907E-01	1.68711E-01	6.31826E-04
5	1.87816E-01	9.08235E-01	1.70581E-01	6.35319E-04
10	1.90473E-01	9.08633E-01	1.73070E-01	6.39937E-04
15	1.91195E-01	9.07801E-01	1.73567E-01	6.40855E-04
20	1.91201E-01	9.07793E-01	1.73571E-01	6.40862E-04
25	1.91058E-01	9.08169E-01	1.73513E-01	6.40755E-04
30	1.91686E-01	9.08418E-01	1.74131E-01	6.41896E-04
35	1.91392E-01	9.08314E-01	1.73844E-01	6.41365E-04
40	1.91515E-01	9.08817E-01	1.74052E-01	6.41749E-04
45	1.91729E-01	9.07860E-01	1.74063E-01	6.41769E-04
50	1.91114E-01	9.08531E-01	1.73633E-01	6.40976E-04
55	1.91314E-01	9.08318E-01	1.73774E-01	6.41237E-04
60	1.91150E-01	9.08166E-01	1.73596E-01	6.40907E-04
65	1.90904E-01	9.07975E-01	1.73336E-01	6.40427E-04
70	1.90859E-01	9.07476E-01	1.73200E-01	6.40177E-04
75	1.88585E-01	9.08752E-01	1.71377E-01	6.36799E-04
80	1.85520E-01	9.07104E-01	1.68286E-01	6.31029E-04
85	1.90759E-01	9.08251E-01	1.73257E-01	6.40283E-04
90	1.91453E-01	9.08249E-01	1.73887E-01	6.41444E-04

ψ	p_n	η	ε	$\sigma(\varepsilon)$
$\theta = 70$				
0	1.74200E-01	9.06917E-01	1.57985E-01	6.79645E-04
5	1.76574E-01	9.06577E-01	1.60078E-01	6.84132E-04
10	1.79459E-01	9.06123E-01	1.62612E-01	6.89525E-04
15	1.79653E-01	9.05624E-01	1.62698E-01	6.89709E-04
20	1.79423E-01	9.06194E-01	1.62592E-01	6.89482E-04
25	1.79731E-01	9.05926E-01	1.62823E-01	6.89974E-04
30	1.79711E-01	9.06461E-01	1.62901E-01	6.90139E-04
35	1.79962E-01	9.06241E-01	1.63089E-01	6.90535E-04
40	1.79631E-01	9.06397E-01	1.62817E-01	6.89959E-04
45	1.79814E-01	9.06553E-01	1.63011E-01	6.90370E-04
50	1.79835E-01	9.06081E-01	1.62945E-01	6.90231E-04
55	1.79565E-01	9.06201E-01	1.62722E-01	6.89759E-04
60	1.79442E-01	9.06337E-01	1.62635E-01	6.89575E-04
65	1.79129E-01	9.06559E-01	1.62391E-01	6.89057E-04
70	1.79654E-01	9.06793E-01	1.62909E-01	6.90155E-04
75	1.77230E-01	9.06647E-01	1.60685E-01	6.85429E-04
80	1.73833E-01	9.05990E-01	1.57491E-01	6.78582E-04
85	1.78939E-01	9.05800E-01	1.62083E-01	6.88402E-04
90	1.79482E-01	9.06202E-01	1.62647E-01	6.89600E-04
$\theta = 75$				
0	1.56371E-01	9.02469E-01	1.41120E-01	7.38406E-04
5	1.60288E-01	9.03361E-01	1.44798E-01	7.47969E-04
10	1.62052E-01	9.03155E-01	1.46358E-01	7.51986E-04
15	1.62238E-01	9.03253E-01	1.46542E-01	7.52459E-04
20	1.62064E-01	9.03267E-01	1.46387E-01	7.52061E-04
25	1.62076E-01	9.02509E-01	1.46275E-01	7.51773E-04
30	1.62335E-01	9.02486E-01	1.46505E-01	7.52364E-04
35	1.61893E-01	9.03430E-01	1.46259E-01	7.51733E-04
40	1.62318E-01	9.02907E-01	1.46558E-01	7.52500E-04
45	1.62026E-01	9.03546E-01	1.46398E-01	7.52089E-04
50	1.62159E-01	9.02941E-01	1.46420E-01	7.52146E-04
55	1.62169E-01	9.02768E-01	1.46401E-01	7.52098E-04
60	1.62182E-01	9.02819E-01	1.46421E-01	7.52148E-04
65	1.61615E-01	9.02639E-01	1.45880E-01	7.50758E-04
70	1.62136E-01	9.03507E-01	1.46491E-01	7.52328E-04
75	1.60151E-01	9.03329E-01	1.44669E-01	7.47635E-04
80	1.57349E-01	9.03088E-01	1.42100E-01	7.40966E-04
85	1.61931E-01	9.02996E-01	1.46223E-01	7.51640E-04
90	1.62162E-01	9.03664E-01	1.46540E-01	7.52455E-04

ψ	p_n	η	ε	$\sigma(\varepsilon)$
$\theta = 80$				
0	1.28271E-01	8.96212E-01	1.14958E-01	8.13644E-04
5	1.33503E-01	8.97433E-01	1.19810E-01	8.30637E-04
10	1.33430E-01	8.97324E-01	1.19730E-01	8.30360E-04
15	1.33451E-01	8.96981E-01	1.19703E-01	8.30266E-04
20	1.33672E-01	8.96463E-01	1.19832E-01	8.30715E-04
25	1.33586E-01	8.95573E-01	1.19636E-01	8.30034E-04
30	1.33610E-01	8.95449E-01	1.19641E-01	8.30052E-04
35	1.33590E-01	8.96175E-01	1.19720E-01	8.30325E-04
40	1.33581E-01	8.96392E-01	1.19741E-01	8.30397E-04
45	1.33604E-01	8.96582E-01	1.19787E-01	8.30558E-04
50	1.33682E-01	8.96471E-01	1.19842E-01	8.30749E-04
55	1.33667E-01	8.96646E-01	1.19852E-01	8.30783E-04
60	1.33495E-01	8.96858E-01	1.19726E-01	8.30347E-04
65	1.33555E-01	8.96544E-01	1.19738E-01	8.30388E-04
70	1.33680E-01	8.96215E-01	1.19806E-01	8.30624E-04
75	1.33000E-01	8.97188E-01	1.19326E-01	8.28959E-04
80	1.31325E-01	8.97681E-01	1.17888E-01	8.23948E-04
85	1.33566E-01	8.96418E-01	1.19731E-01	8.30365E-04
90	1.33638E-01	8.97267E-01	1.19909E-01	8.30981E-04
$\theta = 85$				
0	7.96818E-02	8.78075E-01	6.99666E-02	8.95978E-04
5	8.24203E-02	8.77812E-01	7.23495E-02	9.11108E-04
10	8.24550E-02	8.77029E-01	7.23154E-02	9.10894E-04
15	8.24860E-02	8.76318E-01	7.22840E-02	9.10695E-04
20	8.24443E-02	8.77005E-01	7.23041E-02	9.10822E-04
25	8.24846E-02	8.76214E-01	7.22742E-02	9.10634E-04
30	8.24784E-02	8.75844E-01	7.22382E-02	9.10407E-04
35	8.24530E-02	8.75696E-01	7.22038E-02	9.10190E-04
40	8.24769E-02	8.76437E-01	7.22858E-02	9.10707E-04
45	8.25163E-02	8.76237E-01	7.23038E-02	9.10820E-04
50	8.24704E-02	8.75803E-01	7.22278E-02	9.10341E-04
55	8.24372E-02	8.76673E-01	7.22705E-02	9.10610E-04
60	8.24750E-02	8.76175E-01	7.22625E-02	9.10560E-04
65	8.24926E-02	8.75980E-01	7.22619E-02	9.10556E-04
70	8.24590E-02	8.76557E-01	7.22800E-02	9.10670E-04
75	8.24157E-02	8.77492E-01	7.23191E-02	9.10917E-04
80	8.24848E-02	8.78150E-01	7.24340E-02	9.11640E-04
85	8.24451E-02	8.76435E-01	7.22578E-02	9.10531E-04
90	8.24820E-02	8.75881E-01	7.22444E-02	9.10446E-04

Table B.16. ${}^6\text{LiF}$ sinusoid detector with 100 μm deep perforations, 35 μm wave separation, 130 μm wave period, 40 μm wave amplitude, and no cap

ψ	p_n	η	ε	$\sigma(\varepsilon)$
$\theta = 0$				
0	2.77875E-01	5.11169E-01	1.42041E-01	3.76883E-04
5	2.77888E-01	5.10260E-01	1.41795E-01	3.76557E-04
10	2.78075E-01	5.11502E-01	1.42236E-01	3.77142E-04
15	2.77665E-01	5.11739E-01	1.42092E-01	3.76951E-04
20	2.78014E-01	5.11956E-01	1.42331E-01	3.77268E-04
25	2.77360E-01	5.11552E-01	1.41884E-01	3.76675E-04
30	2.78344E-01	5.11144E-01	1.42274E-01	3.77192E-04
35	2.77239E-01	5.12558E-01	1.42101E-01	3.76963E-04
40	2.77251E-01	5.11122E-01	1.41709E-01	3.76443E-04
45	2.77783E-01	5.11086E-01	1.41971E-01	3.76790E-04
50	2.77870E-01	5.11905E-01	1.42243E-01	3.77151E-04
55	2.77572E-01	5.10945E-01	1.41824E-01	3.76595E-04
60	2.77278E-01	5.11029E-01	1.41697E-01	3.76427E-04
65	2.76885E-01	5.11945E-01	1.41750E-01	3.76497E-04
70	2.77694E-01	5.10141E-01	1.41663E-01	3.76381E-04
75	2.77059E-01	5.10870E-01	1.41541E-01	3.76219E-04
80	2.77520E-01	5.11887E-01	1.42059E-01	3.76907E-04
85	2.77737E-01	5.10375E-01	1.41750E-01	3.76497E-04
90	2.77640E-01	5.11756E-01	1.42084E-01	3.76940E-04
$\theta = 5$				
0	2.82098E-01	5.18270E-01	1.46203E-01	3.83094E-04
5	2.82258E-01	5.16581E-01	1.45809E-01	3.82578E-04
10	2.81811E-01	5.17279E-01	1.45775E-01	3.82534E-04
15	2.81384E-01	5.17442E-01	1.45600E-01	3.82304E-04
20	2.81398E-01	5.17477E-01	1.45617E-01	3.82326E-04
25	2.81726E-01	5.17009E-01	1.45655E-01	3.82375E-04
30	2.81256E-01	5.17646E-01	1.45591E-01	3.82292E-04
35	2.81460E-01	5.15778E-01	1.45171E-01	3.81741E-04
40	2.80553E-01	5.16074E-01	1.44786E-01	3.81234E-04
45	2.80240E-01	5.16564E-01	1.44762E-01	3.81202E-04
50	2.80333E-01	5.14798E-01	1.44315E-01	3.80613E-04
55	2.80248E-01	5.15372E-01	1.44432E-01	3.80768E-04
60	2.80615E-01	5.15710E-01	1.44716E-01	3.81142E-04
65	2.80529E-01	5.15954E-01	1.44740E-01	3.81173E-04
70	2.80434E-01	5.14178E-01	1.44193E-01	3.80452E-04
75	2.80887E-01	5.16069E-01	1.44957E-01	3.81459E-04
80	2.80405E-01	5.15658E-01	1.44593E-01	3.80979E-04
85	2.80884E-01	5.16259E-01	1.45009E-01	3.81527E-04
90	2.81141E-01	5.17637E-01	1.45529E-01	3.82211E-04

ψ	p_n	η	ε	$\sigma(\varepsilon)$
$\theta = 10$				
0	2.85558E-01	5.20731E-01	1.48699E-01	3.88578E-04
5	2.85515E-01	5.20361E-01	1.48571E-01	3.88411E-04
10	2.86452E-01	5.21777E-01	1.49464E-01	3.89577E-04
15	2.85470E-01	5.22111E-01	1.49047E-01	3.89032E-04
20	2.85328E-01	5.20324E-01	1.48463E-01	3.88269E-04
25	2.86278E-01	5.21252E-01	1.49223E-01	3.89262E-04
30	2.84853E-01	5.20844E-01	1.48364E-01	3.88140E-04
35	2.84167E-01	5.20155E-01	1.47811E-01	3.87416E-04
40	2.83296E-01	5.19721E-01	1.47235E-01	3.86660E-04
45	2.84706E-01	5.19708E-01	1.47964E-01	3.87617E-04
50	2.83287E-01	5.18224E-01	1.46806E-01	3.86097E-04
55	2.84345E-01	5.18764E-01	1.47508E-01	3.87019E-04
60	2.83368E-01	5.19152E-01	1.47111E-01	3.86497E-04
65	2.83522E-01	5.19960E-01	1.47420E-01	3.86903E-04
70	2.83765E-01	5.18824E-01	1.47224E-01	3.86646E-04
75	2.83888E-01	5.19867E-01	1.47584E-01	3.87119E-04
80	2.83519E-01	5.19083E-01	1.47170E-01	3.86575E-04
85	2.83536E-01	5.20008E-01	1.47441E-01	3.86932E-04
90	2.84260E-01	5.21642E-01	1.48282E-01	3.88032E-04
$\theta = 15$				
0	2.89782E-01	5.22358E-01	1.51370E-01	3.95866E-04
5	2.88557E-01	5.23030E-01	1.50924E-01	3.95282E-04
10	2.88600E-01	5.25017E-01	1.51520E-01	3.96062E-04
15	2.89577E-01	5.23988E-01	1.51735E-01	3.96343E-04
20	2.88680E-01	5.24719E-01	1.51476E-01	3.96005E-04
25	2.87885E-01	5.21698E-01	1.50189E-01	3.94318E-04
30	2.87460E-01	5.21700E-01	1.49968E-01	3.94028E-04
35	2.87592E-01	5.21231E-01	1.49902E-01	3.93942E-04
40	2.86922E-01	5.19793E-01	1.49140E-01	3.92939E-04
45	2.86565E-01	5.20238E-01	1.49082E-01	3.92863E-04
50	2.86747E-01	5.22314E-01	1.49772E-01	3.93770E-04
55	2.85274E-01	5.21053E-01	1.48643E-01	3.92284E-04
60	2.85027E-01	5.19007E-01	1.47931E-01	3.91343E-04
65	2.85743E-01	5.19547E-01	1.48457E-01	3.92038E-04
70	2.86880E-01	5.21239E-01	1.49533E-01	3.93456E-04
75	2.86377E-01	5.21515E-01	1.49350E-01	3.93215E-04
80	2.86041E-01	5.23002E-01	1.49600E-01	3.93544E-04
85	2.87118E-01	5.20347E-01	1.49401E-01	3.93282E-04
90	2.86896E-01	5.23029E-01	1.50055E-01	3.94142E-04

ψ	p_n	η	ε	$\sigma(\varepsilon)$
$\theta = 20$				
0	2.90714E-01	5.24784E-01	1.52562E-01	4.02931E-04
5	2.90419E-01	5.24380E-01	1.52290E-01	4.02572E-04
10	2.91090E-01	5.23697E-01	1.52443E-01	4.02773E-04
15	2.89904E-01	5.22911E-01	1.51594E-01	4.01650E-04
20	2.90985E-01	5.23687E-01	1.52385E-01	4.02697E-04
25	2.89843E-01	5.24391E-01	1.51991E-01	4.02175E-04
30	2.88550E-01	5.23289E-01	1.50995E-01	4.00855E-04
35	2.88424E-01	5.22418E-01	1.50678E-01	4.00435E-04
40	2.87545E-01	5.21111E-01	1.49843E-01	3.99324E-04
45	2.86981E-01	5.20770E-01	1.49451E-01	3.98801E-04
50	2.86561E-01	5.22238E-01	1.49653E-01	3.99070E-04
55	2.85922E-01	5.19337E-01	1.48490E-01	3.97517E-04
60	2.85880E-01	5.20575E-01	1.48822E-01	3.97961E-04
65	2.86735E-01	5.20927E-01	1.49368E-01	3.98690E-04
70	2.87426E-01	5.21960E-01	1.50025E-01	3.99566E-04
75	2.88134E-01	5.23982E-01	1.50977E-01	4.00832E-04
80	2.90565E-01	5.21835E-01	1.51627E-01	4.01694E-04
85	2.89794E-01	5.23568E-01	1.51727E-01	4.01826E-04
90	2.89248E-01	5.24125E-01	1.51602E-01	4.01660E-04
$\theta = 25$				
0	2.89636E-01	5.26026E-01	1.52356E-01	4.10007E-04
5	2.90085E-01	5.24653E-01	1.52194E-01	4.09790E-04
10	2.90486E-01	5.24662E-01	1.52407E-01	4.10077E-04
15	2.89494E-01	5.24868E-01	1.51946E-01	4.09456E-04
20	2.88795E-01	5.24867E-01	1.51579E-01	4.08961E-04
25	2.88894E-01	5.24566E-01	1.51544E-01	4.08913E-04
30	2.88990E-01	5.22983E-01	1.51137E-01	4.08364E-04
35	2.87412E-01	5.22946E-01	1.50301E-01	4.07233E-04
40	2.86794E-01	5.21702E-01	1.49621E-01	4.06311E-04
45	2.86781E-01	5.20390E-01	1.49238E-01	4.05791E-04
50	2.85928E-01	5.20019E-01	1.48688E-01	4.05042E-04
55	2.85117E-01	5.20628E-01	1.48440E-01	4.04704E-04
60	2.86283E-01	5.19475E-01	1.48717E-01	4.05081E-04
65	2.87373E-01	5.21750E-01	1.49937E-01	4.06739E-04
70	2.88937E-01	5.21802E-01	1.50768E-01	4.07865E-04
75	2.89746E-01	5.23238E-01	1.51606E-01	4.08998E-04
80	2.89883E-01	5.24912E-01	1.52163E-01	4.09747E-04
85	2.91765E-01	5.24878E-01	1.53141E-01	4.11062E-04
90	2.91605E-01	5.25756E-01	1.53313E-01	4.11293E-04

ψ	p_n	η	ε	$\sigma(\varepsilon)$
$\theta = 30$				
0	2.87754E-01	5.23013E-01	1.50499E-01	4.16870E-04
5	2.88306E-01	5.23458E-01	1.50916E-01	4.17448E-04
10	2.89074E-01	5.23485E-01	1.51326E-01	4.18014E-04
15	2.88113E-01	5.24076E-01	1.50993E-01	4.17555E-04
20	2.87929E-01	5.22858E-01	1.50546E-01	4.16936E-04
25	2.87318E-01	5.22599E-01	1.50152E-01	4.16390E-04
30	2.87502E-01	5.21485E-01	1.49928E-01	4.16079E-04
35	2.86350E-01	5.22336E-01	1.49571E-01	4.15584E-04
40	2.86662E-01	5.21632E-01	1.49532E-01	4.15530E-04
45	2.84082E-01	5.21276E-01	1.48085E-01	4.13514E-04
50	2.84734E-01	5.20279E-01	1.48141E-01	4.13592E-04
55	2.83176E-01	5.19963E-01	1.47241E-01	4.12334E-04
60	2.83758E-01	5.18121E-01	1.47021E-01	4.12025E-04
65	2.85212E-01	5.21633E-01	1.48776E-01	4.14478E-04
70	2.86919E-01	5.22524E-01	1.49922E-01	4.16071E-04
75	2.88548E-01	5.22052E-01	1.50637E-01	4.17062E-04
80	2.90474E-01	5.24061E-01	1.52226E-01	4.19256E-04
85	2.91401E-01	5.24058E-01	1.52711E-01	4.19924E-04
90	2.91348E-01	5.24126E-01	1.52703E-01	4.19912E-04
$\theta = 35$				
0	2.85616E-01	5.21119E-01	1.48840E-01	4.26263E-04
5	2.85427E-01	5.20963E-01	1.48697E-01	4.26059E-04
10	2.85860E-01	5.21678E-01	1.49127E-01	4.26673E-04
15	2.85969E-01	5.21109E-01	1.49021E-01	4.26522E-04
20	2.86191E-01	5.22218E-01	1.49454E-01	4.27142E-04
25	2.85551E-01	5.21854E-01	1.49016E-01	4.26515E-04
30	2.84711E-01	5.21894E-01	1.48589E-01	4.25904E-04
35	2.84922E-01	5.21680E-01	1.48638E-01	4.25974E-04
40	2.83477E-01	5.21111E-01	1.47723E-01	4.24661E-04
45	2.81616E-01	5.20421E-01	1.46559E-01	4.22983E-04
50	2.80909E-01	5.18221E-01	1.45573E-01	4.21559E-04
55	2.81875E-01	5.16814E-01	1.45677E-01	4.21710E-04
60	2.81189E-01	5.18537E-01	1.45807E-01	4.21898E-04
65	2.82194E-01	5.18041E-01	1.46188E-01	4.22448E-04
70	2.84502E-01	5.20031E-01	1.47950E-01	4.24986E-04
75	2.86563E-01	5.21425E-01	1.49421E-01	4.27094E-04
80	2.87739E-01	5.23624E-01	1.50667E-01	4.28871E-04
85	2.88226E-01	5.22531E-01	1.50607E-01	4.28785E-04
90	2.89603E-01	5.23945E-01	1.51736E-01	4.30389E-04

ψ	p_n	η	ε	$\sigma(\varepsilon)$
$\theta = 40$				
0	2.81524E-01	5.18826E-01	1.46062E-01	4.36658E-04
5	2.81768E-01	5.19569E-01	1.46398E-01	4.37160E-04
10	2.81431E-01	5.19925E-01	1.46323E-01	4.37048E-04
15	2.81948E-01	5.19117E-01	1.46364E-01	4.37110E-04
20	2.82105E-01	5.20157E-01	1.46739E-01	4.37669E-04
25	2.82471E-01	5.20889E-01	1.47136E-01	4.38261E-04
30	2.82577E-01	5.22360E-01	1.47607E-01	4.38961E-04
35	2.81725E-01	5.19191E-01	1.46269E-01	4.36967E-04
40	2.80904E-01	5.18736E-01	1.45715E-01	4.36139E-04
45	2.78720E-01	5.17616E-01	1.44270E-01	4.33971E-04
50	2.78434E-01	5.18712E-01	1.44427E-01	4.34207E-04
55	2.78065E-01	5.15764E-01	1.43416E-01	4.32685E-04
60	2.77694E-01	5.17343E-01	1.43663E-01	4.33058E-04
65	2.79269E-01	5.16448E-01	1.44228E-01	4.33908E-04
70	2.81786E-01	5.19494E-01	1.46386E-01	4.37142E-04
75	2.83585E-01	5.21121E-01	1.47782E-01	4.39222E-04
80	2.84215E-01	5.21767E-01	1.48294E-01	4.39982E-04
85	2.84618E-01	5.20635E-01	1.48182E-01	4.39816E-04
90	2.84750E-01	5.19877E-01	1.48035E-01	4.39598E-04
$\theta = 45$				
0	2.76180E-01	5.17930E-01	1.43042E-01	4.49769E-04
5	2.76404E-01	5.18556E-01	1.43331E-01	4.50223E-04
10	2.76777E-01	5.18898E-01	1.43619E-01	4.50675E-04
15	2.77670E-01	5.19786E-01	1.44329E-01	4.51788E-04
20	2.78133E-01	5.18550E-01	1.44226E-01	4.51626E-04
25	2.78387E-01	5.18092E-01	1.44230E-01	4.51633E-04
30	2.77822E-01	5.17464E-01	1.43763E-01	4.50900E-04
35	2.77271E-01	5.17822E-01	1.43577E-01	4.50608E-04
40	2.76030E-01	5.15564E-01	1.42311E-01	4.48618E-04
45	2.75325E-01	5.14933E-01	1.41774E-01	4.47771E-04
50	2.73445E-01	5.14374E-01	1.40653E-01	4.45997E-04
55	2.73097E-01	5.14758E-01	1.40579E-01	4.45880E-04
60	2.73320E-01	5.13098E-01	1.40240E-01	4.45341E-04
65	2.75422E-01	5.14785E-01	1.41783E-01	4.47785E-04
70	2.77877E-01	5.17002E-01	1.43663E-01	4.50744E-04
75	2.79553E-01	5.19061E-01	1.45105E-01	4.53001E-04
80	2.80141E-01	5.16979E-01	1.44827E-01	4.52566E-04
85	2.79430E-01	5.18459E-01	1.44873E-01	4.52639E-04
90	2.78512E-01	5.16513E-01	1.43855E-01	4.51045E-04

ψ	p_n	η	ε	$\sigma(\varepsilon)$
$\theta = 50$				
0	2.69716E-01	5.13881E-01	1.38602E-01	4.64357E-04
5	2.70639E-01	5.13485E-01	1.38969E-01	4.64971E-04
10	2.70269E-01	5.16030E-01	1.39467E-01	4.65803E-04
15	2.71203E-01	5.14747E-01	1.39601E-01	4.66026E-04
20	2.72262E-01	5.15434E-01	1.40333E-01	4.67246E-04
25	2.72639E-01	5.14596E-01	1.40299E-01	4.67191E-04
30	2.72715E-01	5.14966E-01	1.40439E-01	4.67424E-04
35	2.71204E-01	5.14679E-01	1.39583E-01	4.65997E-04
40	2.69532E-01	5.13520E-01	1.38410E-01	4.64033E-04
45	2.68323E-01	5.13173E-01	1.37696E-01	4.62836E-04
50	2.66961E-01	5.10801E-01	1.36364E-01	4.60592E-04
55	2.66850E-01	5.11047E-01	1.36373E-01	4.60606E-04
60	2.66833E-01	5.09922E-01	1.36064E-01	4.60085E-04
65	2.69721E-01	5.11922E-01	1.38076E-01	4.63474E-04
70	2.72032E-01	5.13638E-01	1.39726E-01	4.66235E-04
75	2.73914E-01	5.15852E-01	1.41299E-01	4.68853E-04
80	2.73334E-01	5.15417E-01	1.40881E-01	4.68158E-04
85	2.73592E-01	5.14408E-01	1.40738E-01	4.67921E-04
90	2.73881E-01	5.14833E-01	1.41003E-01	4.68360E-04
$\theta = 55$				
0	2.61481E-01	5.08714E-01	1.33019E-01	4.81572E-04
5	2.62229E-01	5.10264E-01	1.33806E-01	4.82994E-04
10	2.62996E-01	5.12232E-01	1.34715E-01	4.84632E-04
15	2.63948E-01	5.11059E-01	1.34893E-01	4.84952E-04
20	2.64669E-01	5.11628E-01	1.35412E-01	4.85884E-04
25	2.64947E-01	5.10925E-01	1.35368E-01	4.85806E-04
30	2.65528E-01	5.11283E-01	1.35760E-01	4.86508E-04
35	2.63903E-01	5.10085E-01	1.34613E-01	4.84448E-04
40	2.62275E-01	5.07971E-01	1.33228E-01	4.81950E-04
45	2.60346E-01	5.08896E-01	1.32489E-01	4.80612E-04
50	2.59817E-01	5.07746E-01	1.31921E-01	4.79580E-04
55	2.58474E-01	5.06244E-01	1.30851E-01	4.77632E-04
60	2.59402E-01	5.06307E-01	1.31337E-01	4.78518E-04
65	2.62445E-01	5.08804E-01	1.33533E-01	4.82501E-04
70	2.64590E-01	5.11663E-01	1.35381E-01	4.85828E-04
75	2.65028E-01	5.10467E-01	1.35288E-01	4.85662E-04
80	2.65261E-01	5.09615E-01	1.35181E-01	4.85470E-04
85	2.65336E-01	5.12075E-01	1.35872E-01	4.86709E-04
90	2.65722E-01	5.12419E-01	1.36161E-01	4.87227E-04

ψ	p_n	η	ε	$\sigma(\varepsilon)$
$\theta = 60$				
0	2.51091E-01	5.03718E-01	1.26479E-01	5.02950E-04
5	2.51475E-01	5.02690E-01	1.26414E-01	5.02821E-04
10	2.52974E-01	5.05076E-01	1.27771E-01	5.05512E-04
15	2.53878E-01	5.06992E-01	1.28714E-01	5.07374E-04
20	2.54757E-01	5.04932E-01	1.28635E-01	5.07218E-04
25	2.54555E-01	5.06771E-01	1.29001E-01	5.07940E-04
30	2.54593E-01	5.04664E-01	1.28484E-01	5.06920E-04
35	2.54068E-01	5.06526E-01	1.28692E-01	5.07331E-04
40	2.51781E-01	5.03227E-01	1.26703E-01	5.03395E-04
45	2.49758E-01	5.03027E-01	1.25635E-01	5.01268E-04
50	2.49875E-01	5.01331E-01	1.25270E-01	5.00541E-04
55	2.49204E-01	5.01918E-01	1.25080E-01	5.00161E-04
60	2.49652E-01	4.99840E-01	1.24786E-01	4.99572E-04
65	2.51867E-01	5.03111E-01	1.26717E-01	5.03422E-04
70	2.54094E-01	5.05034E-01	1.28326E-01	5.06609E-04
75	2.54665E-01	5.05704E-01	1.28785E-01	5.07515E-04
80	2.54982E-01	5.06091E-01	1.29044E-01	5.08025E-04
85	2.55342E-01	5.05256E-01	1.29013E-01	5.07963E-04
90	2.54811E-01	5.06006E-01	1.28936E-01	5.07811E-04
$\theta = 65$				
0	2.36926E-01	4.94597E-01	1.17183E-01	5.26573E-04
5	2.37499E-01	4.96242E-01	1.17857E-01	5.28084E-04
10	2.39374E-01	4.96879E-01	1.18940E-01	5.30506E-04
15	2.40780E-01	4.96869E-01	1.19636E-01	5.32055E-04
20	2.40468E-01	4.98258E-01	1.19815E-01	5.32453E-04
25	2.40468E-01	4.97343E-01	1.19595E-01	5.31964E-04
30	2.40267E-01	4.96881E-01	1.19384E-01	5.31494E-04
35	2.40419E-01	4.97585E-01	1.19629E-01	5.32040E-04
40	2.39205E-01	4.96821E-01	1.18842E-01	5.30287E-04
45	2.35503E-01	4.93484E-01	1.16217E-01	5.24399E-04
50	2.35934E-01	4.94405E-01	1.16647E-01	5.25367E-04
55	2.36293E-01	4.94898E-01	1.16941E-01	5.26029E-04
60	2.36661E-01	4.91162E-01	1.16239E-01	5.24447E-04
65	2.38936E-01	4.96053E-01	1.18525E-01	5.29580E-04
70	2.40013E-01	4.96319E-01	1.19123E-01	5.30914E-04
75	2.40869E-01	4.96361E-01	1.19558E-01	5.31882E-04
80	2.41032E-01	4.97668E-01	1.19954E-01	5.32763E-04
85	2.40816E-01	4.96998E-01	1.19685E-01	5.32165E-04
90	2.41009E-01	4.96828E-01	1.19740E-01	5.32286E-04

ψ	p_n	η	ε	$\sigma(\varepsilon)$
$\theta = 70$				
0	2.17044E-01	4.81073E-01	1.04414E-01	5.52526E-04
5	2.18405E-01	4.84559E-01	1.05830E-01	5.56262E-04
10	2.20971E-01	4.84792E-01	1.07125E-01	5.59655E-04
15	2.21677E-01	4.84701E-01	1.07447E-01	5.60494E-04
20	2.20923E-01	4.83517E-01	1.06820E-01	5.58857E-04
25	2.20920E-01	4.84845E-01	1.07112E-01	5.59620E-04
30	2.20947E-01	4.85374E-01	1.07242E-01	5.59961E-04
35	2.21383E-01	4.84030E-01	1.07156E-01	5.59736E-04
40	2.20606E-01	4.86025E-01	1.07220E-01	5.59903E-04
45	2.16476E-01	4.80450E-01	1.04006E-01	5.51445E-04
50	2.17109E-01	4.81394E-01	1.04515E-01	5.52795E-04
55	2.18715E-01	4.82372E-01	1.05502E-01	5.55399E-04
60	2.17168E-01	4.78924E-01	1.04007E-01	5.51448E-04
65	2.20177E-01	4.83452E-01	1.06445E-01	5.57874E-04
70	2.21144E-01	4.84255E-01	1.07090E-01	5.59561E-04
75	2.21530E-01	4.84278E-01	1.07282E-01	5.60065E-04
80	2.21448E-01	4.84755E-01	1.07348E-01	5.60236E-04
85	2.21252E-01	4.84149E-01	1.07119E-01	5.59639E-04
90	2.21650E-01	4.84151E-01	1.07312E-01	5.60143E-04
$\theta = 75$				
0	1.89214E-01	4.62198E-01	8.74544E-02	5.81290E-04
5	1.91810E-01	4.62377E-01	8.86885E-02	5.85377E-04
10	1.93477E-01	4.63513E-01	8.96792E-02	5.88637E-04
15	1.93338E-01	4.62649E-01	8.94476E-02	5.87877E-04
20	1.93304E-01	4.62543E-01	8.94114E-02	5.87758E-04
25	1.93240E-01	4.62674E-01	8.94072E-02	5.87744E-04
30	1.93057E-01	4.63860E-01	8.95514E-02	5.88218E-04
35	1.93529E-01	4.63654E-01	8.97305E-02	5.88806E-04
40	1.93376E-01	4.64526E-01	8.98281E-02	5.89126E-04
45	1.89844E-01	4.60834E-01	8.74865E-02	5.81397E-04
50	1.90243E-01	4.60852E-01	8.76739E-02	5.82019E-04
55	1.92234E-01	4.62518E-01	8.89116E-02	5.86113E-04
60	1.90481E-01	4.60001E-01	8.76214E-02	5.81844E-04
65	1.92098E-01	4.61305E-01	8.86157E-02	5.85137E-04
70	1.93427E-01	4.64327E-01	8.98133E-02	5.89077E-04
75	1.93630E-01	4.63947E-01	8.98340E-02	5.89145E-04
80	1.93687E-01	4.63853E-01	8.98423E-02	5.89172E-04
85	1.93458E-01	4.64187E-01	8.98006E-02	5.89036E-04
90	1.93461E-01	4.62415E-01	8.94592E-02	5.87915E-04

ψ	p_n	η	ε	$\sigma(\varepsilon)$
$\theta = 80$				
0	1.48122E-01	4.20102E-01	6.22263E-02	5.98621E-04
5	1.51067E-01	4.22458E-01	6.38195E-02	6.06236E-04
10	1.51203E-01	4.22831E-01	6.39333E-02	6.06776E-04
15	1.51404E-01	4.22521E-01	6.39713E-02	6.06956E-04
20	1.51327E-01	4.20754E-01	6.36714E-02	6.05532E-04
25	1.51327E-01	4.22202E-01	6.38905E-02	6.06573E-04
30	1.51220E-01	4.22551E-01	6.38982E-02	6.06609E-04
35	1.51375E-01	4.22150E-01	6.39029E-02	6.06632E-04
40	1.51198E-01	4.21390E-01	6.37134E-02	6.05732E-04
45	1.49307E-01	4.21808E-01	6.29789E-02	6.02230E-04
50	1.50329E-01	4.22767E-01	6.35542E-02	6.04974E-04
55	1.51155E-01	4.22248E-01	6.38249E-02	6.06261E-04
60	1.49814E-01	4.19383E-01	6.28294E-02	6.01515E-04
65	1.50367E-01	4.19822E-01	6.31274E-02	6.02939E-04
70	1.51231E-01	4.22343E-01	6.38713E-02	6.06482E-04
75	1.51424E-01	4.22954E-01	6.40454E-02	6.07308E-04
80	1.51345E-01	4.22868E-01	6.39989E-02	6.07087E-04
85	1.51474E-01	4.22214E-01	6.39544E-02	6.06876E-04
90	1.51435E-01	4.23316E-01	6.41048E-02	6.07589E-04
$\theta = 85$				
0	8.47926E-02	3.18205E-01	2.69814E-02	5.56396E-04
5	8.56718E-02	3.17723E-01	2.72199E-02	5.58850E-04
10	8.57015E-02	3.17036E-01	2.71705E-02	5.58343E-04
15	8.57228E-02	3.17254E-01	2.71959E-02	5.58604E-04
20	8.56746E-02	3.16940E-01	2.71537E-02	5.58170E-04
25	8.57128E-02	3.17738E-01	2.72342E-02	5.58997E-04
30	8.56706E-02	3.17871E-01	2.72322E-02	5.58977E-04
35	8.56918E-02	3.17503E-01	2.72074E-02	5.58722E-04
40	8.56883E-02	3.18192E-01	2.72653E-02	5.59316E-04
45	8.57004E-02	3.18907E-01	2.73305E-02	5.59984E-04
50	8.56641E-02	3.18098E-01	2.72496E-02	5.59155E-04
55	8.56600E-02	3.17466E-01	2.71941E-02	5.58586E-04
60	8.56824E-02	3.17577E-01	2.72108E-02	5.58757E-04
65	8.54542E-02	3.16237E-01	2.70238E-02	5.56833E-04
70	8.56680E-02	3.17590E-01	2.72073E-02	5.58721E-04
75	8.57062E-02	3.17763E-01	2.72343E-02	5.58998E-04
80	8.57170E-02	3.17518E-01	2.72167E-02	5.58818E-04
85	8.56901E-02	3.17433E-01	2.72009E-02	5.58655E-04
90	8.56870E-02	3.16938E-01	2.71575E-02	5.58209E-04

Appendix C

Cargo Detector Calculation Scripts and Codes

File Name	Description	Page
cgo.pl	Script for determining the optimum front, back, and radial polyethylene thicknesses for a cargo detector irradiated end-on	279
pcgo.pl	Script for determining the optimum front, back, and radial polyethylene thicknesses for a cargo detector irradiated from the side	283
crtspk.k.pl	Script for determining k_{eff} for a sphere of Pu as a function of the radius and ^{240}Pu content	289
RvsF.f90	Program written to extract the subcritical radii as a function of the ^{240}Pu content	291
crtspf.f.pl	Script for calculating the surface flux leaving a subcritical sphere as a function of the ^{240}Pu content	289

cgo.pl: Cargo Detector End-on Irradiation Optimization Script

```
#!/usr/bin/perl
$sdis=300; # distance of source from detector cm
$tcap=0.0020; # cap thickness in cm
$tdet=0.0100;
$rdet=0.315; # detector radius in cm

$nps = 1000000;
$dnps = 500000;

$dr=1; # radial poly thickness step
$df=1; # front poly thickness step
$db=1; # back poly thickness step

$RMIN=0; # minimum radial poly thickness
$FMIN=0; # minimum front poly thickness
$BMIN=0; # minimum back poly thickness

$RMAX=0; # maximum radial poly thickness
$FMAX=10; # maximum front poly thickness
$BMAX=10; # maximum back poly thickness

for($rthk=$RMIN;$rthk<=$RMAX;$rthk++)
{
  open(DATFIL,">datafile_`$rthk`");
  if($rthk==0)
  {
    $rp=0.000000001;
  }
  else
  {
    $rp=$rthk*$dr;
  }
  for($fthk=$FMIN;$fthk<=$FMAX;$fthk++)
  {
    if($fthk==0)
    {
      $fp=0.000000001;
    }
    else
    {
      $fp=$fthk*$df;
    }
    for($bthk=$BMIN;$bthk<=$BMAX;$bthk++)
    {
      if($bthk==0)
      {
        $bp=0.000000001;
      }
      else
      {
        $bp=$bthk*$db;
      }

      open(INFILE,">`$rthk`$fthk`$bthk`");

      print INFILE "CARGO DETECTOR INPUT FILE\n";
      print INFILE "c 34567890123456789012345678901234567890123456789012345678901234567890\n";
      print INFILE "c 1 2 3 4 5 6 7 8\n";
      print INFILE "c *****\n";
      print INFILE "c Cell Cards\n";
      print INFILE "c *****\n";
      print INFILE "1001 2 5.73e-2 -101 u=1\n";
      print INFILE "1002 3 -2.33 101 u=1\n";
    }
  }
}
```

```

print INFILE "c \n";
print INFILE "2001 0          -201 202 -203 204          lat=1 fill=1 u=2\n";
print INFILE "c \n";
print INFILE "3001 2  5.73e-2  -301 302 -303\n";
print INFILE "3002 0          -301 303 -304          fill=2\n";
print INFILE "c \n";
print INFILE "4001 1  -0.92   -301 -302 402\n";
print INFILE "4002 1  -0.92   -301 304 -403\n";
print INFILE "4003 1  -0.92   301 -401 402 -403\n";
print INFILE "c \n";
print INFILE "9991 0          -999 (401:-402:403)\n";
print INFILE "9992 0          999\n";
print INFILE "\n";
print INFILE "c *****\n";
print INFILE "c          Surface Cards\n";
print INFILE "c *****\n";
print INFILE "101 cy  0.0015\n";
print INFILE "c \n";
print INFILE "201 px  0.0025\n";
print INFILE "202 px -0.0025\n";
print INFILE "203 pz  0.0025\n";
print INFILE "204 pz -0.0025\n";
print INFILE "c \n";
print INFILE "301 cy  ",$rdet,"\n";
print INFILE "302 py  0.0000\n";
print INFILE "303 py  ",$tcap,"\n";
print INFILE "304 py  ",$tcap+$tdet,"\n";
print INFILE "c \n";
print INFILE "401 cy  ",$rp+$rdet,"\n";
print INFILE "402 py  ",-$fp,"\n";
print INFILE "403 py  ",$bp+$tcap+$tdet,"\n";
print INFILE "c \n";
print INFILE "999 so  350\n";
print INFILE "\n";
print INFILE "c *****\n";
print INFILE "c          Data Cards\n";
print INFILE "c *****\n";
print INFILE "imp:n 1 1 1 1 1 1 1 1 0\n";
print INFILE "c \n";
print INFILE "mode n\n";
print INFILE "c \n";
print INFILE "rand gen=2 stride=418439\n";
print INFILE "c \n";
print INFILE "nps ",$nps,"\n";
print INFILE "c \n";
print INFILE "sdef pos=0 ",-$sdis," 0 \n";
print INFILE "    erg=d1 \n";
print INFILE "    vec=0 1 0\n";
print INFILE "    dir=d2\n";
print INFILE "sp1 -3 0.799 4.903\n";


```

```

print INFILE "c          0.5  1.5  2.5  3.5  4.5  5.5  6.5  7.5  8.5  9.5\n";
print INFILE "c wwg  4  0  0  4j  0\n";
print INFILE "wwp:n  5  3  5  0  -1  0\n";
print INFILE "c \n";
print INFILE "m1  1001.66c  0.666667\n";
print INFILE "      6000.66c  0.333333\n";
print INFILE "c \n";
print INFILE "m2  3006.66c  1.000000\n";
print INFILE "c \n";
print INFILE "m3  14028.66c  0.922297\n";
print INFILE "      14029.66c  0.046832\n";
print INFILE "      14030.66c  0.030872\n";

```

```
close(INFILE);
```

```
# loop until statistical checks passed
```

```

$PASSED = 0;
$iter = 0;
while(not $PASSED)
{
  if(not -e "runtpe")
  {
    system "mpirun -n 11 mcnp5.mpi i=$rthk$fthk$bthk wwinp=cgowim2";
  }
  else
  {
    open(CFILE,">cont");
    print CFILE "continue\n";
    print CFILE "nps ",$nps + $iter*$dnps," \n";
    print CFILE " \n";
    close(CFILE);

    system "mpirun -n 11 mcnp5.mpi c i=cont";
  }

  open(OUTFIL,"<outp");

  while($line=<OUTFIL>)
  {
    if($line =~ /\^smultiplier\sbin:\s+-1\.00000E\+00\s+2\s+105/)
    {
      $line=<OUTFIL>;
      if($line =~ /\^s+(\d\.\d+E[+-]\d+)\s(\d\.\d+)/)
      {
        $val = $1*$1;
        $err = $1*$2;
      }
    }

    if($line =~ /\^spassed?(s+(yes|no)){10}/)
    {
      print $line;
      if($line =~ /\^spassed?(s+yes){10}/)
      {
        $PASSED = 1;
        system "rm outp runtpe $rthk$fthk$bthk";
      }
      else
      {
        system "rm outp";
        $iter+=1
      }
    }
  }
}

print DATFIL $fp,"\t\t",$bp,"\t\t",$val,"\t\t",$err,"\n";

```

```
    }  
    print DATFIL "\n";  
  }  
  close(DATFIL);  
}
```

pcgo.pl: Cargo Detector Side Irradiation Optimization Script

```
#!/usr/bin/perl
$sdis=300; # distance of source from detector cm
$tcap=0.0020; # cap thickness in cm
$tdet=0.0100;
$rdet=0.315; # detector radius in cm

$nps = 2500000;
$dnps = 500000;

$dr=1; # radial poly thickness step
$df=1; # front poly thickness step
$db=1; # back poly thickness step

$RMIN=10; # minimum radial poly thickness
$FMIN=10; # minimum front poly thickness
$BMIN=10; # minimum back poly thickness

$RMAX=10; # maximum radial poly thickness
$FMAX=10; # maximum front poly thickness
$BMAX=10; # maximum back poly thickness

for($rthk=$RMIN;$rthk<=$RMAX;$rthk++)
{
  open(DATFIL,">datafile_{$rthk}");
  if($rthk==0)
  {
    $rp=0.000000001;
  }
  else
  {
    $rp=$rthk*$dr;
  }
  for($fthk=$FMIN;$fthk<=$FMAX;$fthk++)
  {
    if($fthk==0)
    {
      $fp=0.000000001;
    }
    else
    {
      $fp=$fthk*$df;
    }
    for($bthk=$BMIN;$bthk<=$BMAX;$bthk++)
    {
      if($bthk==0)
      {
        $bp=0.000000001;
      }
      else
      {
        $bp=$bthk*$db;
      }

      open(INFILE,">{$rthk}{$fthk}{$bthk}");

      print INFILE "CARGO DETECTOR INPUT FILE\n";
      print INFILE "c 34567890123456789012345678901234567890123456789012345678901234567890\n";
      print INFILE "c 1 2 3 4 5 6 7 8\n";
      print INFILE "c *****\n";
      print INFILE "c Cell Cards\n";
      print INFILE "c *****\n";
      print INFILE "1001 2 5.73e-2 -101 u=1\n";
      print INFILE "1002 3 -2.33 101 u=1\n";
    }
  }
}
```

```

print INFILE "c \n";
print INFILE "2001 0          -201 202 -203 204          lat=1 fill=1 u=2\n";
print INFILE "c \n";
print INFILE "3001 2  5.73e-2  -301 302 -303\n";
print INFILE "3002 0          -301 303 -304          fill=2\n";
print INFILE "c \n";
print INFILE "4001 1  -0.92   -301 -302 402\n";
print INFILE "4002 1  -0.92   -301 304 -403\n";
print INFILE "4003 1  -0.92   301 -401 402 -403\n";
print INFILE "c \n";
print INFILE "9991 0          -999 (401:-402:403)\n";
print INFILE "9992 0          999\n";
print INFILE "\n";
print INFILE "c *****\n";
print INFILE "c          Surface Cards\n";
print INFILE "c *****\n";
print INFILE "101 cy  0.0015\n";
print INFILE "c \n";
print INFILE "201 px  0.0025\n";
print INFILE "202 px -0.0025\n";
print INFILE "203 pz  0.0025\n";
print INFILE "204 pz -0.0025\n";
print INFILE "c \n";
print INFILE "301 cy  ",$rdet,"\n";
print INFILE "302 py  0.0000\n";
print INFILE "303 py  ",$tcap,"\n";
print INFILE "304 py  ",$tcap+$tdet,"\n";
print INFILE "c \n";
print INFILE "401 cy  ",$rp+$rdet,"\n";
print INFILE "402 py  ",-$fp,"\n";
print INFILE "403 py  ",$bp+$tcap+$tdet,"\n";
print INFILE "c \n";
print INFILE "999 so  350\n";
print INFILE "\n";
print INFILE "c *****\n";
print INFILE "c          Data Cards\n";
print INFILE "c *****\n";
print INFILE "imp:n 1 1 1 1 1 1 1 1 0\n";
print INFILE "c \n";
print INFILE "mode n\n";
print INFILE "c \n";
print INFILE "rand gen=2 stride=418439\n";
print INFILE "c \n";
print INFILE "nps ",$nps,"\n";
print INFILE "c \n";
print INFILE "sdef pos=0 0 ", -$sdis,"\n";
print INFILE "      erg=d1 \n";
print INFILE "      vec=0 0 1\n";
print INFILE "      dir=d2\n";
print INFILE "sp1 -3 0.799 4.903\n";
$r1 = sqrt( ($bp+$tcap+$tdet)**2 + ($rp+$rdet)**2 );
$r2 = sqrt( ($fp)**2 + ($rp+$rdet)**2 );
if($r1>=$r2)
{
  $theta = atan2($r1,$sdis-$rp-$rdet);
}
else{
  $theta = atan2($r2,$sdis-$rp-$rdet);
}
}
$costheta = cos($theta);
$fsa = 0.5*(1-$costheta);
print INFILE "si2 -1 ",$costheta," 1\n";
print INFILE "sp2  0 ",1-$fsa," ",$fsa,"\n";
print INFILE "sb2  0 0 1\n";
print INFILE "c \n";
print INFILE "f4:n (1001 3001)\n";
print INFILE "fm4 -1 2 105\n";
print INFILE "sd4  1\n";

```

```

print INFIL "c \n";
print INFIL "mesh geom=xyz ref= 0,0,-300 origin=-11.5,-11.5,-300.5\n";
print INFIL "    imesh= -10.5 -9.5 -8.5 -7.5 -6.5 -5.5 -4.5 -3.5 -2.5 -1.5 -0.5\n";
print INFIL "          0.5 1.5 2.5 3.5 4.5 5.5 6.5 7.5 8.5\n";
print INFIL "          9.5 10.5 11.5\n";
print INFIL "    jmesh= -10.5 -9.5 -8.5 -7.5 -6.5 -5.5 -4.5 -3.5 -2.5 -1.5 -0.5\n";
print INFIL "          0.5 1.5 2.5 3.5 4.5 5.5 6.5 7.5 8.5\n";
print INFIL "          9.5 10.5 11.5\n";
print INFIL "    kmesh= -200.5 -100.5 -50.5 -25.5 -11.5 -10.5 -9.5 \n";
print INFIL "          -8.5 -7.5 -6.5 -5.5 -4.5 -3.5 -2.5 -1.5 -0.5\n";
print INFIL "          0.5 1.5 2.5 3.5 4.5 5.5 6.5 7.5 8.5\n";
print INFIL "          9.5 10.5 11.5\n";
print INFIL "wvg 4 0 0 4j 0\n";
print INFIL "c wwp:n 5 3 5 0 -1 0\n";
print INFIL "c \n";
print INFIL "m1 1001.66c 0.666667\n";
print INFIL "    6000.66c 0.333333\n";
print INFIL "c \n";
print INFIL "m2 3006.66c 1.000000\n";
print INFIL "c \n";
print INFIL "m3 14028.66c 0.922297\n";
print INFIL "    14029.66c 0.046832\n";
print INFIL "    14030.66c 0.030872\n";

close(INFIL);

# run mcnp in analog and generate ww
system "mpirun -n 25 mcnp5.mpi i=$rthk$fthk$bthk";

# check if all tests are passed
$PASSED = 0;

open(OUTFIL,"<outp");

while($line=<OUTFIL>)
{
  if($line =~ /\smultiplier\sbin:\s+-1\.00000E\+00\s+2\s+105/)
  {
    $line=<OUTFIL>;
    if($line =~ /\s+(\d\.\d+E[+-]\d+)\s(\d\.\d+)/)
    {
      $val = sprintf("%6.4E",$1*1);
      $err = sprintf("%6.4E",$1*$2);
    }
  }

  if($line =~ /\spassed\?(\s+(yes|no)){10}/)
  {
    print $line;
    if($line =~ /\spassed\?(\s+yes){10}/)
    {
      $PASSED = 1;
      system "rm outp runtpe $rthk$fthk$bthk";
    }
    else
    {
      system "rm outp runtpe $rthk$fthk$bthk";
      system "mv wwout wwinp";
    }
  }
}

# if not passed reprint the input file and use the weight windows
print "*****\n";
print "*          W-W NEEDED          *\n";
print "*****\n";

if(not $PASSED)

```



```

{
open(INFILE,">$rthk$fthk$bthk");

print INFILE "CARGO DETECTOR INPUT FILE\n";
print INFILE "c 34567890123456789012345678901234567890123456789012345678901234567890\n";
print INFILE "c      1      2      3      4      5      6      7      8\n";
print INFILE "c *****\n";
print INFILE "c
                                Cell Cards\n";
print INFILE "c *****\n";
print INFILE "1001 2 5.73e-2 -101                                u=1\n";
print INFILE "1002 3 -2.33      101                                u=1\n";
print INFILE "c \n";
print INFILE "2001 0                                -201 202 -203 204      lat=1 fill=1 u=2\n";
print INFILE "c \n";
print INFILE "3001 2 5.73e-2 -301 302 -303\n";
print INFILE "3002 0                                -301 303 -304      fill=2\n";
print INFILE "c \n";
print INFILE "4001 1 -0.92      -301 -302 402\n";
print INFILE "4002 1 -0.92      -301 304 -403\n";
print INFILE "4003 1 -0.92      301 -401 402 -403\n";
print INFILE "c \n";
print INFILE "9991 0                                -999 (401:-402:403)\n";
print INFILE "9992 0                                999\n";
print INFILE "\n";
print INFILE "c *****\n";
print INFILE "c
                                Surface Cards\n";
print INFILE "c *****\n";
print INFILE "101 cy 0.0015\n";
print INFILE "c \n";
print INFILE "201 px 0.0025\n";
print INFILE "202 px -0.0025\n";
print INFILE "203 pz 0.0025\n";
print INFILE "204 pz -0.0025\n";
print INFILE "c \n";
print INFILE "301 cy ",$rdet,"\n";
print INFILE "302 py 0.0000\n";
print INFILE "303 py ",$tcap,"\n";
print INFILE "304 py ",$tcap+$tdet,"\n";
print INFILE "c \n";
print INFILE "401 cy ",$rp+$rdet,"\n";
print INFILE "402 py ",-$fp,"\n";
print INFILE "403 py ",$bp+$tcap+$tdet,"\n";
print INFILE "c \n";
print INFILE "999 so 350\n";
print INFILE "\n";
print INFILE "c *****\n";
print INFILE "c
                                Data Cards\n";
print INFILE "c *****\n";
print INFILE "imp:n 1 1 1 1 1 1 1 1 1 0\n";
print INFILE "c \n";
print INFILE "mode n\n";
print INFILE "c \n";
print INFILE "rand gen=2 stride=418439\n";
print INFILE "c \n";
print INFILE "nps ",$nps,"\n";
print INFILE "c \n";
print INFILE "sdef pos=0 0 ",-$sdis,"\n";
print INFILE "      erg=d1 \n";
print INFILE "      vec=0 0 1\n";
print INFILE "      dir=d2\n";
print INFILE "sp1 -3 0.799 4.903\n";
$r1 = sqrt( ($bp+$tcap+$tdet)**2 + ($rp+$rdet)**2 );
$r2 = sqrt( ($fp)**2 + ($rp+$rdet)**2 );
if($r1>=$r2)
{
    $theta = atan2($r1,$sdis-$rp-$rdet);
}
else{

```

```

    $theta = atan2($r2,$sdis-$rp-$rdet);
}
$costheta = cos($theta);
$fsa = 0.5*(1-$costheta);
print INFILE "si2 -1 ", $costheta, " 1\n";
print INFILE "sp2 0 ", 1-$fsa, " ", $fsa, "\n";
print INFILE "sb2 0 0 1\n";
print INFILE "c \n";
print INFILE "f4:n (1001 3001)\n";
print INFILE "fm4 -1 2 105\n";
print INFILE "sd4 1\n";
print INFILE "c \n";
print INFILE "c mesh geom=xyz ref= 0,0,-300 origin=-11.5,-11.5,-300.5\n";
print INFILE "c imesh= -10.5 -9.5 -8.5 -7.5 -6.5 -5.5 -4.5 -3.5 -2.5 -1.5 -0.5\n";
print INFILE "c 0.5 1.5 2.5 3.5 4.5 5.5 6.5 7.5 8.5\n";
print INFILE "c 9.5 10.5 11.5\n";
print INFILE "c jmesh= -10.5 -9.5 -8.5 -7.5 -6.5 -5.5 -4.5 -3.5 -2.5 -1.5 -0.5\n";
print INFILE "c 0.5 1.5 2.5 3.5 4.5 5.5 6.5 7.5 8.5\n";
print INFILE "c 9.5 10.5 11.5\n";
print INFILE "c kmesh= -200.5 -100.5 -50.5 -25.5 -11.5 -10.5 -9.5 \n";
print INFILE "c -8.5 -7.5 -6.5 -5.5 -4.5 -3.5 -2.5 -1.5 -0.5\n";
print INFILE "c 0.5 1.5 2.5 3.5 4.5 5.5 6.5 7.5 8.5\n";
print INFILE "c 9.5 10.5 11.5\n";
print INFILE "c wwg 4 0 0 4j 0\n";
print INFILE "wvp:n 5 3 5 0 -1 0\n";
print INFILE "c \n";
print INFILE "m1 1001.66c 0.666667\n";
print INFILE " 6000.66c 0.333333\n";
print INFILE "c \n";
print INFILE "m2 3006.66c 1.000000\n";
print INFILE "c \n";
print INFILE "m3 14028.66c 0.922297\n";
print INFILE " 14029.66c 0.046832\n";
print INFILE " 14030.66c 0.030872\n";

close(INFILE);

# loop until statistical checks passed
$PASSED = 0;
while(not $PASSED)
{
    if(not -e "runtp")
    {
        system "mpirun -n 25 mcnp5.mpi i=$rthk$ftk$bthk";
    }
    else
    {
        open(CFILE, ">cont");
        print CFILE "continue\n";
        print CFILE "nps ", $nps + $iter*$dnps, "\n";
        print CFILE "\n";
        close(CFILE);

        system "mpirun -n 25 mcnp5.mpi c i=cont";
    }

    open(OUTFIL, "<outp");

    while($line=<OUTFIL>)
    {
        if($line =~ /\smultiplier\sbin:\s+-1\.00000E+00\s+2\s+105/)
        {
            $line=<OUTFIL>;
            if($line =~ /\s+(\d\.\d+E[+-]\d+)\s+(\d\.\d+)/)
            {
                $val = sprintf("%6.4E", $1*1);
                $err = sprintf("%6.4E", $1*$2);
            }
        }
    }
}

```

```

    }

    if($line =~ /\spassed\?(s+(yes|no)){10}/)
    {
        print $line;
        if($line =~ /\spassed\?(s+yes){10}/)
        {
            $PASSED = 1;
            system "rm outp runtpe $rthk$fthk$bthk";
        }
        else
        {
            system "rm outp";
        }
    }
}
}
}

# print results
    print DATFIL $fp, "\t\t", $bp, "\t\t", $val, "\t\t", $err, "\n";

}

    print DATFIL "\n";

}

close(DATFIL);

}

```

crtspk.pl: Criticality Calculation Script

```
#!/usr/bin/perl

$RMIN = 1;
$RMAX = 20;
$dr = 0.5;

$CMIN = 0;
$CMAX = 20;
$dc = 0.01;

open(KFILE,">koutput");

for($scint=$CMIN;$scint<=$CMAX;$scint++)
{
  if($scint != 0)
  {
    $f240 = $scint * $dc;
  }
  if($scint == 0)
  {
    $f240 = 1e-30;
  }
  for($rint=$RMIN;$rint<=$RMAX;$rint++)
  {
    $r = $rint * $dr;

    open (INFILE,">cs_-$scint-$rint");

    print INFILE "Critical Plutonium Shere input file\n";
    print INFILE "c 34567890123456789012345678901234567890123456789012345678901234567890\n";
    print INFILE "c      1      2      3      4      5      6      7      8\n";
    print INFILE "c *****\n";
    print INFILE "c                      Cell Cards\n";
    print INFILE "c *****\n";
    print INFILE "1000 1 -16.9 -100\n";
    print INFILE "c \n";
    print INFILE "9999 0          100\n";
    print INFILE "\n";
    print INFILE "c *****\n";
    print INFILE "c                      Surface Cards\n";
    print INFILE "c *****\n";
    print INFILE "100 so ",$r,"\n";
    print INFILE "\n";
    print INFILE "c *****\n";
    print INFILE "c                      Data Cards\n";
    print INFILE "c *****\n";
    print INFILE "imp:n 1 0\n";
    print INFILE "c \n";
    print INFILE "mode n\n";
    print INFILE "c \n";
    print INFILE "kcode 1500 1 30 900 \n";
    print INFILE "sdef pos=0 0 0 \n";
    print INFILE "  par=1\n";
    print INFILE "  erg=d1\n";
    print INFILE "  rad=d2\n";
    print INFILE "sp1 -3 0.799 4.903\n";
    print INFILE "si2 0 ",$r,"\n";
    print INFILE "sp2 -21 2\n";
    print INFILE "c \n";
    print INFILE "m1 94239.66c ",1-$f240,"\n";
    print INFILE " 94240.66c ",$f240,"\n";

    close(INFILE);

    system "mcp5 i=cs_-$scint-$rint";
  }
}
```

```

open(OUTFIL,"<outp");

while($line=<OUTFIL>)
{
  if($line =~ /^s\|s\sthe\sfinal\sestimated\scombined\scollision\/absorption\/track-length\skeff
    \s=\s(\d\.\d+)\swith\san\sestimated\sstandard\sdeviation\s(\d\.\d+)\s+\|\/)
  {
    $k = $1*1;
    $kerr = $2*1;
  }
}

system "rm cs_$scint-$rint outp runtpe srctp";

print KFILE $f240,"\t\t",$r,"\t\t",$k,"\t\t",$kerr,"\n";
}
print KFILE "\n";
}

```

RvsF.f90: Critical Radius Interpolation

```
program RvsF
  use spline_mod
  implicit none

  character(len=80) :: line

  real :: error
  real, dimension(20) :: f, r, k, err, r2s
  real, dimension(21) :: fs, rs
  integer :: i, j, l, ios

  logical :: eof = .false.

  open(unit=1,status="old",file="koutput")

  j=0
  do while( .not. eof )
    j=j+1
    read(1,'(a80)', iostat=ios) line

    if (ios == -1)then
      eof = .true.
      cycle
    endif

    i=0
    do while(line /= "")
      i = i + 1
      read(line,*) f(i), r(i), k(i), err(i)

      read(1,'(a80)',iostat=ios)line
      if(ios== -1) eof=.true.
    enddo

    fs(j) = f(1)

    call spline(k,r,0.0,0.0,r2s)
    call splint(k,r,r2s,0.9,rs(j))

  enddo

  do l=1,j-1
    write(*,'(2(2x,g12.5))') fs(l), rs(l)
  enddo

  write(*,*) '# ', (fs(l), l=1,j-1)
  write(*,*)
  write(*,*) '# ', (rs(l), l=1,j-1)

end program RvsF
```

crtsp_h.f90: Subcritical Flux Calculation Script

```
#!/usr/bin/perl

$pi = 3.14159265359;

$RMIN = 0;
$RMAX = 20;

@cdat = (1.E-30, 0.01, 0.02, 0.03, 0.04, 0.05, 0.06, 0.07, 0.08, 0.09,
         0.1, 0.11, 0.12, 0.13, 0.14, 0.15, 0.16, 0.17, 0.18, 0.19, 0.2);

open(FFILE,">foutput");
open(SFILE,">soutput");

for($rint=$RMIN;$rint<=$RMAX;$rint++)
{
    $f240 = $cdat[$rint];
    $r = 1.4617*$f240+5.14113;

    open (INFILE,">csf_$rint");

    print INFILE "Critical Plutonium Sphere input file\n";
    print INFILE "c 34567890123456789012345678901234567890123456789012345678901234567890\n";
    print INFILE "c      1      2      3      4      5      6      7      8\n";
    print INFILE "c *****\n";
    print INFILE "c
        Cell Cards\n";
    print INFILE "c *****\n";
    print INFILE "1000 1 -16.9 -100\n";
    print INFILE "c \n";
    print INFILE "9999 0      100\n";
    print INFILE "\n";
    print INFILE "c *****\n";
    print INFILE "c
        Surface Cards\n";
    print INFILE "c *****\n";
    print INFILE "100 so ",$r,"\n";
    print INFILE "\n";
    print INFILE "c *****\n";
    print INFILE "c
        Data Cards\n";
    print INFILE "c *****\n";
    print INFILE "imp:n 1 0\n";
    print INFILE "c \n";
    print INFILE "mode n\n";
    print INFILE "c \n";
    print INFILE "nps 5000000\n";
    print INFILE "c \n";
    print INFILE "sdef pos=0 0 0 \n";
    print INFILE "      par=1\n";
    print INFILE "      erg=d1\n";
    print INFILE "      rad=d2\n";
    print INFILE "nonu\n";
    print INFILE "sp1 -3 0.799 4.903\n";
    print INFILE "si2 0 ",$r,"\n";
    print INFILE "sp2 -21 2\n";
    print INFILE "c \n";
    print INFILE "f2:n 100\n";
    print INFILE "e2 ";
    $j=0;
    for ($i=0;$i<=100;$i++)
    {
        $j+=1;
        print INFILE 10*(-3+$i/100*4)," ";
        if($j==3 || $i==100)
        {
            print INFILE "\n";
            $j=0;
            if($i!=100)

```

```

    {
        print INFILE "      ";
    }
}
print INFILE "c \n";
print INFILE "m1  94239.66c  ",1-$f240,"\n";
print INFILE "      94240.66c  ",$f240,"\n";

close(INFILE);

system "mpirun -n 25 mcnp5.mpi i=csf_$rint";

open(OUTFIL,"<outp");

while($line=<OUTFIL>)
{
    if($line =~ /\ssurface\s+100/)
    {
        while($line=<OUTFIL>)
        {
            if($line =~ /\s+(\d\.\d+E[+-]\d+)\s+(\d\.\d+E[+-]\d+)\s+(\d\.\d+)/)
            {
                $energy = $1*$1;
                $f = $2*$1*(4.0/3.0*$pi*$r*$r*$r)*16.9*(920*$f240+2.2e-2*(1-$f240));
                $ferr = $2*$3*(4.0/3.0*$pi*$r*$r*$r)*16.9*(920*$f240+2.2e-2*(1-$f240));
                print SFILE $f240,"\t\t",$r,"\t\t",$energy,"\t\t",$f,"\t\t",$ferr,"\n";
            }
            if($line =~ /\s+total\s+(\d\.\d+E[+-]\d+)\s+(\d\.\d+)/)
            {
                $f = $1*$1*(4.0/3.0*$pi*$r*$r*$r)*16.9*(920*$f240+2.2e-2*(1-$f240));
                $ferr = $1*$2*(4.0/3.0*$pi*$r*$r*$r)*16.9*(920*$f240+2.2e-2*(1-$f240));
                print FFILE $f240,"\t\t",$r,"\t\t",$f,"\t\t",$ferr,"\n";
            }
        }
    }
}
print SFILE "\n";

system "rm csf_$rint outp runtpe";
}

```


Appendix D

Cargo Detector Tabulated Data

Description	Page
End-on irradiation for 1 cm radial poly. thck.	296
End-on irradiation for 2 cm radial poly. thck.	300
End-on irradiation for 3 cm radial poly. thck.	304
End-on irradiation for 4 cm radial poly. thck.	308
End-on irradiation for 5 cm radial poly. thck.	312
End-on irradiation for 6 cm radial poly. thck.	316
End-on irradiation for 7 cm radial poly. thck.	320
End-on irradiation for 8 cm radial poly. thck.	324
End-on irradiation for 9 cm radial poly. thck.	328
End-on irradiation for 10 cm radial poly. thck.	332
Side irradiation for 1 cm radial poly. thck.	336
Side irradiation for 2 cm radial poly. thck.	340
Side irradiation for 3 cm radial poly. thck.	344
Side irradiation for 4 cm radial poly. thck.	348
Side irradiation for 5 cm radial poly. thck.	352
Side irradiation for 6 cm radial poly. thck.	356
Side irradiation for 7 cm radial poly. thck.	360
Side irradiation for 8 cm radial poly. thck.	364
Side irradiation for 9 cm radial poly. thck.	368
Side irradiation for 10 cm radial poly. thck.	372
α -phase criticality values	376
δ -phase criticality values	387

Description	Page
α -phase Pu sphere flux	398
δ -phase Pu sphere flux	399

Table D.1. End-on irradiation for 1 cm radial poly. thck.

Back Poly. Thck. (cm)	Detector Resp.	Relative Error
Front Poly. Thck. = 1 cm		
1	1.6108E-10	7.1035E-12
2	2.1410E-10	8.1571E-12
3	2.5004E-10	1.0227E-11
4	2.5700E-10	1.0357E-11
5	2.6072E-10	1.0429E-11
6	2.6216E-10	1.0460E-11
7	2.6216E-10	1.0460E-11
8	2.6217E-10	1.0460E-11
9	2.6217E-10	1.0460E-11
10	2.6217E-10	1.0460E-11
Front Poly. Thck. = 2 cm		
1	2.0626E-10	8.7454E-12
2	2.3723E-10	7.4965E-12
3	2.6884E-10	1.0458E-11
4	2.7165E-10	9.8881E-12
5	2.7184E-10	9.8676E-12
6	2.7189E-10	9.8695E-12
7	2.7189E-10	9.8696E-12
8	2.7190E-10	9.8699E-12
9	2.7190E-10	9.8699E-12
10	2.7190E-10	9.8699E-12
Front Poly. Thck. = 3 cm		
1	1.8312E-10	6.2993E-12
2	2.1922E-10	6.7519E-12
3	2.3396E-10	7.1358E-12
4	2.3837E-10	7.2227E-12
5	2.3872E-10	7.2332E-12
6	2.3898E-10	7.2173E-12
7	2.3907E-10	7.2200E-12
8	2.3908E-10	7.2201E-12
9	2.3908E-10	7.2201E-12
10	2.3908E-10	7.2201E-12

Back Poly. Thck. (cm)	Detector Resp.	Relative Error
Front Poly. Thck. = 4 cm		
1	1.5823E-10	7.9908E-12
2	1.8690E-10	8.9340E-12
3	1.9658E-10	9.1412E-12
4	1.9933E-10	9.1690E-12
5	2.0004E-10	9.1817E-12
6	2.0022E-10	9.1901E-12
7	2.0022E-10	9.1903E-12
8	2.0022E-10	9.1903E-12
9	2.0022E-10	9.1903E-12
10	2.0022E-10	9.1903E-12
Front Poly. Thck. = 5 cm		
1	1.2029E-10	6.5801E-12
2	1.3719E-10	7.1339E-12
3	1.4229E-10	7.2143E-12
4	1.4334E-10	7.2386E-12
5	1.4359E-10	7.2511E-12
6	1.4359E-10	7.2515E-12
7	1.4361E-10	7.2525E-12
8	1.4361E-10	7.2526E-12
9	1.4361E-10	7.2526E-12
10	1.4361E-10	7.2526E-12
Front Poly. Thck. = 6 cm		
1	9.5686E-11	6.2100E-12
2	1.0715E-10	6.5253E-12
3	1.0952E-10	6.5928E-12
4	1.1072E-10	6.6099E-12
5	1.1072E-10	6.6102E-12
6	1.1073E-10	6.6106E-12
7	1.1073E-10	6.6106E-12
8	1.1073E-10	6.6107E-12
9	1.1073E-10	6.6107E-12
10	1.1073E-10	6.6107E-12

Back Poly. Thck. (cm)	Detector Resp.	Relative Error
Front Poly. Thck. = 7 cm		
1	7.0076E-11	5.4099E-12
2	7.5197E-11	5.5195E-12
3	7.9450E-11	5.8475E-12
4	7.9824E-11	5.8511E-12
5	7.9925E-11	5.8505E-12
6	7.9929E-11	5.8508E-12
7	7.9930E-11	5.8509E-12
8	7.9930E-11	5.8509E-12
9	7.9930E-11	5.8509E-12
10	7.9930E-11	5.8509E-12
Front Poly. Thck. = 8 cm		
1	4.5399E-11	4.4446E-12
2	5.1821E-11	4.9696E-12
3	5.2873E-11	5.0017E-12
4	5.3384E-11	5.0234E-12
5	5.3619E-11	5.0241E-12
6	5.3620E-11	5.0242E-12
7	5.3620E-11	5.0242E-12
8	5.3620E-11	5.0242E-12
9	5.3620E-11	5.0242E-12
10	5.3620E-11	5.0242E-12
Front Poly. Thck. = 9 cm		
1	2.4269E-11	2.0483E-12
2	2.6508E-11	2.3327E-12
3	2.8334E-11	2.4990E-12
4	2.9096E-11	2.5546E-12
5	2.9424E-11	2.5628E-12
6	2.9427E-11	2.5631E-12
7	2.9427E-11	2.5631E-12
8	2.9427E-11	2.5631E-12
9	2.9427E-11	2.5631E-12
10	2.9427E-11	2.5631E-12

Back Poly. Thck. (cm)	Detector Resp.	Relative Error
Front Poly. Thck. = 10 cm		
1	2.1436E-11	2.0021E-12
2	2.2863E-11	2.0897E-12
3	2.3558E-11	2.1131E-12
4	2.3899E-11	2.1390E-12
5	2.3904E-11	2.1395E-12
6	2.3905E-11	2.1395E-12
7	2.3905E-11	2.1395E-12
8	2.3905E-11	2.1395E-12
9	2.3905E-11	2.1395E-12
10	2.3905E-11	2.1395E-12

Table D.2. End-on irradiation for 2 cm radial poly. thck.

Back Poly. Thck. (cm)	Detector Resp.	Relative Error
Front Poly. Thck. = 1 cm		
1	5.7606E-10	1.7916E-11
2	1.1656E-09	4.2661E-11
3	1.4627E-09	4.7537E-11
4	1.6253E-09	4.9573E-11
5	1.7249E-09	5.1920E-11
6	1.7536E-09	5.2256E-11
7	1.7610E-09	5.2479E-11
8	1.7657E-09	5.2440E-11
9	1.7659E-09	5.2448E-11
10	1.7659E-09	5.2448E-11
Front Poly. Thck. = 2 cm		
1	1.0820E-09	3.8304E-11
2	1.6541E-09	4.7969E-11
3	2.0101E-09	5.3870E-11
4	2.1205E-09	3.7108E-11
5	2.1812E-09	3.7734E-11
6	2.2015E-09	3.7865E-11
7	2.2089E-09	3.7993E-11
8	2.2093E-09	3.7999E-11
9	2.2097E-09	3.7785E-11
10	2.2114E-09	3.7815E-11
Front Poly. Thck. = 3 cm		
1	1.3992E-09	4.3796E-11
2	1.9204E-09	5.2042E-11
3	2.1640E-09	5.5399E-11
4	2.2744E-09	5.6859E-11
5	2.3135E-09	5.7374E-11
6	2.3217E-09	5.7579E-11
7	2.3265E-09	5.7465E-11
8	2.3268E-09	5.7471E-11
9	2.3279E-09	5.7500E-11
10	2.3282E-09	5.7505E-11

Back Poly. Thck. (cm)	Detector Resp.	Relative Error
Front Poly. Thck. = 4 cm		
1	1.4804E-09	4.3819E-11
2	1.9110E-09	4.7775E-11
3	2.1312E-09	5.0723E-11
4	2.2243E-09	5.1826E-11
5	2.2621E-09	5.2480E-11
6	2.2723E-09	5.2490E-11
7	2.2717E-09	4.7024E-11
8	2.2730E-09	4.7050E-11
9	2.2782E-09	5.2626E-11
10	2.2739E-09	4.7070E-11
Front Poly. Thck. = 5 cm		
1	1.2895E-09	4.3584E-11
2	1.6618E-09	4.9023E-11
3	1.8240E-09	5.1073E-11
4	1.8875E-09	5.1719E-11
5	1.9154E-09	5.2100E-11
6	1.9296E-09	5.2291E-11
7	1.9329E-09	5.2382E-11
8	1.9329E-09	5.2382E-11
9	1.9329E-09	5.2382E-11
10	1.9329E-09	5.2382E-11
Front Poly. Thck. = 6 cm		
1	1.1068E-09	4.1504E-11
2	1.3978E-09	4.7105E-11
3	1.5133E-09	4.4794E-11
4	1.5663E-09	4.5737E-11
5	1.5868E-09	4.6018E-11
6	1.5927E-09	4.6188E-11
7	1.5936E-09	4.6214E-11
8	1.5943E-09	4.6234E-11
9	1.5947E-09	4.6246E-11
10	1.5947E-09	4.6246E-11

Back Poly. Thck. (cm)	Detector Resp.	Relative Error
Front Poly. Thck. = 7 cm		
1	8.2340E-10	3.3265E-11
2	1.0575E-09	3.9022E-11
3	1.1412E-09	4.0400E-11
4	1.1717E-09	4.1009E-11
5	1.1815E-09	4.0999E-11
6	1.1844E-09	4.1100E-11
7	1.1881E-09	4.1226E-11
8	1.1881E-09	4.1226E-11
9	1.1881E-09	4.1226E-11
10	1.1881E-09	4.1226E-11
Front Poly. Thck. = 8 cm		
1	6.6387E-10	3.2264E-11
2	8.3031E-10	3.4707E-11
3	8.7794E-10	3.5557E-11
4	8.7964E-10	3.6681E-11
5	8.8348E-10	3.6753E-11
6	8.8863E-10	3.6789E-11
7	8.9586E-10	3.7178E-11
8	8.9657E-10	3.7118E-11
9	8.9657E-10	3.7118E-11
10	8.9658E-10	3.7118E-11
Front Poly. Thck. = 9 cm		
1	5.0660E-10	2.2493E-11
2	6.0291E-10	2.5262E-11
3	6.5113E-10	2.7608E-11
4	6.8864E-10	3.2366E-11
5	6.9231E-10	3.2400E-11
6	6.9770E-10	3.2513E-11
7	6.9819E-10	3.2536E-11
8	6.9819E-10	3.2536E-11
9	6.9819E-10	3.2536E-11
10	6.9819E-10	3.2536E-11

Back Poly. Thck. (cm)	Detector Resp.	Relative Error
Front Poly. Thck. = 10 cm		
1	3.7659E-10	2.2972E-11
2	4.5059E-10	2.2710E-11
3	4.8913E-10	2.3576E-11
4	5.0586E-10	2.6254E-11
5	5.1025E-10	2.6329E-11
6	5.1335E-10	2.6386E-11
7	5.1411E-10	2.6374E-11
8	5.1411E-10	2.6374E-11
9	5.1411E-10	2.6374E-11
10	5.1411E-10	2.6374E-11

Table D.3. End-on irradiation for 3 cm radial poly. thck.

Back Poly. Thck. (cm)	Detector Resp.	Relative Error
Front Poly. Thck. = 1 cm		
1	1.2257E-09	5.9934E-11
2	2.7499E-09	9.1297E-11
3	3.9592E-09	9.6208E-11
4	4.6939E-09	1.0514E-10
5	5.1996E-09	1.2687E-10
6	5.3873E-09	1.2876E-10
7	5.4483E-09	1.2912E-10
8	5.4941E-09	1.2966E-10
9	5.5126E-09	1.2955E-10
10	5.5251E-09	1.2984E-10
Front Poly. Thck. = 2 cm		
1	2.5073E-09	7.5721E-11
2	4.4829E-09	1.0938E-10
3	5.9022E-09	1.3162E-10
4	6.6693E-09	1.4005E-10
5	7.0358E-09	1.4353E-10
6	7.2292E-09	1.4531E-10
7	7.3125E-09	1.4625E-10
8	7.3334E-09	1.4667E-10
9	7.3375E-09	1.4675E-10
10	7.3456E-09	1.4618E-10
Front Poly. Thck. = 3 cm		
1	3.8232E-09	1.0552E-10
2	5.9230E-09	1.1313E-10
3	7.1467E-09	1.4722E-10
4	7.7888E-09	1.5344E-10
5	8.0964E-09	1.5545E-10
6	8.1934E-09	1.5649E-10
7	8.2337E-09	1.5644E-10
8	8.2587E-09	1.5692E-10
9	8.3242E-09	1.2486E-10
10	8.2736E-09	1.5720E-10

Back Poly. Thck. (cm)	Detector Resp.	Relative Error
Front Poly. Thck. = 4 cm		
1	4.2123E-09	1.1036E-10
2	6.1861E-09	1.3609E-10
3	7.2806E-09	1.4707E-10
4	7.8091E-09	1.5228E-10
5	8.0387E-09	1.5354E-10
6	8.1493E-09	1.5484E-10
7	8.1952E-09	1.5489E-10
8	8.2086E-09	1.5514E-10
9	8.2195E-09	1.5535E-10
10	8.2209E-09	1.5537E-10
Front Poly. Thck. = 5 cm		
1	4.5028E-09	1.0897E-10
2	5.9970E-09	1.2774E-10
3	6.8827E-09	1.3696E-10
4	7.3360E-09	1.5552E-10
5	7.4848E-09	1.5643E-10
6	7.5559E-09	1.5716E-10
7	7.5805E-09	1.5768E-10
8	7.5910E-09	1.5713E-10
9	7.5938E-09	1.5719E-10
10	7.5996E-09	1.5731E-10
Front Poly. Thck. = 6 cm		
1	4.1040E-09	1.1327E-10
2	5.3453E-09	1.2829E-10
3	5.9224E-09	1.3385E-10
4	6.2021E-09	1.3645E-10
5	6.3321E-09	1.3804E-10
6	6.3798E-09	1.3844E-10
7	6.4134E-09	1.3853E-10
8	6.4209E-09	1.3869E-10
9	6.4282E-09	1.3885E-10
10	6.4363E-09	1.3902E-10

Back Poly. Thck. (cm)	Detector Resp.	Relative Error
Front Poly. Thck. = 7 cm		
1	3.4805E-09	1.0302E-10
2	4.4797E-09	1.0751E-10
3	4.9130E-09	1.1251E-10
4	5.1647E-09	1.1517E-10
5	5.2836E-09	1.1624E-10
6	5.3108E-09	1.1631E-10
7	5.3485E-09	1.1713E-10
8	5.3643E-09	1.1694E-10
9	5.3713E-09	1.1709E-10
10	5.3735E-09	1.1714E-10
Front Poly. Thck. = 8 cm		
1	2.7970E-09	7.5240E-11
2	3.5983E-09	8.4559E-11
3	4.0425E-09	9.3382E-11
4	4.2196E-09	9.7050E-11
5	4.2797E-09	9.8006E-11
6	4.3307E-09	1.0220E-10
7	4.3434E-09	1.0207E-10
8	4.3704E-09	1.0270E-10
9	4.3718E-09	1.0274E-10
10	4.3740E-09	1.0279E-10
Front Poly. Thck. = 9 cm		
1	2.3202E-09	8.5847E-11
2	2.9323E-09	9.6473E-11
3	3.2052E-09	1.0000E-10
4	3.3470E-09	1.0208E-10
5	3.3945E-09	1.0217E-10
6	3.4203E-09	1.0261E-10
7	3.4292E-09	1.0288E-10
8	3.4293E-09	1.0288E-10
9	3.4307E-09	1.0292E-10
10	3.4307E-09	1.0292E-10

Back Poly. Thck. (cm)	Detector Resp.	Relative Error
Front Poly. Thck. = 10 cm		
1	1.8199E-09	7.6798E-11
2	2.3559E-09	9.0936E-11
3	2.6061E-09	9.4862E-11
4	2.7038E-09	9.5985E-11
5	2.7304E-09	9.6110E-11
6	2.7462E-09	9.6391E-11
7	2.7340E-09	8.0106E-11
8	2.7515E-09	9.6301E-11
9	2.7515E-09	9.6301E-11
10	2.7529E-09	9.6352E-11

Table D.4. End-on irradiation for 4 cm radial poly. thck.

Back Poly. Thck. (cm)	Detector Resp.	Relative Error
Front Poly. Thck. = 1 cm		
1	1.5829E-09	8.4686E-11
2	4.1090E-09	1.4669E-10
3	6.5537E-09	1.8547E-10
4	8.1940E-09	2.0813E-10
5	9.0863E-09	2.1716E-10
6	9.5145E-09	2.2074E-10
7	9.7534E-09	2.2238E-10
8	9.8890E-09	2.2349E-10
9	9.9239E-09	2.2329E-10
10	9.9465E-09	2.2380E-10
Front Poly. Thck. = 2 cm		
1	4.2309E-09	1.4512E-10
2	8.3346E-09	2.0753E-10
3	1.1033E-08	2.1846E-10
4	1.2770E-08	2.3241E-10
5	1.3793E-08	2.3999E-10
6	1.4309E-08	2.6615E-10
7	1.4548E-08	2.4586E-10
8	1.4688E-08	2.6879E-10
9	1.4749E-08	2.4632E-10
10	1.4780E-08	2.6900E-10
Front Poly. Thck. = 3 cm		
1	6.5191E-09	1.5972E-10
2	1.0490E-08	2.2239E-10
3	1.3334E-08	2.6136E-10
4	1.4801E-08	2.7233E-10
5	1.5649E-08	2.7856E-10
6	1.6058E-08	2.8262E-10
7	1.6330E-08	2.8414E-10
8	1.6426E-08	2.8581E-10
9	1.6488E-08	2.8525E-10
10	1.6513E-08	2.8568E-10

Back Poly. Thck. (cm)	Detector Resp.	Relative Error
Front Poly. Thck. = 4 cm		
1	8.0633E-09	1.3546E-10
2	1.2194E-08	1.7315E-10
3	1.4190E-08	2.6536E-10
4	1.5511E-08	2.7764E-10
5	1.6672E-08	2.0174E-10
6	1.7036E-08	2.0443E-10
7	1.7228E-08	2.0501E-10
8	1.7297E-08	2.0411E-10
9	1.7328E-08	2.0447E-10
10	1.7340E-08	2.0461E-10
Front Poly. Thck. = 5 cm		
1	8.3250E-09	2.0396E-10
2	1.1930E-08	2.4576E-10
3	1.4294E-08	2.7301E-10
4	1.5411E-08	2.8047E-10
5	1.6007E-08	2.8653E-10
6	1.6323E-08	2.8892E-10
7	1.6441E-08	2.8936E-10
8	1.6478E-08	2.9001E-10
9	1.6512E-08	2.9061E-10
10	1.6528E-08	2.8923E-10
Front Poly. Thck. = 6 cm		
1	8.3342E-09	2.0335E-10
2	1.1659E-08	2.4368E-10
3	1.3361E-08	2.5787E-10
4	1.4160E-08	2.6479E-10
5	1.4610E-08	2.6883E-10
6	1.4873E-08	2.7068E-10
7	1.4986E-08	2.7124E-10
8	1.5068E-08	2.7424E-10
9	1.5093E-08	2.7469E-10
10	1.5120E-08	2.7366E-10

Back Poly. Thck. (cm)	Detector Resp.	Relative Error
Front Poly. Thck. = 7 cm		
1	7.3952E-09	1.8266E-10
2	9.9132E-09	2.1115E-10
3	1.1446E-08	2.3006E-10
4	1.2179E-08	2.3627E-10
5	1.2560E-08	2.3989E-10
6	1.2733E-08	2.4065E-10
7	1.2847E-08	2.4282E-10
8	1.2876E-08	2.4206E-10
9	1.2888E-08	2.4229E-10
10	1.2906E-08	2.4263E-10
Front Poly. Thck. = 8 cm		
1	6.4271E-09	1.7674E-10
2	8.4591E-09	2.0217E-10
3	9.5753E-09	2.1544E-10
4	1.0125E-08	2.1972E-10
5	1.0442E-08	2.2345E-10
6	1.0589E-08	2.2555E-10
7	1.0628E-08	2.2531E-10
8	1.0649E-08	2.2576E-10
9	1.0663E-08	2.2606E-10
10	1.0670E-08	2.2621E-10
Front Poly. Thck. = 9 cm		
1	5.3664E-09	1.6260E-10
2	7.0791E-09	1.8689E-10
3	7.8419E-09	1.9605E-10
4	8.2800E-09	2.0203E-10
5	8.4767E-09	2.0344E-10
6	8.6273E-09	2.0619E-10
7	8.6820E-09	2.0750E-10
8	8.7010E-09	2.0795E-10
9	8.7151E-09	2.0829E-10
10	8.7211E-09	2.0843E-10

Back Poly. Thck. (cm)	Detector Resp.	Relative Error
Front Poly. Thck. = 10 cm		
1	4.1316E-09	1.4419E-10
2	5.3898E-09	1.6439E-10
3	6.0219E-09	1.7223E-10
4	6.3162E-09	1.7559E-10
5	6.4640E-09	1.7776E-10
6	6.5569E-09	1.7900E-10
7	6.5909E-09	1.7927E-10
8	6.6127E-09	1.7920E-10
9	6.6281E-09	1.7962E-10
10	6.6345E-09	1.7980E-10

Table D.5. End-on irradiation for 5 cm radial poly. thck.

Back Poly. Thck. (cm)	Detector Resp.	Relative Error
Front Poly. Thck. = 1 cm		
1	1.7890E-09	1.0877E-10
2	5.4204E-09	1.7941E-10
3	9.0331E-09	2.5744E-10
4	1.1816E-08	2.9658E-10
5	1.3439E-08	3.1313E-10
6	1.4493E-08	3.2174E-10
7	1.5201E-08	3.2985E-10
8	1.5499E-08	3.3168E-10
9	1.5606E-08	3.3240E-10
10	1.5678E-08	3.3394E-10
Front Poly. Thck. = 2 cm		
1	5.4589E-09	2.1235E-10
2	1.1219E-08	2.9953E-10
3	1.5630E-08	3.4542E-10
4	1.8657E-08	3.7315E-10
5	2.0284E-08	3.8539E-10
6	2.1424E-08	3.9206E-10
7	2.2032E-08	3.9878E-10
8	2.2271E-08	4.0088E-10
9	2.2410E-08	4.0114E-10
10	2.2473E-08	4.0227E-10
Front Poly. Thck. = 3 cm		
1	8.4824E-09	2.5278E-10
2	1.5538E-08	3.4494E-10
3	2.0138E-08	3.8665E-10
4	2.3208E-08	4.1774E-10
5	2.5026E-08	4.3044E-10
6	2.5875E-08	4.3470E-10
7	2.6372E-08	4.3778E-10
8	2.6605E-08	4.4164E-10
9	2.6711E-08	4.4072E-10
10	2.6796E-08	4.4213E-10

Back Poly. Thck. (cm)	Detector Resp.	Relative Error
Front Poly. Thck. = 4 cm		
1	1.1958E-08	2.5950E-10
2	1.8254E-08	3.7239E-10
3	2.2738E-08	4.1382E-10
4	2.5296E-08	4.3509E-10
5	2.6668E-08	4.4536E-10
6	2.7544E-08	4.5172E-10
7	2.7961E-08	4.5297E-10
8	2.8197E-08	4.5679E-10
9	2.8273E-08	4.5519E-10
10	2.8320E-08	4.5595E-10
Front Poly. Thck. = 5 cm		
1	1.2739E-08	3.1467E-10
2	1.8524E-08	3.7974E-10
3	2.2301E-08	4.1257E-10
4	2.4287E-08	4.2745E-10
5	2.5529E-08	4.3655E-10
6	2.6219E-08	4.4049E-10
7	2.6501E-08	4.4257E-10
8	2.6690E-08	4.4572E-10
9	2.6723E-08	4.4360E-10
10	2.6746E-08	4.4399E-10
Front Poly. Thck. = 6 cm		
1	1.3061E-08	3.1608E-10
2	1.8088E-08	3.7261E-10
3	2.1090E-08	3.9860E-10
4	2.2941E-08	4.1294E-10
5	2.3945E-08	4.1904E-10
6	2.4416E-08	4.2240E-10
7	2.4768E-08	4.2848E-10
8	2.4938E-08	4.2894E-10
9	2.4987E-08	4.2977E-10
10	2.5035E-08	4.3061E-10

Back Poly. Thck. (cm)	Detector Resp.	Relative Error
Front Poly. Thck. = 7 cm		
1	1.1827E-08	2.8149E-10
2	1.6366E-08	3.4369E-10
3	1.9240E-08	3.7326E-10
4	2.0744E-08	3.8583E-10
5	2.1410E-08	3.8966E-10
6	2.1754E-08	3.9375E-10
7	2.1980E-08	3.9565E-10
8	2.2100E-08	3.9559E-10
9	2.2140E-08	3.9630E-10
10	2.2153E-08	3.9653E-10
Front Poly. Thck. = 8 cm		
1	1.0684E-08	2.6816E-10
2	1.4627E-08	3.1009E-10
3	1.6890E-08	2.9389E-10
4	1.8023E-08	3.0460E-10
5	1.8635E-08	3.0935E-10
6	1.8910E-08	3.1013E-10
7	1.9068E-08	3.1081E-10
8	1.9122E-08	3.1169E-10
9	1.9171E-08	3.1248E-10
10	1.9208E-08	3.1117E-10
Front Poly. Thck. = 9 cm		
1	9.2525E-09	2.7017E-10
2	1.2693E-08	3.1352E-10
3	1.4477E-08	3.3152E-10
4	1.5303E-08	3.3972E-10
5	1.5754E-08	3.4344E-10
6	1.6059E-08	3.4686E-10
7	1.6180E-08	3.4625E-10
8	1.6262E-08	3.4800E-10
9	1.6291E-08	3.4700E-10
10	1.6309E-08	3.4738E-10

Back Poly. Thck. (cm)	Detector Resp.	Relative Error
Front Poly. Thck. = 10 cm		
1	7.8125E-09	2.4609E-10
2	1.0294E-08	2.7690E-10
3	1.1630E-08	2.9308E-10
4	1.2332E-08	2.9967E-10
5	1.2733E-08	3.0431E-10
6	1.2958E-08	3.0710E-10
7	1.3085E-08	3.0882E-10
8	1.3123E-08	3.0838E-10
9	1.3179E-08	3.0971E-10
10	1.3182E-08	3.0978E-10

Table D.6. End-on irradiation for 6 cm radial poly. thck.

Back Poly. Thck. (cm)	Detector Resp.	Relative Error
Front Poly. Thck. = 1 cm		
1	2.0955E-09	1.3202E-10
2	6.0966E-09	2.2923E-10
3	1.0504E-08	3.0358E-10
4	1.4659E-08	3.6062E-10
5	1.7309E-08	4.2754E-10
6	1.8712E-08	4.3973E-10
7	1.9689E-08	4.4693E-10
8	2.0205E-08	4.0005E-10
9	2.0538E-08	4.5593E-10
10	2.0641E-08	4.0251E-10
Front Poly. Thck. = 2 cm		
1	6.2538E-09	1.8886E-10
2	1.3044E-08	2.7131E-10
3	1.9170E-08	3.5657E-10
4	2.3905E-08	3.9683E-10
5	2.6742E-08	4.1450E-10
6	2.8540E-08	4.2810E-10
7	2.9544E-08	4.3135E-10
8	3.0095E-08	4.3638E-10
9	3.0382E-08	4.3750E-10
10	3.0499E-08	4.3614E-10
Front Poly. Thck. = 3 cm		
1	1.1352E-08	3.6325E-10
2	1.9881E-08	4.6720E-10
3	2.6480E-08	5.3225E-10
4	3.0758E-08	5.6595E-10
5	3.3454E-08	5.8879E-10
6	3.4932E-08	6.0083E-10
7	3.5783E-08	6.0474E-10
8	3.6207E-08	6.0827E-10
9	3.6507E-08	6.0967E-10
10	3.6597E-08	6.1117E-10

Back Poly. Thck. (cm)	Detector Resp.	Relative Error
Front Poly. Thck. = 4 cm		
1	1.4811E-08	3.9397E-10
2	2.3596E-08	5.1674E-10
3	2.9571E-08	5.6776E-10
4	3.3196E-08	5.9422E-10
5	3.5494E-08	6.1050E-10
6	3.6978E-08	6.2123E-10
7	3.7668E-08	6.2528E-10
8	3.8042E-08	6.2769E-10
9	3.8244E-08	6.3103E-10
10	3.8322E-08	6.2848E-10
Front Poly. Thck. = 5 cm		
1	1.6487E-08	3.6765E-10
2	2.5235E-08	5.1227E-10
3	3.0752E-08	5.5968E-10
4	3.4182E-08	5.9135E-10
5	3.6188E-08	6.0434E-10
6	3.7386E-08	6.1313E-10
7	3.8075E-08	6.1681E-10
8	3.8382E-08	6.2178E-10
9	3.8561E-08	6.2084E-10
10	3.8634E-08	6.2201E-10
Front Poly. Thck. = 6 cm		
1	1.6792E-08	3.4927E-10
2	2.4701E-08	4.1991E-10
3	2.9696E-08	5.6423E-10
4	3.2469E-08	5.8445E-10
5	3.4170E-08	5.9798E-10
6	3.4946E-08	6.0108E-10
7	3.5524E-08	6.0746E-10
8	3.5751E-08	6.0776E-10
9	3.5909E-08	6.0687E-10
10	3.5962E-08	6.0775E-10

Back Poly. Thck. (cm)	Detector Resp.	Relative Error
Front Poly. Thck. = 7 cm		
1	1.5565E-08	3.7511E-10
2	2.2555E-08	4.7816E-10
3	2.6460E-08	5.1333E-10
4	2.8858E-08	5.3388E-10
5	3.0067E-08	5.4421E-10
6	3.0796E-08	5.4817E-10
7	3.1137E-08	5.5113E-10
8	3.1341E-08	5.5160E-10
9	3.1411E-08	5.5283E-10
10	3.1453E-08	5.5358E-10
Front Poly. Thck. = 8 cm		
1	1.4194E-08	3.7614E-10
2	1.9659E-08	4.3840E-10
3	2.2835E-08	4.7268E-10
4	2.4873E-08	4.9248E-10
5	2.5936E-08	5.0316E-10
6	2.6463E-08	5.0545E-10
7	2.6817E-08	5.0684E-10
8	2.6942E-08	5.0921E-10
9	2.7004E-08	5.1037E-10
10	2.7050E-08	5.0853E-10
Front Poly. Thck. = 9 cm		
1	1.3485E-08	3.4118E-10
2	1.8190E-08	3.6563E-10
3	2.1121E-08	3.9286E-10
4	2.2673E-08	4.0358E-10
5	2.3465E-08	4.1064E-10
6	2.3901E-08	4.1349E-10
7	2.4139E-08	4.1518E-10
8	2.4255E-08	4.1476E-10
9	2.4338E-08	4.1618E-10
10	2.4362E-08	4.1659E-10

Back Poly. Thck. (cm)	Detector Resp.	Relative Error
Front Poly. Thck. = 10 cm		
1	1.0557E-08	3.2200E-10
2	1.4345E-08	3.7011E-10
3	1.6769E-08	4.0749E-10
4	1.7951E-08	4.1825E-10
5	1.8540E-08	4.2642E-10
6	1.8871E-08	4.2837E-10
7	1.9072E-08	4.3103E-10
8	1.9228E-08	4.3455E-10
9	1.9269E-08	4.3549E-10
10	1.9319E-08	4.3467E-10

Table D.7. End-on irradiation for 7 cm radial poly. thck.

Back Poly. Thck. (cm)	Detector Resp.	Relative Error
Front Poly. Thck. = 1 cm		
1	2.5466E-09	1.8947E-10
2	7.3793E-09	3.3502E-10
3	1.2840E-08	4.3785E-10
4	1.8083E-08	4.9367E-10
5	2.1685E-08	5.3563E-10
6	2.3711E-08	5.5246E-10
7	2.5099E-08	4.9445E-10
8	2.6057E-08	5.7325E-10
9	2.6461E-08	5.7685E-10
10	2.6745E-08	5.8037E-10
Front Poly. Thck. = 2 cm		
1	7.0318E-09	3.3472E-10
2	1.5135E-08	4.7677E-10
3	2.2407E-08	5.6914E-10
4	2.7924E-08	6.2271E-10
5	3.1833E-08	6.5895E-10
6	3.4140E-08	6.7939E-10
7	3.5662E-08	6.9184E-10
8	3.6452E-08	6.9623E-10
9	3.6979E-08	6.9890E-10
10	3.7151E-08	6.9844E-10
Front Poly. Thck. = 3 cm		
1	1.2614E-08	4.3390E-10
2	2.2217E-08	5.6209E-10
3	3.0191E-08	6.4911E-10
4	3.5960E-08	6.5448E-10
5	3.9670E-08	6.8233E-10
6	4.1693E-08	6.9210E-10
7	4.2825E-08	7.6657E-10
8	4.3430E-08	7.6871E-10
9	4.3918E-08	7.7297E-10
10	4.4142E-08	7.7691E-10

Back Poly. Thck. (cm)	Detector Resp.	Relative Error
Front Poly. Thck. = 4 cm		
1	1.6646E-08	4.8772E-10
2	2.7765E-08	6.1916E-10
3	3.5679E-08	6.9218E-10
4	4.0719E-08	7.3702E-10
5	4.4443E-08	6.7997E-10
6	4.5902E-08	7.8033E-10
7	4.7088E-08	7.8638E-10
8	4.7515E-08	7.8876E-10
9	4.8190E-08	7.0357E-10
10	4.8038E-08	7.9262E-10
Front Poly. Thck. = 5 cm		
1	1.9703E-08	5.1818E-10
2	3.0279E-08	6.3284E-10
3	3.7397E-08	6.9933E-10
4	4.1650E-08	6.4975E-10
5	4.4607E-08	7.3155E-10
6	4.6216E-08	6.6089E-10
7	4.7066E-08	6.6363E-10
8	4.7618E-08	6.6665E-10
9	4.7879E-08	6.6552E-10
10	4.8041E-08	6.6777E-10
Front Poly. Thck. = 6 cm		
1	2.1212E-08	4.9001E-10
2	3.0786E-08	5.9109E-10
3	3.7335E-08	6.4963E-10
4	4.0987E-08	6.7628E-10
5	4.3387E-08	7.2022E-10
6	4.4732E-08	7.2913E-10
7	4.5424E-08	7.3586E-10
8	4.5725E-08	7.3617E-10
9	4.5907E-08	7.3911E-10
10	4.6000E-08	7.3600E-10

Back Poly. Thck. (cm)	Detector Resp.	Relative Error
Front Poly. Thck. = 7 cm		
1	1.9592E-08	5.2507E-10
2	2.8021E-08	6.2206E-10
3	3.3902E-08	6.7803E-10
4	3.7458E-08	7.1545E-10
5	3.9214E-08	7.2546E-10
6	4.0138E-08	7.3051E-10
7	4.0721E-08	7.3297E-10
8	4.0964E-08	7.3735E-10
9	4.1116E-08	7.3598E-10
10	4.1236E-08	7.3813E-10
Front Poly. Thck. = 8 cm		
1	1.8347E-08	5.0455E-10
2	2.6630E-08	6.1249E-10
3	3.1133E-08	6.5691E-10
4	3.3657E-08	6.7314E-10
5	3.5282E-08	6.8448E-10
6	3.6100E-08	6.9312E-10
7	3.6594E-08	6.9530E-10
8	3.6862E-08	6.9669E-10
9	3.7011E-08	6.9950E-10
10	3.7058E-08	6.9669E-10
Front Poly. Thck. = 9 cm		
1	1.6986E-08	4.7221E-10
2	2.3177E-08	5.4234E-10
3	2.7136E-08	5.8613E-10
4	2.9780E-08	6.1644E-10
5	3.1161E-08	6.2945E-10
6	3.1920E-08	6.3521E-10
7	3.2213E-08	6.3782E-10
8	3.2531E-08	6.4086E-10
9	3.2645E-08	6.4311E-10
10	3.2688E-08	6.4069E-10

Back Poly. Thck. (cm)	Detector Resp.	Relative Error
Front Poly. Thck. = 10 cm		
1	1.4058E-08	4.2596E-10
2	1.9604E-08	5.1166E-10
3	2.2483E-08	5.4185E-10
4	2.4267E-08	5.5813E-10
5	2.5169E-08	5.6630E-10
6	2.5724E-08	5.7107E-10
7	2.6019E-08	5.7242E-10
8	2.6166E-08	5.7304E-10
9	2.6240E-08	5.7465E-10
10	2.6290E-08	5.7576E-10

Table D.8. End-on irradiation for 8 cm radial poly. thck.

Back Poly. Thck. (cm)	Detector Resp.	Relative Error
Front Poly. Thck. = 1 cm		
1	2.6655E-09	2.3270E-10
2	7.8086E-09	3.1235E-10
3	1.4080E-08	5.2378E-10
4	1.9075E-08	5.3220E-10
5	2.3269E-08	6.5386E-10
6	2.5800E-08	6.7597E-10
7	2.7498E-08	6.9569E-10
8	2.8518E-08	7.0439E-10
9	2.8991E-08	7.0738E-10
10	2.9371E-08	7.1077E-10
Front Poly. Thck. = 2 cm		
1	7.5193E-09	3.5566E-10
2	1.6205E-08	5.0235E-10
3	2.4728E-08	6.2068E-10
4	3.1445E-08	7.9555E-10
5	3.5989E-08	8.4575E-10
6	3.8666E-08	8.6226E-10
7	4.0471E-08	8.7823E-10
8	4.1402E-08	8.8185E-10
9	4.2016E-08	8.8654E-10
10	4.2284E-08	8.8797E-10
Front Poly. Thck. = 3 cm		
1	1.3915E-08	5.3154E-10
2	2.4065E-08	6.6420E-10
3	3.4054E-08	7.9347E-10
4	4.0519E-08	8.5090E-10
5	4.5227E-08	8.8645E-10
6	4.7955E-08	9.0635E-10
7	4.9528E-08	9.1627E-10
8	5.0504E-08	9.2422E-10
9	5.1043E-08	9.2899E-10
10	5.1425E-08	9.3080E-10

Back Poly. Thck. (cm)	Detector Resp.	Relative Error
Front Poly. Thck. = 4 cm		
1	1.7598E-08	5.6489E-10
2	3.0219E-08	6.8294E-10
3	3.9106E-08	8.3295E-10
4	4.5547E-08	8.9272E-10
5	5.0166E-08	9.2806E-10
6	5.2644E-08	9.4759E-10
7	5.4090E-08	9.5740E-10
8	5.4816E-08	9.6475E-10
9	5.5224E-08	9.6642E-10
10	5.5492E-08	9.6556E-10
Front Poly. Thck. = 5 cm		
1	2.2230E-08	6.2467E-10
2	3.4804E-08	7.3786E-10
3	4.3863E-08	8.1585E-10
4	4.9408E-08	8.5476E-10
5	5.3520E-08	8.8308E-10
6	5.5318E-08	8.9062E-10
7	5.6409E-08	8.9691E-10
8	5.7058E-08	9.0151E-10
9	5.7357E-08	9.0624E-10
10	5.7579E-08	9.0398E-10
Front Poly. Thck. = 6 cm		
1	2.3741E-08	6.7425E-10
2	3.5083E-08	8.0340E-10
3	4.3427E-08	8.8591E-10
4	4.8478E-08	9.2594E-10
5	5.1666E-08	9.5582E-10
6	5.3404E-08	9.6661E-10
7	5.4515E-08	9.7036E-10
8	5.5155E-08	9.7625E-10
9	5.5439E-08	9.8127E-10
10	5.5550E-08	9.7768E-10

Back Poly. Thck. (cm)	Detector Resp.	Relative Error
Front Poly. Thck. = 7 cm		
1	2.3457E-08	6.5913E-10
2	3.4239E-08	7.8408E-10
3	4.1045E-08	8.4962E-10
4	4.5560E-08	8.8843E-10
5	4.7967E-08	9.0658E-10
6	4.9444E-08	9.1966E-10
7	5.0340E-08	9.3129E-10
8	5.0756E-08	9.3390E-10
9	5.0990E-08	9.3312E-10
10	5.1099E-08	9.3512E-10
Front Poly. Thck. = 8 cm		
1	2.1977E-08	6.2195E-10
2	3.1081E-08	7.3351E-10
3	3.6812E-08	7.8041E-10
4	3.9399E-08	7.6040E-10
5	4.1374E-08	7.7782E-10
6	4.2496E-08	7.8193E-10
7	4.3104E-08	7.8881E-10
8	4.3563E-08	7.9285E-10
9	4.3806E-08	7.9290E-10
10	4.3968E-08	7.9582E-10
Front Poly. Thck. = 9 cm		
1	1.9202E-08	5.9336E-10
2	2.6877E-08	6.9342E-10
3	3.1755E-08	7.4624E-10
4	3.4462E-08	7.6850E-10
5	3.6005E-08	7.8130E-10
6	3.7084E-08	7.8988E-10
7	3.7623E-08	7.9760E-10
8	3.7877E-08	7.9920E-10
9	3.8170E-08	8.0157E-10
10	3.8251E-08	8.0327E-10

Back Poly. Thck. (cm)	Detector Resp.	Relative Error
Front Poly. Thck. = 10 cm		
1	1.6585E-08	4.6604E-10
2	2.3574E-08	5.9170E-10
3	2.7693E-08	6.3418E-10
4	3.0128E-08	6.5679E-10
5	3.1492E-08	6.6764E-10
6	3.2282E-08	6.7470E-10
7	3.2693E-08	6.7675E-10
8	3.2953E-08	6.7883E-10
9	3.3092E-08	6.8169E-10
10	3.3162E-08	6.7982E-10

Table D.9. End-on irradiation for 9 cm radial poly. thck.

Back Poly. Thck. (cm)	Detector Resp.	Relative Error
Front Poly. Thck. = 1 cm		
1	2.1968E-09	2.1880E-10
2	7.9757E-09	4.5621E-10
3	1.3409E-08	5.6855E-10
4	1.8720E-08	6.5893E-10
5	2.3604E-08	7.3408E-10
6	2.6319E-08	7.6325E-10
7	2.8284E-08	7.8065E-10
8	2.9312E-08	7.9143E-10
9	3.0096E-08	8.0057E-10
10	3.0518E-08	8.0263E-10
Front Poly. Thck. = 2 cm		
1	7.8251E-09	4.4212E-10
2	1.7234E-08	6.3595E-10
3	2.6701E-08	6.8088E-10
4	3.4784E-08	8.7307E-10
5	3.9480E-08	9.1593E-10
6	4.2889E-08	9.4785E-10
7	4.5166E-08	9.6656E-10
8	4.6586E-08	9.7830E-10
9	4.7489E-08	8.9753E-10
10	4.7665E-08	9.8667E-10
Front Poly. Thck. = 3 cm		
1	1.3658E-08	5.6408E-10
2	2.5324E-08	7.5973E-10
3	3.6291E-08	8.9275E-10
4	4.3454E-08	9.6034E-10
5	4.9493E-08	1.0196E-09
6	5.3059E-08	1.0453E-09
7	5.5048E-08	1.0624E-09
8	5.6213E-08	1.0681E-09
9	5.6812E-08	1.0737E-09
10	5.7128E-08	1.0740E-09

Back Poly. Thck. (cm)	Detector Resp.	Relative Error
Front Poly. Thck. = 4 cm		
1	1.9168E-08	6.4214E-10
2	3.2758E-08	8.3205E-10
3	4.4448E-08	9.7342E-10
4	5.1874E-08	1.0479E-09
5	5.6734E-08	1.0893E-09
6	5.9725E-08	1.1169E-09
7	6.1778E-08	1.1367E-09
8	6.2762E-08	1.1485E-09
9	6.3380E-08	1.1472E-09
10	6.3809E-08	1.1486E-09
Front Poly. Thck. = 5 cm		
1	2.2877E-08	6.8861E-10
2	3.6255E-08	8.0849E-10
3	4.5858E-08	9.4010E-10
4	5.2365E-08	9.4780E-10
5	5.6900E-08	9.8437E-10
6	5.9418E-08	9.9822E-10
7	6.0870E-08	1.0104E-09
8	6.1752E-08	1.0127E-09
9	6.2281E-08	1.0152E-09
10	6.2548E-08	1.0195E-09
Front Poly. Thck. = 6 cm		
1	2.4933E-08	7.1308E-10
2	3.7774E-08	9.0280E-10
3	4.6600E-08	9.3666E-10
4	5.2808E-08	9.9279E-10
5	5.6467E-08	1.0221E-09
6	5.8679E-08	1.0327E-09
7	5.9875E-08	1.0418E-09
8	6.1008E-08	1.1103E-09
9	6.1515E-08	1.1134E-09
10	6.1676E-08	1.1163E-09

Back Poly. Thck. (cm)	Detector Resp.	Relative Error
Front Poly. Thck. = 7 cm		
1	2.4701E-08	6.3728E-10
2	3.5949E-08	7.5133E-10
3	4.4178E-08	8.2613E-10
4	4.9175E-08	8.9498E-10
5	5.1897E-08	9.1858E-10
6	5.3812E-08	9.3095E-10
7	5.5133E-08	9.0419E-10
8	5.5320E-08	9.4044E-10
9	5.5602E-08	9.4524E-10
10	5.5782E-08	9.4272E-10
Front Poly. Thck. = 8 cm		
1	2.3047E-08	7.0294E-10
2	3.3281E-08	8.3536E-10
3	4.0057E-08	9.1730E-10
4	4.3963E-08	9.4959E-10
5	4.6421E-08	9.7019E-10
6	4.8087E-08	9.8578E-10
7	4.8897E-08	9.9261E-10
8	4.9476E-08	9.9447E-10
9	4.9696E-08	9.9889E-10
10	4.9842E-08	9.9684E-10
Front Poly. Thck. = 9 cm		
1	2.1694E-08	5.3366E-10
2	3.1281E-08	6.4126E-10
3	3.7338E-08	7.0196E-10
4	4.0650E-08	7.2358E-10
5	4.2899E-08	7.4215E-10
6	4.4193E-08	7.5128E-10
7	4.4820E-08	7.5298E-10
8	4.5120E-08	7.5801E-10
9	4.5375E-08	7.5775E-10
10	4.5514E-08	7.6008E-10

Back Poly. Thck. (cm)	Detector Resp.	Relative Error
Front Poly. Thck. = 10 cm		
1	1.8785E-08	5.2787E-10
2	2.6072E-08	6.3616E-10
3	3.1558E-08	6.5326E-10
4	3.3829E-08	7.4086E-10
5	3.5525E-08	7.5667E-10
6	3.5897E-08	8.2563E-10
7	3.6348E-08	8.2511E-10
8	3.6697E-08	8.3302E-10
9	3.6821E-08	8.3215E-10
10	3.6936E-08	8.3474E-10

Table D.10. End-on irradiation for 10 cm radial poly. thck.

Back Poly. Thck. (cm)	Detector Resp.	Relative Error
Front Poly. Thck. = 1 cm		
1	2.1713E-09	2.1431E-10
2	7.5024E-09	4.6440E-10
3	1.4339E-08	6.4383E-10
4	1.9301E-08	6.0798E-10
5	2.4088E-08	6.6724E-10
6	2.7352E-08	7.0295E-10
7	3.0168E-08	8.2961E-10
8	3.1078E-08	7.3967E-10
9	3.2021E-08	7.5571E-10
10	3.2635E-08	7.6365E-10
Front Poly. Thck. = 2 cm		
1	7.4445E-09	4.3476E-10
2	1.7592E-08	6.3684E-10
3	2.7939E-08	7.1523E-10
4	3.5393E-08	8.9898E-10
5	4.1479E-08	9.6231E-10
6	4.5264E-08	9.9129E-10
7	4.7265E-08	1.0068E-09
8	4.8801E-08	1.0151E-09
9	4.9542E-08	1.0206E-09
10	5.0017E-08	1.0203E-09
Front Poly. Thck. = 3 cm		
1	1.4469E-08	6.4530E-10
2	2.7718E-08	8.8974E-10
3	3.9063E-08	1.0547E-09
4	4.8196E-08	1.1567E-09
5	5.4017E-08	1.2046E-09
6	5.7481E-08	1.2358E-09
7	5.9714E-08	1.2480E-09
8	6.1331E-08	1.2634E-09
9	6.2157E-08	1.2680E-09
10	6.2715E-08	1.2731E-09

Back Poly. Thck. (cm)	Detector Resp.	Relative Error
Front Poly. Thck. = 4 cm		
1	1.9417E-08	7.2814E-10
2	3.3319E-08	9.2293E-10
3	4.4065E-08	1.0399E-09
4	5.1949E-08	1.1325E-09
5	5.7357E-08	1.1758E-09
6	6.0543E-08	1.2109E-09
7	6.2682E-08	1.2223E-09
8	6.3751E-08	1.2304E-09
9	6.4570E-08	1.2333E-09
10	6.7469E-08	9.5806E-10
Front Poly. Thck. = 5 cm		
1	2.4633E-08	7.9318E-10
2	3.8361E-08	9.7436E-10
3	4.8902E-08	1.1541E-09
4	5.6399E-08	1.1731E-09
5	6.1143E-08	1.2779E-09
6	6.4465E-08	1.3022E-09
7	6.5961E-08	1.3126E-09
8	6.6923E-08	1.3184E-09
9	6.7677E-08	1.3197E-09
10	6.7961E-08	1.3252E-09
Front Poly. Thck. = 6 cm		
1	2.6829E-08	8.3171E-10
2	4.0224E-08	9.2917E-10
3	5.0476E-08	1.1408E-09
4	5.7527E-08	1.1563E-09
5	6.1672E-08	1.1964E-09
6	6.4271E-08	1.2083E-09
7	6.5839E-08	1.2246E-09
8	6.6590E-08	1.2253E-09
9	6.7141E-08	1.2287E-09
10	6.7477E-08	1.2348E-09

Back Poly. Thck. (cm)	Detector Resp.	Relative Error
Front Poly. Thck. = 7 cm		
1	2.6405E-08	6.7596E-10
2	3.9516E-08	8.1008E-10
3	4.8336E-08	8.8939E-10
4	5.3143E-08	1.1692E-09
5	5.6298E-08	1.1991E-09
6	5.8416E-08	1.2209E-09
7	5.9765E-08	1.2252E-09
8	6.0543E-08	1.2351E-09
9	6.1001E-08	1.2383E-09
10	6.1170E-08	1.2417E-09
Front Poly. Thck. = 8 cm		
1	2.5373E-08	8.2210E-10
2	3.6417E-08	9.6141E-10
3	4.4676E-08	1.0722E-09
4	4.9738E-08	1.1191E-09
5	5.2536E-08	1.1032E-09
6	5.4413E-08	1.1155E-09
7	5.5309E-08	1.1228E-09
8	5.5924E-08	1.1241E-09
9	5.6452E-08	1.1742E-09
10	5.6418E-08	1.1284E-09
Front Poly. Thck. = 9 cm		
1	2.4239E-08	7.9503E-10
2	3.4042E-08	9.2936E-10
3	4.0527E-08	1.0091E-09
4	4.4775E-08	1.0656E-09
5	4.7164E-08	1.0848E-09
6	4.8806E-08	1.1030E-09
7	4.9579E-08	1.1106E-09
8	5.0106E-08	1.1123E-09
9	5.0280E-08	1.1112E-09
10	5.0493E-08	1.1159E-09

Back Poly. Thck. (cm)	Detector Resp.	Relative Error
Front Poly. Thck. = 10 cm		
1	2.1825E-08	6.7877E-10
2	3.1047E-08	7.8860E-10
3	3.6485E-08	8.4281E-10
4	4.0263E-08	8.7370E-10
5	4.2543E-08	8.9766E-10
6	4.3688E-08	9.0435E-10
7	4.4352E-08	9.1366E-10
8	4.4821E-08	9.1435E-10
9	4.5132E-08	9.2070E-10
10	4.5317E-08	9.1993E-10

Table D.11. Side irradiation for 1 cm radial poly. thck.

Back Poly. Thck. (cm)	Detector Resp.	Relative Error
Front Poly. Thck. = 1 cm		
1	1.4408E-10	8.0253E-12
2	2.2118E-10	1.6323E-11
3	2.9269E-10	1.9903E-11
4	3.2022E-10	2.4176E-11
5	3.2159E-10	2.3862E-11
6	3.4884E-10	3.1780E-11
7	3.4468E-10	3.0263E-11
8	3.0218E-10	2.4779E-11
9	3.5673E-10	3.2142E-11
10	4.1231E-10	2.9769E-11
Front Poly. Thck. = 2 cm		
1	2.0458E-10	1.4055E-11
2	3.0769E-10	1.8523E-11
3	3.8883E-10	2.3563E-11
4	4.5425E-10	3.8657E-11
5	4.8768E-10	4.6281E-11
6	4.7817E-10	4.2175E-11
7	4.5551E-10	3.9493E-11
8	4.0343E-10	3.6228E-11
9	4.3760E-10	3.9996E-11
10	4.4634E-10	3.9055E-11
Front Poly. Thck. = 3 cm		
1	2.6536E-10	1.5603E-11
2	3.8698E-10	2.7940E-11
3	4.4533E-10	2.7744E-11
4	4.8054E-10	4.1471E-11
5	6.0496E-10	5.8318E-11
6	5.3215E-10	4.4009E-11
7	5.0036E-10	4.5583E-11
8	4.7967E-10	4.3410E-11
9	4.7643E-10	4.5928E-11
10	5.0506E-10	4.5556E-11

Back Poly. Thck. (cm)	Detector Resp.	Relative Error
Front Poly. Thck. = 4 cm		
1	3.0564E-10	2.4727E-11
2	4.1522E-10	3.3674E-11
3	4.4780E-10	3.6809E-11
4	5.2364E-10	4.3567E-11
5	6.4425E-10	6.2492E-11
6	5.6638E-10	4.5253E-11
7	5.2337E-10	4.6528E-11
8	5.2482E-10	4.8389E-11
9	5.0226E-10	4.6760E-11
10	5.4197E-10	4.8560E-11
Front Poly. Thck. = 5 cm		
1	3.3502E-10	2.7573E-11
2	5.3179E-10	4.7223E-11
3	6.5362E-10	6.1701E-11
4	6.7072E-10	6.1907E-11
5	6.9192E-10	6.7808E-11
6	5.8163E-10	4.5658E-11
7	5.3944E-10	4.7309E-11
8	5.3996E-10	4.8758E-11
9	5.0871E-10	4.9040E-11
10	5.4488E-10	4.8603E-11
Front Poly. Thck. = 6 cm		
1	3.6668E-10	2.7538E-11
2	4.7072E-10	4.1329E-11
3	5.5699E-10	4.9238E-11
4	5.9229E-10	5.0108E-11
5	6.0993E-10	5.0502E-11
6	5.8460E-10	4.5716E-11
7	5.5521E-10	5.0635E-11
8	5.3967E-10	5.0621E-11
9	5.2585E-10	5.0429E-11
10	5.4520E-10	5.0049E-11

Back Poly. Thck. (cm)	Detector Resp.	Relative Error
Front Poly. Thck. = 7 cm		
1	3.1494E-10	2.7117E-11
2	4.1288E-10	3.5962E-11
3	4.8789E-10	4.0056E-11
4	5.1492E-10	4.1245E-11
5	5.2253E-10	4.1437E-11
6	5.3697E-10	4.6019E-11
7	5.5574E-10	5.0628E-11
8	5.3971E-10	5.0625E-11
9	5.4688E-10	5.3484E-11
10	5.5122E-10	5.0381E-11
Front Poly. Thck. = 8 cm		
1	3.5084E-10	3.0103E-11
2	4.5421E-10	4.3559E-11
3	5.1074E-10	4.7090E-11
4	5.4503E-10	5.0906E-11
5	5.5313E-10	5.3156E-11
6	5.5889E-10	5.3262E-11
7	5.6188E-10	5.3323E-11
8	5.4504E-10	5.0907E-11
9	5.4688E-10	5.3485E-11
10	5.5518E-10	5.0577E-11
Front Poly. Thck. = 9 cm		
1	3.7321E-10	3.3514E-11
2	4.7123E-10	4.5804E-11
3	5.4141E-10	5.0568E-11
4	5.4876E-10	5.1693E-11
5	5.5737E-10	5.1892E-11
6	5.5888E-10	5.1920E-11
7	5.6099E-10	5.1948E-11
8	5.6099E-10	5.1948E-11
9	5.5053E-10	5.3621E-11
10	5.5518E-10	5.0577E-11

Back Poly. Thck. (cm)	Detector Resp.	Relative Error
Front Poly. Thck. = 10 cm		
1	3.2544E-10	2.7630E-11
2	4.5172E-10	3.4963E-11
3	4.8236E-10	4.4812E-11
4	5.1369E-10	4.6489E-11
5	5.2323E-10	4.6776E-11
6	5.2929E-10	4.6948E-11
7	5.3011E-10	4.6968E-11
8	5.3361E-10	4.7118E-11
9	5.3361E-10	4.7118E-11
10	5.5518E-10	5.0577E-11

Table D.12. Side irradiation for 2 cm radial poly. thck.

Back Poly. Thck. (cm)	Detector Resp.	Relative Error
Front Poly. Thck. = 1 cm		
1	3.8147E-10	2.2240E-11
2	9.0306E-10	3.7929E-11
3	1.4433E-09	7.6931E-11
4	1.7397E-09	9.5860E-11
5	1.6418E-09	1.1624E-10
6	1.9371E-09	1.4141E-10
7	2.2092E-09	1.9706E-10
8	1.8120E-09	1.6688E-10
9	2.0753E-09	1.9653E-10
10	2.2770E-09	1.3116E-10
Front Poly. Thck. = 2 cm		
1	9.9085E-10	4.3498E-11
2	1.7219E-09	6.2331E-11
3	2.3770E-09	9.7456E-11
4	2.7127E-09	1.2261E-10
5	2.8180E-09	1.2878E-10
6	3.0724E-09	1.6253E-10
7	3.2892E-09	2.3814E-10
8	2.8074E-09	2.1055E-10
9	2.9698E-09	2.3818E-10
10	3.3908E-09	2.6957E-10
Front Poly. Thck. = 3 cm		
1	1.3875E-09	6.9651E-11
2	2.3568E-09	9.4038E-11
3	3.0282E-09	1.1113E-10
4	3.4341E-09	1.3771E-10
5	3.4346E-09	1.6967E-10
6	3.6305E-09	1.8951E-10
7	3.9709E-09	2.5493E-10
8	3.5082E-09	2.4487E-10
9	3.6064E-09	2.6038E-10
10	4.2127E-09	3.6650E-10

Back Poly. Thck. (cm)	Detector Resp.	Relative Error
Front Poly. Thck. = 4 cm		
1	1.9085E-09	1.0687E-10
2	2.9320E-09	1.3135E-10
3	3.4954E-09	1.4086E-10
4	3.8516E-09	1.4598E-10
5	3.9405E-09	1.8560E-10
6	4.1794E-09	2.1273E-10
7	4.3272E-09	2.6266E-10
8	3.9148E-09	2.5681E-10
9	4.0945E-09	2.6696E-10
10	4.3364E-09	2.9227E-10
Front Poly. Thck. = 5 cm		
1	2.1886E-09	1.3832E-10
2	3.0842E-09	1.6346E-10
3	3.7152E-09	1.8167E-10
4	4.1198E-09	1.9198E-10
5	4.1903E-09	1.5798E-10
6	4.4172E-09	2.0982E-10
7	4.6208E-09	2.7263E-10
8	4.1216E-09	2.2998E-10
9	4.4119E-09	2.7530E-10
10	4.6864E-09	3.0134E-10
Front Poly. Thck. = 6 cm		
1	1.9790E-09	1.2626E-10
2	2.9373E-09	1.6537E-10
3	3.5832E-09	1.8346E-10
4	4.0492E-09	1.6764E-10
5	4.3494E-09	1.7398E-10
6	4.6846E-09	2.2580E-10
7	4.7490E-09	2.7639E-10
8	4.2984E-09	2.3426E-10
9	4.5048E-09	2.7705E-10
10	4.8795E-09	3.0594E-10

Back Poly. Thck. (cm)	Detector Resp.	Relative Error
Front Poly. Thck. = 7 cm		
1	2.0632E-09	1.6464E-10
2	2.9732E-09	2.1348E-10
3	3.5397E-09	2.3185E-10
4	4.0039E-09	2.4704E-10
5	4.2393E-09	2.5436E-10
6	4.4980E-09	2.6358E-10
7	4.8108E-09	2.7758E-10
8	4.4466E-09	2.3967E-10
9	4.4934E-09	2.4624E-10
10	5.0267E-09	3.3830E-10
Front Poly. Thck. = 8 cm		
1	2.3504E-09	1.6805E-10
2	3.2360E-09	2.2976E-10
3	3.9736E-09	2.6186E-10
4	4.3006E-09	2.7223E-10
5	4.4268E-09	2.5675E-10
6	4.5931E-09	2.6180E-10
7	4.6478E-09	2.6260E-10
8	4.4930E-09	2.4082E-10
9	4.6042E-09	2.8040E-10
10	5.0573E-09	3.3884E-10
Front Poly. Thck. = 9 cm		
1	2.2953E-09	2.1668E-10
2	3.3533E-09	2.6525E-10
3	3.8643E-09	2.6935E-10
4	4.1996E-09	2.8137E-10
5	4.5134E-09	3.0827E-10
6	4.7797E-09	3.1833E-10
7	4.9592E-09	3.2681E-10
8	4.9835E-09	3.2742E-10
9	4.6330E-09	2.8122E-10
10	5.0698E-09	3.3866E-10

Back Poly. Thck. (cm)	Detector Resp.	Relative Error
Front Poly. Thck. = 10 cm		
1	2.3954E-09	2.3403E-10
2	3.4173E-09	3.1849E-10
3	4.2491E-09	3.4205E-10
4	4.7764E-09	3.8545E-10
5	4.6671E-09	3.3697E-10
6	4.9188E-09	3.6301E-10
7	4.8572E-09	3.4195E-10
8	4.9733E-09	3.6405E-10
9	4.9733E-09	3.6405E-10
10	5.1187E-09	3.4244E-10

Table D.13. Side irradiation for 3 cm radial poly. thck.

Back Poly. Thck. (cm)	Detector Resp.	Relative Error
Front Poly. Thck. = 1 cm		
1	5.4099E-10	3.7166E-11
2	1.7189E-09	6.6176E-11
3	3.0113E-09	1.3069E-10
4	4.1225E-09	1.3852E-10
5	5.2793E-09	2.2754E-10
6	5.3969E-09	2.7200E-10
7	5.7060E-09	2.9728E-10
8	5.6261E-09	3.3756E-10
9	5.5640E-09	3.3328E-10
10	5.7998E-09	3.7757E-10
Front Poly. Thck. = 2 cm		
1	1.5892E-09	6.4999E-11
2	3.4154E-09	1.1715E-10
3	5.5041E-09	1.7833E-10
4	6.4806E-09	1.9442E-10
5	7.9255E-09	2.7977E-10
6	8.3283E-09	2.8483E-10
7	8.7701E-09	3.6396E-10
8	8.5149E-09	4.1212E-10
9	8.5315E-09	4.9312E-10
10	8.9832E-09	5.4259E-10
Front Poly. Thck. = 3 cm		
1	2.9482E-09	1.2205E-10
2	5.2470E-09	1.6790E-10
3	7.5310E-09	2.0861E-10
4	8.7329E-09	2.1919E-10
5	1.0009E-08	3.0928E-10
6	1.0484E-08	3.8161E-10
7	1.0799E-08	4.0173E-10
8	1.1089E-08	4.8459E-10
9	1.1331E-08	5.6653E-10
10	1.1366E-08	5.9444E-10

Back Poly. Thck. (cm)	Detector Resp.	Relative Error
Front Poly. Thck. = 4 cm		
1	3.8608E-09	1.4671E-10
2	6.6271E-09	1.6303E-10
3	8.6673E-09	1.9501E-10
4	1.0185E-08	2.3527E-10
5	1.1605E-08	3.3306E-10
6	1.2063E-08	4.0533E-10
7	1.2296E-08	4.2299E-10
8	1.2496E-08	5.0734E-10
9	1.2503E-08	5.8637E-10
10	1.2626E-08	6.1614E-10
Front Poly. Thck. = 5 cm		
1	5.1751E-09	2.3340E-10
2	8.1127E-09	2.9125E-10
3	1.0184E-08	3.2078E-10
4	1.1787E-08	3.4888E-10
5	1.2700E-08	3.3401E-10
6	1.2844E-08	4.1486E-10
7	1.3307E-08	4.4179E-10
8	1.3505E-08	5.2401E-10
9	1.3472E-08	6.0758E-10
10	1.3816E-08	6.3828E-10
Front Poly. Thck. = 6 cm		
1	5.4659E-09	2.4706E-10
2	8.4423E-09	3.3769E-10
3	1.0814E-08	3.8173E-10
4	1.2433E-08	4.0782E-10
5	1.3253E-08	4.1745E-10
6	1.3645E-08	4.2710E-10
7	1.3835E-08	4.4827E-10
8	1.4224E-08	5.1207E-10
9	1.3956E-08	6.1408E-10
10	1.4849E-08	6.9937E-10

Back Poly. Thck. (cm)	Detector Resp.	Relative Error
Front Poly. Thck. = 7 cm		
1	5.9135E-09	3.2879E-10
2	8.7637E-09	3.9699E-10
3	1.0986E-08	4.4163E-10
4	1.2521E-08	4.4576E-10
5	1.3537E-08	4.5621E-10
6	1.4126E-08	4.6333E-10
7	1.4241E-08	4.5997E-10
8	1.4683E-08	5.4327E-10
9	1.4293E-08	6.2033E-10
10	1.4968E-08	6.6307E-10
Front Poly. Thck. = 8 cm		
1	5.9360E-09	3.3776E-10
2	8.7953E-09	4.1162E-10
3	1.1134E-08	4.6874E-10
4	1.2683E-08	5.0351E-10
5	1.3621E-08	4.9991E-10
6	1.4384E-08	5.3940E-10
7	1.4592E-08	5.1803E-10
8	1.4959E-08	5.4751E-10
9	1.4633E-08	6.2923E-10
10	1.5260E-08	6.6685E-10
Front Poly. Thck. = 9 cm		
1	6.1059E-09	4.2985E-10
2	8.8696E-09	4.7541E-10
3	1.1156E-08	5.5670E-10
4	1.2319E-08	5.7900E-10
5	1.3237E-08	5.9565E-10
6	1.3898E-08	6.1150E-10
7	1.4064E-08	5.7802E-10
8	1.4292E-08	5.8455E-10
9	1.4771E-08	6.3219E-10
10	1.5814E-08	7.2428E-10

Back Poly. Thck. (cm)	Detector Resp.	Relative Error
Front Poly. Thck. = 10 cm		
1	6.2266E-09	3.6674E-10
2	9.9212E-09	5.9230E-10
3	1.1824E-08	6.0186E-10
4	1.3506E-08	6.7262E-10
5	1.4601E-08	6.9499E-10
6	1.5221E-08	7.0625E-10
7	1.5573E-08	7.1169E-10
8	1.5759E-08	7.1388E-10
9	1.5919E-08	7.1637E-10
10	1.6013E-08	7.3978E-10

Table D.14. Side irradiation for 4 cm radial poly. thck.

Back Poly. Thck. (cm)	Detector Resp.	Relative Error
Front Poly. Thck. = 1 cm		
1	5.7244E-10	4.7970E-11
2	2.0769E-09	1.1984E-10
3	3.9329E-09	1.7423E-10
4	5.8212E-09	2.3750E-10
5	7.3271E-09	3.0114E-10
6	7.9241E-09	3.3440E-10
7	9.2077E-09	4.0974E-10
8	9.0036E-09	3.9706E-10
9	1.0099E-08	5.4939E-10
10	9.8651E-09	5.2877E-10
Front Poly. Thck. = 2 cm		
1	1.8587E-09	1.0149E-10
2	4.6535E-09	1.6892E-10
3	7.7554E-09	2.5128E-10
4	9.8923E-09	3.0666E-10
5	1.2077E-08	3.3334E-10
6	1.3391E-08	4.4725E-10
7	1.4188E-08	5.0792E-10
8	1.4025E-08	5.0068E-10
9	1.6407E-08	6.3495E-10
10	1.5095E-08	6.7476E-10
Front Poly. Thck. = 3 cm		
1	4.1863E-09	1.8462E-10
2	7.6390E-09	2.4521E-10
3	1.1046E-08	2.9713E-10
4	1.3428E-08	3.5718E-10
5	1.6555E-08	4.5360E-10
6	1.7354E-08	5.0848E-10
7	1.7941E-08	5.6155E-10
8	1.7851E-08	5.6409E-10
9	2.0438E-08	7.0305E-10
10	1.9467E-08	7.7478E-10

Back Poly. Thck. (cm)	Detector Resp.	Relative Error
Front Poly. Thck. = 4 cm		
1	5.7325E-09	2.3045E-10
2	9.9338E-09	3.1093E-10
3	1.3370E-08	3.5698E-10
4	1.6112E-08	3.8508E-10
5	1.9642E-08	4.9302E-10
6	2.0147E-08	5.4397E-10
7	2.0934E-08	6.0498E-10
8	2.1045E-08	6.2924E-10
9	2.3632E-08	8.1768E-10
10	2.2250E-08	8.2548E-10
Front Poly. Thck. = 5 cm		
1	7.5437E-09	2.8213E-10
2	1.2561E-08	3.7682E-10
3	1.6660E-08	4.3484E-10
4	1.9810E-08	4.9327E-10
5	2.1765E-08	5.1582E-10
6	2.2245E-08	5.6948E-10
7	2.2975E-08	6.3181E-10
8	2.3409E-08	6.7652E-10
9	2.5883E-08	7.8166E-10
10	2.4792E-08	8.7021E-10
Front Poly. Thck. = 6 cm		
1	7.9399E-09	3.1362E-10
2	1.2738E-08	3.8595E-10
3	1.6690E-08	4.8569E-10
4	1.9426E-08	5.1674E-10
5	2.1901E-08	5.4971E-10
6	2.3728E-08	5.8608E-10
7	2.4177E-08	6.4552E-10
8	2.4629E-08	6.9208E-10
9	2.7223E-08	7.9491E-10
10	2.5939E-08	8.8194E-10

Back Poly. Thck. (cm)	Detector Resp.	Relative Error
Front Poly. Thck. = 7 cm		
1	8.9238E-09	3.9622E-10
2	1.4119E-08	5.0970E-10
3	1.7913E-08	5.6963E-10
4	2.0632E-08	6.0452E-10
5	2.2654E-08	6.2978E-10
6	2.3986E-08	6.4523E-10
7	2.5178E-08	6.5715E-10
8	2.5437E-08	6.9952E-10
9	2.8360E-08	8.7631E-10
10	2.6955E-08	9.0030E-10
Front Poly. Thck. = 8 cm		
1	9.2369E-09	3.7502E-10
2	1.3842E-08	4.5403E-10
3	1.7413E-08	5.0499E-10
4	2.0351E-08	5.3931E-10
5	2.2613E-08	6.6707E-10
6	2.3939E-08	6.8466E-10
7	2.4860E-08	6.9609E-10
8	2.6084E-08	7.0687E-10
9	2.8962E-08	8.8334E-10
10	2.7541E-08	9.0886E-10
Front Poly. Thck. = 9 cm		
1	1.0087E-08	4.9226E-10
2	1.4970E-08	5.6138E-10
3	1.9458E-08	6.8297E-10
4	2.2310E-08	7.8530E-10
5	2.4260E-08	8.1271E-10
6	2.5499E-08	8.2871E-10
7	2.6513E-08	8.4047E-10
8	2.7016E-08	8.4831E-10
9	2.9507E-08	8.9407E-10
10	2.8036E-08	9.1677E-10

Back Poly. Thck. (cm)	Detector Resp.	Relative Error
Front Poly. Thck. = 10 cm		
1	1.0338E-08	5.9234E-10
2	1.5753E-08	7.0887E-10
3	1.9993E-08	7.9970E-10
4	2.3337E-08	8.7749E-10
5	2.5429E-08	9.1800E-10
6	2.6856E-08	9.4266E-10
7	2.7712E-08	9.5885E-10
8	2.8272E-08	9.6691E-10
9	2.8572E-08	9.7144E-10
10	2.8473E-08	9.2538E-10

Table D.15. Side irradiation for 5 cm radial poly. thck.

Back Poly. Thck. (cm)	Detector Resp.	Relative Error
Front Poly. Thck. = 1 cm		
1	5.3430E-10	5.0812E-11
2	2.2206E-09	1.2368E-10
3	4.0276E-09	1.9494E-10
4	6.4358E-09	2.7931E-10
5	8.9116E-09	2.9676E-10
6	1.0957E-08	4.4596E-10
7	1.1574E-08	4.5715E-10
8	1.2814E-08	5.4586E-10
9	1.2737E-08	6.4575E-10
10	1.2899E-08	6.6042E-10
Front Poly. Thck. = 2 cm		
1	2.3165E-09	1.5799E-10
2	5.5508E-09	2.2703E-10
3	8.8619E-09	2.6408E-10
4	1.1837E-08	3.7879E-10
5	1.5300E-08	3.9780E-10
6	1.7358E-08	5.5373E-10
7	1.7965E-08	5.6409E-10
8	2.0188E-08	5.6122E-10
9	1.9327E-08	7.6922E-10
10	2.0565E-08	8.3495E-10
Front Poly. Thck. = 3 cm		
1	4.2648E-09	2.1409E-10
2	8.8397E-09	3.0851E-10
3	1.3196E-08	3.2065E-10
4	1.7114E-08	4.4668E-10
5	2.1335E-08	5.5470E-10
6	2.3348E-08	6.3741E-10
7	2.4142E-08	7.0976E-10
8	2.5694E-08	7.1173E-10
9	2.4970E-08	8.7893E-10
10	2.7554E-08	9.7817E-10

Back Poly. Thck. (cm)	Detector Resp.	Relative Error
Front Poly. Thck. = 4 cm		
1	6.8240E-09	2.9343E-10
2	1.2156E-08	3.8048E-10
3	1.7356E-08	4.3216E-10
4	2.0895E-08	4.8895E-10
5	2.5511E-08	5.1022E-10
6	2.7667E-08	6.9443E-10
7	2.8284E-08	7.2406E-10
8	2.9702E-08	8.6730E-10
9	2.9836E-08	9.4282E-10
10	3.2200E-08	1.0497E-09
Front Poly. Thck. = 5 cm		
1	8.8008E-09	3.1067E-10
2	1.5322E-08	4.6425E-10
3	2.0541E-08	5.3406E-10
4	2.4952E-08	5.3896E-10
5	2.8793E-08	5.3842E-10
6	3.0932E-08	7.3309E-10
7	3.1214E-08	7.5851E-10
8	3.2697E-08	5.9835E-10
9	3.3035E-08	9.8443E-10
10	3.5485E-08	1.1036E-09
Front Poly. Thck. = 6 cm		
1	1.0204E-08	4.0715E-10
2	1.6375E-08	5.0434E-10
3	2.2293E-08	5.9745E-10
4	2.6657E-08	6.5575E-10
5	3.0055E-08	6.9428E-10
6	3.3131E-08	7.5538E-10
7	3.3244E-08	7.7792E-10
8	3.4951E-08	7.8290E-10
9	3.5066E-08	1.0064E-09
10	3.8075E-08	1.1385E-09

Back Poly. Thck. (cm)	Detector Resp.	Relative Error
Front Poly. Thck. = 7 cm		
1	1.0746E-08	4.6528E-10
2	1.7085E-08	5.7748E-10
3	2.2606E-08	6.6687E-10
4	2.6649E-08	7.1951E-10
5	2.9865E-08	7.5560E-10
6	3.2322E-08	7.8542E-10
7	3.5189E-08	8.4454E-10
8	3.6510E-08	7.9592E-10
9	3.6802E-08	1.0268E-09
10	3.9961E-08	1.1709E-09
Front Poly. Thck. = 8 cm		
1	1.1994E-08	5.3132E-10
2	1.8748E-08	6.5994E-10
3	2.4513E-08	7.4765E-10
4	2.9392E-08	8.2298E-10
5	3.2578E-08	8.5679E-10
6	3.5057E-08	8.8693E-10
7	3.6429E-08	8.9980E-10
8	3.7255E-08	6.3333E-10
9	3.8083E-08	1.0397E-09
10	4.1283E-08	1.1890E-09
Front Poly. Thck. = 9 cm		
1	1.2666E-08	5.5098E-10
2	1.9474E-08	7.2443E-10
3	2.5853E-08	8.4798E-10
4	2.9865E-08	9.1388E-10
5	3.3183E-08	9.7558E-10
6	3.5416E-08	9.9873E-10
7	3.7181E-08	1.0225E-09
8	3.8277E-08	1.0335E-09
9	3.8847E-08	1.0450E-09
10	4.1816E-08	1.1918E-09

Back Poly. Thck. (cm)	Detector Resp.	Relative Error
Front Poly. Thck. = 10 cm		
1	1.3414E-08	5.3521E-10
2	2.0897E-08	6.7707E-10
3	2.7714E-08	9.8661E-10
4	3.2338E-08	1.0801E-09
5	3.6041E-08	1.1389E-09
6	3.8903E-08	1.1943E-09
7	4.0438E-08	1.2212E-09
8	4.1704E-08	1.2386E-09
9	4.2473E-08	1.2444E-09
10	4.2325E-08	1.1978E-09

Table D.16. Side irradiation for 6 cm radial poly. thck.

Back Poly. Thck. (cm)	Detector Resp.	Relative Error
Front Poly. Thck. = 1 cm		
1	5.1792E-10	4.9202E-11
2	2.0559E-09	1.3179E-10
3	4.3261E-09	2.3707E-10
4	7.1545E-09	3.5558E-10
5	9.3329E-09	3.7891E-10
6	1.1539E-08	3.5772E-10
7	1.2963E-08	5.6132E-10
8	1.3422E-08	6.0131E-10
9	1.4474E-08	7.0056E-10
10	1.5275E-08	5.5905E-10
Front Poly. Thck. = 2 cm		
1	1.9280E-09	1.4749E-10
2	5.0977E-09	2.3857E-10
3	9.3980E-09	3.5149E-10
4	1.3063E-08	4.6244E-10
5	1.5875E-08	4.9053E-10
6	1.8825E-08	6.2875E-10
7	2.1296E-08	7.2620E-10
8	2.2158E-08	7.7333E-10
9	2.3282E-08	7.9858E-10
10	2.4435E-08	7.0862E-10
Front Poly. Thck. = 3 cm		
1	4.4639E-09	2.5757E-10
2	9.5738E-09	3.7242E-10
3	1.4447E-08	4.3486E-10
4	1.8502E-08	5.3287E-10
5	2.1769E-08	5.6599E-10
6	2.4870E-08	7.0631E-10
7	2.7425E-08	8.2276E-10
8	2.9272E-08	6.9961E-10
9	3.1118E-08	7.0950E-10
10	3.1713E-08	8.0867E-10

Back Poly. Thck. (cm)	Detector Resp.	Relative Error
Front Poly. Thck. = 4 cm		
1	6.9556E-09	3.2761E-10
2	1.3445E-08	4.5849E-10
3	1.8714E-08	5.2211E-10
4	2.3313E-08	5.8748E-10
5	2.6847E-08	6.7655E-10
6	3.0365E-08	7.8645E-10
7	3.2630E-08	8.9732E-10
8	3.4846E-08	9.5477E-10
9	3.5495E-08	9.5837E-10
10	3.6625E-08	8.5702E-10
Front Poly. Thck. = 5 cm		
1	8.7589E-09	3.9765E-10
2	1.5803E-08	4.7567E-10
3	2.1746E-08	5.7844E-10
4	2.6807E-08	6.3265E-10
5	3.0925E-08	6.6799E-10
6	3.4250E-08	8.2885E-10
7	3.6575E-08	9.4729E-10
8	3.9687E-08	1.0160E-09
9	3.9682E-08	1.0079E-09
10	4.0756E-08	8.9664E-10
Front Poly. Thck. = 6 cm		
1	1.0925E-08	4.7631E-10
2	1.8610E-08	6.3460E-10
3	2.4474E-08	7.1221E-10
4	2.9828E-08	7.8446E-10
5	3.4164E-08	8.3359E-10
6	3.7097E-08	8.5695E-10
7	3.9632E-08	9.8288E-10
8	4.2489E-08	1.0537E-09
9	4.2683E-08	1.1439E-09
10	4.3696E-08	9.2199E-10

Back Poly. Thck. (cm)	Detector Resp.	Relative Error
Front Poly. Thck. = 7 cm		
1	1.2394E-08	5.7136E-10
2	2.0501E-08	7.2367E-10
3	2.6859E-08	8.1653E-10
4	3.2349E-08	8.8312E-10
5	3.6843E-08	9.4317E-10
6	3.9934E-08	9.7839E-10
7	4.1925E-08	1.0104E-09
8	4.5059E-08	1.0814E-09
9	4.5120E-08	1.1821E-09
10	4.5534E-08	9.3801E-10
Front Poly. Thck. = 8 cm		
1	1.4526E-08	6.3479E-10
2	2.2574E-08	7.2913E-10
3	2.9236E-08	6.7828E-10
4	3.4398E-08	7.2924E-10
5	3.9526E-08	9.4468E-10
6	4.1969E-08	7.9742E-10
7	4.3937E-08	8.1284E-10
8	4.6693E-08	1.0973E-09
9	4.6666E-08	1.2040E-09
10	4.7251E-08	9.5448E-10
Front Poly. Thck. = 9 cm		
1	1.4028E-08	6.2706E-10
2	2.3027E-08	8.4277E-10
3	3.0128E-08	9.5204E-10
4	3.5836E-08	1.0500E-09
5	4.0168E-08	1.1247E-09
6	4.3061E-08	1.1540E-09
7	4.5329E-08	1.1740E-09
8	4.6817E-08	1.1892E-09
9	4.7747E-08	1.2128E-09
10	4.8428E-08	9.6371E-10

Back Poly. Thck. (cm)	Detector Resp.	Relative Error
Front Poly. Thck. = 10 cm		
1	1.4828E-08	6.9991E-10
2	2.3079E-08	8.8623E-10
3	3.0735E-08	1.0204E-09
4	3.6325E-08	1.1261E-09
5	4.0305E-08	1.1769E-09
6	4.3372E-08	1.2231E-09
7	4.5157E-08	1.2508E-09
8	4.6542E-08	1.2660E-09
9	4.7990E-08	1.2861E-09
10	4.9271E-08	9.7064E-10

Table D.17. Side irradiation for 7 cm radial poly. thck.

Back Poly. Thck. (cm)	Detector Resp.	Relative Error
Front Poly. Thck. = 1 cm		
1	4.3142E-10	4.2926E-11
2	1.6552E-09	1.5443E-10
3	3.7893E-09	2.4631E-10
4	6.5446E-09	3.2985E-10
5	8.6861E-09	4.1085E-10
6	1.0331E-08	5.0932E-10
7	1.3894E-08	6.3220E-10
8	1.3871E-08	5.8398E-10
9	1.5898E-08	7.5514E-10
10	1.6396E-08	8.2142E-10
Front Poly. Thck. = 2 cm		
1	1.4853E-09	1.4170E-10
2	4.4599E-09	2.3192E-10
3	8.0361E-09	3.6323E-10
4	1.2601E-08	4.6496E-10
5	1.5320E-08	5.2240E-10
6	1.7801E-08	6.5151E-10
7	2.2168E-08	7.8253E-10
8	2.1952E-08	7.1562E-10
9	2.4473E-08	9.2263E-10
10	2.5522E-08	1.0821E-09
Front Poly. Thck. = 3 cm		
1	3.7977E-09	2.5027E-10
2	8.4334E-09	3.7697E-10
3	1.2743E-08	4.4599E-10
4	1.8146E-08	5.4076E-10
5	2.1845E-08	6.2040E-10
6	2.4971E-08	7.6662E-10
7	2.9227E-08	8.9142E-10
8	3.0076E-08	9.2936E-10
9	3.1222E-08	1.0241E-09
10	3.3117E-08	1.2022E-09

Back Poly. Thck. (cm)	Detector Resp.	Relative Error
Front Poly. Thck. = 4 cm		
1	6.6443E-09	2.5448E-10
2	1.2919E-08	4.4184E-10
3	1.8308E-08	4.9982E-10
4	2.3233E-08	6.0406E-10
5	2.7167E-08	7.4982E-10
6	3.0604E-08	8.3550E-10
7	3.4801E-08	9.5008E-10
8	3.5626E-08	9.2271E-10
9	3.7766E-08	1.1217E-09
10	3.9630E-08	1.2959E-09
Front Poly. Thck. = 5 cm		
1	8.3102E-09	3.5402E-10
2	1.5755E-08	4.5217E-10
3	2.1665E-08	5.7628E-10
4	2.6877E-08	7.1493E-10
5	3.1538E-08	7.9475E-10
6	3.5101E-08	8.4594E-10
7	3.8754E-08	9.8822E-10
8	4.0328E-08	8.7916E-10
9	4.2168E-08	1.1976E-09
10	4.4146E-08	1.3862E-09
Front Poly. Thck. = 6 cm		
1	1.1184E-08	5.0999E-10
2	1.8815E-08	5.4565E-10
3	2.5576E-08	7.5960E-10
4	3.0961E-08	8.2977E-10
5	3.5948E-08	6.0392E-10
6	3.7944E-08	9.0686E-10
7	4.2078E-08	1.0225E-09
8	4.3953E-08	1.0241E-09
9	4.5136E-08	1.2322E-09
10	4.7342E-08	1.4155E-09

Back Poly. Thck. (cm)	Detector Resp.	Relative Error
Front Poly. Thck. = 7 cm		
1	1.2522E-08	4.2324E-10
2	2.0264E-08	5.3294E-10
3	2.6488E-08	7.4167E-10
4	3.2677E-08	8.2019E-10
5	3.7997E-08	9.4613E-10
6	4.1754E-08	1.0397E-09
7	4.4568E-08	1.0518E-09
8	4.6567E-08	1.1362E-09
9	4.8851E-08	1.1284E-09
10	4.9723E-08	1.4370E-09
Front Poly. Thck. = 8 cm		
1	1.3306E-08	4.0450E-10
2	2.2862E-08	8.4820E-10
3	2.9669E-08	8.9896E-10
4	3.6021E-08	1.0302E-09
5	4.0187E-08	1.0850E-09
6	4.3940E-08	1.1249E-09
7	4.6726E-08	1.1541E-09
8	4.8732E-08	1.1647E-09
9	5.0244E-08	1.2862E-09
10	5.2134E-08	1.4650E-09
Front Poly. Thck. = 9 cm		
1	1.4627E-08	5.5145E-10
2	2.3670E-08	7.8110E-10
3	3.1761E-08	1.0608E-09
4	3.8037E-08	1.1677E-09
5	4.2155E-08	1.2183E-09
6	4.5755E-08	1.2583E-09
7	4.8401E-08	1.2972E-09
8	5.0620E-08	1.0225E-09
9	5.1735E-08	1.3037E-09
10	5.3208E-08	1.4739E-09

Back Poly. Thck. (cm)	Detector Resp.	Relative Error
Front Poly. Thck. = 10 cm		
1	1.5129E-08	5.5374E-10
2	2.3869E-08	7.0174E-10
3	3.1431E-08	8.0149E-10
4	3.8797E-08	1.1096E-09
5	4.2308E-08	1.2523E-09
6	4.5462E-08	1.2911E-09
7	4.8016E-08	1.3205E-09
8	5.0570E-08	1.3603E-09
9	5.2116E-08	1.3759E-09
10	5.4312E-08	1.4827E-09

Table D.18. Side irradiation for 8 cm radial poly. thck.

Back Poly. Thck. (cm)	Detector Resp.	Relative Error
Front Poly. Thck. = 1 cm		
1	2.9586E-10	2.8462E-11
2	1.4821E-09	1.4421E-10
3	3.6279E-09	1.9155E-10
4	6.1377E-09	2.9645E-10
5	7.6662E-09	4.2931E-10
6	1.0432E-08	5.4352E-10
7	1.0584E-08	5.4613E-10
8	1.3637E-08	7.6776E-10
9	1.4416E-08	7.1216E-10
10	1.5612E-08	7.0409E-10
Front Poly. Thck. = 2 cm		
1	1.5855E-09	1.4983E-10
2	4.4971E-09	2.9456E-10
3	8.9725E-09	4.8182E-10
4	1.1509E-08	5.3289E-10
5	1.4286E-08	5.7287E-10
6	1.8365E-08	7.1073E-10
7	1.8520E-08	7.2412E-10
8	2.2634E-08	9.4612E-10
9	2.2794E-08	8.8897E-10
10	2.4635E-08	9.0903E-10
Front Poly. Thck. = 3 cm		
1	4.0436E-09	3.1297E-10
2	8.9084E-09	4.4987E-10
3	1.4080E-08	5.5618E-10
4	1.7133E-08	6.4761E-10
5	1.9881E-08	6.6006E-10
6	2.4655E-08	8.1607E-10
7	2.5514E-08	8.5471E-10
8	2.9919E-08	1.0621E-09
9	3.0317E-08	1.0520E-09
10	3.2338E-08	1.0057E-09

Back Poly. Thck. (cm)	Detector Resp.	Relative Error
Front Poly. Thck. = 4 cm		
1	5.9798E-09	3.5341E-10
2	1.1978E-08	4.5997E-10
3	1.7710E-08	6.3404E-10
4	2.2411E-08	7.2835E-10
5	2.5997E-08	7.5130E-10
6	3.0335E-08	8.8579E-10
7	3.1738E-08	9.4896E-10
8	3.5967E-08	1.1401E-09
9	3.7267E-08	1.1665E-09
10	3.8348E-08	1.0814E-09
Front Poly. Thck. = 5 cm		
1	8.1000E-09	4.5117E-10
2	1.4891E-08	5.9861E-10
3	2.0816E-08	7.0150E-10
4	2.6233E-08	7.7648E-10
5	3.0327E-08	8.0063E-10
6	3.5096E-08	9.4409E-10
7	3.6248E-08	1.0077E-09
8	4.0844E-08	1.1967E-09
9	4.2465E-08	1.2315E-09
10	4.3170E-08	1.1310E-09
Front Poly. Thck. = 6 cm		
1	9.9476E-09	3.9193E-10
2	1.7647E-08	5.5236E-10
3	2.5112E-08	6.6548E-10
4	3.1072E-08	7.3331E-10
5	3.5767E-08	7.7257E-10
6	3.8985E-08	9.9023E-10
7	3.9581E-08	1.0410E-09
8	4.5282E-08	1.0958E-09
9	4.6253E-08	1.2303E-09
10	4.7172E-08	1.1793E-09

Back Poly. Thck. (cm)	Detector Resp.	Relative Error
Front Poly. Thck. = 7 cm		
1	1.0816E-08	5.3647E-10
2	1.7983E-08	6.9235E-10
3	2.6058E-08	8.6250E-10
4	3.1395E-08	9.3557E-10
5	3.5654E-08	9.9118E-10
6	3.9523E-08	1.0355E-09
7	4.2734E-08	1.0812E-09
8	4.7547E-08	1.2695E-09
9	4.9239E-08	1.2654E-09
10	4.9679E-08	1.2022E-09
Front Poly. Thck. = 8 cm		
1	1.3474E-08	5.4703E-10
2	2.1532E-08	7.9453E-10
3	2.9839E-08	8.8622E-10
4	3.6348E-08	9.0144E-10
5	4.1269E-08	1.0813E-09
6	4.5116E-08	1.1189E-09
7	4.7915E-08	1.1500E-09
8	5.0033E-08	1.1357E-09
9	5.1321E-08	1.3497E-09
10	5.2044E-08	1.2230E-09
Front Poly. Thck. = 9 cm		
1	1.3989E-08	7.2885E-10
2	2.3535E-08	9.2961E-10
3	3.0946E-08	1.0491E-09
4	3.7306E-08	1.1043E-09
5	4.2642E-08	1.2238E-09
6	4.5782E-08	1.2544E-09
7	4.8479E-08	1.2799E-09
8	5.0720E-08	1.2477E-09
9	5.2802E-08	1.3623E-09
10	5.3815E-08	1.2485E-09

Back Poly. Thck. (cm)	Detector Resp.	Relative Error
Front Poly. Thck. = 10 cm		
1	1.5496E-08	7.0196E-10
2	2.4580E-08	9.0700E-10
3	3.2467E-08	1.0779E-09
4	3.7854E-08	1.1432E-09
5	4.2293E-08	1.2730E-09
6	4.6164E-08	1.3203E-09
7	4.9544E-08	1.3625E-09
8	5.1870E-08	1.3486E-09
9	5.3627E-08	1.3675E-09
10	5.5203E-08	1.2586E-09

Table D.19. Side irradiation for 9 cm radial poly. thck.

Back Poly. Thck. (cm)	Detector Resp.	Relative Error
Front Poly. Thck. = 1 cm		
1	2.2052E-10	2.1743E-11
2	1.0965E-09	1.0680E-10
3	2.8551E-09	2.6238E-10
4	4.6247E-09	2.4326E-10
5	6.2361E-09	3.9163E-10
6	8.7926E-09	5.2580E-10
7	1.0821E-08	6.1682E-10
8	1.2518E-08	7.0349E-10
9	1.2370E-08	6.9151E-10
10	1.3770E-08	8.2068E-10
Front Poly. Thck. = 2 cm		
1	1.1523E-09	6.7525E-11
2	3.1317E-09	2.6808E-10
3	6.3875E-09	3.9603E-10
4	9.8201E-09	4.2619E-10
5	1.2257E-08	5.7238E-10
6	1.5714E-08	6.5527E-10
7	1.8242E-08	7.8621E-10
8	2.0196E-08	8.7449E-10
9	2.0301E-08	8.1001E-10
10	2.2024E-08	9.8666E-10
Front Poly. Thck. = 3 cm		
1	2.6797E-09	2.5484E-10
2	6.1947E-09	3.9461E-10
3	1.0684E-08	5.0215E-10
4	1.5107E-08	5.2117E-10
5	1.7730E-08	6.7375E-10
6	2.2459E-08	8.1750E-10
7	2.5153E-08	9.0803E-10
8	2.6628E-08	1.0172E-09
9	2.7624E-08	9.4751E-10
10	2.9373E-08	1.1456E-09

Back Poly. Thck. (cm)	Detector Resp.	Relative Error
Front Poly. Thck. = 4 cm		
1	4.5787E-09	3.3791E-10
2	9.8472E-09	3.8010E-10
3	1.4807E-08	4.5161E-10
4	1.9633E-08	5.7722E-10
5	2.3138E-08	7.1266E-10
6	2.8285E-08	8.8531E-10
7	3.0758E-08	1.0058E-09
8	3.2494E-08	1.1015E-09
9	3.3730E-08	1.1772E-09
10	3.5467E-08	1.2484E-09
Front Poly. Thck. = 5 cm		
1	6.4180E-09	4.1332E-10
2	1.1762E-08	5.5989E-10
3	1.7490E-08	6.7862E-10
4	2.2667E-08	7.6162E-10
5	2.7535E-08	8.5358E-10
6	3.2939E-08	9.4866E-10
7	3.4640E-08	1.0634E-09
8	3.6765E-08	1.1654E-09
9	3.8276E-08	1.1827E-09
10	4.0364E-08	1.3280E-09
Front Poly. Thck. = 6 cm		
1	9.4333E-09	5.5751E-10
2	1.5793E-08	6.7435E-10
3	2.2103E-08	8.2443E-10
4	2.7459E-08	8.6496E-10
5	3.2704E-08	9.5168E-10
6	3.7437E-08	1.0632E-09
7	3.9336E-08	1.1407E-09
8	3.9960E-08	1.1988E-09
9	4.1725E-08	1.2225E-09
10	4.3921E-08	1.3747E-09

Back Poly. Thck. (cm)	Detector Resp.	Relative Error
Front Poly. Thck. = 7 cm		
1	1.0257E-08	5.7848E-10
2	1.7244E-08	7.5872E-10
3	2.3852E-08	8.7775E-10
4	3.0070E-08	9.8029E-10
5	3.4273E-08	1.0282E-09
6	3.8251E-08	1.0978E-09
7	4.2276E-08	1.1753E-09
8	4.2688E-08	1.2337E-09
9	4.4419E-08	1.1638E-09
10	4.6992E-08	1.4051E-09
Front Poly. Thck. = 8 cm		
1	1.1606E-08	6.5573E-10
2	2.0034E-08	8.9553E-10
3	2.7699E-08	1.0387E-09
4	3.3842E-08	1.1269E-09
5	3.8264E-08	1.1938E-09
6	4.2479E-08	1.2701E-09
7	4.5052E-08	1.3020E-09
8	4.4981E-08	1.2550E-09
9	4.6307E-08	1.2179E-09
10	4.8899E-08	1.4230E-09
Front Poly. Thck. = 9 cm		
1	1.2923E-08	6.5647E-10
2	2.0557E-08	7.8529E-10
3	2.7848E-08	9.0505E-10
4	3.3407E-08	9.8217E-10
5	3.8396E-08	1.0444E-09
6	4.2028E-08	1.2188E-09
7	4.5382E-08	1.3297E-09
8	4.7418E-08	1.3514E-09
9	4.8046E-08	1.3645E-09
10	5.0508E-08	1.4395E-09

Back Poly. Thck. (cm)	Detector Resp.	Relative Error
Front Poly. Thck. = 10 cm		
1	1.3572E-08	7.0984E-10
2	2.1556E-08	9.7434E-10
3	2.7927E-08	1.0892E-09
4	3.4198E-08	1.2106E-09
5	3.8587E-08	1.2695E-09
6	4.3293E-08	1.3551E-09
7	4.6707E-08	1.4059E-09
8	4.8308E-08	1.4299E-09
9	5.0112E-08	1.4583E-09
10	5.1471E-08	1.4463E-09

Table D.20. Side irradiation for 10 cm radial poly. thck.

Back Poly. Thck. (cm)	Detector Resp.	Relative Error
Front Poly. Thck. = 1 cm		
1	1.9321E-10	1.9128E-11
2	8.7529E-10	8.6129E-11
3	2.5612E-09	2.3461E-10
4	4.4633E-09	3.7849E-10
5	5.8865E-09	4.4914E-10
6	7.7532E-09	5.2644E-10
7	8.9097E-09	5.9695E-10
8	1.0554E-08	6.7548E-10
9	1.0226E-08	6.3709E-10
10	1.1565E-08	6.1757E-10
Front Poly. Thck. = 2 cm		
1	9.1263E-10	8.9255E-11
2	3.0928E-09	3.0000E-10
3	5.5179E-09	3.4984E-10
4	8.7281E-09	5.1321E-10
5	1.1668E-08	6.2657E-10
6	1.4078E-08	6.9548E-10
7	1.4972E-08	7.5308E-10
8	1.6378E-08	8.0416E-10
9	1.6654E-08	8.1103E-10
10	1.8155E-08	8.3333E-10
Front Poly. Thck. = 3 cm		
1	2.0035E-09	1.8472E-10
2	5.1112E-09	2.5760E-10
3	8.8282E-09	5.2793E-10
4	1.3004E-08	6.3591E-10
5	1.7349E-08	7.7378E-10
6	1.9707E-08	7.9815E-10
7	2.1372E-08	8.7413E-10
8	2.3876E-08	1.0028E-09
9	2.3377E-08	1.0192E-09
10	2.5446E-08	9.1605E-10

Back Poly. Thck. (cm)	Detector Resp.	Relative Error
Front Poly. Thck. = 4 cm		
1	3.9986E-09	2.5551E-10
2	8.0400E-09	3.8753E-10
3	1.2802E-08	4.7494E-10
4	1.7784E-08	7.5762E-10
5	2.2330E-08	8.5971E-10
6	2.5320E-08	9.0140E-10
7	2.6669E-08	9.6276E-10
8	2.9144E-08	1.0900E-09
9	2.8288E-08	1.0891E-09
10	3.1535E-08	1.1069E-09
Front Poly. Thck. = 5 cm		
1	6.5244E-09	4.8868E-10
2	1.2344E-08	6.9498E-10
3	1.7393E-08	7.9140E-10
4	2.2397E-08	8.7125E-10
5	2.6186E-08	9.2698E-10
6	2.9387E-08	8.7572E-10
7	3.1380E-08	1.0355E-09
8	3.3473E-08	1.1481E-09
9	3.3503E-08	1.1860E-09
10	3.6200E-08	1.0751E-09
Front Poly. Thck. = 6 cm		
1	7.7809E-09	5.1821E-10
2	1.4283E-08	7.1985E-10
3	1.9644E-08	6.3842E-10
4	2.6063E-08	9.3828E-10
5	3.0291E-08	9.2084E-10
6	3.3862E-08	9.1428E-10
7	3.5389E-08	1.0511E-09
8	3.7191E-08	1.1976E-09
9	3.7412E-08	1.2533E-09
10	3.9840E-08	1.1673E-09

Back Poly. Thck. (cm)	Detector Resp.	Relative Error
Front Poly. Thck. = 7 cm		
1	1.0425E-08	6.5154E-10
2	1.6920E-08	8.0031E-10
3	2.3664E-08	9.0158E-10
4	2.8452E-08	1.0129E-09
5	3.2762E-08	1.0811E-09
6	3.6928E-08	1.0894E-09
7	3.8711E-08	1.1110E-09
8	3.9989E-08	1.2437E-09
9	4.0663E-08	1.3053E-09
10	4.2497E-08	1.1984E-09
Front Poly. Thck. = 8 cm		
1	1.0850E-08	6.5426E-10
2	1.8305E-08	7.7611E-10
3	2.4125E-08	9.6984E-10
4	2.9596E-08	1.0595E-09
5	3.3828E-08	1.1231E-09
6	3.7425E-08	1.1714E-09
7	4.0033E-08	1.2370E-09
8	4.2691E-08	1.2893E-09
9	4.2702E-08	1.3280E-09
10	4.4298E-08	1.2138E-09
Front Poly. Thck. = 9 cm		
1	1.2016E-08	6.9333E-10
2	1.9414E-08	8.2314E-10
3	2.5214E-08	1.0514E-09
4	3.0553E-08	1.0449E-09
5	3.4556E-08	1.1404E-09
6	3.8786E-08	1.2024E-09
7	4.1201E-08	1.1742E-09
8	4.3035E-08	1.2480E-09
9	4.4246E-08	1.3407E-09
10	4.6135E-08	1.2964E-09

Back Poly. Thck. (cm)	Detector Resp.	Relative Error
Front Poly. Thck. = 10 cm		
1	1.2170E-08	7.8982E-10
2	1.9260E-08	1.0034E-09
3	2.6058E-08	1.0944E-09
4	3.1513E-08	1.1723E-09
5	3.5976E-08	1.1764E-09
6	3.9950E-08	1.2305E-09
7	4.2109E-08	1.3054E-09
8	4.4179E-08	1.3254E-09
9	4.5648E-08	1.3375E-09
10	4.7127E-08	1.2489E-09

Table D.21. α -phase criticality values

Radius	k_{eff}	$\sigma(k_{eff})$
^{240}Pu Frac. = 0.00		
0.5	0.10796	0.00007
1	0.21447	0.00013
1.5	0.31898	0.00017
2	0.42092	0.00024
2.5	0.52058	0.00028
3	0.6191	0.00033
3.5	0.71389	0.00037
4	0.80571	0.00043
4.5	0.89661	0.00046
5	0.98186	0.00048
5.5	1.06481	0.00055
6	1.14307	0.00057
6.5	1.21947	0.00061
7	1.29374	0.00064
7.5	1.36549	0.00068
8	1.43185	0.00071
8.5	1.49697	0.00073
9	1.55801	0.00071
9.5	1.6182	0.00073
10	1.67264	0.00078
^{240}Pu Frac. = 0.01		
0.5	0.10775	0.00007
1	0.2139	0.00012
1.5	0.31829	0.00018
2	0.42031	0.00024
2.5	0.52095	0.00029
3	0.61659	0.00033
3.5	0.71321	0.00036
4	0.80402	0.00039
4.5	0.89421	0.00047
5	0.97817	0.00048
5.5	1.06093	0.00051
6	1.14181	0.00055
6.5	1.21816	0.00061
7	1.29324	0.00061
7.5	1.36255	0.00063
8	1.4304	0.00072
8.5	1.49328	0.00072
9	1.55448	0.00074
9.5	1.61552	0.00074
10	1.66888	0.00077

Radius	k_{eff}	$\sigma(k_{eff})$
^{240}Pu Frac. = 0.02		
1	0.21324	0.00013
1.5	0.31698	0.00018
2	0.4192	0.00024
2.5	0.51863	0.00029
3	0.61669	0.00034
3.5	0.71107	0.00036
4	0.80251	0.00042
4.5	0.89184	0.00047
5	0.97647	0.00052
5.5	1.05968	0.00055
6	1.13835	0.00059
6.5	1.21434	0.00058
7	1.28955	0.00064
7.5	1.36084	0.00067
8	1.42814	0.00072
8.5	1.49111	0.00071
9	1.55368	0.00076
9.5	1.60989	0.00073
10	1.66821	0.00077
^{240}Pu Frac. = 0.03		
0.5	0.10724	0.00007
1	0.21295	0.00013
1.5	0.31703	0.00018
2	0.41862	0.00023
2.5	0.51766	0.00028
3	0.61435	0.00033
3.5	0.70916	0.00037
4	0.80011	0.00041
4.5	0.88886	0.00047
5	0.97519	0.00049
5.5	1.05758	0.00054
6	1.13646	0.00059
6.5	1.21268	0.00061
7	1.28534	0.00064
7.5	1.35563	0.00066
8	1.42473	0.00068
8.5	1.48831	0.00068
9	1.54902	0.00074
9.5	1.60803	0.00079
10	1.66551	0.00076

Radius	k_{eff}	$\sigma(k_{eff})$
^{240}Pu Frac. = 0.04		
0.5	0.10695	0.00007
1	0.21208	0.00013
1.5	0.31567	0.00018
2	0.41693	0.00023
2.5	0.51643	0.00028
3	0.61371	0.00034
3.5	0.7074	0.00037
4	0.79836	0.00043
4.5	0.88673	0.00043
5	0.97232	0.00049
5.5	1.05362	0.00053
6	1.13388	0.00056
6.5	1.21073	0.00061
7	1.28365	0.00065
7.5	1.35296	0.00065
8	1.42168	0.00069
8.5	1.48584	0.00069
9	1.54667	0.00075
9.5	1.60432	0.00073
10	1.6606	0.00078
^{240}Pu Frac. = 0.05		
0.5	0.10664	0.00007
1	0.21191	0.00012
1.5	0.31539	0.00018
2	0.41584	0.00023
2.5	0.51506	0.00027
3	0.61179	0.00033
3.5	0.7058	0.00037
4	0.79676	0.00042
4.5	0.88591	0.00045
5	0.97072	0.00049
5.5	1.053	0.00053
6	1.13207	0.00056
6.5	1.20699	0.00059
7	1.28038	0.00064
7.5	1.35071	0.00068
8	1.41833	0.00068
8.5	1.48386	0.00069
9	1.54437	0.00074
9.5	1.6024	0.00076
10	1.65691	0.00078

Radius	k_{eff}	$\sigma(k_{eff})$
^{240}Pu Frac. = 0.06		
0.5	0.10643	0.00007
1	0.21116	0.00013
1.5	0.31411	0.00017
2	0.41518	0.00023
2.5	0.51375	0.00028
3	0.60978	0.00033
3.5	0.70421	0.00037
4	0.79535	0.00042
4.5	0.88215	0.00046
5	0.96788	0.00049
5.5	1.04957	0.00052
6	1.1285	0.00055
6.5	1.20471	0.00059
7	1.27915	0.00064
7.5	1.34886	0.00067
8	1.41574	0.0007
8.5	1.47885	0.00069
9	1.53936	0.00074
9.5	1.5982	0.00075
10	1.65308	0.00075
^{240}Pu Frac. = 0.07		
0.5	0.10626	0.00007
1	0.21069	0.00012
1.5	0.31354	0.00019
2	0.41394	0.00022
2.5	0.51182	0.00028
3	0.60812	0.00032
3.5	0.70236	0.00038
4	0.79313	0.0004
4.5	0.88179	0.00045
5	0.96601	0.0005
5.5	1.04836	0.00053
6	1.12688	0.00056
6.5	1.2029	0.00057
7	1.27511	0.00065
7.5	1.3447	0.00064
8	1.4134	0.00069
8.5	1.47552	0.00073
9	1.53726	0.00074
9.5	1.5952	0.00075
10	1.65114	0.00076

Radius	k_{eff}	$\sigma(k_{eff})$
^{240}Pu Frac. = 0.08		
0.5	0.10585	0.00007
1	0.2103	0.00013
1.5	0.31265	0.00019
2	0.41323	0.00023
2.5	0.51162	0.00029
3	0.60721	0.00033
3.5	0.70015	0.00038
4	0.7911	0.00043
4.5	0.87902	0.00046
5	0.96439	0.00052
5.5	1.04442	0.00051
6	1.12385	0.00057
6.5	1.19987	0.00063
7	1.27133	0.00061
7.5	1.34242	0.00064
8	1.41073	0.00067
8.5	1.47339	0.0007
9	1.53381	0.00074
9.5	1.59345	0.00076
10	1.64753	0.00073
^{240}Pu Frac. = 0.09		
0.5	0.10549	0.00007
1	0.2099	0.00012
1.5	0.31184	0.00018
2	0.41193	0.00023
2.5	0.51022	0.00027
3	0.60564	0.00033
3.5	0.69819	0.00038
4	0.78845	0.00042
4.5	0.87678	0.00045
5	0.96192	0.00048
5.5	1.04255	0.00053
6	1.12081	0.00056
6.5	1.19538	0.00058
7	1.26901	0.00065
7.5	1.34037	0.00066
8	1.40533	0.00073
8.5	1.46951	0.00069
9	1.53054	0.00072
9.5	1.58916	0.00075
10	1.64294	0.00072

Radius	k_{eff}	$\sigma(k_{eff})$
^{240}Pu Frac. = 0.1		
0.5	0.10544	0.00007
1	0.20912	0.00012
1.5	0.31086	0.00019
2	0.411	0.00024
2.5	0.50874	0.00028
3	0.60393	0.00032
3.5	0.69714	0.00038
4	0.78682	0.00042
4.5	0.8751	0.00045
5	0.95881	0.00049
5.5	1.04029	0.00053
6	1.11908	0.00057
6.5	1.19523	0.00061
7	1.26702	0.00061
7.5	1.33472	0.00064
8	1.40347	0.00068
8.5	1.466	0.00073
9	1.52701	0.00071
9.5	1.58567	0.00075
10	1.64123	0.00075
^{240}Pu Frac. = 0.11		
0.5	0.10507	0.00007
1	0.20872	0.00012
1.5	0.30979	0.00017
2	0.4098	0.00024
2.5	0.50729	0.00029
3	0.602	0.00032
3.5	0.69488	0.00036
4	0.78462	0.00041
4.5	0.87125	0.00046
5	0.95659	0.0005
5.5	1.03872	0.00054
6	1.11527	0.00057
6.5	1.19322	0.0006
7	1.26454	0.00065
7.5	1.33237	0.00065
8	1.39818	0.00067
8.5	1.46289	0.00071
9	1.52266	0.0007
9.5	1.58231	0.00074
10	1.63591	0.00077

Radius	k_{eff}	$\sigma(k_{eff})$
^{240}Pu Frac. = 0.12		
0.5	0.10486	0.00007
1	0.20815	0.00012
1.5	0.30914	0.00018
2	0.40912	0.00023
2.5	0.50586	0.00027
3	0.6013	0.00033
3.5	0.6926	0.00034
4	0.7824	0.00041
4.5	0.8699	0.00046
5	0.95409	0.00049
5.5	1.03519	0.00054
6	1.11236	0.00055
6.5	1.18847	0.00058
7	1.26066	0.00064
7.5	1.32994	0.00066
8	1.39577	0.00068
8.5	1.45914	0.00068
9	1.51967	0.00071
9.5	1.57828	0.00076
10	1.63523	0.00078
^{240}Pu Frac. = 0.13		
0.5	0.10454	0.00007
1	0.20746	0.00012
1.5	0.30884	0.00018
2	0.40748	0.00022
2.5	0.50464	0.00027
3	0.59888	0.00034
3.5	0.6909	0.00037
4	0.78149	0.00041
4.5	0.86719	0.00044
5	0.95077	0.00048
5.5	1.03301	0.00054
6	1.11185	0.00054
6.5	1.18604	0.00062
7	1.25735	0.00062
7.5	1.32642	0.00066
8	1.39308	0.00067
8.5	1.45745	0.0007
9	1.51682	0.00073
9.5	1.57653	0.00073
10	1.63074	0.00078

Radius	k_{eff}	$\sigma(k_{eff})$
^{240}Pu Frac. = 0.14		
0.5	0.10422	0.00007
1	0.20714	0.00013
1.5	0.30773	0.00018
2	0.40625	0.00023
2.5	0.5035	0.00029
3	0.5982	0.00031
3.5	0.68911	0.00037
4	0.77866	0.00041
4.5	0.86549	0.00046
5	0.9487	0.00051
5.5	1.03034	0.00054
6	1.10784	0.00056
6.5	1.18289	0.00059
7	1.25383	0.00064
7.5	1.32367	0.00065
8	1.38979	0.00068
8.5	1.45369	0.00071
9	1.5144	0.00069
9.5	1.57089	0.00075
10	1.62843	0.00071
^{240}Pu Frac. = 0.15		
0.5	0.10393	0.00007
1	0.20613	0.00013
1.5	0.30711	0.00018
2	0.40608	0.00023
2.5	0.50138	0.00028
3	0.5972	0.00033
3.5	0.6884	0.00037
4	0.77676	0.00041
4.5	0.86353	0.00044
5	0.94742	0.00051
5.5	1.02769	0.00054
6	1.10525	0.00055
6.5	1.1798	0.00058
7	1.25201	0.00062
7.5	1.32099	0.00065
8	1.38783	0.00067
8.5	1.44983	0.00073
9	1.51008	0.00075
9.5	1.56891	0.00075
10	1.62247	0.00076

Radius	k_{eff}	$\sigma(k_{eff})$
^{240}Pu Frac. = 0.16		
0.5	0.10383	0.00007
1	0.20573	0.00012
1.5	0.30656	0.00017
2	0.40451	0.00023
2.5	0.50094	0.00029
3	0.59469	0.00033
3.5	0.686	0.00038
4	0.77511	0.00041
4.5	0.86095	0.00045
5	0.94468	0.00051
5.5	1.02595	0.00051
6	1.1021	0.00054
6.5	1.1764	0.00059
7	1.24776	0.0006
7.5	1.31813	0.00065
8	1.38251	0.00068
8.5	1.44732	0.0007
9	1.50706	0.00071
9.5	1.56507	0.00071
10	1.62073	0.00075
^{240}Pu Frac. = 0.17		
0.5	0.10353	0.00007
1	0.2054	0.00013
1.5	0.30553	0.00018
2	0.40342	0.00023
2.5	0.49982	0.00027
3	0.59324	0.00033
3.5	0.68366	0.00036
4	0.77224	0.00039
4.5	0.85768	0.00042
5	0.94259	0.00049
5.5	1.02124	0.00053
6	1.09977	0.00055
6.5	1.17505	0.00057
7	1.24659	0.0006
7.5	1.31374	0.00066
8	1.38119	0.00065
8.5	1.44308	0.00068
9	1.50389	0.00069
9.5	1.5624	0.00072
10	1.61696	0.00075

Radius	k_{eff}	$\sigma(k_{eff})$
^{240}Pu Frac. = 0.18		
0.5	0.10334	0.00007
1	0.20482	0.00012
1.5	0.30458	0.00018
2	0.40258	0.00022
2.5	0.49794	0.00028
3	0.59163	0.00032
3.5	0.68265	0.00037
4	0.7707	0.00042
4.5	0.85725	0.00044
5	0.94051	0.0005
5.5	1.0196	0.00052
6	1.09692	0.00055
6.5	1.17292	0.00058
7	1.24252	0.00059
7.5	1.31137	0.00063
8	1.3782	0.00067
8.5	1.43974	0.00067
9	1.50231	0.00071
9.5	1.55935	0.00075
10	1.61375	0.00075
^{240}Pu Frac. = 0.19		
0.5	0.1029	0.00007
1	0.20415	0.00012
1.5	0.30384	0.00017
2	0.40132	0.00023
2.5	0.49713	0.00028
3	0.58989	0.00033
3.5	0.68086	0.00037
4	0.76892	0.00041
4.5	0.85506	0.00045
5	0.93769	0.00048
5.5	1.01818	0.00051
6	1.09501	0.00054
6.5	1.16856	0.00057
7	1.24119	0.00063
7.5	1.30793	0.00064
8	1.37348	0.00068
8.5	1.43671	0.00068
9	1.4958	0.00073
9.5	1.5528	0.00071
10	1.61003	0.00076

Radius	k_{eff}	$\sigma(k_{eff})$
^{240}Pu Frac. = 0.2		
0.5	0.10272	0.00007
1	0.20349	0.00013
1.5	0.30312	0.00017
2	0.40037	0.00022
2.5	0.49488	0.00027
3	0.58807	0.00032
3.5	0.67887	0.00035
4	0.76723	0.00039
4.5	0.85257	0.00043
5	0.93598	0.00047
5.5	1.01546	0.00051
6	1.09008	0.00058
6.5	1.16531	0.00059
7	1.23688	0.00062
7.5	1.30486	0.00065
8	1.37247	0.00069
8.5	1.43472	0.00072
9	1.49344	0.0007
9.5	1.55141	0.00074
10	1.60695	0.00074

Table D.22. δ -phase criticality values

Radius	k_{eff}	$\sigma(k_{eff})$
^{240}Pu Frac. = 0.00		
0.5	0.09511	0.00006
1	0.18914	0.00011
1.5	0.28149	0.00016
2	0.37257	0.00021
2.5	0.46169	0.00025
3	0.54897	0.0003
3.5	0.63465	0.00033
4	0.71767	0.00038
4.5	0.79939	0.00043
5	0.87762	0.00047
5.5	0.95434	0.0005
6	1.02679	0.0005
6.5	1.10015	0.00052
7	1.17056	0.00058
7.5	1.23549	0.00062
8	1.30127	0.00063
8.5	1.36212	0.00066
9	1.42209	0.00067
9.5	1.47941	0.00069
10	1.53259	0.00067
^{240}Pu Frac. = 0.01		
0.5	0.09492	0.00007
1	0.18848	0.00011
1.5	0.28082	0.00017
2	0.3713	0.0002
2.5	0.46066	0.00026
3	0.54829	0.00029
3.5	0.63301	0.00035
4	0.71635	0.00039
4.5	0.79712	0.00042
5	0.87559	0.00043
5.5	0.95069	0.00051
6	1.02591	0.00052
6.5	1.09781	0.00054
7	1.1669	0.00058
7.5	1.23347	0.0006
8	1.29828	0.00064
8.5	1.36017	0.00067
9	1.41992	0.00067
9.5	1.47694	0.00069
10	1.53247	0.00074

Radius	k_{eff}	$\sigma(k_{eff})$
^{240}Pu Frac. = 0.02		
0.5	0.09474	0.00006
1	0.18802	0.00012
1.5	0.27991	0.00017
2	0.37063	0.00021
2.5	0.45924	0.00025
3	0.54683	0.0003
3.5	0.6311	0.00033
4	0.71384	0.00037
4.5	0.79618	0.00041
5	0.87306	0.00045
5.5	0.95025	0.00048
6	1.02347	0.00054
6.5	1.09516	0.00055
7	1.16555	0.00059
7.5	1.2306	0.00062
8	1.29395	0.00064
8.5	1.35733	0.00068
9	1.41665	0.00068
9.5	1.47327	0.0007
10	1.52906	0.00072
^{240}Pu Frac. = 0.03		
0.5	0.09441	0.00006
1	0.18773	0.00011
1.5	0.2795	0.00016
2	0.36998	0.00021
2.5	0.45827	0.00025
3	0.5449	0.00029
3.5	0.62955	0.00035
4	0.71236	0.00039
4.5	0.7927	0.0004
5	0.87193	0.00045
5.5	0.94731	0.00048
6	1.0208	0.00053
6.5	1.09293	0.00058
7	1.16176	0.00058
7.5	1.2274	0.00062
8	1.29204	0.00063
8.5	1.35502	0.00064
9	1.41365	0.00069
9.5	1.46986	0.0007
10	1.52571	0.0007

Radius	k_{eff}	$\sigma(k_{eff})$
^{240}Pu Frac. = 0.04		
0.5	0.0941	0.00006
1	0.18735	0.00011
1.5	0.27864	0.00016
2	0.36849	0.00021
2.5	0.45755	0.00024
3	0.54369	0.0003
3.5	0.62849	0.00033
4	0.71171	0.00038
4.5	0.79211	0.00042
5	0.86932	0.00045
5.5	0.9456	0.00049
6	1.01927	0.00051
6.5	1.09038	0.00055
7	1.15947	0.00055
7.5	1.22482	0.00062
8	1.28982	0.00064
8.5	1.35158	0.00067
9	1.41043	0.00069
9.5	1.46847	0.00068
10	1.52138	0.00072
^{240}Pu Frac. = 0.05		
0.5	0.09398	0.00006
1	0.18655	0.00011
1.5	0.27828	0.00016
2	0.36759	0.00022
2.5	0.45582	0.00024
3	0.54285	0.00029
3.5	0.62717	0.00033
4	0.70907	0.00038
4.5	0.78985	0.00041
5	0.86703	0.00046
5.5	0.94416	0.00049
6	1.01732	0.00053
6.5	1.08794	0.00053
7	1.15694	0.00058
7.5	1.22351	0.00061
8	1.28768	0.00062
8.5	1.34881	0.00066
9	1.40831	0.00066
9.5	1.46367	0.0007
10	1.51896	0.00073

Radius	k_{eff}	$\sigma(k_{eff})$
^{240}Pu Frac. = 0.06		
0.5	0.09388	0.00006
1	0.18626	0.00011
1.5	0.2775	0.00016
2	0.36722	0.00019
2.5	0.45478	0.00025
3	0.54155	0.00029
3.5	0.62528	0.00035
4	0.70783	0.00038
4.5	0.7867	0.00042
5	0.86452	0.00043
5.5	0.94055	0.00049
6	1.01398	0.00052
6.5	1.08507	0.00056
7	1.15426	0.00057
7.5	1.21979	0.00059
8	1.28435	0.00065
8.5	1.34507	0.00064
9	1.40361	0.00068
9.5	1.46076	0.0007
10	1.51574	0.00071
^{240}Pu Frac. = 0.07		
0.5	0.09364	0.00006
1	0.18565	0.00011
1.5	0.27682	0.00016
2	0.36562	0.00021
2.5	0.45394	0.00026
3	0.53951	0.0003
3.5	0.62375	0.00033
4	0.70524	0.00038
4.5	0.78603	0.00042
5	0.86365	0.00043
5.5	0.93906	0.00048
6	1.0125	0.00052
6.5	1.08255	0.00054
7	1.15235	0.00057
7.5	1.21799	0.00059
8	1.28091	0.00064
8.5	1.34363	0.00065
9	1.40253	0.00065
9.5	1.45849	0.00071
10	1.51401	0.00074

Radius	k_{eff}	$\sigma(k_{eff})$
^{240}Pu Frac. = 0.08		
0.5	0.09322	0.00007
1	0.18539	0.00012
1.5	0.27604	0.00017
2	0.36494	0.00021
2.5	0.45266	0.00026
3	0.53816	0.0003
3.5	0.62207	0.00035
4	0.70378	0.00038
4.5	0.78299	0.0004
5	0.86152	0.00047
5.5	0.93659	0.00048
6	1.00931	0.00051
6.5	1.08049	0.00054
7	1.14737	0.00055
7.5	1.21362	0.00061
8	1.27833	0.00063
8.5	1.34023	0.00068
9	1.39917	0.00067
9.5	1.45639	0.00069
10	1.50973	0.00071
^{240}Pu Frac. = 0.09		
0.5	0.09318	0.00006
1	0.18473	0.00012
1.5	0.2752	0.00016
2	0.36443	0.0002
2.5	0.45138	0.00024
3	0.53715	0.00029
3.5	0.62093	0.00033
4	0.70245	0.00038
4.5	0.78145	0.00041
5	0.8591	0.00042
5.5	0.93409	0.00048
6	1.00825	0.00052
6.5	1.07713	0.00057
7	1.14533	0.00057
7.5	1.21133	0.00061
8	1.27507	0.00062
8.5	1.33743	0.00067
9	1.39589	0.00066
9.5	1.45362	0.0007
10	1.50606	0.0007

Radius	k_{eff}	$\sigma(k_{eff})$
^{240}Pu Frac. = 0.1		
0.5	0.09285	0.00006
1	0.18467	0.00011
1.5	0.27445	0.00016
2	0.36317	0.0002
2.5	0.45027	0.00025
3	0.53606	0.00029
3.5	0.6196	0.00033
4	0.70045	0.00036
4.5	0.77934	0.0004
5	0.85695	0.00044
5.5	0.93218	0.00048
6	1.00477	0.00051
6.5	1.07431	0.00054
7	1.14278	0.00056
7.5	1.20718	0.00057
8	1.27194	0.00061
8.5	1.33347	0.00064
9	1.39241	0.00069
9.5	1.44919	0.00067
10	1.50421	0.00074
^{240}Pu Frac. = 0.11		
0.5	0.09266	0.00007
1	0.18394	0.00011
1.5	0.27404	0.00016
2	0.36246	0.00021
2.5	0.4494	0.00025
3	0.53461	0.00029
3.5	0.61811	0.00034
4	0.69801	0.00037
4.5	0.77755	0.00042
5	0.85522	0.00047
5.5	0.92919	0.00048
6	1.00155	0.00052
6.5	1.07197	0.00055
7	1.1402	0.00057
7.5	1.20543	0.00059
8	1.26931	0.00065
8.5	1.3314	0.00065
9	1.38908	0.00069
9.5	1.44683	0.0007
10	1.49903	0.00069

Radius	k_{eff}	$\sigma(k_{eff})$
^{240}Pu Frac. = 0.12		
0.5	0.09253	0.00006
1	0.18371	0.00012
1.5	0.27345	0.00016
2	0.36178	0.0002
2.5	0.44761	0.00025
3	0.53356	0.00029
3.5	0.61604	0.00034
4	0.69702	0.00037
4.5	0.77624	0.0004
5	0.85255	0.00044
5.5	0.9288	0.00048
6	1.0008	0.00049
6.5	1.06984	0.00054
7	1.13745	0.00058
7.5	1.20336	0.0006
8	1.26704	0.00063
8.5	1.32781	0.00068
9	1.38658	0.00068
9.5	1.44323	0.00071
10	1.49667	0.00071
^{240}Pu Frac. = 0.13		
0.5	0.09227	0.00006
1	0.18299	0.00011
1.5	0.27279	0.00016
2	0.36047	0.0002
2.5	0.44729	0.00025
3	0.53239	0.0003
3.5	0.61419	0.00034
4	0.69507	0.00036
4.5	0.7739	0.0004
5	0.8496	0.00042
5.5	0.92556	0.00045
6	0.99762	0.00053
6.5	1.06809	0.00053
7	1.13467	0.00058
7.5	1.20116	0.00063
8	1.26212	0.00059
8.5	1.32421	0.00066
9	1.38191	0.00067
9.5	1.43985	0.0007
10	1.49356	0.00073

Radius	k_{eff}	$\sigma(k_{eff})$
^{240}Pu Frac. = 0.14		
0.5	0.09183	0.00006
1	0.18254	0.00011
1.5	0.27187	0.00016
2	0.35945	0.0002
2.5	0.44531	0.00025
3	0.53001	0.0003
3.5	0.61241	0.00033
4	0.69381	0.00038
4.5	0.77276	0.0004
5	0.84828	0.00044
5.5	0.92257	0.00047
6	0.99554	0.00048
6.5	1.06395	0.00053
7	1.13241	0.00058
7.5	1.19867	0.0006
8	1.26026	0.00063
8.5	1.32117	0.00064
9	1.37976	0.00067
9.5	1.43619	0.00068
10	1.49017	0.00073
^{240}Pu Frac. = 0.15		
0.5	0.09175	0.00006
1	0.18217	0.00011
1.5	0.27151	0.00016
2	0.35868	0.00021
2.5	0.44477	0.00025
3	0.52866	0.00031
3.5	0.611	0.00033
4	0.69232	0.00038
4.5	0.77039	0.00039
5	0.84642	0.00043
5.5	0.92071	0.00049
6	0.99295	0.0005
6.5	1.06214	0.00054
7	1.12925	0.00056
7.5	1.19451	0.0006
8	1.25809	0.00061
8.5	1.3185	0.00066
9	1.37728	0.00068
9.5	1.43346	0.00071
10	1.4852	0.00071

Radius	k_{eff}	$\sigma(k_{eff})$
^{240}Pu Frac. = 0.16		
0.5	0.09145	0.00006
1	0.18166	0.00012
1.5	0.27038	0.00016
2	0.35773	0.00021
2.5	0.44319	0.00025
3	0.52753	0.00028
3.5	0.60992	0.00035
4	0.68871	0.00038
4.5	0.76851	0.00042
5	0.84471	0.00044
5.5	0.9187	0.0005
6	0.98976	0.00048
6.5	1.05942	0.00055
7	1.12715	0.00057
7.5	1.19224	0.00059
8	1.25449	0.00059
8.5	1.31517	0.00066
9	1.37423	0.00065
9.5	1.42945	0.00068
10	1.48384	0.00069
^{240}Pu Frac. = 0.17		
0.5	0.09123	0.00006
1	0.18103	0.00011
1.5	0.26977	0.00016
2	0.35677	0.00021
2.5	0.44239	0.00025
3	0.52579	0.00028
3.5	0.60796	0.00032
4	0.68829	0.00036
4.5	0.76631	0.0004
5	0.84248	0.00043
5.5	0.91648	0.00046
6	0.98713	0.00052
6.5	1.05524	0.00052
7	1.12354	0.00058
7.5	1.18829	0.00058
8	1.25159	0.0006
8.5	1.31252	0.00065
9	1.37104	0.00068
9.5	1.42668	0.00068
10	1.48076	0.0007

Radius	k_{eff}	$\sigma(k_{eff})$
^{240}Pu Frac. = 0.18		
0.5	0.09108	0.00006
1	0.18062	0.00011
1.5	0.26942	0.00016
2	0.35565	0.00021
2.5	0.4418	0.00024
3	0.5247	0.00029
3.5	0.60672	0.00032
4	0.68603	0.00037
4.5	0.7637	0.0004
5	0.83905	0.00045
5.5	0.91309	0.00048
6	0.98483	0.00049
6.5	1.05367	0.00053
7	1.12186	0.00058
7.5	1.18605	0.00059
8	1.24677	0.00063
8.5	1.30946	0.00069
9	1.36662	0.00068
9.5	1.42291	0.00066
10	1.47678	0.00072
^{240}Pu Frac. = 0.19		
0.5	0.09074	0.00006
1	0.18054	0.00011
1.5	0.26798	0.00015
2	0.35472	0.0002
2.5	0.43955	0.00024
3	0.52286	0.0003
3.5	0.60465	0.00033
4	0.68397	0.00036
4.5	0.76241	0.00041
5	0.83763	0.00044
5.5	0.91098	0.00048
6	0.98171	0.0005
6.5	1.05137	0.00052
7	1.11792	0.00059
7.5	1.18307	0.0006
8	1.24489	0.00062
8.5	1.30481	0.00063
9	1.36492	0.00065
9.5	1.42003	0.00069
10	1.47383	0.00071

Radius	k_{eff}	$\sigma(k_{eff})$
^{240}Pu Frac. = 0.2		
0.5	0.09055	0.00007
1	0.1799	0.00011
1.5	0.26752	0.00015
2	0.35408	0.0002
2.5	0.43907	0.00026
3	0.5222	0.0003
3.5	0.60314	0.00033
4	0.68294	0.00036
4.5	0.76045	0.00039
5	0.83531	0.00044
5.5	0.9091	0.00047
6	0.97928	0.00052
6.5	1.04896	0.00053
7	1.11484	0.00055
7.5	1.17873	0.00059
8	1.24403	0.00062
8.5	1.30246	0.00064
9	1.35989	0.00067
9.5	1.41641	0.00067
10	1.47072	0.00074

Table D.23. α -phase Pu sphere surface flux

^{240}Pu Frac.	Radius ($k_{eff} = 0.9$) (cm)	Flux, ϕ ($\text{cm}^{-2} \text{s}^{-1}$)	$\sigma(\phi)$
0.00	4.51987	5.96295	0.01132
0.01	4.5330043	2512.00	4.77280
0.02	4.5461386	5035.07	9.56664
0.03	4.5592729	7592.93	14.4265
0.04	4.5724072	10119.9	19.2278
0.05	4.5855415	12715.1	24.1587
0.06	4.5986758	15283.0	29.0378
0.07	4.6118101	17913.1	34.0350
0.08	4.6249444	20554.9	39.0543
0.09	4.6380787	23210.7	44.1004
0.1	4.651213	25880.3	49.1727
0.11	4.6643473	28490.3	54.1316
0.12	4.6774816	31147.8	59.1809
0.13	4.6906159	33894.5	64.3996
0.14	4.7037502	36486.5	69.3244
0.15	4.7168845	39197.8	74.4758
0.16	4.7300188	41897.1	79.6046
0.17	4.7431531	44730.9	84.9888
0.18	4.7562874	47379.6	90.0212
0.19	4.7694217	49934.5	94.8756
0.2	4.782556	52673.6	100.079

Table D.24. δ -phase Pu sphere surface flux

^{240}Pu Frac.	Radius ($k_{eff} = 0.9$) (cm)	Flux, ϕ ($\text{cm}^{-2} \text{s}^{-1}$)	$\sigma(\phi)$
0.00	5.14113	6.01415	0.01142
0.01	5.155747	2537.26	4.82081
0.02	5.170364	5085.56	9.66256
0.03	5.184981	7644.80	14.5251
0.04	5.199598	10208.1	19.3955
0.05	5.214215	12799.1	24.3183
0.06	5.228832	15370.3	29.2036
0.07	5.243449	18032.1	34.2610
0.08	5.258066	20676.8	39.2860
0.09	5.272683	23378.3	44.4189
0.1	5.2873	25968.7	49.3405
0.11	5.301917	28607.3	54.3539
0.12	5.316534	31260.4	59.3948
0.13	5.331151	34023.0	64.6437
0.14	5.345768	36576.9	69.4961
0.15	5.360385	39295.9	74.6623
0.16	5.375002	41988.3	79.7778
0.17	5.389619	44793.2	85.1071
0.18	5.404236	47444.4	90.1444
0.19	5.418853	49950.9	94.9067
0.2	5.43347	52681.5	100.094